



**Platelets as components of the circulating immune
system: role as scavenging cells**

Anisha Rose Chacko

**This dissertation is submitted for the degree of
*Doctor of Philosophy***

**The University of Hull and The University of York
Hull York Medical School (HYMS)**

September 2020

Abstract

Although platelets are widely known for their role in haemostasis, an increasing body of evidence demonstrates platelets to encompass a role as immune cells. This underappreciated function involves numerous cell surface receptors and a series of intracellular signalling events which ultimately enable platelets to migrate, scavenge and aggregate at the site of infection, thus promoting immunologic responses.

At the same time microorganisms have evolved to develop a variety of virulence factors which enable them to survive and evade host defence systems, in many cases by interfering with the signalling machinery that regulates remodelling of the cytoskeleton (Rho GTPases). One such example is the cytotoxic necrotising factor 1 (CNF1), a toxin secreted by certain *Escherichia coli* strains and whose effects in platelets remain unclear.

We hypothesise that Rho GTPases (which are key regulators of the actin cytoskeleton), platelet receptors such as FcγRIIA and GPIIb/IIIa (which aid platelet-bacteria and platelet-matrix interactions) and downstream tyrosine kinase (TK) signalling molecules critically influence platelet scavenging and migration properties. In this thesis we aim to adapt, optimise, and make use of the quantification capabilities of assays to gain insight into the molecular mechanisms involved in platelet scavenging and migration properties through the use of a panel of specific inhibitors.

We found inhibition of RhoA, Rac1 and Cdc42 to significantly impair the ability of platelets to scavenge bacteria and migrate on fibrinogen, suggesting that Rho GTPases are critically involved in regulating such platelet immunologic functions. The same was found to be true for various TK signalling molecules (Src, Syk and BTK). These results were complemented with platelet aggregation tests which revealed significant changes elicited by inhibitors in the ability of platelets to aggregate in response to bacteria.

We also hypothesise that CNF1, which targets Rho GTPases by rendering them constitutively active, will lead to major modifications in Rho signalling and consequently affect platelet functions, thus contributing to the pathogenesis of *E. coli* infection.

We demonstrate indirectly for CNF1 to be taken up and processed by platelets, where it modifies Rho GTPases and induces an increase in F-actin. We found morphological alterations in toxin-treated platelets as well as slightly reduced integrin activation and granule secretion upon stimulation with various agonists.

In summary, our data revealed platelets to encompass immune functions (scavenging and migration) that aid the prevention of infections progressing to conditions such as sepsis, and for this to be tightly regulated by a number of Rho GTPases and TK signalling molecules. However, our data also emphasised how microorganism have evolved and adapted to evade and modify platelet functions to aid their survival in the host.

Publications

Poster presentations:

- Chacko, A.R., DJ Riley, J Wei, A Colarusso, ML Tutino., & F Rivero., 2020. The bacterial toxin cytotoxic necrotising factor 1 and its effects on platelet function. International Society on Thrombosis and Hemostasis, *Virtual conference, UK*.
- Chacko, A.R., DJ Riley, J Wei, A Colarusso, ML Tutino., & F Rivero., 2019. Effects of the bacterial toxin cytotoxic necrotising factor 1 on platelet function. The platelet society conference, *Cambridge, UK*.
- Chacko, A.R., & Rivero, F., 2019. Scavenging of bacteria by platelets. Allam Lecture, *Hull, UK*.
- Chacko, A.R., Riley, D., & Rivero, F., 2018. Migration and Clearance of bacteria by platelets. *North of England Cell Biology Forum 15th Annual Meeting, Huddersfield, UK*
- Chacko, A.R., Riley, D., Pieters, J., & Rivero, F., 2018. Migration and Clearance of bacteria by platelets. *4th European platelet network, Bruges, Belgium*.
- Chacko, A.R., Riley, D., & Rivero, F., 2018. Migration and Clearance of bacteria by platelets. *7th HYMS Postgraduate Research Conference, Hull, UK*. (Winner of best poster presentation award).

Table of contents

Abstract	2
Publications	4
Table of contents	5
List of figures	10
List of tables	14
Abbreviations	15
Acknowledgements	19
Author's declaration	21
Chapter 1. Introduction	22
1.1 Platelets: an overview.....	22
1.1.1 Platelet formation and production.....	22
1.2 Platelet ultrastructure.....	24
1.2.1 The plasma membrane and membrane systems.....	25
1.2.2 Organelles and granules.....	26
1.2.3 The platelet cytoskeleton.....	31
1.2.3.1 Structural changes of activated platelets.....	32
1.3 The actin cytoskeleton.....	35
1.3.1 Overview on actin.....	35
1.3.2 Mechanism of actin polymerisation and depolymerisation.....	35
1.3.3 Actin-binding proteins.....	38
1.3.4 Formation of actin structures.....	41
1.4 Rho GTPases.....	46
1.4.1 RhoA.....	48
1.4.2 Rac1.....	49
1.4.3 Cdc42.....	49
1.4.4 Regulation of Rho GTPases.....	50
1.5 Role of platelets in haemostasis.....	51
1.5.1 Platelet adhesion.....	51
1.5.2 Platelet activation.....	53
1.5.3 Platelet secretion.....	54
1.5.4 Platelet aggregation.....	54
1.6 Platelet signalling via receptors.....	56
1.6.1 Tyrosine kinase receptor.....	56
1.6.1.1 Inhibitors of tyrosine kinase signalling pathway.....	57

1.6.2 G-protein coupled receptors	59
1.6.3 Integrin $\alpha_{IIb}\beta_3$	63
1.7 Role of platelets in infection and immunity	64
1.7.1 General overview of platelets as immune cells.....	64
1.7.2 Platelets and their role in sepsis.....	68
1.7.3 Platelets are motile cells with scavenging abilities	69
1.8 Platelet-bacteria interplay	71
1.8.1 Bacteria can interact with platelet receptors.....	71
1.8.2 Platelet-bacteria: focus on <i>S. aureus</i>	76
1.8.2.1 <i>S. aureus</i> virulence factors.....	77
1.8.3 Platelet-bacteria: focus on <i>E. coli</i>	82
1.8.3.1 <i>E. coli</i> virulence factors.....	83
1.8.3.2 The cytotoxic necrotising factor	86
1.8.3.3 Cellular uptake of CNF1 toxins	88
1.8.3.4 Molecular mechanisms of CNF1 toxins	89
1.9 Aims of the study.....	91
Chapter 2. Materials and methods	93
2.1 Materials.....	93
2.1.1 Fluorescent dyes.....	93
2.1.2 Primary antibodies.....	93
2.1.3 Secondary antibodies	94
2.1.4 Bacterial species	94
2.1.5 Inhibitors.....	95
2.1.6 Chemicals.....	95
2.1.7 Sterilisation.....	96
2.2 Ethics.....	96
2.3 Platelet biology methods.....	97
2.3.1 Isolation of human platelets.....	97
2.3.2 Isolation of mouse platelets	99
2.3.3 Platelet counting.....	99
2.3.4 Assessing platelet functionality via light transmission aggregometry	100
2.4 Microbiology and immunocytochemistry methods	102
2.4.1 Preparation of bacteria for scavenging studies.....	102
2.4.2 Preparation of coverslips	103
2.4.3 Fixing and staining of cells	104
2.4.5 Mounting of coverslips	105

2.4.6 Microscopy and image analysis	105
2.4.7 Determination of the area platelets migrated on Alexa488 fibrinogen	105
2.4.8 Image analysis of bacteria scavenged by platelets	107
2.5 Biochemistry methods	114
2.5.1 Expression and purification of His- and GST-tagged cytotoxic necrotising factor 1 proteins	114
2.5.1.1 Small scale expression of His- and GST-tagged proteins	114
2.5.1.2 Lysate preparation from bacterial expression	117
2.5.1.3 Large scale expression of His-tagged and GST-tagged proteins	117
2.5.1.4 Purification and dialysis of CNF1.....	118
2.5.2 Determining protein concentration	119
2.5.3 SDS polyacrylamide gel electrophoresis	120
2.5.3.1 Polyacrylamide gel preparation	121
2.5.3.2 Performing electrophoresis	122
2.5.4 Coomassie blue staining	122
2.5.5 Western blotting procedures.....	123
2.5.6 Stripping and reprobing PVDF membranes	124
2.5.7 Determination of actin in the Triton insoluble pellet	124
2.5.8 Fluorescence activated cell sorting.....	125
2.5.8.1 Sample preparation for FACS.....	125
2.6 Statistical analysis	126
Chapter 3. Characterisation of platelet's ability to scavenge bacteria.	127
3.1 Introduction	127
3.2 Optimisation of bacterial coverage.....	133
3.2.1 Treatment of coverslips to determine maximal bacterial coverage.....	133
3.2.2 Effect of buffers on bacterial distribution and coverage on coverslips	139
.....	141
3.2.3 Determining the optimal density of bacteria required for maximal coverage on coverslips	142
3.3 Optimisation of conditions for scavenging	144
3.3.1 Effect of the platelet preparation on the ability to scavenge <i>S. aureus</i>	144
3.3.2 The effects of anticoagulants in the ability of platelets to scavenge bacteria	148
3.3.3 The effect of platelet concentration on bacterial scavenging	151
3.4 The ability of platelets to scavenge bacteria increases over time.....	154
3.5 Effect of pH and plasma concentration on the scavenging properties of platelets	158
3.6 Molecular mechanisms regulating scavenging of bacteria by platelets	165

3.6.1 Cytoskeletal inhibitors diminish the scavenging properties of platelets	165
3.6.2 Inhibition of platelet surface receptors FcγRIIIa and GPIIb/IIIa inhibits platelet aggregation and hinders platelet scavenging properties.	171
3.6.3 Inhibition of tyrosine kinase signalling pathways inhibits platelet aggregation and alters platelet scavenging properties	176
3.6.4 The effect of secondary mediator inhibitors on platelet aggregation and scavenging properties.	180
3.7 Supplementation of IgGs and fibrinogen on WPs' ability to scavenge.	184
3.8 Discussion	188
Chapter 4. Investigating platelet migration on Alexa488 fibrinogen.....	198
4.1 Introduction	198
4.2 Optimisation of conditions for platelet migration assay	201
4.2.1 Treatment of coverslips for optimal Alexa488 fibrinogen coating.....	201
4.2.2 The effect of platelet concentration on the ability of platelets to migrate	204
4.2.3 The ability for platelets to migrate on Alexa488 FG increases with time	206
4.2.4 The effect of platelet preparation on the ability of platelets to migrate	209
4.2.5 The effect of anticoagulants on the ability of platelets to migrate.....	212
4.3 Effect of plasma concentration on the migration properties of platelets	215
4.4 Molecular mechanisms regulating migration of platelets on Alexa488 fibrinogen	219
4.4.1 Cytoskeletal inhibitors diminish the migration properties of platelets.....	219
4.4.2 Inhibition of platelet surface receptors FcγRIIIa and GPIIb/IIIa modifies platelet migration capacity	224
4.4.3 Inhibition of tyrosine kinase signalling pathways alters the capacity of platelets to migrate.....	227
4.5 The ability of mouse platelets to migrate.....	231
4.5.1 Optimisation of the conditions required for mouse platelets to migrate on Alexa488 FG	231
4.5.2 A comparison of human and mouse plasma on the ability of mouse platelets to migrate	233
4.5.3 A comparison of fresh and frozen plasma on the ability of mouse platelets to migrate	236
4.5.4 The importance of coronin in the ability of mouse platelets to migrate	238
4.6 Discussion	240
Chapter 5. Effects of the bacterial toxin Cytotoxic Necrotising Factor 1 on platelet function.....	246
5.1 Introduction	246
5.2 Recombinant protein production and purification of CNF1 toxin.....	250
5.3 Does CNF1 modify Rho GTPase signalling pathways in platelets	253

5.3.1 Optimisations of conditions for commercially available Rho GTPase antibodies	253
5.3.2 CNF1 induces a mobility shift of Rho in platelets	255
5.3.3 CNF1 does not affect the stability of Rho GTPases in platelets	256
5.4 The effect of CNF1 on the amount of F-actin	258
5.5 The effect of CNF1 on platelet spreading and morphology.....	260
5.5.1 The effects of CNF1 on the morphology of human platelets and their ability to spread on FG and collagen.....	260
5.5.2 The effects of CNF1 on the morphology of mouse platelets and its ability to spread on FG	264
5.6 Effects of CNF1 on secretion and integrin activation	267
5.6.1 The effects of CNF1 intoxication on platelet receptor activation.....	267
5.6.2 Effects of CNF1 on integrin activation	268
5.6.3 The effect of CNF1 on platelet granule secretion.....	270
5.7 Discussion.....	273
Chapter 6. Discussion.....	278
6.1 General discussion	278
6.2 Future work.....	287
Appendices.....	289
References	294

List of figures

Chapter 1. Introduction

1.1 A schematic representation of the steps involved in the production of platelets from megakaryocytes.....	23
1.2 A summary of the structural elements found within a platelet in the equatorial plane	24
1.3 Platelet dense granule content	29
1.4 Schematic representation of the platelet cytoskeleton in its quiescent state.	32
1.5 Transmission electron microscopy of platelets adhered to glass	34
1.6 A schematic diagram of the sequential steps for the polymerisation and depolymerisation of actin filaments.....	37
1.7 Actin structures in platelets.....	41
1.8 The signalling pathway involved in the formation of filopodia in platelets	43
1.9 Lamellipodia formation in platelets.....	44
1.10 Stress fibre formation in platelets	45
1.11 The regulation and activation cycle for Rho GTPases	46
1.12 Platelet adhesion and activation on ECM at sites of vascular endothelial damage....	52
1.13 Schematic representation of platelet activation and the signalling pathways involved	54
1.14 Model of tyrosine kinase mediated signalling pathway in platelets.....	57
1.15 Mechanisms by which bacteria bind to platelet integrin GPIIb-IIIa	73
1.16 Mechanisms by which bacteria bind to platelet GPIb.....	74
1.17 Molecules involved in the interaction between platelets and <i>S. aureus</i> and their effect on platelet functions	78
1.18 Examples of specialised virulence factors of different <i>E. coli</i> pathotypes	83
1.19 Molecular structure of CNF1	86
1.20 Cellular uptake and processing of CNF1 by target cells	89
1.21 CNF1-mediated activation of Rho GTPases	90

Chapter 2. Materials and methods

2.1 Light transmission aggregation principle.....	101
2.2 Selection of area of Alexa488 FG coating.	106
2.3 Image of a platelet scavenging Alexa488 FG and the corresponding analysis	106
2.4 A step by step protocol used to analyse the number of bacteria scavenged by platelets.....	109
2.5 Histogram showing the pixel intensity value per bacterium	110
2.6 Correlation in the number of bacteria determined using the formula and manual counting	111
2.7 Correlation between number of bacteria in cluster between Z-stack image and single plane image.....	112
2.8 Bacterial density in scavenged clusters and non-scavenged areas.	113

Chapter 3. Characterisation of platelet's ability to scavenge bacteria

3.1 Immobilisation of <i>S. aureus</i> Newman on glass coverslips	136
3.2 Immobilisation of <i>E. coli</i> RS218 on glass coverslips.	138
3.3 Effect of solutions on bacterial attachment to glass coverslips,	141
3.4 Optimisation of the density of <i>S. aureus</i> Newman	143
3.5 Difference between washed platelets and platelet rich plasma in scavenging immobilised <i>S. aureus</i> Newman.....	148
3.6 Effect of anticoagulant on the capacity of platelets to scavenge bacteria.....	151
3.7 The effect of platelet density on the ability of platelets to scavenge <i>S. aureus</i> Newman.	153
3.8 Time dependent changes in the ability of platelets to scavenge <i>S. aureus</i> Newman .	157
3.9 The effect of plasma concentration on the pH of platelet suspensions.....	159
3.10 Effect of the concentration of plasma on platelets' ability to scavenge <i>S. aureus</i> Newman	163
3.11 Cytoskeleton inhibitors block platelet aggregation. (A) Representative LTA trace...167	
3.12 The effect of cytoskeletal inhibitors on platelet functions.....	170
3.13 The effect of platelet surface receptor inhibitors on platelet functions	175
3.14 The effect of BTK, Src and Syk signalling inhibitors on platelet scavenging and aggregation.	179

3.15 The effect apyrase and indomethacin on platelet scavenging ability and aggregation	182
3.16 The effect of supplementing WP with FG and/or IgG on platelet scavenging and aggregation properties	187

Chapter 4. Investigation platelet migration on fibrinogen

4.1 Effect of silanisation of coverslips on platelet adhesion and migration	203
4.2 The effect of platelet density on the ability of platelets to migrate on Alexa488 FG.	205
4.3 Time-dependent effects on the ability of platelets to migrate on Alexa488 FG.....	208
4.4 Difference between human washed platelets and platelet rich plasma in their ability to migrate	212
4.5 Effect of anticoagulant on the capacity of platelets to migrate on Alexa488 FG	214
4.6 Effect of the concentration of plasma on platelets' ability to migrate	218
4.7 The effect of cytoskeletal inhibitors on platelet migration on Alexa488 FG.....	223
4.8 The effect of platelet surface receptor inhibitors on platelet functions.....	226
4.9 The effect of BTK, Src and Syk signalling inhibitors on the ability of platelets to migrate	230
4.10 Difference between mouse washed platelets and platelet rich plasma in their ability to migrate	233
4.11 The difference between resuspending mouse platelets in human or mouse plasma on their ability to migrate.....	235
4.12 The effects of diluting platelets in frozen plasma on the capacity of platelets to migrate.....	237
4.13 The difference between KO and WT coronin mouse models in their ability to migrate on Alexa488 FG	239

Chapter 5. Effect of bacterial toxin Cytotoxic necrotising factor 1 on platelet function

5.1 Expression and purification of GST-tagged CNF1 toxin	250
5.2 Expression and purification of his-tagged CNF1 toxin.....	251
5.3 Expression and purification of CNF1 C688S. Bacterial total lysates were obtained before (NI) and after (I) induction of expression with 0.5 mM IPTG. Bacterial.	252
5.4 Optimisation of conditions for Rho GTPase antibodies in platelets.	254

5.5 Electrophoretic shift of platelet RhoA upon exposure to CNF1	256
5.6 CNF1 effects on the stability of Rho GTPases in platelets	257
5.7 The effect of CNF1 on the F-actin concentration of thrombin-stimulated platelets...	259
5.8 The effect of CNF1 on the morphology and ability of human washed platelets to spread on fibrinogen and collagen	262
5.9 The effect of CNF1 on the morphology and ability of mouse washed platelets to spread on fibrinogen	266
5.10 Flow cytometric analysis of the expression of platelet surface receptors in platelets treated with CNF1	268
5.11 Flow cytometric analysis of integrin activation in platelets treated with CNF1.....	269
5.12 Flow cytometric analysis of alpha granule secretion in platelets treated with CNF.	271

Chapter 6. General discussion

6.1 A schematic model of the platelet signalling cascade for platelet scavenging induced by <i>S. aureus</i> Newman.....	281
6.2 A schematic model of the platelet signalling cascade for platelet migration	283
6.3 A schematic model of the effect of CNF1 on platelet signalling pathways	285

Appendix

7.1 Immobilisation of <i>S. aureus</i> Newman and <i>E. coli</i> RS218 on glass coverslips.....	289
7.2 The extent to which plasma affects the attachment of bacteria and platelets to the coverslips in a scavenging assay	290
7.3 The effects of an extended platelet incubation time on the ability of platelets to migrate	291
7.4 Platelets express p37/67 and Lu/BCAM laminin receptors required for CNF1 binding	292
7.5 The effect of CNF1 on the ability of human washed platelets to spread on fibrinogen over time	293

List of tables

Chapter 1. Introduction

1.1 Examples of alpha granule content and their functions in platelets.	28
1.2 Examples of actin-binding proteins in platelets.	40
1.3 Examples of effector proteins and the Rho GTPases that activate them.	47
1.4 Summary of some of the functions reported for Rho GTPase in platelets	48
1.5 Key agonists acting via GPCRs on human and mouse platelets.	60
1.6 Examples of platelet products and how they function as immune cells.....	66
1.7 Some of the effects reported upon treating cells with CNF1.....	87

Chapter 2. Materials and methods

2.1.1 Fluorescent dyes.....	93
2.1.2 Primary antibodies.....	93
2.1.3 Secondary antibodies	94
2.1.4 Bacterial species	94
2.1.5 Inhibitors.....	95
2.1.6 Polyacrylamide gel composition for SDS-PAGE	121

Abbreviations

α -granule	Alpha granule
δ -granules	Dense granule
ACD	Acid citrate dextrose
ACAL	Acalabrutinib
ADP	Adenosine diphosphate
ATP	Adenosine triphosphate
Alexa488 FG	Alexa488 fibrinogen conjugate
Apy	Apyrase
ATP	Adenosine triphosphate
BCA	Bicinchoninic acid
BCR	B-cell receptor
BHI	Brain heart infusion
BTK	Bruton tyrosine kinase
CASIN	Cdc42 activity-specific inhibitor
C1fA	Clumping factor A
CLL	Chronic lymphoid leukaemia
CML	Chronic myeloid leukaemia
CNF1	Cytotoxic necrotising factor 1
COX	Cyclo-oxygenase
DAG	Diacylglycerol
Das	Dasatinib
DMS	Demarcation membrane system
DMSO	Dimethyl sulfoxide
DTS	Dense tubular system
ECM	Extracellular matrix
F-actin	Filamentous actin
FA	Focal adhesion
FACS	Fluorescence activated cell sorting
FG	Fibrinogen
FITC	Fluorescein isothiocyanate phalloidin

FnBP	Fibronectin binding proteins
G-actin	Globular actin
GAPs	GTPase activating proteins
GEFs	Guanine nucleotide exchange factors
Gly	Glycogen
GM	Granulomere
GP	Glycoprotein
GPCR	G-protein coupled receptors
GR	Golgi remnants
GTP	Guanosine-5'-triphosphate
HM	Hyalomeres
HMDS	Hexamethyldisilazane
Ibrut	Ibrutinib
IE	Infective endocarditis
Indo	Indomethacin
IP	Prostaglandin receptor
IP3	Inositol tris-phosphate
IPTG	Isopropyl β - d-1-thiogalactopyranoside
ITAM	Immunoreceptor tyrosine-based activation motif
Lat-A	Latrunculin A
LB	Lysogeny broth
LTA	Light transmission aggregometry
MLC	Myosin light chain
Mit	Mitochondria
MKs	Megakaryocytes
MSCRAMM	Microbial surface components recognizing adhesive matrix molecules
MT	Microtubule
MTB	Modified Tyrode's buffer
OCS	Open canicular system
PAK	p21-activated kinases

PAMPs	Pathogen associated molecular patterns
PAR	Protease-activated receptor
PDI	Protein-disulphide isomerase
PF4	Platelet factor 4
PDGF	Platelet-derived growth factor
PGI ₂	Prostaglandin
PLC	Phospholipase C
PI3K	Phosphoinositide-3-kinase
PIC	Protein inhibitor cocktail
PIP ₂	Phosphatidylinositol-(4,5)-bisphosphate
PKC	Protein kinase C
PMSF	Phenylmethylsulfonyl fluoride
PPP	Platelet poor plasma
PREX1	PIP3-dependent Rac exchanger 1 protein
PRP	Platelet rich plasma
PRT318	PRT-060318
PS	Phosphatidylserine
PVDF	Polyvinylidene Fluoride
RANTES	Regulated on activation, normal T cell expressed and secreted
RGD	Arginine-Glycine-Aspartic acid
RhoGDI	Rho-guanine nucleotide dissociation inhibitor
Rib	Ribosomes
ROCK	Rho-associated kinases
<i>S. aureus</i>	Staphylococcus aureus
SD	Serine/aspartate
SDS	Sodium dodecyl sulfate
SDS-PAGE	Sodium dodecyl sulfate polyacrylamide gel electrophoresis
SFK	Src family kinase
Src	S-locus receptor kinase
Syk	Spleen tyrosine kinase
TBS-T	Tris buffered saline with Tween 20

TGF- β	Transforming growth factor- β
TK	Tyrosine kinase
TKI	Tyrosine kinase inhibitors
TLRs	Toll-like receptors
TP	Thromboxane receptor
TPO	Thrombopoietin
TRITC	Tetramethylrhodamine B isothiocyanate phalloidin
TxA2	Thromboxane A2
VEGF	Vascular endothelial growth factor
vWF	Von Willebrand's factor
WASp	Wiskott–Aldrich syndrome protein
WP	Washed platelets

Acknowledgements

First and foremost, I thank my God, Esho and my amma Mathav for constantly being with me throughout my life. They have blessed me immensely and continue to do so every single second of my life. Even when I wander away, your love and mercy has protected me.

Next, I would like to thank my supervisor Dr Francisco Rivero, who has guided me and supported me every step of the way. I feel privileged and blessed to have him as my supervisor, his patient and humble nature helped me immensely to stay optimistic during every hardship I faced. Without his guidance and reassurance, I would not have been able to complete this. I would also like to extend my gratitude to my TAP members: Dr Monica Arman and Dr Nathalie Signoret for all their advice and encouragement.

I would also like to express my deepest gratitude to all members of the platelet group, both past and present who helped me to remain sane and jovial. I would like to thank in particular Dr Jawad-ji who from day one ensured I was relaxed and happy and answered every single silly question I asked. Thank you for being like an older brother to me and thank you for being super welcoming and sharing all your funny and crazy childhood stories. Thank you especially for teaching me so much about science and life in such a short period of time. I am forever indebted to you for all the kindness and support you have given me. I hope to see you as Professor Jawad one day :). I would also like to thank Yusra who has been present in all my ups and downs for the past four years. I thank God for helping me meet such an amazing soul. Thank you for all the spontaneous adventures, the crazy singing sessions, for picking me up when I was lost, for listening to all my meltdowns and for generally being there for me. I wish you the best of everything life has to offer.

Moving away from home for the first time was indeed daunting and it is only right I thank the Malayalees in Hull (both in the University and outside) for helping me feel at home. I am fortunate to have met some incredible people and gained some amazing friends. Their mere presence has brightened many gloomy days. I am not mentioning any names but some in particular have gone above and beyond to ensure I remain happy and safe. I am

extremely lucky and blessed to have met you and all the countless memories will be cherished for a lifetime. Thank you all!

Also, my sincere thanks to all those who have encouraged me, prayed for me, made me smile, believed in me when I doubted myself, my friends, relatives, and all those in between. It genuinely means a lot and I remain forever grateful.

Finally, I cannot express into words the gratitude and love I have for my family. Without their unconditional love and prayers, I would not be where I am today. The sacrifices they have made for me is immeasurable and the support unfathomable. No amount of thank you will ever account for all that you have done for me and for everything you all are still doing for me. I am beyond blessed to be born with such loving parents and sister. There is so much I would like to mention but no number of words or pages will suffice for the depth of gratitude I have for you. I love you more than anything in the world and I am nothing without you.

To you- Pappa, Amma and Anitta, I dedicate this thesis.

Author's declaration

I confirm that this work is original and that if any passage(s) or diagram(s) have been copied from academic papers, books, the Internet, or any other sources these are clearly identified by the use of quotation marks and the reference(s) is fully cited. I certify that, other than where indicated, this is my own work and does not breach the regulations of HYMS, the University of Hull or the University of York regarding plagiarism or academic conduct in examinations. I have read the HYMS Code of Practice on Academic Misconduct, and state that this piece of work is my own and does not contain any unacknowledged work from any other sources.

Chapter 1. Introduction

1.1 Platelets: an overview

Platelets are small, anucleate, discoid cell fragments which are part of the blood constituents (Harker *et al.*, 2000; Meijden & Heemskerk, 2019). Platelets are small in size, generally 2 μm – 5 μm in diameter and have a short life span. They are typically in circulation for around 7 to 10 days in humans and comparatively less in mice, before being removed by the spleen and liver (Quach., 2018; Harker *et al.*, 2000). Platelets play a critical role in maintaining haemostasis by initiating blood coagulation upon vascular endothelial damage (Ghoshal and Bhattacharyya, 2014). Apart from their central role in preventing blood loss, emerging body of evidence suggests platelets to contribute to a wide spectrum of functions, including angiogenesis, cancer progression and inflammation (Menter *et al.*, 2014; Schlesinger, 2018).

1.1.1 Platelet formation and production

Platelets are formed from progenitor cells known as megakaryocytes (MK) through a well-regulated process. MK are highly specialised myeloid cells which reside primarily in the bone marrow but can also be found in the liver and spleen (Ogawa, 1993; Patel *et al.*, 2005). In addition to this, recent reports have proposed platelet biogenesis to occur in the lungs, though the mechanisms remain largely unclear (Looney, 2018).

MKs are large polyploid cells $\approx 50 \mu\text{m}$ to $100 \mu\text{m}$ in diameter, which arise from haemopoietic stem cells and are characterised by the presence of a multilobulated nucleus (Pang *et al.*, 2005). Immature precursor cells develop within the bone marrow and undergo endomitosis whereby they enlarge their diameter considerably, and this is regulated by thrombopoietin (TPO) (Patel *et al.*, 2005). Following nuclear endomitosis, a cascade of events occurs: breakdown of the nuclear envelope; replication of chromosomes; an increase in the concentration of ribosomes to facilitate the production of platelet-specific proteins; enlargement and maturation of the cytoplasm as well as the formation and expansion of organelles; generation of a demarcation membrane system (DMS) consisting of a network of cisternae and tubules; and the extension of DMS giving rise to structures known as proplatelets (Patel *et al.*, 2005; Thon & Italiano, 2010). This is then followed by the

extrusion of the nucleus from the mass of proplatelets and ultimately the release of individual platelets into the bloodstream from the bone marrow sinusoids (Patel *et al.*, 2005). An overview on the formation of platelets from MKs is summarised in Figure 1.1.

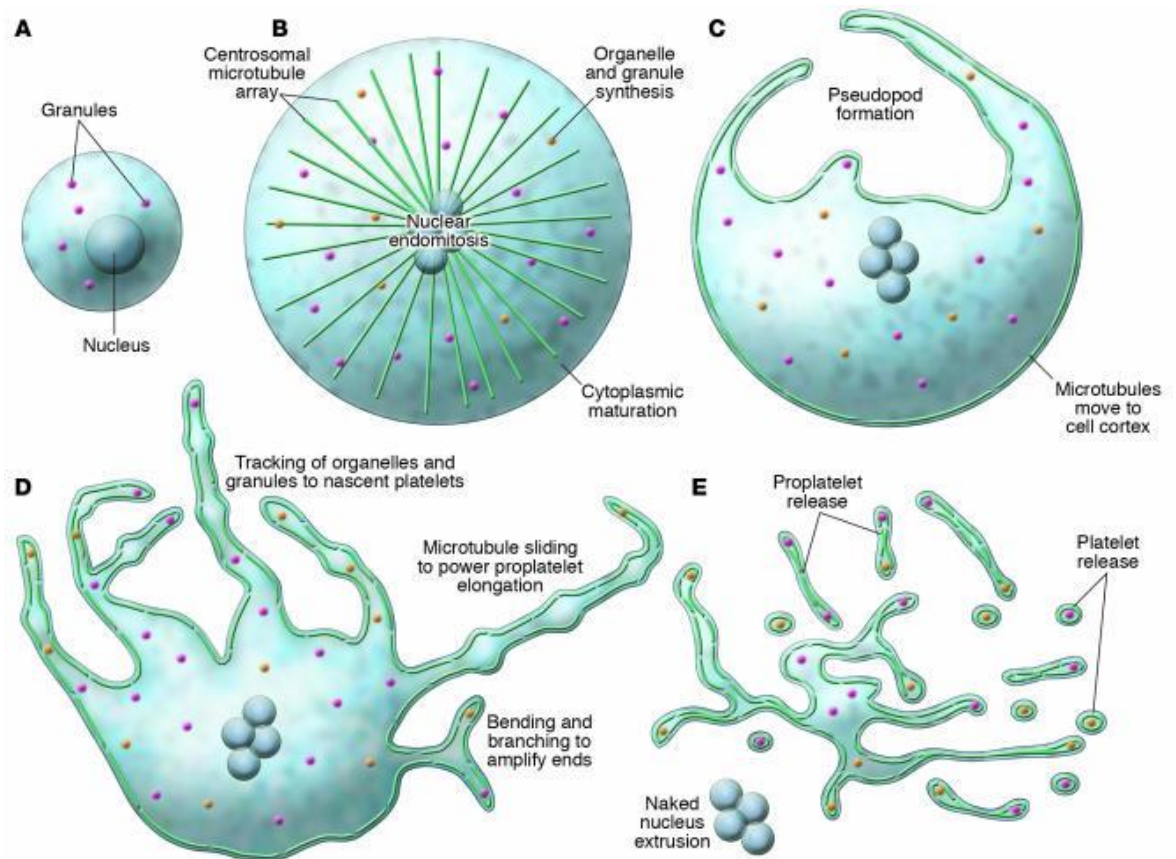


Figure 1.1 A schematic representation of the steps involved in the production of platelets from megakaryocytes.

Immature MKs (A) undergo numerous steps including nuclear endomitosis which facilitates the synthesis of organelles along with the maturation and expansion of cytoplasmic and cellular components (B). This is followed by the translocation of microtubules (MTs) to the cell cortex and the rearrangement/disassembly of centrosomes (C). Proplatelet production occurs as the cytoplasm of MKs begins to erode at one side of the pole. The reorganisation of MTs such that the overlapping MTs start to slide, drives proplatelet elongation. Translocation of organelles into proplatelet ends also occurs simultaneously (D). Subsequently, proplatelets continue to branch and bend outwards, causing the amplification of proplatelet ends. This step is followed by nuclear extrusion which mediates platelet release i.e. proplatelets become separated from the remaining cell mass via rapid retraction and are released into the bloodstream as platelets (E) (Patel *et al.*, 2005).

1.2 Platelet ultrastructure

A number of distinct structural features has been characterised in platelets predominately via transmission electron microscopy (Behnke, 1968). These features include: a demarcation plasma membrane with a spectrin-based membrane frame; the open canalicular system (OCS); the dense tubular system (DTS); the cytoskeleton formed primarily of actin; a cluster of MTs networks; several cytoplasmic organelles such as mitochondria and peroxisomes; and a range of granules which have the capacity to secrete their contents upon certain stimuli (White, 1972). The OCS is a network system of membrane that is contiguous with the plasma membrane. The DTS is an internal network of smooth endoplasmic reticulum residuals. The cytoskeleton is formed primarily of actin and a cluster of MT networks. Figure 1.2 depicts some of the major structures of human platelets and these are described in greater detail in the subsequent sections.

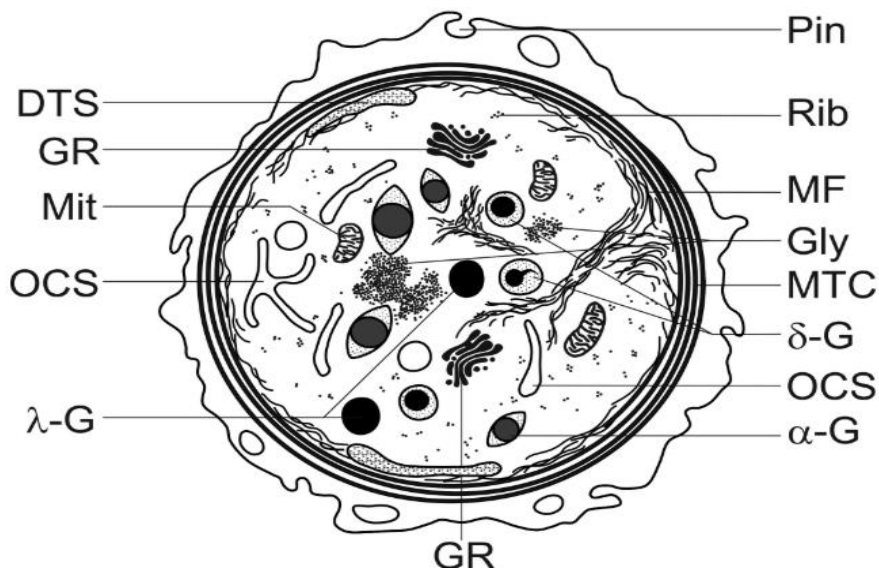


Figure 1.2 A summary of the structural elements found within a platelet in the equatorial plane. The peripheral zone is composed of an exterior coat and a submembrane area which when it protrudes inwards forms the open canalicular- and dense tubular- systems (OCS, DTS). Microfilaments (MF), glycogen granules (Gly) and microtubule coil (MTC) are found in the sol-gel zone. Additionally, structures such as platelet granules (α , δ , and λ), ribosomes (Rib), golgi remnants (GR) and mitochondria (Mit) are also found embedded in the sol-gel region. The regions which encompasses these elements are collectively referred to as the organelle zone (Neumüller et al., 2015).

1.2.1 The plasma membrane and membrane systems

The outermost layer of platelets consists of a thick (20-30 nm) amorphous coating referred to as the glycocalyx, which is rich in carbohydrates and glycoproteins (GPs) (White, 1979). The glycocalyx is adhesive and has the capacity to rapidly respond to haemostatic demands as well as aid the transport of plasma proteins such as fibrinogen and albumin into platelet granules (Fritsma, 2015). The plasma membrane of platelets consists of the typical membrane unit, primarily made up of an asymmetrical phospholipid bilayer in which GPs, glycolipids and cholesterol as well as Na⁺ and Ca²⁺-ATPase pumps regulating the internal ionic composition of platelets are embedded (Thon and Italiano, 2012).

The asymmetric organisation of phospholipids is maintained by enzymes known as flippases, which actively shift negatively charged phospholipids, for example phosphatidylserine (PS) and phosphatidylinositol (PI), to the inner leaflet of the plasma membrane, thus ensuring the surface of the platelet remains in a non-procoagulant state (Thon & Italiano, 2012). However, upon vascular injury, stimulation of platelets occurs and results in aminophospholipids to be revealed on the surface of platelets and this process is aided by enzymes such as ATP-dependent floppases and scramblases which ultimately stimulate platelet-surface based coagulation activity (Heemskerk *et al.*, 2002).

Microdomains rich in sphingolipids and cholesterol known as lipid rafts (containing proteins such as flotillin 1 and 2, stomatin and ganglioside) are also found within the plasma membrane of platelets (Thon and Italiano, 2012). Lipid rafts have been observed to play a critical role in platelet signalling processes. Indeed, a broad range of distinct surface receptors involved in a variety of platelet functions including platelet activation, aggregation, antimicrobial defence, coagulation and platelet granule content release are also found densely distributed on the biomolecular leaflet of platelets (Blair and Flaumenhaft, 2009). Platelet receptors will be described in subsequent sections.

As depicted in Figure 1.2, platelets contain two membrane systems, OCS and DTS, which are both perceptible in the resting platelet (Zucker-Franklin, 1997). The OCS consists of invaginations which are continuous with the plasma membrane and has been observed to

perform three critical functions in platelets (Behnke, 1970). The first involves the participation of OCS in the exchange of components from the external environment into the platelet, along with an exchange of released granular content from within the platelet to its external environment (Klement *et al.*, 2009). Secondly, the OCS has been reported to contain a vast number of internal membranes which can potentially evaginate to facilitate cytoskeletal membrane reorganisation and platelet shape change allowing the formation of actin structures such as filopodia which aid platelet spreading upon adhesion to a stimulating surface (Escolar *et al.*, 1989). Last of all, the OCS has been found to serve as a storage system for membrane GPs such as GPIb/IX, which upon thrombin-mediated activation of platelets becomes sequestered in the OCS (Michelson, 1992; Thon & Italiano, 2012).

The DTS on the other hand is a network of smooth endomembrane systems and appears to be in close juxtaposition with the OCS in particular regions (White, 1972). It was first discovered histochemically by White, (1972) who was able to distinguish the structure as it displayed peroxidase activity. The DTS was found to contribute to the stimulation and modulation of platelet activity and it is largely believed to be involved in the storage and sequestration of ionized calcium (Gerrard *et al.*, 1978). The DTS has also been described to harbour several enzymes such as calreticulin and protein-disulphide isomerase (PDI) which are essential for processes such as the folding of proteins (Heijnen and Korporaal, 2017). It has also been proposed for DTS to modulate actin cytoskeleton rearrangement as well as influence the secretion of platelet granule content (Thon & Italiano, 2012; White, 1972).

1.2.2 Organelles and granules

Like most cells in the body, platelets too contain numerous organelles within its structure. These organelles are involved in a diverse range of activities and play a critical role in maintaining both cellular and vascular integrity (Richardson *et al.*, 2005). A fascinating feature of platelets is the vast number of active biomolecules that are stored within their alpha- and dense granules (α - and δ - granules) (Flaumenhaft, 2003b). These biologically active molecules are released from the platelet granules upon vascular injury and are involved in the recruitment of various cells in the body.

Alpha granules

The most abundant secretory organelles within platelets are the α -granules (~50–80 per platelet) (Thon and Italiano, 2012). These spherically shaped granules are typically 200-500 nm in diameter and constitute approximately 10% of the platelet volume. Upon platelet activation α -granules fuse with the platelet membrane prior to secreting its content. Numerous adhesive proteins involved in primary haemostasis are found within the α -granules. These adhesive proteins are critically involved in aiding platelet adhesion as well as allowing the formation of a stable thrombus to arrest bleeding (Heijnen and Korporaal, 2017).

In addition to the adhesive proteins, several mediators as well as chemokines involved in mechanisms such as wound repair, angiogenesis, coagulation and inflammation have also been identified to be stored within the α -granules, with platelet factor 4 (PF4), β -thromboglobulin, and a molecule known as 'regulated on activation, normal T cell expressed and secreted' (RANTES) being the most abundant (Deuel *et al.*, 1981; Folkman *et al.*, 2001). It has been shown that the α -granular content is acquired from endogenous protein synthesis as well as exogenous plasma proteins (Heijnen and Korporaal, 2017). A list of some of the common molecules stored within α -granules and their roles upon secretion into the blood stream is listed in Table 1.1.

Table 1.1 Examples of alpha granule content and their functions in platelets.

Type of molecule	Examples	Involved in	Reference
Adhesive proteins	vWF Fibrinogen Fibronectin Vitronectin Thrombospondin	Primary haemostasis/ thrombus formation.	(Sander <i>et al.</i> , 1983), (Blair and Flaumenhaft, 2009), (Wencel-Drake <i>et al.</i> , 1986).
Cytokines	PF4 β -Thromboglobulin RANTES	Recruitment of other cells.	(Deuel <i>et al.</i> , 1981).
Mediators	PF4 β -Thromboglobulin Interleukin-8 (IL-8) Platelet-derived growth factor (PDGF) Transforming growth factor- β (TGF- β) Vascular endothelial growth factor (VEGF)	Coagulation, wound repair, inflammation, and angiogenesis.	(Folkman <i>et al.</i> , 2001), (Maynard <i>et al.</i> , 2007).

Dense granules

δ granules are the second most abundant secretory organelle in a platelet (3-8 per platelet) (Flaumenhaft and Sharda, 2018). Similar to α granules, they are generally spherically shaped and 200 nm in diameter (Heijnen and Korporaal, 2017). Moreover, like α -granules, δ granules also contain a myriad number of biological molecules which are predominantly involved in the recruitment of platelets to the site of vascular injury (Gerrard *et al.*, 1977). Examples of molecules stored and secreted by the δ granules are illustrated in Figure 1.3. These haemostatically active molecules are released upon platelet activation. Adenosine diphosphate (ADP) secreted from δ granules play a critical role in activating P2Y12 receptors on the platelet surface which in turn triggers a feedback mechanism for the platelet activation cycle (Section 1.5) (Heijnen and Korporaal, 2017).

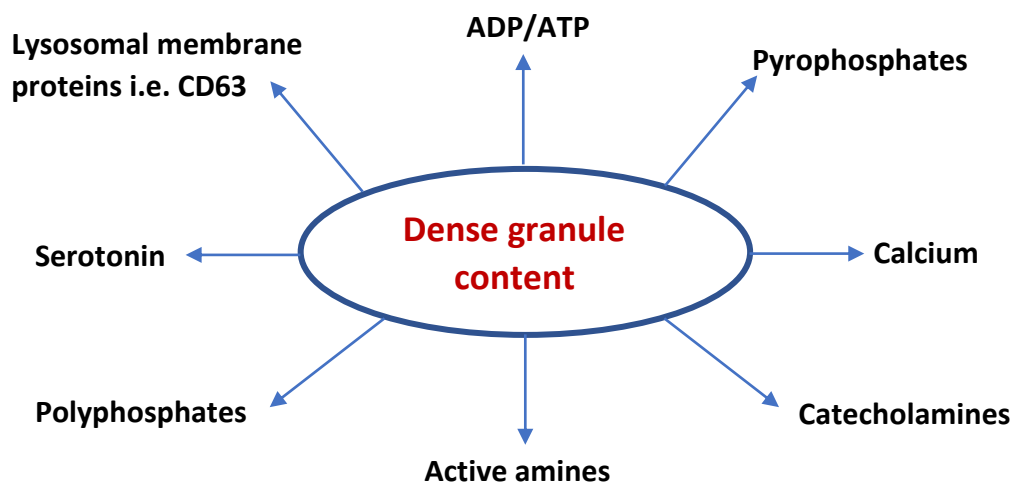


Figure 1.3 Platelet dense granule content. δ granules of platelets contain a wide array of molecules including active amines, adenosine di- and tri- phosphate (ADP and ATP), cations such as calcium, catecholamines and serotonin. These molecules are secreted following platelet activation and play critical roles as mediators in preventing excess blood loss.

Lysosomal granule

Lysosomal granules are found within platelets in very few numbers (1-3 lysosomes per platelet) and are 200-250 nm in diameter (Sharda and Flaumenhaft, 2018). Many enzymes including cathepsins, β -hexosaminidase, β -galactosidase, β -glucuronidase, arylsulfatase as well as acid phosphatase, collectively known as acid hydrolases, are found within this granule (Heijnen and Korporaal, 2017). Like δ granules, lysosomes express LAMP1/2 and

CD63 which are translocated to the plasma membrane surface of platelets upon activation (Israels *et al.*, 1992). Lysosomes' primary function in platelets involves the degradation of phagocytic and cytosolic materials (Behnke, 1992). Secreted lysosomal granule content has been reported to partake in a number of additional processes such as receptor cleavage, support fibrinolysis and induce the breakdown of components in the extracellular matrix (Heijnen and Korporaal, 2017).

Mitochondria

Platelets contain a relatively small number of mitochondria (approximately 7 per platelet) which are approximately 200 nm in diameter (Morgenstern, 1997). They are easily identified through electron microscopy due to their classic cisternae and double membrane structures (Alberts *et al.*, 2002). As with most cells, mitochondria in platelets participate in energy metabolism to ensure adequate energy content in platelets is maintained by providing ATP via oxidative phosphorylation (Thon and Italiano, 2012). Mitochondria in platelets along with glucose ensures necessary amounts of ATP are maintained for essential platelet events such as adhesion, aggregation, secretion, and contraction (Garcia-Souza and Oliveira, 2014). Increasing number of studies have reported additional roles of mitochondria in platelets, in that they are involved in the regulation of internal signals via reactive oxygen species production (Zharikov and Shiva, 2013). Additionally, mitochondria have been found to release cytochrome c which is a key molecule involved in triggering apoptotic pathways in platelets (Lopez *et al.*, 2007).

Other organelles

Platelets also contain a small number of single-membrane organelles known as peroxisomes which are considered to have developed from endoplasmic reticulum (Tabak *et al.*, 2003). Peroxisomes contain the enzyme catalase and is believed to be involved in lipid metabolism with many studies reporting its role in the synthesis of the potent phospholipid activator platelet-activating factor (PAF) (Heijnen and Korporaal, 2017). Platelets have also been found to possess a few glycosomes containing glycogen particles as well as some Golgi remnants.

1.2.3 The platelet cytoskeleton

Platelets contain a highly specialised and well-defined internal cytoskeleton which supports the maintenance of the discoid shape of resting platelets. In quiescent platelets, this elaborate cytoskeletal system is composed of three key elements: spectrin-based membrane skeleton, actin cytoskeleton and a marginal ring of microtubule coils (Figure 1.4) (Nachmias, 1980). These elements along with the acto-myosin cortex helps maintain cellular integrity as well as cellular morphology when platelets are subjected to high shear forces in particular blood vessels (Thon and Italiano, 2010).

A number of molecules can interact directly or indirectly with components of the platelet cytoskeleton to regulate its functions. The platelet cytoskeleton has the capacity to actively contract in response to specific stimuli, thus lead to profound alterations in cells' morphology, cell-cell and cell-substrate interactions (Fox, 1993). Signalling molecules and secondary messengers are contained within the platelet cytoplasm in compartments associated with the membrane cytoskeleton (Sigismund *et al.*, 2012). Studies have shown that upon platelet stimulation, these signalling molecules and secondary mediators get recruited and activated resulting in the reorganisation and remodelling of cytoskeletal elements thus supporting dynamic changes within platelets and promoting platelet activation and adhesion mechanisms to occur (Fox, 2001). Studies have also revealed the significant role of the platelet cytoskeleton in regulating cellular processes such as endocytosis and secretion (Sigismund *et al.*, 2012).

The remarkable ability of the platelet cytoskeleton to carry out such dynamic functions in response to cellular requirements is only possible due to the presence of several proteins that have the ability to rapidly polymerise and depolymerise accordingly (Fox, 2001). These filaments and associated proteins also aid the formation of various actin structures upon platelet activation which will be described in the subsequent sections, but first a brief overview on the general components of the platelet cytoskeleton and their role in the reorganisation of cytoskeletal elements in platelets is outlined.

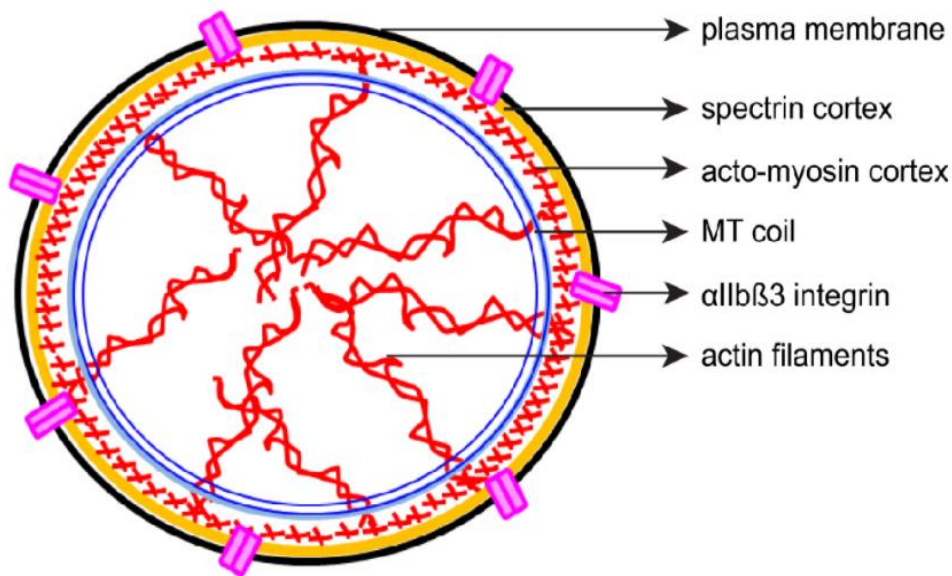


Figure 1.4 Schematic representation of the platelet cytoskeleton in its quiescent state.

Platelets contain a highly specialised and well-defined cytoskeleton which helps maintain the discoid shape of inactive platelets as they circulate in the bloodstream along with other vascular cells. Quiescent discoid platelets contain a plasma membrane with bound transmembrane surface receptors such as $\alpha\text{IIb}\beta\text{3}$ integrins, underneath this lies the spectrin cortex which provides the framework for the cytoskeleton. The spectrin cortex is joined to an actomyosin cortex. Actin and myosin components together provide tension which also aids the maintenance of the discoid shape. A marginal band consisting of dynamic MT coils are found beneath the actomyosin cortex. A large quantity of filamentous actin is found within the platelet cytoplasm, which also helps maintain the shape of the platelet under conditions such as high shear rates (Paknikar, 2016).

1.2.3.1 Structural changes of activated platelets

Binding of agonists to their respective receptors orchestrates a multitude of signalling events intracellularly which leads to a number of structural changes within platelets, allowing them to carry out critical functions in order to maintain haemostasis. These signalling events resulting in the activation of platelets contribute to biochemical and morphological modifications including the incredible change in shape of platelets from discoid to spherical via the reorganisation of platelet cytoskeleton and the release of platelet granular content.

The majority of morphological changes that occur upon platelet activation has been identified and visualised via electron microscopy studies, with the transformation of platelets from disc to spherical shape being the most notable (Figure 1.5) (Neumüller *et al.*,

2015). These changes in platelet morphology are also present when the cells interact with foreign surfaces such as glass (White & Burris, 1984). Upon stimulation of platelets, the circumferential MTs which help maintain the discoid platelet shape contract to the centre of the platelet with the aid of the actomyosin cytoskeleton, into compartments known as granulomeres (Peters *et al.*, 2012). This drives the movement of platelet granules to the centre of the platelet.

Studies have reported platelets to achieve spreading within 10 to 12 minutes by initially forming pseudopodia which extend and retract giving rise to the formation of hyalomeres which aid the adhesion and spreading of platelets on damaged surfaces (Allen *et al.*, 1979). This is commonly followed by the release of platelet granular content via exocytosis in response to a strong platelet stimulus and this results in irreversible activation (Behnke, 1970). Ensuing these events, platelets transform into a flat shape with extension of several actin structures such as filopodia and lamellipodia (section 1.2.3.5) as a result of platelet cytoskeleton remodelling. This gives platelets a fried-egg like appearance whereby a protuberance can be observed in the centre of the cell as platelet granules are squeezed into the middle region of a platelet (Allen *et al.*, 1979). These changes in platelet shape leading to an increased surface area is essential as it promotes the ability of these cells to securely attach to their extracellular matrix as well as other platelets to allow the formation of a platelet plug and thus seal the damaged area on a vessel. In fact, a 420% increase in the surface area of platelets has been reported previously upon platelet activation/spreading (Allen *et al.*, 1979; Cerecedo, 2013).

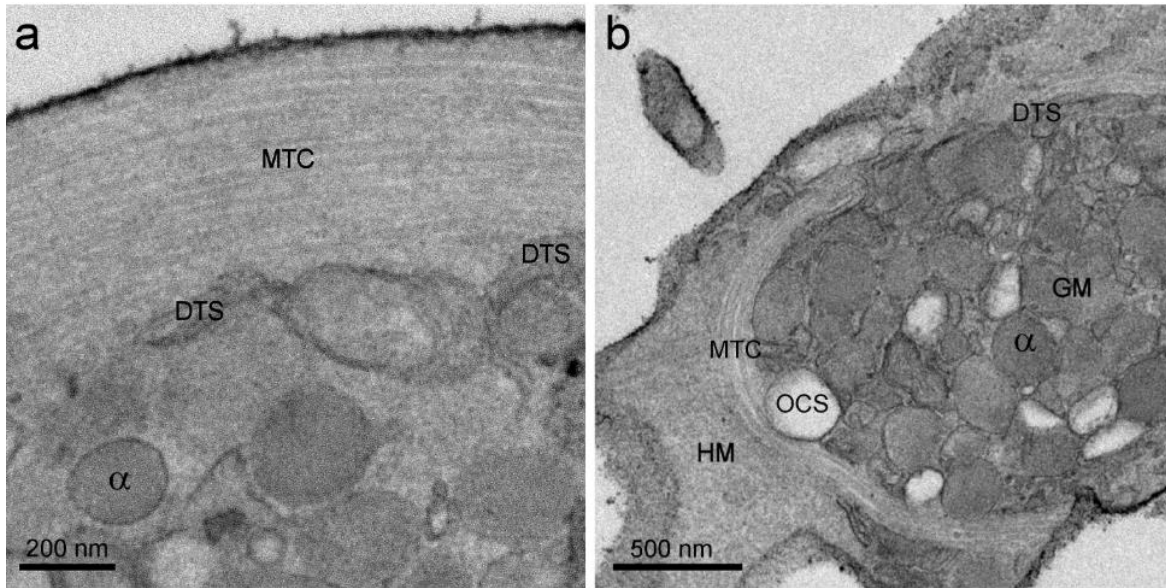


Figure 1.5 Transmission electron microscopy of platelets adhered to glass. Quiescent platelets with their discoid shape incubated for 5 min prior to fixation (a), shows microtubular coil (MTC) in close proximity with the DTS, and the random distribution of α granules (α) within the cell. Activated platelets with their spherical shape incubated for 15 min prior to fixation shows the presence of hyalomeres (HM) and granulomere (GM). MTC appears to have retracted into the centre of the cell along with α granules and openings to the OCS can also be observed (b) (Neumüller *et al.*, 2015).

1.3 The actin cytoskeleton

1.3.1 Overview on actin

Actin is a 42 kDa protein and is the most abundant protein in platelets with around two million molecules present per platelet (Thon and Italiano, 2012). Two forms of actin are found within platelets: polymeric filamentous actin (F-actin) also known as actin filaments, and monomeric globular actin (G-actin) (Bearer *et al.*, 2002). The linear actin filaments present in platelets in their resting state are formed from the assembly of around 40% of the actin subunits (Lefebvre *et al.*, 1993). The remainder of the monomeric actin is generally stored in a 1:1 complex with β 4-thymosin. These G-actin- β 4-thymosin complexes then undergo extensive rearrangement to become F-actin (70%) upon platelet activation to promote processes such as cell spreading (Fox *et al.*, 1985).

F-actin can interact with a variety of proteins and assemble further to form a network of bundles. A relatively large number of proteins are considered to be involved in this actin crosslinking, for instance filamin and α -actinin (Bearer *et al.*, 2002). Therefore, the mechanism by which platelets undergo shape change from discoid to a flattened 'fried egg-like structure' is an incredibly complex and extremely rapid process which involves numerous actin-binding proteins (Bearer *et al.*, 2002). Essentially actin acts as a building block which can be constructed into several higher order structures with the assistance of a wide variety of actin-binding proteins.

1.3.2 Mechanism of actin polymerisation and depolymerisation

Intrinsically actin is composed of two domains, one facilitates the binding of ATP and ADP molecules while the other acts as a site for the binding of divalent cations (Kabsch *et al.*, 1990). In a eukaryotic organism, actin continually polymerises and depolymerises according to the cells' requirements.

The binding of ATP to the cleft on G-actin promotes actin polymerisation via sequential steps involving nucleation and elongation processes (Figure 1.6) (Pollard and Cooper, 1986). The initial step involves the actual accumulation of ATP bound G-actin complexes into short oligomers. These unstable oligomers then continue to accrue to a particular

length of approximately three to four repeating units and a (stable) nucleus is formed, this step is referred to as 'nucleation' and is followed by the elongation stage whereby oligomers formed during the nucleation stage acts as a seed on which additional ATP bound G-actin monomers are added (Bearer, 1995). It is also important to note that an actin filament consists of two ends: a fast-growing barbed (plus) end and a slow-growing pointed (minus) end.

The conversion of ATP-G-actin monomers into new F-actin continues, resulting in an increase in length of the actin filaments formed. These actin filaments then combine in a linear or branched manner to form structures that protrude from the platelet: filopodia and lamellipodia (Bearer *et al.*, 2002). These actin-rich structure formations are tightly regulated by the family of Rho GTPases and the details are discussed in the subsequent sections (1.4).

Actin polymerisation is essential for numerous platelet functions for instance spreading, however depolymerisation of actin and capping of actin filaments is equally important to aid morphological changes that occur upon stimulation of platelets (Bender *et al.*, 2010). Actin depolymerisation occurs primary through the hydrolysis of bound ATP to ADP following the incorporation of G-actin bound ATP into the actin filaments during the elongation stage thus hindering elongation processes (Fox & Phillips, 1981). In essence, ATP-G-actin gets hydrolysed to ADP which in turn gives rise to ADP-F-actin. Ultimately, an equilibrium is reached where the rate of ATP-G-actin addition becomes equivalent to the rate of ADP-G-actin disassociation and this phase is known as 'treadmilling' (Weber, 1999). Numerous proteins are involved in the stabilisation of existing filaments and depolymerisation of actin and they synergistically act by 1) sequestering monomers, 2) capping the barbed end and 3) stabilising filaments (Bearer *et al.*, 2002).

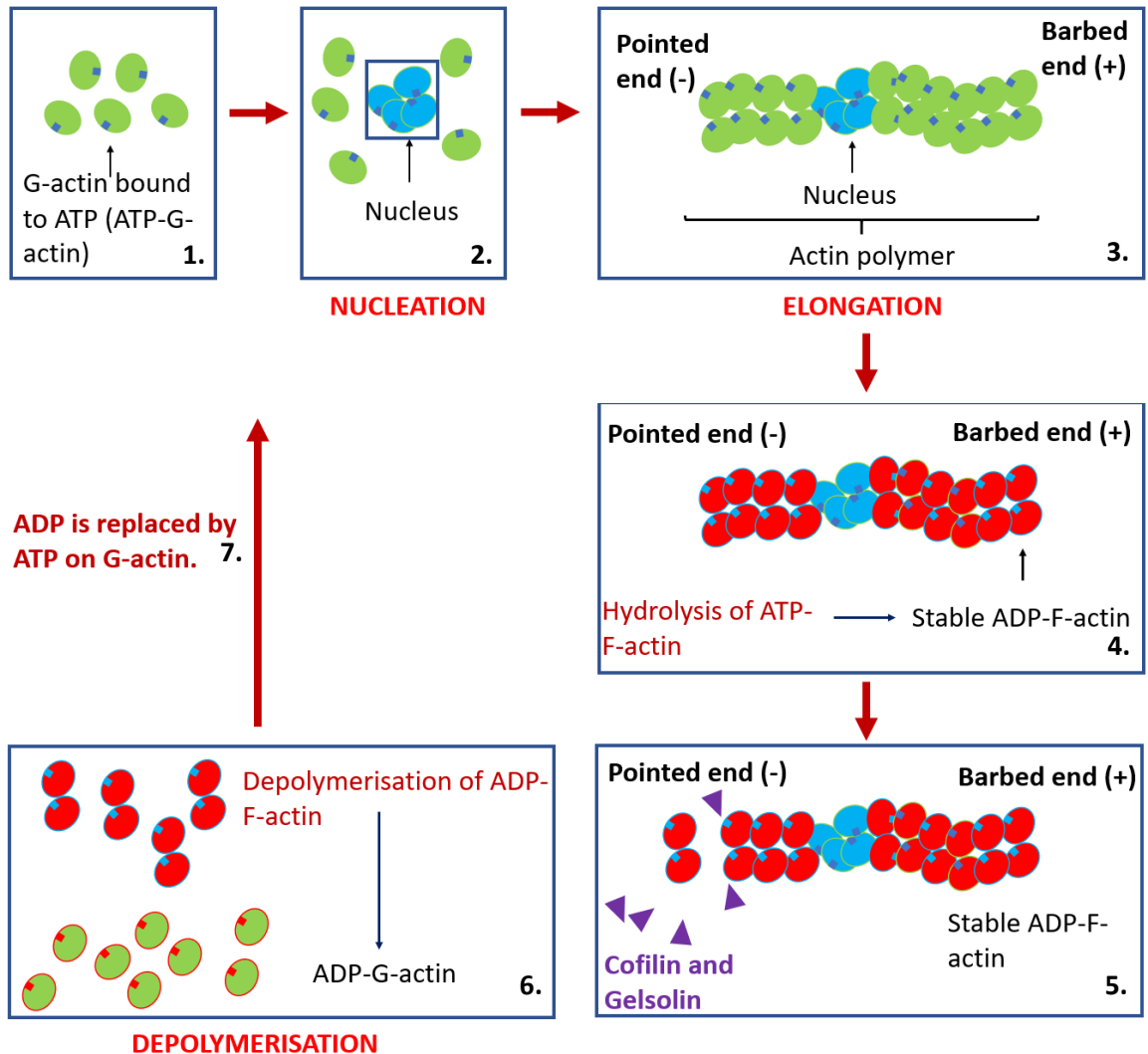


Figure 1.6 A schematic diagram of the sequential steps for the polymerisation and depolymerisation of actin filaments. 1) ATP is bound to G-actin and forms oligomers. 2) Oligomers aggregate (blue, 3-4 oligomers) to form a nucleus during a stage referred to as nucleation, which can occur de novo and/or be mediated by Arp2/3. 3) The nucleus serves as a 'seed' on which additional ATP-bound-G-actin gets attached and these then continue to elongate. Polymerisation also continues forming actin filaments. 4) Hydrolysis of ATP results in ADP-bound-F-actin formation (red). 5) Actin depolymerising proteins such as cofilin and gelsolin then interact with the F-actin resulting in the removal of actin monomers from the structure. 6) ADP-F-actin continues to depolymerise and form ADP-G-actin. 7) This cycle then continues as ADP-G-actin gets replaced with ATP to produce further actin filaments. Figure adapted from (Mullins *et al.*, 1998).

1.3.3 Actin-binding proteins

A number of accessory platelet proteins that control actin dynamics mediates the remodelling of the platelet actin cytoskeleton via assembly and disassembly of actin filaments (Michelson, 2013). Upon activation, platelets generally 'round off' whereby they alter their cytoskeleton and appear spherical before structures rich in F-actin start protruding from the platelet surface (Bearer *et al.*, 2002). This 'rounding off' step in platelets is dependent on the disassembly of actin filaments which are present in platelets in their resting state. Table 1.2 outlines some of the common actin-binding proteins reported to partake in the regulation of actin filament polymerisation and depolymerisation.

Gelsolin is a protein which aids the disassembly of actin filaments by binding to filaments in the fast-growing end thus preventing further elongation (Bearer *et al.*, 2002). Cofilin and ADF are other proteins which in combination with gelsolin act to enhance depolymerisation of the actin filaments in platelets (Bearer *et al.*, 2002). The compact platelet cytoskeleton therefore starts to break down due to the depolymerisation of actin filaments, which in turn allows the formation of new F-actin structures via deformation of the plasma membrane (Bearer *et al.*, 2002). This causes the release of monomers of G-actin from the 'slow growing end' of the filaments. In addition to this, a loss of affinity of proteins involved in monomer sequestration such as thymosin β 4 occurs (Hartwig & DeSisto, 1991). All of the above events synergistically result in an increase in G-actin monomers in platelets, mainly through the catalysis of ADP to ATP (Bearer *et al.*, 2002).

On the contrary, molecules such as Arp2/3 complex has been found to promote actin polymerisation via actin filament nucleation (Li *et al.*, 2002). F-actin assembly processes is driven through the uncapping and unattachment of filamentous actin which previously attached to the fast-growing end via gelsolin (Glenn *et al.*, 1996). F-actin assembly has been reported to occur via *de novo* nucleation processes in the presence of nucleation promoting factors like Arp2 and 3, and WASp (Bearer *et al.*, 2002). The Arp2/3 complex itself is structurally similar to actin and combines to of form dimers like actin and so it has been suggested for the Arp2/3 complex to initiate actin polymerisation by allowing the

attachment of G-actin molecules to itself through the formation of additional nucleation sites (Bearer *et al.*, 2002). Studies have also shown Arp2/3 complex to partake in instigating branching of F-actin filaments (Svitkina and Borisy, 1999). Members of the WASp and cortactin family also regulate actin polymerisation as it has been reported to regulate the binding of Arp2/3 complex and stimulate the nucleation process thus promoting actin polymerisation (Bearer *et al.*, 2002).

Formin proteins are also expressed in platelets and they play a key role in actin nucleation and elongation giving rise to structures such as lamellipodia, filopodia and stress fibres which play a crucial role in platelet functions such as adhesion and spreading (Zuidsherwoude *et al.*, 2019). mDia1 is one of the most studied type of formin protein in platelets. The activation of mDia1 has been reported to occur when GTP bound Rho GTPases binds to the GTPase-binding domain resulting in movement of Diaphanous Auto-regulatory Domain from the N-terminal part of mDia1 (Watanabe *et al.*, 1999).

Table 1.2 Examples of actin-binding proteins in platelets.

Actin-binding protein	Type of activity	Reference
Profilin	Monomer-binding protein which promotes monomer sequestration.	(Shenker <i>et al.</i> , 1991).
Thymosin β 4	Monomer-binding proteins, major G-actin sequestration molecule.	(Huff <i>et al.</i> , 2002).
CapZ and gCap39	Barbed-end capping protein which hinders the addition of actin monomers to filaments.	(Bearer <i>et al.</i> , 2002).
DNase I	Monomer-binding proteins, major G-actin sequestration molecule which inhibits actin polymerisation.	(Jennings <i>et al.</i> , 1981).
Cofilin	Depolymerising protein which severs actin filaments.	(Davidson and Haslam, 1994; Bearer <i>et al.</i> , 2002).
Severin	F-actin end binding protein.	(Barkalow <i>et al.</i> , 1996).
Tropomodulin	Pointed-end capping protein and severs actin filaments.	(Weber <i>et al.</i> , 1994).
Gelsolin	Barbed-end capping protein which hinders the addition of actin monomers to filaments.	(Bearer <i>et al.</i> , 2002).
Coronin	Modulates Arp2/3 and cofilin.	(Riley <i>et al.</i> , 2019).
CAP1	Actin filament severing and depolymerisation.	(Joshi <i>et al.</i> , 2018).
VASP, spectrin	Side binding protein.	(Fox <i>et al.</i> , 1987; Bearer <i>et al.</i> , 2002).
Arp2/3, WASp	Aids nucleation processes.	(Bearer <i>et al.</i> , 2002; Li <i>et al.</i> , 2002).
Microtubule-actin cross-linking factor 1	Regulates and facilitates actin-microtubule interaction.	(Schurr <i>et al.</i> , 2019).
Myosin	Facilitates formation of contractile units.	(Lodish <i>et al.</i> , 2000)

1.3.4 Formation of actin structures

Platelets have the capacity to modify their morphology and spreading profile according to the geometry of the external microenvironment. Moreover, intra- or extra-cellular signals which stimulate processes such as the activation of platelets can cause a series of morphological events resulting in the formation of extensions of the cellular structure and/or formation of actin bundles, which aids the attachment, spreading, migration and eventually contraction of platelets (Cerecedo, 2013). These adaptive morphological alterations depend on the assembly of actin, giving rise to plasma membrane protrusions structures and are regulated by the family of Rho GTPases (Section 1.4) (Dmitrieff and Nédélec, 2016). In humans, four distinctive structures with different morphology exists in spread platelets. Unique sets of actin-binding proteins participate in the formation of these physiologically diverse structures: lamellipodia, filopodia, stress fibres and actin nodules. A schematic overview of the elements involved in the development of three of the actin structures is depicted in Figure 1.7.

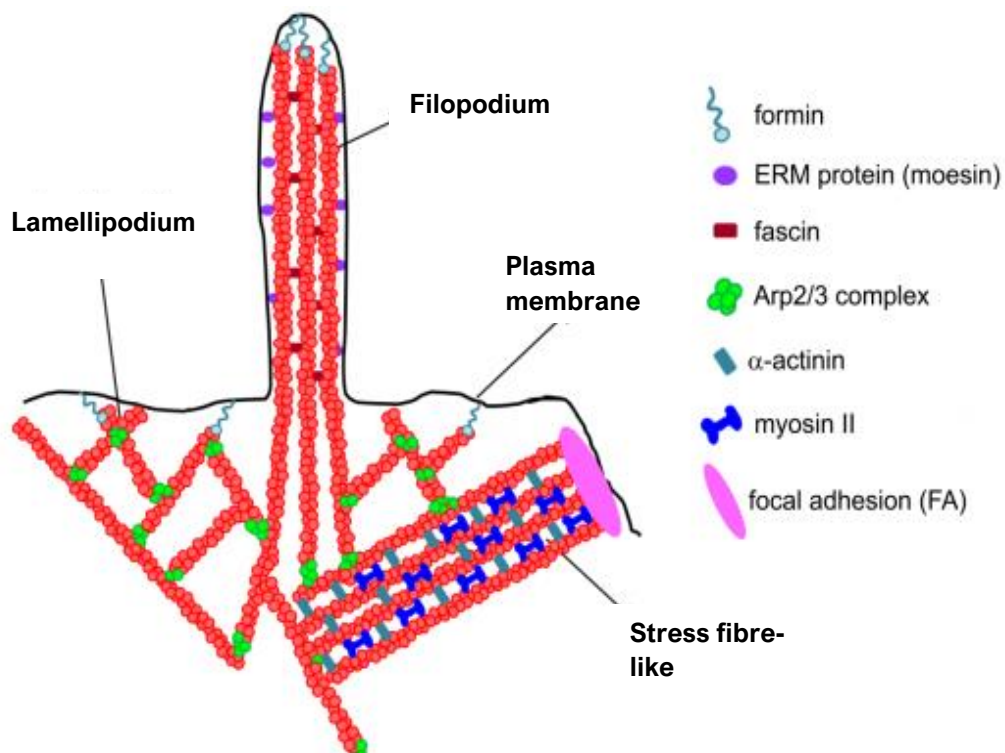


Figure 1.7 Actin structures in platelets. Schematic image of a filopodium, lamellipodium and stress fibre along with the structural elements that partake in their formation upon platelet stimulation (Paknikar, 2016).

Filopodia

Filopodia are thin cell surface protrusions (0.1-0.3 μm) which are abundant in F-actin. A distinct characteristic of filopodia is the presence of long parallel arrangement of actin filament bundles (Hartwig & Desisto, 1988). These elongations of F-actin are linked to the platelet plasma membrane via ERM (ezrin, radixin, moesin) proteins. Filopodia act as antennas and are involved in assessing the external environment of the cell (Nakamura *et al.*, 2000). The molecular mechanisms involved in the formation of filopodia in platelets have not yet been fully clarified, although the involvement of molecules such as members of the Wiskott–Aldrich syndrome protein (WASp), the Arp2/3 complex and the Cdc42 subfamily of the Rho family have been proposed, with Cdc42 being suggested as the major contributor to stimulate actin polymerisation and subsequent formation of filopodia (Nobes and Hall, 1995).

Studies conducted by Carlier *et al.*, (1999) and Nobes & Hall, (1995) on fibroblasts reported the formation of filopodia following the activation of Cdc42. They demonstrated GTP-bound-Cdc42 to interact with and trigger WASp (GTP-binding domain) which in turn stimulated the Arp2/3 complex in the presence of PIP₂ and resulted in the formation of filopodia via actin polymerisation. The molecules reported to participate in the regulation of filopodia in the study are also expressed in platelets thus further suggesting the possibility for a similar pathway to occur in the formation of filopodia in platelets. However, evidence from studies conducted on WASp *-/-* platelets failed to prevent filopodia formation (Falet *et al.*, 2002), hence signifying the possibility of other additional molecular mechanisms to occur for filopodia formation in platelets. Indeed, a number of studies reported the involvement of the Rif pathway (including formins) in driving the generation of filopodia through actin polymerisation independently of Cdc42 and WASp in neuronal cells (Goh *et al.*, 2011). Like neuronal cells, platelets also contain Rif and formins thus suggesting a similar pathway to ensue in platelets by which these proteins are able to promote filopodia formation in platelets independent of Cdc42 (Figure 1.8) (Goggs *et al.*, 2013).

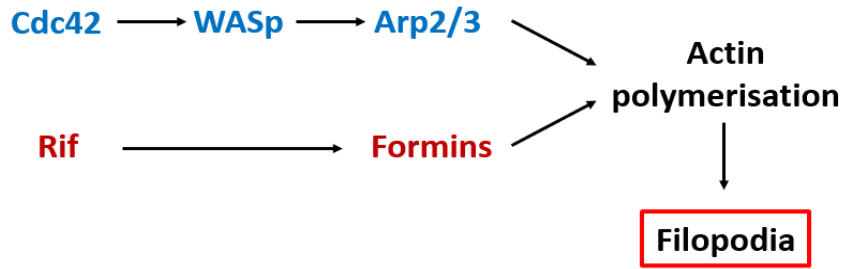


Figure 1.8 The signalling pathway involved in the formation of filopodia in platelets.

Filopodia have been proposed to occur via two mechanisms, one involving Cdc42 activation and subsequent WASp and Arp2/3 complex activation and the other involving Rif molecules and formins. Both trigger actin polymerisation resulting in filopodia formation.

Lamellipodia

Lamellipodia are wave-like projections of plasma membrane that protrude from the platelets (Reeves *et al.*, 2018). These structures are composed of a network of F-actin (0.1-0.2 μm) (Mattila and Lappalainen, 2008). The involvement of Rho family GTPases, namely the Rac subfamily, in the formation of lamellipodia via actin polymerisation was discovered by Ridley *et al.* (1992), who conducted studies on Swiss 3T3 fibroblasts. They found Rac family of GTPases targeted the Arp2/3 complex which in turn participated in F-actin branching mechanisms. Following this, numerous studies have demonstrated the participation of Rac1 and Arp2/3 complexes in lamellipodia formation in platelets (Falet *et al.*, 2002; McCarty *et al.*, 2005). In essence, the formation of lamellipodia in platelets involves the activation of Rac which in turn attaches to WAVE complexes, and results in the uncovering of the VCA regions (mediated by PIP3 and Rac-GTP), Arp 2/3 then binds to the exposed VCA regions and triggers actin polymerisation to commence (Figure 1.9) (Schaks *et al.*, 2019).

It has also been reported recently that p21-activated kinases (PAK) (which are effectors of Rac1 present in platelets) contribute in the stimulation of actin polymerisation and ultimately drive the formation of lamellipodia (Aslan *et al.*, 2013).

It has been proposed that the main role of lamellipodia in platelets is to aid cell spreading at the site of vascular injury (Reeves *et al.*, 2018). Many studies have also reported the

involvement of these structures in relation to cell locomotion functions in various cell lines such as leukocytes (Hartwig, 2006). Platelets have also been reported to utilise these structures to aid directed movement (Aslan and McCarty, 2013).

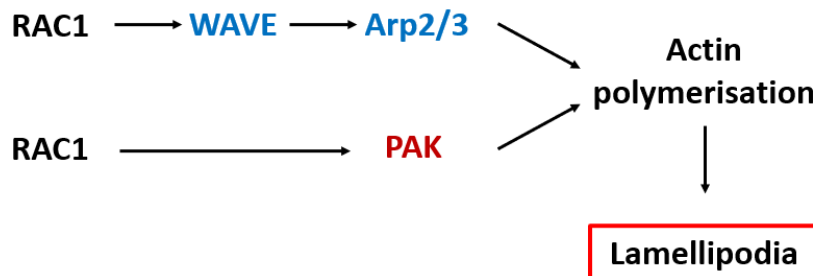


Figure 1.9 Lamellipodia formation in platelets. Lamellipodia have been proposed to occur via two mechanisms, one involving WAVE and Arp2/3 activation and the other involving PAK molecules. Both trigger actin polymerisation resulting in lamellipodia formation.

Stress fibres

Stress fibres are structures composed of bundles of F-actin as well as myosin II and are critical elements that participate in cellular contraction mechanisms in non-muscle cells (Cerecedo, 2013). Cross-linking of proteins such as α -actinin has also been found within stress fibres of spread platelets during cell adhesion (Tanaka and Itoh, 1998). These complex structures have been shown to facilitate cellular contraction activities in various cell lines (Tojkander *et al.*, 2012). Stress fibres are attached to integrin-based structures known as focal adhesions (FAs). FAs along with numerous proteins (talin and vinculin), serve as communication points by which extracellular matrix is connected to the intracellular actin cytoskeleton (Livne and Geiger, 2016).

Early work discovered stress fibre formation to be critically regulated via actomyosin contractility by Rho GTPases, RhoA (Figure 1.10) (Pellegrin and Mellor, 2007). RhoA activation in turn has been found to be mediated by Rho-associated kinases (ROCK) and myosin II pathways (Kato *et al.*, 2001). Moreover, emerging studies have found RhoA to possess the capacity to facilitate the formation of stress fibres via formin effectors: mDia1 and 2 (Figure 1.10) (Goggs *et al.*, 2015). Both pathways stimulate actin polymerisation and thus the generation of stress fibres in platelets. Studies have shown the importance of

stress fibres in platelets in providing cellular integrity, indeed diminished stability of a thrombus was reported in studies where there was an absence of components required for the formation of stress fibre-like structures (Calaminus *et al.*, 2007).

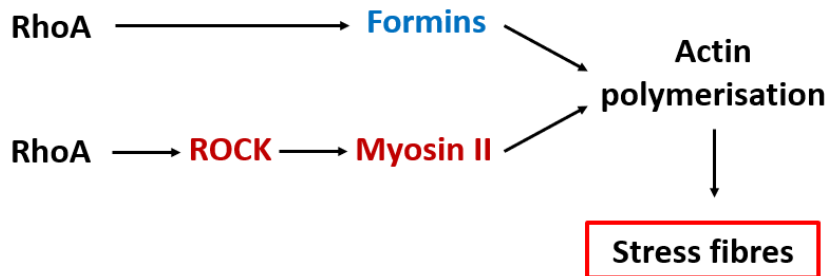


Figure 1.10 Stress fibre formation in platelets. Stress fibre formation has been proposed to occur via two mechanisms, one involving the activation of formin proteins and the other involving ROCK activation and subsequent myosin II activation. Both trigger actin polymerisation resulting in stress fibre formation.

Actin nodules

Actin nodules are described as actin-rich structures made up of punctate regions of actin during early stages of platelet adhesion and cell spreading (Calaminus *et al.*, 2008; Cerecedo, 2013). These highly dynamic structures have been proposed to be the precursor to the formation of platelet structures like lamellipodia and stress fibres as they are present during onset of lamellipodia and stress fibre formation but absent in fully spread platelets (Calaminus *et al.*, 2008). Actin nodules have been proposed to contain mostly filamentous actin and they can be visualised using fluorescently labelled phalloidin, although many aspects including the key roles of actin nodules in platelet functioning is not yet established.

Actin nodules have however been found to possess multiple proteins such as talin and vinculin (components of FA), in abundance (Poulter *et al.*, 2015). Although, little is known about actin nodules, studies have reported a dependency on WASp proteins and the Arp2/3 complex in particular, for their formation (Calaminus *et al.*, 2008). This is further supported by Poulter *et al.*, (2015) who conducted studies on WASp^{-/-} mice and they found impaired actin nodules formation and diminished ability for platelet-platelet interactions resulting in bleeding disorders similar to that of Wiskott–Aldrich syndrome patients.

1.4 Rho GTPases

Rho family of GTP binding proteins also known as Rho GTPases are a family of small (21 kDa) signalling G-proteins (Goggs *et al.*, 2015). Rho GTPases have a prominent role in eukaryotic cells as they act as molecular switches which regulate a diverse range of intracellular signalling pathways (Hodge and Ridley, 2016). They are well-known for their critical involvement in regulating the actin cytoskeleton. In addition to this, Rho GTPases influence a wide variety of mechanisms including transcription factor activity, cell polarity and microtubule dynamics (as reviewed by Hodge and Ridley, 2016).

Rho GTPase activity depends on the binding of either GTP or GDP, which ultimately switches the Rho effector functions on/off accordingly thus resulting in the activation and inhibition of downstream functions such as actin cytoskeletal reorganisation (Figure 1.11) (Aslan and McCarty, 2013). Guanine exchange factors (GEFs) aids the binding of GTP to Rho GTPases in order to activate these proteins and stimulate downstream signalling of specific effectors; GTPase activating proteins (GAPs) acts on Rho GTPases to bring about the opposite effect i.e. GAPs promote the hydrolysis of GTP to GDP on Rho GTPases, thus inhibiting GTPase activity by inactivating Rho GTPase (Figure 1.11) (Aslan, 2019).

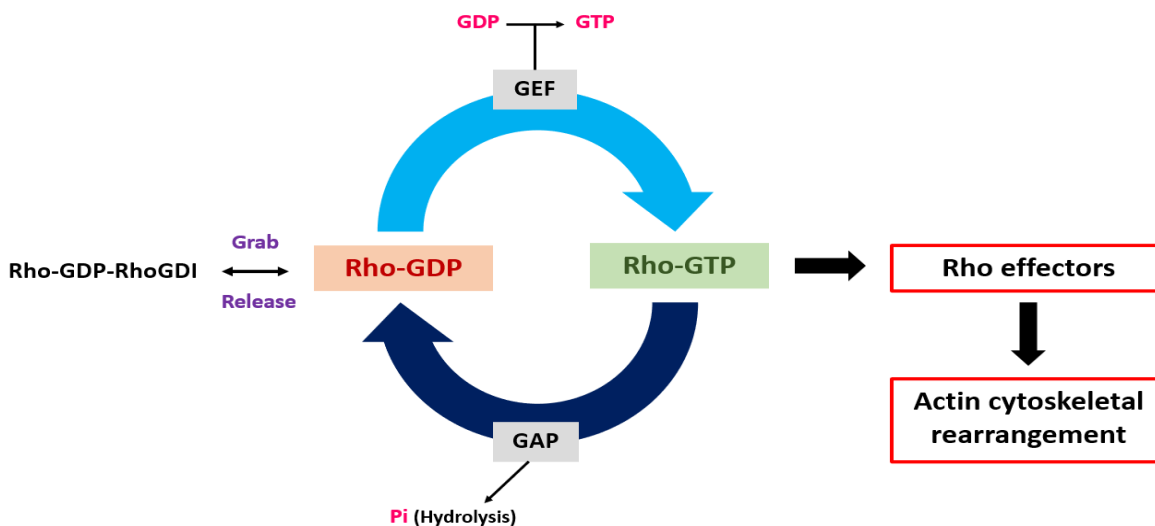


Figure 1.11 The regulation and activation cycle for Rho GTPases. Rho GTPases when bound to GTP interacts with downstream effector proteins which in turn regulate actin cytoskeletal rearrangement mechanisms. Guanine nucleotide exchange factor (GEFs) and GTPase activating proteins (GAPs) regulate the activity of Rho GTPases. GEFs activate Rho GTPases by catalysing and facilitating the exchange of GDP to GTP. On the contrary, GAPs inhibit downstream signalling by inducing the hydrolysis of GTP-bound Rho into GDP. RhoGDI proteins have also been demonstrated to regulate Rho GTPases.

The role of Rho GTPases, specifically RhoA, Rac and Cdc42 subfamilies, in regulating the platelet actin cytoskeleton is extensively researched. Processes such as cell-cell adhesion, secretion of granular content and the regulation of phosphoinositide-3-kinase (PI3K) and phospholipase C (PLC) are some examples of platelet activities regulated by Rho GTPases (Akbar *et al.*, 2007; Fukata *et al.*, 1999). The ability of Rho GTPases to regulate such diverse functions is accomplished primarily through the interaction of a broad selection of effector proteins with the GTP-loaded activated GTPase (Table 1.3).

Table 1.3 Examples of effector proteins and the Rho GTPases that activate them.

Effector	Rho GTPase	Biological function
FilaminA	RhoA, Rac1 and Cdc42	Regulation of the actin cytoskeleton, in particular the actin filament cross-linking.
FMNL1	Rac1	Regulation of the actin cytoskeleton, cell polarity & cytokinesis
IQGAP1,2	Rac1, Cdc42	Cell–cell interactions, Regulation of the platelet actin cytoskeleton.
ROCK1,2	RhoA	Regulates the cytoskeleton, blockage of cell contact inhibition
PPP1R12A	RhoA	Myosin light chain inactivation which mediates cytoskeletal remodelling.
N-WASP	Cdc42	Regulation of the actin cytoskeletal via Arp2/3 complex.
WAVE/Scar1,2	Rac1, Cdc42	Regulation of the actin cytoskeletal via Arp2/3 complex.
DIAPH1,2	RhoA, Rac1	Regulation of the actin cytoskeletal via profilin and IRSp53.
PKCα	RhoA, Rac1, Cdc42	Signal transduction
PIK3R1	Rac1, Cdc42	Regulation of PIK3C activity and signal transduction.

The above list of RhoA, Rac1 and Cdc42 effectors and their known biological effects was compiled from the following references: (Bishop & Hall, 2000; Bustelo *et al.*, 2007; Goggs *et al.*, 2015).

The use of mouse models and a number of inhibitors targeting specific Rho GTPases has greatly broadened our understanding about the critical roles Rho GTPases play in regulating platelet function. Findings from such studies is summarised in Table 1.4.

Table 1.4 Summary of some of the functions reported for Rho GTPase in platelets

Rho GTPase	Physiological function	References
RhoA	Platelet shape change	(Calaminus <i>et al.</i> , 2007)
	Platelet aggregation	(Pleines <i>et al.</i> , 2012)
	Reactive oxygen species generation	(Akbar <i>et al.</i> , 2016)
	Platelet activation and thrombosis	(Williams <i>et al.</i> , 2015)
	Secretion of platelet granular content	(Pleines <i>et al.</i> , 2012)
	Platelet production	(Suzuki <i>et al.</i> , 2013)
Rac1	Secretion of platelet granular content	(Akbar <i>et al.</i> , 2007)
	Calcium mobilisation	(Pleines <i>et al.</i> , 2009)
	Clot retraction	(Stefanini <i>et al.</i> , 2012)
	Activation of GPIIb/IIIa	(Akbar <i>et al.</i> , 2016)
	Platelet spreading	(McCarty <i>et al.</i> , 2005)
	Platelet aggregation	(Dwivedi <i>et al.</i> , 2010)
	Activation of PLC γ 2	(Pleines <i>et al.</i> , 2009)
Cdc42	Secretion of platelet granular content	(Akbar <i>et al.</i> , 2016)
	Platelet spreading	(Akbar <i>et al.</i> , 2009)
	Filopodia formation	(Antkowiak <i>et al.</i> , 2016)
	Platelet production	(Pleines <i>et al.</i> , 2010)
	Regulation of platelet aggregates	(Pleines <i>et al.</i> , 2009)

Table adapted from (Aslan and McCarty, 2013).

1.4.1 RhoA

RhoA activation in platelets can result in cytoskeletal remodelling. Indeed numerous studies have demonstrated that platelet stimulation which in turn activates RhoA, to modify the platelet cytoskeleton resulting in an initial sphering characteristic (Choi *et al.*,

2017). It was also found for cyclic adenosine monophosphate (cAMP)-dependent signalling in platelets to target RhoA and Rho kinase-MLC phosphatase pathways thus resulting in platelet shape change, hence reinforcing the participation of RhoA in modulating platelet functions (Aburima *et al.*, 2013).

A number of studies have also examined the effects of RhoA on platelet function by utilising platelets deficient in RhoA (Pleines *et al.*, 2012; Aslan and McCarty, 2013). These studies confirmed information acquired via pharmacological means in that they reinforced the requirement of RhoA in processes such as integrin activation, secretion of platelet granular content and clot retraction. They highlighted *in vivo* haemostatic and thrombotic defects in the absence of RhoA in platelets.

1.4.2 Rac1

Three isoforms of Rac are found in mammals (Rac1, 2 and 3) and they all possess a similar structural arrangement with over 89% similarity in the amino acid identity between the isoforms (Goggs *et al.*, 2015). Rac1 is ubiquitously expressed and has emerged as a key player in coordinating platelet cytoskeletal reorganisation leading to the formation of protrusion structures such as lamellipodia, which aid cellular processes (see section 1.3.4). In platelets only Rac1 and Rac2 have been found to be expressed, with Rac1 being the widely studied isoform (McCarty *et al.*, 2005). Data obtained from mice platelets lacking both Rac1 and Rac2 and a number of studies on various cell types utilising constitutively active Rac as well as dominant negative mutants of Rac, have confirmed further the role of Rac in the formation of lamellipodia (Burrige & Wennerberg, 2004; Gu *et al.*, 2003). Recently the application of Rac1 inhibitors such as NSC23766 has also aided the characterisation of the role of Rac1 in mediating secretion-dependent aggregation in platelets (Dwivedi *et al.*, 2010).

1.4.3 Cdc42

Like RhoA and Rac, Cdc42 has been extensively studied and discovered to act as signal mediator of numerous pathways in mammals (Moon & Zheng, 2003; Wang *et al.*, 2006). It was first uncovered as a critical gene element which contributed to actin cytoskeleton

rearrangement in *Saccharomyces cerevisiae*. In platelets, Cdc42 is expressed extensively (with over 28000 copies) and it has been established as an essential regulator of filopodia formation (see section 1.3.4) (Burkhart *et al.*, 2012). Akbar *et al.*, (2011) used knockout models of Cdc42 deletion to demonstrate the critical role of Cdc42 in platelets. They found platelets from mouse lacking Cdc42 were unable to form filopodia when spread on fibrinogen or collagen related peptide (CRP), as well as a significant reduction in platelet count.

1.4.4 Regulation of Rho GTPases

GEF with particular relevance to platelets includes p115RhoGEF and PIP3-dependent Rac exchanger 1 protein (PREX-1) (Aslan and McCarty, 2013). p115RhoGEF has been associated with activating RhoA and the stimulation of downstream ROCK which both having a combined effect in facilitating shape change in platelets. Proteins known as Vav have also been found to mediate platelet functions and have been characterised mainly as a Rac GEFs, although studies have demonstrated the promiscuous ability for Vav protein isoforms to interact with and activate a number of Rho family members including RhoA and Cdc42 proteins (Hornstein *et al.*, 2004).

The role of the majority of GAPs identified in platelets is largely unknown and unexplored. Although, emerging evidence have found GAPs such as oligophrenin1 and Nadrin to exert effects on Rac and Cdc42 and thus have been proposed to regulate downstream effectors and in turn platelet functions (Elders *et al.*, 2012).

In addition to GEFs and GAPs, emerging body of evidence has suggested for a further protein to partake in the regulation of Rho GTPase activity: Rho-guanine nucleotide dissociation inhibitor (RhoGDI). RhoGDI proteins act in similar ways to GAPs, in that they sequester Rho GTPases to particular intracellular sites thus restricting enzymatic activity of GTPases while also regulating their expression (DerMardirossian and Bokoch, 2005). Like GAPs, the roles of RhoGDIs as a plausible inhibitory regulation candidate of platelet activity remains largely uncharacterised, and again as with GAPs, platelets were used to aid the discovery of the first RhoGDI for Cdc42 (Leonard *et al.*, 1992).

1.5 Role of platelets in haemostasis

Under normal conditions, platelets circulate in blood vessels which are surrounded by a continuous monolayer of endothelial cells. Platelets move freely within the vasculature in an inactive state, however, the exposure of protein components in the subendothelial layer upon vascular injury stimulates platelet adhesion to the site and triggers the activation of platelets through a multitude of signalling molecules and pathways which manifest in the formation of a haemostatic plug, which in turn maintains haemostasis (Stalker *et al.*, 2012). The role of platelets in the context of haemostasis is fundamental and the steps involved in the process, namely adhesion, activation, secretion, and aggregation are described briefly below.

1.5.1 Platelet adhesion

Platelet adhesion mechanisms to a large extent depend upon the type of blood vessel and the shear rate environment that platelets are around. Platelets flowing in arteriole circulation are under relatively high shear rates (300-800/s) whilst lower shear rates occur in the venous system (20-200/s) (Goto *et al.*, 1995). Following damage to the vascular endothelial layer, extracellular matrix (ECM) proteins such as collagen, vWF, fibronectin and laminin become exposed to circulating platelets (Jobling and Eyre, 2013). This results in the rapid activation and adhesion of platelets to the site of vascular damage in order to arrest blood loss (Figure 1.12). The initial binding of platelets to exposed adhesive macromolecules occurs via an array of receptors expressed on the surface of the platelet (Section 1.6).

Tethering of platelets to the site of injury is primarily mediated through platelet receptors which interact with vWF bound to collagen (Varga-Szabo *et al.*, 2008). At high shear rates, this reversible binding of immobilised vWF to the GPIb α subunit of the GPIbV-IX receptor complex via its A1 domain is critical to slow the velocity of flowing platelets and promote firm adhesion to the site of vascular damage (Andre *et al.*, 2000). Several studies have highlighted the significance of this interaction between vWF and GPIb α , and demonstrated severe bleeding disorders in patients with conditions such as Bernard-Soulier syndrome

where they lack vWF and GPIb-IX-V complex, respectively, thus suggesting tethering of platelets under high shear rates is a crucial mechanism (Berndt & Andrews, 2011).

This tethering action permits GPVI and GP α IIb β 3 on platelets to bind to collagen (a potent thrombotic factor) thus stimulating platelet activation and downstream signalling which results in the stable irreversible adhesion of platelets to the site of injury via synergistic binding of numerous integrins to their ligands (Figure 1.12) (Hou *et al.*, 2015).

As for platelets flowing under low shear rate, they have been found to directly interact predominantly with collagen, laminin and fibronectin and this interaction is generally sufficient to initiate immediate firm platelet adhesion to the site of injury (Varga-Szabo *et al.*, 2008).

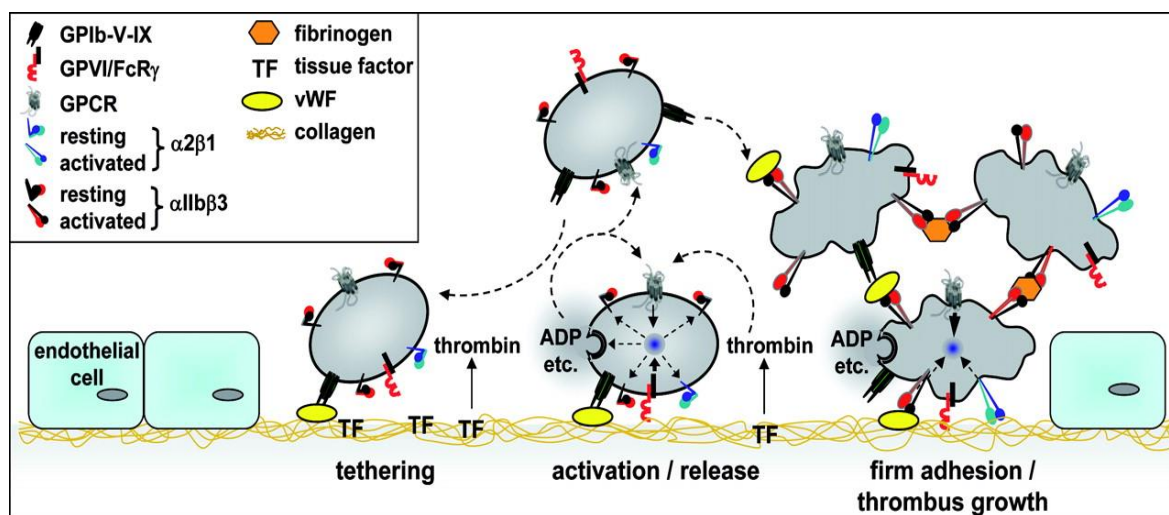


Figure 1.12 Platelet adhesion and activation on ECM at sites of vascular endothelial damage. The association between GPIb α and vWF facilitates platelet tethering, thus allowing GPVI interaction with collagen. GPVI-collagen interaction shifts platelet integrins to a high-affinity state and results in the release of ADP and Thromboxane (TXA₂). Exposed tissue factor (TF) generates the formation of thrombin which results in platelet activation resulting in firm adhesion of platelets to the site of vascular injury (Varga-Szabo *et al.*, 2008).

1.5.2 Platelet activation

Platelet activation occurs simultaneously as platelets adhere to ECM proteins exposed upon damage to the vascular endothelial layer. A range of stimuli such as ADP, TXA₂, thrombin and collagen all contribute to the activation of platelets through various distinct mechanisms (Figure 1.13). Thrombin in particular, is a potent activator of platelets and it is generated following the exposure of tissue factors to plasma coagulation factors. On the other hand, specific molecules like nitric oxide and prostacyclin released by the endothelium lead to platelet inhibition (Figures 1.13). A variety of platelet receptors and ligands are involved in recognising the wide array of stimuli and compounds and thus lead to signalling downstream. Platelet activation pathways as a result of interaction with such substrates through the numerous platelet receptors are outlined in Section 1.6. Platelet activation commonly results in a dramatic morphological change of platelets, from a discoid to a spherical shape as previously mentioned. Platelets reorganise their cytoskeleton to achieve this in order to firstly increase their surface area for adhesion and secondly, to stimulate inactivated platelets into their active form (Vorchheimer and Becker, 2006).

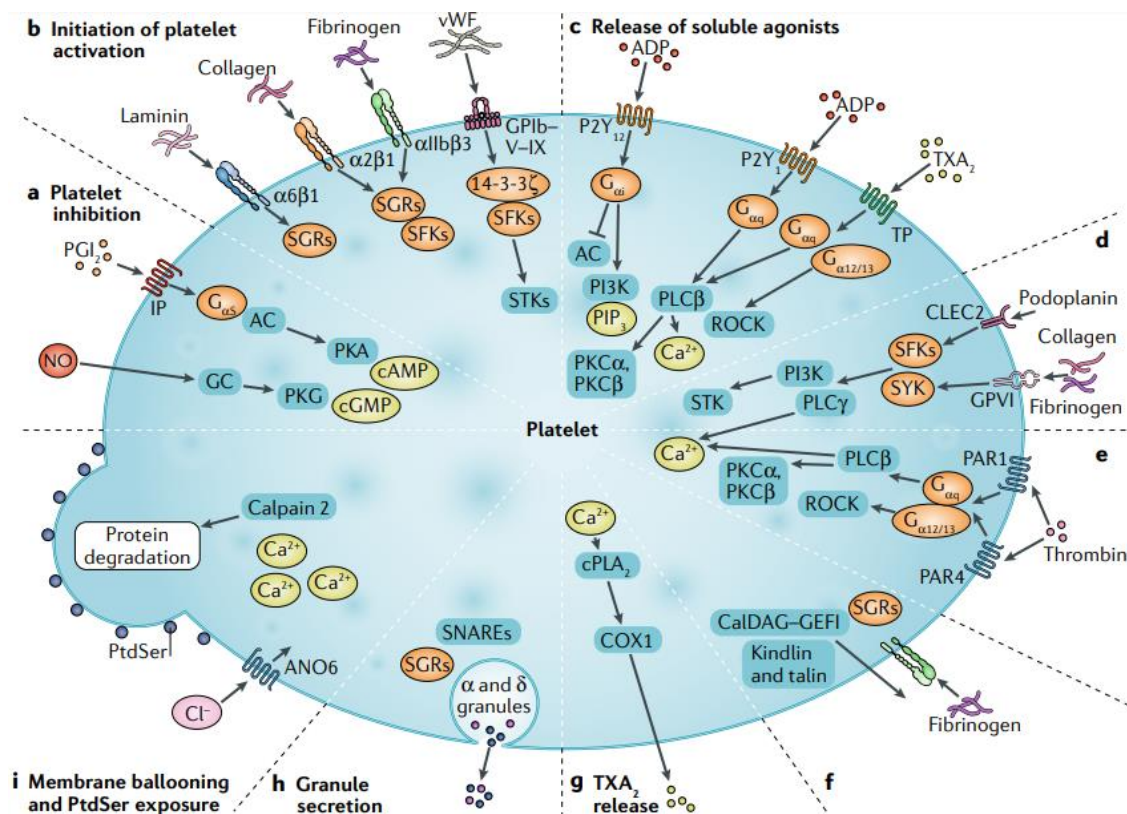


Figure 1.13 Schematic representation of platelet activation and the signalling pathways

involved. a) NO and PGI₂ lead to platelet inhibition via triggering guanylate cyclase (GC) and adenylyl cyclase (AC), respectively, which in turn stimulates protein kinases. b) Integrins and GPIb-V-IX bind to their respective ECM ligands i.e., fibrinogen and collagen thus initiating platelet activation; this process involves the participation of various small G-protein regulators (SGRs), SRC-family kinases (SFKs), and serine/threonine-protein kinases (STKs). c) Agonists such as ADP and TXA₂ stimulate P₂Y₁₂/P₂Y₁ and the TXA₂ G-protein coupled receptors, respectively. d) Platelet activation activity is amplified through GPVI and C-type lectin-like receptor 2 (CLEC2), both of which can trigger PI3K and PLC γ , as well as initiate Ca²⁺ release into the cytoplasm via PTK pathways involving SFK and SYK proteins. e) G α q-coupled receptors PAR1 and PAR4 in humans are activated via thrombin, which serves as a strong platelet agonist. f) The integrin receptor α IIb β 3 changes conformation from a low-affinity to high-affinity state. g) Activation of cyclooxygenase 1 (COX1) and cytosolic phospholipase A2 (cPLA2) result in release of TXA₂. h) Platelet granule secretion is stimulated by secondary messengers such as Ca²⁺ and involves SNAREs. i) Ballooning of the membrane and exposure of phosphatidylserine occurs as concentration of Ca²⁺-mobilizing agents increase (van der Meijden & Heemskerk, 2019).

1.5.3 Platelet secretion

Following platelet activation, secretion of platelet granular content via the OCS into the external environment is a common course and is critical in amplifying the activation process. Molecules such as ADP and polyphosphates contained in the dense granules are important components that contribute to haemostasis by aiding the second wave of platelet aggregation (Johnston-Cox *et al.*, 2011).

Numerous cytokines, anti- and pro-inflammatory mediators and proteins are found in the α granules of platelets (Golebiewska and Poole, 2015). Degranulation of these compartments and the formation of TXA₂ as well as ROS, increases platelet activation and inside-out signalling of α IIb β 3 integrin which in turn recruits additional platelets and thus aids the regulation and formation of a stable thrombus (Jin *et al.*, 2002).

1.5.4 Platelet aggregation

Platelet aggregation ultimately aids the formation of a thrombus via numerous platelet-platelet and platelet-vessel wall interactions in order to arrest bleeding. Thus far, studies have confirmed platelet aggregation mechanisms at the site of vascular injury depends upon the shear rates the platelets are flowing under (Rana *et al.*, 2019). Likewise, the

formation of a thrombus and aggregation of platelets are also dependent on the interaction between soluble fibrinogen and $\alpha\text{IIb}\beta\text{3}$. Bennett *et al.*, (1999) found cytoskeletal proteins exerted a constricting impact on the $\alpha\text{IIb}\beta\text{3}$ integrin when platelets were in their quiescent state, hence a decreased affinity for ligands was observed. However, they also found upon platelet activation by haemostatic agonists that the constricting effects on the integrin was alleviated by the activation of inside-out signalling cascade (Bennett & Vilaire, 1979).

In essence, subsequent to platelet activation following endothelial injury, $\alpha\text{IIb}\beta\text{3}$ on the surface of platelets undergoes a conformational change via inside-out signalling cascade and as a result the receptor acquires a high affinity form for binding ligands such as fibrinogen (Bennett *et al.*, 2009). This high-affinity fibrinogen receptor is then capable of interacting with the platelet cytoskeleton and facilitate platelet spreading, aggregation and clot retraction (Jobling and Eyre, 2013). The mechanisms of $\alpha\text{IIb}\beta\text{3}$ integrin mediated platelet signalling and adhesion is discussed further in Section 1.6.3.

1.6 Platelet signalling via receptors

The adhesion of platelets to the ECM of the damaged endothelium and the formation of a stable platelet plug are essential to maintain primary haemostasis. These processes can be summarised by three phases: initiation, extension and stabilisation and are regulated by various signalling pathways. The key receptors and signalling pathways are described in the following subheadings.

1.6.1 Tyrosine kinase receptor

According to current models, the initial interaction of collagen and vWF with their respective receptors results in a characteristic clustering of GPVI which in turn induces intracellular signalling via phosphorylation of FcR γ -chain at immunoreceptor tyrosine-based activation motif (ITAM) (Abdul, 2017; Senis *et al.*, 2014). Since these receptors do not possess any intrinsic kinase activity; they rely on protein tyrosine kinase cascade and signalling which is mediated by Src family kinases: Lyn and Fyn (Figure 1.14) (Moroi and Jung, 2004). The precise mechanisms leading to the activation of members of the SFKs remains widely undiscovered, although they have been reported to be in close proximity or attached to proline rich domain of the cytoplasmic tail of GPVI by the Src homology-3 domain (Abdul, 2017). These results propose the model shown in Figure 1.14, whereby GPVI on platelet exists as a complex with the FcR γ -chain.

It is believed for the phosphorylation of FcR γ -chain by Lyn and Fyn to lead to the assembly of a GPVI signalosome (ITAM motif) whereby Syk protein tyrosine kinases via SH2 domain interact with residues on ITAM (Mkaddem *et al.*, 2017). This stimulation of ITAM and activation of Syk triggers the activation and phosphorylation of adaptor proteins such as LAT, Btk, Gads and SLP-76, which in turn generates a signalosome (Pasquet *et al.*, 1999). The formation of a GPVI signalosome stimulates phosphorylation of PLC- γ 2, which in turn when activated results in the hydrolysis of phosphatidylinositol 4, 5 bisphosphate (PIP2) into inositol 1, 4, 5 trisphosphate (IP3) and diacylglycerol (DAG) (Lapetina and Siess, 1983). The formed IP3 then diffuses through the cytoplasmic matrix and binds to IP3 receptors on the DTS (Varga-Szabo *et al.*, 2009). This results in an increase in cytosolic Ca^{2+} causing activation of the calcium channel Orai1 (Jooss *et al.*, 2019).

DAG formed from the hydrolysis of PIP2 triggers potent platelet activation through activating protein kinase C (PKC) isoforms (Stalker *et al.*, 2012). Both IP3 and DAG signalling function to mediate granule secretion, shape change of platelets and activation of integrins.

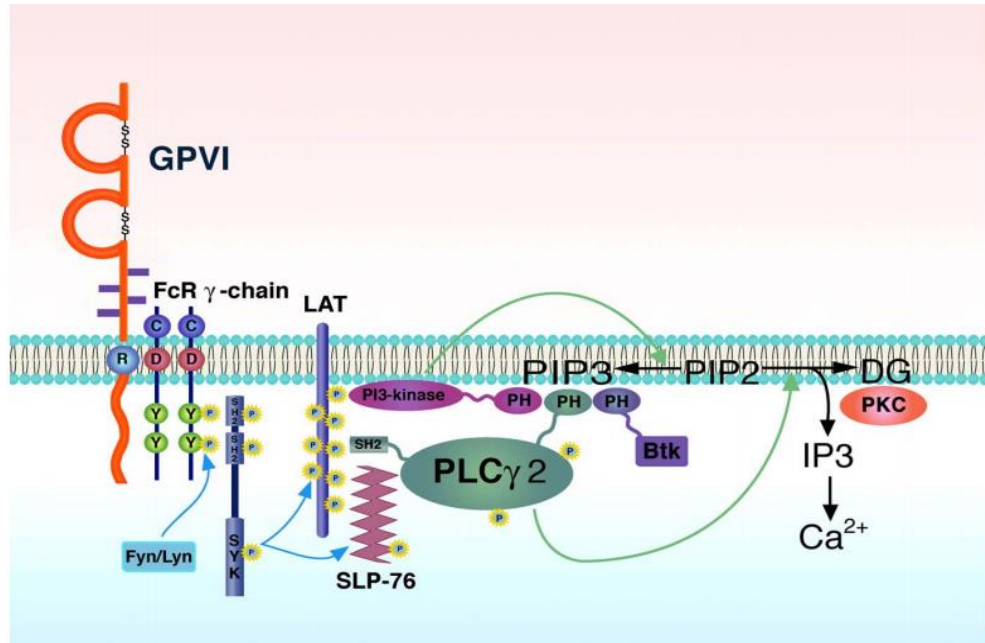


Figure 1.14 Model of tyrosine kinase mediated signalling pathway in platelets. Tyrosine residue (FcR γ chain ITAM) phosphorylation is induced upon collagen-mediated clustering of GPVI receptor on platelets via Fyn and Lyn proteins. This delivers docking sites for Syk and subsequent activation of the protein, which in turn triggers the phosphorylation of adaptor proteins LAT, SLP-76 and Btk, collectively referred to as a signalosome. These signalosomes induce the activation of PLC γ 2 and through the hydrolysis of PIP2, generates IP3 and DAG. IP3 stimulates the efflux of calcium ions from DTS into the cytosol while DAG triggers PKC activity. Together IP3 and DAG mediate platelet shape change, release of platelet granular content and platelet aggregation. Abbreviations: PH, pleckstrin-homology domain; SH2, Src homology 2 domain; C; Cysteine, R; Arginine, D; Aspartic acid Y; Tyrosine (Moroi and Jung, 2004).

1.6.1.1 Inhibitors of tyrosine kinase signalling pathway

The use of platelet signalling inhibitors has allowed us to gain valuable insight into innumerable signalling molecules involved in a diverse range of signalling pathways that influence platelet activation. In addition to this, it has allowed the identification of targets for which novel antiplatelet agents can be developed. Indeed the development of tyrosine kinase inhibitors has revolutionised the management of several cancers, namely chronic myelogenous leukaemia (CML) (Yurttas and Eskazan, 2019). CML is characterised by the

unregulated and constitutively activated form of Abl tyrosine kinase leading to uncontrolled growth of myeloid cells (Sawyers, 1993).

Dasatinib is an example of an FDA approved, potent ATP-competitive inhibitor which targets SFK, and is used widely for the treatment of CML (Senis *et al.*, 2014). Side effects such as gastrointestinal symptoms, fluid retention and myelosuppression have been observed in patients (Gratacap *et al.*, 2009). In addition this, some studies have found off-target effects leading to platelet dysfunction and bleeding diathesis (Kostos *et al.*, 2015; Mustafa *et al.*, 2015). SFKs such as Lyn, Fyn and c-Src are reported to be present in platelets, and it has been proposed for dasatinib to alter platelet functions by inhibiting SFKs (Senis *et al.*, 2014). A number of studies have utilised dasatinib to decipher the molecular mechanisms by which dasatinib alters platelet function, although largely this remains uncovered (Quintás-Cardama *et al.*, 2009; Neelakantan *et al.*, 2012).

PRT-060318 (PRT) is another example of a tyrosine kinase inhibitor. It selectively inhibits Syk tyrosine kinase activity which is downstream of FcγRIIA and has been suggested as an approach to treat Heparin-induced thrombocytopenia (HIT). Although not much is known about the effects of PRT in platelets. Nevertheless, a study utilising transgenic mouse models have shown PRT to inhibit HIT and platelet-mediated thrombosis thus confirming PRT interferes with platelet signalling (Reilly *et al.*, 2011).

Burton tyrosine kinases (BTK) belong to the Tec family of TKs and are downstream of GPVI and the B-cell antigen receptor. Its activation results in subsequent phosphorylation of PLCγ2 downstream. Ibrutinib and acalabrutinib are examples of BTK inhibitors used for the treatment of chronic lymphocytic leukaemia (CLL) (Series *et al.*, 2019). However, they have been observed in a subgroup of patients to result in major haemorrhage and this in turn has been correlated with a loss of platelet activation via GPIb and GPVI (Caron *et al.*, 2017). Thus, indicating BTKs to play a critical role in platelet activation. However, patients with X-linked agammaglobulinemia (linked to a mutation in the BTK gene) have been reported to not bleed excessively (Nicolson *et al.*, 2018) and so the role of BTK in supporting platelet functions remains uncovered.

1.6.2 G-protein coupled receptors

Following activation platelets undergo, among other processes, the release of secondary mediators from their dense granules, production of TxA₂ from arachidonic acid and the generation of thrombin on their surface (Badimon *et al.*, 1988). The release of these soluble molecules stimulates the recruitment of additional platelets in circulation to the site of injury and aids the formation of a thrombus. This phase of recruitment and adhesion of additional platelets to the site of injury is referred to as the extension stage and occurs primarily via G-protein coupled receptors (GPCRs) (Woulfe, 2005).

GPCRs consist of 7 transmembrane domains containing equal number of extracellular and intracellular loops in a serpentine arrangement (Kroeze *et al.*, 2003). The intracellular loops of GPCRs contain the carboxyl-terminal domain while the extracellular loops contains the amino terminus and binding sites for ligands/agonists (Gurbel *et al.*, 2015). GPCRs have the capacity to interact with a wide array of functionally diverse guanine nucleotide-binding proteins known as G proteins which are normally harboured in the intracellular loop (Gurbel *et al.*, 2015). G proteins are heterotrimeric structures consisting of α , β , and γ subunits (Gurbel *et al.*, 2015). The $G\alpha$ subunit is typically bound to GDP and remains tightly associated with β and γ subunits in its inactive state (Kroeze *et al.*, 2003). However, upon activation by agonists, GDP is replaced by GTP resulting in the dissociation of the α subunit from the $\beta\gamma$ subunits. This exposes the surfaces on the individual subunits and facilitates the interaction with effectors (Woulfe, 2005).

Ten forms of G proteins have been identified thus far and they are commonly categorised into four families based on the functions of the α subunit: $G\alpha_i$, $G\alpha_q$, $G\alpha_{12/13}$ and $G\alpha_s$ (Table 1.5) (Woulfe, 2005). Comparatively less is understood about the role of the β and γ subunits (Smyth *et al.*, 2009). Platelet agonists have the potential to bind to a single or several GPCRs and the receptors can then subsequently associate with one or more G proteins (Woulfe, 2005). In general, most agonists bind to GPCRs and stimulates the activation of quiescent platelets. An exception to this is the binding of prostaglandin, which results in inhibitory signalling events and thus dampens the platelet response (Woulfe, 2005).

Table 1.5 Key agonists acting via GPCRs on human and mouse platelets.

Receptor	Agonist	G protein	Associated effector/signalling	Reference
PAR1 (human)	Thrombin	G _q , G ₁₂ /G ₁₃	-PKC activation. -Release of PLC/Ca ²⁺ . -Activation of Rho signalling pathway leading to actin remodelling.	(Shenker <i>et al.</i> , 1991; Offermanns, 2006)
PAR3 (mouse)	Thrombin	None	-A reduction in platelet aggregation and secretion in response to thrombin. -Prolonged bleeding time has also been observed <i>in vivo</i> .	(Kahn <i>et al.</i> , 1998; Keularts <i>et al.</i> , 2000)
PAR4	Thrombin	G _q , G ₁₃	-PKC activation. -Release of PLC/Ca ⁺⁺ . -Activation of Rho signalling pathway leading to actin remodelling. -Complete inhibition of platelet aggregation in response to thrombin.	(Yada <i>et al.</i> , 1989; Shenker <i>et al.</i> , 1991)
P2Y1	ADP	G _q	-PKC activation. -Release of PLC/Ca ⁺⁺ . -Platelet aggregation is reduced slightly in response to ADP.	(Salzman <i>et al.</i> , 1972)
P2Y1	ADP	G _{i2}	-Decrease in cAMP levels. -PI3Ky activation occurs. -Platelet aggregation diminishes drastically in response to ADP. -A reduction in platelet aggregation was observed in response to collagen/ thrombin.	(Brass <i>et al.</i> , 1997; Kahn <i>et al.</i> , 1999)
IP	PGI ₂	G _s	-An increase in cAMP thus diminishes platelets' response to other agonists.	(Jin and Kunapuli, 1998)
TP	TxA ₂	G _q , G ₁₃	-PKC activation. -Release of PLC/Ca ⁺⁺ . -Activation of Rho signalling pathway leading to actin remodelling.	(Lenain <i>et al.</i> , 2003)

PAR, Protease-activated receptor; IP, prostaglandin receptor; TP, thromboxane receptor.

Prostaglandin

Platelets in the bloodstream are constantly exposed to PGI₂ and NO. These are compounds released from endothelial cells and aid in maintenance of platelets in their inactive form until and unless platelets are stimulated by agonists upon vascular injury. PGI₂ binds to the prostaglandin receptor (commonly referred to as the IP receptor) on the surface of platelets which is coupled to Gα_s (Baranova *et al.*, 2008). Association of PGI₂ to its receptor mediates the stimulation of adenylyl cyclase and an increased level of cytosolic cAMP is also observed, this then acts to suppress the function of platelets (Salzman *et al.*, 1972). In fact, it has been discovered for all agonists binding to Gα_s-coupled receptors on platelets to inhibit platelet function.

Thrombin and thromboxane.

Thrombin receptors PAR1 and PAR4 in humans and PAR3 and PAR4 in mice are coupled to Gα_q family of receptors. Binding of PARs to Gα_q-subunits triggers PLCβ activation which leads to the catalysis of PIP₂ into IP₃ and DAG (Jin *et al.*, 1998). The resulting IP₃ triggers calcium release which stimulates DAG which in turn activate PKC activity (Offermanns *et al.*, 1997).

Binding of thrombin to PARs can also activate Gα_{12/13}. Upon agonist-mediated activation of Gα_{12/13}, stimulation of small GTPase RhoA is commonly observed as well as the activation of Rho kinases (Moers *et al.*, 2003). Studies have previously reported the stimulation of RhoA and ROCK to promote the phosphorylation of myosin light chain (MLC). MLC in turn has been proposed to be involved in the regulation of contractile events in platelets via reorganisation of actin cytoskeletal components related to platelet shape change and secretion of granular content (Moers *et al.*, 2003).

Like thrombin, the TXA₂ receptor (TP) is also coupled to Gα_q and Gα_{12/13} subunits and activation of this receptor by TXA₂ results in the stimulation of the above-mentioned signalling cascade through similar mechanisms to that triggered by thrombin (Fitzgerald, 1991).

ADP

ADP serves as an autocrine and paracrine stimulus since ADP can either be released from within the dense granule of platelets following platelet activation or it can be released from damaged endothelial cells at the site of vascular injury (Rivera *et al.*, 2009). Hence ADP plays a role in both recruiting additional platelets to the site of injury as well as stabilising the haemostatic plug to prevent blood loss. ADP binds to two families of purinergic GPCRs, P2Y₁ and P2Y₁₂, which are coupled to G α_q and G α_i respectively (Rivera *et al.*, 2009). P2Y₁ and P2Y₁₂ knockout mice studies have enabled to identify the possible complementary and different functions of these receptors in the formation of a thrombus.

P2Y₁ coupled to G α_q acts in similar ways to that mentioned for thrombin-mediated PAR-G α_q stimulation whereby an increase in cytosolic calcium concentration results in integrin activation and subsequent aggregation. This is reinforced by data from mice knockout studies where P2Y₁ deficient mice injected with ADP showed impaired platelet response including the lack of ability to cause shape change and induce platelet aggregation (Jirouskova *et al.*, 2007).

On the contrary, it has been reported that ADP mediated activation of P2Y₁₂ receptor coupled to G α_i inhibits the stimulation of adenylyl cyclase thus preventing the formation of cAMP (Jin *et al.*, 2002). It was also found for P2Y₁₂-G α_i activation to stimulate PI3K activity which as a result triggered Akt and protein kinase B thus mediating calcium mobilisation and secretion of platelet granular content as well as facilitating the signalling involved in integrin activation (García *et al.*, 2010). Data from inhibitor studies and P2Y₁₂^{-/-} mice studies revealed hinderance in platelet aggregation in response to ADP (Offermanns *et al.*, 1997). Interestingly, results from P2Y₁₂^{-/-} platelets showed P2Y₁-associated responses to be intact i.e. platelet shape change and activation of PLC remained unaltered, however an absence in ADP mediated inhibition of cAMP formation was observed (Foster *et al.*, 2001).

1.6.3 Integrin $\alpha_{IIb}\beta_3$

The final stage to prevent blood loss at the site of vascular breach is through the formation of an efficient thrombus and this is referred to as the stabilisation stage. This stage involves heterodimeric transmembrane integrins which aid the interaction between platelets and extracellular ligands, thus coordinating various intracellular signalling events which affects diverse physiological processes (Joo, 2012).

Platelet express a number of integrins which are all composed of α - and β -subunits and contain an N-terminal globular head domain, a distinct transmembrane domain and a small cytoplasmic tail domain (Joo, 2012). The dominant integrin (60,000-80,000 per platelet) involved in platelet aggregation is $\alpha_{IIb}\beta_3$ and common ligands for this integrin include fibrinogen, fibronectin, vWF and vitronectin. A critical characteristic of $\alpha_{IIb}\beta_3$ is the ability for the integrin to modulate its affinity according to platelet requirement.

In resting platelets the integrin has low affinity for fibrinogen however upon activation via ADP, thrombin or TXA₂, the integrin undergoes a conformational change and becomes a high affinity receptor for fibrinogen (Joo, 2012). This process of transforming into a high affinity integrin requires information from within the cell to be transmitted to the extracellular domain of the integrin and is referred to as 'inside-out' signalling. Low affinity state of $\alpha_{IIb}\beta_3$ is maintained primarily by the interactions within the cytoplasmic tail domain of α and β subunits. Some proteins such as talin, kindlin, myosin, Src, Syk, TKs and Fyn are able to interact with and disrupt the cytoplasmic subunits of $\alpha_{IIb}\beta_3$ thus facilitate a conformational change via the transmembrane region of the receptor, resulting in the conversion of the integrin from a 'bent' low affinity receptor to a 'stretched' high affinity form (Stalker *et al.*, 2012).

Upon activation of $\alpha_{IIb}\beta_3$, the receptor can then bind to agonists such as fibrinogen with high affinity and thus induce intracellular signalling events within the cell, triggering molecules such as SFKs which result in processes such as cytoskeletal remodelling and this is referred to as 'outside-in' signalling (Durrant *et al.*, 2017).

1.7 Role of platelets in infection and immunity

1.7.1 General overview of platelets as immune cells

Although the primary role of platelets is understood to be preventing excess blood loss, platelets have been observed to contribute to a wide array of functions and processes that extend beyond maintaining haemostasis. An increasing body of evidence suggest platelets to play an important immune function role: platelets are capable of recruiting immune cells such as leukocytes to the site of endothelial injury and are also efficient at storing, producing and secreting a variety of bioactive molecules (Smyth *et al.*, 2009). These secreted bioactive molecules can then serve as mediators which attract and regulate innate immune cells. Some secreted molecules also encompass bactericidal properties i.e. antimicrobial peptides, reactive oxygen species, defensins and proteases (Hoylaerts *et al.*, 2018). In essence, platelets have been reported to partake in host defence mechanism via direct and indirect methods.

Platelets themselves possess numerous receptors which enable them to serve a direct effector function in innate immunity. It has been discovered for platelets to be among the first cells to recognise the entry of microbial pathogens in the bloodstream (Yeaman, 2010). Platelets express a number of receptors that act as pattern recognition receptors (PRRs) which survey the internal environment for pathogen associated molecular patterns (PAMPs). The detection of PAMPs by platelets is an effective host defence element that enables the orchestration of a rapid response to potential invading pathogens.

It has been demonstrated that platelets express toll-like receptors (TLRs) which act as PRRs seeking out PAMPs such as a variety of lipopolysaccharide (LPS) isoforms on bacteria (Hamzeh-Cognasse *et al.*, 2015). In certain cases the interaction between LPS and TLR has been shown to modulate the secretion of cytokines and anti-microbial peptides from the platelet granules, thus promoting the clearance of pathogens (Vallance *et al.*, 2017). A number of platelet receptors can interact with bacterial components and this will be discussed in subsequent sections (1.8.1). However, it is also important to note that numerous pathogens have evolved various mechanism to not only evade the immune functions of platelets but also modify various platelet activities (see section 1.8.2-1.8.3).

In addition to platelet receptors which aid platelet-bacteria interaction, platelets are capable of secreting a myriad of anti-microbial products (known commonly as platelet microbicidal products (PMPs)) which can have direct anti-bacterial effects, reinforcing the role of the platelet as an immune cell (Sonmez and Sonmez, 2017). So far, four families of PMPs have been identified to aid host defence system and these include kinocidins (i.e. CXCL-4,7,5), defensins (human β -defensin II), thymosin β 4, and derivatives such as thrombocidins and fibrinopeptide A/B (Sonmez and Sonmez, 2017).

A number of studies have also reported platelets to internalise and kill microbes, in particular *E. coli*, HIV and *S. aureus* (Youssefian *et al.*, 2002). Although great speculation exists on the true capacity of platelets to engulf and destroy microbes. Nevertheless, a study by Antczak *et al.*, (2011) described platelets to engulf IgG coated beads and result in the secretion of soluble CD40L and RANTES. This was further supported by Riaz. *et al.*, (2012) who found platelets to participate in host protection mechanisms by killing IgG-opsonised *E. coli*.

In addition to the above secreted platelet molecules, platelets can also mediate the recruitment of other host innate immune cells to the site of infection and thus aid/coordinate the removal and destruction of microbes. These platelet products and their immune function are listed in Table 1.6.

Table 1.6 Examples of platelet products and how they function as immune cells.

Molecule	Function	Reference
Proinflammatory lipids: -TXA2 and PAF	-Promotes inflammation & procoagulant. Monocyte activation and results in T cell differentiation.	(Bussolino <i>et al.</i> , 1989; Fillon <i>et al.</i> , 2006)
Chemokines: -MIP-1 α , monocyte chemotactic protein-3 & RANTES. -PF4 and β -thromboglobulin, NAP-2, IL-8	-Recruit and activate leukocytes and lymphocytes. Potentiates the production of immunoglobulins. -PMN recruitment.	(Kameyoshi <i>et al.</i> , 1994; Gear and Camerini, 2003) (Cognasse <i>et al.</i> , 2007)
Growth factors: -PDGF & TGF β	-Modulates immune cells.	(Assoian and Sporn, 1986).
Immune mediators: -Histamine -Serotonin	-Proinflammatory regulator of leukocytes & lymphocytes. Induces release of granular content. - Proinflammatory regulator & results in T cell and monocytes activation.	(Ali <i>et al.</i> , 1998) (Herr <i>et al.</i> , 2017)
Cytokine: -IL-1 β	-Amplifies inflammation & antigen presentation by DC.	(Brown and McIntyre, 2011)
Microbicidal proteins: - PMP1 & PMP2	- lyses bacteria	(Yeaman <i>et al.</i> , 1998)

- Defensins	- Triggers the release of neutrophil extracellular traps.	(Kraemer <i>et al.</i> , 2011)
Nucleotide: -ATP, ADP & GTP	-Activates purinergic receptors on immune cells and enhances chemotaxis of macrophages.	(Kronlage <i>et al.</i> , 2010)
Interaction with complement receptors: -PAF	-Phagocytosis of RBC bound to complement receptor 1 is enhanced by monocytes.	(Bussolino <i>et al.</i> , 1989)
Platelet-leukocyte interaction: -P-selectin -GP Iba	-P-selectin from platelets can interact with PSGL-1 on leukocytes. Enhances transendothelial migration of neutrophils. Induces complement activation. -Interacts with Mac-1 and stimulates microvascular inflammation.	(Lam <i>et al.</i> , 2011) (Wang <i>et al.</i> , 2005)
Lysosomal granules: -Protease & glycosidase	-Breaks down microbial pathogens.	(Sonmez and Sonmez, 2017)
Other molecules: -NO -Thrombospondin -vWF	-antithrombotic, serves as a reactive oxygen species. -Stimulates aggregates of macrophage and platelets. -PMN extravasation.	(Silverstein and Nachman, 1987) (Morrell <i>et al.</i> , 2014)

PAF: platelet activating factor, MIP-1: macrophage inflammatory protein, PF4: platelet factor 4, NAP-2: neutrophil activating peptide 2, IL-8: interleukin-8, PDGF: platelet derived growth factor, TGF: transforming growth factor, PMN: polymorphonuclear leucocytes, DC: dendritic cell.

1.7.2 Platelets and their role in sepsis

The normal host response to invading pathogen involves a complicated process by which microbes are firstly identified and confined and eventually neutralised. This method involves a number of pro-inflammatory molecules including cytokines, chemokines, NO synthases, and adhesion molecules (Assinger *et al.*, 2019). In addition to this, a number of cells are also activated and recruited to the site of infection i.e., neutrophils, monocytes, and macrophages. This eventually leads to the cardinal signs of local inflammation for example, warmth, pain, protein-rich edema, and hyperaemia (Assinger *et al.*, 2019). A fine balance between pro- and anti-inflammatory mediators regulates the inflammatory processes and ensures homeostasis is re-established.

Sepsis occurs as a result of dysregulated host immune response to infection as well as uncontrolled levels of inflammation, ultimately leading to organ dysfunction (Vardon-Bounes *et al.*, 2019). The manifestation of sepsis involves an early hyper-inflammatory phase also known as the systemic inflammatory response syndrome which is closely associated with patients acquiring symptoms such as a fever and is also characterised by hyper-metabolism, which in turn can lead to septic shock and secondary complications (Assinger *et al.*, 2019). Bacteria and bacterial products contribute to aggravated inflammation thus resulting in multiple organ failure in patients. Gram-positive bacteria, namely *S. aureus* and *S. pneumoniae* are the frequently isolated forms of bacteria from blood of patients with sepsis (Assinger *et al.*, 2019).

Although, platelets are now being accepted to have an immune function role, studies have also provided evidence that suggests platelets to contribute to the pathophysiology of sepsis, since they have the capacity to modulate the function of several cells as well as their own (Vardon-Bounes *et al.*, 2019). It has been shown for platelets to regulate leukocyte function which in turn are critical partakers in the inflammatory cascade (as reviewed by Kral *et al.*, 2016).

In addition to this, platelets can also interact with host immune cells either directly or indirectly via the release of chemokines and cytokines from platelet granular content,

hence platelets have the ability to exert immunomodulatory effect (Schrottmaier *et al.*, 2015). Furthermore, Assinger *et al.*, (2019) proposed platelets to partake in the differentiation of monocytes into macrophages and ultimately regulate their effector functions. All of the above-mentioned processes support platelets to result in excessive inflammatory response and thus promote the advancement of sepsis in patients.

1.7.3 Platelets are motile cells with scavenging abilities

Originally, many investigators argued for a nucleus to be fundamental for migration in cells and so they disregarded platelets as motile cells due to the lack of a nucleus, in fact a study conducted by Clark, (1942) showed the removal of the nucleus from an amoebae to correlate with impaired motility.

Contrary to this, Euteneuer & Schliwa, (1984) reported unimpaired locomotion in experimentally derived (enucleated) metazoan cells and so suggested migration of cells to not be dependent on the nucleus itself rather the machinery associated with motility to be found within the cytoplasm. This study gave rise to the potential of platelets to encompass the capacity to migrate since it contains all the essential contractile features and enzymatic machinery involved in cellular locomotion (chemokine receptors, PI3K, Rho GTPases) (Bettex-Galland and Lüscher, 1959). Indeed, it was in the early 1970s that Löwenhaupt and co-workers (1978) reported platelets recruited to the sites of endothelial injury to have the capacity to 'change position'.

Numerous studies have since supported the notion of platelets as motile cells that constantly scavenge the local microenvironment (Gaertner *et al.*, 2017, Petito *et al.*, 2017, Valone *et al.*, 1974). Cell polarisation is believed to be key in aiding chemotaxis and primarily requires the formation of two cellular structures postulated to be regulated by Rho GTPases; a leading edge and trailing edge (Petito *et al.*, 2017). These structures allow the cell to form new adhesion sites at the leading edge while at the same time allows detachment from adhesion sites at the trailing edge (Petito *et al.*, 2017).

The ability of platelets to actively migrate lends support to the role of platelets in host defence. Certainly, a study conducted by Czapiga *et al.*, (2005) demonstrated the ability of platelets to move positions using functional N-formyl peptide receptors thus supporting the immunologic functions of platelets. Similarly, Kraemer *et al.*, (2011) also agreed with the idea of platelets as motile cell since they found high shear flow and SDF-1 to induce migration of adherent platelets.

1.8 Platelet-bacteria interplay

It has been long known that bacteria interact with platelets and stimulate the formation of platelet aggregates. In fact the earliest study was conducted in 1901 by Levaditi, who reported platelets to form 'clumps' in response to *Vibrio cholerae* in rabbits. Nevertheless, it was only in the 1970s that investigations into the mechanisms on how bacteria initiates platelet aggregation was examined (Clawson *et al.*, 1975; Clawson & White, 1971b, 1971a). Platelet-bacteria interplay can be classified into three stages: initial recognition and binding of bacteria to platelet receptors; activation of platelets resulting in downstream signalling; platelet aggregation and granule content release enabling platelets to coordinate an immune response (Kerrigan, 2015).

It is essential to further deepen our knowledge on platelet-bacteria relationships since a number of cardiovascular diseases allegedly have infectious origins thus an insight into the mechanisms involved may perhaps aid the development of therapeutic interventions that could potentially prevent the advancement of such disease and as a result, lower mortality rates (Hamzeh-Cognasse *et al.*, 2015).

The scope of this thesis focuses primarily on investigating the effects of *S. aureus* and *E. coli* on platelet function and so the majority of information mentioned herein will be regarding these organisms in relation to platelets.

1.8.1 Bacteria can interact with platelet receptors

Platelet receptors and bacterial interactions are at the forefront of recent research and significant advances has been made in identifying molecular mechanisms involved and the effect this interaction has on downstream signalling pathways in platelets. Thus far, two methods by which bacteria interact with platelets has been reported: (1) direct binding of bacteria to receptors on the surface of the platelets; (2) bacteria indirectly binding to receptors on platelets via a plasma protein (Hamzeh-Cognasse *et al.*, 2015). A diverse range of platelet receptors are recognised to interact with bacteria and thus stimulate platelet activation and aggregation. Some platelet components involved in bacteria-platelet binding are described below.

Integrin α IIb β 3

Platelet integrin α IIb β 3 (GPIIb/IIIa) is the most abundant integrin expressed on the surface of platelets and is known commonly to bind fibrinogen (Deppermann & Kubes, 2018). It has however, been widely reported to partake in the binding of bacteria to platelets via both direct and indirect mechanisms (Figure 1.15) (Hamzeh-Cognasse *et al.*, 2015). Essentially GPIIb/IIIa binds to ligands that have a specific amino acid sequence: RGD (Deppermann & Kubes, 2018). In line with this finding, a variety of bacterial species has been reported to possess RGD-like motif such as the serine/aspartate (SD) family of proteins, on their cell wall enabling the organism to bind directly to the GPIIb/IIIa. SdrG from the SD family of proteins was discovered on the surface of *Staphylococcus epidermidis* and was reported to be involved in the binding of the bacterium to the platelet integrin and subsequently stimulate platelet aggregation (Arciola *et al.*, 2004). Likewise, Coburn *et al.*, (1993) discovered *Borrelia burgdorferi* binding to platelet to be mediated by GPIIb/IIIa and revealed that the ability of the organism to attach to platelets diminished upon the addition of a synthetic RGD peptide, therefore reinforcing the participation of platelet integrin in establishing the binding of bacteria to platelet components.

Certain bacteria, namely staphylococci and streptococci species, possess several plasma protein binding molecules which can bind to an intermediate plasma protein (i.e. fibrinogen) which in turn associates with GPIIb/IIIa and Fc γ RIIa resulting in the indirect binding of the bacterium to the platelet integrin (Kerrigan, 2015). M protein and FbsA are examples of fibrinogen binding proteins expressed on the bacterial cell wall of streptococci organisms and is a well characterised model of indirect binding of bacteria to platelet integrin causing subsequent bacteria-mediated platelet aggregation (Brennan *et al.*, 2009; Kerrigan, 2015). However, it has also been shown that indirect binding of bacteria to platelets does not always result in the activation of the cells, rather a co-stimulus is required which is accomplished as bacteria binding IgG crosslinks and interacts with Fc γ RIIa (reciprocal receptor) (Kerrigan, 2015).

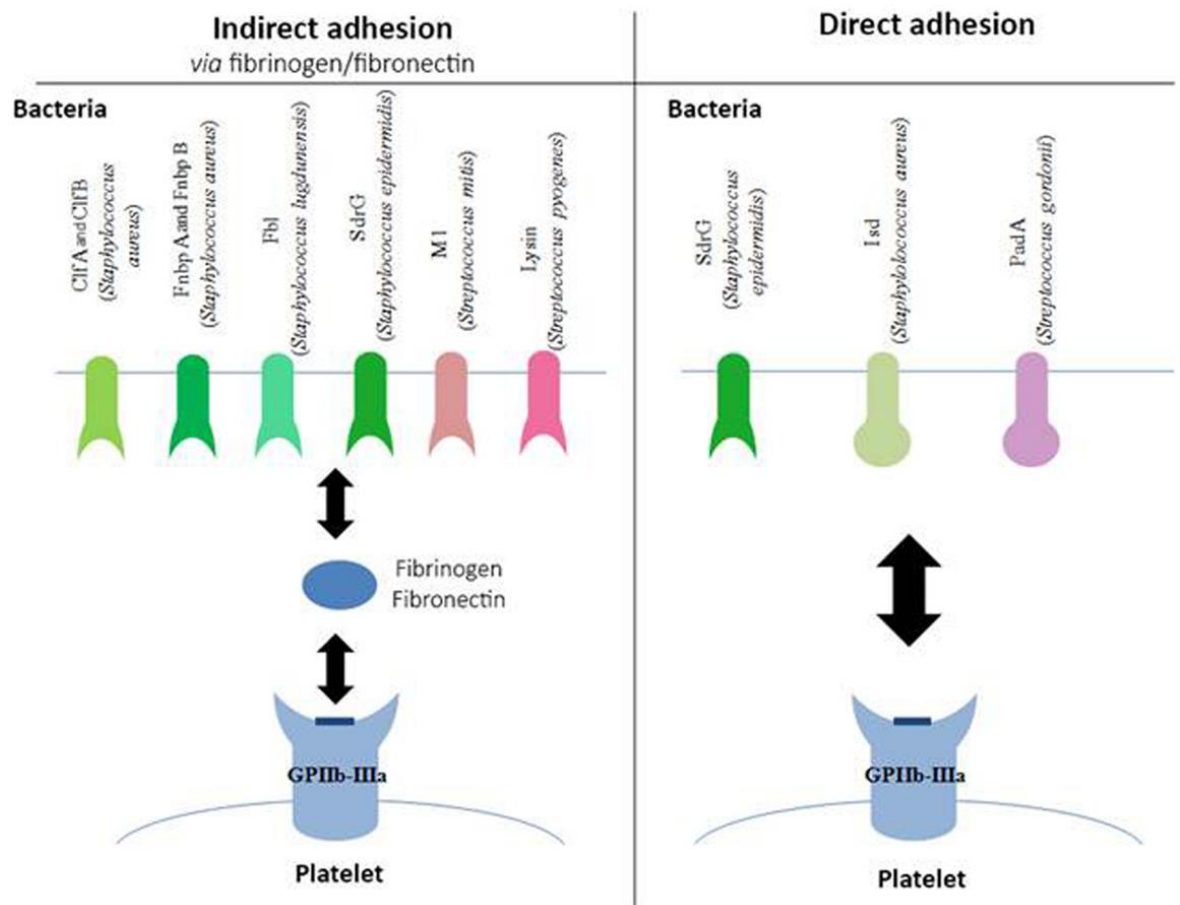


Figure 1.15 Mechanisms by which bacteria bind to platelet integrin GPIIb-IIIa. Schematic diagram demonstrating the mechanisms by which bacterial proteins interact either indirectly via plasma proteins or directly, with the platelet GPIIb-IIIa (Hamzeh-Cognasse *et al.*, 2015).

Glycoprotein Ib

Glycoprotein Ib (GPIb) is another example of a receptor found exclusively on the platelet membrane and on megakaryocytes. GPIb has been found to partake in the binding of several types of bacteria to platelets (Figure 1.16) (Hamzeh-Cognasse *et al.*, 2015). Studies have revealed many streptococci species to interact directly with the sialic acid of the glycoprotein via serine-rich proteins expressed on the bacterium such as serine-rich protein A expressed by *S. sanguinis*, or hemagglutinin salivary antigen expressed by *S. gordonii* (Kerrigan *et al.*, 2002; Plummer *et al.*, 2005). Staphylococcal accessory regulator protein expressed by *S. aureus* has also been discovered to bind directly to GPIb (Siboo *et al.*, 2005). On the other side, *S. aureus* protein A was found to interact indirectly with GPIb via vWF, which itself is a ligand of GPIb (O'Seaghda *et al.*, 2006).

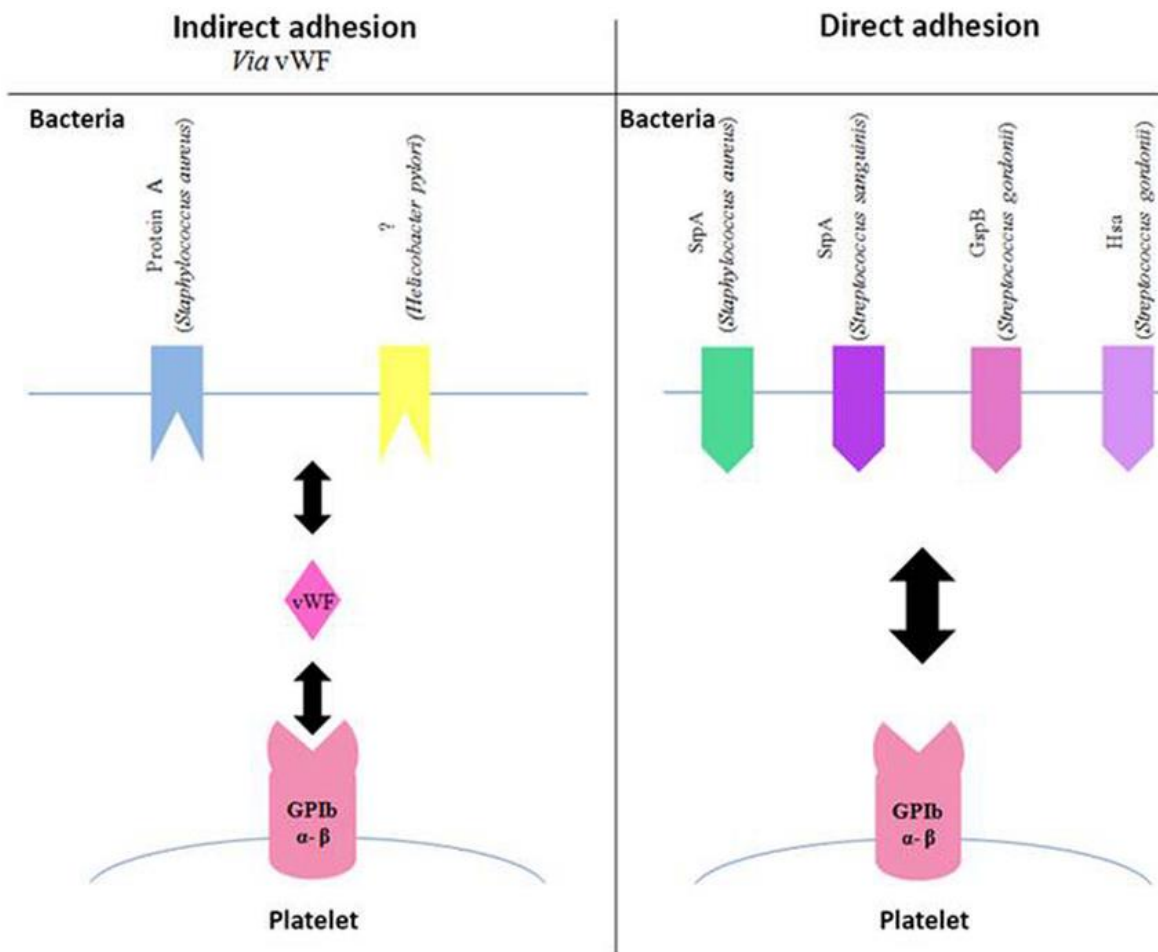


Figure 1.16 Mechanisms by which bacteria bind to platelet GPIb. Schematic diagram showing the mechanisms by which bacterial elements interact either indirectly via vWF or directly with platelet GPIb, leading to bacteria-platelet attachment (Hamzeh-Cognasse *et al.*, 2015).

Toll like receptors (TLRs)

Pathogen associated molecular patterns (PAMPs) such as molecules in the cell wall of the bacteria (i.e. lipoteichoic acid), are generally recognised by toll like receptors (TLRs) (O'Neill, 2006). TLR1-9 have been found in platelets and many pathogens have been observed to interact with some of these receptors to induce aggregation of platelets (Semple and Freedman, 2010). *S. pneumoniae* was found to stimulate platelet aggregation and subsequent release of dense granule content following the attachment of the bacteria to platelets via TLR2 (Keane *et al.*, 2010), whereas enterohemorrhagic *E. coli* was reported to bind to TLR4 via lipopolysaccharides (TLR4 ligand) expressed on the bacterium (Ståhl *et al.*, 2006).

Fc receptor

Fc receptor FcγRIIIa has been identified as a critical receptor for the interaction of bacteria with platelets and subsequent bacteria-mediated platelet activation/ aggregation (Speth *et al.*, 2013). FcγRIIIa is the low-affinity receptor for the Fc fragment of IgG (Qiao *et al.*, 2015). In platelet, FcγRIIIa interaction with immune complexes stimulates a plethora of signalling pathways intracellularly leading to events such as platelet activation and aggregation.

A variety of pathogens including, but not limited to, *S. aureus*, *S. epidermidis*, *H. pylori*, *S. pyogenes* have been identified to interact with platelets via the Fc receptor (Brennan *et al.*, 2009; Byrne *et al.*, 2003; Kerrigan *et al.*, 2002). Interestingly, in all the cases mentioned above it was established that IgG-complexes bound to bacteria was necessary for the interaction with the receptor. Moreover, it was noted in all the studies that the antibody alone proved to be insufficient in stimulating platelet aggregation/activation in response to the pathogen, rather the engagement of an additional platelet receptor for instance GPIb, GPIIb/IIIa or TLRs was required (Kerrigan and Cox, 2010). The requirement of receptor clustering to induce platelet activation has therefore been proposed.

Complement receptors

Several studies have proven platelets to interact with the complement system (Verschoor and Langer, 2013). Likewise, a number of studies have also demonstrated for bacteria to interact with complement proteins via both the conventional and alternative pathway (Gadjeva, 2014). Certain bacteria possess adhesive proteins that can bind directly to complement receptors on the surface of platelets under pathological environments i.e. SpA proteins on *S. aureus* bacterium interacts directly with gC1q-R (Nguyen *et al.*, 2000). gC1q-R is a receptor for C1q which functions as a receptor for organisms coated in complement factors. CD62P is another example of a receptor that is expressed on the surface of platelets following platelet activation and it has been shown to bind C3b which is an inflammatory mediator (Hamad *et al.*, 2010).

1.8.2 Platelet-bacteria: focus on *S. aureus*

S. aureus is a Gram-positive commensal bacterium which commonly resides asymptotically in the human anterior nares and on skin (Miajlovic *et al.*, 2007). However, upon alterations to the niche in which the organism persists, these bacteria have the capacity to transform into pathogenic organisms and result in superficial infections as well as a number of clinical conditions including infective endocarditis (IE) and bacteraemia, which can lead to detrimental outcomes and ultimately death if left untreated (Ondusko and Nolt, 2018).

Platelets have been postulated to be at the interface of conditions such as IE. In fact, IE is characterised by the generation of a platelet-bacteria thrombi on the surface of a heart valve and is typically attributable to *S. aureus* (Fowler *et al.*, 2005). It has been shown for bacteria to attach to the endothelium of the vasculature thus increasing the permeability of the valvular cells. This in turn results in the exposure of tissue factors found within the subendothelial surface hence resulting in the activation and recruitment of platelets to the site (Hamzeh-Cognasse *et al.*, 2015). The attachment of circulating platelets to the subendothelial layer along with the activation of platelets initiates the formation of a thrombus which has the potential to lead to arterial ischemia as well as a pulmonary embolism (Leask *et al.*, 2003).

The ability of *S. aureus* to bind to platelets and initiate the activation of these cells followed by subsequent aggregation is a multi-step process which has widely been demonstrated to play a central role in the pathogenesis of IE, although many aspects such as the effect of *S. aureus* in altering certain platelet functions remain largely unexplored (Fowler *et al.*, 2005; Kerrigan *et al.*, 2007). Nonetheless, numerous microbial surface component reacting with adhesive matrix molecules have been identified to stimulate the attachment of *S. aureus* to platelets and thus trigger platelet activation (Kerrigan and Cox, 2010).

Binding of *S. aureus* to receptors on the surface of the platelets occurs either directly or indirectly via bridging molecules such as fibrinogen (Miajlovic *et al.*, 2007) (section 1.8.1). While the initial binding of bacteria to platelets is considered pivotal for the stimulation of

platelets, the receptors and surface molecules involved in this bacteria-platelet association were mostly unknown until recently. The use of mutant forms of *S. aureus* (deficient in particular surface molecules) has allowed a better understanding of the participating components involved in the interaction between *S. aureus* and platelets (O'Brien *et al.*, 2002). Evidence from such studies suggests bacteria-platelet adherence and activation to be multifactorial and provided novel insight into the various virulence factors produced and secreted by the organism.

1.8.2.1 *S. aureus* virulence factors

S. aurei possess an elaborate and broad range of virulence factors which allow the organism to cause a variety of pathogenic infections. These diverse array of virulence factors are expressed in different amounts at different anatomical areas and affect distinct signalling pathways/processes during the evolution of the given infection (Yeaman and Bayer, 2000). It is also important to note that these molecules expressed on *S. aureus* can vary considerably between different strains of the species as well as the different growth stages of the bacteria. This was demonstrated by Kerrigan & Cox, (2010) and Saravia-Otten *et al.*, (1997) who both showed *S. aureus* in the stationary stage of growth to cause aggregation of platelets via predominantly clumping factor A (ClfA), whereas fibronectin binding proteins (FnBP) were found to be the main pro-aggregant molecule during the exponential stages of growth. A brief overview of some of the virulence factors of *S. aureus* that affects platelet function is presented below and depicted in Figure 1.17.

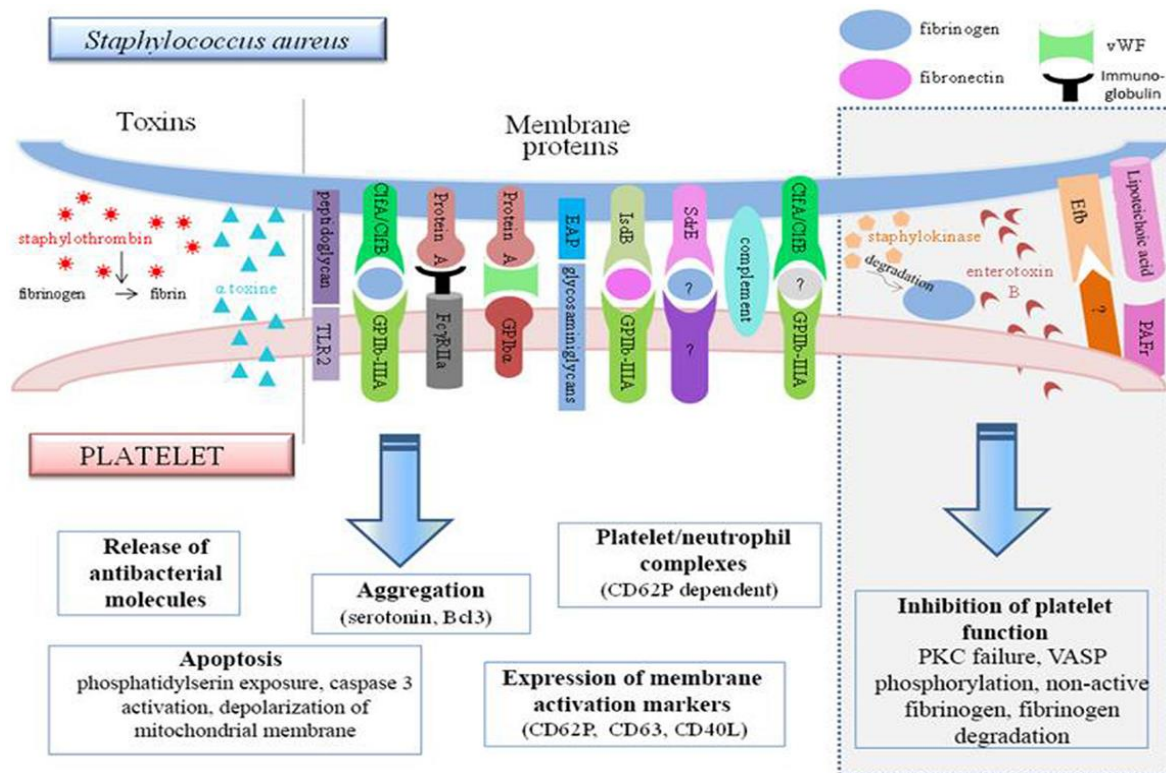


Figure 1.17 Molecules involved in the interaction between platelets and *S. aureus* and their effect on platelet functions. *S. aureus* can adhere to platelets either directly (via receptors on the surface of the platelet) or indirectly (via plasma proteins). *S. aureus* can also simulate the activation of platelets through the release of toxins, whereas certain bacterial virulence factors can result in the inhibition of several platelet functions (shown in the grey box on the far right of the image) (Hamzeh-Cognasse *et al.*, 2015).

Protein A

Protein A has been widely recognised as a common molecule expressed on the surface of *S. aureus* and has been demonstrated to act as a major virulence for the bacteria in various pathological conditions (Herbert *et al.*, 2010). Protein A from *S. aureus* has been discovered to mediate platelet activation as it can bind to FcγRIIa of platelets causing the release of serotonin and thus trigger platelet aggregation (Herbert *et al.*, 2010; Hamzeh-Cognasse *et al.*, 2015).

These *S. aureus* adhesins have also been reported to interact with gC1qR/p33 protein expressed on the platelet membranes (Nguyen *et al.*, 2000). A study by Pawar *et al.*, (2004) investigated the role of protein A in inducing *S. aureus*-mediated platelet aggregation under flow. They, along with Viela *et al.*, (2019) found the protein to interact with vWF under

high shear rates, which in turn interacted with GPIIb/IIIa therefore stimulating platelet adhesion and ultimately triggering platelet aggregation. This was further supported by Kerrigan & Cox, (2010) who used specific antibodies to block vWF and observed a partial inhibition in the activation of platelets by *S. aureus*. Although the interaction between protein A is important to initiate platelet adhesion, the absence of complete inhibition of platelet activation suggests the potential involvement of other pathways in the attachment of *S. aureus* to platelets (Kerrigan and Cox, 2010).

Clumping factors

Clumping factors are virulence factors that are retained by *S. aureus* which can essentially result in platelet aggregation. ClfA and ClfB have been reported to participate in the binding of the organism to platelets via fibrinogen, which associates with GPIIb/IIIa integrin on the platelet surface (Fitzgerald *et al.*, 2006). Essentially, ClfA contains a 500 residues of fibrinogen-binding region which protrudes from the surface of the bacterium and partakes in the binding and activation of platelets via SD repeats (O'Brien *et al.*, 2002).

S. aureus can cause the aggregation of platelets following platelet activation. As mentioned previously, the initial interaction of the organism with platelets causes a conformational change and an increase in the expression of GPIIb/IIIa integrins to its active form, which subsequently readily attaches to fibrinogen and fibronectin (Calvete, 1999; Jackson *et al.*, 2003). One end of the γ chain on the bivalent fibrinogen binds to ClfA while the other end interacts with the platelet integrin (Farrell *et al.*, 1992; Miajlovic *et al.*, 2007). Upon bacteria-mediated binding of fibrinogen/ fibronectin to the platelet integrin via a fibrinogen bridge, platelet activation and aggregation occurs as nearby platelets interact with each other via bound fibrinogen (Moreillon and Que, 2004). This leads to outside-in signalling of integrin α IIb β 3 which activates and stimulates a myriad of intracellular signalling pathways through the activation of molecules such as: transmembrane proteins; adaptor molecules which in turn recruits kindlin which couple with the β 3 tail of the integrin and leads to actin cytoskeletal changes via ILK/PINCH/Parvin complex; kinases such as FAKs which recruit p130Cas and Crk which leads to the activation of Rac; phosphates such as PI3K which is then hydrolysed into PIP3 and results in integrin activation; and Rho GTPases i.e. p190Rho which shuts down RhoA and promotes platelet spreading to occur.

The use of artificial molecules which occupy the necessary site of ClfA on fibrinogen was shown to block aggregation entirely, thus suggesting the dominance of ClfA in spite of the large array of other elements present in the vasculature (Hamzeh-Cognasse *et al.*, 2015). Other studies have also reported an increase in *S. aureus* adherence to platelets in a manner which increased in the presence of fibrinogen, thus confirming that ClfA requires fibrinogen molecules to induce adherence to platelets (Herrmann *et al.*, 1993; Loughman *et al.*, 2005).

Bacteria mediated platelet aggregation is usually preceded by a 'lag phase'. Lag phase relates to the time required for bacteria-mediated platelet binding and the stimulation of activation signals. Thus, variations in lag times may perhaps relate to the affinity of adhesion elements on the surface of the bacterial cell for receptors on the surface of platelets (O'Brien *et al.*, 2002). The lag phase is considerably shortened in organisms expressing ClfA and FnBPA and since *S. aureus* expresses both molecules, the lag phase for this organism was found to be between 1 and 3 minutes (Loughman *et al.*, 2005; Kerrigan *et al.*, 2007).

Iron-regulated surface determinant proteins

S. aureus has limited iron supply *in vivo* and so some strains of *S. aureus* express iron-regulated surface determinant (Isd) proteins which generally aid the capture and internalisation of a haem group from flowing haemoglobin (Torres *et al.*, 2006). IsdA, IsdB and IsdH are examples of proteins that are expressed by *S. aureus* which also play a role in promoting the adhesion of the bacterium to platelets as well as contributing in the evasion of phagocytosis (Kerrigan *et al.*, 2007; Zapotoczna *et al.*, 2013). Studies utilising mutated strains of *S. aureus* lacking specific surface Isds found IsdB to be the key player in directly interacting with GPIIb/IIIa and mediating platelet adhesion (Miajlovic *et al.*, 2010). It was also found for IsdB to partake in signalling leading to the induction of platelet aggregation (Miajlovic *et al.*, 2007).

Staphylokinase

Staphylokinase is a plasminogen activator protein produced in various *S. aureus* strains which contributes to the virulence of the microorganism (Chen *et al.*, 2007). This enzyme

binds to fibrin indirectly via fibrin binding of plasmin(ogen). This then results in the degradation of plasmin and fibrinogen, thereby inhibiting platelet aggregation mechanisms (Suehiro *et al.*, 1993).

Prothrombin activating molecules

Another typical factor that contributes to *S. aureus* virulence is that it contains prothrombin activating molecules. *S. aureus* stores and secretes staphylocoagulase and vWF-binding protein, which result in the formation of staphylothrombin upon interacting with human prothrombin (Miale, 1949). Although the complete mechanism of the effects of staphylothrombin on platelets is not fully elucidated, some studies have shown this enzymatic complex to interfere in the conversion of fibrinogen to fibrin and by doing so, the complex facilitated the induction and stabilisation of bacteria-mediated platelet aggregation (Hamzeh-Cognasse *et al.*, 2015).

Alpha-toxins

In addition to the interaction between various platelet receptors and *S. aureus* membrane elements, a number of studies have shown evidence for the involvement of *S. aureus* toxins in modulating platelet function. Alpha-toxins produced by *S. aureus* have been extensively investigated and found to induce the formation of microbicidal proteins upon interactions with the platelet membrane. Studies have also shown the potential of this toxin to cause aggregation of platelets in a dose-dependent manner. It has also been found that platelet-neutrophil complexes via CD62P are formed as a result of these exotoxins and an accumulation of such aggregates leads to diseases such as *S. aureus* haemorrhagic pneumonia.

Lipoteichoic acid

Lipoteichoic acid (LPA) produced by *S. aureus* has been previously shown to inhibit platelet activation and thus prevent the formation of a stable thrombus, although the precise mechanisms are yet to be clarified (Sheu *et al.*, 2000). Nevertheless, some studies have provided insight into the potential molecular pathways of LPA-mediated platelet inhibition. Waller *et al.*, (2013) demonstrated LPA to interact with the platelet activating factor

receptor and thereby result in an increase in intracellular cAMP concentration, and this increase in cAMP was proposed to stimulate VASP, which in turn inhibits platelet aggregation and the generation of a thrombus.

Extracellular Fibrinogen-binding protein

S. aureus organisms are also capable of producing extracellular fibrinogen-binding protein (Efb) and these molecules have been shown to inhibit platelet activation (Shannon and Flock, 2004). It has been highlighted by Posner and co-workers (2016) for Efb to bind to P-selectin receptors on activated platelets and thus inhibit the ability of the platelet receptor to bind to its natural ligand, P-selectin glycoprotein ligand-1 (PSGL-1). The interaction of PSGL-1 and P-selectin receptors in platelets has in turn been shown to be critical for the interaction of platelets with leukocytes (Posner *et al.*, 2016). Inevitably, Efb prevents the formation of platelet-leukocyte complexes and thus hinders platelet functions.

Enterotoxin B

Toxins that hinder the haemostatic role of platelets are also produced by certain *S. aureus* strains. Staphylococcal enterotoxin B is an example of a toxin that results in the overactivation of platelet components i.e. PKC, which is a key enzyme involved in generating the appropriate platelet aggregation response to thrombin (Tran *et al.*, 2006). This was further supported by Page and Pretorius, (2020) who also argued that *Staphylococcus aureus* enterotoxin B to inhibit platelet activation and aggregation.

1.8.3 Platelet-bacteria: focus on *E. coli*

E. coli is a widely researched Gram-negative, facultative anaerobic bacterium which is a common commensal of the gastrointestinal tract (Moriarty *et al.*, 2016). However, pathogenic strains of the bacterium do exist which can lead to both intestinal and extraintestinal infections (Croxen and Finlay, 2010). Examples of pathogenic *E. coli* include enterohemorrhagic *E. coli* (EPEC) and uropathogenic *E. coli* (UPEC) which can lead to a range of diseases including haemolytic uremic syndrome, sepsis, peritonitis and urinary tract infections (UTIs) (Kudinha, 2017; Mora-Rillo *et al.*, 2015). Such pathogenic strains of

E. coli have a specialised set of virulence factors which enable the microorganism to establish itself within the host's environment and aid the progression of disease.

Platelets being highly abundant in the circulation, has the potential to interact with UPEC organisms as UPEC organisms have the capacity to enter the bloodstream where they are able to interact primarily with the Fcy-receptor on the surface of platelets, thus induce platelet activation and platelet dysfunction (Moriarty *et al.*, 2016). As mentioned previously in this thesis, the interaction of UPEC with platelets can occur via direct or indirect mechanisms in similar ways to that depicted in Figure 1.16.

1.8.3.1 *E. coli* virulence factors

Similar to *S. aureus*, strains of *E. coli* possess a variety of distinct virulence factors i.e. adhesins to allow interactions with host cells, toxins, acquisition systems for capturing iron, polysaccharide coats and invasins (Figure 1.18) (Sannes *et al.*, 2004). *E. coli* virulence factors related to platelets are briefly outlined below.

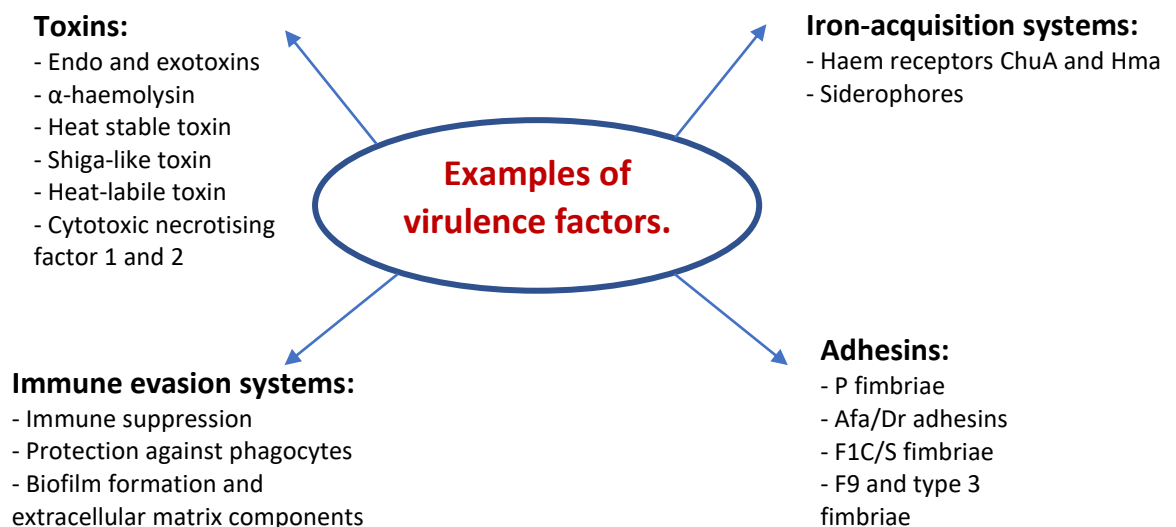


Figure 1.18 Examples of specialised virulence factors of different *E. coli* pathotypes. The above examples were gathered from the following references: (Maslow *et al.*, 1993; Demir and Kaleli, 2004; Mainil, 2013; Wurpel *et al.*, 2014; Van Avondt *et al.*, 2015; Sarowska *et al.*, 2019).

In comparison to platelet activation and modification to platelet activity induced by Gram-positive bacteria, far less has been characterised for Gram-negative bacteria. Nevertheless, a few studies have reported certain strains of *E. coli* to possess a distinct set of virulence factors which can interact with platelets and thus hinder its function. A brief overview on some of these virulence factors and how they affect normal functioning of platelets is outlined below, although for the majority of factors, the precise mechanism of action in platelets is not fully elucidated.

Lipopolysaccharide

Most Gram-negative bacteria contain an outer membrane rich in lipopolysaccharide (LPS) which provides the bacterial cell with structural integrity. A number of studies have shown LPS of certain *E. coli* strains to interact with platelets and subsequently induce platelet activation and aggregation. A study by Zhang *et al.*, (2009) demonstrated platelets to express the required receptor elements to aid interactions with LPS i.e. TLR-4, MD2, MyD88 and CD14. They demonstrated inhibition of LPS-mediated platelet activation upon use of an anti-TLR4 blocking antibody and TLR knockout studies, thus reinforcing that the TLR4 pathway is critical in platelet activation mediated by LPS. In addition to this Zhang *et al.*, (2009) also demonstrated LPS to trigger secretion of platelet granular content, mainly ATP and P-selectin from the α and dense granules hence enhancing the activation of platelets. This was further supported by Ståhl *et al.*, (2006) who also found LPS-mediated platelet activation to occur via the TLR4 pathway by using TLR4 knockout and wildtype mice models. Data from Lenehan *et al.*, (2016) was also in agreement with the above researchers in that they too found a direct link between platelet receptor (TLR4) and the binding of *E. coli* LPS.

In addition to the above, studies have also reported LPS to induce the aggregation of platelets in a Fc γ RIIa- and IgG-dependent manner. Moriarty *et al.*, (2016) revealed *E. coli* to induce platelet aggregation in an all-or-nothing manner, similar to that commonly observed in Gram-positive bacteria. This was further supported by Watson *et al.*, (2016) who observed a critical role of Fc γ RIIa and tyrosine kinases in α IIb β 3-mediated activation of platelets by certain *E. coli* isolates.

Toxins

In addition to LPS, another prominent example of virulence in *E. coli* is the production and secretion of toxins. Some *E. coli* strains have the capacity to produce Shiga toxins which contribute considerably to the virulence of the microorganism and can lead to haemolytic-uremic syndrome (HUS) (Mayer *et al.*, 2012). HUS is characterised by acute renal failure, thrombocytopenia and microangiopathic haemolytic anaemia. It has been discovered from elaborate high-performance thin-layer chromatography studies for this toxin to bind to platelets via globotriaosylceramide receptor as well as a platelet glycolipid termed 0.03 band (Cooling *et al.*, 1998). Additionally, studies have demonstrated internalisation of toxins by platelets, leading to platelet aggregation and in some cases, enhanced binding of platelets to matrixes (Karpman *et al.*, 2001). However, the effect of Shiga toxins in altering platelet function is controversial since some studies have reported Shiga toxins to have no effect in inducing platelet aggregation or secretion of platelet granular content (Yoshimura *et al.*, 1998; Thorpe *et al.*, 1999).

Another example of a toxin which enhances the virulence of certain strains of *E. coli* is α -hemolysin (Deppermann and Kubes, 2016). This toxin has been reported to have the ability to result in degradation of BclxL proteins in platelets (a key regulatory protein for platelet survival) by altering the membrane potential of the platelet mitochondria, thus ultimately leading to the induction of apoptosis (Kraemer *et al.*, 2012).

Additionally, a rising body of evidence has demonstrated a new category of toxin to target the cytoskeletal elements of host cell thus altering its function. These toxins are known as cytotoxic necrotizing factors (CNFs). *E. coli* has been found to have the capacity to produce three forms of CNFs which target Rho GTPases; CNF1, 2 and 3 (Knust and Schmidt, 2010). In this thesis we focus on CNF1 and so the molecular and cellular mechanisms of CNF1 is discussed in greater detail in the subsequent sections.

1.8.3.2 The cytotoxic necrotising factor

CNF1 is produced by certain pathogenic strains of *E. coli*, predominately UPEC (Fabbri *et al.*, 2010). CNF1 is a 110 kDa single-chain AB toxin that targets and modifies the Rho-GTPases proteins resulting in changes to cytoskeletal structures of cells (Knust *et al.*, 2009). The modular structured toxin contains three distinct domains: a N-domain (contains the binding domain of the toxin), middle domain also known as translocation domain (contains hydrophobic structures) and a terminal C-domain (harbours the enzymatic activity of the toxin) (Figure 1.19) (Lemichez *et al.*, 1997).

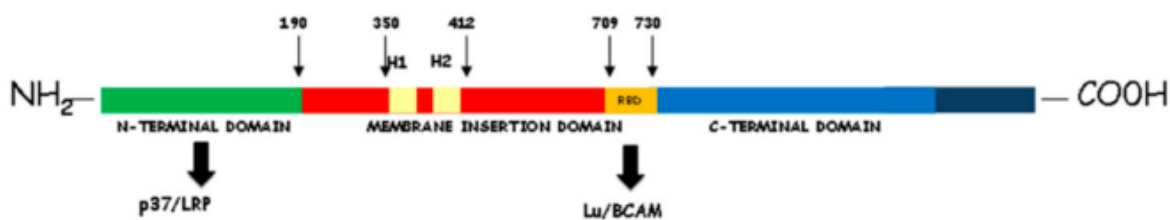


Figure 1.19 Molecular structure of CNF1. Numbers above the schematic image represents amino acid residues. Black arrows indicate the cell-binding domain and receptors.

The toxin was first described by Caprioli *et al.*, (1983) who found it to be dermonecrotic when injected into the skin of rabbits. It has since been reported to cause various modifications to cellular activity including the multinucleation of HeLa cells via inhibition of cytokinesis, decreased stimulation of electrical resistance in Caco 2 cells leading to enhanced cellular permeability, loss of CR3 phagocytosis activity and increased binding of leukocytes to epithelia (Capo *et al.*, 1998; Gerhard *et al.*, 1998; Hofman *et al.*, 2000). As well as the mentioned cellular alterations, emerging body of evidence suggests the toxin to be a potential risk factor in the development of various diseases including cancer (Travaglione *et al.*, 2008). Table 1.6 summaries some of the effects reported upon intoxicating cells with CNF1.

Table 1.7 Some of the effects reported upon treating cells with CNF1

Effect	Cells	Ref
<u>Morphological changes</u>		
Formation of stress fibres	Hep-2, Vero, HEK293, HBEC-5i cells	(Lemichez <i>et al.</i> , 1997), (Messina <i>et al.</i> , 2019)
Increased lamellipodia	Monocytic cells	(Nobes and Hall, 1995)
Cell spreading	Monocytic cells, HBEC-5i	(Nobes and Hall, 1995), (Messina <i>et al.</i> , 2019)
Multinucleation of cells. Blockage of cytodieresis in proliferating cells.	Murine glioma model	(Tantillo <i>et al.</i> , 2018), (Vannini <i>et al.</i> , 2014)
Restricts the activation of RhoA via targeting host cell proteasomal machinery.	Epithelial cells	(Doye <i>et al.</i> , 2002)
Degradation of Rac	HEp-2 carcinoma cell	(Landraud <i>et al.</i> , 2004)
Cell cycle deregulation	Uroepithelial cell line T24	(Falzano <i>et al.</i> , 2006)
Induction of phagocytic behaviour.	Epithelial cells	(Falzano <i>et al.</i> , 2006), (Vannini <i>et al.</i> , 2014)
Increase in F-actin	Monocytic cells	(Nobes and Hall, 1995)
Blockage of mitosis/ cytokinesis	Human colon cancer cells	(Zhang <i>et al.</i> , 2018)
Blocking phagocytic behaviour and apoptosis	Epithelial cells	(Fiorentini <i>et al.</i> , 1997)

1.8.3.3 Cellular uptake of CNF1 toxins

The cellular uptake of CNF1 has been reported to occur via receptor-mediated endocytosis. Thus far, studies have identified two molecules to mediate the uptake of the toxin in endothelial and epithelial cells, these include Lutheran (Lu) adhesion glycoprotein/basal cell adhesion molecule (BCAM) and p37/LRP (Piteau *et al.*, 2014).

Lu/BCAM was identified recently via direct protein-protein interaction analysis and competition studies using endothelial cells and the C-domain of the toxin was found to bind to the receptor (Piteau *et al.*, 2014). Comparatively less known about the mechanisms involved for the latter, although it has been proposed that the N-terminal domain of the toxin to bind to p67 (Fiorentini *et al.*, 1995).

CNF1 in the first instance has been found to bind receptors on the target cells' surface with high affinity. Following CNF1 binding to its receptor, the multidomain toxin is endocytosed and trafficked into early endosomes (Contamin *et al.*, 2000). This is followed by the acidification of this early endosomal compartment through an influx of H⁺. Acidic milieu results in a conformational change on a small region of the toxin such that hydrophobic residues within the middle domain of the toxin becomes exposed. The toxin then via an acid-dependent membrane translocation mechanism, inserts its catalytic activity domain into the cytosol (Contamin *et al.*, 2000). The catalytic domain is then cleaved from the rest of the protein by serine proteases. The released catalytically active C-terminus results in the deamidation of Rho proteins at Gln63/61 thus triggers Rho GTP-binding proteins by blocking GAP-mediated GTP hydrolysis. The uptake of CNF1 into target cells is summarised in Figure 1.20.

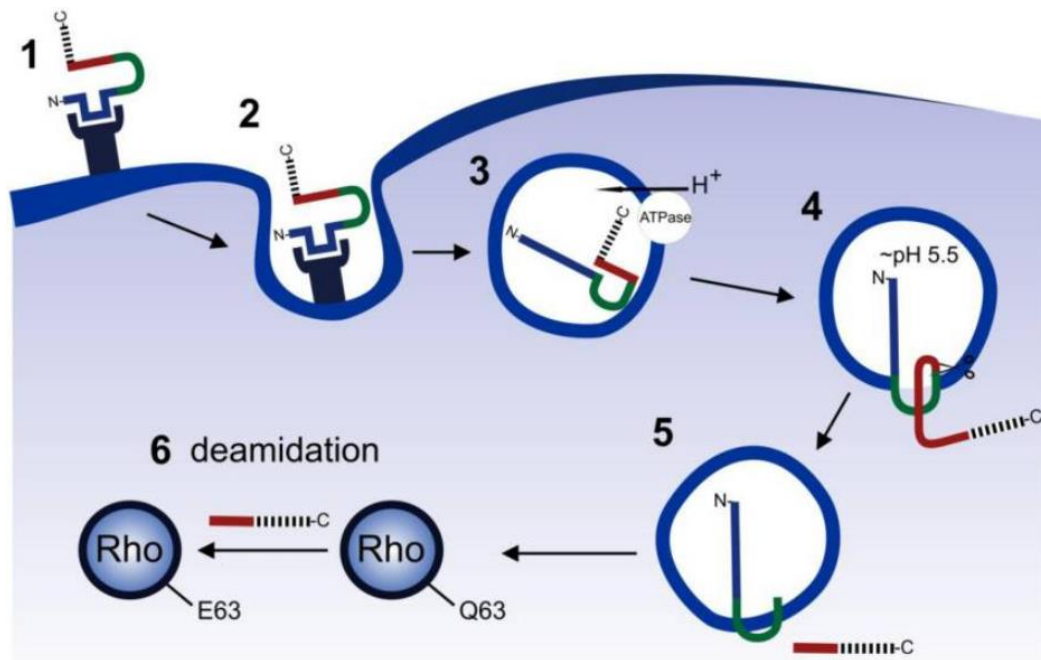


Figure 1.20 Cellular uptake and processing of CNF1 by target cells. 1) CNF1 binds to laminin receptors (Lu/BCAM, p67) on the plasma membrane of the target cells. 2) Receptor mediated endocytosis occurs, and the toxin is enclosed into early endosome vesicles. 3) Influx of H^+ results in acidification of these early endosomes. 4) The acidic environment stimulates a conformational change in CNF1 that subsequently results in the insertion of the translocation domain into the vesicular membrane. 5) A serine protease cleaves the toxin at specific junctions causing the release of the catalytically active C-terminus from the rest of the protein. 6) The catalytic domain of the toxin catalyses the deamidation of Rho proteins at Gln63/61 which in turn results in the permanent activation of Rho proteins (Knust and Schmidt, 2010).

1.8.3.4 Molecular mechanisms of CNF1 toxins

CNF1 induces remodelling of the actin cytoskeleton by constitutively activating Rho GTPases (Lerm *et al.*, 1999). More specifically CNF1 catalyses the deamidation of glutamine residues in Rho at position 63 (or the equivalent glutamine 61 in Rac and Cdc42) into glutamic acid (Figure 1.21) (Flatau *et al.*, 1997; Lemichez *et al.*, 1997). It has been found for CNF1 residues Cys-866 and His-881 to be necessary for the deamidase activity (Meysick *et al.*, 2001).

Glutamine 63 in Rho (or 61 in Rac and Cdc42) is an important modulator of the GTP-GDP cycle, it specifically regulates GAP-stimulated GTPase activity (Boquet, 2001a). Therefore, modification by the toxin means the Rho proteins are locked permanently in the GTP-bound active state since GTP hydrolysis step is prevented (Figure 1.21). This constant

activation of Rho GTPases due to CNF1-intoxicantion has been reported to result in continuous effector activation, leading to characteristic morphological modifications in numerous cells (Fabbri *et al.*, 2010). The most prominent associated effects of CNF1 on mammalian cells includes the formations of actin structures namely lamellipodia and filopodia along with stress fibres (Knust and Schmidt, 2010). Though the molecular mechanism of CNF1 in endothelial and epithelial cells has been studied to some extent, no studies have investigated the effects of CNF1 in platelets.

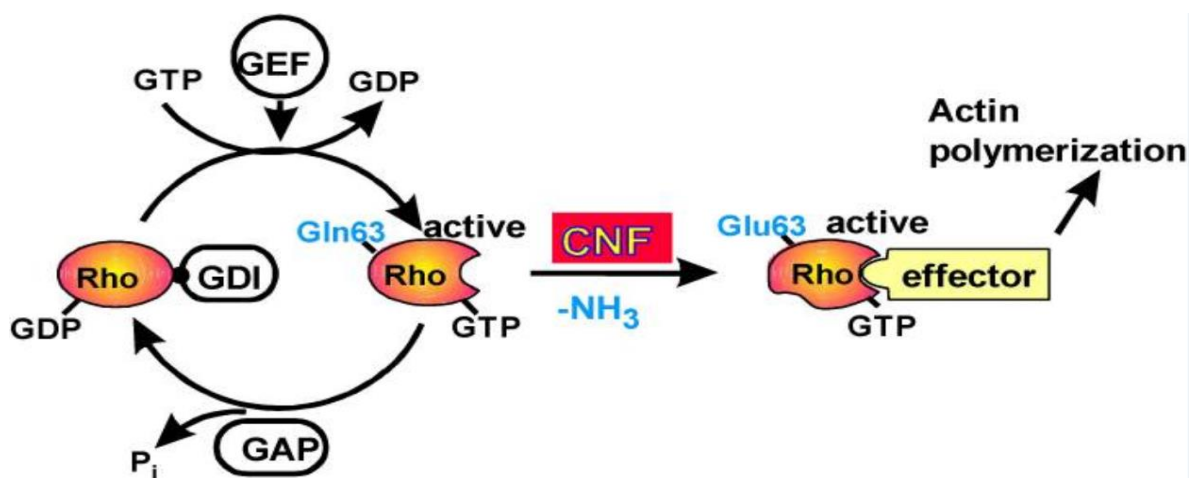


Figure 1.21 CNF1-mediated activation of Rho GTPases (Knust and Schmidt, 2010).

1.9 Aims of the study

Although primarily known for its role in haemostasis, a growing body of evidence places platelets as critical partakers in immune responses and inflammation, since platelets have been reported to rapidly detect, interact with, and aid the elimination of microbial pathogens. In addition to this, they have been found to act as mediators recruiting other immune cells such as neutrophils to the site of infection to allow the rapid removal of pathogens via neutrophil extracellular traps (NET) activity. Despite this, our understanding of platelet-bacteria interactions on a molecular level is rudimentary. It is however believed for platelets to carry out their immune role by mainly utilising their various cell surface receptors as well as through secreting a myriad of bioactive proteins enclosed within their granules (Tomaiuolo *et al.*, 2017). Though, the signalling involved in facilitating immunologic functions of platelets such as scavenging and migration remains elusive.

The generation of specific pharmacological blocking agents and the availability of transgenic mouse strains as experimental tools has paved the way for the discovery of novel pathways, mechanisms and compounds that modify platelet functions. As a result, it has enabled us to gain an in-depth understanding into key regulators of the thrombotic and haemorrhagic propensity of platelets in health and under various disease states.

Therefore, an obvious method to explore the interaction and signalling involved in the field of platelet-bacterial interconnections is through the use of pharmacological agents that inhibit platelet surface receptors enabling us to pinpoint the structures involved in the attachment and downstream regulation of platelet functions (Rivera *et al.*, 2009; Saboor *et al.*, 2013). FcγRIIIa and GPIIb/IIIa has been previously identified to facilitate the binding between platelets and bacteria and/or bacterial components (Worth *et al.*, 2006; Hamzeh-Cognasse *et al.*, 2015). However, the engagement of bacteria to these specific platelet receptors in the context of platelet migration and/or scavenging has not yet been revealed. Likewise, the intracellular signalling pathways that occur downstream of platelet-bacterial engagement and the involvement of Rho GTPases in facilitating platelet migration and scavenging properties are not clearly defined.

Equally, the effects of particular medications such as TK inhibitors used commonly in the treatment of both haematologic and solid malignancies, in modifying platelet immunologic functions remains largely uncovered.

In addition to this, numerous studies have indicated bacteria to have evolved a diverse range of virulence factors that directly target platelet functions. One such example is CNF1 which has been reported to drastically alter cellular functions in many epithelial and endothelial cell lines. Although the effects of the toxin have not been studied in platelets to our knowledge.

Therefore, to advance our knowledge in the field of platelet-bacterial interconnections, and to decipher the molecular mechanisms involved in critical platelet processes such as scavenging and migration, this study aims to do the following:

1. Adapt and optimise a method by which platelet immunologic functions such as scavenging of infectious matter and migration can be quantitatively assessed.
2. Explore the effects of inhibiting key platelet cell surface receptors in altering platelet functions.
3. Investigate the importance of Rho GTPases in facilitating platelets' immunologic roles.
4. Determine the potential effects pharmacological agents that specifically inhibit tyrosine kinase signalling pathway may have on platelet functions, in particular the ability of platelets to scavenge, migrate, adhere and aggregate.
5. Investigate whether CNF1 affects platelet functions via modulation of Rho GTPases.

Chapter 2. Materials and methods

2.1 Materials

2.1.1 Fluorescent dyes

Name	Source
Fluorescein isothiocyanate (FITC) phalloidin	Sigma-Aldrich, cat no. 27072-45-3
Tetramethylrhodamine B isothiocyanate (TRITC) phalloidin	Sigma-Aldrich, cat no. P1951-1MG
Alexa488 fibrinogen conjugate (Alexa488 FG)	Thermofisher, cat no. F13191
Hoechst 33342	Abcam, cat no. 228551

2.1.2 Primary antibodies

Antibody	Host	Dilution used for WB	Blocking agent	Source
GAPDH	Mouse monoclonal	1:6000	Milk	Sigma-Aldrich, cat no. CB1001
RhoA	Rabbit monoclonal	1:500	BSA	Cell Signalling, cat no. 2117
RAC 1/2/3	Rabbit monoclonal	1:1000	Milk	Cell Signalling, cat no. 2465
Cdc42	Rabbit monoclonal	1:1000	BSA	Cell Signalling, cat no. 2462
β - Actin	Mouse monoclonal	1:1000	BSA	Millipore, cat no. MAB1501
CNF1 (NG8)	Mouse monoclonal	1:500	BSA	Santa Cruz, cat no. 52655

2.1.3 Secondary antibodies

Antibody	Host	Dilution used for WB	Source
IR Dye 680CW anti-rabbit IgG, fluorescently labelled.	Goat	1:20,000	Li-Cor, cat no. 827-08365
IR Dye 800CW anti-rabbit IgG, fluorescently labelled.	Goat	1:20,000	Li-Cor, cat no. 926-68171
IR Dye 680RD anti-mouse IgG, fluorescently labelled.	Goat	1:15,000	Li-Cor, cat no. 827-08364
IR Dye 800CW anti-mouse IgG, fluorescently labelled.	Goat	1:15,000	Li-Cor, cat no. 926-32210

2.1.4 Bacterial species

Bacterial Species
<i>Staphylococcus aureus</i> (Newman) (Arman <i>et al.</i> , 2014).
<i>Escherichia coli</i> (RS218) (Watson <i>et al.</i> , 2016).

2.1.5 Inhibitors

Inhibitor	Final Concentration	Inhibits	Source
Casin	10 μ M	Cdc42	Tocris, cat no. 5050
Latrunculin A	20 μ M	Actin polymerisation	Tocris, cat no. 3973
IV.3 antibody	15 μ g/ml	Fc γ RIIA	Stemcell technologies, cat no. 60012
Integrilin/ eptifibatide	9 μ M	α IIb β 3	2B Scientific, cat no. BE0224-1MG
Apyrase	2 U/ml	Platelet aggregation; degrades ADP	Sigma, cat no. A6535
Indomethacin	10 μ M	TXA2 production	Sigma, cat no. I7378
Dasatinib	4 μ M	Src	Cell Guidance Systems, cat no. SM45
NSC23766	70 μ M	Rac1	Tocris, cat no. 2161
Rhosin hydrochloride	30 μ M	RhoA	Tocris, cat no. 5003
PRT-060318	10 μ M	Syk	Med Chem Express, cat no. HY-12974
Ibrutinib	5 μ M	BTK	Cayman Chemical, cat no.16274
Acalabrutinib	15 μ M	A more BTK-specific inhibitor than Ibrutinib	Cayman Chemical, cat no.19899

2.1.6 Chemicals

All reagents and laboratory materials used throughout the study were obtained from Merck/Sigma-Aldrich, unless indicated otherwise.

2.1.7 Sterilisation

Bacterial broth, buffers, cell medium and glassware were autoclaved at 120°C to ensure sterilisation and to decrease the risk of contamination. However, if autoclaving was not possible, 0.2 µm and 0.45 µm filters were used to help eliminate any impurities and contamination.

2.2 Ethics

Human

Ethical approval from Hull York Medical School was granted for all experiments that involved the use of blood from volunteers. Trained phlebotomists obtained venous blood from consenting healthy individuals who confirmed they had not taken any medication which would affect platelet activity i.e., antihistamines/aspirin within two weeks prior to the donation.

Animals

Wildtype C57BL/6 mice along with Coronin 1 deficient mice and their corresponding wildtype mice (Riley *et al.*, 2019) were kept in the appropriate animal facility of the Centre for Cardiovascular and Metabolic Research at the University of Hull, under standard conditions. All work with animals was performed in accordance with UK Home Office regulations, UK Animals (Scientific Procedures) Act of 1986, under the Home Office project licence no. PPL 60/4024.

Microbiology

All microbiology work was carried out in accordance with the protocols established for bacterial work in the laboratory under approval of the University Genetic Modification Safety Committee. Care was taken to ensure controlled use of bacteria whilst also preventing the spread/contamination of bacteria to both individuals and the workplace. All laboratory apparatus used for microbiology work and excess bacteria from experiments were washed with Virkon S disinfectant (Thermo Fisher Scientific, cat no. NC9549978).

2.3 Platelet biology methods

2.3.1 Isolation of human platelets

Blood was obtained from the antecubital vein of healthy donors via a 21-gauge butterfly needle and collected into 20 ml plastic syringes containing filtered anticoagulant at appropriate dilutions. The routinely used anticoagulants for the isolation of platelets are sodium citrate (SC) and acid citrate dextrose (ACD).

Anticoagulants are essential to prevent clotting during apheresis. Likewise, the choice of anticoagulant to use is equally critical for the isolation of platelets. It has been previously reported that whole blood drawn into a syringe containing SC would not be suited for the isolation of washed platelets (WP), as adequate levels of calcium would be present to allow thrombin activation and thus platelet activation during the high-speed centrifugation steps used to obtain WP (Hechler *et al.*, 2019). SC is the preferred anticoagulant for the preparation of platelet rich plasma (PRP), while ACD is used as the anticoagulant of choice for preparing WP from whole blood. ACD acts as a calcium chelator and so prevents activation of coagulation events (Lee and Arepally, 2012).

ACD at a ratio of 1:5 (1 ml ACD for every 4 ml of blood) was in syringes for experiments involving the isolation of WP. SC at a ratio of 1:10 (1 ml SC for every 9 ml of blood) was prepared in syringes for experiments involving the isolation of PRP. Following this, the first 2-3 ml of blood drawn was discarded to avoid artificially activated platelets.

Blood collected in the syringes was then gently mixed and carefully transferred into 15 ml conical tubes. These tubes were then centrifuged immediately in a swing-out rotor at 200xg for 15 min at room temperature (no brakes were applied). This initial centrifugation of whole blood results in the formation of three separate layers: top layer contains PRP, a thin middle buffy coat layer which mainly consists of leukocytes and a bottom layer containing erythrocytes. PRP was then collected and transferred into new 15 ml conical tubes using a Pasteur pipette. Care was taken to avoid disruption to the buffy coat layer, which would result in the contamination of PRP with red blood cells.

To obtain WP, PRP was treated with 0.3 M citric acid at a ratio of 1:50. The addition of citric acid reduces the pH of PRP, thus ensuring that platelets remain in a quiescent state during subsequent centrifugation steps. Citric acid treated PRP was then gently mixed and centrifuged at 800xg for 12 min at room temperature.

The resultant platelet poor plasma (PPP) was discarded, and the pellet of platelets was gently resuspended in 4 ml of wash buffer. The platelets were centrifuged again at 800xg for 12 min at room temperature. The supernatant was discarded, and the sediment of platelets was resuspended in 300-1000 μ l of modified Tyrode's buffer (MTB).

In some experiments, platelets were supplemented with plasma. In such cases, plasma was obtained by centrifuging whole blood for 10 min at 1700xg. Centrifugation at the higher speed results in the formation of three layers, however, unlike previously, the top layer now consists of plasma which is carefully transferred into a clean 15 ml tube.

Buffers and solutions used for the isolation of platelets:

ACD, pH 6.5

29.9 mM tri-sodium citrate

2.9 mM citric acid

72.6 mM NaCl

113.8 mM D-glucose

SC, pH 7.4

29.9 mM tri-sodium citrate

Wash buffer, pH 6.5

0.036 mM citric acid

0.01 mM EDTA

0.005 mM D-glucose

0.005 mM KCl

0.09 mM NaCl

Modified Tyrode's buffer, pH 7.4

150 mM NaCl

5 mM HEPES

0.55 mM NaH₂PO₄

7 mM NaHCO₃

2.7 mM KCl

0.5 mM MgCl₂

5.6 mM D-glucose

All buffers were filtered through a 0.22 µm filter and stored at 4°C.

2.3.2 Isolation of mouse platelets

Whole blood from mice was obtained via cardiac puncture with a 25-gauge needle into a 1 ml syringe containing ACD at a ratio of 1:5. Blood was drawn into the needle slowly to prevent the heart from collapsing. The syringe was gently inverted a few times to allow the blood to mix fully with the anticoagulant. Subsequently, blood was transferred into 2 ml eppendorf tubes and centrifuged immediately at 200xg for 10 min (zero brakes). Centrifugation results in the separation of blood components as described in section 2.2.1, and the upmost layer was carefully transferred into a new 2 ml eppendorf tube. Citric acid was subsequently added to PRP (0.3 M citric acid at a ratio of 1:50). PRP was then recentrifuged at 800xg for 10 min (room temperature). Supernatant (PPP) was discarded, and the platelet rich pellet formed from the second centrifugation step was resuspended in MTB and/or human plasma to the desired platelet concentration.

2.3.3 Platelet counting

Platelets were counted using a Beckman Coulter Z1 Particle Counter. This device measures electrical resistance of cells as they pass through a micro-channel and consequently gives an output for the number of cells present. Platelet count was determined by transferring 2.5 µl of platelet suspension into a Beckman Coulter Accuvette containing 10 ml of isotonic diluent. The electrode of the Beckman counter was then washed with isotonic buffer and the Accuvette containing isotonic buffer with platelet suspension was placed into the

chamber of the counter and the number of platelets was analysed. This step was repeated thrice, and an average platelet count was calculated. Platelets were then diluted to the desired concentration with MTB and/or plasma and incubated at 37°C for 45 min before experimentation.

2.3.4 Assessing platelet functionality via light transmission aggregometry

Light transmission aggregometry (LTA) was first described as a photometric method to test functionality of platelets quantitatively by Born, (1962). LTA is now used as the 'gold standard' method in clinical settings to investigate defects in platelet function in patients (Cattaneo, 2009). This method is essentially based upon the detection of changes in light transmission by a photometer from a light source through a platelet suspension.

The principle of this method is simple. In an unstimulated and quiescent (homogeneous) platelet suspension, platelet aggregation would not be present and so the amount of light transmitted through the turbid sample would be low since the platelet suspension would scatter the passing light from the light source. In an activated platelet sample (or upon addition of platelet agonists such as thrombin), platelet aggregation response occurs, resulting in the presence of platelet aggregates. Hence, the amount of light transmitted straight through the platelet suspension increases (dependent on the size of the aggregates which is proportional to the level of platelet activation), resulting in a higher level of light being detected by the photometer (Figure 2.1A).

Aggregation is widely considered as a late index of platelet activity. Therefore, to ensure platelets were not pre-activated and to establish the functionality/sensitivity of isolated platelets, platelet aggregation (of both PRP and WP) was determined using a Chrono-log aggregometer (model 490 4+4) prior to conducting any experiments. Throughout this study, 250 µl of platelet suspension (both human or mouse) at a concentration of 2.5×10^8 cells/ml were added to an aggregation cuvette and incubated at 37°C for 1 min under stirring conditions (1000 rpm) to allow equilibration. Aggregation was then monitored once the platelets had been stimulated with relevant agonists.

Platelets undergo an initial shape change which is followed by a biphasic stage. The primary wave is reversible whereas the secondary wave is irreversible due to the release of platelet granule content. Upon the addition of potent agonists i.e. thrombin, the distinction between the two waves will be absent (as in Figure 2.1B) since platelet stimulus-response reaction happens instantaneously, prior to aggregation (Zhou and Schmaier, 2005).

All aggregation experiments were monitored for a minimum of 5 min and aggregometers were calibrated for each sample, using 250 μ l of unstimulated platelets (0% aggregation) and either MTB (100% aggregation for WP samples) or PPP (100% aggregation for PRP samples). Aggregation was then plotted as an increase in percentage light transmission through the sample cuvette relative to the percentage light transmission through the non-stimulated platelet sample (control). In some experiments, platelets were pre-incubated with particular inhibitors for a specified amount of time prior to stimulation.

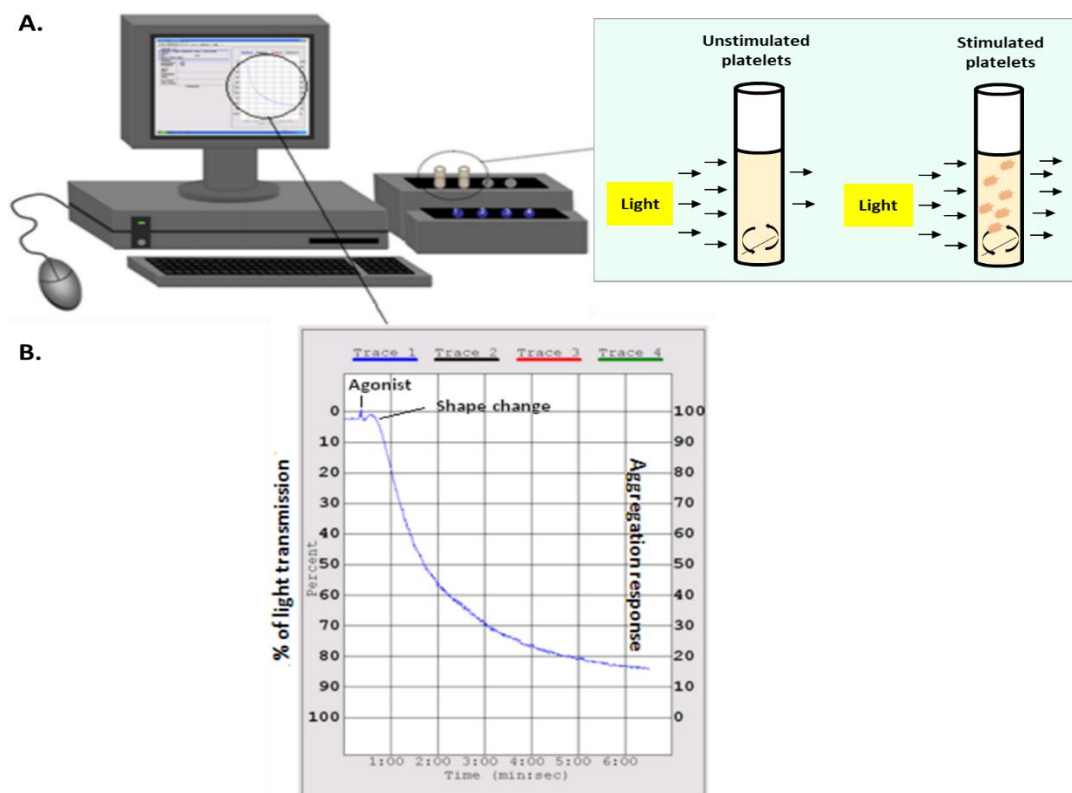


Figure 2.1 Light transmission aggregation principle. An illustration of the basic principle of platelet aggregation via LTA (A). A representative aggregation trace for washed platelets upon stimulation with 0.1 U/ml thrombin (B) (adapted from Khalil, 2018).

2.4 Microbiology and immunocytochemistry methods

The following set of methods outlined below were carried out to visualise specific structures and proteins in cells and to determine their localisation.

2.4.1 Preparation of bacteria for scavenging studies

The composition of the growth medium depends entirely upon the species and strain of bacteria i.e., *Staphylococcus aureus* Newman is cultured in BHI (brain heart infusion) broth whereas *E. coli* RS218 is cultured in LB (lysogeny broth). All bacterial broths were prepared in deionised water, autoclaved at 120°C and cooled to room temperature.

BHI broth (Fluka Analytical, 100912234):

14.8g in 400ml of distilled water (dH₂O)

LB broth:

2g of yeast extract (Sigma-Aldrich, Y1625)

4g of sodium chloride (Sigma-Aldrich, S7653)

4g of peptone

} in 400ml of dH₂O

Bacteria were inoculated from a glycerol stock into a sterile 50 ml conical tube containing 10 ml of the corresponding bacterial broth. *S. aureus* Newman was grown in BHI broth under anaerobic conditions while, *E. coli* RS218 was cultured in LB broth in aerobic conditions. Both bacteria were cultured overnight at 37°C and under shaking conditions (200 rpm) and grown to the stationary phase. The following day, the conical tubes containing bacterial culture were centrifuged at 4000 rpm for 10 min (zero brakes) at room temperature. The resultant supernatant containing the growth media was discarded, and the bacterial pellet was resuspended in 10 ml of PBS (137 mM NaCl, 10 mM phosphate, 2.7 mM KCl; pH 7.4). PBS was selected as the buffer to resuspend the bacteria, since it limits bacterial growth as it is nutritionally inert, thus allows the concentration of bacteria prepared to remain fixed. The resuspended bacterial pellet was then centrifuged again for 10 min at 4000 rpm and as aforementioned, the supernatant was discarded. Bacterial pellet was then thoroughly resuspended in 1 ml of PBS. Following this, small aliquots of the

bacterial suspension were added to a cuvette containing PBS until the desired optical density was achieved spectrophotometrically. Jenway Visible Spectrophotometer (Cole-Palmer, 632621) was used to aid this step.

2.4.2 Preparation of coverslips

Glass coverslips were placed into 24 well plates and 15% hydrochloric acid was deposited onto the coverslips for 1 h. The acid was then removed, and coverslips were submerged in dH₂O for a further 1 h. Subsequently, coverslips were air dried and 200 µl of hexamethyldisilazane (HMDS) (Sigma-Aldrich, cat no. 440191) was added to silanise the coverslips for 1 min (unless otherwise stated). HMDS was then aspirated and the coverslips were left to air dry once more. Following this, the coverslips were thoroughly washed with dH₂O and placed on glass plates coated with a layer of parafilm and placed in a humid chamber ready for immunostaining experiments. In some instances, poly-L-lysine was used to coat coverslips. In such cases, coverslips were coated with 200 µl of poly-L-lysine (1:1 ratio with dH₂O) for 15 min and washed with PBS twice.

For fibrinogen scavenging assays, glass coverslips (non-treated, acid washed and/or silanated with HMDS or poly-L-lysine treated) were coated with different concentrations of Alexa488 labelled fibrinogen (Alexa488 FG) (Thermofisher Scientific, UK), in combination with 2 mg/ml of heat inactivated fatty acid free bovine serum albumin (BSA) (Biowest, P6156-100GR) for 15 min at room temperature. However, for some CNF1 experiments, coverslips were incubated with either 10-100 µg/ml non-labelled fibrinogen (FG) (Enzyme research, Swansea, UK) in PBS or 100 µg/ml of collagen (Kollagenreagens Horm) in PBS, either at 4°C overnight or for 1 h at room temperature. The FG/collagen treated coverslips were then washed with PBS twice before blocking with 5 mg/ml of heat inactivated fatty acid free BSA for 1 h at room temperature, in order to prevent non-specific binding of platelets to the coverslips.

For all platelet scavenging-bacteria experiments, the desired concentration of bacteria was prepared from an overnight culture as described in section 2.4.1. Bacteria were then placed on glass coverslips (non-treated, acid washed and/or silanated with HMDS, and poly-

L-lysine treated) for 1-2 h at room temperature. The bacteria were then removed using an aspirator, and coverslips were washed with PBS twice to remove any additional unattached/loosely attached bacteria from the surface of the coverslips. Care was taken to not apply excessive force since this may result in detachment of bound bacteria and thus lead to uneven distribution of bacteria on the coverslip. The direction from where the liquid was aspirated was also fixed for the rinsing step (from the bottom, right corner of each coverslip) to standardise the washing method. Coverslips were then blocked with 5 mg/ml of heat inactivated, fatty acid free BSA for 1 h at room temperature.

2.4.3 Fixing and staining of cells

Pre-prepared coverslips (coated with either Alexa488 FG or bacteria, section 2.4.2) were washed twice with PBS and washed platelets and/or PRP from mice or humans (isolated and diluted to the desired concentration as described in section 2.3.1) were placed on top of the coverslips. Coverslips were then incubated for different amounts of time (0 -180 min) in a humid chamber at 37°C according to the experimental design.

At given timepoints, all relevant coverslips were washed with 200 µl of PBS to remove any unbound cells. 200 µl of 4% paraformaldehyde (PFA) in PBS was then added for 10 min at room temperature to fix the cells via crosslinking proteins. The coverslips containing fixed platelets and/or bacteria were then washed with PBS twice and 100 µl of 0.3% Triton X-100 in PBS were added for 5 min to permeabilise the cells. After the permeabilisation step, coverslips were once again washed with PBS twice and relevant fluorescent dyes and/or antibodies were added to the coverslips and incubated for the required amount of time. Excess dye which may cause interference when imaging, was removed by washing the coverslips with PBS. Coverslips were then washed again with PBS three times and once with dH₂O before mounting them onto glass coverslips (see section 2.4.5).

Preparation of 4% PFA

4g of paraformaldehyde was added to 90 ml of PBS and placed on a heat block at ~60°C, under stirring conditions until PFA dissolved completely. pH was then adjusted to 7.4 and the total volume of the solution was adjusted to 100 ml with dH₂O.

2.4.5 Mounting of coverslips

After washing, the coverslips were lifted carefully from the parafilm using a tweezer and pipette tip and excess dH₂O was removed by carefully dabbing the edge of the coverslip onto tissue paper. The coverslips were then placed (platelets side faced down) onto glass slides containing 3 µl of ProLong Diamond Antifade Mountant (GE Healthcare). Glass slides were then thoroughly labelled with necessary experimental details and stored in the dark at 4°C overnight, prior to imaging with a fluorescence microscope.

2.4.6 Microscopy and image analysis

A Zeiss Axio Observer (Zeiss, Cambridge, UK) fluorescence microscope equipped with a x40 and x63 oil immersion objective (1.4 NA) and AxioCam 506 camera was used to visualise and document all glass slides (unless otherwise stated). Zen Pro software (Carl Zeiss, Cambridge, UK), CorelDRAW 2017 (Corel) and ImageJ software (NIH, Bethesda, USA) was used to process and analyse all the images gathered. Care was taken to ensure different areas of the coverslip were imaged and in a random manner to avoid bias/false outcomes. Wherever possible, 100-200 platelets were analysed from each coverslip.

2.4.7 Determination of the area platelets migrated on Alexa488 fibrinogen

In experiments where Alexa488 FG was utilised, areas with an even fibrinogen coating were selected for imaging. Areas with scratches, exceptionally bright blotches (presumably clusters of labelled fibrinogen) or inadequate fibrinogen coating were omitted (Figure 2.2). ImageJ software was used to determine the area of Alexa488 fibrinogen scavenged by platelets. The area of each platelet and the total area cleared by the platelet (area of the platelets combined with the area of Alexa488 FG cleared by the platelet), were calculated by using the 'free hand selection' tool and the analysis tool available on the ImageJ software. An example is illustrated in Figure 2.3. Microsoft Excel was then used to determine the area of Alexa488 FG cleared by platelets by applying the following equation:

$$\frac{\text{Total area cleared by platelet}}{\text{Platelet area}} = \text{Normalised clearance}$$

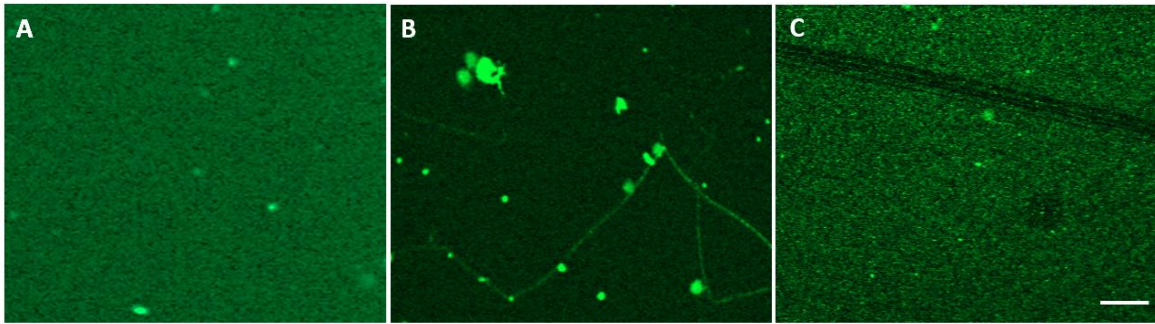


Figure 2.2 Selection of area of Alexa488 FG coating. Examples of fluorescence images where glass coverslips were coated with 40 $\mu\text{g/ml}$ of Alexa488 FG (green) for 1h, fixed with 4% PFA for 10 min, permeabilised with TritonX100 for 5 min and mounted onto coverslips using Antifade diamond. Areas of even and complete Alexa488 FG coating (A) were selected wherever possible for platelet imaging. Areas where fibrinogen formed clusters (B) and areas with scratches (C) were avoided. Images were taken on a Zeiss ApoTome.2 fluorescence microscope with a x63 oil immersion objective. Scale bar represents 5 μm .

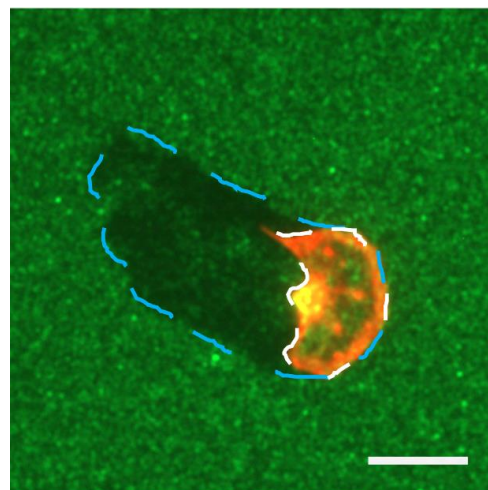


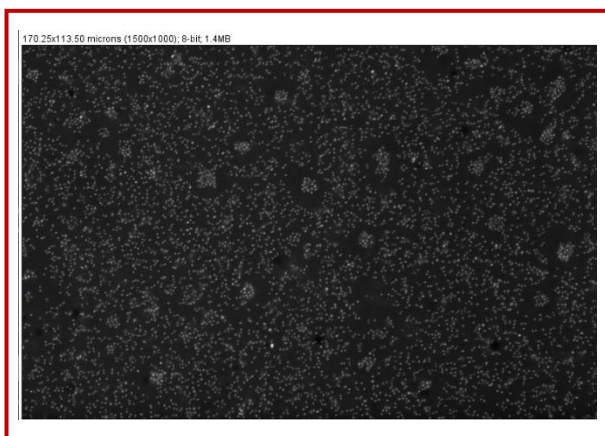
Figure 2.3 Image of a platelet scavenging Alexa488 FG and the corresponding analysis. A representative example of a human platelet spread on 40 $\mu\text{g/ml}$ of Alexa488 FG (green) for 1 h, fixed with 4% PFA for 10 min, permeabilised with TritonX100 for 5 min, stained with 1 $\mu\text{g/ml}$ TRITC phalloidin (actin, red) and mounted onto a coverslips using Antifade diamond mounting medium. Free hand tool from the ImageJ software was used to draw around the platelet (white discontinuous line) and the total area of Alexa488 FG cleared i.e.; area of Alexa488 FG cleared in combination with the area of the platelet (blue discontinuous line). Image was taken with a Zeiss ApoTome.2 fluorescence microscope at x63 magnification and zoomed. Scale bar equals 5 μm .

2.4.8 Image analysis of bacteria scavenged by platelets

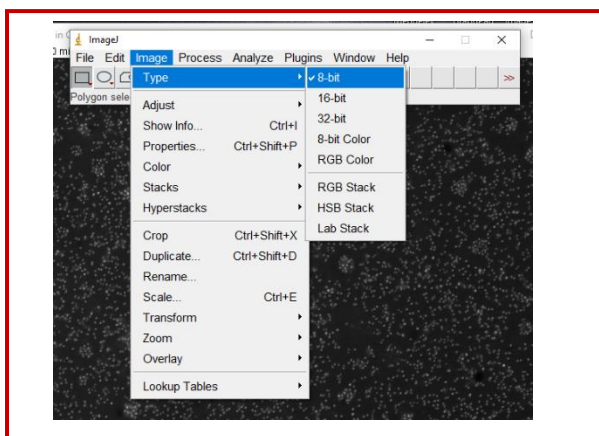
ImageJ software was used to determine the number of bacteria scavenged by platelets. Images were acquired as mentioned in section 2.4.6. The bacterial species used in this study, specifically *S. aureus* Newman, appear as grape-like structures when viewed through a microscope. Moreover, these cells when immobilised on glass coverslips typically do not stay on a single focal plane, and so could considerably affect the measurement of intensity between clusters of bacteria. Initially, Z-stack images from platelet-bacterial studies were obtained via a Zeiss ApoTome.2 fluorescence microscope equipped with 40x oil immersion objective. Z-slices were taken at 0.15 μm intervals, ensuring the stacks covers the entire sections of both the bacteria and the platelet. Following this, central Z-slices from the Z stack run were selected, deconvolved and saved as a maximum intensity projection image. An elaborate explanation of the series of steps performed to analyse the bacterial clusters from such experiments is depicted in Figure 2.4.

Images were opened with ImageJ software (step 1) as separate channels and converted into 8-bit images (step 2). The Set Scale tool on the Analyze tab was then used to remove the pre-existing scale from the image (step 3). After this, the integrated density and area were determined by applying the 'Set Measurements' application on the Analyze tab (step 4). The background intensity was then calculated (step 5) by applying the settings of step 3 and 4 on randomly selected areas within the image (using the free hand tool). The background intensity per pixel was calculated by dividing intensity by area and an average was calculated. In step 6, single individual bacteria were circled using the 'free hand' tool. In order to allow each bacterium to be circled precisely, the selected image can be zoomed prior to sketching the outline of each bacterium. To allow accurate representation of the population, a total of 300 single bacteria were circled. The above-mentioned parameters (area and integrated density) were used to calculate the average intensity of a single bacterium by subtracting the background (which is the area multiplied by the average background obtained in step 5) from the intensity. This procedure was then repeated on bacterial clusters scavenged by platelets and all the accompanying calculations were conducted on Microsoft Excel to determine the number of bacteria scavenged by each platelet (step 7).

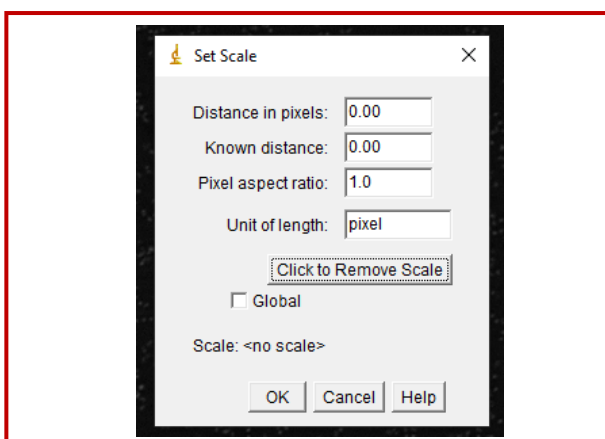
Step 1.



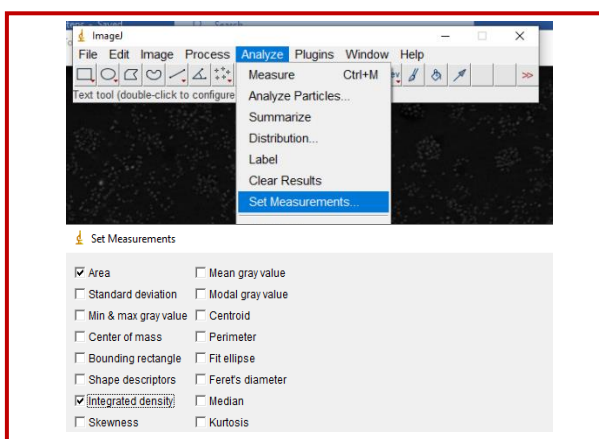
Step 2.



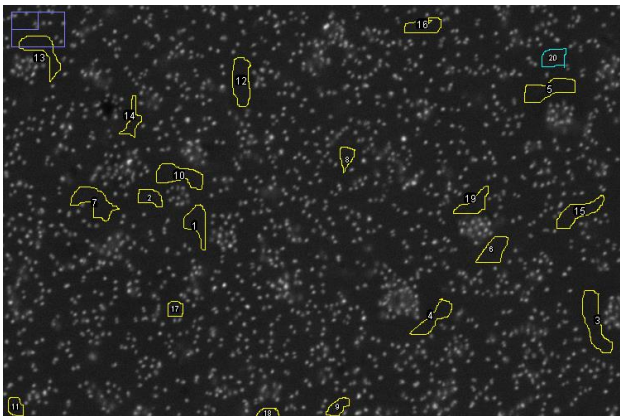
Step 3.



Step 4.

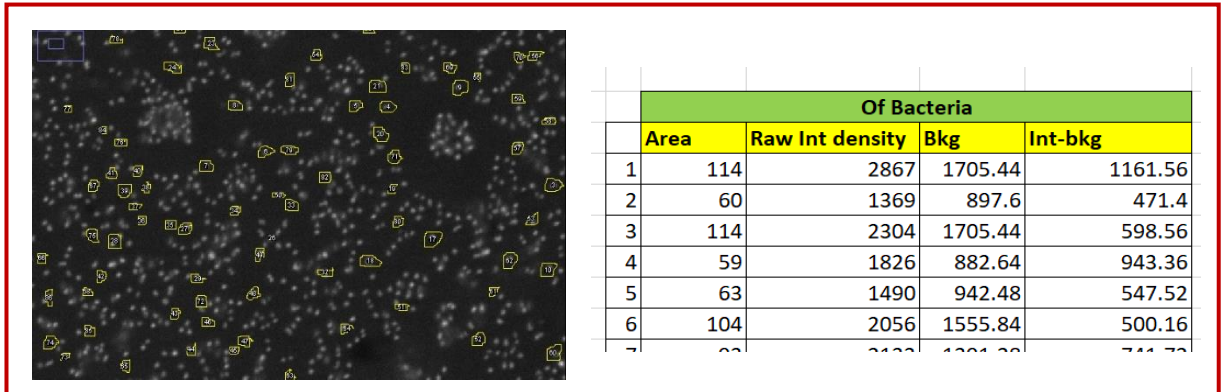


Step 5.



Of background			
	Area of background	Raw intensity of background	Dens/area
1	1992	30179	15.15
2	925	14196	15.35
3	1630	25494	15.64
4	1187	18146	15.29
5	1460	23046	15.78
6	1567	24009	15.32
7	574	8886	15.47

Step 6.



Step 7.

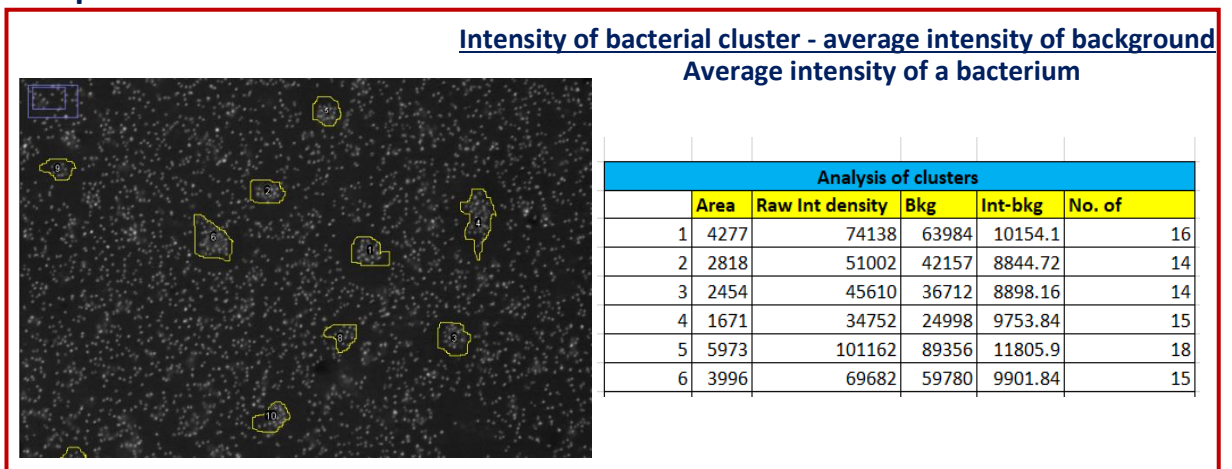


Figure 2.4 A step by step protocol used to analyse the number of bacteria scavenged by platelets. Step 1. Images displaying the bacterial channel (Hoechst 33342 which binds to bacterial DNA) were opened and processed using ImageJ software and the following steps were conducted to quantify the intensity of bacteria scavenged by platelets. Step 2. Images were converted into 8-bit image file by selecting 8-bit from the drop-down list under the tap labelled 'image'. Step 3. 'Set scale option' under the analysis tool available on the ImageJ software was then used to remove pre-existing scale from the image. Step 4. 'Set measurements' options under the analysis tab was selected to choose the different parameters to identify in each image: area and integrated density. Step 5. The 'free-hand' tool was chosen to enable the outlining of regions of different areas where there was an absence of bacteria in order to calculate background intensity. Step 6. The previous step was repeated but this time approximately 300 single bacteria were circled to determine their intensity and calculate the average intensity of a bacterium. Step 7. All areas where platelets had scavenged bacteria into clusters were carefully circled and the parameters used to determine the number of bacteria per cluster. All calculations were performed in parallel on Microsoft Excel 2017 to accompany the steps performed on the ImageJ software.

A histogram showing the distribution of the intensity of a bacterium in one experiment shown in Figure 2.5. From this graph it can be seen that the intensity of the bacteria is distributed normally and peaked within class 5 which corresponds to an average pixel intensity value between 21-25.

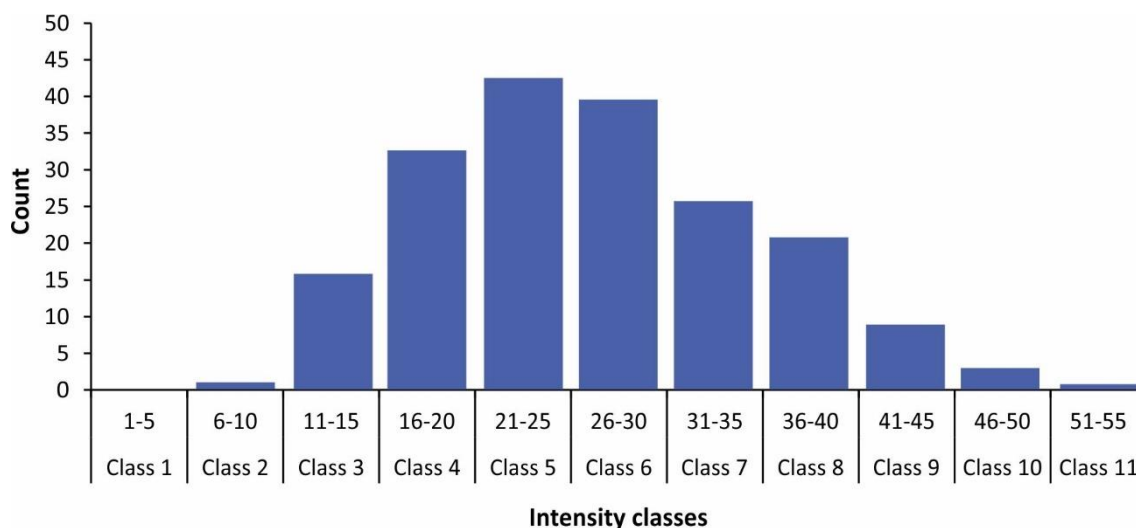


Figure 2.5 Histogram showing the pixel intensity value per bacterium. Glass coverslips were treated with poly-L-lysine for 15 min. *S. aureus* Newman bacteria were diluted to OD_(600nm) 1.0 in PBS from an overnight grown suspension culture. 200 µl of *S. aureus* bacterial suspension were then added to glass coverslips for 1 h. The coverslips were washed with PBS and bacterial cells were fixed with 4% PFA for 10 min, permeabilised with 0.3% Triton X100 for 5 min and subsequently stained with 15 µg/ml Hoechst 33342 for 15 min at room temperature. Glass coverslips were then mounted onto glass slides with ProLong Antifade Mountant. Images were obtained with a Zeiss ApoTome.2 fluorescence microscope equipped with a 40x oil immersion objective. A total of 200 bacteria were scored. Bacterial intensity was then determined as described in figure 2.4 and classed as indicated above.

In addition to the above, in order to ensure the number of bacteria scavenged by platelets determined by using the formula is reliable and matches the results obtained via manual counting, the steps detailed in Figure 2.4 were conducted on a population of small groups of bacteria (consisting of 8 to 117 individual bacteria). Care was taken to ensure only regions where one could manually distinguish each individual bacterium (within the bacterial cluster) were selected. Figure 2.6A illustrates a good correlation between the two methods of analysing the number of bacteria present in a given area ($R=0.9934$). These results confirm the formula to be accurate in determining the number of bacteria and so it

can be presumed for the formula to also be reliable in determining the number of bacteria in a cluster where it is hard to distinguish individual bacteria.

Figure 2.6B shows the intensity of the bacterial clusters to increase linearly within a broad range that includes the maximum expected in clusters collected by platelets.

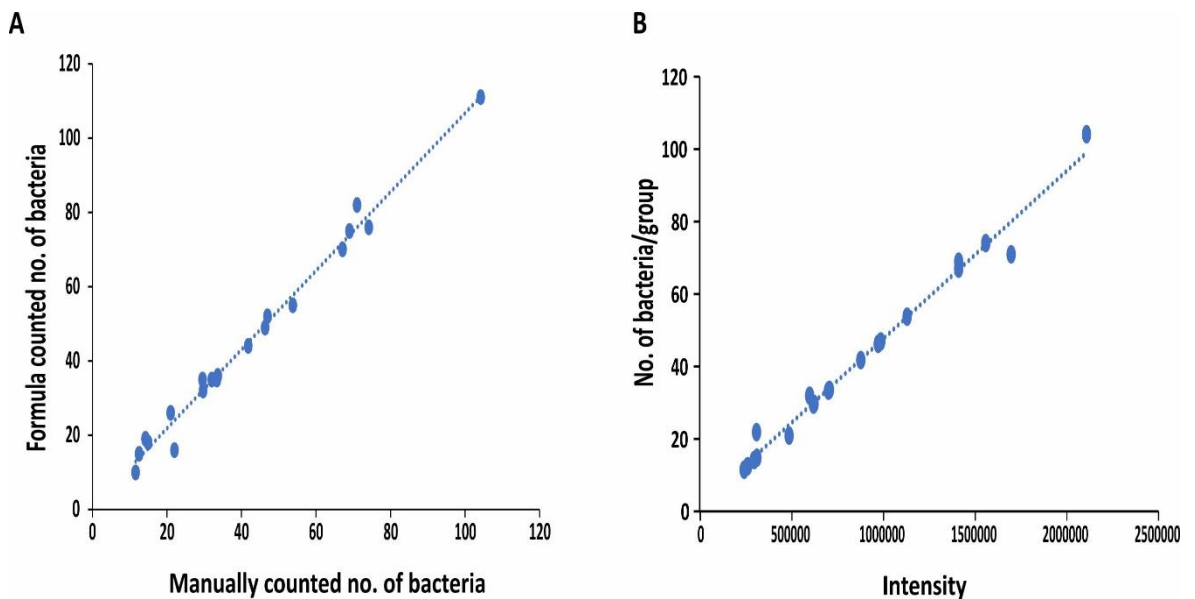


Figure 2.6 Correlation in the number of bacteria determined using the formula and manual counting. (A) The number of bacteria present in a given area was calculated via manually counting groups of bacteria on ImageJ software and via a formula on Microsoft Excel, as described in figure 2.4. $R=0.9934$. (B) The relationship between bacteria and intensity signals when counted manually is demonstrated to be linear within a broad range of bacteria.

As a proof of principle all the above-mentioned series of steps to analyse the amount of bacteria scavenged by platelets were conducted on images obtained from Z-stacks slices. However, taking adequate numbers of Z-stack sections for all the bacterial experiments conducted and the different experimental conditions within each experiment (including the duplicate coverslips etc.) was unfeasible due to time and space constraints. Therefore, to ensure accurate conclusions were drawn from platelet-bacterial experiments and that too in a time efficient and space efficient manner, the aforementioned steps were repeated however this time images were obtained from Zeiss ApoTome.2 fluorescence microscope with a 40x oil immersion objective both as a single plane or as a Z-stack (Figure 2.7A).

The results obtained from images taken via the two formats mentioned above were found to be comparable in terms of intensity of the bacterial clusters scavenged by platelets (Figure 2.7B). It was therefore decided to proceed taking images with 40x magnification (without the Z-stack function) since this method proved to be more feasible for the study of platelet-bacteria interactions in terms of platelet scavenging properties. Hence, for each experimental condition, steps 1-7 illustrated in Figure 2.4 were followed on single plane images to determine the intensity of bacteria scavenged by platelets.

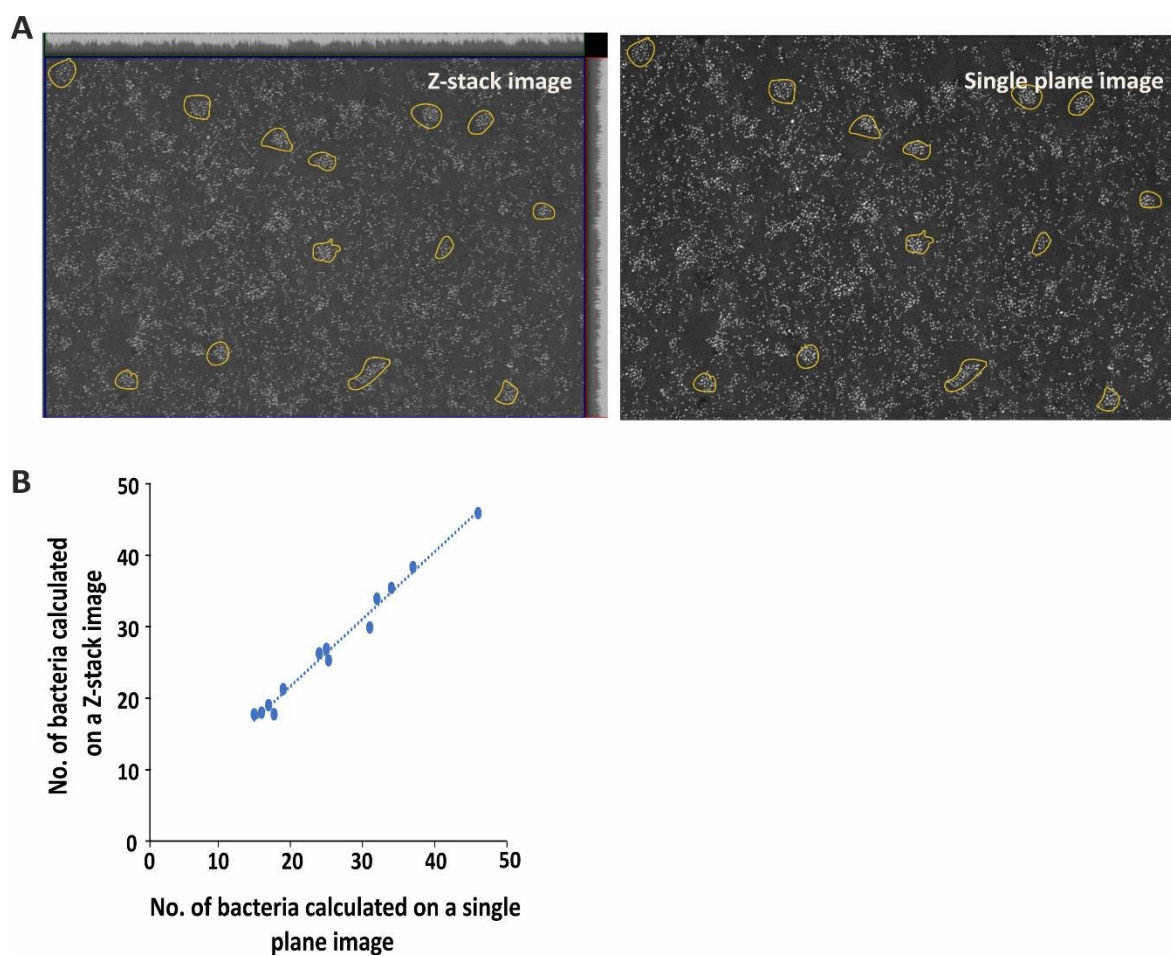


Figure 2.7 Correlation between number of bacteria in cluster between Z-stack image and single plane image. (A) Representative Z-stack (maximum projection) or single plane images obtained from Zeiss ApoTome.2 fluorescence microscope with a 40x oil immersion objective. (B) The correlation between the number of bacteria per cluster between the two types of images was calculated on Microsoft excel. $R=0.99308$.

When determining bacterial clusters scavenged by platelets, we select clusters by eye based on the high densities of bacteria within a cluster which is generally in combination with the presence of a halo devoid of bacteria surrounding a cluster. However, in order to validate whether the density of bacteria within a cluster is above the density of bacteria in a non-scavenged area, the following was conducted:

Number of bacteria in a cluster was determined as outlined in Figure 2.4, the same steps were repeated to calculate the number of bacteria in a region outside of the cluster (ensuring the area measured does not touch or include a potential halo surrounding clustered bacteria). The average densities of both scavenged bacteria in a cluster and non-scavenged bacteria were then calculated.

Figure 2.8 demonstrates a clear difference in bacteria/ μm^2 between both samples (0.53 ± 0.07 bacteria/ μm^2 in a non-cluster area vs 1.51 ± 0.09 bacteria/ μm^2 in a cluster). This observation can be used to verify quantitatively during the analysis that a given region can be considered a cluster of scavenged bacteria.

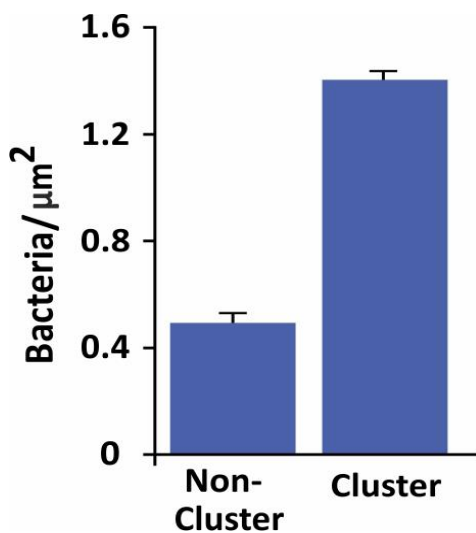


Figure 2.8 Bacterial density in scavenged clusters and non-scavenged areas. The number of bacteria present in a cluster and in an area devoid of cluster was calculated as described in figure 2.4. Bacteria/ μm^2 was calculated for 50 regions from five different coverslips of both bacteria in a cluster and in areas devoid of cluster. Data are presented as means \pm SEM.

2.5 Biochemistry methods

2.5.1 Expression and purification of His- and GST-tagged cytotoxic necrotising factor 1 proteins

2.5.1.1 Small scale expression of His- and GST-tagged proteins

In order to ensure the optimum conditions for the production of recombinant proteins, the toxin was initially produced on a small scale. Small scale expression of proteins allows us to determine the effectiveness of the expression prior to progressing onto large scale expression.

His-tagged CNF1 toxin

A small sample from *E. coli* glycerol stock (CNF1-H8) was picked using a sterile pipette tip and grown overnight at 37°C in 5 ml of LB medium (see section 2.4.1) supplemented with 50 µg/mL of kanamycin, under shaking conditions (200 RPM). The following day, small amounts from the overnight bacterial culture were transferred into a new 50 ml conical tube containing 15 ml of fresh LB medium (in the presence of kanamycin at the above-mentioned concentration) until $OD_{600} = 0.1$ was achieved. The bacterial culture was then placed in a shaker (200 RPM) at 20°C and grown until $OD_{600} = 0.8$ was reached. Upon achieving $OD_{600} = 0.8$, 1 ml of the culture sample was transferred into an eppendorf tube and cell lysates were prepared (see section 2.5.1.2). Isopropyl β- d-1-thiogalactopyranoside (IPTG) at a final concentration of 0.5 mM was supplemented to the remainder of the bacterial culture to induce protein expression. The induced bacterial culture was then incubated overnight at 15°C under shaking conditions (200 RPM).

The next day, 1 ml from the overnight grown induced bacterial sample was aliquoted into an eppendorf tube and a lysate was prepared (section 2.5.1.2). Following the production of the his-tagged recombinant proteins, the rest of the bacterial culture was centrifuged (4500xg) at 4 °C for 30 min in order to harvest the cells. The pellets obtained were washed with 5 ml of PBS and subsequently resuspended in 1 ml of cold lysis buffer supplemented with protein inhibitor cocktail (PIC) and phenylmethylsulfonyl fluoride (PMSF). The suspension was then incubated on ice for 30 min, after which the cells were lysed via

sonication (1 min cycles, 100% amplitude, 30 sec pauses in between each cycle, for a total of 5 min at 4 °C) (Ultrasonic Processor, Ultrasound Technology, UP200S).

Following the sonication procedure, the lysate was centrifuged at 13,000xg for 30 min at 4 °C, in order to separate the soluble supernatant and insoluble pellet fractions. A 25 µl sample was obtained and processed to form lysates from both the pellet and supernatant fractions, by adding equal volumes of 2x Laemmli buffer to the samples and boiling them for 5 min. Samples obtained through the series of steps mentioned above (non-induced, induced, pellet and supernatant) were resolved via SDS polyacrylamide gel electrophoresis on a 10% SDS gel as outlined in section 2.4.3.3. The gels were then evaluated via Coomassie blue staining method (section 2.5.4).

The following buffers were used at various stages during the production and purification of his-tagged CNF1 toxins. All buffers were stored at 4°C until use.

Lysis buffer (1)

50 mM phosphate buffer pH 8.0

150 mM NaCl

20 mM imidazole (Melford, B4005)

15% glycerol (added fresh)

1 mM PMSF (added fresh) (Thermofisher, 36978)

Protein inhibitor cocktail (PIC) (added fresh) (Merck, 4693116001)

Wash buffer (Same recipe as lysis buffer but 50 mM imidazole is used instead of 20 mM)

Elution buffer (500 mM imidazole)

Dialysis buffer

50 mM Tris pH 8.0

200 mM NaCl

30% glycerol

2 mM dithiothreitol

GST-tagged CNF1 toxin

The same steps conducted for the expression of His-tagged CNF1 was conducted for the expression of GST-tagged CNF1 toxin, with slight differences in the procedure i.e. 100 µg/mL of Ampicillin was supplemented to LB medium instead of Kanamycin. Also, following induction of protein expression with 0.5 mM IPTG, bacterial culture was incubated overnight at 21°C under shaking conditions (200 RPM).

The following buffers were used at various stages during the production and purification of GST-tagged CNF1 toxins. All buffers were stored at 4°C until use.

Lysis Buffer (2)

20 mM Tris-HCL, pH 7.3

10 mM NaCl

5 mM MgCl₂

Lysis Buffer (3)

Same as lysis buffer 2 with an addition of 1% Triton X-100

Lysis Buffer (4)

1% triton X

5mM DTT

1 mM PMSF (added fresh)

PIC (added fresh)

High salt buffer

50 mM Tris-HCl, pH 7.5

150 mM NaCl

5 mM MgCl₂

Elution Buffer

10 mM reduced glutathione

0.5 M Tris-HCl, pH 9.0

2.5.1.2 Lysate preparation from bacterial expression

Bacterial suspensions (500 μ l) of a known OD₆₀₀ were collected into eppendorf tubes and spun at 15,000xg for 1 min at room temperature. The supernatant obtained following the centrifugation step was discarded and the pellet was resuspended in the below outlined quantities of Laemmli buffer:

50 μ l of Laemmli buffer was added for every unit of absorbance i.e. for an OD₆₀₀ of 0.8, 40 μ l of Laemmli buffer would be used to lyse the cells pelleted following the centrifugation step described above. The lysates were then boiled at 95 °C for 5 min and stored at -20 °C.

Laemmli buffer

4% sodium dodecylsulfate (SDS)

20% glycerol

0.004% bromophenol blue

0.125M Tris-Cl, pH 6.8

10% 2-mercaptoethanol

2.5.1.3 Large scale expression of His-tagged and GST-tagged proteins

Once a standard protocol for small scale His- and GST-tagged protein production was established, CNF1 toxin was then produced on a large scale to yield more amounts of the recombinant proteins to allow comprehensive exploration of the toxin's properties.

In order to increase the quantities of soluble CNF1 produced, the protocol outlined in section 2.5.1.1 was followed but on a larger scale, i.e. bacteria were initially inoculated in 250 ml of LB medium in the presence of either kanamycin or ampicillin for His- and GST-tagged protein, respectively (see section 2.5.1.1). The following day, bacterial suspension from the overnight grown culture was added to flasks containing a total of 2 litre of LB medium + antibiotic until OD₆₀₀= 0.1 was achieved. The protocol described in section 2.5.1.1 was then essentially followed. Pellet from the centrifugation step was however resuspended in 40 ml of cold lysis buffer (1) for his-tagged protein batch or 40 ml of cold lysis buffer (4) for GST-tagged protein, and kept on ice for 30 min.

Unlike the sonication methods employed to disrupt the cells when conducting the small-scale expression of the recombinant proteins, French press technique was used to break the bacterial plasma membrane in order to isolate the proteins. To ensure efficient bacterial lysis, the French press cycle was repeated 3 to 4 times on 15 ml of bacterial suspensions. Samples were then centrifuged and as before, a sample was collected at each stage of the process (see section 2.5.1.1). Following this, the lysates were resolved via SDS polyacrylamide gel electrophoresis on a 10% gel as outlined in section 2.5.3, and then evaluated via Coomassie blue staining method (see section 2.5.4).

2.5.1.4 Purification and dialysis of CNF1

His-tagged CNF1 toxin

The supernatant obtained from the last centrifugation step described in section 2.5.1.1, was incubated for 2 h at 4°C with Ni-NTA agarose bead slurry (Qiagen, 109226119), with gentle agitation. Beads were pre-equilibrated using wash buffer (see section 2.5.1.1), through a repeated cycle of resuspending beads in wash buffer, incubating the beads on ice for 5 min, followed by centrifuging the beads for 5 min at 1000xg at 4°C and finally discarding the supernatant carefully.

After the 2 h incubation period, the beads were centrifuged at 1000xg at 4°C for 30 min and washed four times with wash buffer. Subsequently, proteins bound to the beads were eluted through a series of elution steps as described by Irie & Ohgi, (2001). The recipe for the elution buffer can be found in section 2.5.1.1. A sample of the beads was lysed in 2x Laemmli buffer and boiled for 5 min at 95°C.

Samples were then dialysed to remove any remaining imidazole. Each eluted sample was carefully pipetted into a 10 cm dialysis tubing and the ends of each tubing were secured with plastic clips. The tubes were then placed in a plastic beaker containing 1 litre of dialysis buffer (recipe as described in section 2.5.1.1) under stirring conditions at 4°C. Dialysis buffer was replaced with fresh buffer every 10 h, this was done a total of three times and the resulting protein was collected, aliquoted and stored at -20°C until further use. Again, a sample from each step (supernatant, elution 1-4, beads control, dialysed samples) was

collected, lysed (by the addition of 2x Laemmli buffer) and resolved on a 10% gel. This was then followed by analysis via Coomassie blue staining.

GST-tagged CNF1 toxin

The supernatant obtained from the last centrifugation step described in section 2.5.1.1, was incubated for 1 h at 4°C with 300 µl of glutathione Sepharose beads (Sigma-Aldrich, GE17-0756-05) with gentle rolling (9 RPM). Beads were pre-equilibrated using PBS through a repeated cycle of resuspending beads in PBS, incubating the beads on ice for 5 min, followed by centrifuging the beads for 5 min at 3000xg at 4°C and finally discarding the supernatant carefully.

Following the 1 h incubation period, the beads were centrifuged at 500xg at 4°C for 5 min. After this, the supernatant was discarded and pellet was resuspended in 1 ml of lysis buffer (4) and placed on a roller at 9 RPM for 5 min. The sample was again centrifuged at the above setting and SN discarded. Pellet obtained from this centrifugation step was resuspended in 1 ml of lysis buffer (3) and again placed on the roller for 5 min. This cycle was repeated twice more, with lysis buffer (2) and high salt buffer used to resuspend the pellet. Subsequently, proteins bound to the beads were eluted with corresponding elution buffer detailed above for GST-tagged proteins As with His-tagged proteins, a sample of the beads was lysed in 2x Laemmli buffer and boiled for 5 min at 95°C.

2.5.2 Determining protein concentration

To determine the concentration of protein in samples, a Pierce™ Bicinchoninic acid (BCA) protein assay kit (ThermoFisher scientific, cat no. 23225) was utilised. This protein concentration determination kit is based upon the principles outlined by Lowery *et al.* (1951). BCA protein kit is a colorimetric assay which quantitatively calculates the amount of protein in a sample via two stages. The first involves the reduction of Cu^{+2} into Cu^{+1} by proteins in an alkaline medium, this step is widely known as the biuret reaction and results in the formation of a light blue complex. In the second stage of the colorimetric assay, BCA reacts with the Cu^{+1} formed during the first stage of the assay, this results in the development of a concentrated purple colour. This purple-coloured reaction complex of BCA-copper is water soluble and has maximum absorbance

of light at 562 nm. Therefore, a spectrophotometer was used to detect the change in light absorption.

A standard curve was prepared with increasing concentrations of BSA (0, 25, 125, 250, 500, 750, 1000, 1500, 2000 µg/ml), diluted in the same lysis buffer as the one used to produce the protein samples. Lysis buffer at a ratio of 1:1 was then used to lyse an aliquot of protein sample and was diluted in PBS at the following ratios, 1:25, 2:25 and 5:25. Following this, 25 µl of each diluted protein sample (of unknown concentration), along with 25 µl of BSA standards were added in triplicates into the respective wells of a 96 well microplate (Nunclon). 200 µl of the BCA reagent solution was then added to each well and mixed carefully. The 96 well plate was then immediately incubated at 37°C for 30 min. Absorbance for all the samples, including the standard protein samples was measured at 562 nm with a Tecan plate reader. Absorbances obtained for the standard BSA samples were then used to plot a standard curve, and the concentrations of the protein samples were determined from the curve.

2.5.3 SDS polyacrylamide gel electrophoresis

SDS-Polyacrylamide Gel Electrophoresis (SDS-PAGE) is the most widely used analytical technique to separate specific protein of interest from a mixture of charged macromolecules. SDS-PAGE was first described by Laemmli (1970) and the principles of this method rely predominantly upon the fact that each protein molecule has a fixed molecular size and becomes charged upon the addition of SDS and β-mercaptoethanol, which under certain conditions when an electric current is applied, will move and separate from other proteins primarily based upon mass.

SDS is an ionic detergent which intercalates hydrophobic protein sites, consequently, proteins breakdown into their subunits. Samples are exposed to SDS both before and during SDS-PAGE. On the other hand, β-mercaptoethanol present in the sample buffer breaks disulfide bonds, thus disrupting the protein structure. The addition of SDS and β-mercaptoethanol to samples ultimately results in a conformational change of proteins and confers a negative charge on polypeptide subunits (Kar *et al.*, 2012). Since each protein

becomes negatively charged (meaning all proteins now have the same charge density), the electrophoretic ability of proteins depends entirely upon the molecular weight of the protein i.e., the smaller the protein, the faster it will travel through the porous polyacrylamide gel. This therefore allows the differentiation of proteins according to their molecular size. All SDS-PAGE experiments conducted in this study were in a discontinuous buffer system.

SDS-PAGE requires the denaturation of sample proteins. Therefore, platelets and other cells (both basal and samples treated with necessary compounds depending on the experimental design) were prepared to 30-50 µg/ml, lysed in 1:1 with 2x Laemmli buffer (see section 2.5.1.2) and boiled for 5 minutes at 95°C.

2.5.3.1 Polyacrylamide gel preparation

The composition of the gels varied according to the size and other properties of the protein under examination. Polyacrylamide gels consist of two components: stacking and separating gel, which differ in pH. Stacking gel is casted on top of the separating gel and this ensures that the loaded proteins are compacted into a single band prior to entering the separating gel. Table 2.1.6 details the reagents utilized to make up the different percentage gels. 1.5 mm thick glass plates and gel combs were used to cast gels.

2.1.6 Polyacrylamide gel composition for SDS-PAGE

Components	Separating gel		Stacking gel (4%)
	10 %	15%	
30% Acrylamide-Bisacrylamide (Carl Roth, Germany)	10 ml	15 ml	830 µl
1.5 M Tris HCl (pH 8.8) (Sigma, UK)	7.5 ml	7.5 ml	N/A
10% SDS (Melrose, UK)	300 µl	300 µl	50 µl
Distilled water	11.9 ml	6.9 ml	3.4 ml
10 % ammonium persulfate (APS) (Sigma, UK)	300 µl	300 µl	50 µl
TEMED (Sigma, UK)	30 µl	30 µl	10 µl
0.5 M Tris-HCl pH 6.8 (Sigma, UK)	N/A	N/A	630 µl

2.5.3.2 Performing electrophoresis

Polyacrylamide gels were placed into chambers in the MiniPROTEAN® (BioRad, UK) electrophoresis tanks, containing running buffer in both the inner and outer compartments. Protein samples were then carefully loaded into casted polyacrylamide gels alongside 4 µl of pre-stained protein ladder (with pre-determined protein sizes) (EZ-RUN Pre-stained Rec Protein Ladder, Fisher Bioreagents, cat no. BP3603-500), which allows the monitoring of protein separation during the run and provides an approximation of protein sizes. Electrophoresis was then performed at 70 V for 20 min followed by 100-120 V until the bromophenol blue dye front reached the end of the gel. These were the optimal running conditions, which provided maximum resolution of proteins used in this study. Following gel electrophoresis, Coomassie blue staining or western blotting was done to evaluate the separated proteins.

Running buffer: 25 mM Tris base, 192 mM glycine, 0.1% SDS (w/v)

2.5.4 Coomassie blue staining

Coomassie blue staining is a method by which proteins resolved on a polyacrylamide gel via electrophoresis can be visualised and analysed, since the dye binds to proteins via Van der Waals attractions. After SDS-PAGE, gels were immersed completely in Coomassie-Brilliant-Blue R250 solution (ThermoFisher Scientific, 20278), overnight at room temperature on a shaker at 10 rpm. The following day, protein bands on the gels were visualised by destaining the gel from excess dye. This was achieved through a repeated cycle of placing the gel in boiling water for 5 min and then replacing the water with room temperature water for 5 min until protein bands were visible and/or excess dye was removed. Odyssey CLx imaging device (Li-Cor, Germany) was then used to scan the destained gel.

Coomassie blue staining solution

0.1% (w/v) Coomassie-Brilliant-Blue R 250

50% (v/v) Methanol

10% (v/v) Acetic acid

2.5.5 Western blotting procedures

Western blotting is a commonly used method which allows denatured and resolved proteins from SDS polyacrylamide gels to be transferred onto a membrane (Towbin *et al.*, 1979). An identical replica of the protein bands from the gels forms onto the membrane through effective transfer methods, which then enables the detection and characterisation of a variety of proteins, in particular, proteins of low abundance which may not be detected otherwise (Kurien and Scofield, 2006). Bio-Rad Trans-blot Turbo transfer system (Bio-Rad laboratories, Hertfordshire, UK) was used to electroblot proteins from the polyacrylamide gel onto pre-cut adsorbent polyvinylidene fluoride (PVDF) membrane (Bio-Rad laboratories, Immun-Blot® PVDF Membrane, 1620255), in a semi-dry manner. To do so, a piece of PVDF membrane was soaked in 100% methanol in order to activate it (diazo groups) and equilibrated with Bio-Rad transfer buffer. Pre-cut Bio-Rad Blot filter paper (1703968) was also drenched in Bio-Rad transfer buffer and this, along with the gel and membrane were assembled in the following order: (+) filter paper, PVDF membrane, gel and filter paper (-), ensuring no air bubbles were trapped between the layers. The proteins were subsequently transferred using the Turbo-blot for 10 min at 20 V.

After the transfer, the PVDF membranes were blocked to prevent binding of antibodies non-specifically. Depending on the primary antibodies used in certain experiments, membranes were either soaked in 5% (w/v) BSA/ Tris buffered saline with Tween 20 [TBS-T (recipe outlined below)] or 5% (w/v) milk powder/TBS-T for 1h with gentle shaking. Membranes were then incubated overnight with the primary antibody at a suitable concentration. The following day, membranes were washed with TBS-T three times for 8 min each and incubated with corresponding fluorescently labelled secondary antibodies diluted to the appropriate concentration, for 1 h with gentle agitation. The membranes were once again washed with TBS-T three times for 15 min each before proteins were visualised with Odyssey CLx imaging device.

TBS-T: 150 mM, NaCl 10 mM, Tris-HCl (pH 8.0), 0.1% Tween 20

2.5.6 Stripping and reprobing PVDF membranes

Primary and secondary antibodies can be removed from a western blot membrane via a technique known as stripping, whereby an antigen binding site of an antibody becomes inactive by using a low pH buffer. This method allows a single blot to be investigated sequentially with numerous antibodies such as a loading control antibody to ensure equal amounts of protein were loaded in each well prior to SDS-PAGE. Moreover, stripping can be advantageous in that it allows: limited samples to be conserved, prevents having to perform SDS-PAGE again and saves more reagents and materials from being used.

In order to strip a membrane of the antibodies, the membrane was first re-activated with 100% methanol, if dried beforehand, otherwise the membranes were directly submerged in stripping buffer for 10 min with mild agitation. The membrane was subsequently washed three times with TBS-T for 5 min each, followed by two PBS washes (10 min each). The PVDF membrane was then blocked with either 5% BSA or 5% milk for 1 h at room temperature as outlined in section 2.5.5 and reprobbed with primary or secondary antibodies at appropriate concentrations.

Stripping buffer, pH 2.2

15g glycine

1g SDS

10 ml Tween20 (v/v)

bring volume up to 1L of dH₂O

2.5.7 Determination of actin in the Triton insoluble pellet

Platelets were isolated as described in section 2.3.1 and incubated at 37°C in the absence or presence of *E. coli* bacterial toxin (CNF1 at 1 µM) for 4 h. Following this, aliquots of each sample were transferred to eppendorf tubes, placed on a heat block set to 37°C and stimulated with 0.1 U/ml of thrombin. At given time intervals (0, 30 and 60 sec) thrombin-incubated platelets were lysed with lysis buffer and placed on ice for 15 min. The samples were then centrifuged at 15,600xg for 15 min at 4°C in order to separate the insoluble and soluble fractions (containing F-actin and G-actin respectively). The supernatant obtained

from the centrifugation step was removed and a further 200 µl of lysis buffer was added to the pellet, followed by centrifugation for 5 min at 15,600xg (washing step). As per above, the supernatant was discarded, and the pellet was then resuspended with 30 µl of Laemmli buffer (section 2.5.1.2) and lysed for 5 min at 95°C. SDS-page and western blotting was then conducted on the samples as outlined in section 2.5.3 and 2.5.5.

Lysis buffer composition:

100 mM Tris-HCl pH 7.4, 10 mM EGTA, 2% Triton X-100, and 0.1 mM PMSF and PIC (added fresh prior to use).

2.5.8 Fluorescence activated cell sorting

Fluorescence activated cell sorting (FACS) allows the rapid separation and analysis, of a group of cells into sub-groups, with the aid of fluorescently labelled antibodies which recognise certain antigens. Therefore, specific cells within a heterogenous sample such as whole blood, can be identified through staining the population with certain fluorophore-conjugated antibodies. Hence, populations of cells with distinct characteristics are detected as the sample flows past a light source, since fluorescence is emitted from bound antibodies, which in turn, is directly proportional to the total number of antigens present on/in cells.

Flow cytometers contains numerous detectors and emission filters which effectively capture fluorescence within the visible and infrared spectrum. Therefore, this allows the simultaneous recognition of several antigens on the same cell when antibodies are coupled to fluorophores with distinct emission properties.

2.5.8.1 Sample preparation for FACS

FACS was used in this study to detect receptor levels, integrin activation and secretion in human platelets treated with CNF1 toxin. A well-established protocol by Metcalfe *et al.*, (1997) was followed, whereby blood from healthy donors was diluted, incubated with antibodies/agonists and fixed prior to analysis. For the thesis, PRP prepared with sodium

citrate in the absence or presence of CNF1 (1 μ M) was stimulated with the following at 37°C:

- Thrombin in the presence of 10 μ M Gly-Pro-Arg-Pro-NH₂ (0.1 and 0.01 U/ml)
- CRP (5 and 0.5 μ g/ml)
- ADP (10 μ M)
- U46619 (3 μ M)
- A combination of ADP (10 μ M) and U46619 (3 μ M)

Along with the above, platelets were also incubated with the following antibodies for the detection of integrin activation and secretion: FITC-conjugated CD62P-P-selectin antibody (BD Bioscience, cat no. 550866), PAC-1 (Emfret, Würzburg, Germany) and APC/Cy7-conjugated anti-CD63 (Biolegend, cat no. 353009). In order to investigate receptor expression, isolated platelets were incubated with FITC-conjugated antibodies directed against the following platelet surface receptors: GPIb (CD42b), GPVI, integrin α 2 (CD49b) (Emfret, Eibelstadt, Germany), integrin α IIb (CD41) (BD Biosciences, Oxford, UK).

Subsequent to sample incubation, platelets were fixed with PFA for 10 min and analysed using a BD LSR Fortessa™ flow cytometer (BD Bioscience) along with FlowJo software.

2.6 Statistical analysis

All data was initially expressed as average \pm either standard error of the mean (SEM) or standard deviation (SD) and analysed using both GraphPad software (La Jolla, CA, USA) and Microsoft Excel 2017. Paired and unpaired Student's t-test or analysis of variance (ANOVA) in conjunction with Bonferroni post-hoc test was conducted on the SEM/SD values to test for statistical differences between groups. Results where P value was <0.05 were considered statistically significant.

Chapter 3. Characterisation of platelet's ability to scavenge bacteria.

3.1 Introduction

The central role of platelets as cells participating in haemostasis to minimise blood loss upon endothelial damage has been widely acknowledged. However, platelets are in circulation at extremely high concentrations (150,000 to 400,000 platelets per μl of blood), quantities which are far greater than the amount of platelets required for maintaining routine haemostasis (Alves and Grimalt, 2018). It has been suggested that platelet count is maintained at such high concentrations in the vasculature because in addition to the primary role of platelets in haemostasis, these cells potentially encompass an immune role in response to infection (Alves & Grimalt, 2018). Nevertheless, the emphasis of platelets' role in haemostasis has previously to an extent overshadowed the prospect of these cells to perhaps participate in host defence.

William Osler (1908) was the first person to suggest an association between infectious organisms and cardiovascular disease, although it was mainly disregarded until the 1970s. It was during the early 1970s that a number of studies were conducted by Clawson and White, where they demonstrated platelet degranulation, aggregation and thrombi formation in response to bacterial agents (Clawson and White, 1971, 1980; Clawson *et al.*, 1975). Following this, several investigators have reported the involvement of platelets in host defence against infection and platelets are now considered as sentinels of the circulatory system, especially since they have been shown to express a selection of functional immunoreceptors which are essential for specific defence mechanisms (D'Atri & Schattner, 2017).

A range of methodologies have been used by researchers to investigate the possibility of platelets to behave as immune cells, although initially the ideology of platelets to contribute to innate immunity arose mainly from platelet aggregation studies (Clawson *et al.*, 1975; Clawson *et al.*, 1980; Forrester *et al.*, 1985). Since then, there has been significant advancements in the methods deployed to study the association and effect of bacteria on platelet functions, although some researchers (Arman *et al.*, 2014; Kerrigan, 2015) still

continue to conduct LTA tests to establish platelet-bacteria associations, since LTA is currently still considered 'gold standard' for testing platelet functions. Moreover, it offers the ability to examine a number of variables in a time-efficient manner to obtain a large amount of data regarding various aspects of platelet biochemistry. Some researchers have however used a number of different methods and some have even developed novel techniques to demonstrate platelet-bacteria interactions i.e. a study conducted by Pawar *et al.*, (2004) reported platelet activation and modifications to platelet-bacteria interactions by creating a fluid-mechanical environment typical of the vasculature, whereas Shannon (2017) employed flow cytometry techniques to show platelet integrin activation and granule release in response to different pathogenic bacteria.

Microscopy techniques have also been used extensively throughout literature as a critical tool allowing in-depth analysis of biological processes and platelet structures on a cellular level as well as to offer insight into novel platelet mechanisms. Fluorescence microscopy in particular has allowed the investigation and discovery of various cellular features and discrete platelet processes in response to bacteria, for example a study conducted by Riaz *et al.*, (2012) employed microscopy techniques to demonstrate the capacity of platelets to partake in host defence response by binding to and killing *E. coli*. Whereas, micropatterned arrays of immobilised bacteria and the use of platelet-bacteria co-culture techniques were used by Palankar *et al.*, (2018) to show platelet-mediated killing of pathogens. The results from these studies have enabled the reinforcement of platelets to potentially partake in host defence mechanisms against infection.

A comprehensive study conducted by Gaertner *et al.*, (2017) also utilised microscopy methods to analyse the movement of platelets on fibrin(ogen) coated matrix. They also observed platelets to have the ability to migrate and collect fibrin-bound bacteria. Thus, the outcome of the study supported the notion of platelets as cells capable of migrating, which then trap and aid the clearance of microbes. We believe this approach represents a method capable of providing systematic insight into the different platelet responses mediated by bacteria and so it was decided to incorporate technical aspects from this study in combination with simple aggregation techniques to investigate platelet-bacteria interactions in this chapter.

Platelet migration is an active process, and it has been postulated for Rho proteins to be pivotal in aiding platelet shape change to occur and thus the movement of platelets on a non-infectious matrix (Czapiga *et al.*, 2015). Therefore, in this chapter it was decided to use various cytoskeletal inhibitors to investigate the effects they have on the ability of platelets to scavenge infectious matter.

A recent review of literature on the topic of platelet-bacteria interactions revealed bacteria to encompass the capacity to interact directly and/or indirectly with a number of platelet surface receptors and for this association to be strain-specific (Kerrigan, 2015). The interaction of platelets with microorganisms is generally considered as the primary step of host defence. In this chapter we aim to clarify this interaction between bacteria and platelets by utilising compounds that inhibit platelet receptors. It has been previously shown for the Newman strain to express ClfA and ClfB as well as fibronectin-binding protein A, which in turn binds to fibrinogen and IgG (Arman *et al.*, 2014). Subsequently, resulting in the cross-linking of GP IIa/IIIb and FcγRIIA receptor (Arman & Krauel, 2015, Cox *et al.*, 2011).

Therefore, monoclonal antibody IV.3 (IV.3 ab), which has broadly been used to block FcγRIIa on platelets thus allowing the study of the receptor in the activation/inhibition of secondary mediators, was also utilised in this study. Veri *et al.*, (2007) and Arman *et al.*, (2014) have both reported an inhibition in platelet aggregation in response to bacteria upon blocking FcγRIIa with IV.3 ab. Likewise, Cox *et al.*, (2011) and Keane *et al.*, (2010) also used IV.3 antibody to determine the effects it would have in modifying platelet functions. Indeed, both studies found an absence in platelet spreading and dense granule release upon the addition of the inhibitor to platelets. These studies highlight FcγRIIa to be critical in aiding platelet-bacteria interactions.

Eptifibatide, also known as integrilin, is a relatively small molecule which has been used to inhibit GPIIb/IIIa. It has been reported for integrilin to bind to the platelet integrin α IIb β 3, thus resulting in the inhibition of platelet aggregation by averting the attachment of molecules such as fibrinogen, vWF, and other adhesive ligands (O'Shea and Tcheng, 2002).

The use of inhibitors: IV.3 ab and integrilin has aided the discovery of certain platelet functioning aspects although other factors such as the ability of platelets to scavenge for infectious matter and thereby potentially promote thrombosis has not yet been fully defined. Nor has the effect of impeding parameters such as pH and plasma concentration in the context of platelet scavenging properties on infectious matter, been evaluated previously. Therefore, it was decided to focus on these different parameters, since targeting such critical aspects along with platelet surface adhesion molecules could provide valuable knowledge into the mechanisms involved in platelet-bacterial scavenging, and thus aid the innovation of therapeutic opportunities. Also, because the effects of such interactions on the balance between infection and immunity per se are not fully elucidated.

In addition to investigating potential platelet receptors in aiding the attachment of bacteria to platelets, this chapter also explores the role of secondary mediators in modifying platelet scavenging properties, since the inhibition of secondary mediators has been previously associated with inhibition of other platelet functions such as aggregation in response to bacteria (Arman *et al.*, 2014). Indomethacin is a well-known cyclo-oxygenase (COX) inhibitor. Apyrase is another example of an enzyme that targets critical molecules involved in maintaining haemostasis. Apyrase catalyses the hydrolysis of ATP into inorganic phosphate compounds: adenosine monophosphate (Moeckel *et al.*, 2014). Essentially, apyrase inhibits the interactions between ADP and ATP at the three P2 receptors of platelets (P2X₁, P2Y₁, and P2Y₁₂), thus terminating platelet aggregation and additional recruitment of platelets (Jin *et al.*, 2002). Both apyrase and indomethacin are inhibitors of secondary mediators, ADP and TXA₂ respectively, and both are used in this chapter.

An understanding of the molecular pathways involved in platelets scavenging and the elimination of bacteria in order to prevent bacterial spreading and progression to sepsis in an individual is fundamental. However, it is equally important to appreciate the effects common therapeutic agents may have in compromising host immunity and hindering platelet activity. It has previously been observed that in leukaemia patients undergoing therapy, the likelihood of developing sepsis is considerably increased, although there is some variability in literature (Tillman *et al.*, 2018). Leukaemia patients are often prescribed

numerous therapeutic agents that have been reported to have off-target effects on platelets (Series *et al.*, 2019).

Acalabrutinib and ibrutinib are FDA approved drugs and they inhibit BTKs. The development and use of BTK inhibitors has allowed the investigation of several intracellular signalling pathways. These therapeutic agents have gained increasing interest as appealing candidates for the treatment of multiple B-cell malignancies. However, they are also examples of therapeutic agents that have been observed to have off-target effects, in that they have been found to disrupt normal platelet functioning (Tillman *et al.*, 2018; Series *et al.*, 2019). PRT318 (PRT) is another example of a therapeutic drug commonly prescribed in the treatment of CLL (Liu and Mamorska-Dyga, 2017). PRT has also been found to alter platelet functioning by specifically targeting and inhibiting the spleen tyrosine kinases (Syk), which are critical components of the B-cell receptor signalling pathway (Liu and Mamorska-Dyga, 2017). Likewise, Dasatinib, a Src-locus receptor kinase (Src) inhibitor, is often administered to leukaemia patients and has been associated with platelet dysfunction, with several investigators reporting disruption in platelet aggregation response (Kostos *et al.*, 2015; Ali *et al.*, 2015; Sahu *et al.*, 2016). It can be proposed from these studies that therapeutic drugs can influence and potentially compromise the immune role of platelets. Still, platelet-immunologic functions in relation to the ability of platelets to scavenge infectious matter upon inhibiting Src and Syk signalling pathways has not been previously reported. Moreover, the use of BTK inhibitors in the management and treatment of haematologic and solid malignancies is escalating and since they have been found to exert variable off-target effects in platelets, the need to investigate the effects of BTK inhibitors is therefore critical to understand and avoid detrimental side effects (Tullemans *et al.*, 2018).

While the investigation and accurate assessment of platelet events is critical for identifying abnormalities in platelet function in response to pathogens, it is also equally important to assess platelet function in evaluating the efficacy of antiplatelet therapies. Taking all of the above into account, in order to develop our understanding of how therapeutic agents may alter platelet-bacteria interactions on a cell biological level, it was decided to adapt and optimise the assay described by Gaertner *et al.*, (2017), with the ultimate goal of

distinguishing key signalling pathways involved in platelet-bacteria interactions. In addition to this, it was anticipated for the modified assay to aid and enhance our understanding into the ability of platelets to scavenge bacterial agents under particular conditions which may occur *in vivo*. Hence, the followings aims were devised for this chapter.

Aims of this chapter are:

- To establish and optimise an assay whereby the capacity of platelets to scavenge and clear bacteria can be determined and quantified.
- To investigate the effect of parameters such as pH and plasma concentration on the ability of platelets to scavenge bacteria.
- To characterise the effects of inhibiting various cytoskeletal elements on the capability of platelets to scavenge and aggregate in response to bacteria.
- To examine the effects of commonly prescribed therapeutic agents in altering normal platelet functions.
- To characterise the dependence of fibrinogen and/or IgG's on the ability of platelets to scavenge infectious agents.

3.2 Optimisation of bacterial coverage

The initial step to optimise an assay that can quantitatively assess the ability of platelets to scavenge bacteria was to determine the optimal conditions required for platelet-infectious agent interactions *in vitro*.

Bacteria was chosen as a model of an infectious agent and since these single celled microorganisms are mainly categorised into two groups, Gram positive and Gram negative, an example from each category was selected for developing the platelet scavenging assay. This was done to allow the identification of any effects the fundamental difference in their cell wall composition may have on the interactions with platelets (Silhavy *et al.*, 2010). *S. aureus* strain Newman was chosen as an example of a Gram-positive bacterium while *E. coli* strain RS218 was chosen from the Gram-negative category (Mai-Prochnow *et al.*, 2016).

Several variables such as treatment of coverslips, the effect of buffers, time of exposure and the concentration of bacteria can all contribute to the efficiency and accuracy of an assay which aims to study platelet-bacterial scavenging interactions. Therefore, given the importance of such factors, it was decided to systematically evaluate a number of conditions and parameters to arrive at an optimised protocol that will permit the preservation and investigation of cellular morphology of both bacteria and platelets.

3.2.1 Treatment of coverslips to determine maximal bacterial coverage

The optimisation of an assay aiming to investigate the scavenging properties of platelets on bacteria requires the immobilisation of bacteria to glass coverslips while simultaneously maintaining the biological properties of bacteria. Immobilisation techniques are critical for microscopy analysis of bacteria, this however poses a challenge due to the morphology and small size of bacterial cells (Meyer *et al.*, 2010). Hence, the initial conditions to optimise were the treatments (if any) required on the glass coverslips to firstly immobilise the bacteria with sufficient strength to avoid their detachment and secondly to ensure a maximal but even coverage of bacteria on coverslips.

Immobilisation techniques generally fall into two categories: physically confining bacteria i.e. in microwells, or the use of particular molecules to aid the firm attachment of bacteria to glass coverslips. An example of the latter is poly-L-lysine, a cationic polymer previously described to aid the attachment of bacteria to glass surfaces without any significant modification to their biological viability (Colville *et al.*, 2000).

To examine the effects of pre-treating glass coverslips with chemicals on bacterial adherence, a study was conducted whereby glass coverslips were prepared under the following conditions on the day of the experiment:

- no treatment
- acid washed with 20% HCl for 1 h followed by dH₂O wash for 1 h
- acid washed and subsequently silaned (section 2.4.2)
- treatment with poly-L-lysine for 15 min

S. aureus Newman and *E. coli* RS218 were cultured overnight (section 2.4.1) and the following day 200 µl of bacterial suspension was added to pre-treated coverslips and incubated at room temperature for 1 h. The coverslips were then washed with PBS to remove unadhered bacteria and the cells were fixed. Although methanol fixation is less harsh on cells, it does not conserve cell wall structures as effectively as PFA (Levin, 2016). Hence 4% PFA was applied to fix the bacterial cells and this was followed by permeabilisation of cells with Triton X100. Bacterial cells were then stained with 15 µg/ml of Hoechst 33342 (stains bacterial DNA), washed with PBS and coverslips mounted (section 2.4.3). Coverslips were subsequently visualised with a fluorescence microscope the following day and the percentage of bacterial coverage was measured.

Figures 3.1 and 3.2 show representative images of *S. aureus* and *E. coli*, respectively, adhering to glass coverslips subject to various treatments and the effect of these treatments on the percentage of surface coverage by the bacteria.

Figure 3.1A shows that Gram-positive bacteria had the capacity to adhere to coverslips to some extent, irrespective of whether the coverslips had been pre-treated with

immobilisation compounds. The quantification of the surface coverage (Figure 3.1B) showed that the greatest bacterial coverage was obtained when the coverslips were treated with poly-L-lysine ($24\pm 2\%$ bacterial coverage), which was 10-fold higher when compared to non-treated coverslips ($2\pm 0\%$ bacterial coverage, $P < 0.001$). It can also be noted that there is only a marginal difference in the percentage coverage of bacteria between the non-treated group and the acid-washed group ($3\pm 2\%$ bacterial coverage), implying that the harsh HCl treatment of coverslips practically has no effect in enhancing immobilisation of bacteria to coverslips.

Contrarily, a two-fold increase in bacterial coverage was observed when coverslips were acid-washed and silaned ($7\pm 1\%$) compared to coverslips treated with acid washing alone. This suggests that the addition of HMDS influences the attachment of *S. aureus* to the glass coverslips significantly ($P < 0.05$), although neither approaches provided overall sufficient bacterial coverage on coverslips as vast areas had regions devoid of bacteria. In addition to this, it is evident in Figure 3.1 that *S. aureus* appeared to form clusters rather than attach evenly throughout the coverslips when immobilised on silaned coverslips.

Overall, it can be deduced from these set of experiments that although a complete degree of coverage of *S. aureus* Newman is difficult to achieve, pre-treating coverslips with poly-L-lysine provides an even surface coverage to study the scavenging properties of platelets.

Efforts were taken to increase bacterial coverage by treating coverslips with poly-L-lysine for a longer period of time (overnight at 4°C) prior to adding the bacteria. Similarly, incubating poly-L-lysine treated coverslips with the bacteria overnight at 4°C was also attempted (Appendices, Figure 7.1). However, neither of these modifications proved to be effective in increasing the percentage coverage of bacteria compared to the conditions shown in Figure 3.1. Therefore, to allow maximal bacterial attachment to glass coverslips and to avoid any formation of clusters, all glass coverslips used to conduct scavenging experiments with *S. aureus* Newman were pre-treated with poly-L-lysine for 15 min at room temperature on the day of experimentation.

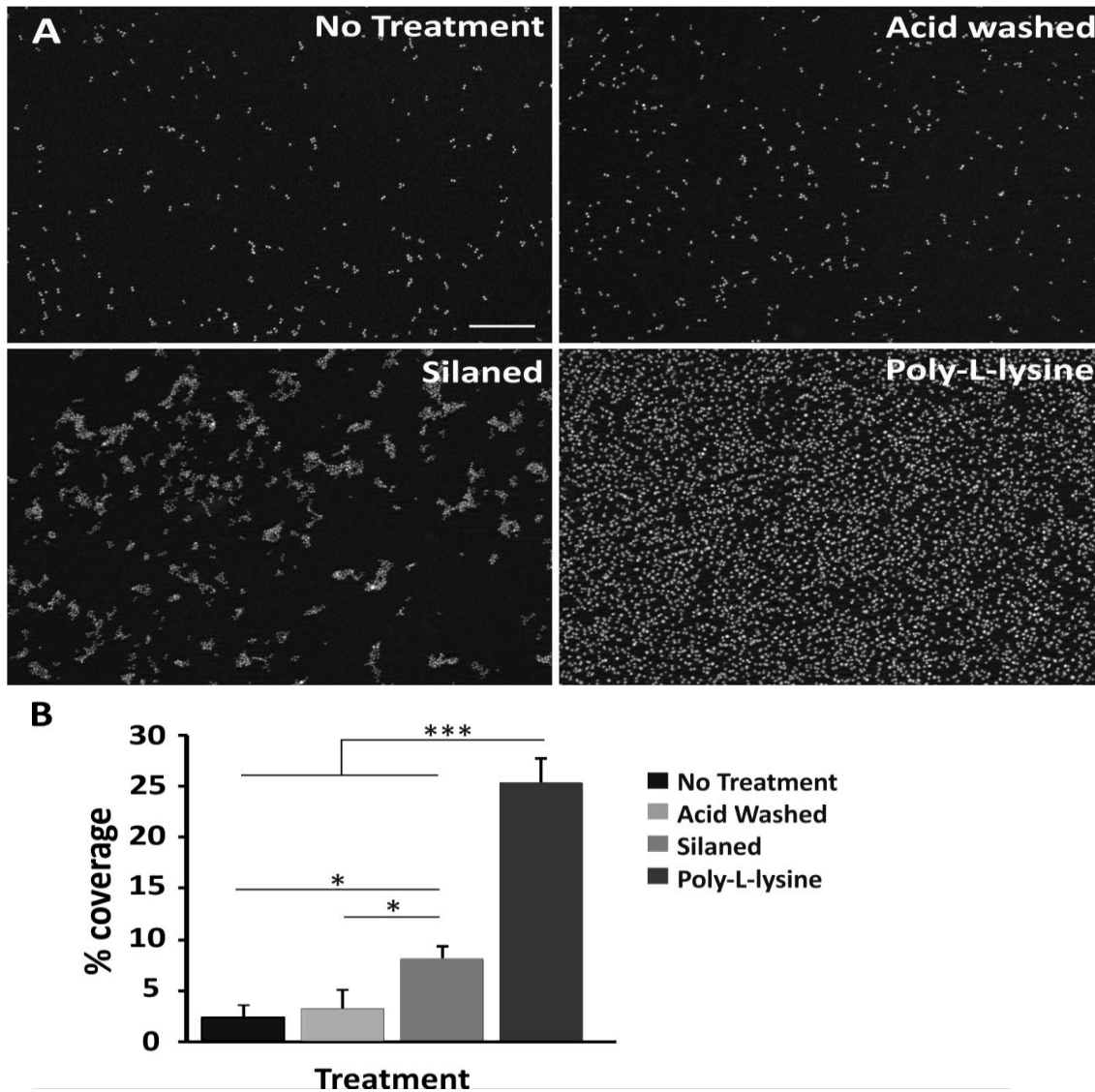


Figure 3.1 Immobilisation of *S. aureus* Newman on glass coverslips. Glass coverslips were prepared by either acid washing with HCl for 1 h followed by dH₂O for 1 h, acid washing with HCl for 1 h then dH₂O for 1 h followed by silanisation with HMDS for 1 min at room temperature or, treatment with poly-L-lysine for 15 min. *S. aureus* Newman bacteria were diluted to OD_(600nm) 1.0 in PBS from an overnight grown suspension culture. 200 µl of bacterial suspension were then added to glass coverslips for 1 h. The coverslips were washed with PBS and bacterial cells were fixed with 4% PFA for 10 min. Cells were then permeabilised with 0.3% Triton X100 for 5 min and subsequently stained with 15 µg/ml Hoechst 33342 (to visualise bacterial DNA) for 15 min at room temperature. Glass coverslips were then mounted onto glass slides with ProLong Antifade Mountant. Images were obtained with a Zeiss ApoTome.2 fluorescence microscope equipped with a 40x oil immersion objective. (A) Representative images from three independent experiments; scale bar represents 20 µm. (B) Percentage coverage of bacteria in each of the treatment conditions was calculated using ImageJ software. A total of 40 fields (image size 165.59 µm x 110.39 µm) per condition was analysed. Data are presented as means ± SEM of three independent experiments. Statistical significance was calculated using a one-way ANOVA (*p < 0.05 and ***p < 0.001).

Unlike *S. aureus* Newman, *E. coli* RS218 placed on glass coverslips did not possess the capacity to adhere effectively, irrespective of the treatment used (Figure 3.2A). No significant difference in bacterial coverage was found between the different immobilisation techniques employed (Figure 3.2B). It can also be observed in Figure 3.2B that when coverslips were treated with poly-L-lysine the percentage coverage of bacteria on the coverslips was below 1%, which is evidently lower compared to *S. aureus* immobilised on coverslips treated by the same method (Figure 3.1B).

In an attempt to increase the coverage of *E. coli*, bacteria were coated overnight at 4°C on poly-L-lysine treated coverslips, as done with *S. aureus*. Nonetheless, the prolonged incubation of bacteria yet again provided inadequate coverage of bacteria on coverslips (Appendices, Figure 7.1).

In summary, poly-L-lysine treatment of coverslips provided an even coverage of *S. aureus* Newman. By contrast, *E. coli* RS218 did not provide reasonable bacterial coverage on glass coverslips regardless of the method utilised and, on this basis, it was decided to exclude *E. coli* from the study as it would evidently be impossible to derive any meaningful conclusions regarding platelet scavenging properties. It was therefore decided to use *S. aureus* Newman as the bacterial model to investigate the scavenging properties of platelets for all subsequent experiments.

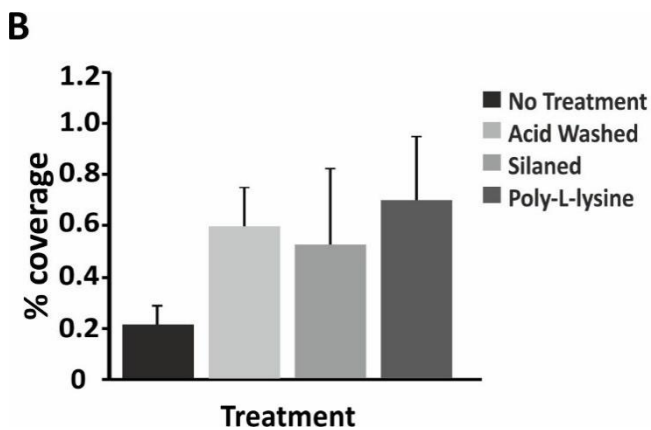
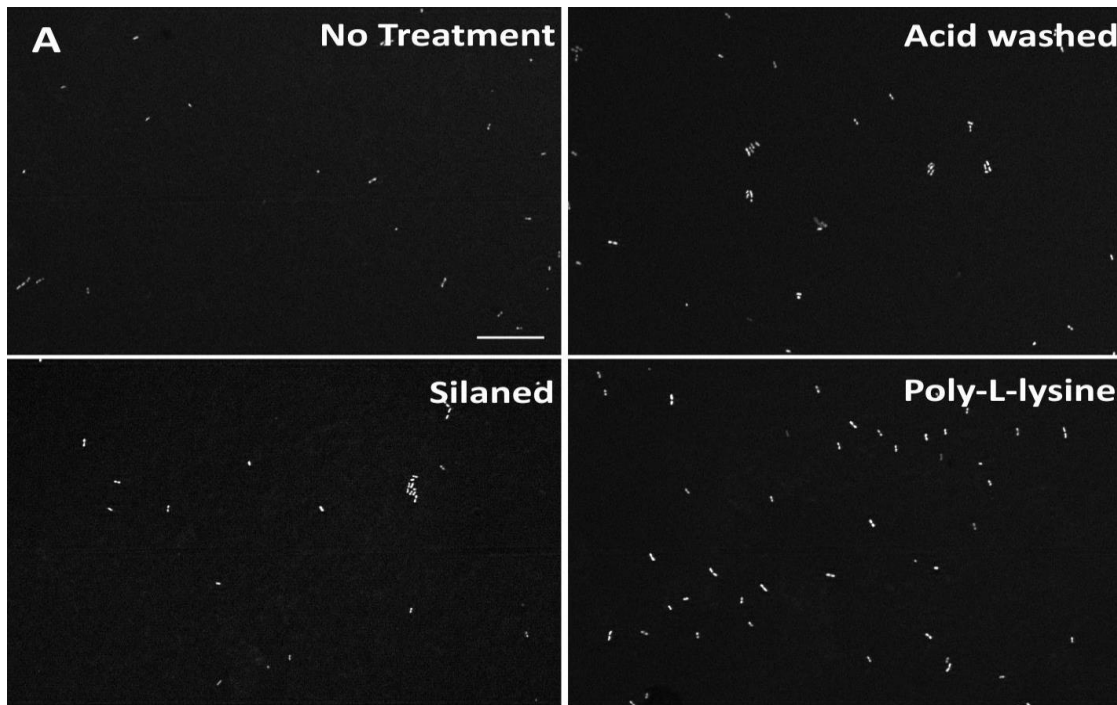


Figure 3.2 Immobilisation of *E. coli* RS218 on glass coverslips. Glass coverslips were prepared by either acid washing with HCl for 1 h followed by dH₂O for 1 h, acid washing with HCl for 1 h then dH₂O for 1 h followed by silanisation with HMDS for 1 min at room temperature or, treatment with poly-L-lysine for 15 min. *E. coli* RS218 bacteria were diluted to OD_(600nm) 1.0 in PBS from an overnight grown suspension culture. 200 µl of bacterial suspension were then added to glass coverslips for 1 h. The coverslips were washed with PBS and bacterial cells were fixed with 4% PFA for 10 min. Cells were then permeabilised with 0.3% Triton X100 for 5 min and subsequently stained with 15 µg/ml Hoechst 33342 (to visualise bacterial DNA) for 15 min at room temperature. Glass coverslips were then mounted onto glass slides with ProLong Antifade Mountant. Images were obtained with a Zeiss ApoTome.2 fluorescence microscope equipped with a 40x oil immersion objective. (A) Representative images from three independent experiments; scale bar represents 20 µm. (B) Percentage coverage of bacteria in each of the treatment conditions was calculated using ImageJ software. A total of 40 fields (image size 165.59 µm x 110.39 µm) per condition was analysed. Data are presented as means ± SEM of three independent experiments. No statistical significance was found.

3.2.2 Effect of buffers on bacterial distribution and coverage on coverslips

The next set of experiments was designed to establish the optimal exposure time and effects of different buffers and solutions on the attachment of *S. aureus* Newman to glass coverslips. Since bacteria are resuspended in PBS and platelets are to be eventually resuspended in either MTB or plasma, it was decided to investigate the effects of these solutions on the ability of bacteria to adhere to coverslips over time.

200 μ l of *S. aureus* Newman was added to poly-L-lysine coated glass coverslips and let to sit at room temperature for 1 h. Following this, unadhered bacteria were aspirated and 200 μ l of PBS, plasma (section 2.3.1) or MTB were then added to the coverslips and incubated at 37°C for 1 or 2 h. Coverslips were then washed, fixed, permeabilised, stained and documented as described in section 3.2.1.

Figure 3.3A shows percentage of bacterial coverage to be comparable between the different treatment groups at 1 h, while a decrease in bacterial coverage was observed upon incubating the bacteria with different solutions, more specifically with MTB and plasma, for 2 h.

As *S. aureus* Newman strain was diluted to OD_(600nm) 1.0 in PBS (nutritionally inert), it was presumed that the exposure of immobilised bacteria on glass coverslips to PBS would not cause any extreme differences in the percentage coverage of bacteria over time. It is therefore not surprising that the addition of PBS had no drastic effects on the bacterial coverage over time (Figure 3.3A). Though, a slight decrease in bacterial coverage was noticed when bacteria remained in PBS for 2 h (24 \pm 1 at 1 h vs. 20 \pm 0% at 2 h), however this was calculated to not be statistically significant (Figure 3.3B).

As previously mentioned, the addition of MTB to immobilised *S. aureus* Newman did not affect the percentage coverage of bacteria (23 \pm 0%) at 1 h relative to control (in this case bacteria treated with PBS for 1 h was used as the control). However, unlike bacteria treated with PBS for 2 h, *S. aureus* Newman exposed to MTB for 2 h showed a substantial decrease of 9% in the percentage bacterial coverage on coverslips (10 \pm 1%) compared to MTB

treatment for 1 h and this difference was found to be significant ($P < 0.05$). It can also be observed that there was a significant difference ($P < 0.01$) in percentage bacterial coverage between bacteria treated with PBS or MTB for 2 h, hence suggesting that *S. aureus* adhere to coverslips more effectively in the presence of PBS rather than MTB for an extended period of time.

Similar results to bacteria treated with MTB were observed upon treating *S. aureus* with plasma. A considerable decrease ($P < 0.001$) in the percentage of bacterial coverage can be seen upon the addition of plasma for 2 h ($8 \pm 3\%$) compared to 1 h ($23 \pm 1\%$) (Figure 3.3B). Treating *S. aureus* with plasma for 2 h gave comparable results to that when bacteria were treated with MTB for 2 h, and again a significant decrease in the percentage of bacterial coverage was observed between PBS-treated bacteria at 2 h and plasma-treated bacteria at 2 h ($P < 0.01$).

The results obtained from these set of experiments suggests that the prolonged exposure time is a critical factor for detachment of bacteria from the glass coverslips. Based on these results it was concluded to carry out all scavenging experiments for a maximum time period of 60 min to limit any possible bacterial detachment as a result of MTB or plasma addition.

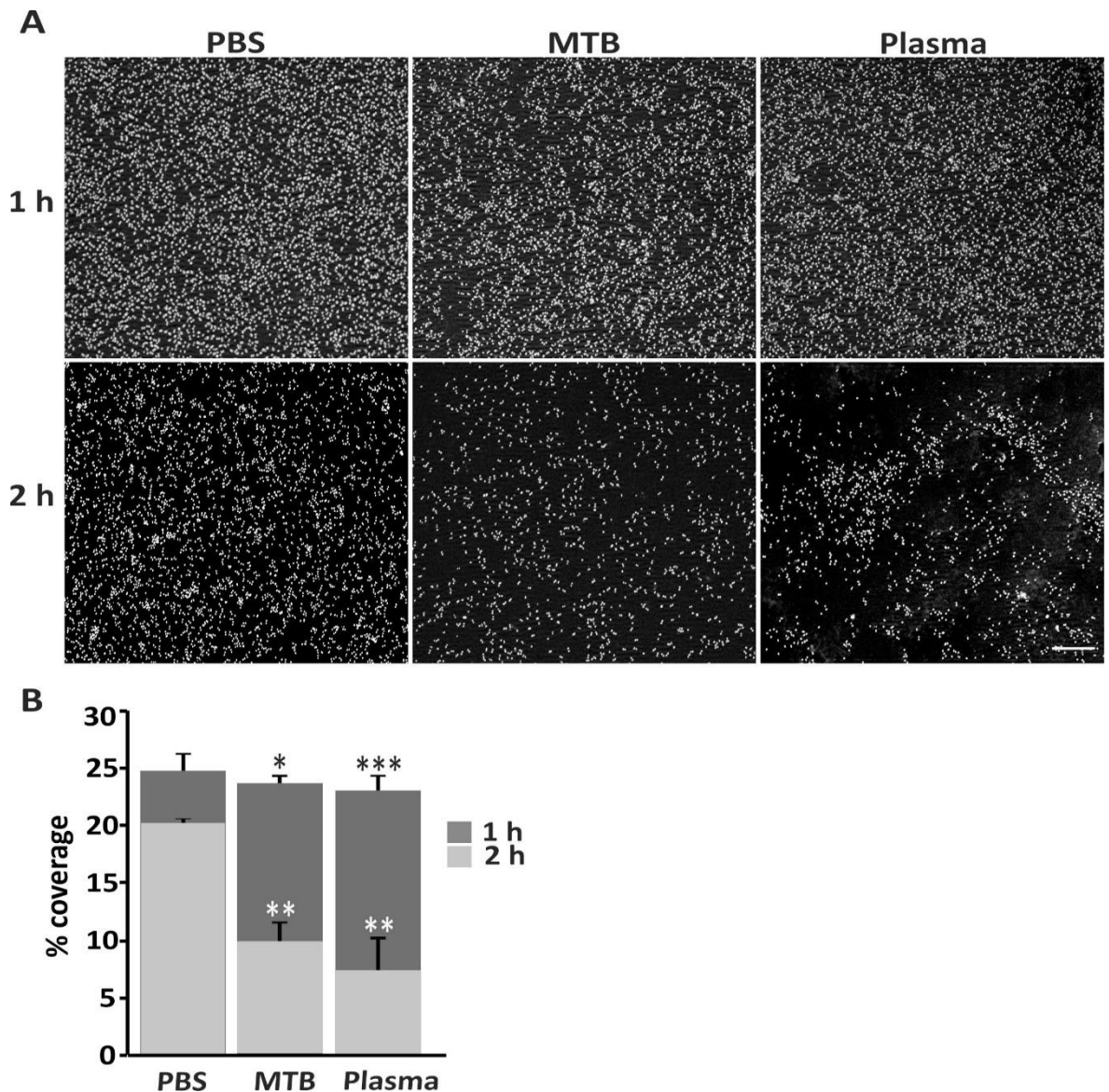


Figure 3.3 Effect of solutions on bacterial attachment to glass coverslips. Glass coverslips were treated with poly-L-lysine for 15 min. *S. aureus* Newman bacteria were diluted to OD_(600nm) 1.0 in either PBS from an overnight grown suspension culture. 200 μ l of *S. aureus* suspension were then added to glass coverslips for 1h. Unadhered bacteria were aspirated and 200 μ l of PBS, MTB or plasma (isolated from whole blood via centrifugation at 1700xg for 10 min) was added to the coverslips for the given timepoints. Coverslips were washed with PBS and bacterial cells were fixed with 4% PFA for 10 min, permeabilised with 0.3% Triton X100 for 5 min and subsequently stained with 15 μ g/ml Hoechst 33342 for 15 min at room temperature. Glass coverslips were then mounted onto glass slides with ProLong Antifade Mountant. Images were obtained with a Zeiss ApoTome.2 fluorescence microscope equipped with a 40x oil immersion objective. (A) Representative images from three independent experiments, scale bar represents 20 μ m. (B) Percentage coverage of bacteria in each of the treatment conditions was calculated using ImageJ software. Data are presented as means \pm SEM of three independent experiments, (* p <0.05, ** p <0.01 and *** p <0.001). Black asterisks indicate the significance between 1h and 2h within the same condition while white asterisks indicate the significance between the conditions relative to PBS at 2h.

3.2.3 Determining the optimal density of bacteria required for maximal coverage on coverslips

Another crucial area of optimisation for the development of the scavenging assay is the density of *S. aureus* Newman bacteria suspension required to provide maximal bacterial coverage. In literature, bacterial suspensions are commonly diluted to OD_(600nm) 1.0 (Chang *et al.*, 2013; Ghali *et al.*, 2016). However, we wanted to assess whether increasing the concentration of bacteria enhances the percentage of coverage on coverslips accordingly.

Three different concentrations of bacteria in PBS were chosen: OD_(600nm) 1.0, 1.25 and 1.5. 200 µl of bacterial suspension were placed on poly-L-lysine treated glass coverslips and the samples were processed as described previously in section 3.2.2.

As can be seen in Figure 3.4A, the percentage of bacterial coverage increased to some extent as the concentration of bacteria increased. Only a marginal (not significant) difference of 2% in the percentage of coverage was observed between bacteria diluted to OD_(600nm) 1.0 and 1.25 (23±1% vs 26±4% respectively) (Figure 3.4B).

The highest percentage of bacterial coverage 34±2% was discovered when bacteria were resuspended at OD 1.5, which was statistically significant compared to the coverage of bacteria resuspended to 1.0 (P<0.05). However, it is notable that *S. aureus* Newman diluted to OD 1.5 tended to form clumps (Figure 3.4A, far right image, arrowheads).

While the higher concentration of bacteria gave a higher percentage of coverage, it was decided not to apply such bacterial concentrations for the purpose of studying scavenging properties of platelets. Since the pre-formed clusters as a result of an excess of bacteria, may interfere with the analysis upon the addition of platelets. It would therefore become challenging to distinguish whether bacteria have clumped as a result of the high concentration or whether platelets were a contributing factor for the cluster-like structures.

Since bacteria prepared to OD 1.0 and OD 1.25 provided similar results and also because the results were not statistically different, OD 1.0 was chosen as the concentration of bacteria to be utilized for all experiments herein, in order to adhere to standard concentrations used frequently in microbiology.

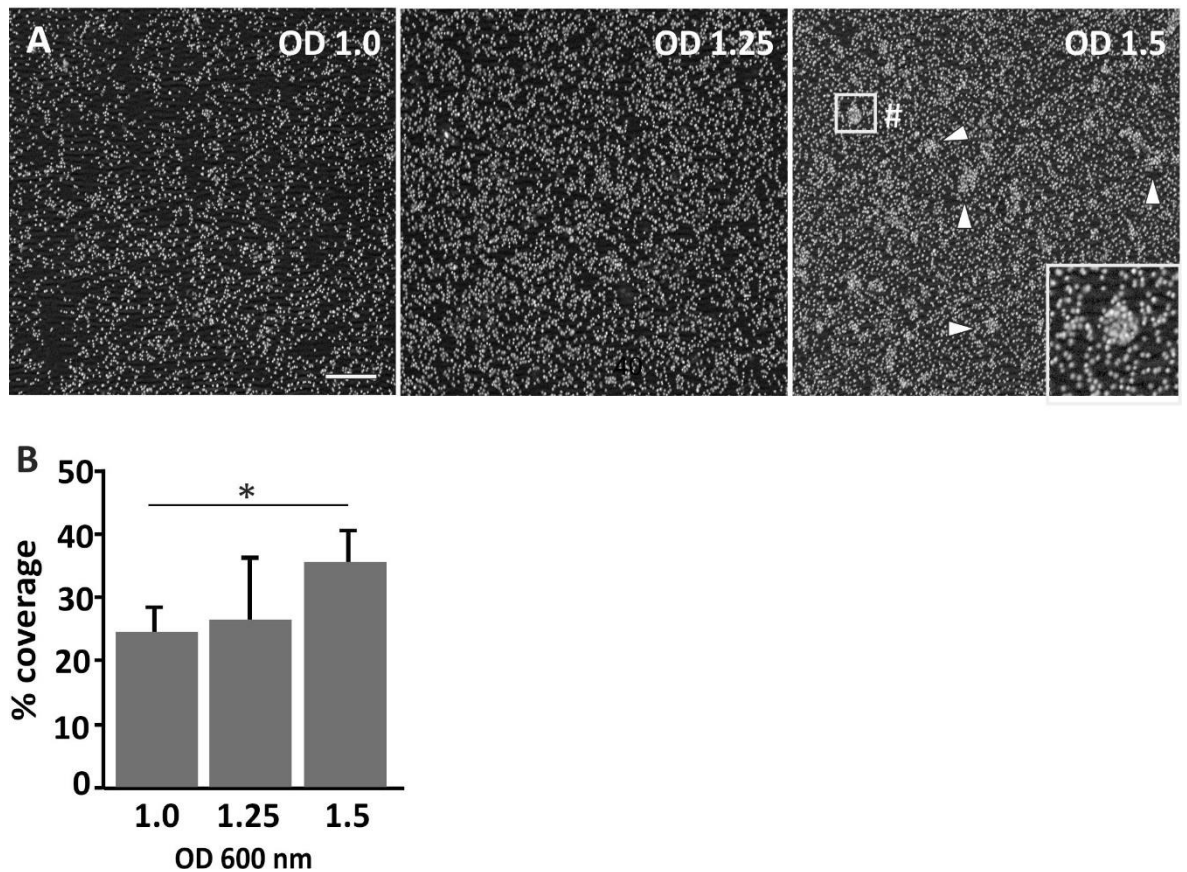


Figure 3.4 Optimisation of the density of *S. aureus* Newman. *S. aureus* Newman bacteria was diluted to OD_(600nm) 1.0, 1.25 and 1.5 in PBS from an overnight grown suspension culture. 200 μ l of bacterial suspension were then added for 1 h at room temperature to glass coverslips pre-treated with poly-L-lysine for 15 min. Cells were then washed with PBS and fixed with 4% PFA for 10 min. Cells were subsequently permeabilised with 0.3% Triton X100 for 5 min and bacterial DNA was stained with 15 μ g/ml Hoechst 33342 (white) for 15 min at room temperature. Coverslips were mounted onto glass slides containing ProLong Antifade Mountant and microscope images were obtained by using Zeiss ApoTome.2 fluorescence microscope equipped with a 40x oil immersion objective. Representative images from three independent experiments are shown; scale bar represents 20 μ m (A). Arrowheads represent clumps of bacteria formed and an example of a bacterial clump formed when bacteria was diluted to OD 1.5 (#) has been enlarged in the bottom left hand corner of panel A. (B) Percentage coverage of bacteria in each of the conditions was calculated by thresholding images on ImageJ software. Data are presented as means of three independent experiments \pm SEM, (* p <0.05).

3.3 Optimisation of conditions for scavenging

Having optimised the basic conditions in terms of sufficient bacterial coating required for an assay which aims to investigate scavenging properties of platelets on an infectious agent, platelets were added to the assay and steps were taken to optimise the capacity of these cells to scavenge bacteria.

3.3.1 Effect of the platelet preparation on the ability to scavenge *S. aureus*

Initially it was decided to assess the ability of platelet rich plasma (PRP) to scavenge bacteria on coverslips since PRP mimics the physiological microenvironment of vascular injury and inflammation *in vivo*. A key element to take into consideration was the potential difference, between PRP and washed platelets (WP) in the ability of platelets to scavenge immobilised *S. aureus* Newman.

Importantly, PRP and WP differ unquestionably in their composition: PRP contains platelets and plasma proteins. WP are resuspended in a buffer devoid of such proteins and are used more commonly for experimentation to exclude their confounding effect (Cazenave *et al.*, 2004). Therefore, by conducting experiments comparing PRP and WP, it will be possible to establish whether the presence of plasma components is mandatory for platelets to scavenge *S. aureus*.

In addition to the above, it was also decided to incorporate an extra category to the experimental design, whereby isolated WP would be resuspended in plasma. This was done partly because the study conducted by Gaertner *et al.*, (2017) had utilized plasma to resuspend WP as plasma proteins proved to be critical for the particular migration characteristic of platelets. So, we postulated that the exclusion of plasma components would result in an absence of platelet scavenging properties. Therefore, to test this hypothesis WP resuspended in plasma were also examined for their ability to scavenge.

PRP and WP were isolated as described in section 2.3.1. Plasma from the same healthy donor was also isolated and used to resuspend isolated PRP to the required platelet concentration, while MTB was used to resuspend WP (WP-MTB) to eliminate any

confounding effects of plasma on platelet scavenging properties. As mentioned previously, an additional condition whereby WP were resuspended in plasma was also incorporated in the experiment (WP-plasma). Platelet density was set to 1×10^7 /ml since these are standard amounts used in spreading experiments. 200 μ l of platelet suspensions were then placed onto glass coverslips pre-coated with *S. aureus*. The coverslips were then incubated at 37°C for 1 h, fixed with 4% PFA, permeabilised with 0.3% Triton X100 and stained with a combination of 1 μ g/ml TRITC phalloidin (stains F-actin in platelets) and 15 μ g/ml Hoechst 33342 to allow the visualisation of both cells on the coverslip. The coverslips were then mounted onto glass slides and imaged using a fluorescence microscope. The number of adhered platelets and the percentage of scavenging platelets were determined for all the groups. Samples of each platelet preparation were also incubated on fibrinogen (100 μ g/ml) coated coverslips for 1 h as a control of their spreading profile. The coverslips were then processed in parallel as mentioned above but stained with TRITC-phalloidin only.

Figure 3.5A illustrates representative examples of the effects of platelet preparation on the ability of platelets to scavenge *S. aureus* Newman. It can be seen that only PRP possessed the ability to scavenge bacteria.

Figure 3.5B shows the number of adhered platelets on the bacteria compared to the respective control group on fibrinogen. Firstly, it can be seen that the number of platelets in PRP and WP-MTB which are able to adhere to immobilised bacteria are comparable (35 ± 2 and 28 ± 4 platelets/field respectively), whereas a smaller number of platelets was found to have adhered when WP were resuspended in plasma (24 ± 2 platelets/field). Secondly, upon closer review it can be noticed that the number of attached platelets on fibrinogen significantly exceeds the number of platelets adhered on bacteria by two-fold or more, although between the different WP preparation groups, the number of adhered platelets was found to be similar (Figure 3.5B). This is true for even the PRP population where around 35 ± 2 platelets were calculated to have adhered to *S. aureus* Newman compared to a remarkable 61 ± 9 platelets/field on fibrinogen, therefore, indicating that platelets have stronger associations with fibrinogen than they do with bacterial components. Importantly, the fibrinogen controls demonstrate that the different methods of preparing platelets do not affect the adhesion capabilities of the platelets.

Another key observation from these set of experiments is the difference in platelets' ability to scavenge immobilised *S. aureus* bacteria between the preparations. A cluster of bacteria at the core of a platelet in addition to lack of bacteria surrounding the area of the platelet is typically indicative of the platelet scavenging bacteria (Figure 3.5A, top row). It can be seen that there is a visible difference between WP and PRP placed on immobilised *S. aureus* Newman in terms of the ability of platelets to scavenge bacteria. Platelets in PRP were able to scavenge immobilised bacteria effectively ($82\pm 1\%$ of platelets) (Figure 3.5C). Interestingly, WP-MTB were found to completely lack the capacity to scavenge bacteria on glass coverslips (0% of WP scavenged bacteria). Therefore, one may speculate that plasma proteins may play a vital role in regard to scavenging ability of platelets. Surprisingly however, WP resuspended in plasma also significantly lacked the ability to scavenge bacteria (0%) (Figure 3.5C).

LTA was conducted in parallel to the scavenging assays to determine whether it was possible for bacteria to induce platelet aggregation in the conditions of the scavenging assay. Platelets were prepared to 2.5×10^8 /ml in the afore-mentioned solutions and LTA was performed at 37°C under 1000 rpm stirring conditions. *S. aureus* Newman at $\text{OD}_{(600\text{nm})}$ 1.6 was used as the agonist. Unstimulated PRP and WP in the absence of the agonist were analysed as basal conditions. As expected, PRP stimulated with *S. aureus* Newman resulted in platelet aggregation ($85\pm 4\%$ light transmission) (Figure 3.5D). In contrast, WP resuspended in either MTB or plasma failed to aggregate in response to the addition of bacteria (Figure 3.5D). These results along with the differences observed in the scavenging assay indicate that plasma itself is not responsible for these effects; rather we speculate that the process of platelet preparation affects the ability of platelets to scavenge bacteria.

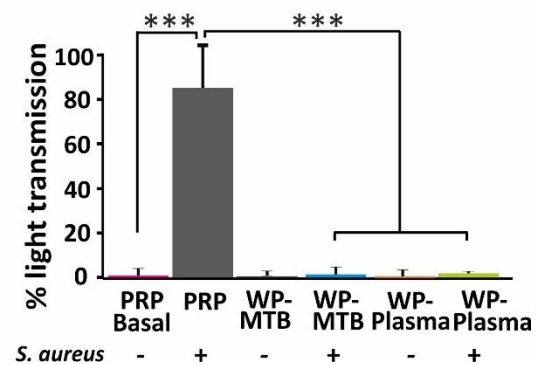
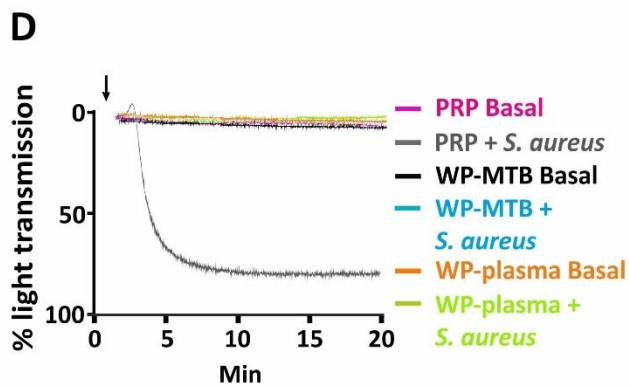
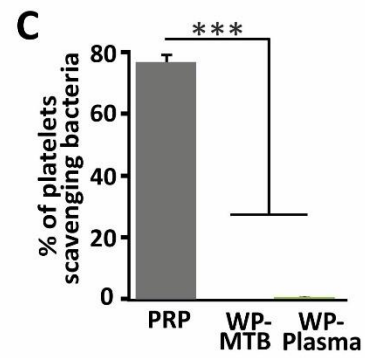
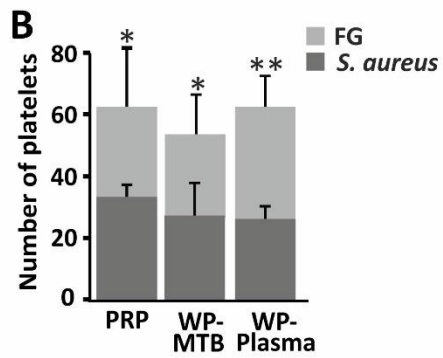
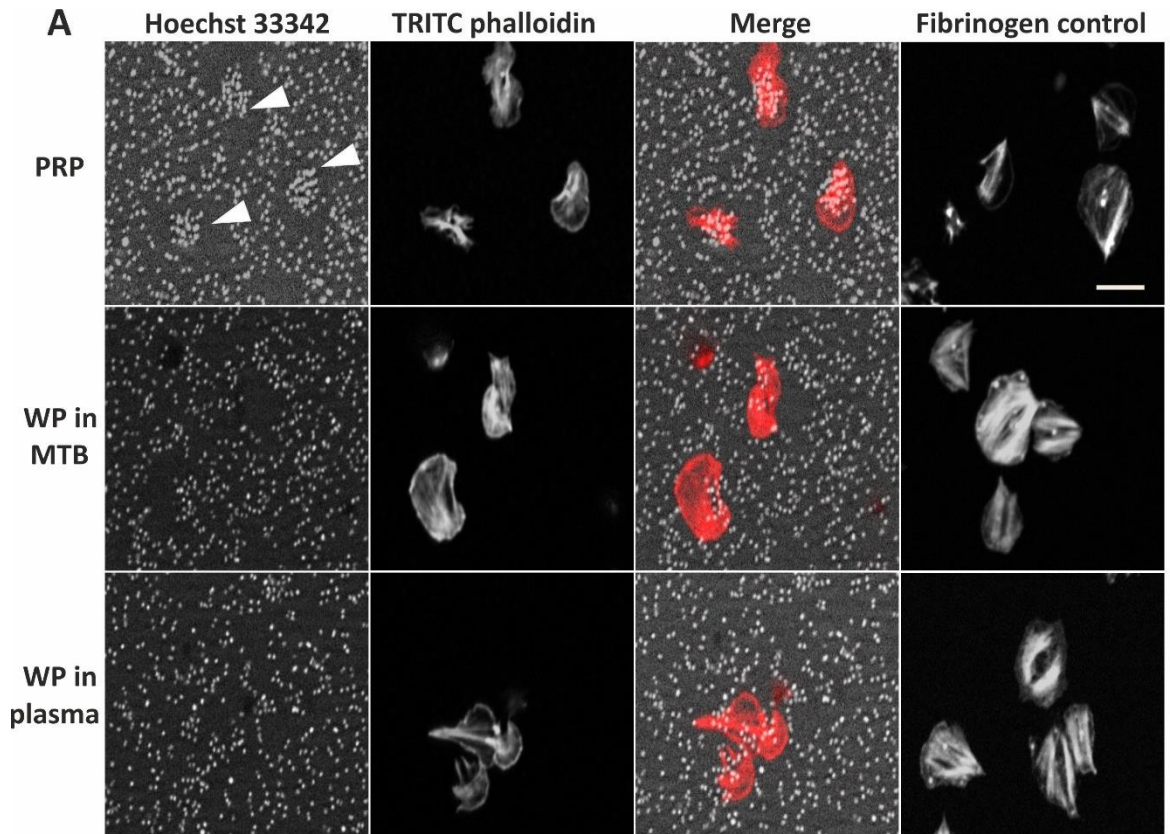


Figure 3.5 Difference between washed platelets and platelet rich plasma in scavenging

immobilised *S. aureus* Newman. 200 μ l of an OD_(600nm) 1.0 *S. aureus* Newman bacterial suspension in PBS were added for 1 h at room temperature to poly-L-lysine coated glass coverslips. Platelets were diluted to 1×10^7 /ml by resuspending PRP in plasma and WP in MTB or plasma and 200 μ l of suspension were added to coverslips and incubated at 37 °C for 1 h. Platelets were also spread on fibrinogen (100 μ g/ml) coated coverslips in parallel. Coverslips were washed with PBS and fixed with 4% PFA for 10 min, permeabilised with 0.3% Triton X100 for 5 min and stained with a combination of 1 μ g/ml TRITC phalloidin (grey; red on the merged image) and 15 μ g/ml Hoechst 33342 (grey) for 30 min at room temperature. Coverslips were mounted onto glass slides with ProLong Antifade Mountant and images were obtained with a Zeiss ApoTome.2 fluorescence microscope equipped with a 40x oil immersion objective. (A) Representative images from three independent experiments. Scale bar represents 20 μ m. Arrowheads indicate examples of clusters of bacteria scavenged by platelets (top panel). (B) Adhesion of cells in each of the conditions was calculated by counting manually. (C) Percentage of scavenging platelets per field was also counted manually from a total of 40 fields (image size 165.59 μ m x 110.39 μ m) per condition. (D) A representative LTA trace for 250 μ l of platelets at 2.5×10^8 /ml, (non)stimulated with OD_(600nm) 1.6 *S. aureus* Newman. LTA was conducted for 20 min; platelets stimulated with 2.5 μ l of *S. aureus* Newman OD_(600nm) 1.6 are indicated. Arrow above the LTA graph indicates the time of addition of bacteria to relevant platelet samples. Data are presented as means \pm SEM of three independent experiments for both scavenging and LTA experiments. Statistical significance was calculated (* $p < 0.05$, ** $p < 0.01$ and *** $p < 0.001$).

3.3.2 The effects of anticoagulants in the ability of platelets to scavenge bacteria

The methodologies, in particular the anticoagulant used for the isolation of platelets differs according to the form of platelets isolated. PRP is routinely prepared in sodium citrate (SC) while acid citrate dextrose (ACD) is the preferred anticoagulant when collecting blood for the isolation of WP. ACD and SC vary considerably in their citrate concentration and pH, which are important variables that could potentially affect platelets' ability to scavenge bacteria. This gave rise to the possibility that the differences observed between WP and PRP in their ability to scavenge bacteria may be as a result of the anticoagulant used for platelet preparation rather than plasma proteins themselves.

Moreover, studies have shown variability in methods used to prepare platelets to lead to differing results in literature; particularly the choice of anticoagulant used (Amaral *et al.*, 2016). Therefore, in order to ensure the effects observed in the previous section (Figure

3.5) were not a result of the anticoagulants used, an experiment was conducted to test the ability of platelets to scavenge bacteria when blood was collected in two different anticoagulants commonly used in our laboratory, SC and ACD. PRP from the same donor was isolated from whole blood drawn into syringes containing either SC or ACD at appropriate concentrations (section 2.3.1). A scavenging assay as well as LTA were then conducted as detailed in the above section (3.3.1). The number of adhered platelets, the percentage of platelets able to scavenge bacteria as well as the number of bacteria per cluster (section 2.4.8) were calculated for these experiments.

It was found from these set of experiments that platelets in PRP, irrespective of the anticoagulant used, had the capacity to scavenge *S. aureus* Newman (Figure 3.6A). The number of adhered platelets on bacteria of PRP isolated in the presence of ACD (37 ± 4 platelet/field) was comparable to that of PRP isolated in the presence of SC (34 ± 6 platelets/field) (Figure 3.6B). Likewise, it can also be seen in Figure 3.6B that equivalent number of cells adhered to fibrinogen coated coverslips (48-50 cells/field). No significant differences was calculated between the two groups in terms of the percentage of platelets able to scavenge bacteria ($78\pm 2\%$ in ACD compared to $81\pm 4\%$ PRP in SC) (Figure 3.6C). Intriguingly, the average number of bacteria scavenged by a platelet were also calculated to be comparable between the two groups with 21 ± 2 compared to 20 ± 1 in the presence of ACD and SC correspondingly (Figure 3.6D). The results collected from these set of experiments confirm that the anticoagulant used for the drawing of whole blood does not essentially play a pivotal role when determining the ability of PRP to scavenge *S. aureus* immobilised on coverslips.

LTA was also conducted in parallel to the scavenging assays to determine whether the ability of bacteria to induce platelet aggregation in the conditions of the scavenging assay. Platelets were prepared in the presence of the two anticoagulants and stimulated with *S. aureus* Newman at OD_(600nm) 1.6 as outlined in section 3.3.1. It can be seen from the aggregation traces obtained that the percentage light transmission between PRP collected in ACD and SC are equivalent (83% compared to 81% respectively) (Figure 3.6E).

Results obtained from LTA along with the similarities observed in the scavenging assay indicate that the choice of anticoagulant does not affect the capacity of platelets to scavenge bacteria. Therefore, it was decided to prepare platelets in the presence of SC for all experiments herein, in order to adhere to standard protocol used frequently for the isolation of platelets in PRP.

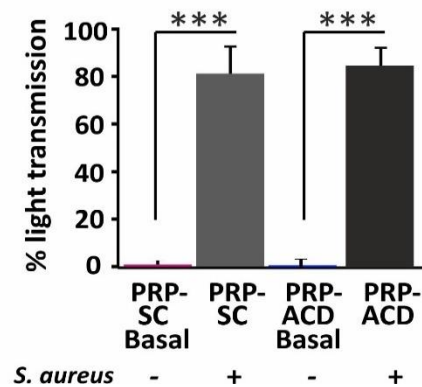
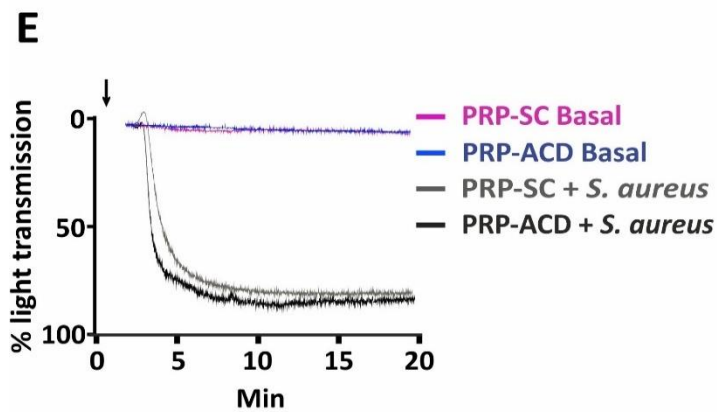
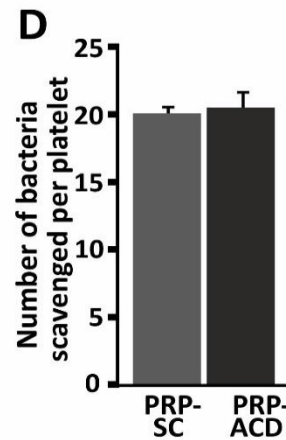
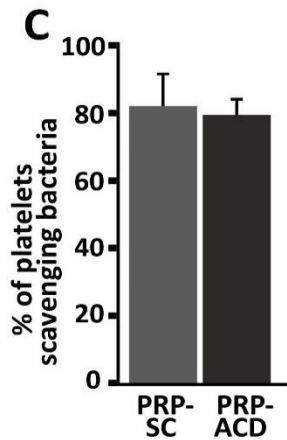
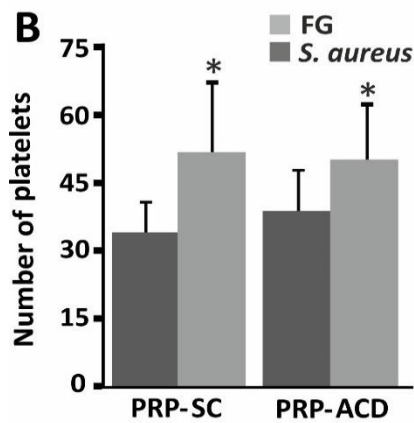
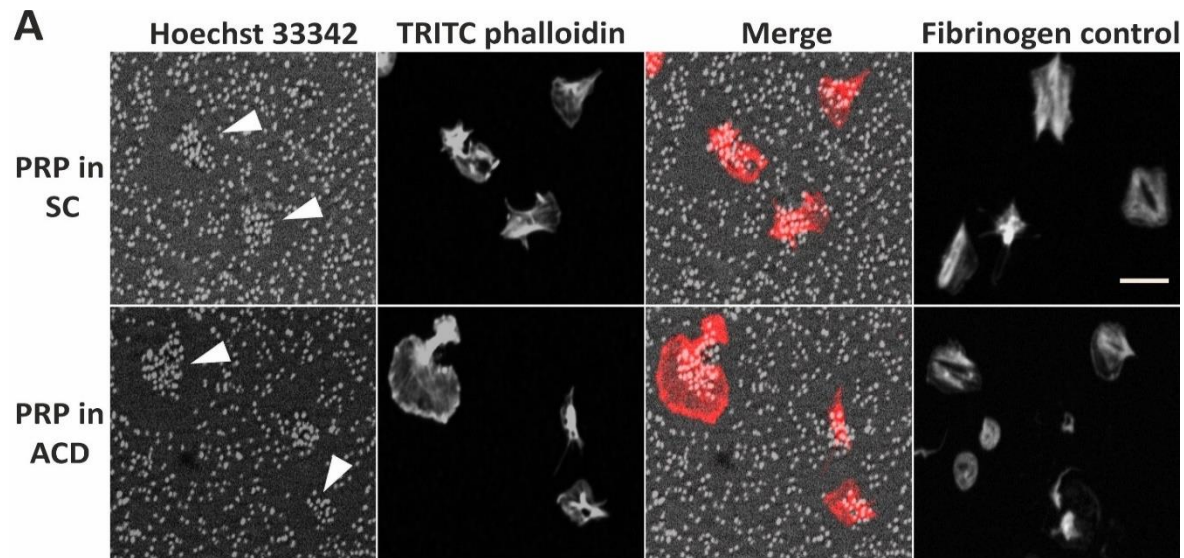


Figure 3.6 Effect of anticoagulant on the capacity of platelets to scavenge bacteria. 200 μ l of an OD_(600nm) 1.0 *S. aureus* Newman suspension in PBS were added for 1 h at room temperature to poly-L-lysine coated glass coverslips. Platelets in PRP were obtained in the presence of either SC or ACD and diluted to 1×10^7 /ml. 200 μ l of platelet suspension was then added to the coverslips and incubated at 37°C for 1 h. Platelets were also spread on fibrinogen (100 μ g/ml) coated coverslips in parallel. Coverslips were washed with PBS and fixed with 4% PFA for 10 min, permeabilised with 0.3% Triton X100 for 5 min and stained with a combination of 1 μ g/ml TRITC phalloidin (grey; red on the merged image) and 15 μ g/ml Hoechst 33342 (grey) for 30 min at room temperature. Coverslips were then mounted onto glass slides with ProLong Antifade Mountant and images were obtained with a Zeiss ApoTome.2 fluorescence microscope equipped with a 40x oil immersion objective. (A) Representative images from three independent experiments. Scale bar represents 20 μ m. Arrowheads indicate examples of clusters of bacteria scavenged by platelets (top panel). (B) Adhesion of cells in each of the conditions was calculated via manually counting cells on ImageJ software. (C) Percentage of scavenging platelets per field was also counted manually from a total of 40 fields (image size 165.59 μ m x 110.39 μ m) per condition. (D) Number of bacteria scavenged by platelets was calculated as outlined in section 2.4.8. (E) A representative LTA trace for 250 μ l of platelets at 2.5×10^8 /ml, (non)stimulated with OD_(600nm) 1.6 *S. aureus* Newman. LTA was conducted for 20 min, platelets stimulated with 2.5 μ l of *S. aureus* Newman OD_(600nm) 1.6 are indicated. Arrow above the LTA graph indicates the time of addition of bacteria to relevant platelet samples. Data are presented as means \pm SEM of three independent experiments for both scavenging and LTA experiments, (* $p < 0.05$ and *** $p < 0.001$).

3.3.3 The effect of platelet concentration on bacterial scavenging

We have established thus far the optimal conditions for assaying scavenging of bacteria in terms of coverslip treatment and bacterial concentration (sections 3.2.1 and 3.2.3). Furthermore, we have shown in this study that platelets possess the capacity to scavenge immobilised *S. aureus* Newman only when prepared as PRP (section 3.3.1). In this section we explore whether any platelet-concentration dependent changes affect the ability of platelets to scavenge bacteria.

Platelet density in PRP was adjusted to two different concentrations, 1×10^7 /ml and 2×10^7 /ml, by diluting in plasma. It was decided to limit the testing concentration of platelets to 2×10^7 /ml, since any concentration higher than this was assumed to result in an excess of platelets on the coverslips, which would then complicate determining accurately the effect of individual platelets.

PRP at the two concentrations indicated above were placed on glass coverslips coated with *S. aureus* Newman. The coverslips were then incubated at 37°C for 1 h. Following the 1 h incubation cells were fixed, permeabilised and stained for visualization as described in previous sections.

It is apparent from Figure 3.7A that platelets at the two different concentrations were able to scavenge *S. aureus* Newman (scavenged bacteria are indicated with arrowheads). As anticipated, the number of platelets adhered to bacteria increased significantly as the concentration of platelets increased (from 31 ± 3 platelets/field at 1×10^7 /ml to 68 ± 4 platelets/field at 2×10^7 /ml; $P < 0.001$) (Figure 3.7B). Moreover, as previously revealed, the number of adhered platelets on coverslips coated with 100 µg/ml fibrinogen (control) was significantly higher (two-fold; $P < 0.001$) when compared to their respective concentration spread on *S. aureus* Newman.

Interestingly, the total percentage of platelets able to scavenge bacteria remained constant regardless of the increasing concentration of platelets: $82 \pm 2\%$ at 1×10^7 platelets/ml vs $76 \pm 7\%$ at 2×10^7 platelets/ml (Figure 3.7C). This confirms that platelet concentration does not alter the ability of platelets to scavenge.

However, it is critical to note that on coverslips with PRP prepared to 2×10^7 /ml, regions with overlapping platelets were often found at a cluster of cleared bacteria. An example is shown in Figure 3.7A (yellow dashed circled area). The analysis of such cells proved to be complicated since there was difficulty in determining which platelet was responsible for scavenging a particular area of bacteria. Therefore, the quantification of bacterial clusters was not undertaken because increasing platelet density does not seem to affect their ability to scavenge bacteria but complicates the quantitative analysis of individual platelets, and so it was decided for platelets to be prepared to 1×10^7 /ml for all subsequent bacteria-scavenging assays.

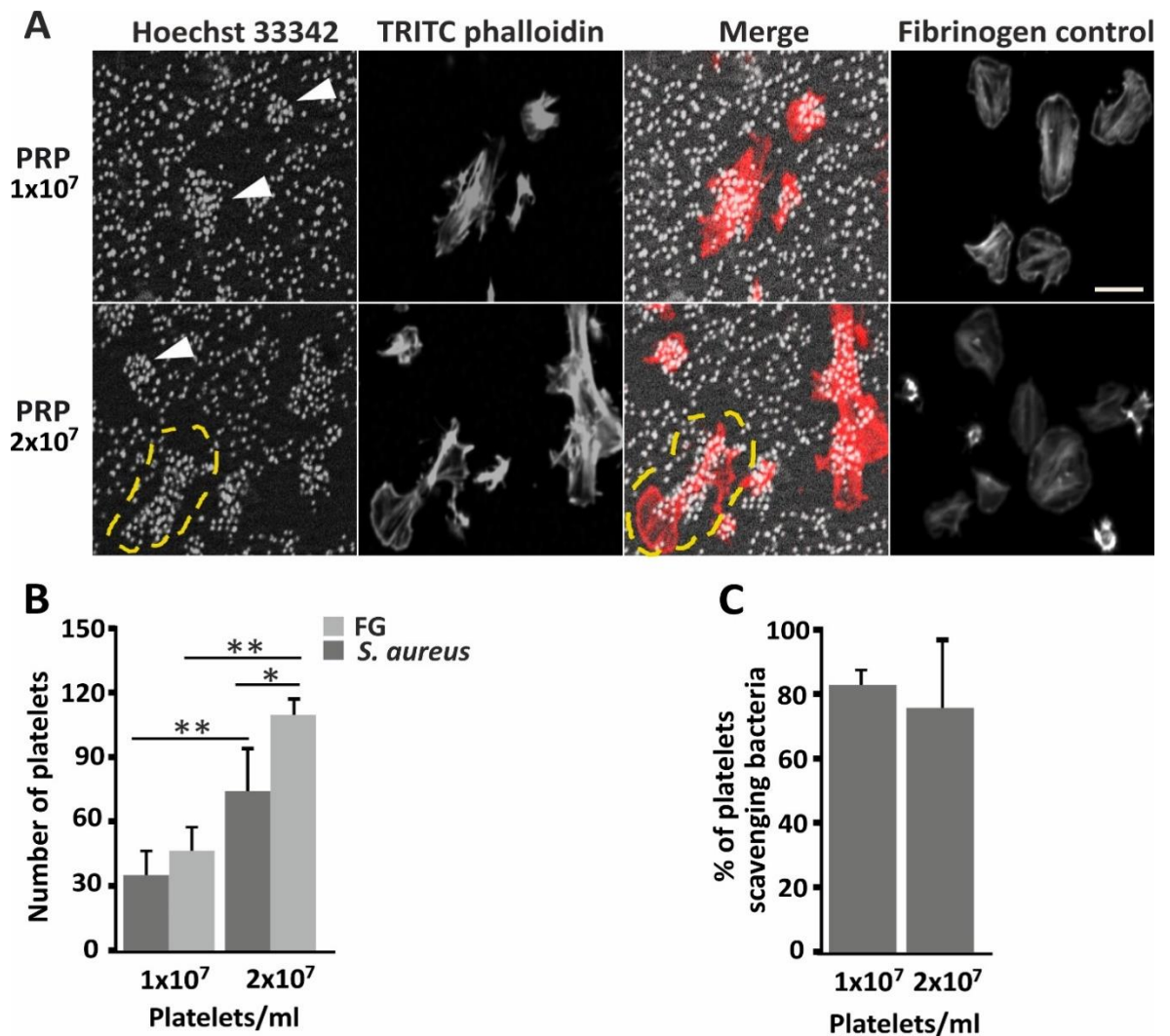


Figure 3.7 The effect of platelet density on the ability of platelets to scavenge *S. aureus*

Newman. 200 μ l of an OD_(600nm) 1.0 *S. aureus* Newman suspension in PBS were added for 1 h at room temperature to poly-L-lysine coated glass coverslips. Platelets were diluted to either 1x10⁷/ml or 2x10⁷/ml by resuspending PRP in plasma. 200 μ l of platelet suspension was then added to the coverslips and incubated at 37°C for 1 h. Platelets were also spread on fibrinogen (100 μ g/ml) coated coverslips in parallel. Coverslips were washed with PBS and fixed with 4% PFA for 10 min, permeabilised with 0.3% Triton X100 for 5 min and stained with a combination of 1 μ g/ml TRITC phalloidin (grey; red on the merged image) and 15 μ g/ml Hoechst 33342 (grey) for 30 min at room temperature. Coverslips were mounted onto glass slides with ProLong Antifade Mountant and images were obtained with a Zeiss ApoTome.2 fluorescence microscope equipped with a 40x oil immersion objective. (A) Representative images from three independent experiments. Scale bar represents 20 μ m. Arrowheads indicate examples of clusters of scavenged bacteria by platelets. Yellow dashed line represents overlap in the area of bacteria scavenged. (B) Adhesion of cells in each of the conditions was counted manually on ImageJ software. (C) Percentage of scavenging platelets per field was also calculated manually from a total of 40 fields (image size 165.59 μ m x 110.39 μ m) per condition. Data are presented as means \pm SEM of three independent experiments, (*p<0.05 and **p<0.01).

3.4 The ability of platelets to scavenge bacteria increases over time

Platelets undergo a series of events whereby they adhere to a matrix, spread and then eventually migrate and scavenge. These steps all require time to progress from one to the other (Bordon, 2018; & Gaertner *et al.*, 2017).

In section 3.2.2 (Figure 3.3) we established that incubating bacteria for longer than 1 h in the presence of MTB or plasma resulted in a significant decrease in the overall percentage coverage of bacteria on coverslips. Consequently, we have since studied the capacity of platelets to scavenge bacteria when incubated for 60 min (section 3.3, Figure 3.5). We were, however, curious to find out whether incubating platelets with immobilised bacteria for a shorter period of time would still lead to the scavenging properties showcased at 60 min incubation and whether the number of bacteria scavenged increased in a time dependent manner.

Thus, the examination of a time course (15, 30 and 60 min) was decided. Scavenging assay were conducted as described previously in section 3.3 and at given timepoints, coverslips were fixed, processed, and analysed as per section 3.3.1.

Figure 3.8A shows representative examples of platelets scavenging *S. aureus* Newman over time. It is apparent that the ability of platelets to scavenge *S. aureus* Newman is only evident at 30 and 60 min (arrowheads). As expected, the number of adhered platelets on both *S. aureus* Newman and fibrinogen increased in a time dependent manner. In fact, more than two-fold increase in the number of platelets adhered on bacteria was observed between 15 min and 60 min (11 ± 5 at 15 min vs 34 ± 6 at 60 min, $P<0.01$) (Figure 3.8B). A similar trend was observed in the FG control groups, in that a significant increase ($P<0.05$) in the number of adhered platelets was observed between 15 and 60 min (17 ± 3 vs 48 ± 6 respectively).

Likewise, morphologically, the surface area of platelets increased as the time platelets incubated on bacteria increased ($9\pm5 \mu\text{m}^2$ at 15 min, $22\pm8 \mu\text{m}^2$ at 30 min and $29\pm3 \mu\text{m}^2$ at 60 min), with a significant increase in platelet area between 15 and 60 min ($P<0.05$) (Figure

3.8C). The same was observed for platelets spread on fibrinogen with the mean surface area of platelets calculated to be $12\pm 2 \mu\text{m}^2$ at 15 min compared to $32\pm 4 \mu\text{m}^2$ at 60 min ($P<0.05$).

In terms of platelet scavenging ability, it can be observed from Figure 3.8D that no scavenging was apparent at 15 min. However, following 30 min incubation of platelets on bacteria, the percentage of scavenging platelets increased significantly ($58\pm 6\%$; $P<0.001$). At 60 min $83\pm 4\%$ of platelets were able to scavenge *S. aureus* Newman, which was significantly higher than the percentage of scavenging cells observed at 30 min ($P<0.05$) and in agreement with the experiments of previous sections.

As for the mean number of bacteria scavenged by platelets, it can be seen in Figure 3.8E that platelets incubated for 60 min scavenged on average 23 ± 4 bacteria, which was significantly higher ($P<0.05$) than platelets at 30 min, where the average number of scavenged bacteria was found to be 12 ± 9 . Therefore, it can be assumed that the capacity of platelets to scavenge bacteria increases with time and that the optimal time for the greatest number of bacteria scavenged by platelet was found to be at 60 min (Figure 3.8E).

In summary, the data from these experiments showed that scavenging of bacteria is indeed time dependent, strengthening the notion that platelets progress through distinct phases before attaining the ability to scavenge matter. Since the percentage of scavenging platelets along with the mean number of bacteria scavenged was observed to be greatest at 60 min, it was decided to continue using 1 h incubation time for subsequent experiments.

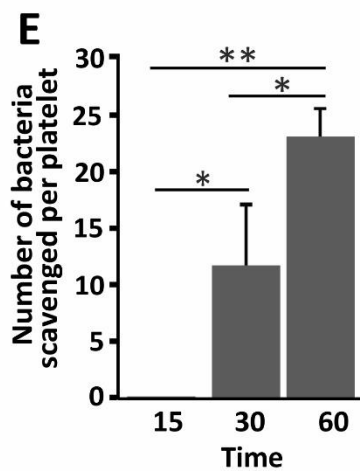
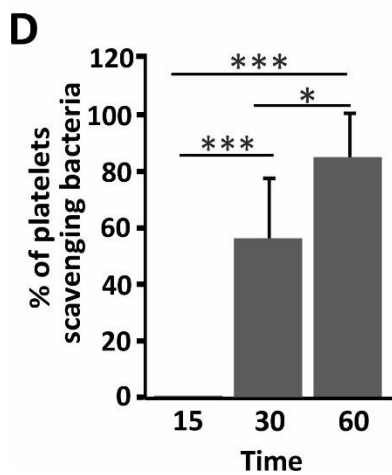
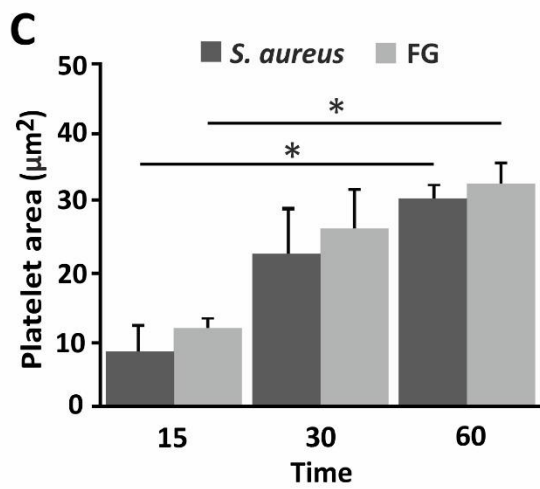
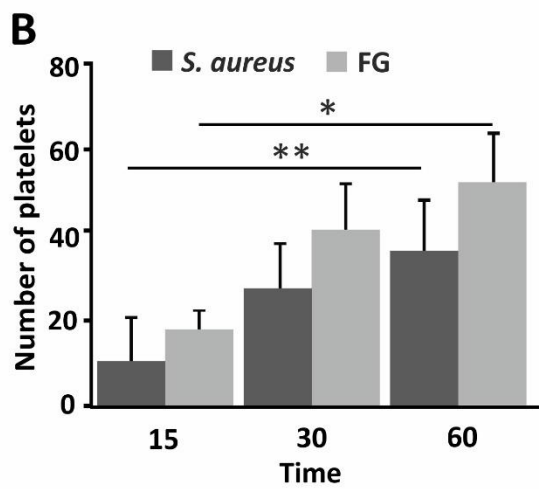
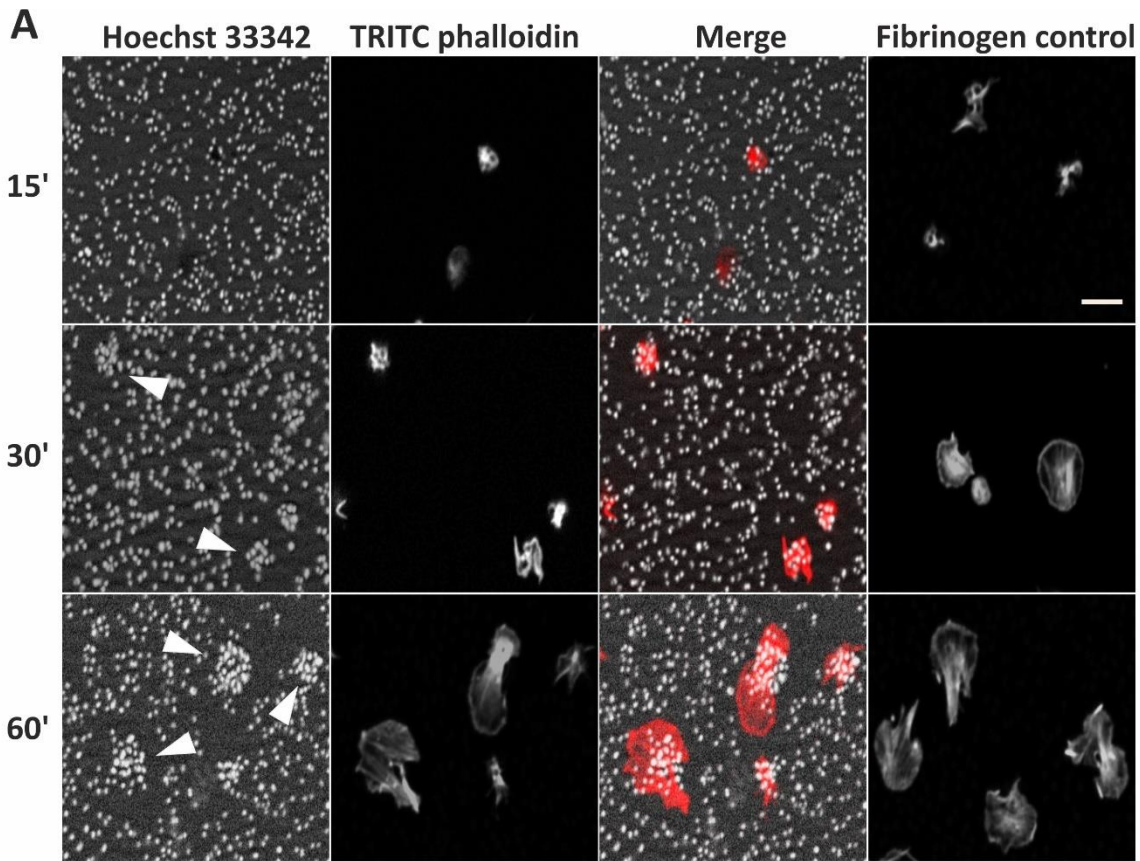


Figure 3.8 Time dependent changes in the ability of platelets to scavenge *S. aureus*

Newman. 200 μ l of an OD_(600nm) 1.0 *S. aureus* suspension in PBS were added for 1 h at room temperature to poly-L-lysine coated glass coverslips. Platelets in PRP were diluted to 1×10^7 /ml. 200 μ l of platelet suspension was then added to the coverslips and incubated at 37 °C for the indicated timepoints. Platelets were also spread on fibrinogen (100 μ g/ml) coated coverslips in parallel. Coverslips were washed with PBS and fixed with 4% PFA for 10 min. The cells were then permeabilised with 0.3% Triton X100 for 5 min and stained with a combination of 1 μ g/ml TRITC phalloidin (grey; red on the merged image) and 15 μ g/ml Hoechst 33342 (grey) for 30 min at room temperature. Following this, coverslips were mounted onto glass slides with ProLong Antifade Mountant and images were obtained with a Zeiss ApoTome.2 fluorescence microscope equipped with a 40x oil immersion objective. (A) Representative images from three independent experiments. Scale bar represents 20 μ m. Arrowheads indicate examples of clusters of scavenged bacteria by platelets. (B) Adhesion of cells at each timepoint were calculated via manual counting. (C) Surface area of platelets were calculated by thresholding images on ImageJ software. (D) Percentage of scavenging platelets per field was counted manually from a total of 40 fields (image size 165.59 μ m x 110.39 μ m) per condition. (E) Average number of bacteria scavenged by platelets was calculated as outlined in section 2.4.8. Data are presented as means \pm SEM of three independent experiments, (* $p < 0.05$, ** $p < 0.01$ and *** $p < 0.001$).

3.5 Effect of pH and plasma concentration on the scavenging properties of platelets

We have identified in previous sections (3.3.1) that plasma is critical in facilitating platelet scavenging properties. Next, it was decided to investigate this further and test the ability of platelets in PRP to scavenge bacteria when exposed to varying proportions of plasma.

Resuspending PRP in different proportions of buffer inevitably means the concentration of plasma proteins present in the final platelet suspension may vary considerably between the different groups and this in turn could potentially affect the pH of the final platelet suspension. It has been widely accepted for pH to play a pivotal role in modifying cellular activity and a number of early studies have confirmed the possibility of this in context of platelet aggregation (Djaldetti *et al.*, 1979; Green *et al.*, 1978). Therefore, it was decided to first determine the pH of platelets resuspended in different proportions of plasma with the hypothesis in mind that the pH may have an effect.

PRP isolated from whole blood was diluted to 1×10^7 platelets/ml in varying proportions of plasma and/or MTB, such that the following final percentages of plasma in the platelet suspension were obtained: 0 (essentially equivalent to WP), 5, 10, 20, 50, 100%. The pH of plasma and MTB were also tested. pH readings were taken immediately upon resuspending platelets as well as after 1h and 2h of incubation at 37°C.

Figure 3.9 shows the pH values obtained for platelets resuspended in different proportions of plasma over time. It can be seen that the pH of MTB remained constant at pH 7.4 with time. By contrast, the pH of plasma increased proportionally with time from 7.46 when pH was measured at 0h to pH 7.72 and 7.88 at 1h ($P < 0.05$) and 2 h ($P < 0.001$), respectively.

An increase in pH over time was observed in all samples containing platelets (Figure 3.9). It was also revealed that the pH of platelet suspension increased as the proportion of plasma used to resuspend platelets increased, thus suggesting a probable association between proportion of plasma used and pH. In fact, it is demonstrated in Figure 3.9 that platelets resuspended in up to 10% plasma had very little changes in pH over time. However,

platelets resuspended in higher proportions of plasma demonstrated an increase in pH with time proportional to the concentration of plasma, with pH of 7.60 and 7.72 observed for platelet suspensions resuspended in 20% and 50% plasma ($P < 0.05$ when compared to 0h control), respectively, at 2h. As for platelets resuspended in 100% plasma the pH values recorded were above the physiological pH of blood at 1h ($P < 0.05$) and more evidently at 2h ($P < 0.001$).

As previously mentioned, data from a number of studies have demonstrated the influence of pH on platelet functions. The results published implies that changes in pH, regardless of how small, should not be considered trivial with regards to their effects on the properties of platelets. Henceforth, it was decided to examine the effect of resuspending platelets in various proportions of plasma on their scavenging properties.

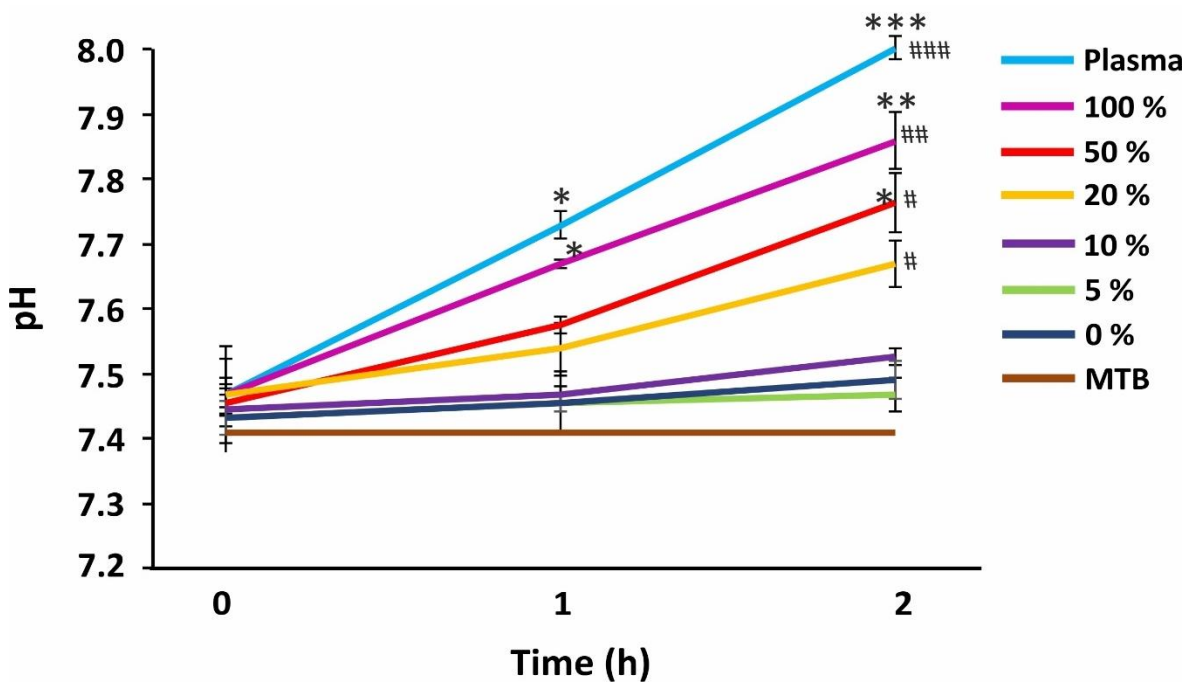


Figure 3.9 The effect of plasma concentration on the pH of platelet suspensions. PRP was diluted to 1×10^7 /ml in variable proportions of plasma and MTB such that the final percentage of plasma in PRP was as indicated. pH readings were then taken at 0, 1 and 2h post incubation at 37°C. The pH of MTB and plasma were also tested. Results are presented as means \pm SEM from three independent experiments, (* $p < 0.05$, ** $p < 0.01$ and *** $p < 0.001$). Asterisks indicates the significance between 1h and 2h within the same condition while hash sign indicates the significance between the conditions relative to 0% at 2h.

PRP and plasma were obtained from healthy blood donors and platelets were diluted to 1×10^7 /ml in MTB or plasma to obtain suspensions varying in the final concentrations of plasma (0, 5, 10, 20, 50 and 100%). Bacterial scavenging assays were then conducted as described in section 3.3.1.

Along with the scavenging assay, a separate set of *S. aureus* coated coverslips were prepared and different percentages of plasma (in the absence of platelets) were added. These coverslips were processed in the same way. This was performed to allow the observation of any effects of plasma proportions on bacterial adherence to coverslips.

It is evident from Figure 3.10A that platelets in the presence of plasma have the ability to scavenge bacteria, and as expected platelets resuspended in MTB lacked the capacity to scavenge *S. aureus* Newman. Figure 3.10B demonstrates the number of platelets per field adhered on *S. aureus* Newman. It can be observed that the results obtained were comparable (with the number of adhered platelets ranging from 28-34/field between platelets resuspended in varying proportions of plasma) and no statistical difference was found.

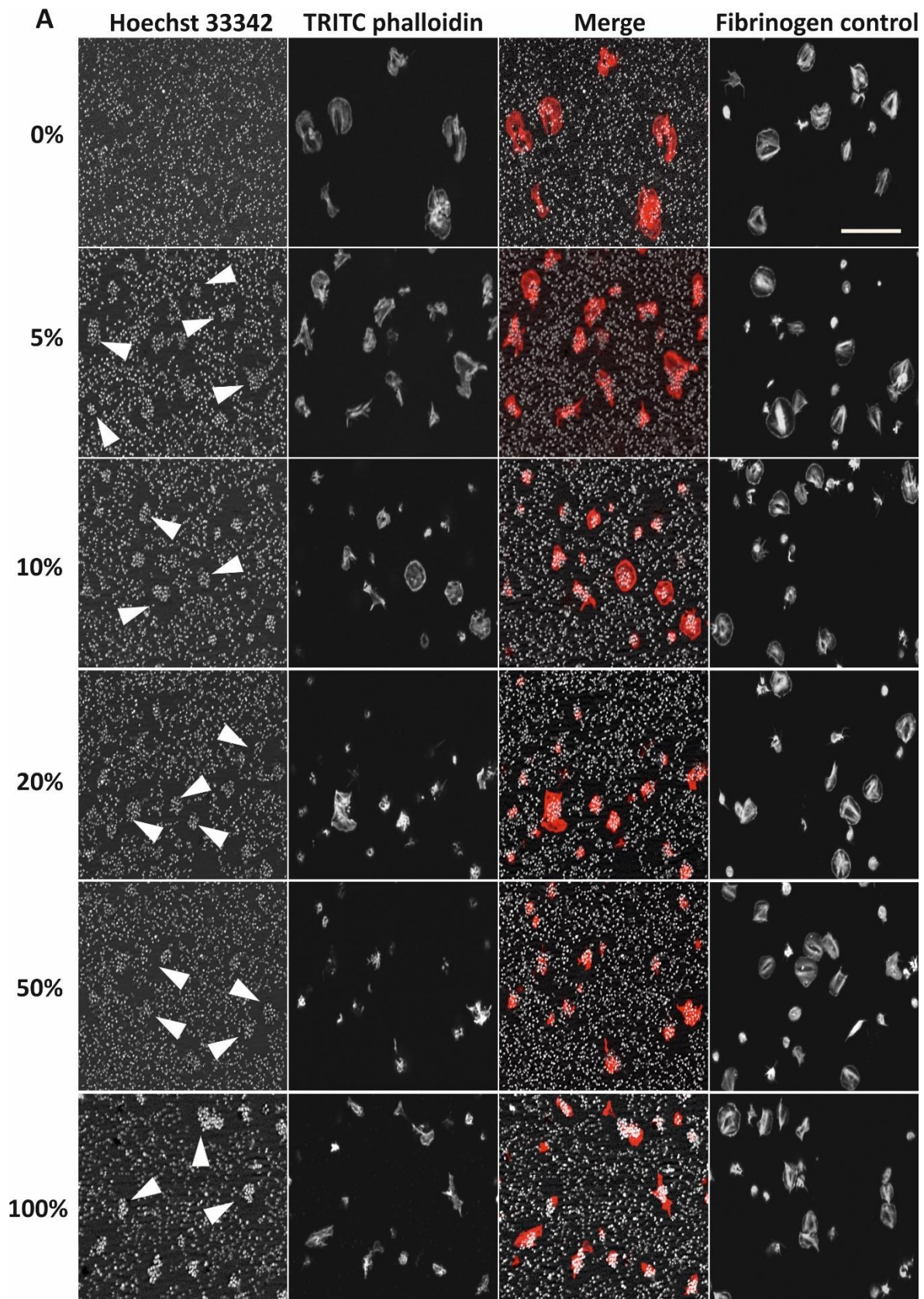
Similarly, the surface area of platelets resuspended in different proportions of plasma and placed on bacteria were also found to be comparable between the different groups of platelets, with surface area of platelets ranging from 29 to 34 μm^2 (Figure 3.10C). The same was found for platelets spread on fibrinogen whereby the surface area of platelets ranged from 32 to 39 μm^2 .

At closer examination it can be observed that there is a small difference in the ability of platelets to scavenge bacteria between PRP resuspended in different proportions of plasma (Figure 3.10D). Although statistically insignificant, it was found that the percentage of platelets able to scavenge bacteria correlated inversely with the proportion of plasma used to resuspend platelets ($94 \pm 4\%$ with 5% plasma vs $82 \pm 3\%$ with 100% plasma). Similarly, minimal differences were observed between the results obtained for the number of bacteria scavenged by platelets (Figure 3.10E).

As with the percentage of platelets able to scavenge bacteria, the numbers of bacteria scavenged per platelet was also found to be inversely proportional to the proportion of plasma used to resuspend platelets, though again statistically this was calculated to be insignificant. The mean number of bacteria scavenged by a platelet was found to be between 21-26.

The results obtained from this part of the experiment suggests that platelets are able to scavenge bacteria given plasma is present. Moreover, since no significant differences were observed between the ability of platelets to scavenge and the number of bacteria scavenged per platelet, it can be assumed that the presence of plasma acts as an all or nothing factor when determining the ability of platelets to scavenge.

Figure 3.10F illustrates the coverage of bacteria to be comparable between platelets resuspended in different proportions of plasma. This is confirmed in Figure 3.10G where the percentage of bacterial coverage on coverslips was found to be unaffected by the different proportions of plasma as no apparent changes were observed between the groups, with percentage bacterial coverage ranging between 21 and 26%.



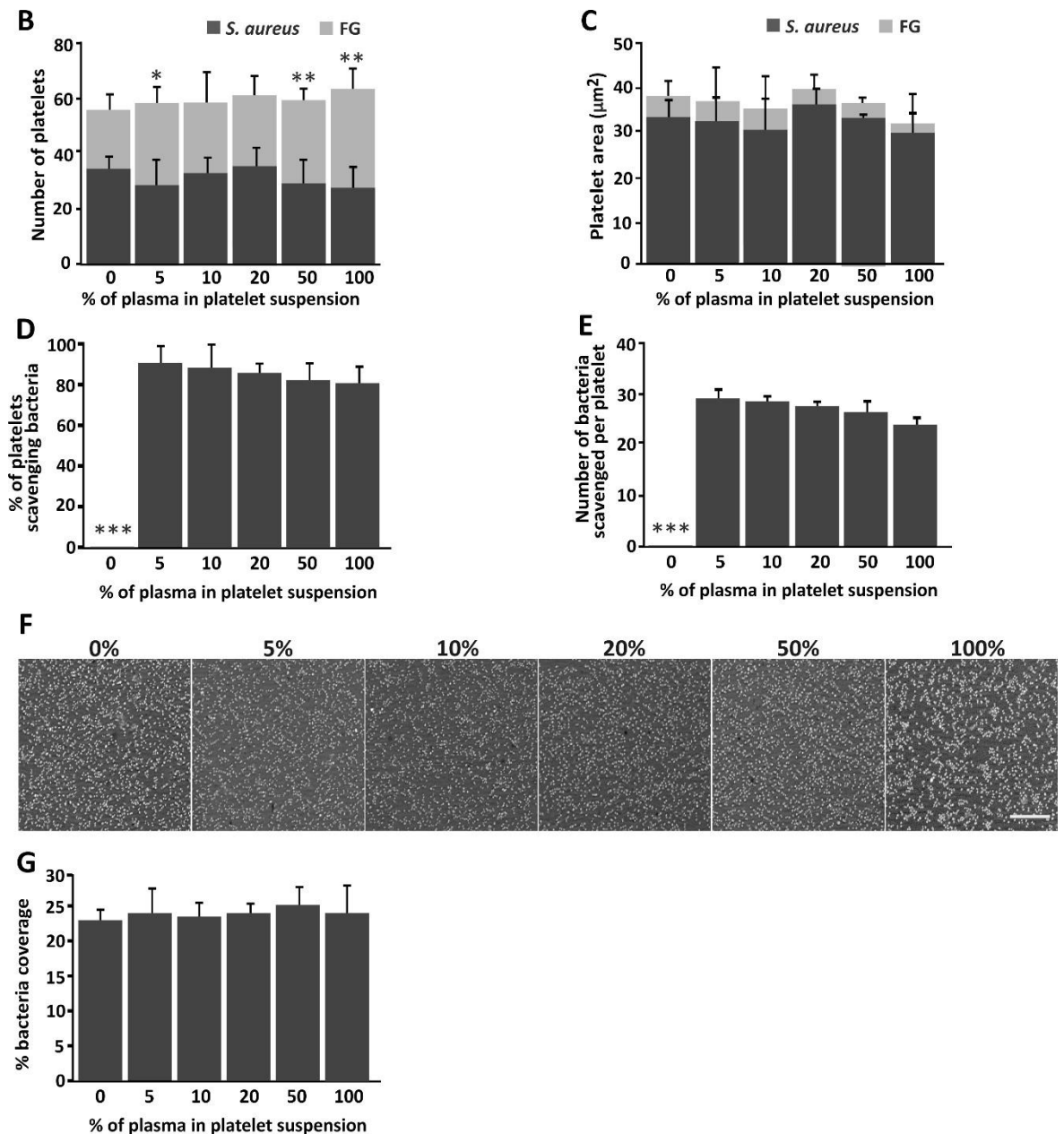


Figure 3.10 Effect of the concentration of plasma on platelets' ability to scavenge *S. aureus* Newman. PRP was diluted to 1×10^7 /ml in varying proportions of plasma and MTB such that the final percentage of plasma was as indicated. 200 μl of platelet suspension were then placed on coverslips containing immobilised *S. aureus* Newman or fibrinogen (100 $\mu\text{g}/\text{ml}$, control) and incubated at 37°C for 1 h. Cells were subsequently washed with PBS, fixed, permeabilised and incubated with a combination of 1 $\mu\text{g}/\text{ml}$ TRITC phalloidin (grey, red on the merged image) and 15 $\mu\text{g}/\text{ml}$ Hoechst 33342 (grey) for 30 min at room temperature. Coverslips were then mounted onto microscope slides and microscope images were obtained by using Zeiss ApoTome.2 fluorescence microscope equipped with a 40x oil immersion objective. (A) Representative images from three independent experiments. Arrowheads indicate examples of clusters of bacteria scavenged by platelets. Scale bar represents 20 μm . (B) Number of platelets per field and (C) the surface area of platelets was determined. (D) Percentage of platelets scavenging bacteria and (E) the number

of bacteria scavenged per platelet were calculated as outlined in section 2.3.8. (F) Varying proportions of plasma diluted with MTB were placed on coverslips coated with *S. aureus* Newman. Coverslips were processed as above but stained only with 15 µg/ml Hoechst 33342. Scale bar represents 20 µm. (G) Bacterial coverage on coverslips was calculated by thresholding images on ImageJ software. Data are presented as means ± SEM of three independent experiment each performed in duplicate, (* $p < 0.05$, $p < 0.01$ and *** $p < 0.001$).

The results obtained from these set of experiments suggests that the proportion of plasma and in turn the pH does not alter the scavenging properties of platelets significantly. In addition to this, data revealed the presence of plasma to be critical for the scavenging ability of platelets since platelets in the absence of plasma failed to scavenge (Figure 3.10). Likewise, we observed that the maximal ability of platelets to scavenge was already attained when platelets in PRP were diluted in as low as 5% plasma, which is the proportion nearest to the physiological pH of blood. Therefore, it was decided for PRP to be diluted in MTB while ensuring a minimum of 5% final plasma proportion is attained in platelets for all subsequent experiments.

In parallel with the above, an experiment was conducted to study the components present in the aspirated suspension following incubation of platelets on bacteria and to inspect the extent to which plasma affects the attachment of both bacteria and platelets to the coverslips. Therefore, unbound cells and medium from each coverslip were carefully pipetted into separate labelled microcentrifuge tubes following the 1 h incubation of platelets on bacteria at 37°C. These were then spun briefly onto poly-L-lysine coated coverslips to allow the determination of the content present in the aspirated mixture. All coverslips were then processed as previously mentioned.

The fluorescence microscopy images revealed nothing extraordinary. The microscopy results are presented in the Appendices (Figure 7.2). As expected, bacteria and platelets were present in the mixture which can be assumed to be potentially the cells that were washed off since they were loosely bound or unbound. No differences between the various percentages of plasma samples were observed.

3.6 Molecular mechanisms regulating scavenging of bacteria by platelets

Having established a method to analyse quantitatively scavenging of *S. aureus* Newman by platelets, the aim was to understand the molecular mechanisms involved in the process of platelet-scavenging of bacteria. We used an approach that involves examining the effects of inhibitors of specific signalling pathways on this process.

In the subsequent sections we aim to investigate the involvement of Rho GTPases, specifically RhoA, Rac1 and Cdc42 in aiding platelet-scavenging of bacteria. In addition to this, we intend to focus on tyrosine kinase (TK) signalling pathway in platelets and how inhibition of certain molecules/receptors may potentially modify the ability of platelets to scavenge bacteria.

To this end, in the ensuing sections, inhibitors of critical cytoskeletal structures and platelet TK signalling pathways were utilised to determine the role of these elements in the ability of platelets to scavenge infectious agents. Furthermore, since LTA continues to be used as the reference method to allow rapid determination of platelet function in patients, we conducted LTA in parallel with scavenging assays to explore any potential effects of the inhibitors in modifying platelet functions.

3.6.1 Cytoskeletal inhibitors diminish the scavenging properties of platelets

Upon platelet activation, cells undergo morphological changes which are predominately mediated by cytoskeletal proteins. Rho family GTPases are master regulators of the actin cytoskeleton (Finkenstaedt-Quinn *et al.*, 2015; Shin *et al.*, 2017) and numerous studies have shown evidence of their critical involvement in regulating the remodelling of the actin cytoskeleton and ultimately modifying platelet aggregation and spreading response (Akbar *et al.*, 2016 & Shang *et al.*, 2012a).

Rhosin is an example of a Rho GTPase inhibitor, and it has been described to target the attachment of RhoA to GEFs such as LBC, DBL, p115 and LARG, leading to alterations in a number of platelet functions such as aggregation and spreading (Shang *et al.*, 2012b).

Similarly, NSC 23766 is another example of an inhibitor that targets the actin cytoskeleton. NSC 23766 selectively inhibits Rac1-GEF interaction and thus inhibits Rac1 activation by Rac-specific GEFs such as TrioN and Tiam1 (Levay *et al.*, 2013).

Another pharmacological agent which interferes with the regulation of the actin cytoskeleton is the Cdc42 activity-specific inhibitor CASIN. CASIN has been reported to specifically inhibit endogenous Cdc42 activity by binding to it and obstructing GTP loading exchange reactions (Akbar *et al.*, 2016). Comparably latrunculin A (Lat-A) also targets actin cytoskeleton organisation, however unlike Rho GTPase inhibitors mentioned previously, Lat-A has direct effects on the actin cytoskeleton as it binds to and sequesters monomeric actin, which results in the disassembly of the resting actin cytoskeleton, which in turn ultimately regulates platelet processes i.e. granule content secretion and spreading (Coué, Brenner *et al.*, 1987; Rosado *et al.*, 2000; Spector *et al.*, 1999).

Although the above compounds directly or indirectly alter the actin cytoskeleton reorganisation and thus platelet activation, at present no studies investigating the effects of such pharmacologic agents in relation to platelet scavenging properties has been conducted. Therefore, in order to provide insight into the field and to allow a better understanding of the molecular mechanisms involved, as well as the differential role(s) of Rho GTPases during platelet scavenging, it was decided to incorporate the inhibitors into the scavenging assay.

The initial step was to determine the appropriate concentration of the inhibitors to use in the scavenging assay. Therefore, literature was thoroughly reviewed for information on the inhibitors and it was decided to use: Rhosin at 30 μ M (Shang *et al.*, 2012a; Akbar *et al.*, 2016a), NSC 23766 at 70 μ M (Pandey *et al.*, 2009; Dütting *et al.*, 2015), CASIN at 10 μ M (Akbar *et al.*, 2010; Antkowiak *et al.*, 2016) and Lat-A at 20 μ M (Woronowicz *et al.*, 2010).

To ensure the concentrations of inhibitor chosen were suitable, an LTA experiment was conducted whereby PRP was incubated at 37°C with the above inhibitors at the indicated concentrations for 10 min (except for Lat-A, which was incubated for 30 min). Following the incubation, standard LTA was performed with TRAP-6 (3 μ M) as the agonist.

Results from this experiment demonstrated that treating the platelets with the cytoskeletal inhibitors at the mentioned concentrations inhibited TRAP-6-induced platelet aggregation (Figure 3.11). Therefore, having confirmed the concentration of inhibitors used were suitable to block TRAP-6-mediated platelet aggregation response, assays were conducted with the above inhibitors to explore their effects on the scavenging properties of platelets.

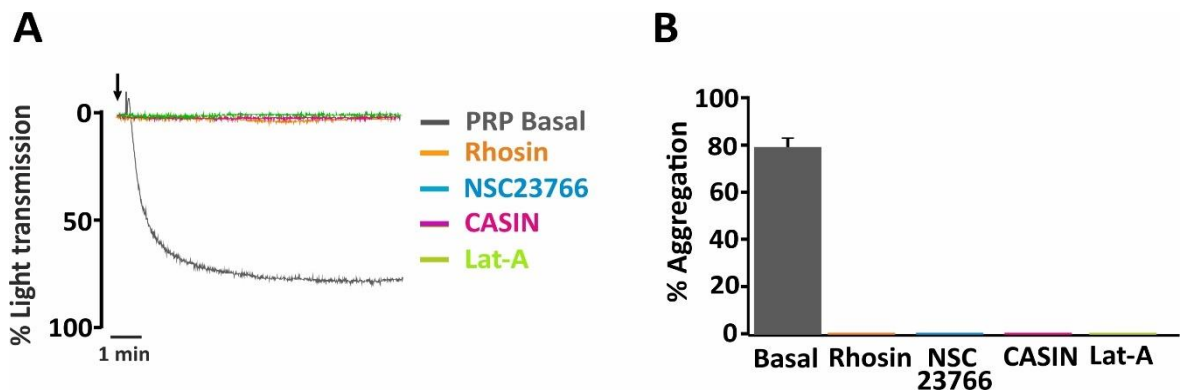


Figure 3.11 Cytoskeleton inhibitors block platelet aggregation. (A) Representative LTA trace. PRP (2.5×10^8 /ml) was incubated with cytoskeletal inhibitors rhosin ($30 \mu\text{M}$), NSC23766 ($70 \mu\text{M}$) or CASIN ($10 \mu\text{M}$) for 10 min, or Lat-A ($20 \mu\text{M}$) for 30 min prior to stimulation with TRAP-6 ($3 \mu\text{M}$). LTA was conducted for 10 min. (B) Data are presented as means \pm SEM of two independent experiments.

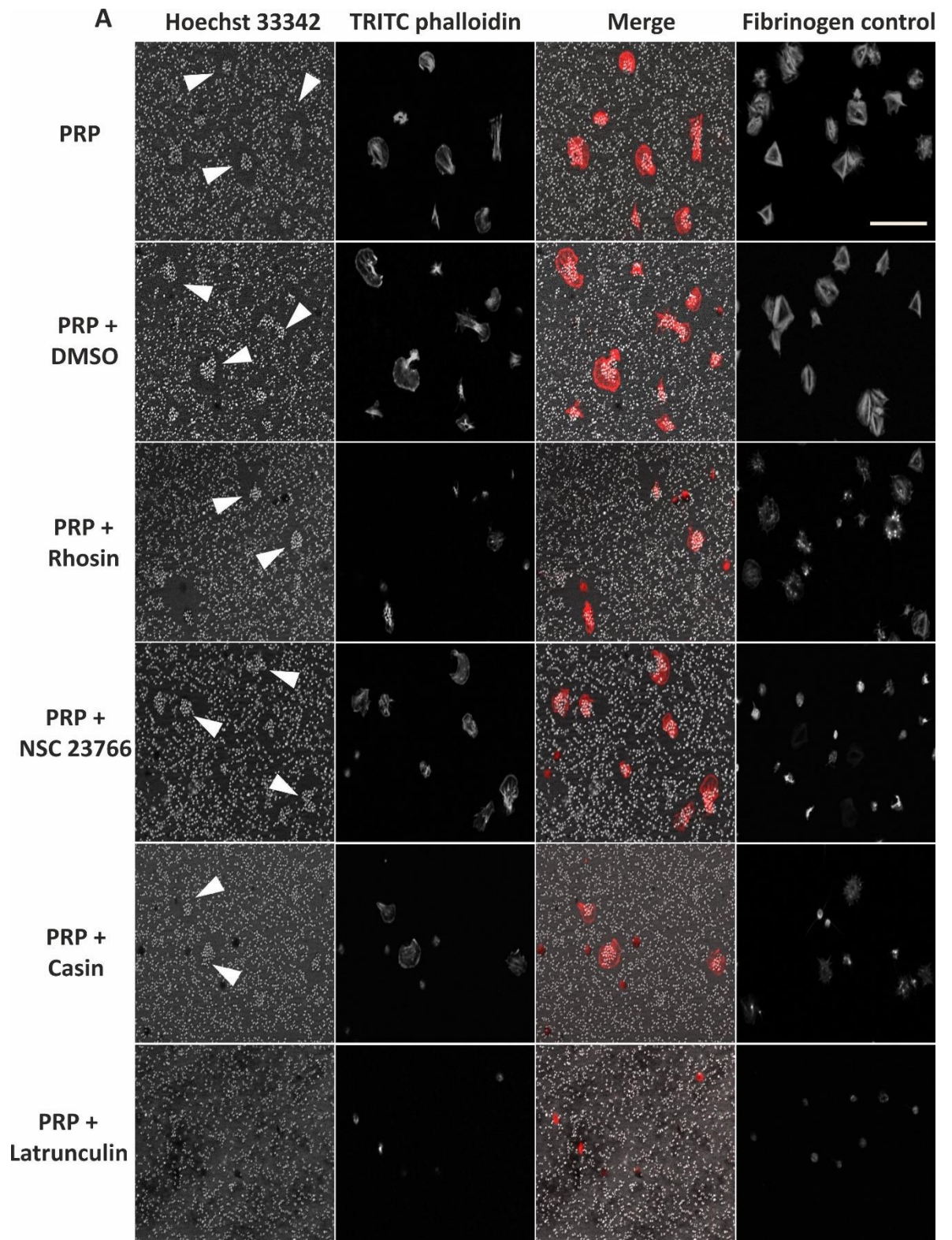
PRP was diluted to 1×10^7 cells/ml with MTB to a final plasma proportion of 5%. Platelets were then treated with the inhibitors at the concentrations, time and temperature indicated above. Dimethyl sulfoxide (DMSO) was used to prepare the inhibitor stocks and so one set of platelets (referred to as PRP-DMSO) was given DMSO to a final 1:1000 dilution. This was done to ensure any effects observed in the platelet inhibitor groups were in fact due to the inhibitors themselves and not caused by the presence of DMSO. After incubation, platelets were placed on *S. aureus* Newman coated coverslips and incubated for 1 h at 37°C . Platelets were also spread on $100 \mu\text{g/ml}$ fibrinogen in parallel. Coverslips were then processed as detailed in section 3.4.

Representative examples of the effect of cytoskeletal inhibitors on the ability of platelets to scavenge bacteria and spread on fibrinogen is shown in Figure 3.12A. As for the ability of platelets to adhere to bacteria and fibrinogen, it can be seen in Figure 3.12B that only Lat-A caused a significant decrease in the number of platelets per field on *S. aureus* Newman (a mere 7 ± 6 platelets/field) compared to the control (38 ± 4 platelets/field;

P<0.01). A similar observation was made for platelets treated with Lat-A inhibitors and then spread on fibrinogen (36 ± 3 platelets/field in the Lat-A treated vs 58 ± 5 in the control; P<0.05). With regard to platelet surface area, it can be observed in Figure 3.12C that a substantial reduction in surface area was found among all cytoskeletal inhibitor-treated platelet groups that were incubated on *S. aureus* Newman. This difference in surface area was most striking when platelets were treated with Lat-A since a complete lack in ability to spread was noted upon placing Lat-A-treated platelets on bacteria ($4\pm 1 \mu\text{m}^2$, P<0.001). Data obtained from un(treated) platelets spread on fibrinogen illustrates similar results to that obtained for platelets incubated on bacteria, in that a significant decrease in surface area was found within all inhibitor-treated platelet groups.

In the matter of platelet scavenging capacity, we observed that PRP in the absence of inhibitors, scavenged bacteria to the same capacity as formerly found in this study (Figure 3.9 and Figure 3.10). However, it is interesting to note that all Rho GTPase inhibitors impaired the capacity of platelet to scavenge immobilised *S. aureus* Newman to some extent. Rhosin caused a more than two-fold decrease in the ability of platelets to scavenge *S. aureus* Newman ($39\pm 6\%$ of scavenging platelets compared to $89\pm 6\%$ in the control; P<0.01). A decrease in the ability of platelets to scavenge was also observed upon treatment with NSC 23766 ($60\pm 6\%$) and CASIN in ($54\pm 5\%$, P<0.05). Platelets treated with Lat-A completely lacked the ability to scavenge bacteria (P<0.001) (Figure 3.12D). Surprisingly, we observed that the number of bacteria scavenged per platelet was comparable between all populations (except Lat-A platelets, that did not scavenge at all), with bacteria scavenged ranging from 18 to 25 per platelet (Figure 3.12E), suggesting the possibility of an all or nothing response.

As for PRP supplemented with DMSO, it can be noted from Figure 3.12 that PRP-DMSO had comparable results in terms of platelet adhesion (38 ± 4 platelets/field), surface area ($28\pm 1 \mu\text{m}^2$), scavenging profile ($82\pm 2\%$ of scavenging platelets) and the number of bacteria scavenged per cluster (23 ± 2), when compared to that of PRP in the absence of DMSO. Therefore, any alterations observed in the inhibitor treated platelet groups are solely an effect of the inhibitors. For the purpose of the subsequent set of experiments, PRP refers to PRP supplemented with DMSO.



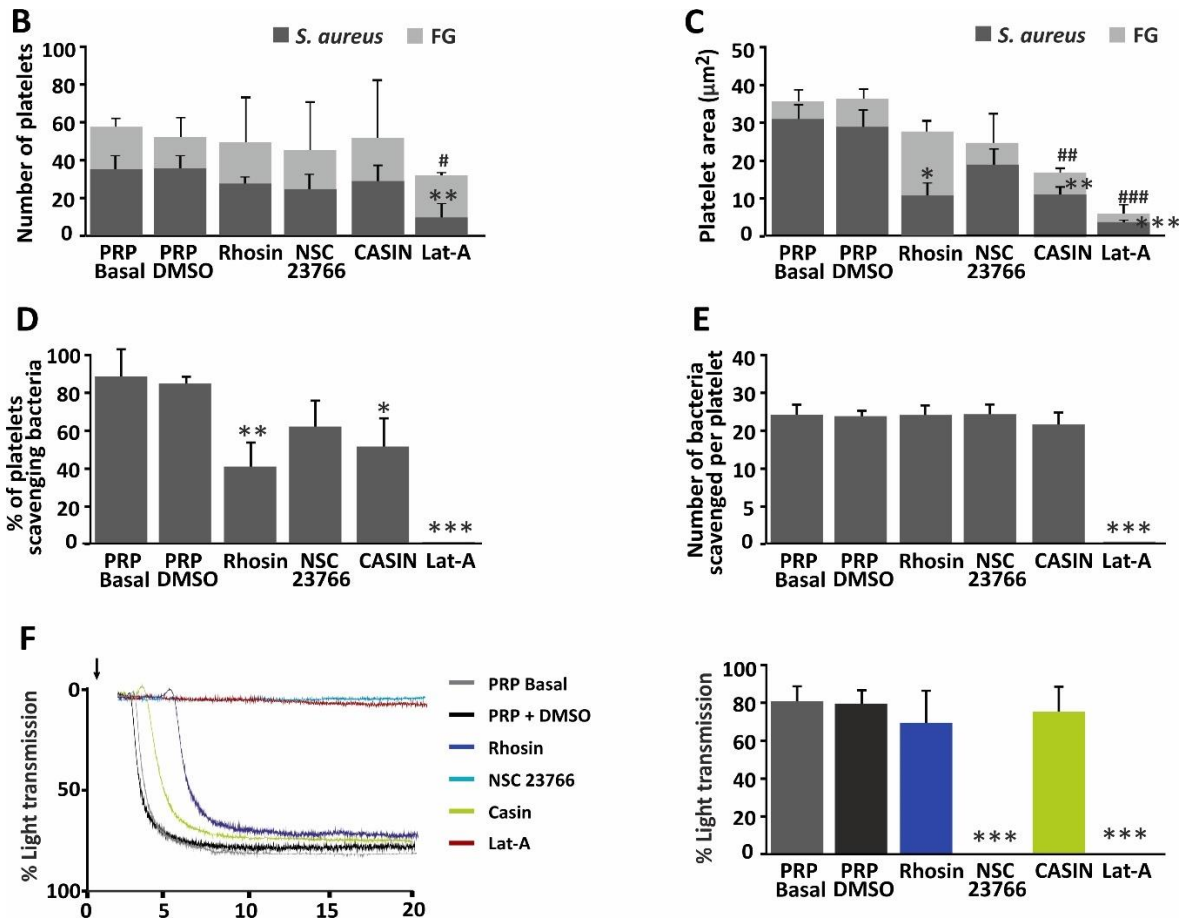


Figure 3.12 The effect of cytoskeletal inhibitors on platelet functions. PRP was diluted with MTB to 1×10^7 platelets/ml and 5% plasma and incubated with Rhosin (30 μ M), NSC 23766 (70 μ M) or CASIN (10 μ M) for 10 min, or Lat-A (20 μ M) for 30 min. PRP-DMSO received 1:1000 DMSO. 200 μ l of platelet suspension was then placed on coverslips containing immobilised *S. aureus* Newman or fibrinogen (100 μ g/ml) and incubated at 37°C for 1 h. Cells were subsequently washed with PBS, fixed, permeabilised and incubated with a combination of 1 μ g/ml TRITC phalloidin (grey; red on the merged image) and 15 μ g/ml Hoechst 33342 (grey) for 30 min at room temperature. Coverslips were mounted onto glass slides and microscope images were obtained by using a Zeiss ApoTome.2 fluorescence microscope equipped with a 40x oil immersion objective. (A) Representative images. Scale bar represents 20 μ m. Arrowheads indicate examples of clusters of scavenged bacteria by platelets. (B) The number of platelets per field and the (C) the surface area of platelets was determined. (D) Percentage of platelets scavenging bacteria and (E) the number of bacteria scavenged per platelet were calculated using ImageJ, as outlined in section 2.3.8. (F) PRP (2.5×10^8 /ml) was incubated with DMSO, Rhosin (30 μ M), NSC 23766 (70 μ M) or CASIN (10 μ M) for 10 min, or Lat-A (20 μ M) for 30 min. LTA was then conducted for 20 min and *S. aureus* Newman (OD_{600nm} 1.6) was the agonist used. Representative LTA traces are shown. Scavenging and LTA data are presented as means \pm SEM of five independent experiments. Statistical significance was calculated using one-way ANOVA (* $p < 0.05$, ** $p < 0.01$ and *** $p < 0.001$). Asterisks indicate the significance between the populations incubated on bacteria relative to the corresponding PRP basal, while the hash signs indicate the significance between the populations incubated on fibrinogen relative to PRP basal.

LTA on PRP treated with the above inhibitors at the indicated concentrations was performed alongside the scavenging assays to examine the effects of the inhibitors on platelet aggregation in response to bacteria. *S. aureus* Newman (OD_(600nm) 1.6) was used as the agonist and all LTA traces were run for a total of 20 min (Figure 3.12F).

In these experiments the lag time for the onset of platelet aggregation in the control groups (basal and DMSO treated platelets), in response to bacteria was around 2-3 min which agrees with literature (Arman *et al.*, 2014). Platelets showed comparable results in the maximum aggregation obtained in response to *S. aureus* in the absence and presence of DMSO confirming that DMSO at the concentration used here does not alter platelet function.

In terms of maximum platelet aggregation, Figure 3.12F illustrates bacteria to induce aggregation in Rhosin and CASIN-treated platelets to a similar degree to that of control groups (64±6% and 72±5% light transmission respectively). By contrast, treatment with NSC 23766 and Lat-A resulted in abolition of *S. aureus* Newman induced platelet aggregation.

Collectively, all this data suggests that disruption to the platelet actin cytoskeleton and its components has profound effects on the ability of platelets to scavenge *S. aureus* Newman and to aggregate in response to the bacteria.

3.6.2 Inhibition of platelet surface receptors FcγR11a and GPIIb/IIIa inhibits platelet aggregation and hinders platelet scavenging properties.

In the next set of experiments, we intended to investigate the effects of FcγR11a and GPIIb/IIIa, two major receptors involved in mediating platelet-bacteria interactions, in altering the scavenging properties of platelets. To address this, we used inhibitors IV.3 antibody and integrilin which target receptors FcγR11a and GPIIb/IIIa, respectively.

PRP was isolated and diluted as mentioned in section 3.6.1. Platelets were then treated with 15 µg/ml IV.3 antibody or 9 µM integrilin for 9 min and 2 min, respectively. Following incubation with the inhibitors, platelet scavenging assay and LTA were performed as

described in section 3.6.1. Platelets were also spread on 100 µg/ml fibrinogen in parallel. Coverslips were then processed as detailed in section 3.3.1. Both inhibitors were initially diluted from stocks in DMSO, PRP in the presence of 1:1000 DMSO was used as the control in all experiments. It has been established in the previous section for DMSO at the given concentration to not alter platelet functions.

Representative examples of the effect of inhibiting platelet surface receptors on the ability of platelets to scavenge bacteria and spread on fibrinogen are shown in Figure 3.13A. Arrowheads indicate clusters of bacteria scavenged by individual platelets. It is possible to see that the incubation of PRP with IV.3 ab diminishes the ability of platelets to scavenge whereas this characteristic is abolished in integrilin-treated platelets.

It can be seen in Figure 3.13B that there was a moderate decrease in the number of adhered platelets when treated with IV.3 ab (21 ± 4 platelets/field), although the differences were not statistically significant when compared to uninhibited platelets (36 ± 7 platelets/field). The same was found for platelets treated with integrilin (22 ± 6 platelet/field). No significant alterations were found in the numbers of platelets adhered to fibrinogen.

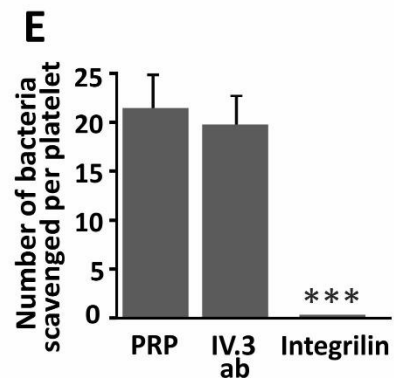
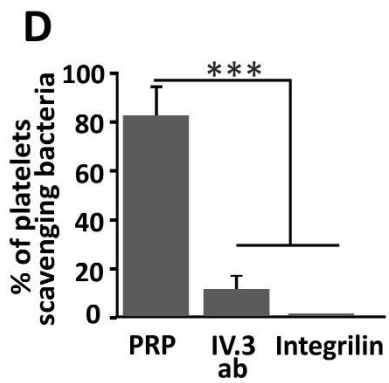
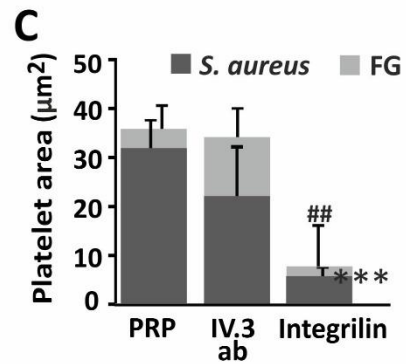
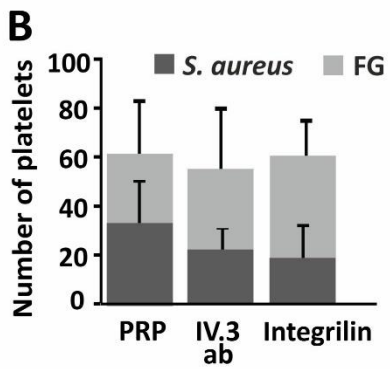
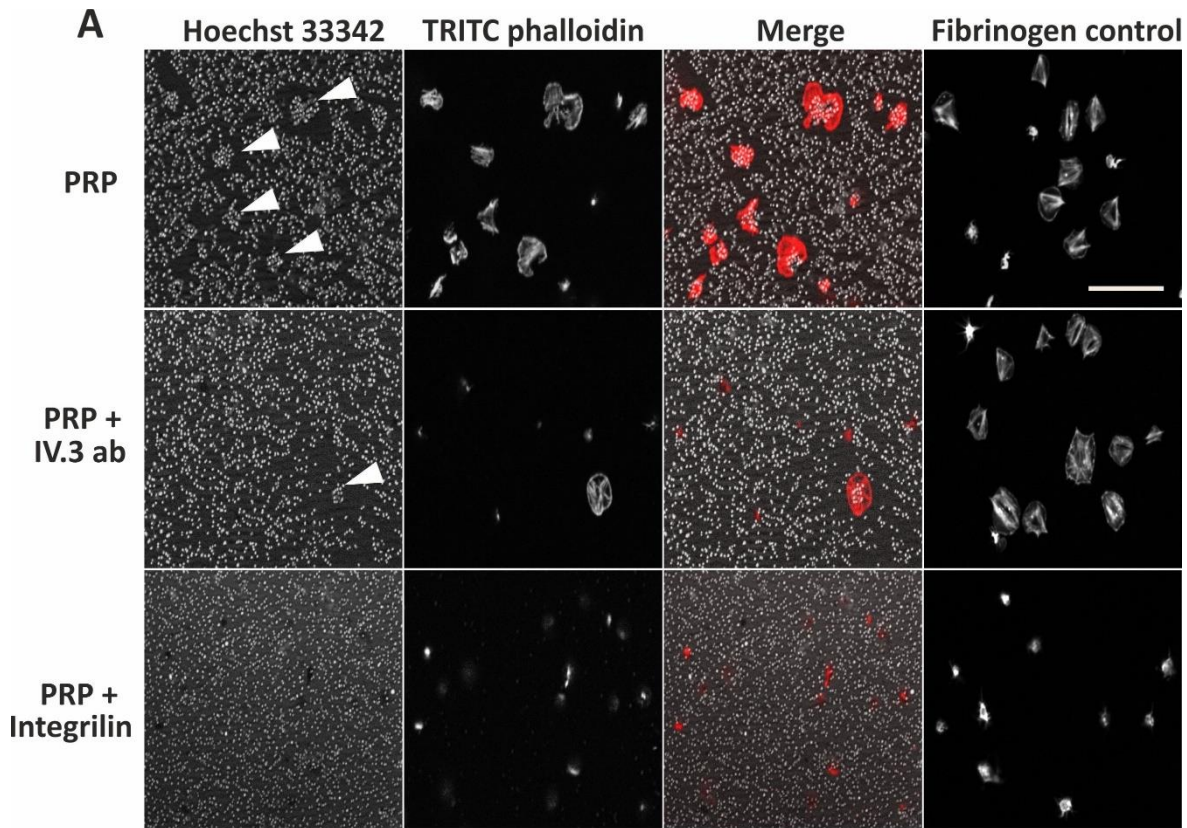
Figure 3.13C shows a decrease in surface area of platelets when incubated with IV.3 ab and placed on bacteria ($22 \pm 8 \mu\text{m}^2$) compared to untreated platelets ($31 \pm 5 \mu\text{m}^2$), although it was statistically insignificant. However, the surface area of untreated platelets and IV.3 ab-treated platelets were found to be comparable when spread on fibrinogen ($35 \pm 4 \mu\text{m}^2$ vs $34 \pm 5 \mu\text{m}^2$ respectively). We found a significant reduction in surface area of platelets with integrilin treatment compared to control both on bacteria ($6 \pm 2 \mu\text{m}^2$, $P < 0.001$) and fibrinogen ($8 \pm 7 \mu\text{m}^2$, $P < 0.01$).

Treatment of platelets with IV.3 ab resulted in a significant reduction in the ability of platelets to scavenge, since only $10 \pm 3\%$ platelets retained the ability to scavenge *S. aureus* Newman (compared to $81 \pm 5\%$ in the control; $P < 0.001$). Intriguingly, platelets treated with integrilin were found to completely lack the ability to scavenge *S. aureus* Newman ($P < 0.001$) (Figure 3.13D).

As for the number of bacteria scavenged per platelet, it was calculated for IV.3 ab treated platelets to scavenge 19 ± 4 bacteria, which was similar to the data obtained for uninhibited platelets (22 ± 5 bacteria/platelet) (Figure 3.13E).

Results gathered and evaluated from LTA traces further emphasises the importance of FcγRIIIa and GPIIb/IIIa in mediating platelet-bacteria interaction and subsequent downstream signalling. Since, both integrilin and IV.3 ab treated platelets displayed complete inhibition of *S. aureus* Newman induced platelet aggregation ($P < 0.001$ relative to control) (Figure 3.13F). The aggregation traces obtained were comparable to that of previously published results in literature, thus further supporting the notion that platelet receptors are critical modulators in platelet activation and aggregation induced by *S. aureus* Newman.

Together, data from these set of experiments reveal that inhibiting platelet receptors, specifically FcγRIIIa and GPIIb/IIIa, impedes platelet scavenging properties suggesting that these receptors are critically involved in initiating signalling which targets aspects of platelet scavenging functions.



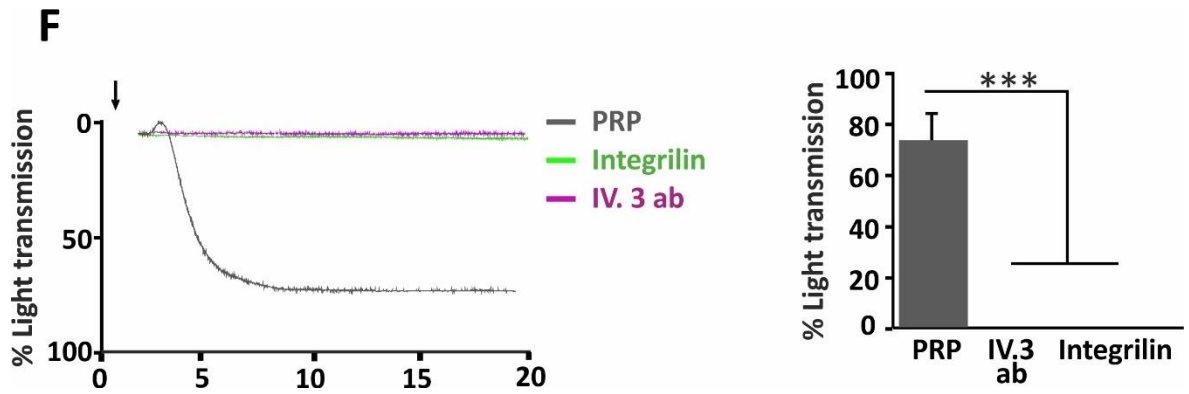


Figure 3.13 The effect of platelet surface receptor inhibitors on platelet functions. PRP was diluted with MTB to 1×10^7 platelets/ml and 5% plasma and incubated with IV.3 ab ($15 \mu\text{g/ml}$) or integrilin ($9 \mu\text{M}$) for 9 min and 2 min, respectively. PRP control received 1:1000 DMSO. $200 \mu\text{l}$ of platelet suspension were then placed on coverslips containing immobilised *S. aureus* Newman or fibrinogen ($100 \mu\text{g/ml}$) and was incubated at 37°C for 1 h. Cells were subsequently washed with PBS, fixed, permeabilised and incubated with a combination of $1 \mu\text{g/ml}$ TRITC phalloidin (grey; red on the merged image) and $15 \mu\text{g/ml}$ Hoechst 33342 (grey) for 30 min at room temperature. Coverslips were then mounted onto glass slides with ProLong Antifade Mountant and microscope images were obtained by using a Zeiss ApoTome.2 fluorescence microscope equipped with a 40x oil immersion objective. (A) Representative images. Scale bar represents $20 \mu\text{m}$. Arrowheads indicate examples of clusters of scavenged bacteria by platelets. (B) The number of platelets per field and the (C) the surface area of platelets was determined. (D) Percentage of platelets scavenging bacteria and (E) the number of bacteria scavenged per platelet were calculated using ImageJ, as outlined in section 2.3.8. (F) PRP with DMSO ($2.5 \times 10^8/\text{ml}$) was incubated with the platelet receptor inhibitors IV.3 ab ($15 \mu\text{g/ml}$) or integrilin ($9 \mu\text{M}$) for 9 min and 2 min, respectively. *S. aureus* Newman ($\text{OD}_{600\text{nm}}$ 1.6) was used as the agonist. LTA was conducted for 20 min. Representative LTA traces are shown. Scavenging and LTA data are presented as means \pm SEM of five independent experiments. Statistical significance was calculated using one-way ANOVA (** $p < 0.01$ and *** $p < 0.001$). Asterisks indicate the significance between the populations incubated on bacteria relative to the corresponding PRP basal, while the hash signs indicate the significance between the populations incubated on fibrinogen relative to PRP basal.

3.6.3 Inhibition of tyrosine kinase signalling pathways inhibits platelet aggregation and alters platelet scavenging properties

Having established the importance of platelet surface receptors in inducing bacteria-mediated platelet aggregation and scavenging properties we next aimed to explore the effects of a number of therapeutic drugs which have been identified to target critical tyrosine signalling pathways, and whether they modify platelet functions: scavenging and aggregation properties specifically. To address this, we used inhibitors PRT318 (PRT), dasatinib and ibrutinib which target Syk, Src and BTK, respectively. Acalabrutinib, a more BTK-specific inhibitor than ibrutinib was also utilised in the experiment.

PRP obtained from healthy donors was diluted to either 2.5×10^8 or 1×10^7 cells/ml and incubated with $5 \mu\text{M}$ ibrutinib for 5 min, $15 \mu\text{M}$ acalabrutinib for 5 min, $4 \mu\text{M}$ dasatinib for 2 min or $10 \mu\text{M}$ PRT for 2 min. After incubation, platelet scavenging assays and LTA were performed as described previously in section 3.4.1. Platelets were also spread on $100 \mu\text{g/ml}$ fibrinogen in parallel. Coverslips were then processed as detailed in section 3.3.1.

Figure 3.14A illustrates representative examples of scavenging properties of platelets treated with BTK, Src or Syk signalling inhibitors. It is evident for TK signalling inhibitor-platelets to lack the ability to scavenge *S. aureus* Newman, except for acalabrutinib-treated platelets. The capacity of (un)inhibited platelets to adhere and spread on fibrinogen is also shown.

A decrease in the number of platelets adhered to *S. aureus* Newman was observed in all inhibitor-treated platelet groups (Figure 3.14B). Both PRT and ibrutinib-treated platelets showed a significant decrease in adhesion (11 ± 4 and 17 ± 3 platelets/field, respectively) when compared to control (37 ± 4 platelets/field; $P < 0.05$). No significant alterations were found in the numbers of platelets adhered to fibrinogen.

In the matter of platelet surface area, it can be seen in Figure 3.14C that there was a significant decrease in the surface area of platelets treated with PRT ($13 \pm 5 \mu\text{m}^2$, $P < 0.05$) or dasatinib ($8 \pm 3 \mu\text{m}^2$, $P < 0.01$) compared to control platelets ($30 \pm 4 \mu\text{m}^2$) and a marginal but

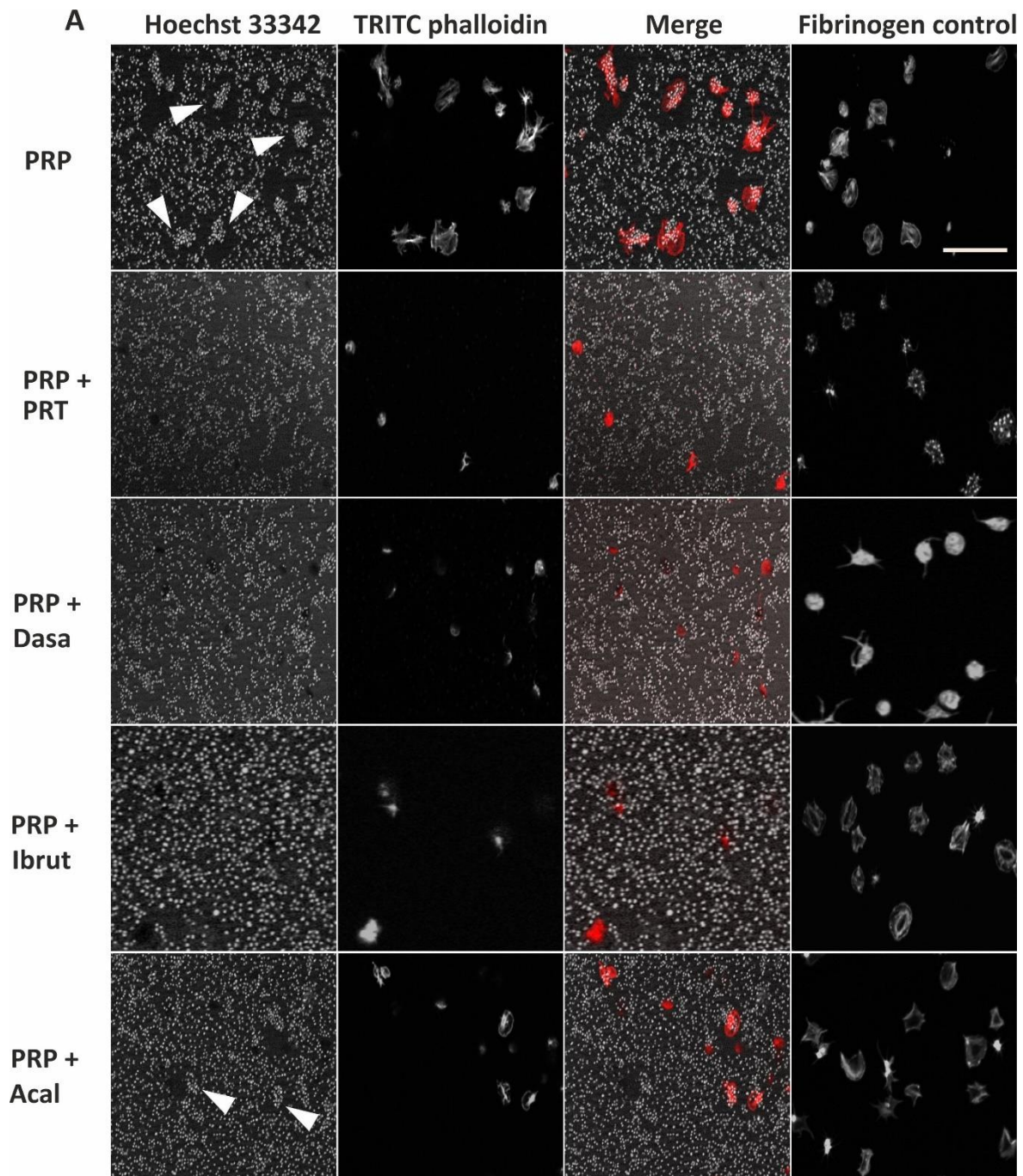
not significant decrease in platelets treated with BTK inhibitors. Only slight differences in the surface area of platelets spread on fibrinogen was observed between the different inhibitor-treated platelet groups when compared to the control group (Figure 3.14C).

Coherent with earlier data obtained, Figure 3.14D shows uninhibited platelets to possess the ability to scavenge *S. aureus* Newman ($81\pm 5\%$ scavenging platelets/field). By comparison, a complete lack in ability to scavenge *S. aureus* Newman ($P<0.001$) was found upon incubating platelets with PRT, dasatinib or ibrutinib. Acalabrutinib-treated platelets demonstrated a drastically reduced ability when compared to uninhibited platelets. In fact, only $8\pm 3\%$ of platelets had the capacity to scavenge bacteria.

The average number of bacteria scavenged per platelet was found to be comparable between control platelets (22 ± 2 bacteria/platelet) and platelets treated with acalabrutinib (20 ± 1 bacteria/platelet) (Figure 3.14E).

Interestingly, aggregation induced by *S. aureus* Newman was completely inhibited by all TK inhibitors ($P<0.001$) (Figure 3.14F).

The results obtained from this set of experiments confirm that TK inhibitors to induce varying degree of modifications in the capacity of platelets to scavenge bacteria and aggregate when exposed to bacteria. Thus, the data gathered reinforces TK molecules to play a critical role in facilitating platelet functions.



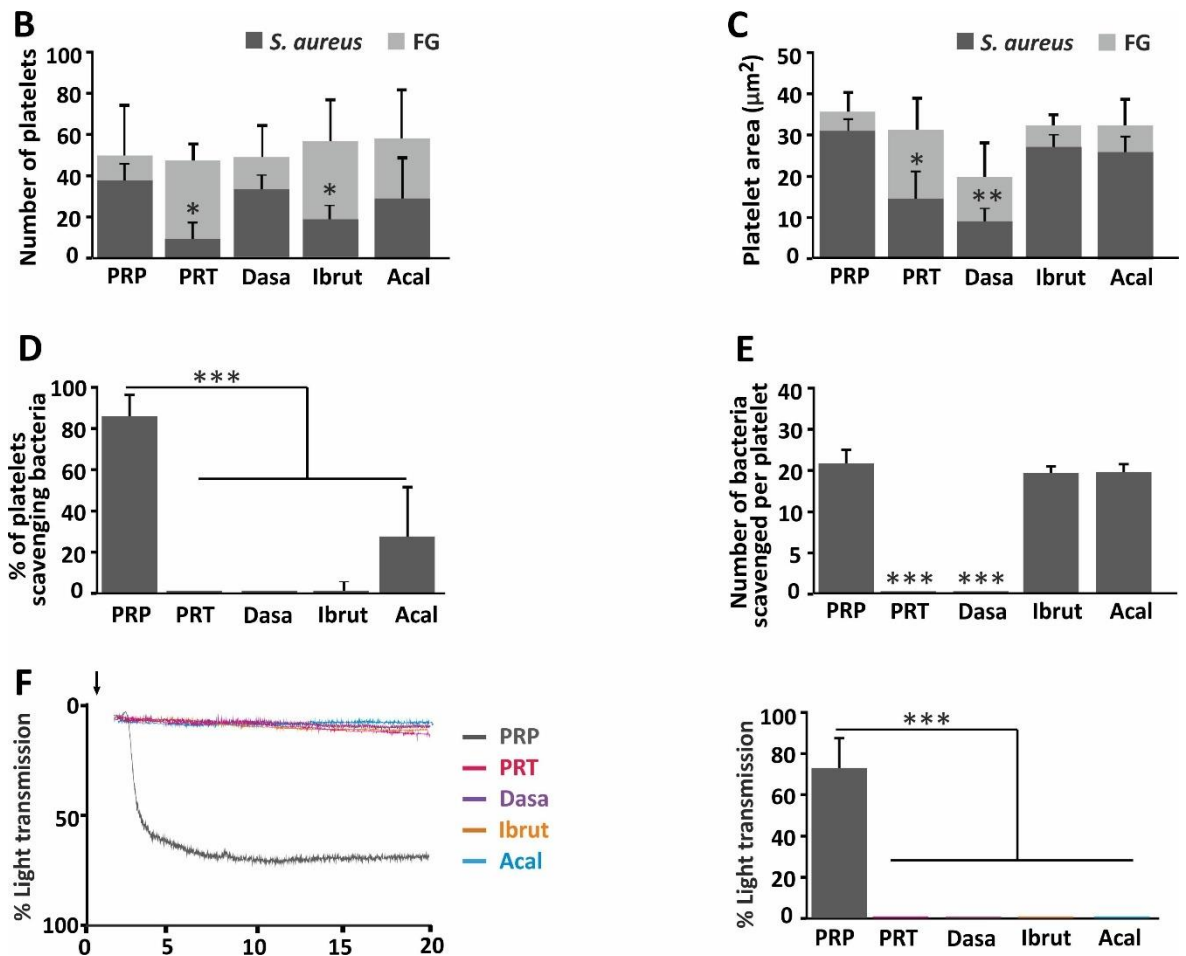


Figure 3.14 The effect of BTK, Src and Syk signalling inhibitors on platelet scavenging and aggregation. PRP was diluted with MTB to 1×10^7 platelets/ml and 5% plasma and incubated with $5 \mu\text{M}$ Ibrutinib (Ibrut) or $15 \mu\text{M}$ acalabrutinib (Acal) for 5 min; or $4 \mu\text{M}$ dasatinib (Dasa) or $10 \mu\text{M}$ PRT318 (PRT) for 2 min. PRP control received 1:1000 DMSO. $200 \mu\text{l}$ of platelet suspension was then placed on coverslips treated with immobilised *S. aureus* Newman or fibrinogen ($100 \mu\text{g/ml}$) and incubated at 37°C for 1 h. Cells were subsequently washed with PBS, fixed, permeabilised and incubated with a combination of $1 \mu\text{g/ml}$ TRITC phalloidin (grey; red on the merged image) and $15 \mu\text{g/ml}$ Hoechst 33342 (grey) for 30 min at room temperature. Coverslips were then mounted onto glass slides with ProLong Antifade Mountant and microscope images were obtained by using a Zeiss ApoTome.2 fluorescence microscope equipped with a $40\times$ oil immersion objective. (A) Representative images. Scale bar represents $20 \mu\text{m}$. Arrowheads indicate examples of clusters of scavenged bacteria by platelets. (B) The number of platelets per field and the (C) the surface area of platelets was determined. (D) Percentage of platelets scavenging bacteria and (E) the number of bacteria scavenged per platelet were calculated using ImageJ, as outlined in section 2.3.8. (F) PRP in the presence of DMSO ($2.5 \times 10^8/\text{ml}$) was incubated with the tyrosine kinase receptor inhibitors: $5 \mu\text{M}$ Ibrutinib (Ibrut) or $15 \mu\text{M}$ acalabrutinib (Acal) for 5 min; or $4 \mu\text{M}$ dasatinib (Dasa) or $10 \mu\text{M}$ PRT318 (PRT) for 2 min prior to addition of *S. aureus* Newman ($\text{OD}_{(600\text{nm})}$ 1.6). LTA was conducted for 20 min. Representative LTA traces are shown. Scavenging and LTA data are presented as means \pm SEM of five independent experiments. Statistical significance was calculated using one-way ANOVA (* $p < 0.05$, ** $p < 0.01$ and *** $p < 0.001$).

3.6.4 The effect of secondary mediator inhibitors on platelet aggregation and scavenging properties.

It has been proposed by Arman *et al.*, (2014) that bacterial activation of platelets is mediated through the FcγRIIIa pathway. They also suggested a possibility of secretion of secondary mediators from platelets to act as a feedback mechanism reinforcing activation via an IgG-dependent pathway. Apyrase and indomethacin are commonly used inhibitors of secondary mediators, ADP and TXA₂ respectively. It was decided to use both inhibitors in the next set of experiments to explore their effects in modifying platelet functions, in particular platelet scavenging and aggregation in response to bacteria.

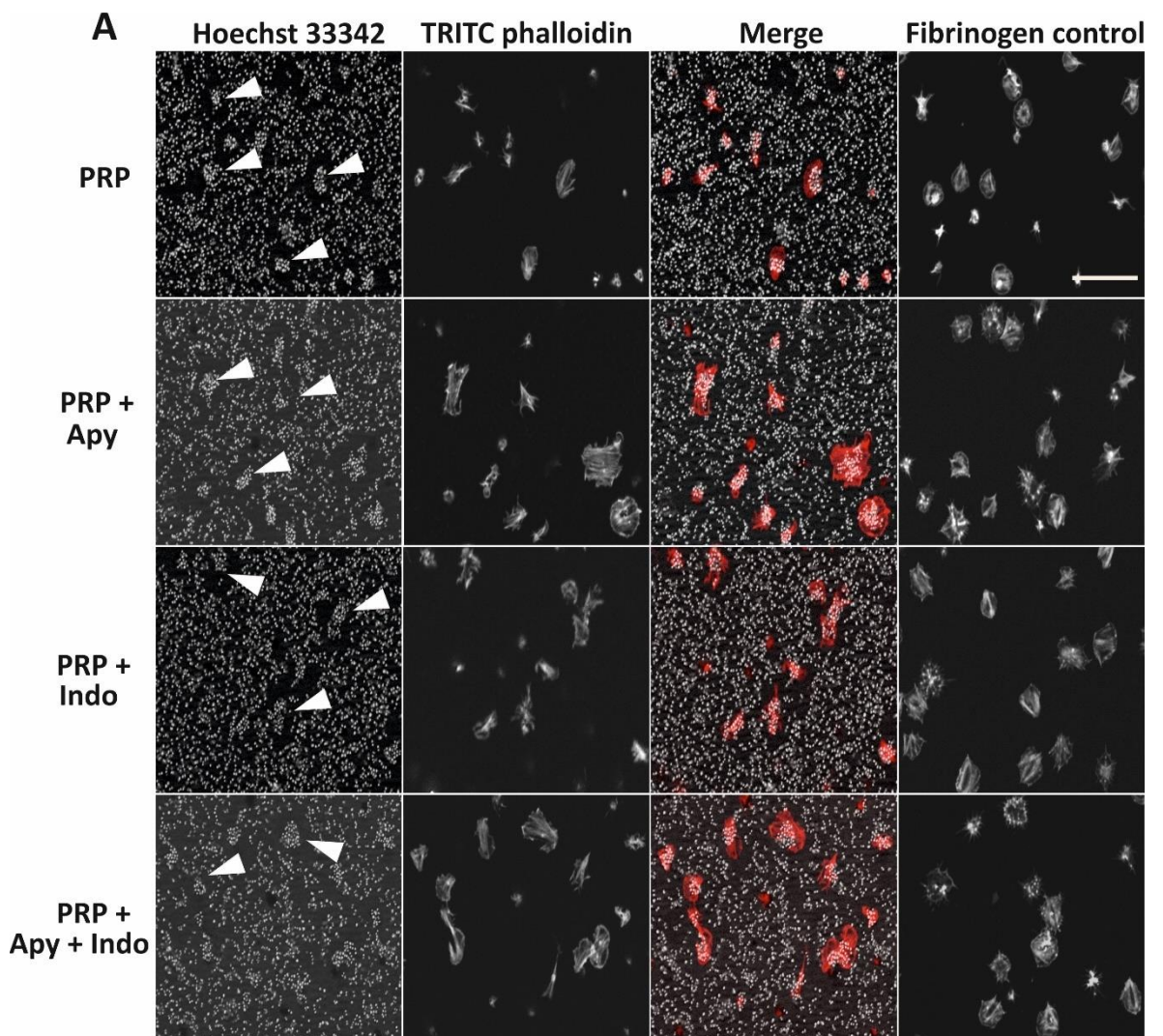
PRP was prepared as outlined in section 3.6.2 and incubated with either 2 U/ml apyrase for 2 min, 10 μM indomethacin for 10 min, or a combination of both inhibitors. After incubation, platelet scavenging assay was performed as described in section 3.5.1. Likewise, LTA was also performed in parallel (section 3.5.1) with *S. aureus* Newman as the agonist.

Figure 3.15A shows representative images of the ability of platelets to scavenge bacteria when treated with secondary mediator inhibitors. The capacity of (un)inhibited platelets to adhere and spread on fibrinogen is also shown.

As highlighted in Figure 3.15B, uninhibited PRP was found to adhere to bacteria as reported in previous sections, with 32 ± 5 platelets calculated to adhere to bacteria per field. As for platelets treated with secondary mediator inhibitors, a small but not significant reduction in the number of cells per field was found in all groups compared to control: 28 ± 9 with apyrase and 26 ± 7 with indomethacin. It was hypothesised that the combination of apyrase and indomethacin would result in a significant reduction in the number of adhered platelets, however, our data again showed a small but not significant decrease (Figure 3.15B). Similar results in the number of adhered platelets were found for cells spread on fibrinogen.

As for the mean surface area, platelets treated with secondary mediator inhibitors, alone or in combination, were considerably similar when compared to the control group for both platelets on bacteria ($25\text{-}29\ \mu\text{m}^2$) and platelets spread on fibrinogen ($31\text{-}36\ \mu\text{m}^2$) (Figure 3.15C).

There was no significant difference in the ability of platelets to scavenge *S. aureus* Newman between the different treatment groups. The percentage of platelets able to scavenge bacteria was calculated to range between 64 and 71% for all platelet groups (Figure 3.15D). Moreover, the results for the average number of bacteria scavenged per platelet were also found to be similar, with all platelet groups scavenging from 17 to 23 bacteria per platelet (Figure 3.15E).



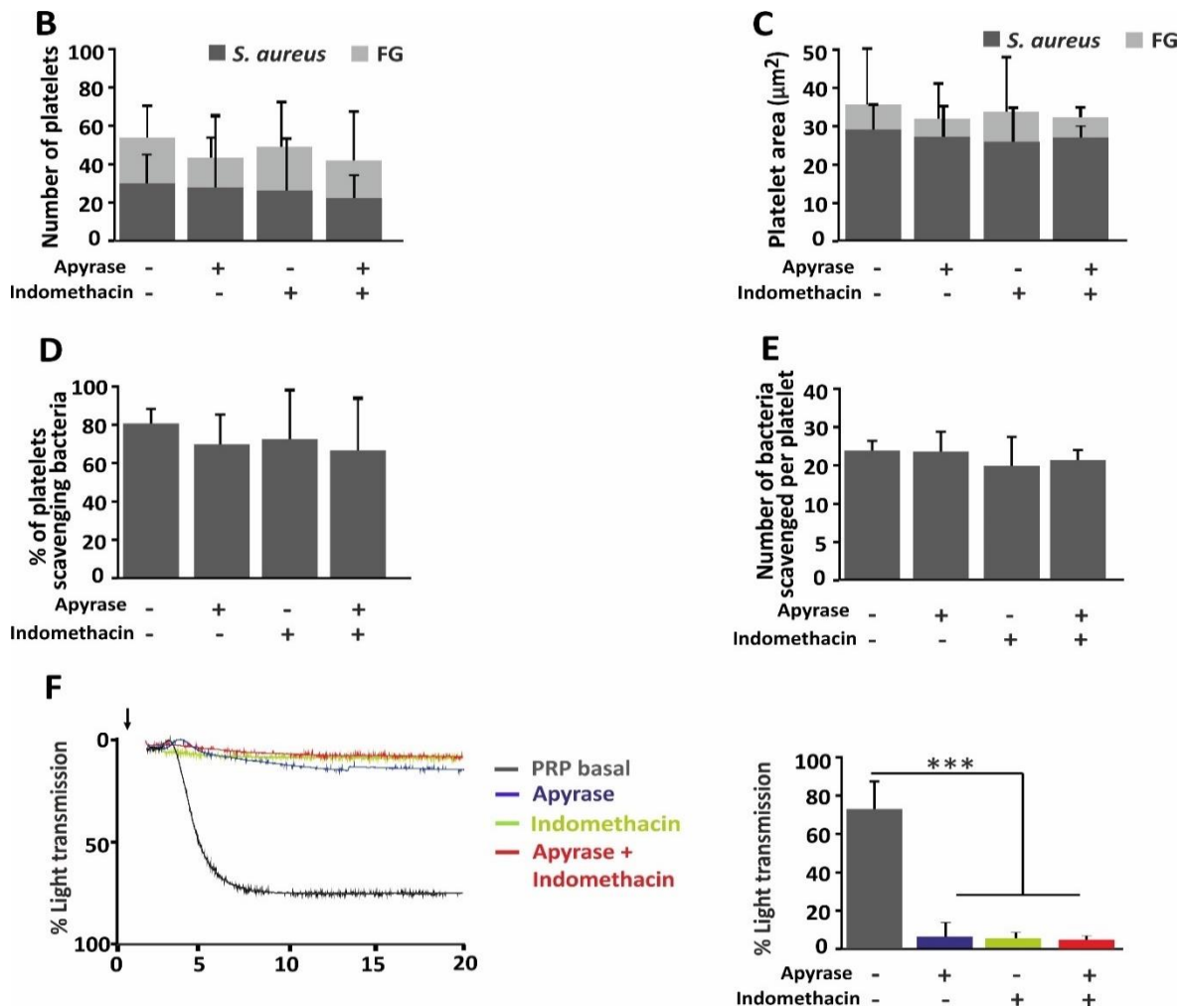


Figure 3.15 The effect apyrase and indomethacin on platelet scavenging ability and aggregation. PRP was diluted with MTB to 1×10^7 platelets/ml and 5% plasma and incubated with either 2 U/ml apyrase for 2 min or 10 μ M indomethacin for 10 min, or in combination of both inhibitors. PRP control received 1:1000 DMSO. 200 μ l of platelet suspension were then placed on coverslips containing immobilised *S. aureus* Newman or fibrinogen (100 μ g/ml) and incubated at 37°C for 1 h. Cells were subsequently washed with PBS, fixed, permeabilised and incubated with a combination of 1 μ g/ml TRITC phalloidin (grey; red on the merged image) and 15 μ g/ml Hoechst 33342 (grey) for 30 min at room temperature. Coverslips were mounted onto glass slides with ProLong Antifade Mountant and microscope images were obtained by using a Zeiss ApoTome.2 fluorescence microscope equipped with a 40x oil immersion objective. (A) Representative images. Scale bar represents 20 μ m. Arrowheads indicate examples of clusters of scavenged bacteria by platelets. (B) The number of platelets per field and the (C) the surface area of platelets was determined. (D) Percentage of platelets scavenging bacteria and (E) the number of bacteria scavenged per platelet were calculated using ImageJ, as outlined in section 2.3.8. (F) PRP with DMSO (2.5×10^8 /ml) was incubated with the secondary mediator inhibitors 2 U/ml apyrase for 2 min or 10 μ M indomethacin for 10 min, or a combination of both inhibitors prior to addition of *S. aureus* Newman ($OD_{(600nm)} 1.6$). LTA was conducted for 20 min. Representative LTA traces are shown. Scavenging and LTA data are presented as means \pm SEM of five independent experiments. Statistical significance was calculated using one-way ANOVA (***) $p < 0.001$.

As for the LTA data obtained following the incubation of platelets with the secondary mediator inhibitors, a considerable inhibition in bacteria-induced platelet aggregation (<10% maximum aggregation in all inhibitor treated groups) was observed compared to uninhibited platelets (Figure 3.15F). Upon incubation of platelets with apyrase, it was found for platelets to have a maximum aggregation of 6% in response to *S. aureus* Newman, this was comparable to the results obtained when platelets were treated with indomethacin (5%). Interestingly, the combination of inhibitors did not abolish platelet aggregation, rather the maximum platelet aggregation was comparable to that of when platelets were treated with the inhibitors separately (Figure 3.15F).

The data gathered from these experiments suggests that neither ADP nor TXA₂- mediated signalling is required for adhesion to and scavenging of *S. aureus*, however both are needed for aggregation upon interaction with the bacteria.

3.7 Supplementation of IgGs and fibrinogen on WPs' ability to scavenge.

Previously in this chapter it was discovered for WPs to lack the ability to scavenge *S. aureus* Newman (Figure 3.5). It was also evident from the accompanying LTA trace that the induction of platelet aggregation in response to bacteria was absent in WP, while the opposite was true for platelets in PRP. This suggests that platelets require something that is removed upon the washing stages of the protocol for obtaining washed platelets. In fact studies have reported supplementation of specific plasma components to restore bacteria-induced aggregation in WP (Arman *et al.*, 2014). It has also been reported for FcγRIIA activation to be dependent on IgG as well as the engagement of αIIbβ3 (Arman *et al.*, 2014). Therefore, it was decided to examine whether the supplementation with fibrinogen and/or IgG would support scavenging of bacteria by WP.

WP obtained from healthy donors was diluted to 1×10^7 cells/ml in MTB and incubated with either 2 U/ml fibrinogen for 12 min, 10 μM IgG for 10 min, or a combination of both. Following incubation, platelet scavenging assay was performed as described in section 3.5.1. A separate sample of PRP at the above density was prepared and processed alongside WP samples as a positive control as described in the previous sections.

Consistent with results obtained earlier in the thesis, WP completely lacked the ability to scavenge bacteria while the opposite was found for PRP (Figure 3.16A). Remarkably, WP supplemented with fibrinogen and/or IgG was found to reverse the effect observed in untreated WP. Figure 3.16A also shows platelets to be spread when placed on fibrinogen irrespective of the treatment supplemented on WP.

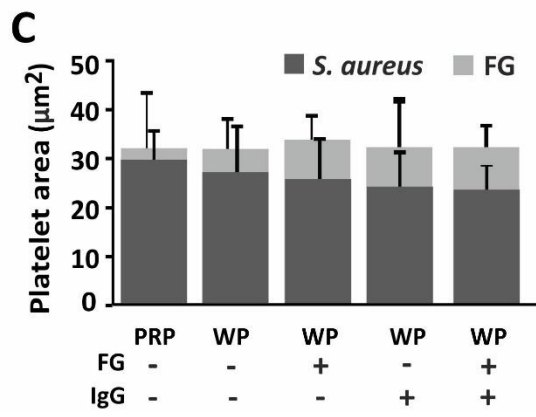
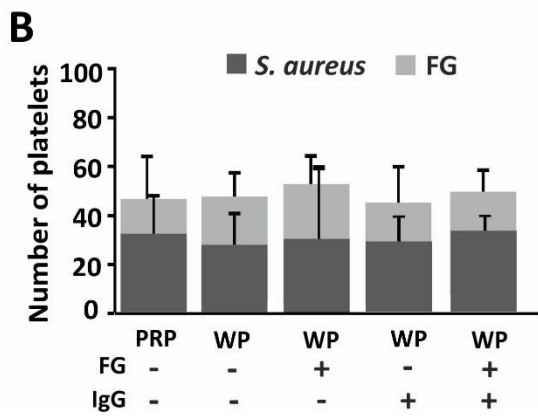
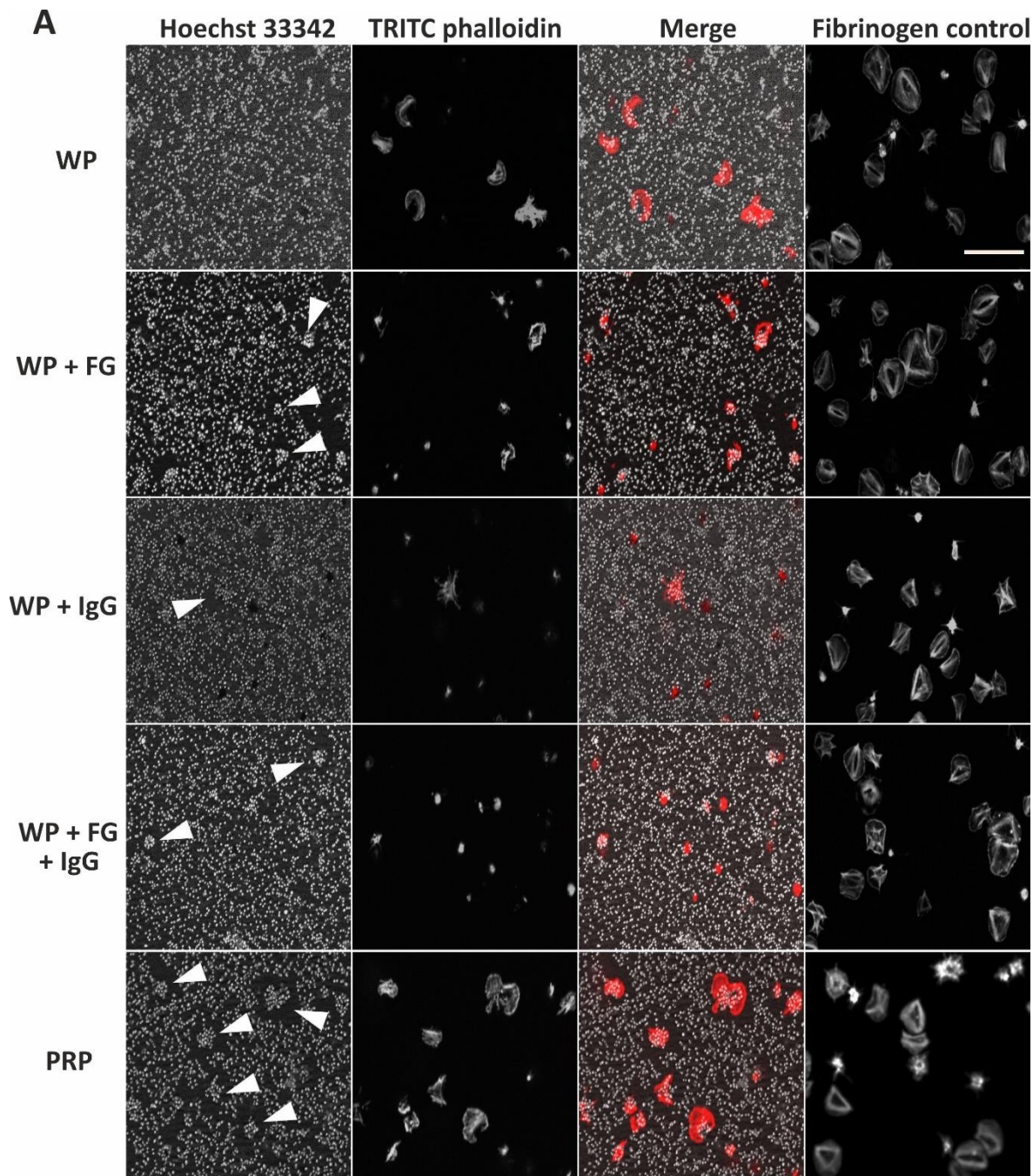
The number of platelets adhered to *S. aureus* Newman coated coverslips were found to be comparable between the WP groups as well as the PRP control group, with platelets/field ranging from 29 to 32 between the groups (Figure 3.16B). Equally, the number of platelets/field in the fibrinogen control groups were also found to be similar, with platelets/field ranging between 41 to 49. Overall, a larger number of platelets were found to adhere to fibrinogen compared to bacteria in all the platelet groups including controls.

The same was found in terms of surface area of platelets (Figure 3.16C). A decrease in the surface area of WP supplemented with fibrinogen and/or IgG was found when placed on bacteria compared to the corresponding untreated WP control as well as PRP, although the differences were not significant. Only marginal differences were found in the surface area of platelets spread on fibrinogen, ranging from 31 to 34 μm^2 .

Figure 3.16D illustrates the differences in the percentage of platelets able to scavenge bacteria per field. Scavenging was absent in the non-treated WP group, as expected. However, when WP were supplemented with IgG, a small proportion of platelets recovered the ability to scavenge bacteria ($8\pm 2\%$ platelets scavenging/field). Remarkably, WP supplemented with fibrinogen were found to have their ability to scavenge bacteria partially restored ($22\pm 9\%$ of platelets scavenged). When WP were supplemented with a combination of IgG and FG we observed a significant increase ($P < 0.05$) in the percentage of platelets able to scavenge *S. aureus* Newman ($35\pm 2\%$ platelets scavenging/field). The mean number of bacteria scavenged per platelets was also found to be comparable for WP supplemented with FG and/or IgG, in fact the results obtained were similar to that of the PRP control group (Figure 3.16E).

LTA was performed in parallel to the scavenging assay to examine the ability of WP (in the absence and presence of supplemented plasma components) to aggregate in response to *S. aureus* Newman. Platelets were prepared as outlined in previous sections and supplemented with FG and/or IgG at the concentration and time mentioned for the corresponding scavenging experiment. Figure 3.16F demonstrates recovery of full aggregation to bacteria in WP supplemented with both fibrinogen and IgGs. Comparable results were found when WP were supplemented with IgG alone, although a prolonged lag time for aggregation was observed. On the other hand, WP treated with FG alone was unable to restore full aggregation, as the maximum aggregation in response to bacteria was found to be 23%.

Data from these set of experiments reveals the important roles of plasma components in restoring scavenging properties of WP. The results obtained also suggest that both IgG and fibrinogen are required to assist aggregation in WP in response to bacteria.



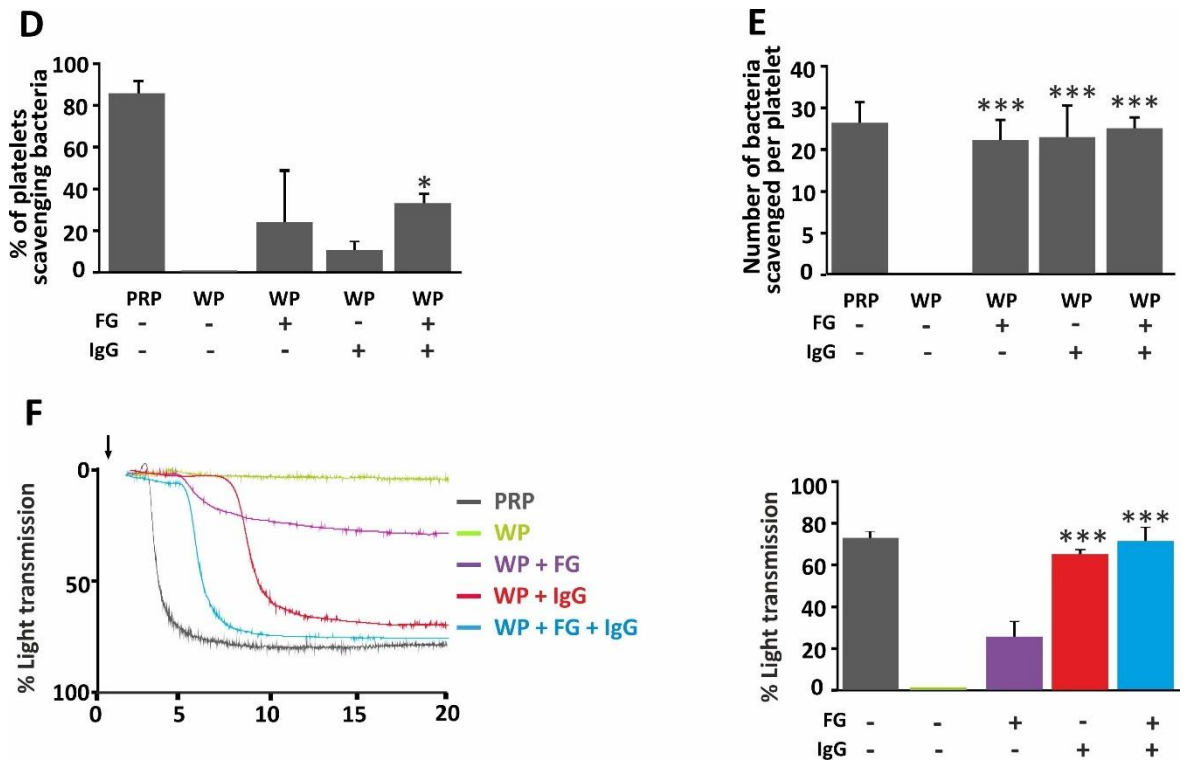


Figure 3.16 The effect of supplementing WP with FG and/or IgG on platelet scavenging and aggregation properties. PRP and WP were diluted 1×10^7 platelets/ml and 5% plasma or MTB respectively. WP were then incubated with either 2 U/ml Fibrinogen (FG) for 12 min or 10 μ M IgG for 10 min, or in combination with both. 200 μ l of platelet suspension was then placed on coverslips containing immobilised *S. aureus* Newman or fibrinogen (100 μ g/ml) and incubated at 37°C for 1 h. Cells were subsequently washed with PBS, fixed, permeabilised and incubated with a combination of 1 μ g/ml TRITC phalloidin (grey; red on the merged image) and 15 μ g/ml Hoechst 33342 (grey) for 30 min at room temperature. Coverslips were mounted onto glass slides containing ProLong Antifade Mountant and microscope images were obtained by using Zeiss ApoTome.2 fluorescence microscope equipped with a 40x oil immersion objective. (A) Representative images. Scale bar represents 20 μ m. Arrowheads indicate examples of clusters of scavenged bacteria by platelets. (B) The number of platelets per field and the (C) the surface area of platelets was determined. (D) Percentage of platelets scavenging bacteria and (E) the number of bacteria scavenged per platelet were calculated using ImageJ, as outlined in section 2.3.8. (F) PRP and WP (2.5×10^8 /ml) were incubated with: 2 U/ml Fibrinogen (FG) for 12 min or 10 μ M IgG for 10 min, or in combination with both prior to addition of *S. aureus* Newman (OD_{600nm} 1.6). LTA was conducted for 20 min. Representative LTA traces are shown. Scavenging and LTA data are presented as means \pm SEM of three independent experiments. Statistical significance between groups were calculated relative to WP control group. One-way ANOVA was conducted (* $p < 0.05$ and *** $p < 0.001$).

3.8 Discussion

The capacity of platelets to encompass immunologic functions has been long debated in literature. Nevertheless, the notion of platelets as host defence cells has become increasingly acknowledged over the past three decades since platelets have been found to contain a myriad of anti-microbial mediators which once released have direct effects on invading pathogens (Tang *et al.*, 2002). In addition to this, numerous studies have also demonstrated the ability of secreted platelet granular content to coordinate the recruitment of other host immune cells to the site of infection (Sonmez & Sonmez, 2017). Recent studies have even proposed that platelets contribute to host defence through a novel process of platelet migration and scavenging. Indeed, a platelet-migration assay developed by Gaertner *et al.*, (2017) demonstrated platelets to actively move and collect fibrin(ogen) bound particles including bacteria, thus supporting the idea of platelets to have roles beyond thrombosis. However, fundamental questions regarding the importance of plasma and the underlying signalling mechanisms involved, remained unaddressed. In this chapter we explored the molecular mechanisms and the signalling pathways involved in the process of platelet scavenging of bacteria. In order to fulfil this purpose, we first aimed to adapt, optimise, and establish a basic methodology for the quantitative analysis and determination of platelets' ability to scavenge bacteria.

With this in mind we first wished to demonstrate sufficient bacterial coverage on coverslips for studying platelet-scavenging mechanisms without compromising the biological properties of the microorganism. We utilised both *S. aureus* and *E. coli* organisms since these microorganisms are examples of the most common type of Gram-positive and -negative bacteria resulting in a range of community- and hospital-acquired infections and are known generally to contribute to morbidity and mortality worldwide (Bachir and Abouni, 2015). Moreover, they have been used extensively in microscopy studies to aid the discovery of numerous fundamental signalling pathways, hence by using these organisms it would allow us to reveal our data in the context of the pertinent literature associated with platelet-bacterial interactions.

Two categories of immobilisation methods have been reported: the use of physical apparatus to confine cells and the use of chemical molecules to aid the attachment of cells to surfaces (Wang *et al.*, 2019). The former approach allows higher throughput; however, the technique is not always favourable, especially for this study since motility of bacteria cannot be analysed by this approach. Thus, chemical confinement methods were tested. The use of HMDS to silane coverslips was tested since this method was used to enhance Alexa488 FG coating on coverslips in the study conducted by Gaertner *et al.*, (2017). The use of poly-L-lysine to immobilise bacteria was also tested as a number of studies have proven enhancement in the attachment of bacteria upon treatment with this compound. It has also been shown for poly-L-lysine to increase electrostatic interaction between the cells' membrane (which has an overall negative charged) and the positively charged surface of the glass coverslip thus enhancing the availability of positively charged binding sites for cells to attach (Colville *et al.*, 2010).

Indeed, we found the treatment of coverslips with HMDS to drastically improve the percentage of *S. aureus* coverage on coverslips compared to control ($P < 0.05$) (Figure 3.1), although treatment of coverslips with poly-L-lysine proved to be significantly more effective at providing a greater bacterial coverage on coverslips ($P < 0.001$). By contrast, it was found for all methods of immobilising *E. coli* RS218 to coverslips to be unsuccessful. Sufficient bacterial coverage was not achieved even upon treating coverslips with poly-L-lysine (Figure 3.2). It is known that the attachment of bacteria to coverslips relies largely upon the interactions between the bacterium itself and the adhesive molecules deposited on the coverslip (Wang *et al.*, 2019). It is also known that the two bacterial organisms differ considerably in terms of the structure and composition of their LPS layers. Therefore, we speculated that *E. coli* did not adhere to coverslips effectively since they may lack the ability to interact with the adhesive molecules on the coverslips as a result of the composition of their cell wall structure. Therefore, since *E. coli* RS218 did not provide reasonable coverage on coverslips regardless of the method utilised, it was decided to exclude *E. coli* RS218 from the study as it would evidently be impossible to derive any meaningful conclusions regarding platelet scavenging properties.

Next, we showed evidence of the effects of solutions and buffers on the ability of *S. aureus* to adhere to coverslips. Bacteria were originally diluted to desired concentration in PBS and so it was assumed that incubation of bacteria with PBS over time would not result in any drastic changes to the percentage of bacterial coverage on coverslips, although Dutta & Willcox (2013) have previously proved incubation with PBS for an extended period of time to lead to a decrease in the number of immobilised bacteria. Despite this, we found no substantial differences in coverage between 1 and 2 h incubation of bacteria with PBS (Figure 3.3). However, the incubation times used in our study were shorter than that reported by Dutta & Willcox (2013) hence possibly why there was no difference in bacterial adherence was observed.

On the other hand, coverslips coated with bacteria and incubated with MTB or plasma resulted in a significant decrease ($P < 0.001$) in the percentage coverage following the 2 h incubation period. A likely suggestion for the decrease in coverage could be due to interference of compounds present in MTB and plasma which perhaps ultimately leads to modification of bacterial adherence properties. This notion is supported by An & Friedman, (1997, 1998) who have reported proteins found within plasma to impair the association of *S. aureus* species to surfaces when exposed to the protein for a prolonged amount of time.

As with any platelet function test, it is instrumental to consider the platelet preparation and isolation methods for the assessment of platelet scavenging properties. Generally, the preparation of whole blood samples are the best way to mimic physiological conditions, however, this was not compatible for this study since whole blood sample requires continuous mixing on a roller to prevent the sample from clotting and so incubation of whole blood for a period of 1 h under static conditions for the scavenging assay would not be feasible. PRP and WP are commonly used in literature to study platelet properties. There are numerous advantages and limitations of using either and the choice of preparation vary greatly in literature with many studies opting for WP preparations to study intrinsic properties of platelets due to the enhanced stability and lack of plasma components which could potentially interfere, while many others argue PRP preparation to be more physiologically relevant and provides a more accurate overview of the mechanisms that occur *in vivo* (Hechler *et al.*, 2019).

Since both platelet preparations have been widely used in literature and because the presence of plasma has been reported to be critical in some studies (Sun *et al.*, 2001), we decided to test both platelet preparations in parallel to examine the effects they would have on platelet functions. An additional group whereby WP were resuspended in plasma was also incorporated into the study to analyse whether substituting plasma would promote WP to scavenge bacteria. It was shown in Figure 3.5B for an increased number of platelets to adhere to fibrinogen compared to bacteria. This increase in adherence could imply there is increased opportunities for fibrinogen to engage with platelet receptors compared to bacteria.

We also proved platelet scavenging to be present in the PRP group only ($82\pm 1\%$ of platelets) (Figure 3.5C). Contrary to expectation, WP-plasma failed to scavenge, this was particularly interesting since the presence of plasma failed to reverse the effect seen in WP-MTB. Similarly, consistent with previous observations (Arman *et al.*, 2014) we demonstrated PRP stimulated with *S. aureus* Newman to induce platelet aggregation ($85\pm 4\%$ light transmission) whereas WP-plasma failed to produce a response. These results gave rise to the possibility of perhaps the difference in anticoagulants used to draw blood for the preparation of PRP vs WP may influence the ability of platelets to scavenge since the anticoagulants differ considerably in pH and calcium concentration (Callan *et al.*, 2009).

Sodium citrate (SC) cannot be used to prepare WP since adequate residuals of calcium remains which can result in thrombin generation and thus platelet activation during the centrifugation steps (Hechler *et al.*, 2019). Hence, we tested platelet scavenging properties of PRP prepared in the presence of SC or ACD. However, no difference in terms of platelet scavenging ability was found between the two groups (Figure 3.6), thus we speculated for the difference in scavenging ability observed in Figure 3.5 to perhaps be due to the washing steps involved for the preparation of WP.

While the presence of plasma has been previously reported to influence the normal functioning of platelets (Chaimoff *et al.*, 1978; Germanovich *et al.*, 2018; Han & Ardlie, 1974), the effects of plasma deprivation in relation to the ability of platelets to scavenge bacteria has been scarcely explored. Therefore, in order to understand to which

extent, the presence of plasma is critical in facilitating platelet scavenging we tested platelets in varying proportions of plasma. Plasma was confirmed to be critical, since platelets in the absence of plasma failed to scavenge, however platelets retained the capacity to scavenge in as low as 5% plasma (Figure 3.10). This was particularly interesting since WP had a pH value comparable to platelets resuspended in 5% plasma (Figure 3.9), indicating the difference in scavenging properties between the two conditions is not due to pH.

Plasma contains a countless number of proteins and other biomolecules, some which are still unexplored, thus we hypothesize that WP-plasma failed to scavenge since a component(s) in plasma along with the preparation method used for the isolation of WP interfered to suppress platelets from scavenging. In fact, Han and Ardlie, (1974) reported environmental factors such as pH, calcium concentration of buffers, components in air that alter pH of plasma and, temperature while preparing platelets to interfere with platelet aggregation responses. Hence, we postulated these factors could have also interfered with our study resulting the data observed.

Although WP-plasma failed to scavenge, we found supplementing WP with FG or IgGs restored platelet scavenging properties and bacteria-induced platelet aggregation response in WP (Figure 3.16D-F). This suggests plasma (or plasma components) are essentially required, even if a minimum to facilitate scavenging properties of platelets. This also reinforces the likelihood of wash steps for the isolation of WP along with components in plasma may have contributed to the lack of scavenging observed in WP-plasma group.

This is supported by initial studies in the 1970s where they found that fibroblasts do not proliferate in plasma containing medium whereas exposing the cells to serum enabled active proliferation hence supporting the notion that elements present in plasma but absent in serum could affect cells ability to function normally (Balk *et al.*, 1973). Ross *et al.*, (1974) also demonstrated the same to be true for smooth muscle cells. Likewise, Gaertner *et al.*, (2017) identified supplementation of albumin and calcium to be critical for shape change in WP.

Our next aim was to investigate the molecular mechanism involved in platelet scavenging since this has not been previously established. It is well known that the use of inhibitors allows in-depth analysis of various pathways, structures and molecular mechanisms involved in the normal functioning of platelets, as well as providing insight into what may occur during various disease states (Kiefer & Becker, 2009; Meadows & Bhatt, 2007).

RhoA, Rac1 and Cdc42 are three major Rho GTPases that coordinate the rapid remodelling of the actin cytoskeleton upon external stimuli (Aslan & MCCarty, 2013). They play a vital role in platelet physiology and aid processes such as haemostasis and thrombosis. It has also been previously defined for aggregation response in platelets to involve Rho GTPases and ultimately actin dynamic (Aslan & MCCarty, 2013) However, the molecular mechanisms involving the regulation of platelet functions by Rho GTPases are extremely complex and ever evolving. Over the past decade the use of inhibitors which specifically perturbate actin assembly units has risen substantially and aided the discovery of many interdependent signal transduction molecules and proteins which modify platelet functions (Huzoor *et al.*, 2016; Yusuf *et al.*, 2017).

Platelet scavenging is an active process and Gaertner *et al.*, (2017) have demonstrated platelets to adopt a characteristic shape upon locomotion, which in turn requires the remodelling of the actin cytoskeleton. Pollard & Cooper, (2009) have also shown shape change and movement in eukaryotic cells to generally involve the assembly and disassembly of actin filaments.

We found platelets adhesion was largely unaffected by the presence of Rho GTPase inhibitors thus implying these elements may not be critical partakers in platelet adhesion processes and suggests the required receptors involved are still present. However, we observed a reduction in platelet surface area upon inhibiting platelet cytoskeletal elements, thus indicating the requirement of actin polymerisation to be key for platelet spreading (Figure 3.12B). This is consistent with findings from Gaertner *et al.*, (2017) who showed a decrease in platelet area upon inhibiting actin polymerisation. Yusuf *et al.*, (2017) also showed a decrease in platelet surface area upon treatment with Rhosin. However, it was observable in Figure 3.12 that Lat-A treatment significantly reduced the ability of

platelet to adhere and spread, hence indicating some actin structures which are key in facilitating adhesion/spreading is disrupted by Lat-A, which is in agreement with findings by Jiroušková *et al.*, (2007).

We also found considerable impairment in the ability of platelets to scavenge bacteria upon inhibiting specific Rho GTPases, especially when platelets were treated with RhoA and Cdc42 inhibitors (Figure 3.12A and D). RhoA and Cdc42 are major Rho GTPases that act as molecular switches to regulate and drive functions such as platelet shape change (Aslan and McCarty, 2013). Since, platelet scavenging requires platelet shape change, it is comprehensible that an absence in scavenging was observed upon inhibiting these proteins. The data we found were consistent with previous studies conducted (Aslan & McCarty, 2013; Kraemer *et al.*, 2010) where researchers demonstrated actin polymerisation to be critical for active platelet processes, although they failed to address the scavenging properties of platelets per se.

Additionally, we were able to investigate the effects of the cytoskeletal inhibitors in relation to bacteria-induced platelet aggregation response. It has been previously demonstrated for NSC 23766 and CASIN to inhibit aggregation responses in platelets (Akbar *et al.*, 2007 & 2009). We too found complete inhibition of *S. aureus* Newman-induced platelet aggregation upon treating platelets with NSC 23766 and Lat-A (Figure 3.12F), which also correlated with scavenging results (Figure 3.12A and C-D). However, RhoA and Cdc42 inhibitors failed to abolish platelet aggregation completely in response to bacteria. This contradicts the idea that bacteria induce an 'all-or-nothing' response as proposed by Arman *et al.*, (2014). Although a possible explanation for the partial aggregation we observed could be that the concentration of inhibitor we used was too low to overcome the activation by *S. aureus*. Although in our study we used Rhosin (RhoA inhibitor) at 30 μ M which is in line with the concentration used by Akbar *et al.*, (2010) who reported inhibition of RhoA activation and thus inhibition of platelet shape change upon treating platelets with Rhosin at 30 μ M. However, it is important to note that they used washed platelets treated with apyrase to test the effects of Rhosin, whereas we used PRP therefore, the presence of plasma components may have contributed to the lack of inhibition in platelet aggregation observed. Similarly, we treated platelets with CASIN at 10 μ M to inhibit Cdc42, which is

consistent with concentrations used in literature (Antkowiak *et al.*, 2016). The differences observed in the data obtained could potentially be linked to heterogeneity of platelets since circulating platelets have been reported to differ in age, size and even genetics and this in turn has been shown to cause in variability in platelet response, hence perhaps why differences arose in terms of the ability of platelets scavenge and aggregate (Jobe, 2017).

In addition to cytoskeletal inhibitors, we also reviewed the effects of platelet surface receptor inhibitors on the ability of platelets to adhere, scavenge and aggregate. FcγRIIa has been reported to be a critical receptor for the binding of Newman to platelets (Arman and Krauel, 2015). It has also been shown that Newman binds to platelets indirectly through fibrinogen to GP IIb/IIIa and for this interaction to be essential for platelet-bacterial activation (Arman & Krauel, 2015). Hence, we had initially hypothesised an absence in the ability of platelets to scavenge bacteria as well as inhibition in platelet aggregation upon treating platelets with IV.3 antibody and integrilin which inhibit FcγRIIa and GPIIb/IIIa, respectively. However, we found platelets still possessed the ability to scavenge bacteria when treated with IV.3 ab, although to a significantly lower extent compared to control (Figure 3.13C). This suggests that additional receptors may participate in the engagement of infectious agents to platelets thus allowing functions such as platelet scavenging to be carried out. Interestingly, the inhibition of GPIIb/IIIa resulted in complete inhibition of platelet scavenging, the surface area of platelets was also found to be significantly reduced compared to control. This was intriguing as one would hypothesise platelet scavenging to still occur through FcγRIIa-mediated signalling pathways. As studies have reported activation of FcγRIIa to activate downstream Syk signalling which in turn activates phospholipase C (PLC) signalling pathways (Gross *et al.*, 1999; Kiefer *et al.*, 1998). PLC has been shown to exert its effects on Rho GTPases aiding cytoskeletal rearrangements (Harden *et al.*, 2009). However, studies have also reported FcγRIIa-mediated activation of Src-Syk-PLC axis to then result in inside-out signalling of GPIIb/IIIa causing a conformation change in the receptor (Joo, 2012). Therefore, this implies that although FcγRIIa mediates bacteria-platelet binding, platelet scavenging is critically dependent on integrin αIIbβ3.

Additionally, absence of platelet aggregation upon treatment with either inhibitors was also observed (Figure 3.13F), consistent with previous work by Arman *et al.*, (2014). The

presence of scavenging upon treatment with IV.3 and the absence of aggregation suggest that two different mechanisms are involved for the observations found.

In addition to the role of platelet surface receptors in mediating platelet functions, it has been proposed by Arman *et al.*, (2014) a possibility of secondary mediators from platelets to act as a feedback mechanism reinforcing activation via an IgG-dependent pathway. However, we did not find any alterations in the ability of platelets to scavenge upon inhibition of ADP or TX2A signalling, although moderate inhibition in the ability of platelets to aggregate in response to Newman was observed (Figure 3.15).

TKs are also linked to FcγRIIa and GPIIb/IIIa, and so it was decided to explore TK signalling pathway through the use of specific Btk, Syk and Src inhibitors which are also commonly used for the treatment of CLL. We showed for the first time that PRT and dasatinib, which target Syk and Src respectively, abolish platelet scavenging (Figure 3.14). It has been reported for Syk to be a mediator of signalling pathways downstream of GPIIb/IIIa and inhibition of the pathway has been shown to abrogate platelet functions including cell spreading on fibrinogen, aggregation and shape change (Spalton *et al.*, 2009). Likewise, Séverin *et al.*, (2012) revealed mouse lacking Src to result in impairment to platelet functions. Both Src and Syk are also downstream of FcγRIIa receptors. We therefore postulate for an inhibition of activity of PLCγ2 and PI3K (involved in directly activating Rho proteins) which are downstream of Syk and Src thus preventing platelet shape to occur. These observations are consistent with previous reported data by Senis *et al.*, (2014) who found severe impairment in tyrosine kinase phosphorylation in mouse models lacking Src. Dasatinib and PRT are commonly used for the targeted therapy to treat acute lymphoblastic leukaemia and its mode of action is that it essentially binds to and inhibits the growth promoting elements of Src or Syk-kinases. Since dasatinib and PRT targets a broad spectrum of kinases, it has been linked with potential dysfunction in platelets. The same was found to be true in our study since these drugs inhibited platelet scavenging as well spreading (Figure 3.14), thus this implies that administration of dasatinib to CLL patients potentially predisposes these individuals to bleeding disorders and infection. Platelet aggregation in response to Newman was also found to be inhibited when platelets

were treated with either dasatinib or PRT. This is in agreement with findings from Quintás-Cardama *et al.*, (2009) and Reilly *et al.*, (2011).

A significant reduction in the ability of BTK inhibitor-treated platelets was also observed, along with complete inhibition of platelet aggregation (Figure 3.14 C-F). This lends support to Chen *et al.*, (2018) who found inhibiting BTK signalling to impair platelet aggregation responses. Our scavenging and aggregation data in response to bacteria further confirm the participation of BTKs in the activation of platelets and platelet processes such as scavenging. BTK inhibitors are also used to treat solid malignancies, the data obtained from these experiments highlights the potential off-target effects in platelets when using therapeutic agents that inhibit BTKs for the treatment of malignancies.

Conclusion

We have effectively adapted and optimised conditions for an assay to quantitatively assess platelet scavenging properties. Through the use of specific pharmacologic inhibitors of each of the main Rho GTPases we have established the differential and unique roles of specific Rho GTPases, in the ability of platelets to adhere, scavenge and induce aggregation in response to bacteria. This chapter also offers insights into critical platelet surface receptors and signalling pathways involved in regulating scavenging properties of platelets. We have also demonstrated the potential dangers and off-target side effects of drugs used commonly in the treatment of CLL and how these can lead to dysfunction in platelet scavenging and aggregation responses, thus rendering individuals susceptible to infection.

Chapter 4. Investigating platelet migration on Alexa488 fibrinogen

4.1 Introduction

Platelets, beyond their established functions in haemostasis and thrombosis, play a role as immune cells partaking in the surveillance of intravascular immune regulation and in various inflammatory conditions (Petito *et al.*, 2017). Studies have demonstrated platelets to possess numerous structural and biochemical components typical of inflammatory cells (Arman *et al.*, 2015).

A critical characteristic of 'bona fide' inflammatory cells is their capacity to migrate. Cell migration is key in forming and retaining appropriate processes in organisms such as maintaining immune responses, homeostasis of tissues and establishing sufficient wound repair (Trepap *et al.*, 2012). Largely due to the lack of a nucleus, platelets have been described previously as immotile cells which upon detection of endothelial injury adhere and aggregate to the vessel walls and remain stationary. However, an accumulating body of research has revealed platelets to contain several molecular attributes found commonly in a migrating cell: they express a number of surface receptors for chemokines and adhesive proteins, release chemicals involved in the degradation of the ECM such as matrix metalloproteinases, possess an enzymatic machinery involved in cellular locomotion, and contain cytoskeletal components required for cell migration (Bettex-Galland and Lüscher, 1959).

Movement of platelets was observed by researchers in the field with the use of light microscopy. However, the encountered 'crawling' of platelets was deemed as passive diffusion or Brownian movement, as reviewed by Petito *et al.*, (2017). It was only in the early 1970s, that studies conducted by Löwenhaupt established platelets to be cells with migratory capacity.

These studies by Löwenhaupt *et al.* (1973, 1977) evaluated optimal conditions to examine the ability of platelets to migrate *in vitro*. Numerous factors such anticoagulant, platelet

concentration and buffer composition, to name a few, were assessed to determine their effects on the movement of platelets within a capillary tube towards collagen (chemotaxis).

Not Long Ago, Czapiga *et al.*, (2005) demonstrated activated platelets to encompass migratory and microbicidal properties as they observed gradient-driven chemotaxis of platelets towards a bacterial N-formyl peptide. In addition to this, a recent elaborate study performed by Gaertner *et al.*, (2017) showed platelets placed on fluorescently labelled fibrinogen to utilise their adhesive receptors to probe the microenvironment in the vicinity of the cell and thus result in the migration of platelets towards a stimulus *in vitro*.

Migration of cells is a complex and active method which is generally described as a multi-step process. Cell migration involves the critical platelet cytoskeletal framework, which is composed primarily of spectrin, actin filaments, filamin and adducin (Goggs *et al.*, 2015). A large number of proteins and several intracellular pathways coordinate the assembly and disassembly of cytoskeletal components which has been proposed to aid the migration of platelets (Clemetson *et al.*, 2000; Charest and Firtel, 2007; Jin, 2013). In particular, small GTPases of the Rho family initiate a plethora of effector molecules which regulate the actin dynamics of the platelet cytoskeleton (Yan and Jin, 2012).

Since the discovery of platelets as motile cells, migration of platelets has been studied in several disease states and/or in response to a variety of inhibitors. Pitchford *et al.*, (2008) demonstrated the migration of platelets towards lung tissue upon induction by allergens. Whereas, Löwenhaupt *et al.*, (1977) utilised cytochalasin B to disrupt actin filaments within platelets and found an inhibition in platelet migration. Rho GTPases play a critical role in regulating actin dynamics and it has been mentioned in the Chapter 3 Introduction, various studies that employed Rho inhibitors to research modification in platelet functions. Nevertheless, certain aspects of platelet signalling in terms of platelet migration remain uncovered.

To complicate matters further, leukaemia patients are often prescribed medications that affect the normal functioning of platelets since they interfere with the BTK, Syk and Src pathways. However, the effects of such drugs in altering platelet migration have yet to be

investigated. Similarly, the roles of platelet surface receptors in coordinating downstream signals which ultimately regulate platelet locomotion has also not been previously studied. Therefore, in order to develop our understanding of the molecular mechanism involved in platelet migration and to gain insight into the factors that may affect platelet migration, the below mentioned aims were designed for this chapter.

This chapter complements chapter 3 since major Rho GTPases and TK signalling molecules are to be investigated but in terms of platelet migration rather than platelet scavenging, as previously done in chapter 3, and so most of the background information regarding the molecular mechanisms have already been stated in Chapter 3, Introduction and Discussion.

In this chapter the primary aim is to adapt the basic techniques employed by both Löwenhaupt *et al.*, (1973) and Gaertner *et al.*, (2017) to observe the effects of different parameters on the capacity of platelets to migrate on glass coverslips. As mentioned above, in the previous chapter we established the molecular mechanism for platelet scavenging infectious matter and the importance of Rho proteins in allowing platelets to carry out their function in terms of platelet scavenging. Here we aim to investigate whether these differ from the traditional spreading on non-infectious agents as well as investigating the capacity of platelets to migrate.

Aims of this chapter are:

- To set the conditions required to study platelet migration on fluorescently labelled fibrinogen.
- To determine the importance of plasma components for the migration of platelets on fluorescently labelled fibrinogen to occur.
- To identify the differences, if any, in migrating capacity between mouse and human platelets.
- To establish the effect(s) of a selection of actin cytoskeleton inhibitors on platelet migration ability.
- To understand the alterations in migratory response upon treating platelets with inhibitors of signalling pathways.

4.2 Optimisation of conditions for platelet migration assay

The primary objective of this section was to establish and adapt the conditions of an assay that can quantitatively assess the ability of platelets to migrate on fibrinogen labelled with Alexa488 (Alexa488 FG) and to determine the optimal conditions required to investigate platelet-matrix protein interactions *in vitro*.

As mentioned in the previous chapter (section 3.2 and 3.3), numerous variables such as treatment of coverslips, time of exposure and the concentration of platelets can all contribute to the efficiency and accuracy of an assay which aims to study the migration properties of platelets. Therefore, in similar ways to chapter 3, it was decided to systematically investigate a number of these conditions and parameters to arrive at an optimised protocol that will permit the investigation of cellular morphology as well as the potential of platelets to migrate.

4.2.1 Treatment of coverslips for optimal Alexa488 fibrinogen coating

In the study conducted by Gaertner *et al.*, (2017), the authors treated glass coverslips with HMDS prior to conducting migration assays, though the reason for doing so was not entirely clarified in the study. However, evidence from other studies has suggested silanisation treatments provide a hydrophobic glass surface allowing the firm attachment of particles to coverslips and has been shown to be a reliable strategy for methods such as cell micropatterning (Bautista *et al.*, 2019).

To validate the effects of pre-treating glass coverslips with HMDS on the uniformity of Alexa488 FG and the ability of platelets to migrate, coverslips were prepared under the following conditions on the day of the experiment:

- no treatment
- acid washed and subsequently silanated with HMDS (section 2.4.2)

Coverslips were then coated with 200 μ l of 40 μ g/ml Alexa488 FG in combination with 2 mg/ml of heat inactivated fatty acid free BSA for 15 min at room temperature. 200 μ l of platelets at 1×10^7 cells/ml from PRP were then placed on the prepared coverslips. Plasma

was obtained and used to dilute platelets to the required density as outlined by Gaertner *et al.*, (2017). Coverslips were subsequently processed as outlined in section 2.4.3 and platelets were stained with TRITC-phalloidin (stains F-actin). Coverslips were then washed with PBS, mounted, and visualised with a fluorescence microscope the following day.

Figure 4.1A shows representative images of platelets adhering to both untreated glass coverslips and coverslips subject to HMDS treatment. It is evident that silanisation provides a uniform layer of Alexa488 FG for the visualisation of platelet migration whereas uneven fibrinogen coating and the presence of bright areas (presumably fibrinogen aggregates) were observed when the coverslips were untreated. Though differences in the overall coverslip coating with fibrinogen was observed, interestingly Figure 4.1B demonstrates the number of adhered platelets to be unaffected regardless of the coverslip treatment utilised (23 ± 5 cells/field when coverslips were untreated vs 22 ± 4 cells/field when coverslips were silaned).

Intriguingly, it can be noted in Figure 4.1A and C that the ability of platelets to migrate and scavenge Alexa488 FG (white arrowheads) was only observed when coverslips were silaned with HMDS. An absence in platelet spreading was also observed when coverslips were left untreated. Migrating platelets are identified by 'dark' areas surrounding the platelet which is indicative of Alexa488 FG cleared by the cell. Additionally, clusters of Alexa488 FG are also often found in the centre of a migrating platelet as can be seen in Figure 4.1A.

A significant difference in the percentage of platelets able to displace on Alexa488 FG was observed between silaned coverslips ($71 \pm 2\%$ of cells displaced/field) and non-silaned coverslips (0 cells displaced/field) ($P < 0.001$). Thus, proving silanisation of coverslips to be critical in aiding the migration of platelets on Alexa488 FG.

Since treatment of coverslips with HMDS provided a uniformed layer of Alexa488 FG and more fundamentally since platelet migration was only present upon treating coverslips with HMDS, it was decided to silane all coverslips herein for the investigation of platelet migration capacity.

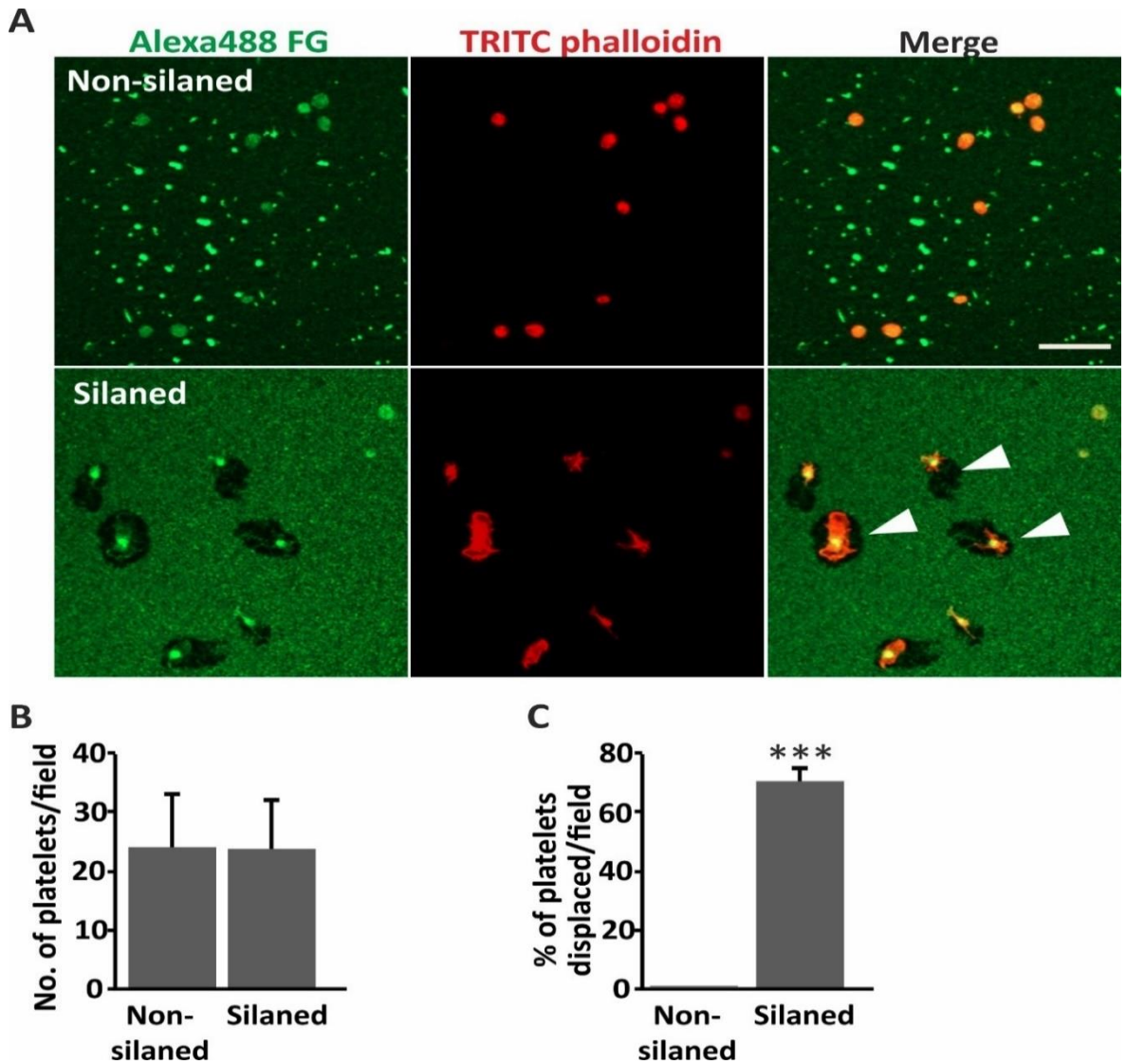


Figure 4.1 Effect of silanisation of coverslips on platelet adhesion and migration. Glass coverslips were either untreated or prepared by acid washing with HCl for 1 h followed by dH₂O for 1 h and then silaned with HMDS for 1 min at room temperature. Coverslips were then coated with 40 µg/ml Alexa488 FG (green) and 2 mg/ml BSA for 15 min. Platelets were isolated and diluted to 1x10⁷/ml by resuspending PRP in plasma. 200 µl of platelet suspension were then added to the coverslips and incubated at 37°C for 1 h. Following this, coverslips were washed with PBS and fixed with 4% PFA for 10 min. Cells were then permeabilised with 0.3% Triton X100 for 5 min and stained with 1 µg/ml TRITC phalloidin (red) for 30 min at room temperature. Coverslips were then mounted onto glass slides with ProLong Antifade Mountant and images were obtained with a Zeiss ApoTome.2 fluorescence microscope equipped with a 60x oil immersion objective. (A) Representative images from three independent experiments. Scale bar represents 10 µm. Arrowheads indicate examples of migrating platelets. (B) Adhesion of cells in each of the conditions and (C) the percentage of platelets displaced was calculated using ImageJ software. Data are presented as means ± SEM of three independent experiments. A minimum total of 40 fields (image size 165.59 µm x 110.39 µm) per experiment was scored, with a minimum of 800 cells analysed, (***)p<0.001).

4.2.2 The effect of platelet concentration on the ability of platelets to migrate

We next decided to investigate whether any platelet-concentration dependent variations would arise in the ability of platelets to migrate on Alexa488 FG.

PRP was isolated from whole blood and platelet density was adjusted to two different concentrations by diluting in plasma: 1×10^7 /ml and 2×10^7 /ml. As in section 3.3.3, it was decided to limit the testing concentration of platelets to 2×10^7 /ml, because any concentration higher than this was thought to result in a surplus of platelets on the coverslips which inevitably may complicate determining accurately the migratory response of individual platelets on Alexa488 FG.

PRP at the two concentrations indicated above was placed on silanated glass coverslips coated with Alexa488 FG for 15 min (as described in section 4.2.1). The coverslips were then incubated at 37°C for 1 h. Platelets were also prepared and spread on unlabelled fibrinogen as a control. Following the 1 h incubation cells were fixed, permeabilised and stained for visualization as described in the preceding section and the difference between cells' ability to migrate on Alexa488 FG was determined.

Figure 4.2A shows that, as anticipated, the number of adhered platelets increased significantly ($P < 0.01$) as the platelet density increased, in both the Alexa488 FG group (22 ± 5 platelets/field at 1×10^7 /ml vs 71 ± 13 platelets/field at 2×10^7 /ml) and in the unconjugated FG control groups (41 ± 13 platelets/field at 1×10^7 /ml vs 88 ± 4 platelets/field at 2×10^7 /ml) (Figure 4.2B).

However, the proportion of platelets able to migrate on Alexa488 FG remained constant between the suspensions prepared to the two different platelet densities (Figure 4.2C). It can be seen that $65 \pm 6\%$ of cells were able to migrate when platelets were diluted to 1×10^7 /ml, which was similar to the percentage of cells able to migrate at 2×10^7 /ml ($56 \pm 1\%$). The same was observed in terms of the average area of Alexa488 FG cleared by individual platelets between the two groups ($2 \pm 0 \mu\text{m}^2$ at 1×10^7 /ml vs $2 \pm 0 \mu\text{m}^2$ at 2×10^7 /ml) (Figure

4.4D). However, it is important to interpret the results with caution for the area of Alexa488 FG cleared for platelets prepared to 2×10^7 /ml since at several regions the area of Alexa488 FG cleared overlapped between platelets (yellow dashed line).

From these experiments we have noticed that increasing the concentration of platelets increased the number of cells adhered, as expected. However, only a marginal difference was observed in terms of platelet migration capabilities between the two platelet densities. Nevertheless, given that our findings demonstrated regions of overlap in the area cleared for platelets prepared to the higher density, it was decided to prepare platelets to 1×10^7 /ml for all subsequent migration experiments in order to avoid confusion when analysing results.

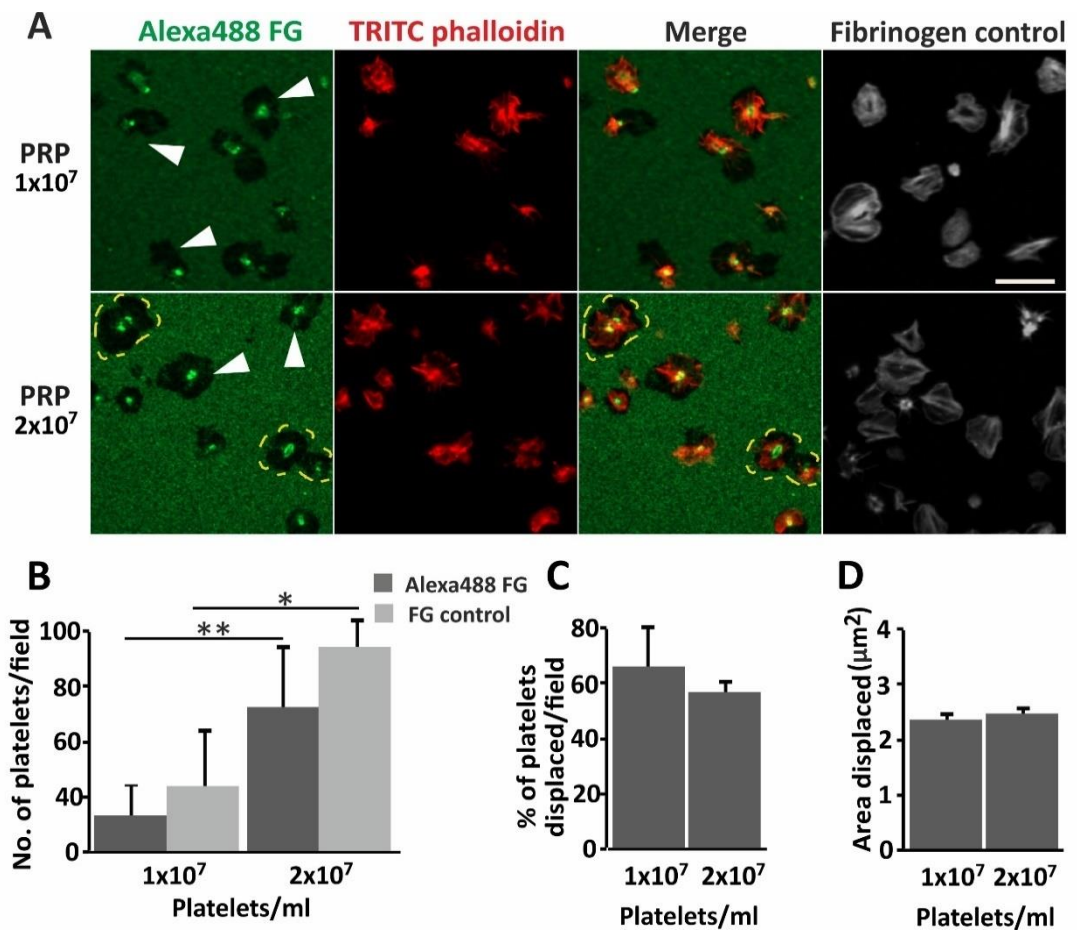


Figure 4.2 The effect of platelet density on the ability of platelets to migrate on Alexa488

FG. Glass coverslips were acid washed with HCl for 1 h followed by dH_2O for 1 h and then silaned with HMDS for 1 min at room temperature. Coverslips were then coated with $40 \mu\text{g/ml}$ Alexa488 fibrinogen (green) and 2 mg/ml BSA for 15 min. Platelets were diluted to either 1×10^7 /ml or 2×10^7 /ml by resuspending PRP in plasma. $200 \mu\text{l}$ of platelet suspension were then added to the coverslips and incubated at 37°C for 1 h. Platelets were

also spread on unconjugated fibrinogen (40 µg/ml) coated coverslips in parallel. Coverslips were then washed with PBS and fixed with 4% PFA for 10 min, permeabilised with 0.3% Triton X100 for 5 min and stained with 1 µg/ml TRITC phalloidin (red; grey on FG control image) for 30 min at room temperature. Coverslips were mounted onto glass slides with ProLong Antifade Mountant and images were obtained with a Zeiss ApoTome.2 fluorescence microscope equipped with a 60x oil immersion objective. (A) Representative images from three independent experiments. Scale bar represents 10 µm. Arrowheads indicate examples of platelet migration. Yellow dashed lines indicate areas where platelet migration overlaps between two platelets. (B) Adhesion of cells in each of the conditions was calculated by manually counting cells on ImageJ software. (C) Percentage of migrating platelets per field was counted manually from a total of 40 fields (image size 165.59 µm x 110.39 µm) per condition. (D) The average area of Alexa488 FG cleared by individual platelets was calculated on ImageJ software as outlined in section 2.4.7. Data are presented as means ±SEM of three independent experiments, (*p<0.05 and **p<0.01).

4.2.3 The ability for platelets to migrate on Alexa488 FG increases with time

In the previous set of experiments, we have established that it is vital to silane coverslips with HMDS in order to observe migration of PRP on Alexa488 FG. Moreover, we have determined the optimal platelet concentration to use to obtain accurate platelet migration results. Here, we aim to determine the optimal time at which platelets migrate on Alexa488 FG. Thus far, all platelet migration experiments were conducted for 60 min. We wanted to investigate any time-dependent effects on platelet migration, so we sought to incubate platelets on Alexa488 FG for reduced timepoints.

Platelets and coverslips were prepared as previously described (section 4.2.1). Platelets were then incubated on Alexa488 FG coated coverslips for 15, 30 and 60 min at 37°C. At indicated time points, cells were processed for the visualisation of platelet migration as described in the previous section and the number of adhered platelets and the percentage of migrating platelets were determined for the different time points.

Representative images of the ability of platelets in PRP to migrate on Alexa488 FG over time are shown in Figure 4.3A. Consistent with previous results, we observed platelet migration at 30 and 60 min and an absence of platelet migration at 15 min, hence suggesting that platelets require time to encompass the ability to displace from their original position.

As anticipated, the number of platelets on Alexa488 FG and unconjugated FG increased over time with a significant differences observed between 15 and 60 min in both the Alexa488 FG and control fibrinogen groups ($P < 0.05$). It is also observable that platelet migration appears to be time dependant as the ability of platelets to migrate increased with time (Figure 4.3C). $49 \pm 12\%$ of platelets were seen to migrate at 30 min and a higher percentage of motile cells were observed at 60 min ($69 \pm 2\%$). These results indicate incubation time to be an important factor in determining the ability of platelets to migrate.

Although a higher percentage of cells were calculated to migrate at 60 min compared to 30 min, Figure 4.3D depicts the average area of Alexa488 FG cleared by migrating platelets to be the same between the two incubation times ($2 \pm 0 \mu\text{m}^2$).

Data from these suggest platelet incubation on Alexa488 FG should exceed 15 min in order to observe migratory characteristics of platelets and that the maximal area for platelets to migrate is approximately $2\text{-}3 \mu\text{m}^2$. Therefore, since maximal percentage of platelets able to migrate was achieved at 60 min, it was decided to incubate platelets on Alexa488 FG for 60 min for all future experiments.

However, to assess whether extending the incubation time of platelets on Alexa488 FG has any effect in increasing the capacity of platelets to migrate, a preliminary study was conducted whereby platelets were incubated on Alexa488 FG coated coverslips for 120 min prior to fixing and staining. Results obtained are shown in Figure 7.3 in the Appendices. No significant difference in the percentage of platelets able to migrate on Alexa488 FG was seen at 120 min compared to 60 min. Consistent with Figure 4.3, the area displaced by platelets were calculated to be within the $2\text{-}3 \mu\text{m}^2$ for both timepoints. Since the results obtained for platelets incubated at 120 min were comparable with that of 60 min, it was decided to continue incubating platelets on Alexa488 FG for 60 min for consistency.

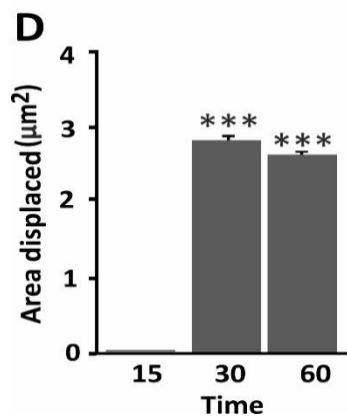
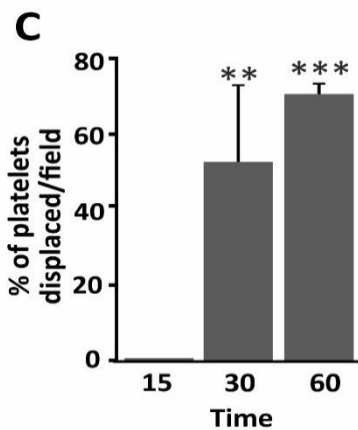
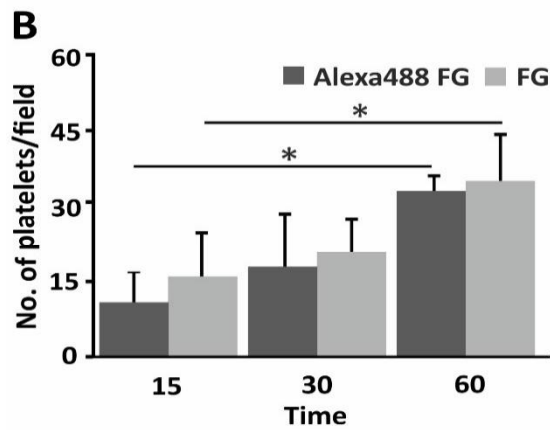
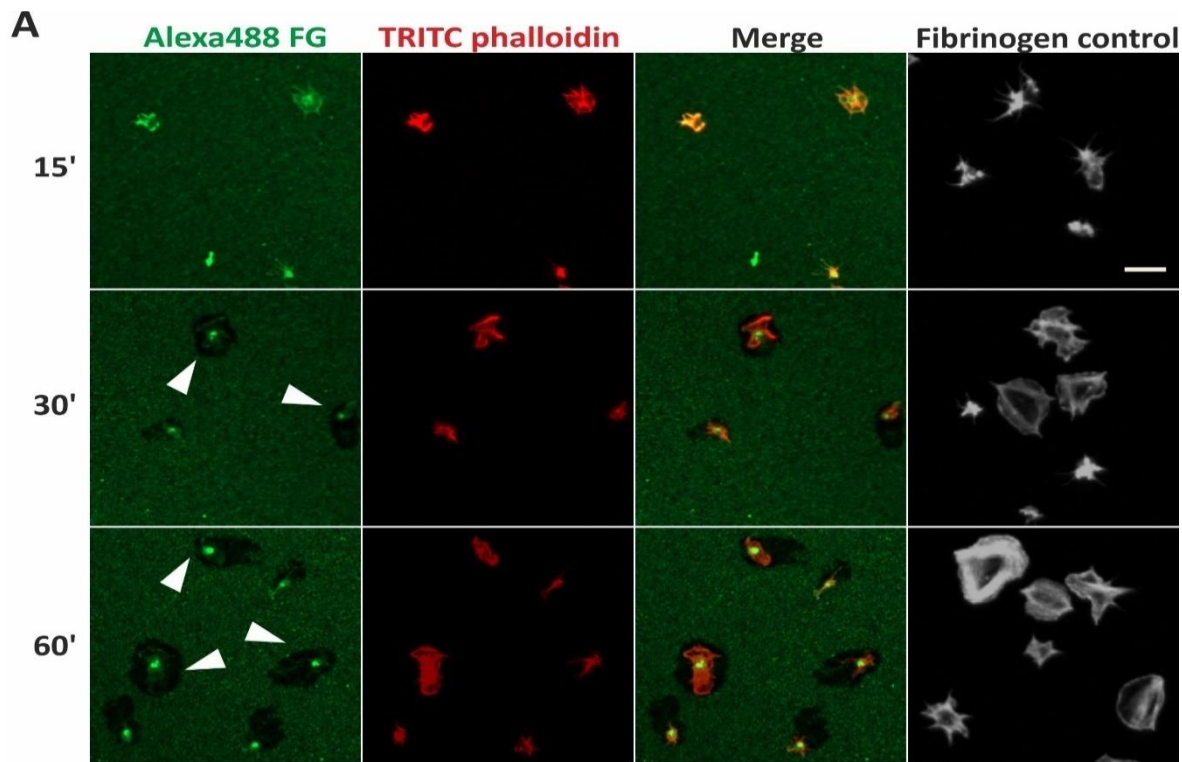


Figure 4.3 Time-dependent effects on the ability of platelets to migrate on Alexa488 FG.

Glass coverslips were acid washed with HCl for 1 h followed by dH₂O for 1 h and then silaned with HMDS for 1 min at room temperature. Following this, coverslips were coated with 40 μg/ml Alexa488 fibrinogen (green)

and 2 mg/ml BSA for 15 min. Platelets were diluted to 1×10^7 /ml by resuspending PRP in plasma and 200 μ l was added to the coverslips and incubated at 37°C for the indicated time. Platelets were also spread on fibrinogen (40 μ g/ml) coated coverslips in parallel. At the relevant timepoints, coverslips were washed with PBS and fixed with 4% PFA for 10 min, permeabilised with 0.3% Triton X100 for 5 min and stained with 1 μ g/ml TRITC phalloidin (red; grey on FG control image) for 30 min at room temperature. Coverslips were then mounted onto glass slides with ProLong Antifade Mountant and images were obtained with a Zeiss ApoTome.2 fluorescence microscope equipped with a 60x oil immersion objective. (A) Representative images from three independent experiments. Scale bar represents 10 μ m. Arrowheads indicate examples of platelet migration. (B) Adhesion of cells in each of the conditions was calculated by manually counting cells on ImageJ software. (C) Percentage of migrating platelets per field was counted manually from a total of 40 fields (image size 165.59 μ m x 110.39 μ m) per condition. (D) The average area of Alexa488 FG cleared by individual platelets was calculated on ImageJ software as outlined in section 2.4.7. Data are presented as means \pm SEM of three independent experiments, (* $p < 0.05$, ** $p < 0.01$ and *** $p < 0.001$). Significance in C and D are relative to 15 min.

4.2.4 The effect of platelet preparation on the ability of platelets to migrate

Numerous studies have demonstrated the critical role of plasma components in altering platelet functions. We too have discovered in the previous chapter that the supplementation of plasma components to WP modified the properties of platelets for scavenging bacteria (Figure 3.17). Therefore, it was decided to test the effect of platelet preparation on the migration ability of platelets.

PRP and WP-plasma were prepared as outlined in section 2.3.1. WP-MTB was also prepared to eliminate the effect of plasma proteins and thus allow the determination of whether plasma components are critical for platelet migration. 200 μ l of platelet suspensions were then placed onto glass coverslips pre-coated with Alexa488 FG and processed as mentioned previously. Samples of each platelet preparation were also incubated on unconjugated fibrinogen (40 μ g/ml) coated coverslips as a control of their spreading profile. The coverslips were then processed in parallel.

As highlighted in Figure 4.4A, WP-MTB completely lacked the capacity to migrate on Alexa488 FG. On the other hand, platelets in PRP and WP-plasma were observed to possess the ability to migrate. Minor differences in the number of adhered platelets were found between the three groups, with 32 ± 6 cells/field in PRP, 53 ± 12 when platelets were

resuspended in MTB and 39 ± 4 in WP-plasma (Figure 4.4B), but these did not reach statistical significance. As observed in previous experiments, there is a slightly higher number of adhered platelets in the respective control groups on unconjugated fibrinogen compared to Alexa488 FG throughout all groups, although the difference was not statistically significant.

Figure 4.4C illustrates the absence in platelet migration upon resuspending WP in MTB. However, unlike WP-MTB, displacement of platelets in PRP and WP-plasma was observed ($P < 0.001$). The lack of displacement of platelets from their position in WP-MTB compared to PRP ($67 \pm 15\%$) and WP-plasma ($40 \pm 8\%$ of platelets migrated) implies that plasma components are indeed critical for platelets to migrate on Alexa488 FG. Although the percentage of platelets able to migrate was higher in PRP compared to WP-plasma, the difference was not statistically significant. The average area of platelet displacement was found to be comparable between WP-plasma ($2 \pm 0 \mu\text{m}^2$) and PRP ($2 \pm 0 \mu\text{m}^2$) (Figure 4.4D).

Since the presence of plasma proved to be key in facilitating platelet migration, it was decided for platelets to be prepared in the presence of plasma for all migration experiments.

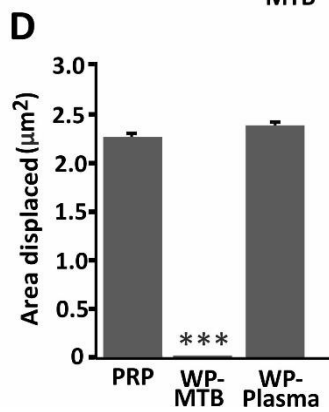
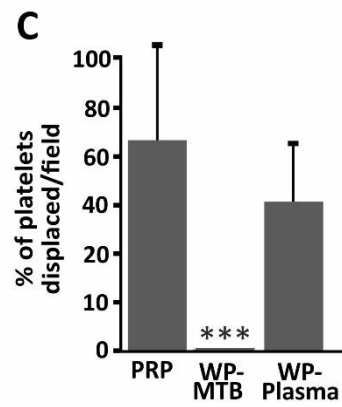
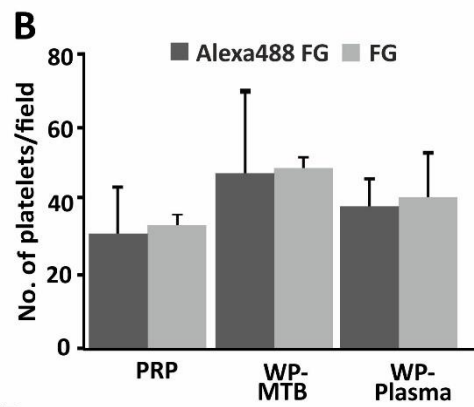
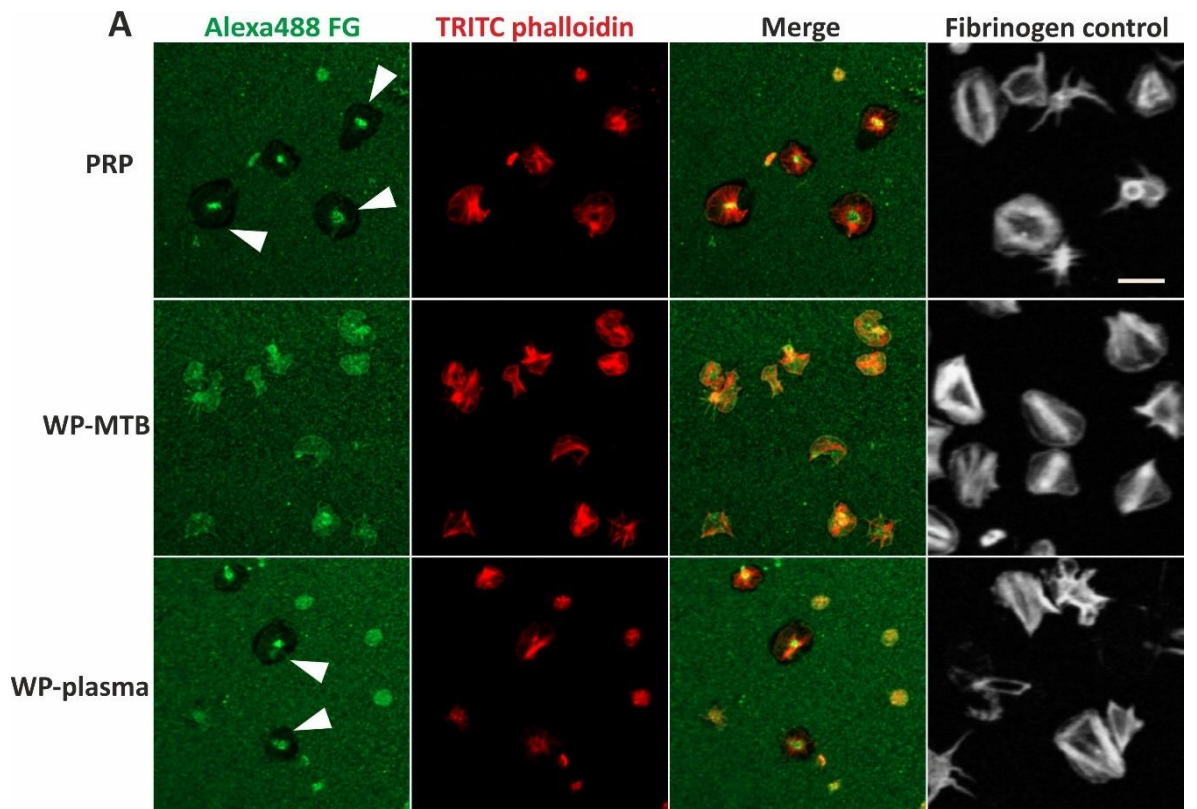


Figure 4.4 Difference between human washed platelets and platelet rich plasma in their ability to migrate.

Glass coverslips were acid washed with HCl for 1 h followed by dH₂O for 1 h and then silanated with HMDS for 1 min at room temperature. Coverslips were then coated with 40 µg/ml Alexa488 fibrinogen (green) and 2mg /ml BSA for 15 min. Platelets were diluted to 1x10⁷/ml by resuspending PRP in plasma and WP in MTB or plasma and 200 µl were added to coverslips and incubated at 37°C for 1 h. Platelets were also spread on fibrinogen (40 µg/ml) coated coverslips in parallel. Coverslips were washed with PBS and fixed with 4% PFA for 10 min, permeabilised with 0.3% Triton X100 for 5 min and stained with 1 µg/ml TRITC phalloidin (red; grey on FG control image) for 30 min at room temperature. Coverslips were then mounted onto glass slides with ProLong Antifade Mountant and images were obtained with a Zeiss ApoTome.2 fluorescence microscope equipped with a 60x oil immersion objective. (A) Representative images from three independent experiments. Scale bar represents 10 µm. Arrowheads indicate examples of platelet migration. (B) Adhesion of cells in each of the conditions was calculated by manually counting cells on ImageJ software. (C) Percentage of migrating platelets per field was counted manually. (D) The average area of Alexa488 FG cleared by individual platelets was calculated on ImageJ software as outlined in section 2.4.7. A total of 40 fields (image size 165.59 µm x 110.39 µm) per condition was analysed. Data are presented as means ±SEM of three independent experiments, (***)p<0.001. Significance in C and D are relative to PRP.

4.2.5 The effect of anticoagulants on the ability of platelets to migrate

Thus far, platelets in PRP were isolated in the presence of SC. In the previous section we found that WP-plasma also possessed the capacity to migrate on Alexa488 FG (Figure 4.4), when compared to PRP. We postulated whether the difference observed was due to the anticoagulant used to isolate platelets, since PRP was isolated in the presence of SC while WP were isolated in the presence of ACD. Therefore, in the next set of experiments we examined the effects of the choice of anticoagulant on the ability of platelets to migrate, to account for buffer compositions in influencing platelet locomotion.

PRP was collected in the presence of ACD or SC and prepared as outlined previously. Platelet migration assay was then conducted as outlined in section 4.2.4.

Movement of platelets on Alexa488 FG was observable in both the ACD and SC groups (Figure 4.5A). It is also possible to see that the number of adhered cells on Alexa488 FG was not significantly different between PRP-ACD (35±4 cells/field) and PRP-SC (24±6 cells/field) (Figure 4.5B). Upon closer analysis of the percentage of cells able to migrate on Alexa488

FG, almost a two-fold increase was found when platelets were prepared in SC ($63\pm 3\%$) compared to ACD ($31\pm 5\%$) ($P < 0.05$) (Figure 4.5C), however the mean area of platelet displacement was found comparable between the two groups ($2\pm 0\mu\text{m}^2$ for PRP-ACD vs $2\pm 0\mu\text{m}^2$ for PRP-SC) (Figure 4.5D).

From the data obtained, it may be assumed that components within the anticoagulants perhaps contribute to the differences observed between platelets prepared in SC and ACD. Therefore, to ensure maximal ability of platelets to migrate, it was decided that if PRP was to be used in future experiments, it would be obtained in the presence of SC.

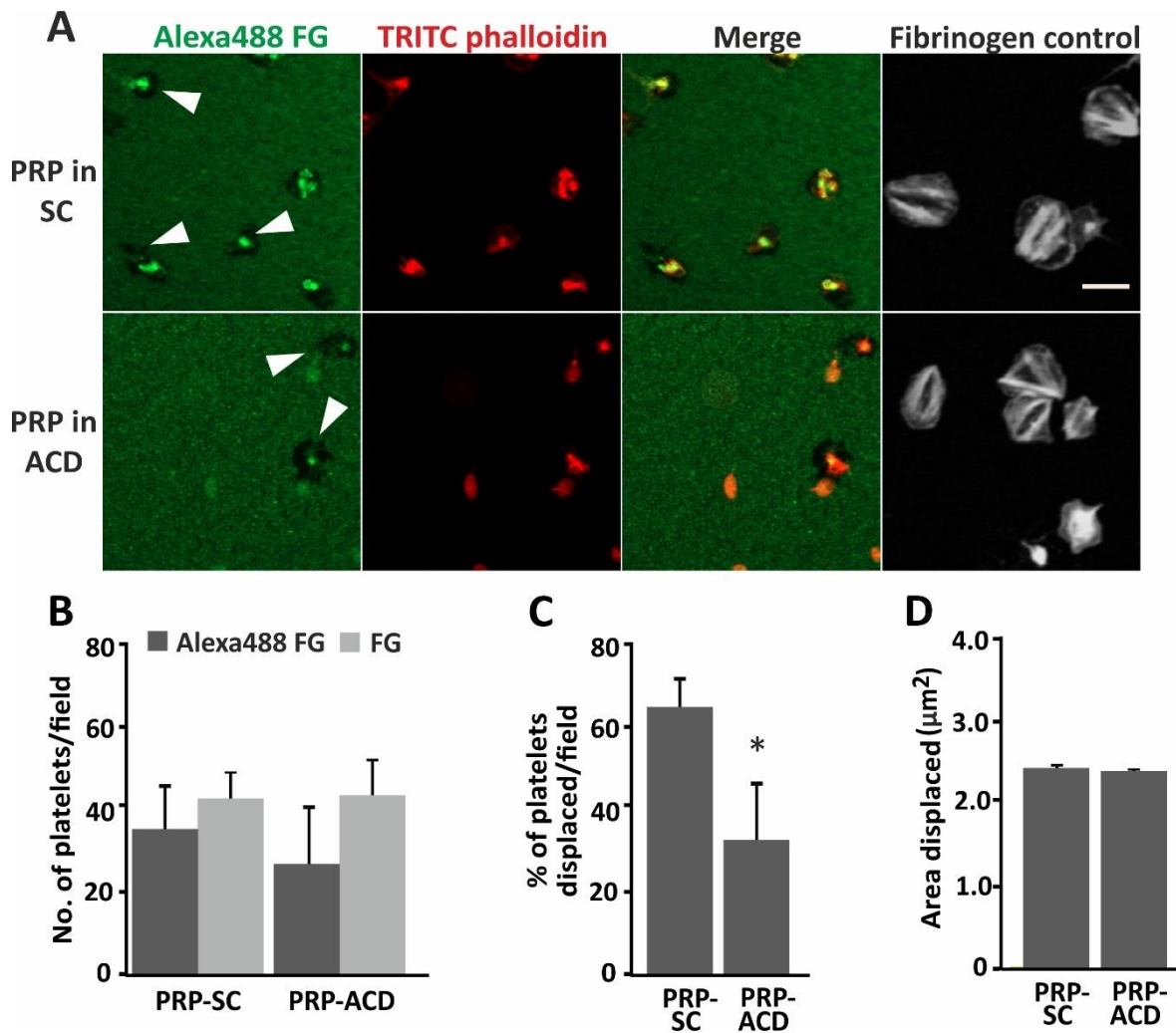


Figure 4.5 Effect of anticoagulant on the capacity of platelets to migrate on Alexa488 FG.

Glass coverslips were acid washed with HCl for 1 h followed by dH₂O for 1 h and then silaned with HMDS for 1 min at room temperature. Coverslips were then coated with 40 $\mu\text{g}/\text{ml}$ Alexa488 fibrinogen (green) and 2mg /ml BSA for 15 min. Platelets in PRP were obtained in the presence of either SC or ACD and diluted to $1 \times 10^7/\text{ml}$. 200 μl of platelet suspension was then added to the coverslips and incubated at 37 $^\circ\text{C}$ for 1 h. Platelets were also spread on fibrinogen (40 $\mu\text{g}/\text{ml}$) coated coverslips in parallel. Coverslips were washed with PBS and fixed with 4% PFA for 10 min, permeabilised with 0.3% Triton X100 for 5 min and stained with 1 $\mu\text{g}/\text{ml}$ TRITC phalloidin (red; grey on the FG control image) for 30 min at room temperature. Coverslips were then mounted onto glass slides with ProLong Antifade Mountant and images were obtained with a Zeiss ApoTome.2 fluorescence microscope equipped with a 60x oil immersion objective. (A) Representative images from three independent experiments. Scale bar represents 10 μm . Arrowheads indicate examples of platelet migration. (B) Adhesion of cells in each of the conditions was calculated by thresholding images on ImageJ software. (C) Percentage of migrating platelets per field was counted manually for all conditions. (D) The average area of Alexa488 FG cleared by individual platelets was calculated on ImageJ software as outlined in section 2.4.7. Data are presented as means \pm SEM of three independent experiments, (* $p < 0.05$).

4.3 Effect of plasma concentration on the migration properties of platelets

In the previous sections (section 4.2.4), it was determined that platelets require the presence of plasma components in order to migrate on Alexa488 FG. Plasma contains a diverse amount of bioactive substances which can modulate the physiological activity of platelets. In the following set of experiments, we wanted to examine the proportion of plasma used to resuspend washed platelets that reverses the capacity of the cells to migrate on Alexa488 FG.

WP and fresh plasma were obtained from healthy blood donors and platelets were diluted to 1×10^7 /ml in combinations of MTB and plasma to obtain suspensions varying in the final concentrations of plasma (0, 25, 50, 75 and 100%). Migration assays were then conducted, and coverslips were processed and analysed as outlined in previous sections.

Figure 4.6A depicts representative images of platelets resuspended in different proportions of plasma and allowed to migrate on Alexa488 FG. It is apparent from these images that platelets were able to migrate on Alexa488 FG in the presence of plasma, irrespective of the amount of plasma used to resuspend the cells.

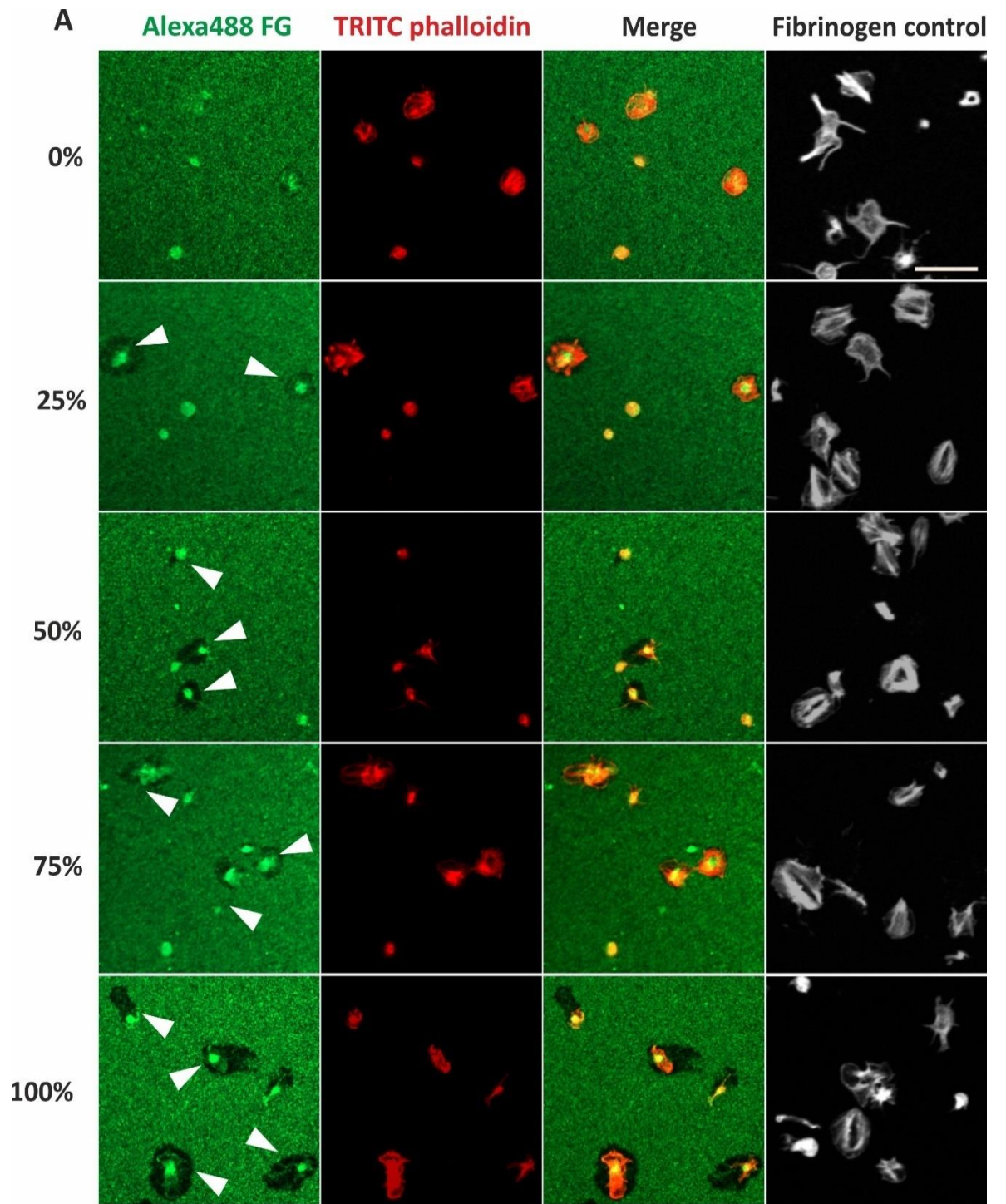
Figure 4.6B confirms that the proportion of plasma used to resuspend platelets does not affect the ability of platelets to adhere to the matrix, as the number of cells/field obtained were comparable between the different platelet suspensions (27 ± 12 cells/field when platelets were resuspended in 100% MTB vs 21 ± 4 cells/field when platelets were resuspended in 100% plasma).

In terms of the ability of platelets to displace from their original position and clear Alexa488 FG, it can be seen in Figure 4.6C that there is a significant difference between different platelet suspension samples. Upon resuspending WP in 25% final plasma volume platelets were found to possess a moderate ability to migrate ($28 \pm 3\%$ cells displaced) ($P < 0.05$). It is also possible to note, that as the percentage of plasma increased, the percentage of cells

able to migrate also increased, with maximal percentage of platelets able to migrate when platelets were resuspended in 100% plasma (70 ± 2 cells displaced).

It is apparent from Figure 4.6D that the area of fibrinogen cleared by platelets remains unaffected by the proportion of plasma since the average area cleared was calculated to be in the range of 2-3 μm^2 between the different populations of migrating platelets.

Essentially, results from these experiments confirmed the notion that plasma is indeed a critical component in permitting the migration of platelets on Alexa488 FG. Resuspending platelets in 100% plasma was determined to be the best conditions and since this is essentially PRP, it was decided to conduct all platelet migration-related investigations into molecular pathways using PRP (diluted to required platelet concentration in plasma) for convenience.



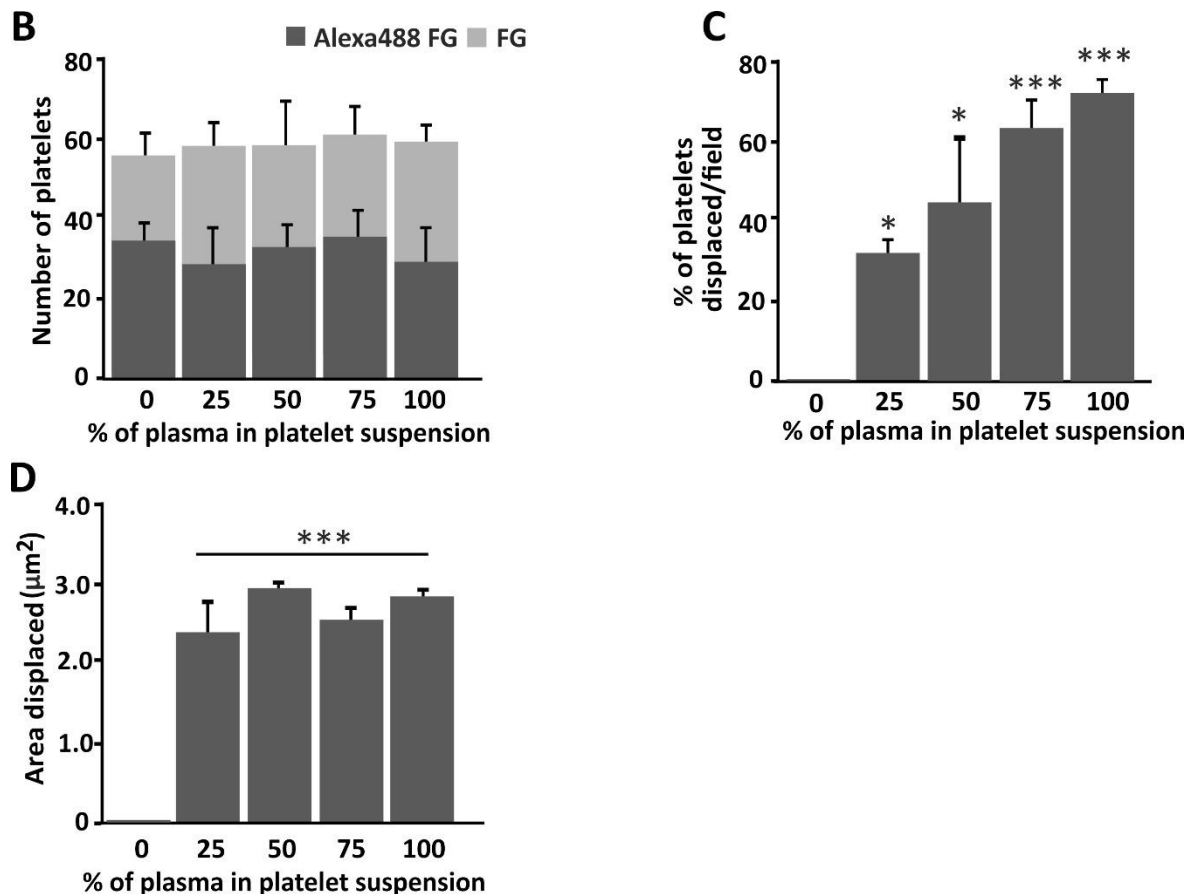


Figure 4.6 Effect of the concentration of plasma on platelets' ability to migrate. Glass coverslips were acid washed with HCl for 1 h followed by dH₂O for 1 h and then silaned with HMDS for 1 min at room temperature. Coverslips were then coated with the 40 µg/ml Alexa488 fibrinogen (green) and 2mg/ml BSA for 15 min. Human WP was isolated from healthy donors and prepared to 1x10⁷/ml in varying proportions of fresh plasma and MTB such that the final percentage of plasma were as indicated. 200 µl of platelet suspension was then added to the coverslips and incubated at 37°C for 1 h. At the relevant timepoints, coverslips were washed with PBS and fixed with 4% PFA for 10 min, permeabilised with 0.3% Triton X100 for 5 min and stained with 1 µg/ml TRITC phalloidin (red) for 30 min at room temperature. Coverslips were mounted onto glass slides with ProLong Antifade Mountant and images were obtained with a Zeiss ApoTome.2 fluorescence microscope equipped with a 60x oil immersion objective. (A) Representative images from three independent experiments. Scale bar represents 10 µm. Arrowheads indicate examples of platelet migration. (B) Adhesion of cells in each of the conditions was calculated by manually counting cells on ImageJ software. (C) Percentage of migrating platelets per field was counted manually for all the conditions. (D) The average area of Alexa488 FG cleared by individual platelets were calculated on ImageJ software as outlined in section 2.4.7. Data are presented as means ±SEM of three independent experiments. Statistical significance was calculated relative to 0%, (*p<0.05 and ***p<0.001).

4.4 Molecular mechanisms regulating migration of platelets on Alexa488 fibrinogen

Thus far we have optimised and established a method for the accurate quantitative analysis of platelet migration capacity. The aim of this section is to gain insight into the molecular mechanisms involved which influence platelet migration processes. In order to do so, we utilised inhibitors of specific signalling pathways and analysed the effects they had on the ability of platelets to migrate.

In the following sections, inhibitors of Rho GTPases, in particular those targeting RhoA, Rac1 and Cdc42 were chosen to examine the involvement of these small GTPases in facilitating platelet migration on Alexa488 FG. Along with this, inhibitors of the tyrosine kinase signalling pathway, used commonly in the treatment of haematologic and solid malignancies, were also chosen to be examined for their effects on the migratory capacity of platelets. It was also decided to analyse the effects of inhibiting major platelet surface receptors GPIIb/IIIa and FcγRIIa, on platelet migration capacity.

4.4.1 Cytoskeletal inhibitors diminish the migration properties of platelets

It is well-recognized for Rho GTPases to be critically involved in the rearrangement of cytoskeletal components which in turn is a key process that influences the migration of platelets. Numerous studies have utilised various compounds to target cytoskeletal components to study various signalling pathways. We too in the previously chapter utilised Rho GTPase inhibitors rhosin, NSC 23766 and CASIN to study the molecular mechanisms involved in platelet-scavenging of bacteria (section 3.6.1).

In this section, it was decided to utilise the same inhibitors; rhosin, NSC 23766 and CASIN for their targeted inhibition of RhoA, Rac1 and Cdc42, respectively. It was also decided to use latrunculin A in this study since this molecule has been reported to directly target the organisation of the actin cytoskeleton.

We have established in Chapter 3 the working concentration of inhibitors to be appropriate for the research of platelet functions (Figure 3.12). PRP was obtained from healthy donors

and diluted to 1×10^7 cells/ml with plasma. Platelets were then treated with cytoskeletal inhibitors rhosin ($30 \mu\text{M}$), NSC23766 ($70 \mu\text{M}$) or CASIN ($10 \mu\text{M}$) for 10 min, or Lat-A ($20 \mu\text{M}$) for 30 min at 37°C . DMSO was used to prepare the inhibitor stocks as done previously and so one set of platelets (referred to as control) was given DMSO to a final 1:1000 dilution. This was performed to confirm any effects detected in the platelet inhibitor populations were owing to the inhibitors themselves and not to the presence of DMSO.

After incubation, 200 μl of inhibitor-treated platelet suspension were placed on Alexa488 FG coated coverslips and incubated for 1 h at 37°C . Platelets were also spread on $40 \mu\text{g/ml}$ fibrinogen in parallel. Coverslips were then processed and analysed as detailed in section 4.2.1.

Figure 4.7A illustrates representative examples of the effect of incubating platelets with cytoskeletal inhibitors on the ability of platelets to migrate on Alexa488 FG and spread on fibrinogen.

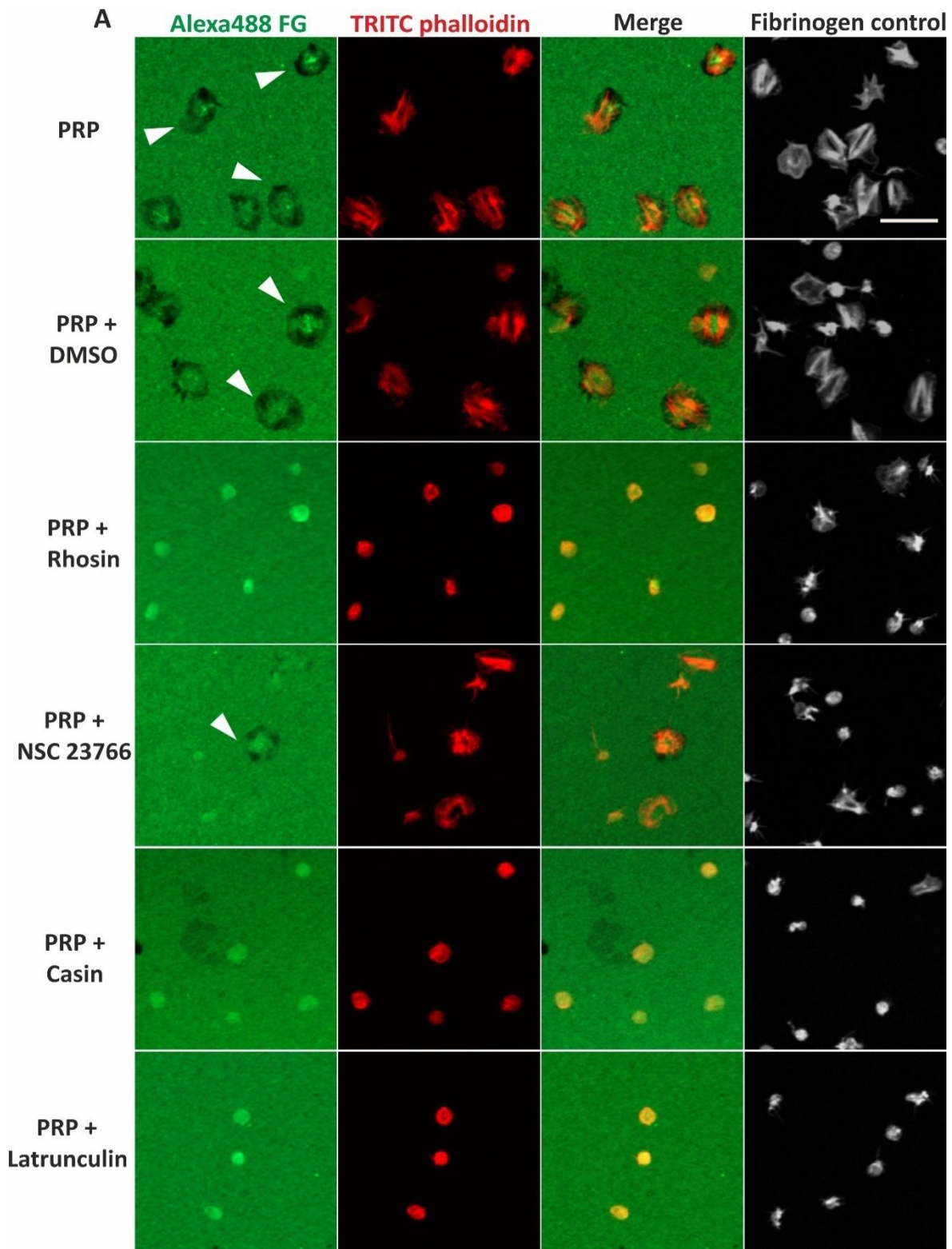
Regarding platelet adhesion, Figure 4.7B demonstrates the number of platelets/field to be comparable between the different groups, except for Lat-A treated platelets where a significant decrease in the number of platelets per field was observed (6 ± 2 platelets/field) compared to the control (25 ± 6 platelets/field; $P < 0.01$). A similar observation was made for platelets treated with Lat-A inhibitor and then spread on fibrinogen (27 ± 1 platelets/field in the Lat-A treated vs 49 ± 4 in the control; $P < 0.05$).

In terms of the ability of platelets to migrate on Alexa488 FG, it can be seen in Figure 4.7C that $65 \pm 3\%$ of platelets had the capacity to migrate in the absence of inhibitors. On the contrary, significant differences in migratory capacity were observed upon cytoskeletal inhibitor treatment, with a complete lack of platelet migration noted upon treating platelets with rhosin, CASIN or Lat-A ($P < 0.001$). As for platelets treated with the Rac1 inhibitor, only $9 \pm 5\%$ of cells were found to possess the ability to migrate which was significantly lower compared to uninhibited platelet group ($P < 0.001$).

Interestingly, we found the area of displacement by platelets to be the same between PRP control group and NSC 23766-treated platelet group ($1 \mu\text{m}^2$) (Figure 4.7D).

In addition to all of the above, it can be seen in Figure 4.7 that uninhibited platelets with the supplementation of DMSO had comparable results in terms of platelet adhesion (27 ± 8 platelets/field), percentage platelet migration ($69 \pm 2\%$) and the area of displacement ($1 \pm 1 \mu\text{m}^2$), when compared to that of PRP in the absence of DMSO. Consequently, this confirms that any changes observed in the inhibitor treated platelet groups are exclusively an effect of the inhibitors. For the purpose of the ensuing set of experiments, PRP in the presence of DMSO is referred to as the control.

The results obtained, reinforces Rho GTPases to be critically involved in regulating platelet functions, specifically platelet migratory capacity.



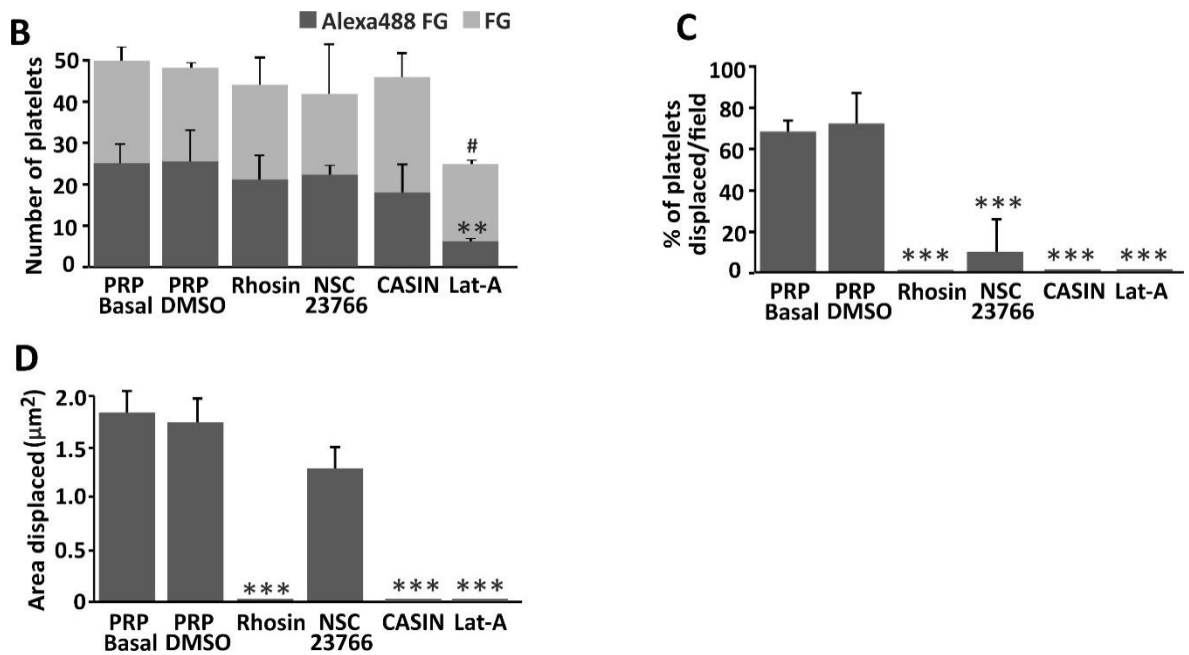


Figure 4.7 The effect of cytoskeletal inhibitors on platelet migration on Alexa488 FG. Glass coverslips were acid washed with HCl for 1 h followed by dH₂O for 1 h and then silanated with HMDS for 1 min at room temperature. Coverslips were then coated with 40 $\mu\text{g}/\text{ml}$ Alexa488 fibrinogen (green) and 2mg /ml BSA for 15 min. Platelets were diluted with plasma to 1×10^7 /ml and incubated with Rhosin (30 μM), NSC 23766 (70 μM) or CASIN (10 μM) for 10 min, or Lat-A (20 μM) for 30 min. PRP DMSO control received 1:1000 DMSO. 200 μl of platelet suspension were then placed on coverslips and incubated at 37°C for 1 h. Platelets were also spread on fibrinogen (40 $\mu\text{g}/\text{ml}$) coated coverslips in parallel. Cells were subsequently washed with PBS, fixed, permeabilised and incubated with 1 $\mu\text{g}/\text{ml}$ TRITC phalloidin (red; grey on FG control image) for 30 min at room temperature. Coverslips were mounted onto glass slides and microscope images were obtained by using a Zeiss ApoTome.2 fluorescence microscope equipped with a 40x oil immersion objective. (A) Representative images from three independent experiments. Scale bar represents 20 μm . Arrowheads indicate examples of Alexa488 FG cleared during platelet migration. (B) The number of platelets per field and (C) the percentage of migrating platelets were calculated manually. (D) The average area of Alexa488 FG cleared by individual platelets was calculated on ImageJ software as outlined in section 2.4.7. Data are presented as means \pm SEM of three independent experiments. Statistical significance was calculated using Kruskal-Wallis (* $p < 0.05$, ** $p < 0.01$ and *** $p < 0.001$). Asterisks indicates the significance between the populations incubated on Alexa488 FG relative to the corresponding PRP basal, while the hash sign indicates the significance between the populations incubated on unconjugated fibrinogen relative to the PRP basal on FG.

4.4.2 Inhibition of platelet surface receptors FcγRIIa and GPIIb/IIIa modifies platelet migration capacity

Platelet receptors are key surface structures used by platelets for the initiation of a number of processes. In the following experimentations, we aimed to explore the contribution of FcγRIIa and GPIIb/IIIa platelet surface receptors in facilitating platelet migration. Since both receptors have been found to promote the binding of platelets to fibrinogen. In order to do so, we utilized inhibitors IV.3 antibody and integrilin which target receptors FcγRIIa and GPIIb/IIIa, respectively.

PRP was isolated and diluted as outlined in section 4.5.1 and platelets were treated with 15 µg/ml IV.3 antibody or 9 µM integrilin for 9 min and 2 min, respectively. After incubation with the inhibitors, platelet migration assay was performed as described previously in section 4.4.1. Platelets were also spread on 40 µg/ml fibrinogen in parallel. Coverslips were then processed and analysed as per the above sections. PRP in the presence of 1:1000 DMSO was used as the control in all experiments since it was revealed in the preceding section for DMSO at the given concentration to not alter platelet migration capabilities (Figure 4.7).

Figure 4.8A shows representative examples of the effect of inhibiting platelet surface receptors on the ability of platelets to migrate on Alexa488 FG and spread on fibrinogen. White arrowheads indicate the area of fibrinogen cleared by individual migrating platelet. An absence in platelet migration can also be seen upon incubating PRP with the GPIIb/IIIa inhibitor.

Figure 4.8B reveals the number of platelets adhered to Alexa488 FG to be comparable between the platelet groups, with 20-25 platelets/field observed in each group. Similarly, no significant difference in the number of platelets/field was found for platelets spread on unconjugated fibrinogen.

In the matter of platelet migration capacity, we found uninhibited platelets in the presence of DMSO to migrate to the same capacity as formerly found in this chapter, with $59 \pm 6\%$

platelets possessing the capacity to migrate (Figure 4.8C). In addition to this, it can be observed that treatment of platelets with IV.3 antibody resulted in a significant reduction in the ability of platelets to migrate, as only $17\pm 2\%$ platelets were found to retain the ability to migrate compared to control ($P < 0.01$), whereas incubating platelets with integrilin resulted in a complete lack of ability for platelets to migrate on Alexa488 FG ($P < 0.001$).

A decrease in the area of Alexa488 FG cleared by individual platelets upon IV.3 ab treatment was found ($1\pm 1 \mu\text{m}^2$) compared to control ($1\pm 1 \mu\text{m}^2$), although the difference was calculated to not be significant (Figure 4.8D).

Results gathered from these set of experiments propose that inhibiting platelet receptors, GPIIb/IIIa more so than FcγRIIa, hinders platelet migratory capacity thus signifying that these receptors are key partakers in initiating platelet signalling necessary for platelet migration.

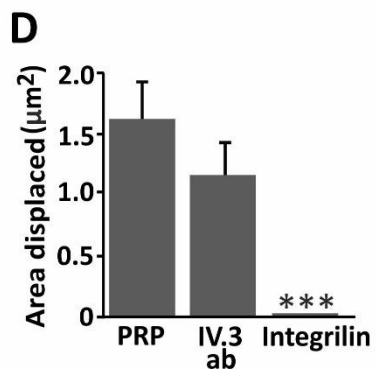
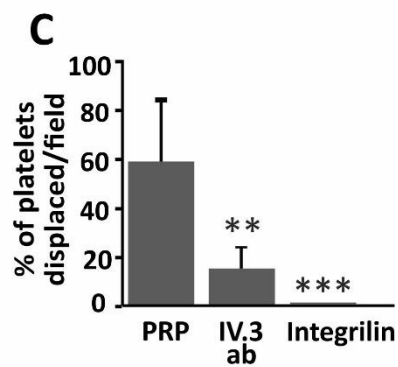
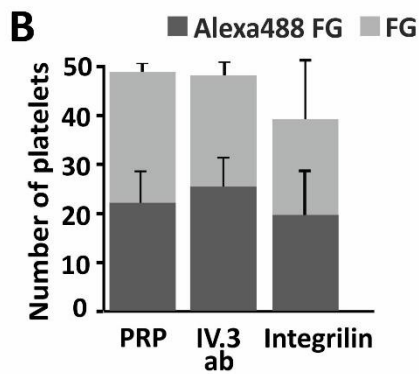
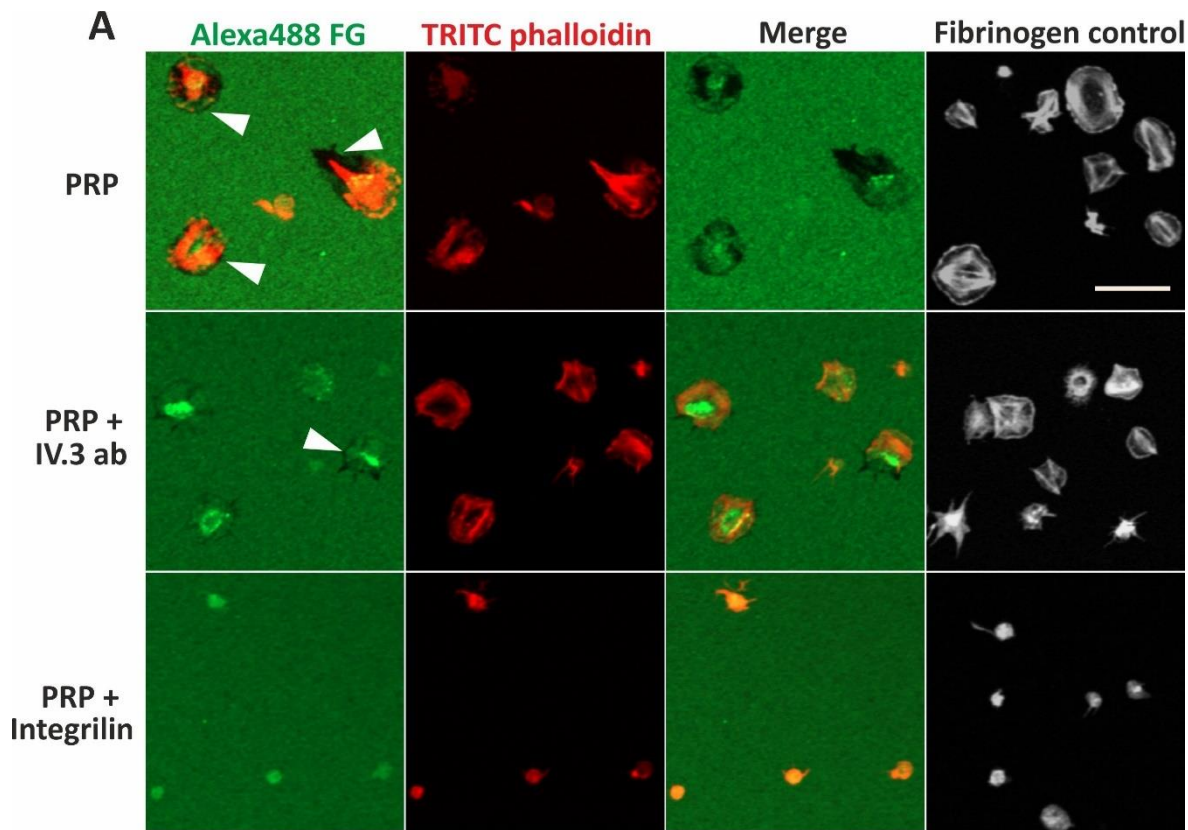


Figure 4.8 The effect of platelet surface receptor inhibitors on platelet functions. Glass coverslips were acid washed with HCl for 1 h followed by dH₂O for 1 h and then silaned with HMDS for 1 min at room temperature. Coverslips were then coated with 40 $\mu\text{g}/\text{ml}$ Alexa488 fibrinogen (green) and 2mg /ml BSA for 15 min. Platelets were diluted with plasma to $1 \times 10^7/\text{ml}$ and incubated with IV.3 ab (15 $\mu\text{g}/\text{ml}$) or

integrilin (9 μM) for 9 min and 2 min, respectively. PRP control received 1:1000 DMSO. 200 μl of platelet suspension were then placed on coverslips and incubated at 37°C for 1 h. Platelets were also spread on fibrinogen (40 $\mu\text{g}/\text{ml}$) coated coverslips in parallel. Cells were subsequently washed with PBS, fixed, permeabilised and incubated with 1 $\mu\text{g}/\text{ml}$ TRITC phalloidin (red; grey on FG control image) for 30 min at room temperature. Coverslips were mounted onto glass slides and microscope images were obtained by using a Zeiss ApoTome.2 fluorescence microscope equipped with a 40x oil immersion objective. (A) Representative images from three independent experiments. Scale bar represents 10 μm . Arrowheads indicate examples of Alexa488 FG cleared during platelet migration. (B) The number of platelets per field and the (C) percentage of migrating platelets were calculated manually. (D) The average area of Alexa488 FG cleared by individual platelets was calculated on ImageJ software as outlined in section 2.4.7. Data are presented as means \pm SEM of three independent experiments, (** $p < 0.01$ and *** $p < 0.001$).

4.4.3 Inhibition of tyrosine kinase signalling pathways alters the capacity of platelets to migrate

The status of platelet surface receptors in facilitating platelet migration on Alexa488 FG has been established in the former section. Here we aim to look at the consequences of various therapeutic drugs which have been identified previously to target numerous platelet signalling pathways, and whether they modify the capacity of platelets to migrate. To address this, we used inhibitors PRT318 (PRT), dasatinib and ibrutinib which target receptors Syk, Src and BTK, respectively. Acalabrutinib, which is a more BTK-specific inhibitor than ibrutinib was also utilised in the next set of experiments to gain insight into the effects of blocking downstream signalling molecules of the Fc γ R1a receptor, which in turn has also been found to stimulate the switch of GPIIb/IIIa from a low affinity to high-affinity state for fibrinogen.

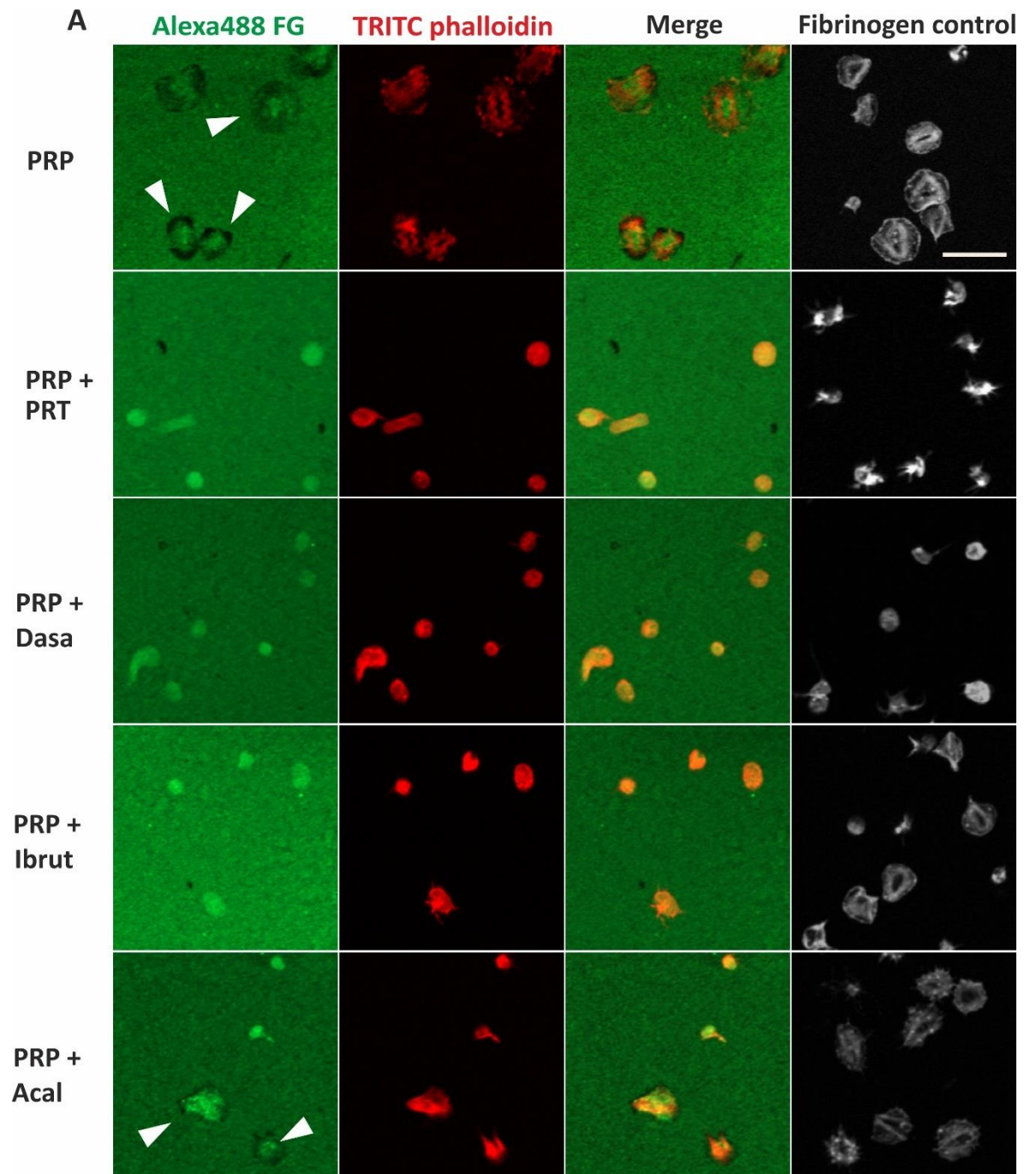
PRP obtained from healthy donors was diluted to 1×10^7 cells/ml in plasma and incubated with 5 μM ibrutinib for 5 min, 15 μM acalabrutinib for 5 min, 4 μM dasatinib for 2 min or 10 μM PRT for 2 min. Following incubation, platelet migration assays was conducted as outlined in section 4.2.1. Platelets were also spread on 40 $\mu\text{g}/\text{ml}$ fibrinogen in parallel. Coverslips were then processed and analysed as detailed in section 4.4.1.

Representative examples of the ability of platelets to migrate in the presence of the above-mentioned signalling inhibitors is shown in Figure 4.9A. A slightly lower number of platelets

was found to adhere to Alexa488 FG in all inhibitor-treated platelet groups, although the difference was calculated to be insignificant (Figure 4.9B). Comparable results were also found between the different platelet groups in terms of the number of platelets adhered/field on unconjugated fibrinogen (42-46 cells/field).

Figure 4.9C shows $64\pm 3\%$ of uninhibited platelets to possess the ability to migrate on Alexa488 FG. By contrast, a significant reduction in the ability of platelets to migrate was observed upon acalabrutinib ($7\pm 4\%$, $P < 0.01$) treatment. A complete lack in ability to migrate was seen for platelets treated with PRT, dasatinib and ibrutinib ($P < 0.001$). However, in terms of area displaced by individual platelets, Figure 4.9D shows results to be similar between uninhibited platelets ($1\pm 0 \mu\text{m}^2$) and acalabrutinib-treated platelets ($1\pm 1 \mu\text{m}^2$).

Together, data from these set of experiments reveal that inhibiting platelet tyrosine signalling pathways hinders platelet migration capacity to varying extents, thus suggesting that these pathways are critically involved in influencing aspects of platelet migratory functions.



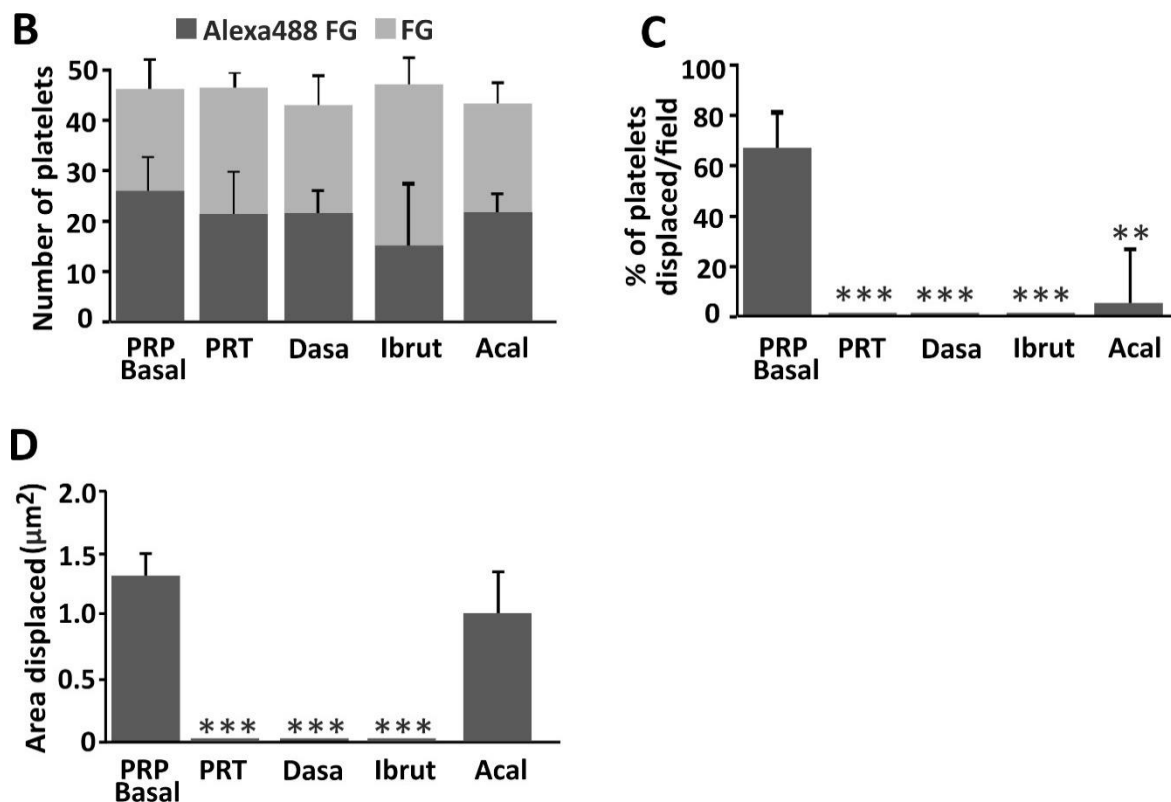


Figure 4.9 The effect of BTK, Src and Syk signalling inhibitors on the ability of platelets to migrate. Glass coverslips were acid washed with HCl for 1 h followed by dH₂O for 1 h and then silanated with HMDS for 1 min at room temperature. Coverslips were then coated with 40 $\mu\text{g}/\text{ml}$ Alexa488 fibrinogen (green) and 2mg /ml BSA for 15 min. Platelets were diluted with plasma to 1×10^7 /ml and incubated with 5 μM Ibrutinib (Ibrut) or 15 μM acalabrutinib (Acal) for 5 min; or 4 μM dasatinib (Dasa) or 10 μM PRT318 (PRT) for 2 min. PRP control received 1:1000 DMSO. 200 μl of platelet suspension were then placed on coverslips and incubated at 37°C for 1 h. Platelets were also spread on fibrinogen (40 $\mu\text{g}/\text{ml}$) coated coverslips in parallel. Cells were subsequently washed with PBS, fixed, permeabilised and incubated with 1 $\mu\text{g}/\text{ml}$ TRITC phalloidin (red; grey on FG control image) for 30 min at room temperature. Coverslips were mounted onto glass slides and microscope images were obtained by using a Zeiss ApoTome.2 fluorescence microscope equipped with a 40x oil immersion objective. (A) Representative images from three independent experiments. Scale bar represents 10 μm . Arrowheads indicate examples of Alexa488 FG cleared during platelet migration. (B) The number of platelets per field and the (C) percentage of migrating platelets were calculated manually. (D) The average area of Alexa488 FG cleared by individual platelets was calculated on ImageJ software as outlined in section 2.4.7. Data are presented as means \pm SEM of three independent experiments. Statistical significance was calculated using a Kruskal-Wallis test, significance is relative to PRP basal (* $p < 0.05$, ** $p < 0.01$ and *** $p < 0.001$).

4.5 The ability of mouse platelets to migrate

A plethora of murine models have been used in literature to aid the study of a variety of platelet functions. This is largely due to the fact that mice are genetically similar to humans and they are susceptible to genetic manipulation. Though murine platelets do differ in terms of size, structure, and number, functionally they are analogous to human platelets. Henceforth, the use of these model systems in research has considerably enhanced our knowledge with respect to the impact of platelets in hemostasis and immunity. In the next set of experiment, we propose to examine the ability of mouse platelets to migrate on Alexa488 FG and whether this differs from the characteristic migration observed in human platelets in the previous sections.

4.5.1 Optimisation of the conditions required for mouse platelets to migrate on Alexa488 FG

It was determined in Figure 4.4 that the presence of plasma proved to be critical for the migration of human platelets on Alexa488 FG. A preliminary test was conducted to investigate whether the same was true for mouse platelets.

Mouse PRP, WP-plasma and WP-MTB were prepared as outlined in section 2.3.2. 200 μ l of platelet suspensions were then placed onto glass coverslips pre-coated with Alexa488 FG in combination with BSA and processed as mentioned in earlier sections. The number of adhered platelets and the percentage of migrating platelets were determined for all the groups. Samples of each platelet preparation were incubated on unconjugated fibrinogen (40 μ g/ml) coated coverslips as a control of their spreading profile and processed in parallel.

It is evident from Figure 4.10A that mouse platelets behave in a similar way to that of human platelets, since platelet migration was only observable upon resuspending platelets in the presence of plasma. No significant difference in the number of platelets was found between the different populations (32-40 cells/field in the different groups) (Figure 4.10B). Comparable results were found among platelets spread on unconjugated fibrinogen with regard to the number of cells/field, though a higher number of platelets were found to have adhered to unconjugated fibrinogen when compared to Alexa488 FG.

Figure 4.10C demonstrates a slightly higher percentage of platelets able to migrate in the PRP group (64% migrating cells) compared to WP-plasma (56% migrating cells) (white arrowheads). As for the area of fibrinogen cleared, it is apparent in Figure 4.10D for the results to be similar between the two groups with platelets migrating on average 1-2 μm^2 in both PRP and WP-plasma.

The results obtained reinforces the pivotal role of plasma in influencing platelet migration in mouse models. Therefore, it was decided for mouse platelets to be prepared in the presence of plasma for the subsequent platelet migration experiments.

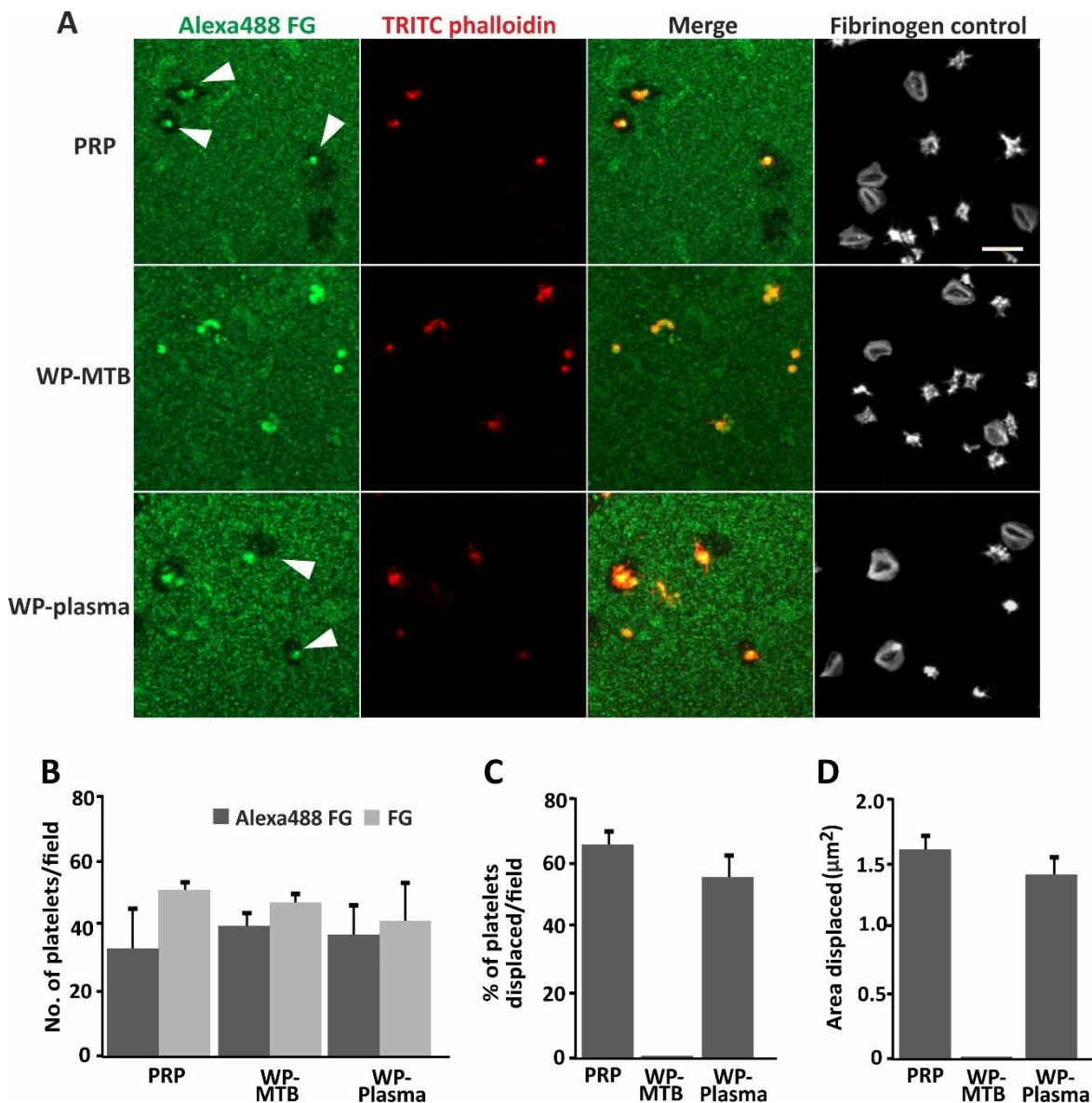


Figure 4.10 Difference between mouse washed platelets and platelet rich plasma in their ability to migrate. Glass coverslips were acid washed with HCl for 1 h followed by dH₂O for 1 h and then silanated with HMDS for 1 min at room temperature. Coverslips were then coated with 40 µg/ml Alexa488 fibrinogen (green) and 2 mg /ml BSA for 15 min. Mouse platelets were diluted to 1x10⁷/ml by resuspending PRP in plasma and WP in MTB or plasma and 200 µl were added to coverslips and incubated at 37 °C for 1 h. Platelets were also spread on fibrinogen (40 µg/ml) coated coverslips in parallel. Coverslips were washed with PBS and fixed with 4% PFA for 10 min, permeabilised with 0.3% Triton X100 for 5 min and stained with 1 µg/ml TRITC phalloidin (red; grey on FG control image) for 30 min at room temperature. Coverslips were then mounted onto glass slides with ProLong Antifade Mountant and images were obtained with a Zeiss ApoTome.2 fluorescence microscope equipped with a 60x oil immersion objective. (A) Representative images from two independent experiments, scale bar represents 20 µm. Arrowheads indicate examples of platelet migration. (B) Adhesion of cells in each of the conditions was calculated by manually counting cells on ImageJ software. (C) Percentage of migrating platelets per field was counted manually. (D) The average area of Alexa488 FG cleared by individual platelets was calculated on ImageJ software as outlined in section 2.4.7. Data are presented as means ±SEM of two independent experiments.

4.5.2 A comparison of human and mouse plasma on the ability of mouse platelets to migrate

Terminal blood collection from a mouse via a cardiac puncture yields around 0.8-1.0 ml of blood (Hoff & Hoff, 2000). Often it is difficult to obtain sufficient amount of blood from mouse models for the isolation of both plasma and platelets. On the contrary, obtaining the necessary amount of blood from human donors for platelet research is much simpler. Therefore, to ensure necessary amount of plasma is available for the investigation of mouse platelet functions, it was decided to assess whether resuspending mouse platelets in human plasma would have any profound effects on the migratory capacity of mouse platelets.

Mouse PRP were diluted to 1x10⁷/ml by resuspending in either human or mouse plasma. Platelet migration assay was then conducted as outlined in section 4.5.1. Samples of each platelet preparation were also incubated on unconjugated fibrinogen (40 µg/ml) coated coverslips as a control of their spreading profile. Coverslips were then processed and analysed in parallel.

Examples of representative images from platelet migration assay conducted on mouse platelets resuspended in human or mouse plasma can be seen in Figure 4.11A. It is observable for platelet migration to be present among both groups.

It is clear from Figure 4.11B for platelet adhesion results to be comparable for platelets on Alexa488 FG between the groups (22 ± 5 platelets/field when platelets were resuspended in mouse plasma vs 23 ± 3 platelets/field upon resuspending platelets in human plasma). Comparable results were also found between the two preparations when platelets were spread on unconjugated fibrinogen.

With respect to the percentage of platelets able to migrate, it was found for 60-70% of platelets in both groups to display migratory capacity (Figure 4.11C). In addition to this, Figure 4.11D demonstrates the area of Alexa488 FG cleared by platelets to also be similar between the two groups ($1 \pm 0 \mu\text{m}^2$ when platelets were resuspended in mouse plasma vs $2 \pm 1 \mu\text{m}^2$ upon resuspending platelets in human plasma).

The results obtained from these set of experiments confirms that resuspending mouse platelets in plasma from either human or mouse species results in no significant difference with regard to observing migratory capabilities of platelets on Alexa488 FG. Therefore, it was decided to resuspend mouse platelets in human plasma for the subsequent experiments since obtaining enough blood from mouse models for the isolation of both plasma and platelets is often problematic.

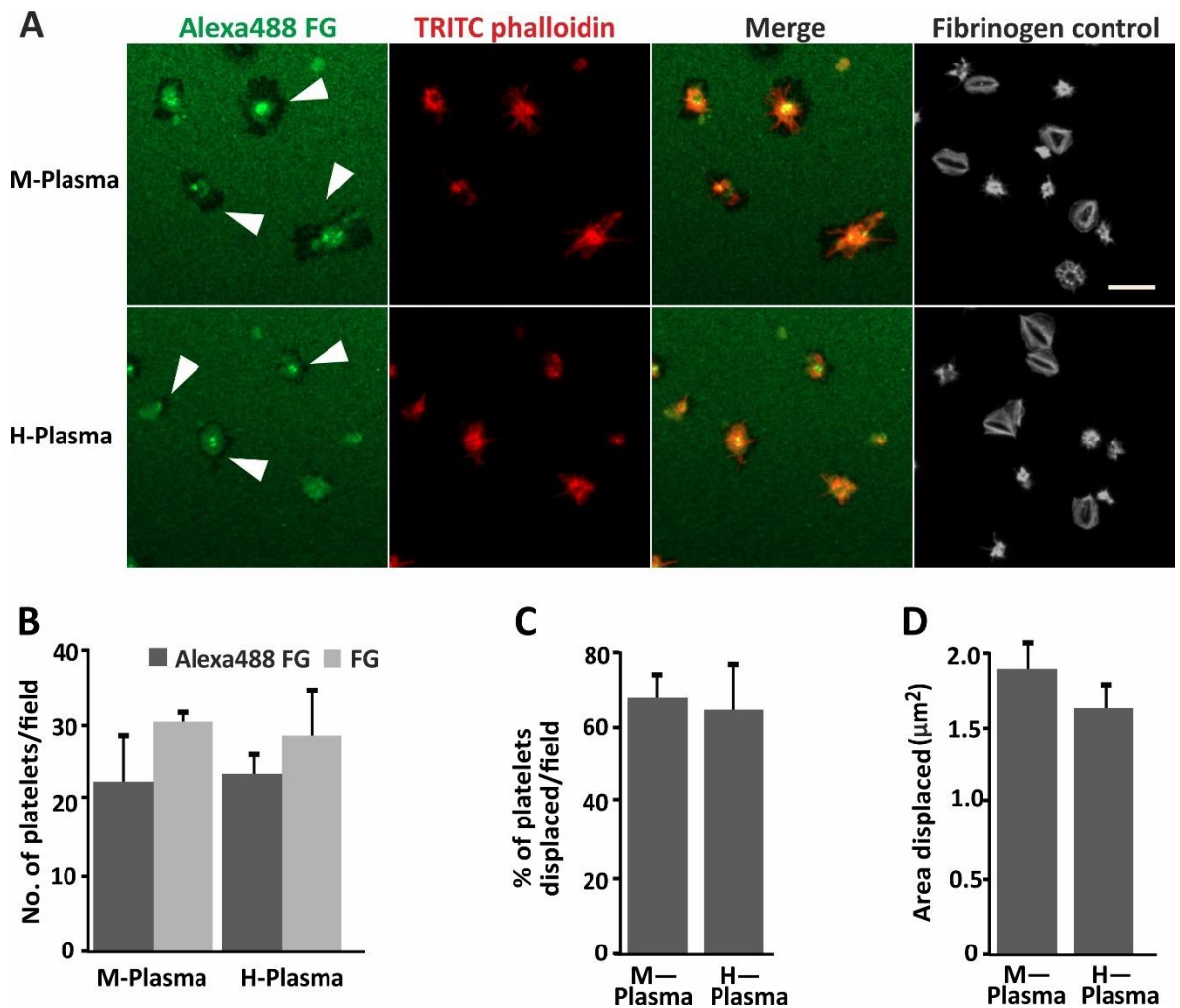


Figure 4.11 The difference between resuspending mouse platelets in human or mouse plasma on their ability to migrate. Glass coverslips were acid washed with HCl for 1 h followed by dH₂O for 1 h and then silaned with HMDS for 1 min at room temperature. Coverslips were then coated with 40 $\mu\text{g}/\text{ml}$ Alexa488 fibrinogen (green) and 2 mg/ml BSA for 15 min. Mouse platelets in PRP were then diluted to $1 \times 10^7/\text{ml}$ by resuspending in either human or mouse plasma. 200 μl of platelet suspension were then added to the coverslips and incubated at 37 $^\circ\text{C}$ for 1 h. Coverslips were washed with PBS and fixed with 4% PFA for 10 min, permeabilised with 0.3% Triton X100 for 5 min and stained with 1 $\mu\text{g}/\text{ml}$ TRITC phalloidin (red; grey on the FG control image) for 30 min at room temperature. Coverslips were mounted onto glass slides with ProLong Antifade Mountant and images were obtained with a Zeiss ApoTome.2 fluorescence microscope equipped with a 60x oil immersion objective. (A) Representative images from three independent experiments. M-plasma: platelets resuspended in mouse plasma, H-plasma: platelets resuspended in human plasma. Scale bar represents 20 μm . Arrowheads indicate examples of platelet migration. (B) Adhesion of cells in each of the conditions was calculated via manual counting (C) Percentage of migrating platelets per field and (D) the average area of Alexa488 FG cleared by individual platelets was either counted manually or calculated on ImageJ software as outlined in section 2.4.7. Data are presented as means \pm SEM of two independent experiments.

4.5.3 A comparison of fresh and frozen plasma on the ability of mouse platelets to migrate

We established in the previous section (4.5.1) that plasma is critical in order for platelets to migrate (Figure 4.10). It has also been found for mouse platelets resuspended in human plasma retained their ability to migrate on Alexa488 FG (Figure 4.11). Generally, obtaining human plasma at the same time as mouse platelets is often difficult due to limited availability of blood from the species at the same time. Studies previously have demonstrated the freezing and thawing of plasma to combat such accessibility issues (Bohoněk, 2018; McIntosh *et al.*, 1990). In this section we sought to determine whether freezing human plasma samples for use at a later time would have any influence on the ability of mouse platelets to migrate.

Plasma from healthy donors were collected and stored at -20°C overnight. The following day mouse platelets were diluted to 1×10^7 /ml in either fresh or frozen-thawed plasma. Platelet migration assay was then conducted as detailed previously.

Figure 4.12A shows representative examples of the effect of resuspending mouse platelets in frozen-thawed plasma compared to plasma processed immediately. A complete absence in platelet migration and spreading upon dilution in frozen plasma was observable when platelets were placed on Alexa488 FG. A small decrease in the number of platelets per field was observed when platelets were diluted in frozen plasma, however the difference was not significant (Figure 4.12B). The same was found for platelets spread on unconjugated fibrinogen. Figure 4.12C and D illustrates a significant difference ($P < 0.001$) between the two groups with regards to platelet migration since platelets resuspended in frozen plasma lacked the capacity to migrate on Alexa488 FG whereas $64 \pm 3\%$ of platelets resuspend in fresh plasma were able to cover $1 \pm 2 \mu\text{m}^2$.

It is clear from the data gathered that fresh plasma is essential to observe the movement of platelets on Alexa488 FG. Hence, it was decided to continue resuspending mouse platelets in fresh human plasma for the next set of experiments.

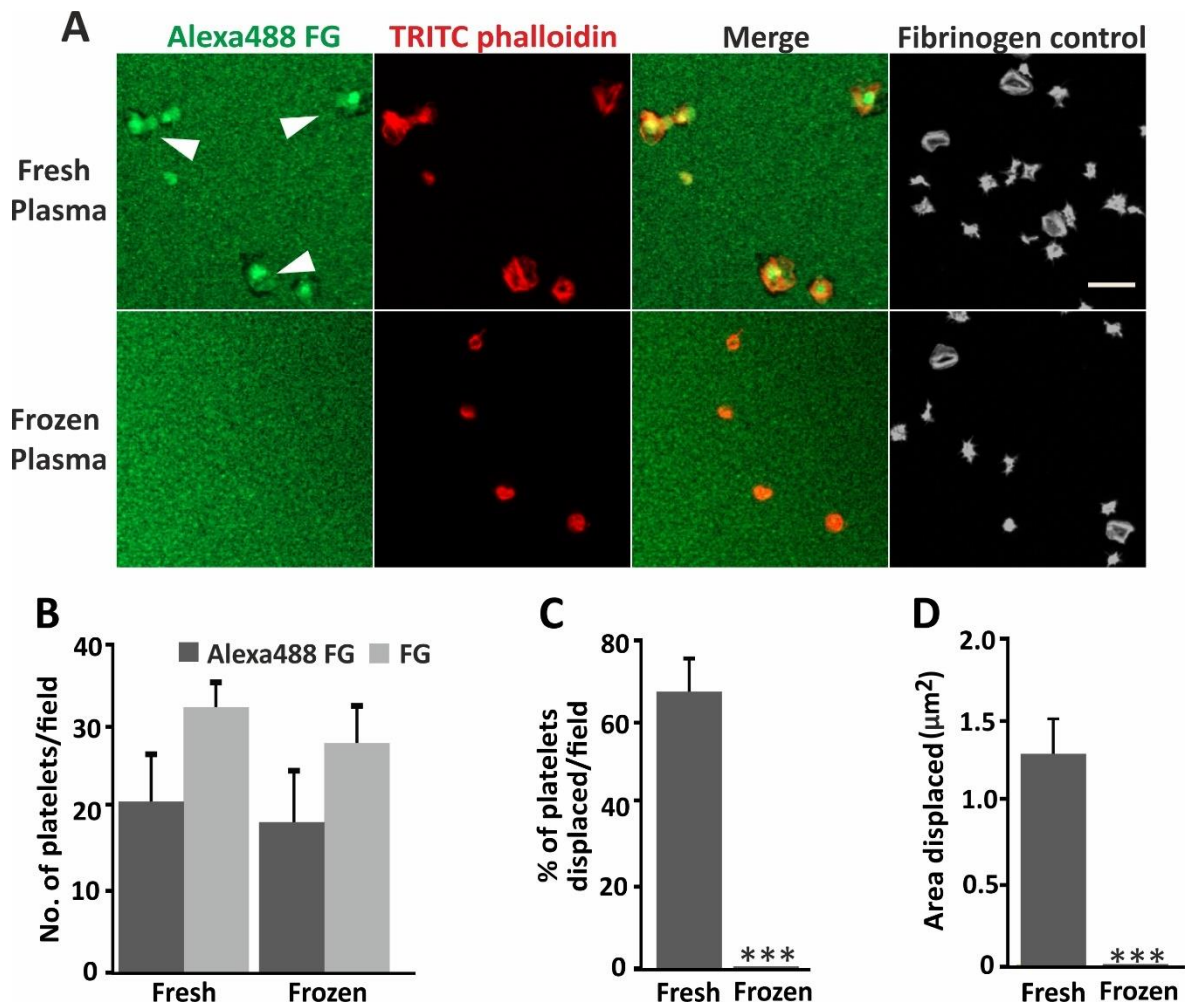


Figure 4.12 The effects of diluting platelets in frozen plasma on the capacity of platelets to migrate. Glass coverslips were acid washed with HCl for 1 h followed by dH₂O for 1 h and then silanated with HMDS for 1 min at room temperature. Coverslips were then coated with 40 $\mu\text{g}/\text{ml}$ Alexa488 fibrinogen (green) and 2mg /ml BSA for 15 min. Plasma was obtained from healthy donors and stored overnight at -20°C . The following day, mouse platelets in PRP was obtained and diluted to $1 \times 10^7/\text{ml}$ in either fresh or frozen-thawed human plasma. 200 μl of platelet suspension were then added to the coverslips and incubated at 37°C for 1 h. Coverslips were washed with PBS and fixed with 4% PFA for 10 min, permeabilised with 0.3% Triton X100 for 5 min and stained with 1 $\mu\text{g}/\text{ml}$ TRITC phalloidin (red; grey on the FG control image) for 30 min at room temperature. Coverslips were mounted onto glass slides with ProLong Antifade Mountant and images were obtained with a Zeiss ApoTome.2 fluorescence microscope equipped with a 60x oil immersion objective. (A) Representative images from three independent experiments. Scale bar represents 20 μm . Arrowheads indicate examples of fibrinogen cleared during platelet migration. (B) Adhesion of cells in each of the conditions was calculated by thresholding images on ImageJ software. (C) Percentage of migrating platelets per field and (D) the average area of Alexa488 FG cleared by individual platelets was either counted manually or calculated on ImageJ software as outlined in section 2.4.7. Data are presented as means \pm SEM of three independent experiments, (***) $p < 0.001$.

4.5.4 The importance of coronin in the ability of mouse platelets to migrate

Numerous proteins and signalling pathways are understood to partake in platelet motility. Coronin, an actin-filament regulatory protein, has been widely studied for its role in cellular processes which rely largely upon rapid reorganisation of the actin cytoskeleton such as endocytosis and cell motility (Gandhi & Goode, 2013; Riley *et al.*, 2020; Rivero, 2008; Xavier *et al.*, 2013). In the following set of experiments, we aimed to investigate the role of coronin in regulating the ability of mouse platelets to migrate on Alexa488 FG using a mouse model of coronin 1 deficiency (Riley *et al.*, 2020).

Platelets from WT and KO coronin mice were diluted to 1×10^7 /ml by resuspending in fresh human plasma. Platelet migration assay was then conducted as outlined in section 4.5.1. Platelets from WT and KO mice were also spread on unconjugated fibrinogen (40 μ g/ml) coated coverslips as a control of their spreading profile. Coverslips were then processed and analysed in parallel.

Representative images of the ability of WT and coronin KO platelets to migrate on Alexa488 FG are shown in Figure 4.13A. It is possible to see comparable results between both groups in term of platelet adhesion: 46 ± 2 and 44 ± 2 cells/field in WT and KO coronin mice respectively (Figure 4.13B). Similar results were found in the fibrinogen control group: 58 ± 7 cells/field in WT vs 53 ± 7 cells/field in KO.

Comparable results between the two groups were also found for the percentage of cells able to migrate on Alexa488 FG ($50 \pm 7\%$ and $57 \pm 9\%$ in WT and KO respectively) (Figure 4.13C). Likewise, Figure 4.13D shows the area of displacement on Alexa488 FG to be similar too between WT ($1 \pm 1 \mu\text{m}^2$) and KO ($2 \pm 1 \mu\text{m}^2$).

From these set of experiments, we conclude that the absence of coronin does not impair the migratory capacity of mouse platelets on Alexa488-FG and the ability of cells to adhere to fibrinogen.

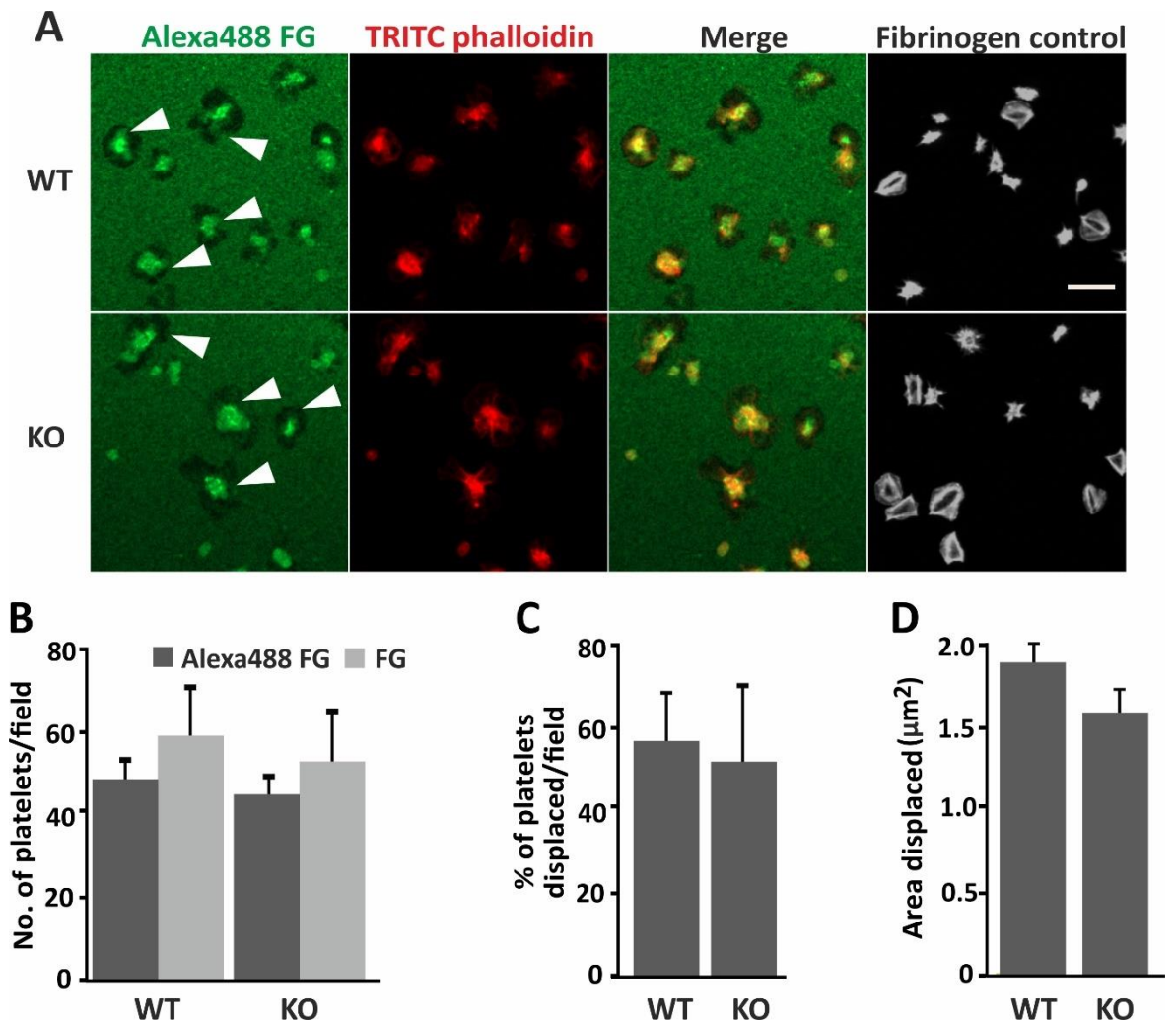


Figure 4.13 The difference between KO and WT coronin mouse models in their ability to migrate on Alexa488 FG. Glass coverslips were acid washed with HCl for 1 h followed by dH₂O for 1 h and then silanated with HMDS for 1 min at room temperature. Coverslips were then coated with 40 $\mu\text{g}/\text{ml}$ Alexa488 fibrinogen (green) and 2mg /ml BSA for 15 min. KO and WT coronin mouse platelets were diluted to $1 \times 10^7/\text{ml}$ in fresh human plasma. 200 μl of platelet suspension were then added to the coverslips and incubated at 37°C for 1 h. Coverslips were washed with PBS and fixed with 4% PFA for 10 min, permeabilised with 0.3% Triton X100 for 5 min and stained with 1 $\mu\text{g}/\text{ml}$ TRITC phalloidin (red; grey on the FG control image) for 30 min at room temperature. Coverslips were mounted onto glass slides with ProLong Antifade Mountant and images were obtained with a Zeiss ApoTome.2 fluorescence microscope equipped with a 60x oil immersion objective. (A) Representative images from three independent experiments. Scale bar represents 20 μm . Arrowheads indicate examples of fibrinogen cleared during platelet migration. (B) Adhesion of cells in each of the conditions was calculated by thresholding images on ImageJ software. (C) Percentage of migrating platelets per field and (D) the average area of Alexa488 FG cleared by individual platelets was either counted manually or calculated on ImageJ software as outlined in section 2.4.7. Data are presented as means \pm SEM of three independent experiments.

4.6 Discussion

Much work has been conducted into the role of platelets as critical cells that arrest bleeding at the site of endothelial injury via processes such as platelet activation, spreading and aggregation. However, some scientists have proposed platelets recruited to sites of vascular damage or inflammation to have the ability to shift their position and ‘migrate’ (Pitchford *et al.*, 2008; Kraemer *et al.*, 2012). This gave rise to the idea of platelets as non-static cells as reviewed by Petito *et al.*, (2017). However, research in this field is not abundant and many questions regarding the underlying mechanisms remain unanswered.

Gaertner and colleagues (2017) supports the notion of platelets as motile cells which actively and continuously scan their microenvironment. Through the use of various methods including live cell microscopy, mouse models and platelet tracking methods they confirmed platelets to possess the ability to migrate. However, considerable ambiguity remains regarding the molecular mechanisms concerned with platelet migration. In this chapter we investigated the molecular mechanisms and the signalling pathways involved in the process of platelet migration on Alexa488 FG. In order to achieve this purpose, we first aimed to adapt the assay utilised by Gaertner *et al.*, (2017), and optimise it for the quantitative analysis and determination of platelets’ ability to migrate.

For this reason, we first wanted to establish appropriate and even coating of Alexa488 FG on coverslips. In consequence, we tested the effect of HMDS silanization of coverslips on Alexa488 FG coating and platelet migration as also done by Gaertner *et al* (2017). We found significant differences between untreated and HMDS-treated coverslips (Figure 4.1). As a matter of fact, platelet migration was absent when coverslips were left untreated. It is known for platelet migration to be governed by the capability of platelets to release the interaction with their adhesions. It is also known for integrin-ligand bond of platelets to be exceptionally strong (Höök *et al.*, 2017), and so the adhesion of platelets to the coverslip is typically released via peeling of the substrate. This was demonstrated by Gaertner *et al* (2017) since they showed migration of platelets to be present only if the cell could remove the substrate (e.g. platelets do not move on covalently bound fibrinogen). Based on this, it is possible to assume that silanization with HMDS effects the coating with fibrinogen in a

way that allows platelets to efficiently remove the ligand when pulling on it. This is supported further by Palecek *et al.*, (1997) who found migration of CHO cells on fibrinogen only when coverslips were silaned. Unfortunately, not much is known about how HMDS affects the alignment/orientation of fibrinogen molecules on coverslips.

Next, we showed evidence of platelet migration to be time-dependent, with maximal platelet migration observed at 60 min (Figure 4.3). This is consistent with work published by Gaertner *et al.*, (2017) who stated platelet migration to be a slow processes. They also reported platelets migrating on fibrinogen to clear the fibrinogen from the surface and transport/deposit it within the open canalicular system of the platelet, commonly central to the platelet. The same was found in our migration assay as clusters of Alexa488 FG were found deposited in the middle of a migrating platelets and there would be a dark area surrounding a migrating platelet which is indicative of cleared Alexa488 FG.

As in chapter 3, we explored the effects of the platelet preparation procedure on the ability of platelets to migrate, specifically the requirement of plasma to facilitate this process. We found plasma to be critical for platelet migratory functions as WP completely failed to migrate, whereas PRP and WP resuspended in plasma encompassed migratory capacity (Figure 4.4). To test this further, we investigated the ability of PRP to migrate upon resuspending platelets in different proportions of plasma and found the percentage of cells able to migrate increased as the proportion of plasma used to resuspend platelets increased (Figure 4.6). The differences observed between the proportions of plasma suggests a component in plasma to critically influence migratory capacity of platelet. We also found resuspending platelets in thawed frozen plasma led to a lack of migration (Figure 4.12), this suggests the critical component(s) in plasma required for platelet migration perhaps losses activity upon freezing. Previous platelet migration studies have used collagen as a chemotactic substance for platelet migration (Löwenhaupt *et al.*, 1973). Keiser *et al.*, (1963) reported for collagen-like protein to be present in plasma. Therefore we propose that this component in plasma may partake in influencing platelets to migrate, hence the reason why WP (lacking such collagen-like substance) were unable to migrate and also the reason why WP resuspended with plasma reversed this effect. To elucidate this, WP should be treated with the collagen-like protein reported by Keiser and migration

capacity evaluated. Other than this, systematic fractionation of plasma could also perhaps reveal the critical compounds involved in platelet migration.

The method we established for determining quantitatively the ability of platelet to migrate is also applicable to mouse platelets and similar results to that of human platelets were found in terms of plasma being essential for platelet migration to occur (Figure 4.10). Hence suggesting comparable mechanism/signalling to occur in mouse with regard to platelet migration capacity.

It has been previously reported that cell polarisation is critical for platelet chemotaxis and that this ultimately leads to the formation of a leading front edge and a trailing edge at the back (Petito *et al.*, 2017). This process requires a number of proteins and intracellular signalling pathways, and it has been reported for the platelet cytoskeleton to play an instrumental role in facilitating the assembly and disassembly of actin to aid migration (Charest and Firtel, 2007; Yan and Jin, 2012). Similarly, Schmidt *et al.*, (2011) have also shown actin polymerisation to be key in mediating platelet migration. Therefore, it was not surprising that Lat-A, which stimulates the disassembly of actin in the resting platelet, completely inhibited platelet migration and significantly reduced platelet adhesion (Figure 4.7). Thus, proving actin polymerisation to be crucial in facilitating platelet migration.

We also established a reduction or absence in platelet migration upon treating platelets with Rho GTPase inhibitors (Figure 4.7). The roles of Rho GTPases, specifically RhoA, Rac1 and Cdc42 in cell migration have been previously demonstrated in many different cell types, including platelets (Infante and Ridley, 2013; Aslan, 2019). We found complete inhibition in the ability of platelets to scavenge upon inhibiting RhoA and Cdc42. Thus, implying these Rho GTPases is be more important in terms of influence scavenging properties compared to Rac1 or perhaps that the concentration of Rac1 inhibitor used was not sufficient, although similar concentration of NSC 23766 have been used by previous researchers (Pandey *et al.*, 2009; Dütting *et al.*, 2015).

We also investigated the importance of coronin in facilitating platelet migration (Figure 4.13). Coronin1 knockout mouse models were utilised to study the role of specific

cytoskeletal components since no inhibitors exist. We report no difference in the ability of platelets to migrate in the absence of coronin thus suggesting coronin1 is dispensable for migratory capacity of platelets. However, the presence of two other classes of coronins have been reported (Coro2 and Coro3) (Riley *et al.*, 2019) and so it is possible that we observed no difference in platelet migration in the knockout mouse model since these additionally coronins may have compensated for the absence of coronin 1 in mouse.

Next, we addressed the roles of surface receptors on platelet migration. It is widely-recognised that GP IIa/IIIb is the major fibrinogen receptor in platelets (Albert & Christopher, 2012). Gaertner *et al.*, (2017) demonstrated activated platelets to use α IIb β 3 integrins to scan their microenvironment to determine the resistance of the substrate in order to choose the direction the platelet should migrate towards. They confirmed this by utilising platelets expressing defective GPIIb/IIIa from individuals with Glanzmann thrombasthenia, and found no migration or spreading in these platelets. Our data also showed an absence in platelet migration and spreading upon treating platelets with integrilin, an inhibitor of GP IIa/IIIb (Figure 4.8), thus confirming platelet migration on fibrinogen to be critically dependent on integrin α IIb β 3. Our data also revealed the effect of IV.3 antibody, which is an inhibitor of the Fc γ RIIa receptor on altering platelet migration capabilities, with a significant reduction in platelet migration detected in the inhibitor-treated platelets (Figure 4.8). This is to some extent consistent with data published by Pitchford and co-workers (2008) who found mice deficient in Fc γ R chain failed to migrate in lung tissues. Although they reported a complete lack in platelet migration whereas we observed the migratory capacity to be reduced in treated platelets but not abolished, the differences observed could potentially be due to immediate environment upon which platelet migration was tested. Pitchford and co-workers tested migration of platelets *in vivo* in tissue where the environment is complex and numerous factors are in interplay, while we investigated migratory capacity of platelet *in vitro* on a defined matrix.

Furthermore, in this chapter we present for the first time the effects of inhibiting components of the tyrosine kinase signalling pathway on the ability of platelets to migrate. We chose inhibitors targeting Syk, Src and BTK that are also commonly used in the treatment of malignancies so that we can explore the effects on platelet migration while

also determining the potential off-target effects of these drugs on platelets' ability to migrate. In this chapter we showed, for an inhibition in platelet migration upon treating platelets with Dasatinib, PRT and Ibrutinib which target Src, Syk and Tec (BTK) family of kinases respectively, while a significant reduction in the migratory capacity of platelets were found upon treatment with acalabrutinib which is a more specific inhibitor of the BTKs (Figure 4.9).

Data from previous studies using mouse models lacking Src showed severe impairment to tyrosine phosphorylation followed by platelet spreading (Séverin *et al.*, 2012). Similarly, Ablooglu *et al.*, (2009) showed disruption in the Src- β 3 interaction to lower inside-out signalling in platelets. This in turn has been shown in this thesis to be critical for platelet migration to occur. Therefore, it is understandable that we found an inhibition in the ability of platelets to migrate upon inhibiting Src in platelets. Oberfell *et al.*, (2002) demonstrated Syk to be associated constitutively with GPIIb/IIIa in platelets. They also established inhibition of Syk to impair platelet spreading and inhibit the phosphorylation of Vav1, Vav3 and SLP-76 which are essentially Syk substrates involved in cytoskeletal regulation. We observed that migration of platelets on Alexa488 FG was abolished upon treatment with PRT which targets Syk. Thus, we propose GPIIb/IIIa to indirectly regulate actin dynamics which in turn mediates platelet migration.

We also found BTK inhibitors ibrutinib and acalabrutinib which have been reported to partake in signalling downstream of ITAM-coupled receptors in platelets (Bradshaw, 2010), to result in alterations to the migratory capacity of platelet. (Figure 4.9). BTK is upstream of PLC γ , which acts to stimulate inside-out signalling of GPIIb/IIIa as well as exerting direct effects on platelet activation and indirectly activates Rho GEFs. Therefore, by inhibiting BTKs, the activity of PLC γ is inhibited and ultimately blocks integrin activation signalling, hence why platelet migration capacity diminished.

Conclusion

Collectively, this chapter has characterised the optimum conditions for an assay to quantitatively assess the migratory capacity of platelets on Alexa488 FG. We have also demonstrated the critical role of the three major cytoskeletal regulators, RhoA, Rac1 and

Cdc42 along with the participation of the actin cytoskeleton itself in platelet migration processes. Moreover, we have shown through the use of inhibitors, GPIIb/IIIa to be fundamental in aiding platelet migration. In addition to this, we demonstrated tyrosine kinases to partake in mediating the ability of platelets to migrate and thus propose the off-target effects of tyrosine kinase inhibitor in the use of CLL to predispose individuals to infection and bleeding complications.

Chapter 5. Effects of the bacterial toxin Cytotoxic Necrotising Factor 1 on platelet function.

5.1 Introduction

The platelet actin cytoskeleton is an integral structure which maintains the discoid shape of the resting platelets (Shin *et al.*, 2017). It is well-known for the platelet cytoskeleton to mediate rapid actin remodelling in response to particular stimuli and so it has been widely accepted for the platelet cytoskeleton to play an instrumental role in supporting physiological platelet functions including cell signalling and spreading.

Several studies have highlighted Rho GTPases RhoA, Rac1 and Cdc42 as master regulators of the platelet actin cytoskeleton Aslan (2019) and Dütting *et al.*, (2017). It has been reported for these low molecular weight GTPases to act as signalling switches which coordinate information from the platelet surface receptors to the numerous intracellular signalling pathways that ultimately control platelet functions (Aslan & McCarty, 2013). We too have established in the previous two chapters the effects of inhibiting key Rho GTPases on the ability of platelets to scavenge bacteria and migrate on matrixes.

An increasing number of studies have also shown the regulation of the platelet actin cytoskeleton by Rho proteins to be critical in allowing platelets to function as potential immune cells (Ridley *et al.*, 1992). Much more information has now become available through the use of Rho protein knockout mouse models. Indeed, Goggs *et al.*, (2015) utilised knockout mouse models to demonstrate defects in spatiotemporal regulation of the cytoskeleton by key Rho GTPases and associated kinases and how this affected the dense granule secretion capacity of platelets. Granular content secretion has in turn been shown to be a key step in allowing platelets to recruit circulating immune cells to the site of infection, thus augmenting host defence mechanisms (Manne *et al.*, 2017). It can be assumed from such studies that Rho GTPases are critical in determining the efficacy of platelets to contribute to a variety of immunological processes and how inhibition of such key regulators could result in an imbalance between infection and immunity, thus giving rise to the possibility of conditions such as sepsis.

In addition to knockout mouse studies, some researchers have emphasized the importance of Rho proteins in maintaining cellular functions through studying modifications exerted by Rho-targeting bacterial proteins. An example of this is C3 transferase produced by *Clostridium botulinum*, which was the first bacterial protein reported to interfere with Rho GTPases resulting in morphological alteration in fibroblast cells (Rubin *et al.*, 1988). Now over 30 bacterial proteins from various microorganisms have been identified to affect the three major Rho GTPases: RhoA, Rac1 and Cdc42 (Boquet & Lemichez, 2003). One such toxin-producing microorganism is *E. coli*.

E. coli has been reported to secrete a variety of molecules which manipulate host immune cell functions and thus enhances survival of the microorganism through the evasion of the host immune system (Billips *et al.*, 2008). A toxin of particular interest to us due to the targeted effects it has on Rho GTPases, is the cytotoxic necrotising factor 1 (CNF1).

CNF1 is a major virulence factor of extraintestinal pathogenic *E. coli* (ExPEC), which is the leading cause of bacteraemia world-wide and a frequent cause of sepsis (Fabbri *et al.*, 2010). This 115kDa single chain AB toxin belongs to the dermonecrotic toxins family and consists of two domains: a receptor binding N-terminal domain which is involved in membrane translocation processes, and a catalytic C-terminal domain encompassing deamidase activity (Fabbri *et al.*, 2010). The enzymatic C-terminal domain of CNF1 targets Rho-GTP binding proteins which act as critical molecular switches that oscillate between an inactive and active form, GDP-bound and GTP-bound state, respectively. More specifically, CNF1 catalyses the deamidation of particular glutamine residues of Rho GTPases into glutamic acid meaning GTP hydrolysis is inhibited, rendering them constitutively active and causing profound morpho-functional alterations and adverse pathologies in the target cell (Fabbri *et al.*, 2010; Williams, *et al.*, 2015).

CNF1 has previously been reported to be internalised into mammalian cells following the binding to target cell-receptors via clathrin- and caveolae-like independent pathways (Boquet, 2001a). Contamin and co-workers (2000) demonstrated the toxin to be packaged into endosomal compartments after which the enzymatic C-domain of the toxin to be

translocated out of the membrane into the cytosol via acidic pH-driven process (Contamin *et al.*, 2000).

Although the mechanism of CNF1 internalisation were proposed in the early 2000, it was only a few years later that cellular receptors for CNF1 [Lutheran (Lu) adhesion glycoprotein/basal cell adhesion molecule (BCAM)] were discovered thus providing novel insight into the mechanisms involved in CNF1 adhesion to target cells (Piteau *et al.*, 2014). Lu/BCAM, a transmembrane adhesion glycoprotein which is a member of the Ig superfamily, was identified as the critical cellular receptor involved in the uptake of CNF1 in a number of epithelial and endothelial cells (Kikkawa and Miner, 2005; Eyler and Telen, 2006). Indeed, co-precipitation studies of surface molecules with tagged toxin verified CNF1-Lu/BCAM interaction via direct protein-protein interaction analysis and competition studies (Reppin *et al.*, 2018). However, while regions close to the C-terminal domain of CNF1 interacts with Lu/BCAM, it was found for the N-terminal region of CNF1 to interact with a 37LRP precursor protein of the non-integrin laminin receptor (67LR) (Piteau *et al.*, 2014). Piteau *et al.*, (2014) concluded for the binding of CNF1 to p37LRP to be vital for the toxin's action, in addition to this they found cells deficient in Lu/BCAM but expressing p37LRP was not able to bind labelled CNF1. Thus implying, CNF1 interacts with two separate proteins via two different domains. Although, CNF1-receptor interactions remain elusive in platelets. Our collaborators in Germany however, conducted two blots on platelet lysates to probe for both of the receptors and found both to be present in platelets (Appendices, Figure 7.4).

We hypothesise that platelets have the potential to interact with CNF1 produced by specific *E. coli* organisms. We propose high concentrations of toxin to be present locally at the site of infection, where platelets will also be present, thus giving rise to the possibility of CNF1 to interact and bind to platelets and ultimately lead to toxin-induced platelet dysfunction. In this chapter, we investigate the ability of CNF1 to hinder platelet function and evaluate the morphological differences that may arise upon treatment of platelets with the toxin.

As mentioned above, once the toxin is taken up by target cells, a number of studies have described CNF1 to target and modify Rho GTPase activity, out of these several have

demonstrated enzymatic effects of CNF1 on RhoA. It is believed that upon release of the enzymatic component of the toxin into the cytosol, CNF1 deamidates Q63 residue of RhoA which can be visualised via an electrophoretic shift and this is considered as an indication, although indirect, of toxin uptake and processing (Piteau *et al.*, 2014). Indeed, Brest *et al.*, (2003) also suggested uptake of the toxin upon observing a mobility shift of Rho in lymphoid cells post CNF1 treatment. Likewise, an electrophoretic shift was observed by Schmidt *et al.*, (1997) upon treating NIH3T3 cells with the toxin.

Many studies have demonstrated morphological and functional alterations in cells upon treatment with CNF1. Fabbri *et al.*, (2010) demonstrated the toxin to induce modification to the actin cytoskeleton of neuronal cells, while Nobes & Hall, (1995) showed morphologic alterations in monocytic cells upon treatment with CNF1. Falzano *et al.*, (1993) revealed intoxication of human epithelial cells with CNF1 to induce phagocytic behaviour in cells. Whereas, Fiorentini *et al.*, (1995) observed induction of actin assembly in epithelial cells treated with CNF1. The molecular and functional effects of CNF1 has been studied to some extent in epithelial cells, fibroblasts, and leukocytes. Meanwhile, no studies have addressed the impact of this toxin on platelet functions. It is therefore of paramount importance that we research how the toxin affects platelets at a molecular level to subvert detrimental effects such as sepsis. Additionally, it may be possible to exploit the activities of the toxin for medical applications as a tool to manage specific cellular pathways thus be used in the prevention and treatment of particular human diseases. Henceforth, to investigate the effects that CNF1 exerts on platelets, the following aims were derived for this chapter:

Aims of this chapter are:

1. To establish the effect(s) CNF1 toxin has on RhoA in platelets and on actin polymerisation.
2. To investigate the morphological alterations that may arise upon treating human and mouse platelets with CNF1 toxin.
3. To examine any functional alterations in platelet secretion in CNF1 toxin-treated platelets.
4. To determine whether toxin treatment results in alteration of platelet integrin activation.

5.2 Recombinant protein production and purification of CNF1 toxin

The expression and purification of sufficient quantities of the full-length CNF1 toxin was the initial step conducted to facilitate production and afterwards allow the detailed investigation of the effects of recombinant CNF1 proteins on platelet functions. Plasmids were kindly provided by Prof G. Schmidt group (University of Freiburg, Germany). Protein expression of GST-tagged CNF1 was conducted as outlined in section 2.5.1

Figure 5.1 shows the Coomassie staining to reveal a band of the expected size (136 kDa) in the induced samples and for this to be recovered in the supernatant sample. However, it can be seen that the protein presented quite extensive degradation products. Therefore, it was decided to investigate a His-tagged protein.

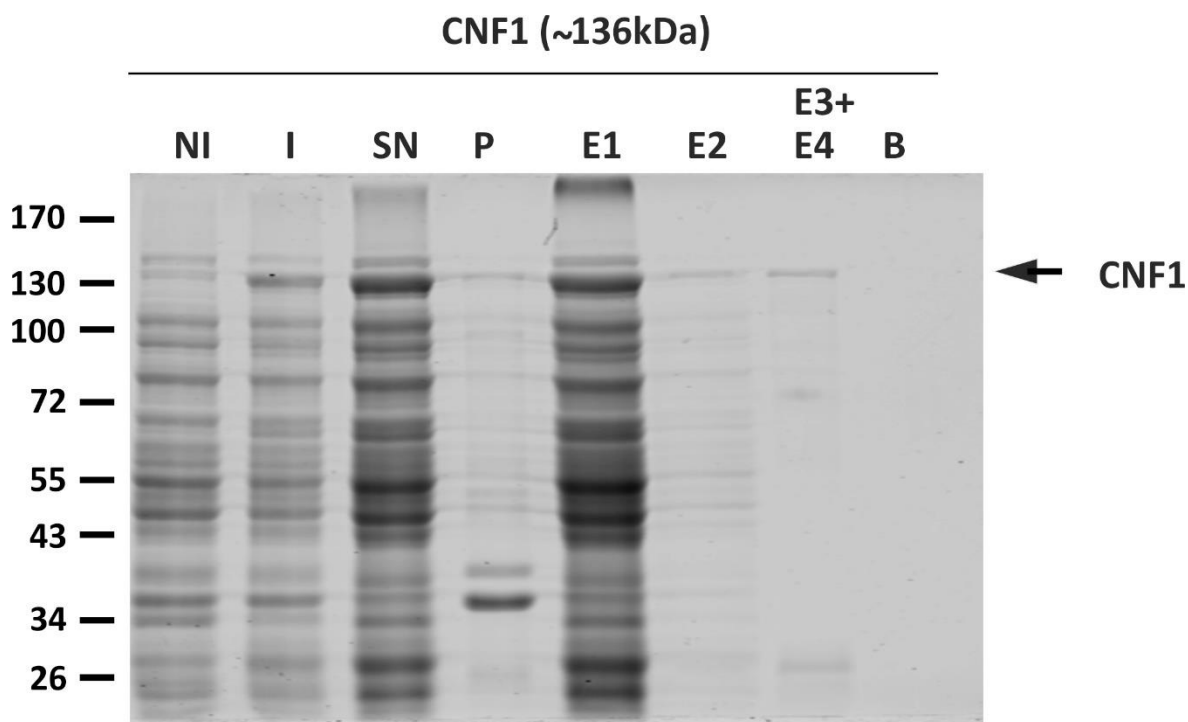


Figure 5.1 Expression and purification of GST-tagged CNF1 toxin. Bacterial total lysates were obtained before (NI) and after (I) induction of expression with 0.5 mM IPTG. Bacterial cells were then lysed via French press. This was followed by the separation of soluble (SN) and insoluble (P) fractions by centrifugation. Bacterial supernatant was then incubated with pre-equilibrated glutathione Sepharose beads for 1 h at 4°C under gentle shaking conditions. After washing, purified GST-tagged CNF1 was eluted (E) several times with different lysis buffer (section 2.5.1). All samples, including (B) beads control were then resolved by SDS-PAGE and the gel was stained with Coomassie-Brilliant-Blue. Arrow indicates CNF1 at the expected molecular weight (136 kDa).

Recombinant protein expression of his-tagged CNF1 was conducted as outlined in section 2.5.1. Plasmids were kindly provided by Dr Colarusso, (University of Naples Federico II, Italy). CNF1 was purified from bacterial supernatants by incubating with pre-equilibrated Ni-NTA agarose. Samples collected from various steps of the procedure were resolved on SDS-PAGE followed by Coomassie staining (Figure 5.2).

It can be seen in Figure 5.2 that Coomassie staining revealed a band of the expected size (115 kDa) in the induced samples. Additionally, it was observed for these bands to be recovered in the supernatant samples. Since the Coomassie staining indicated efficient purification with low amounts of contaminants, it was decided to continue with the His-tagged CNF1 toxin produced.

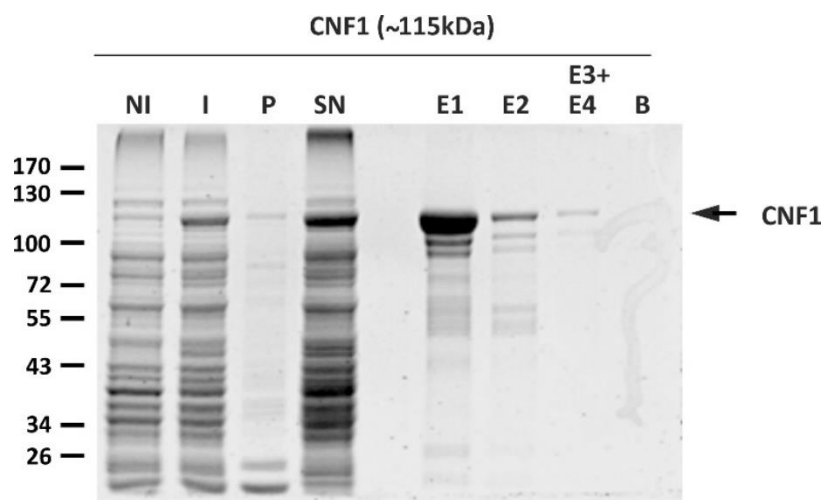


Figure 5.2 Expression and purification of his-tagged CNF1 toxin. Bacterial total lysates were obtained before (NI) and after (I) induction of expression with 0.5 mM IPTG. Bacterial cells were then lysed via French press. This was followed by the separation of soluble (SN) and insoluble (P) fractions by centrifugation. Bacterial supernatant was then incubated with pre-equilibrated Ni-NTA agarose bead for 1 h at 4°C under gentle shaking conditions. After washing, purified his-tagged CNF1 was eluted (E) several times with 500 mM imidazole. All samples, including (B) beads control were then resolved by SDS-PAGE and the gel was stained with Coomassie-Brilliant-Blue. Arrow indicates CNF1 at the expected molecular weight (115 kDa).

Following the successful production of CNF1 toxin, the protein concentration of the purified elutes were determined via BCA protein assay kit as described in section 2.5.2. It was conducted by Paulo Saldanha and was calculated to be 2450.49, 1578.24 and 128.5 µg/ml in E1, E2 and E3+4, respectively. In view of these results, it was decided to go ahead with the his-tagged CNF1 toxin for all subsequent experiments.

It is important to note that 100% purification of the toxin cannot be achieved as the toxin will always carry impurities (other bacterial proteins and molecules i.e. LPS). In order to rule out that observed effects are caused by trace amounts of impurities contaminating the CNF1 preparations, it was decided to perform ensuing experiments in combination with the CNF1 mutant, C688S (lacks catalytic activity). The above-detailed protocol was followed for the expression and purification of CNF1 C688S. Figure 5.3 illustrates a band of the expected size (115kDa) via Coomassie staining. Given that efficient purification with low quantities of impurities was revealed on the Coomassie gel, it was decided to continue with the CNF1 C688S produced as a negative control.

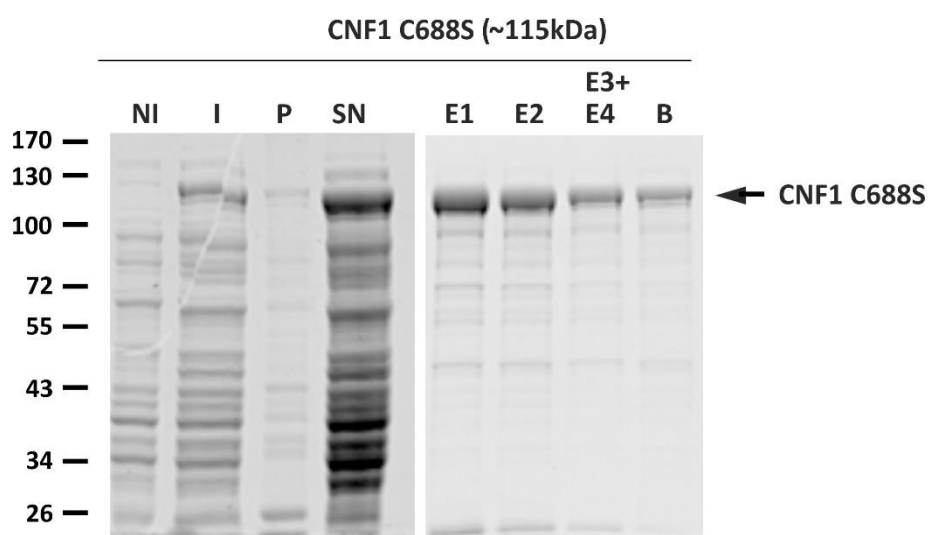


Figure 5.3 Expression and purification of CNF1 C688S. Bacterial total lysates were obtained before (NI) and after (I) induction of expression with 0.5 mM IPTG. Bacterial cells were then lysed via French press. This was followed by the separation of soluble (SN) and insoluble (P) fractions by centrifugation. Bacterial supernatant was then incubated with pre-equilibrated Ni-NTA agarose bead for 1 h at 4°C under gentle shaking conditions. After washing, purified his-tagged CNF1 was eluted (E) several times with 500 mM imidazole. All samples, including (B) beads control were then resolved by SDS-PAGE and the gel was stained with Coomassie-Brilliant-Blue. Arrow indicates CNF1 C688S at the expected molecular weight (115kDa).

5.3 Does CNF1 modify Rho GTPase signalling pathways in platelets

CNF1 is a toxin that results in the permanent activation of Rho GTPases in eukaryotes via deamidation of a critical glutamine residue (Fabbri *et al.*, 2010). In this section we aim to determine the extent to which Rho GTPase signalling is affected by CNF1 in platelets. In order to do so, it is important to first verify that CNF1 deamidates Rho GTPases in platelets and to establish how CNF1 affects the protein levels and activity of the three main Rho GTPases. However, prior to experimentation it was important to optimise the conditions required for the commercially available Rho GTPase antibodies.

5.3.1 Optimisations of conditions for commercially available Rho GTPase antibodies

In the following optimisation experiments, washed platelets were utilised to determine the most effective conditions for each commercially available Rho GTPase antibody. Platelets (1×10^9 /ml) were isolated as outlined in section 2.3.1. Following this whole cell lysates (1 mg protein/ml) were prepared. Different volumes of cell lysates (30, 40 and 50 μ l) were loaded onto a 10% gel and SDS-PAGE was conducted. Proteins from the polyacrylamide gel were transferred onto a PVDF membrane (as in section 2.5.5) and blocked in two different blocking reagents (5% BSA or 5% milk powder). All antibodies were diluted 1:500 as recommended in the manufacture guidelines.

Figure 5.4A shows anti-RhoA antibody to detect a band at the anticipated molecular weight (21 kDa) in both of the blocking methods used. Likewise, platelets incubated with Rac1 antibody is also shown. However, it can be seen that in the case of blocking the PVDF membrane with 5% BSA, only a faint band was detected by Rac1 antibody (Figure 5.4B). On the contrary Rac1 antibody effectively detected bands at the expected molecular weight when the PVDF membrane was blocked with 5% milk powder. The opposite was found for Cdc42 antibody, as it performed better when the membrane was blocked with 5% BSA (Figure 5.4C). Therefore, it was decided to block PVDF membranes in 5% BSA when using RhoA and Cdc42 antibody, and to block with 5% milk powder when using Rac1 antibody. It can also be seen that loading 30 μ l of platelet lysate was sufficient for the detection of a

substantial band for all three antibodies thus it was decided to load 30 μ l of cell lysate for the ensuing experiments.

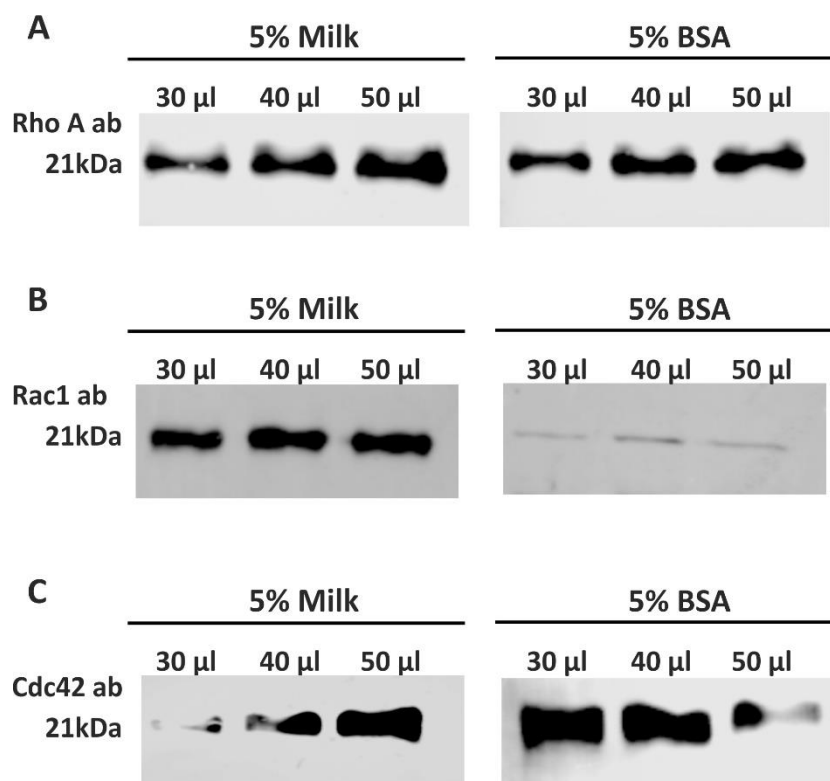


Figure 5.4 Optimisation of conditions for Rho GTPase antibodies in platelets. Washed platelets (1×10^9 /ml) were isolated and lysed in Laemmli buffer. Different volumes of platelet lysates (30, 40 and 50 μ l of 1 mg/ml) were loaded onto a 10% gel and SDS-PAGE was conducted. Proteins were subsequently transferred onto PVDF membranes and blocked with either 5% skimmed milk powder or 5% BSA before probing with 1:500 dilutions of (A) RhoA, (B) Rac1 or (C) Cdc42 antibody overnight at 4°C. The following day, fluorescently labelled secondary antibodies were used to visualise proteins with an Odyssey TM CLx electronic imaging system (Li-Cor).

5.3.2 CNF1 induces a mobility shift of Rho in platelets

A shift in molecular mass of Rho, also referred to as a Rho shift, is indicative of covalent modifications to Rho GTPase and this electrophoretic shift is typical in cells upon treatment with CNF1. Studies have proven for this to be true in epithelial cells, fibroblasts and leukocytes (Schmidt *et al.*, 1997; Gerhard *et al.*, 1998; Brest *et al.*, 2003). However, the effects of the toxin have yet to be examined in platelets hence, it was decided to investigate whether a similar shift in mobility of RhoA would be observed upon treating platelets with the toxin.

Washed platelets (1×10^9 cells/ml) were treated with varying doses of CNF1 toxin (0, 10, 100 and 1000nM) or the catalytically inactive mutant C688S and incubated at 37°C for 4 h. Since an electrophoretic shift has been previously described in HEK cells, it was decided to incorporate HEK cells into the experiment as a positive control. HEK cells were treated with 20 nM of CNF1 for 3 hours (Piteau *et al.*, 2014).

After incubation, platelets and HEK cells were lysed with Laemmli buffer supplemented with 0.1M DTT (section 2.5.1.2). After this, SDS-15% PAGE was conducted (section 2.5.3) and the membranes analysed via western blotting with a RhoA specific antibody (section 2.5.5).

As expected, Figure 5.5 illustrates a shift in motility of RhoA in HEK cells when treated with CNF1 compared to the catalytically inactive control. It can also be distinguished that no difference was observed between platelets treated with 10 or 100 nM of the toxin for 4h compared to control samples. However, upon treating platelets with 1000 nM CNF1, an electrophoretic shift in Rho was observable when compared to control untreated platelets (Figure 5.5, arrowheads).

From these experiments it was established that we need to use 1 μ M concentrations for subsequent experiments. And that 4 h is sufficient time for the toxin to have an effect (at least on RhoA).

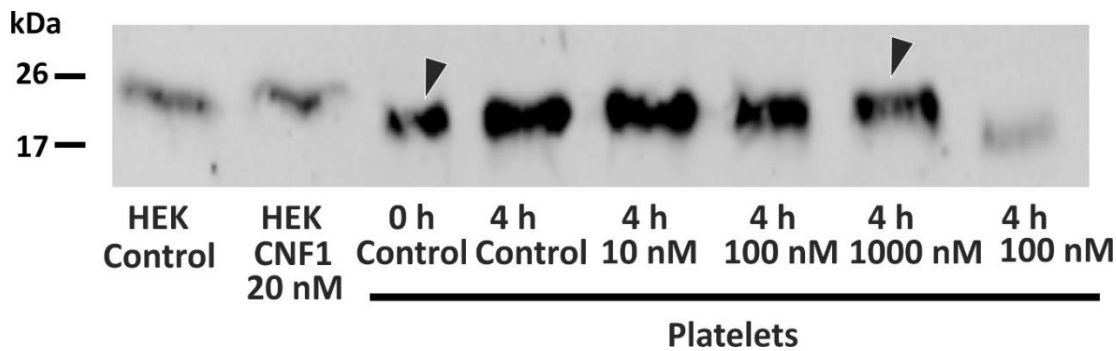


Figure 5.5 Electrophoretic shift of platelet RhoA upon exposure to CNF1. Washed platelets (1×10^9 /ml) were treated with varying concentrations (10, 100 or 1000 nM) of CNF1 or 1000 nM of the catalytically inactive C688S CNF1 mutant as a control for four hours at 37°C. Following incubation, cells were lysed in Laemmli buffer. A separate untreated washed platelet sample was also prepared and lysed immediately (control). HEK cells were also treated with 20 nM of CNF1 toxin (or the C688S mutant) as a positive control and lysed as per above. Samples were resolved by 15% SDS-PAGE (containing 1 M urea), transferred onto a PVDF membrane and probed overnight at 4°C with an anti-RhoA mAb diluted to 1:500. Fluorescently labelled secondary antibodies were used to visualise proteins with an Odyssey TM CLx electronic imaging system (Li-Cor). Molecular masses are indicated on the left-hand side of the figure. An electrophoretic shift in RhoA was indicative of uptake of the toxin by cells and is shown with an arrowhead. A smaller amount of the 100 nM sample was loaded again on the last lane for better visualisation of the shift.

5.3.3 CNF1 does not affect the stability of Rho GTPases in platelets

Studies have shown activated Rho GTPases to be targeted for proteasome degradation (Munro *et al.*, 2004). In fact, a number of studies have also shown Rho GTPase degradation as a result of CNF1 intoxication in epithelial cells (Doye *et al.*, 2002; Lerm *et al.*, 2002). This however, has not yet been previously reported in platelets, thus it was decided to test the stability of these key proteins in platelets upon intoxication with CNF1 toxins.

Washed (1×10^9 /ml) platelets were isolated and then left untreated or treated with 1 μ M of CNF1 and incubated for 0, 2, 4 and 6 h at 37°C. At given timepoints, cells were lysed, and samples analysed by western blot with specific antibodies for RhoA, Rac1 and Cdc42

Since the small GTPases are equivalent in molecular weight, after probing for RhoA the membranes were stripped as outlined in section 2.5.6 and blocked with 5% milk powder before reprobing with Rac1 antibody overnight. The above step was then repeated to visualise the proteins. The membrane was stripped once more and probed with antibodies specific

for Cdc42 as per above. GAPDH was used as a control for equal loading (Figure 5.6A). Western blot analysis indicates that levels of RhoA, Rac1 and Cdc42 in CNF1-treated platelets were not significantly different from the controls for all corresponding timepoints (Figure 5.6B), implying that the toxin does not affect the stability of small Rho GTPases in platelets.

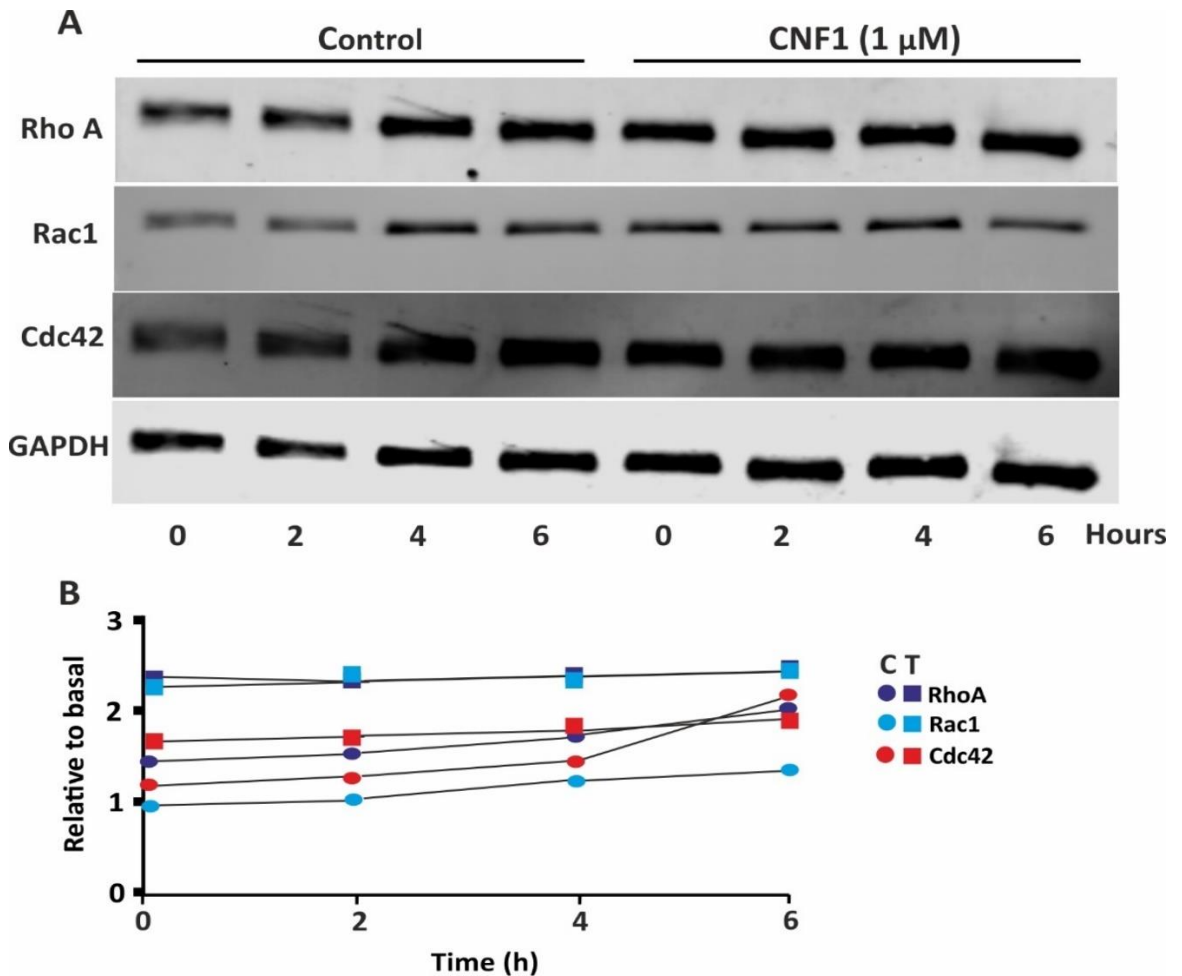


Figure 5.6 CNF1 effects on the stability of Rho GTPases in platelets. Washed platelets (1×10^9 /ml) were incubated at 37°C for 0, 2, 4 and 6 h in the presence and absence of CNF1 ($1 \mu\text{M}$). At the indicated times samples were lysed in one volume of Laemmli buffer. $30 \mu\text{l}$ of the lysates were loaded onto a 10% polyacrylamide gel and separated via SDS-PAGE. Proteins were then transferred onto a PVDF membrane. Following this, membranes were blocked with 5% BSA and probed with specific antibodies for RhoA overnight. Proteins were visualized the following day (secondary antibody, IR Dye 800CW anti-rabbit IgG) with an Odyssey TM CLx electronic imaging system (Li-Cor). Membranes were then stripped and re-probed for antibodies specific for Rac1 and subsequently stripped and re-probed for Cdc42 (secondary antibodies were IR Dye 800CW anti-mouse IgG and IR Dye 680CW anti-rabbit IgG respectively). GAPDH was used as the loading control. (A) Blots from 5 representative experiments. (B) Bands were quantified using ImageStudio lite version 5.2 software. C is control and T is toxin-treated platelets. The means \pm standard deviations of five independent experiments are shown. No statistical significance was found.

5.4 The effect of CNF1 on the amount of F-actin

Rho GTPases are widely recognised for their participation in actin remodelling. Therefore, we hypothesise that upon CNF1 activation of RhoA in platelets, alterations to the level of F-actin will occur. To investigate this, we conducted triton insoluble pellet experiments.

Washed platelets (1×10^9 cells/ml) were incubated with $1 \mu\text{M}$ CNF1 for 4 h. Following the incubation period, control toxin treated platelets were either stimulated with 0.1 U/ml thrombin for 30 or 60 seconds or left unstimulated and lysis buffer was added immediately in order to stop activation. Samples were then immediately processed for extraction of the triton insoluble pellet containing F-actin (section 2.5.7).

Samples were then spun at $15,600 \times g$ at 4°C for 15 min. Following this, the supernatant was discarded leaving the pellet (containing F-actin) which was gently overlaid with lysis buffer and spun again at the above conditions. Supernatant was once again discarded, and the pellet was lysed in Laemmli buffer and processed for western blot analysis. Samples were resolved by SDS10%-PAGE and analysed by western blotting as previously detailed. PVDF membranes were probed with β -actin (1:1000) antibody overnight at 4°C . The following day membranes were probed with appropriate fluorescently-labelled secondary antibodies to allow visualisation of bands and thus permit the determination of the amount of F-actin.

Figure 5.7A shows the bands of β -actin present following SDS-page and western blotting. Data obtained reveals that the level of F-actin increases significantly ($P < 0.01$) from 0 sec to 30 sec in the control group (Figure 5.7B). Similarly, there was an increase in the levels of F-actin between 0 (1.7 relative F-actin) and 30 (2.5 relative F-actin) seconds in the CNF-1 treated platelet group ($P < 0.05$). However, data revealed results between 30 sec and 60 sec to be comparable in both the control and toxin treated group. In addition to this, data shows for a significant difference in the levels of F-actin to be present between the two control groups, i.e. untreated platelets control had F-actin basal levels of 1.0 compared to 1.7 relative F-actin in the basal CNF1-treated platelets ($P < 0.05$). These results are in agreement with CNF1 being taken up by platelets, and resulting in modification to Rho GTPases, causing an increase in basal F-actin.

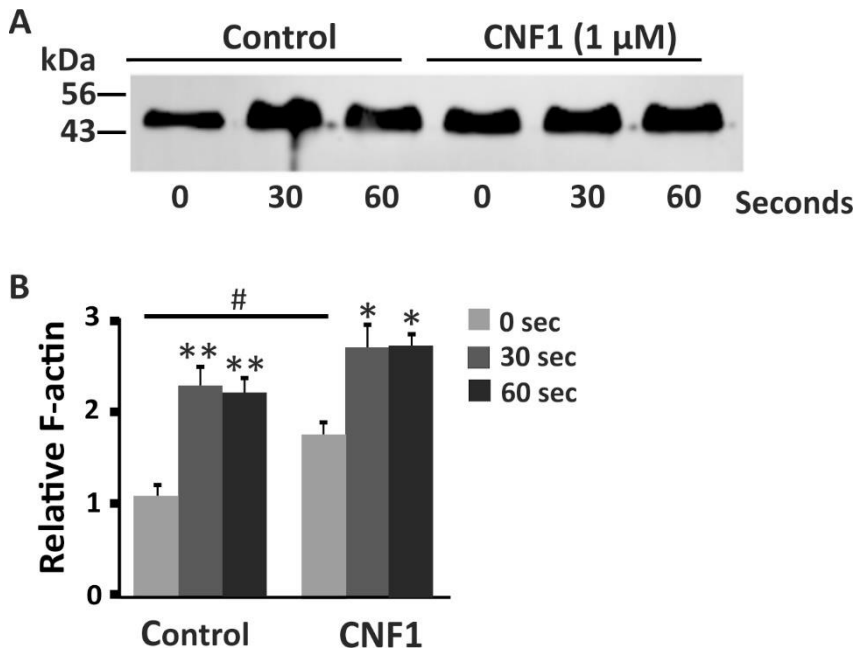


Figure 5.7 The effect of CNF1 on the F-actin concentration of thrombin-stimulated platelets. Washed platelets ($1 \times 10^9/\text{ml}$) were incubated at 37°C for 4 h in the presence or absence of CNF1 ($1 \mu\text{M}$). After incubation, platelet samples were stimulated with 0.1 U/ml of thrombin for 30 or 60 sec or left unstimulated. Lysis buffer was added to samples immediately after stimulation with thrombin and samples were processed for triton insoluble pellet extraction. $30 \mu\text{l}$ of the lysates were loaded onto a 10% polyacrylamide gel and separated via SDS-PAGE. Proteins were then transferred onto a PVDF membrane. Following this, membranes were blocked with 5% BSA and probed with specific antibodies for actin (1:1000) overnight. Proteins were visualized the following day with an Odyssey TM CLx electronic imaging system (Li-Cor). (A) Typical results of five different experiments are shown. Bands obtained were quantified using ImageStudio lite version 5.2 software and ImageJ software. (B) The means \pm standard deviations of six independent experiments are shown. Statistical significance was calculated using one-way ANOVA (* $p < 0.05$ and ** $p < 0.01$). Asterisks indicate significance relative to 0 sec. Hash symbol indicates significance between CNF1-treated platelets and control.

5.5 The effect of CNF1 on platelet spreading and morphology

It is well-established in literature for Rho GTPases to play an integral part in coordinating the activities of the actin cytoskeleton which in turn affects the morphology of the cell (Aslan, 2019; Goggs *et al.*, 2015). In the next set of experiments, we aim to examine the effects of CNF1 on platelet morphology and the dynamics of spreading.

5.5.1 The effects of CNF1 on the morphology of human platelets and their ability to spread on FG and collagen

It was decided to follow the platelet spreading process *in vitro*. Fibrinogen and collagen were chosen as the matrix proteins for investigating the effects of CNF1 on platelet spreading and morphology.

Washed platelets (1×10^9 /ml) were either left untreated or treated with $1 \mu\text{M}$ CNF1 at 37°C for 4 h. Platelets were incubated with CNF1 at high density to economise on toxin usage. Following the incubation, platelets were diluted to 1×10^7 /ml and placed on fibrinogen or collagen ($100 \mu\text{g}/\text{ml}$) coated coverslips for a further 1 h at 37°C . After the incubation, coverslips were processed and documented as described in section 2.6.3-2.4.6. Different parameters such as the number of cells, area and the morphology of cells were then calculated manually or using ImageJ software.

Representative images of the effects of CNF1 on platelet morphology is shown in Figure 5.8A. Our analysis revealed that CNF1 was not able to modify the ability of platelets to adhere to any of the matrixes assayed, since the number of platelets adhered were found to be comparable to the corresponding control groups, 34 ± 13 platelets/field in the control vs 33 ± 11 platelet/field when treated with CNF1 and spread on fibrinogen. Likewise, 29 ± 7 platelets/field in the control vs 22 ± 9 platelet/field when treated with CNF1 and spread on collagen (Figure 5.8B). No difference in the ability of platelets to spread was found between CNF1-treated platelets and untreated platelets spread on both fibrinogen ($30 \pm 3\%$ of cells vs $28 \pm 7\%$ of cells respectively) and collagen ($23 \pm 3\%$ of cells vs $20 \pm 7\%$ of cells respectively) (Figure 5.8C).

Prominent morphological differences among CNF1-treated platelets spread on fibrinogen were observed compared to control groups. A novel characteristic of strands emitting from some platelets was observable among the toxin-treated platelet samples and since these differed from 'typical' morphologies encountered during platelets spreading, it was given the term 'spiky cells' (white arrowheads).

As for platelet morphology, it can be observed from Figure 5.8D that for platelets spread on fibrinogen or collagen, again no difference was observed in the percentage of cells calculated to have stress fibres between control groups and CNF1-treated groups (30±3% of untreated cells had stress fibres vs 27±3% of cells when spread on fibrinogen, likewise 26±4% of untreated cells had stress fibres vs 27±4% of cells when spread on collagen). By contrast, a significant decrease ($P<0.05$) in the number of platelets with actin nodules was observed in the fibrinogen group upon treating platelets with CNF1 (14±4% of cells) compared to control (42±3% of cells) (Figure 5.8E). It is also observable from Figure 5.8E that although a decrease in the percentage of cells with actin nodules was found in CNF1 treated platelets spread on collagen, the difference was assessed to be statistically insignificant.

As mentioned previously, the presence of 'spiky' cells was observable upon treating platelets with the toxin. The data in Figure 5.8F reveals toxin-treated platelets spread on fibrinogen had a significant difference in the proportion of spiky cells present (7±0% of cells) compared to control (0% of cells) ($P<0.01$). On the contrary, although platelets treated with CNF1 and spread on collagen had some degree of spiky cells present (3±3% of cells) compared to the corresponding control group (0% of cells), the difference was found to not be statistically significant.

The results obtained indicate that CNF1 does not have a general effect on platelet adhesion and spreading. However, the toxin appears to modify certain morphological characteristics of platelets and these modifications are more noticeable upon spreading on fibrinogen compared to collagen.

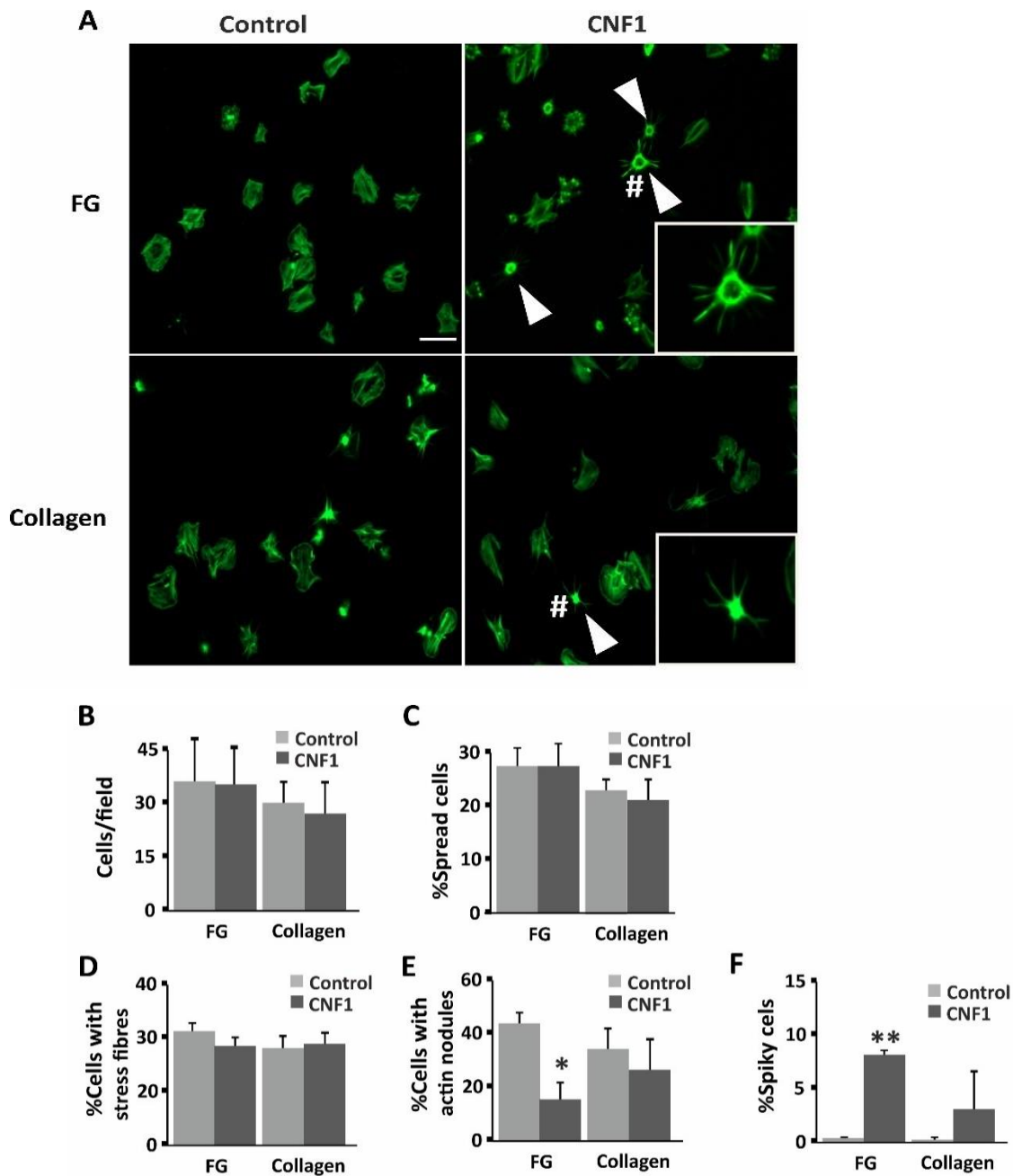


Figure 5.8 The effect of CNF1 on the morphology and ability of human washed platelets to spread on fibrinogen and collagen.

Human washed platelets (1×10^9 /ml) were incubated at 37°C for 4 h in the presence and absence of $1 \mu\text{M}$ CNF1. Following this, the suspension was diluted to 1×10^7 /ml and $200 \mu\text{l}$ of platelet suspension was added to coverslips coated with fibrinogen or collagen ($100 \mu\text{g}/\text{ml}$). Coverslips were incubated at 37°C for one hour, fixed with 4% PFA for 10 min, permeabilised with 0.3% Triton X100 for 5 min and stained with $1 \mu\text{g}/\text{ml}$ FITC phalloidin (green) for 30 min at room temperature. Coverslips were mounted onto glass slides with ProLong Antifade Mountant and images were obtained with a Zeiss ApoTome.2 fluorescence microscope equipped with a 60x oil immersion objective. (A) Representative images from four independent experiments. Scale bar represents $10 \mu\text{m}$. Arrowheads indicate examples of spiky cells. Hash symbols represent spiky cells which is then zoomed and placed at the lower left-hand corner of

appropriate images. (B) Adhesion of cells in each of the conditions and (C) percentage of spread cells were calculated by manually counting cells on ImageJ software. The proportion of cells containing (D) stress fibres, (E) actin nodules and (F) spiky cells was also calculated for each condition. Data are presented as means \pm SEM of four independent experiments, (* $p < 0.05$ and ** $p < 0.01$).

Since significant differences in platelet morphology was observed in platelets treated with CNF1 and spread on fibrinogen, it was decided to conduct a time course experiment to observe whether any differences arose with time. Therefore, washed platelets and coverslips were prepared as mentioned previously and incubated in the presence or absence of 1 μ M CNF1 at 37°C for 4 h. Following this, the platelet suspensions were placed on fibrinogen treated coverslips and incubated again at 37°C for 15, 30, 45 and 60 min. At given timepoints coverslips were fixed, permeabilised and mounted as described previously. Results from the experiments are shown in the Appendices, Figure 7.5.

It is possible to distinguish from Figure 7.5A in the appendices that as expected the number of platelets and the number of spread platelets increased with time in both the control and toxin group. We also observed that the ability of platelets to adhere to fibrinogen was not affected by the presence of the toxin at any timepoint since no difference was found between the number of toxin-treated platelets adhered on fibrinogen when compared to the respective control group.

Figure 7.5C in the appendices shows results to be consistent to that found in Figure 5.8, in that the number of spread cells and cells containing stress fibres between the control group and the toxin-treated group were found to be comparable. It is also possible to see that the number of cells containing stress fibres increased with time for both the control and toxin group, as did the number of cells containing actin nodules. Again, similar to the results obtained in Figure 5.8, a decrease in the number of cells containing actin nodules in CNF1-treated platelets at each of the timepoints compared to the respective control points was found. By contrast, there was an increase in the number of spiky cells in the toxin-treated groups compared to control. The data obtained, confirms the results in Figure 5.8 and suggests that the differences observed in terms of the number of cells with stress fibres,

actin nodules and spiky cells between control group and toxin group is present at all timepoints and that the percentage of cells for each category increases with time.

5.5.2 The effects of CNF1 on the morphology of mouse platelets and its ability to spread on FG

It was established in the previous section from spreading platelets on fibrinogen that CNF1 treatment affects the human platelet cytoskeleton and thus cellular morphology. In this section murine models were employed to study whether the toxin exerts similar effects in mouse models, especially since murine models have genetic similarities to humans. Moreover, if CNF1 is shown to have effects in mouse, one could exploit a mouse model for further studies *in vivo*.

Mouse washed platelets were isolated and (un)treated with 1 μ M CNF1 at 37°C for 4 h. Coverslips were then processed and analysed as described in section 5.5.1. Mouse platelets were not spread on collagen since Figure 5.8 revealed no significant difference in cellular morphology between control and toxin-treated groups when spread on collagen.

Figure 5.9A shows representative images of toxin (un)treated mouse platelet groups spread on fibrinogen. It is possible to see the presence of spiky cells in platelets treated with the toxin (hash symbol). Analysis of the results obtained revealed that CNF1 had no effect on the total number of platelets adhered to the matrix compared to the control group (12 \pm 0 cells/field in the control group vs 12 \pm 4 cells/field in the toxin group) (Figure 5.9B).

In the matter of platelet spreading, the percentage of spread platelets were found to be comparable between untreated platelets (20 \pm 9% of cells) and toxin-treated platelets (21 \pm 3% of cells) (Figure 5.9C). Comparable results between the two groups were also found for the percentage of cells with stress fibres, 5 \pm 1% of untreated cells contained stress fibres vs 6 \pm 1% in toxin-treated cells (Figure 5.9D).

A decrease in the percentage of toxin-treated cells containing actin nodules (71 \pm 4% in the control group compared to 36 \pm 4% in CNF1-treated platelet group) was found among the

two groups, although the difference was calculated to not be significant (Figure 5.9E). The opposite was found in terms of the percentage of spiky cells present, as a significant increase of more than 20% ($P < 0.01$) was found between untreated platelets ($1 \pm 0\%$ of spiky cells) compared to toxin-treated platelets ($29 \pm 2\%$ of spiky cells) (Figure 5.9F).

Taken as a whole, the results found from mouse platelets spread on fibrinogen were comparable to that of human platelets in that CNF1 did not seem to affect platelet adhesion per se. However, data obtained shows modifications to particular morphological attributes to an extent upon CNF1 treatment.

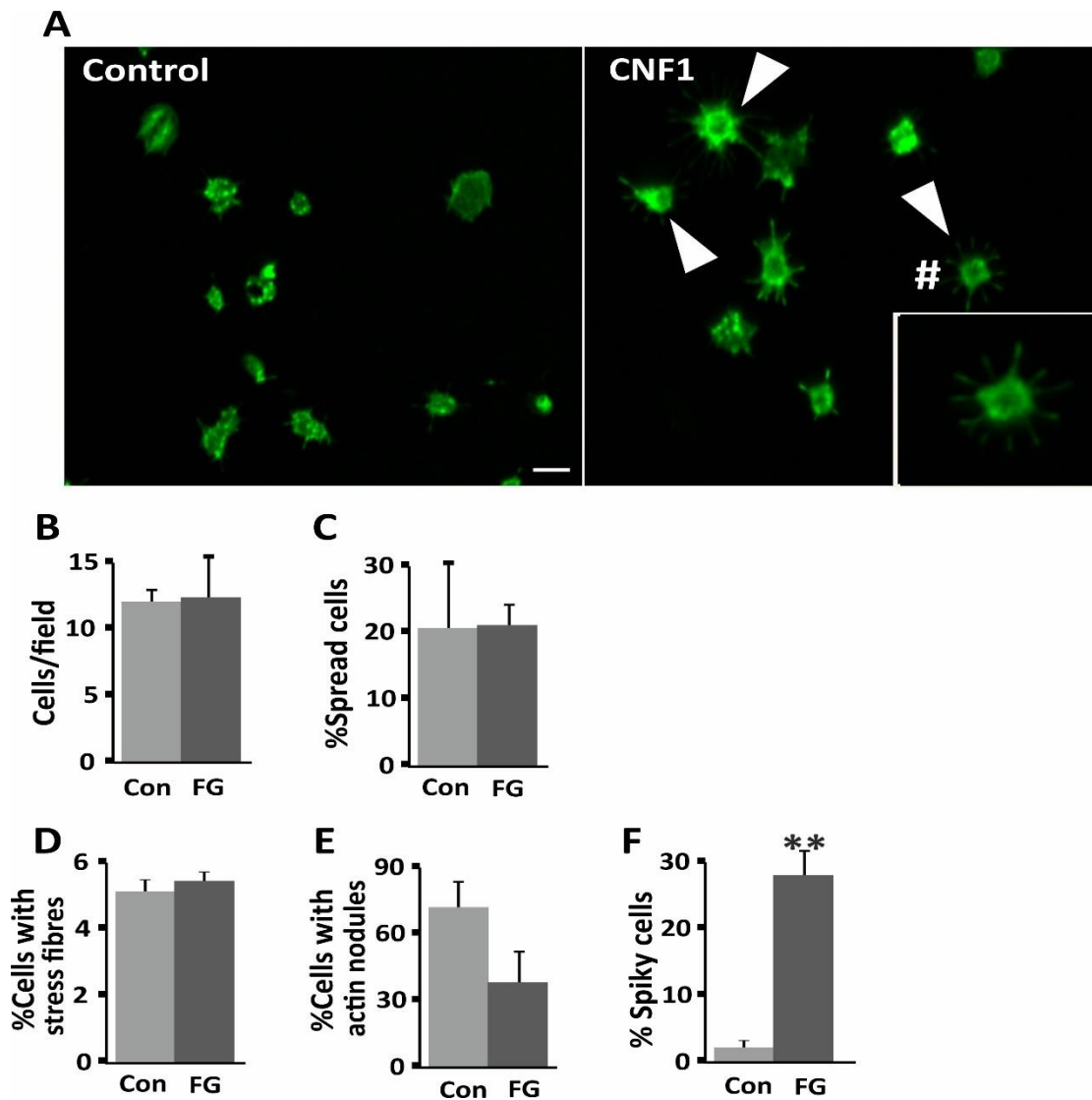


Figure 5.9 The effect of CNF1 on the morphology and ability of mouse washed platelets to spread on fibrinogen. Glass coverslips were coated with 100 $\mu\text{g/ml}$ fibrinogen for 1 h followed by BSA for 1 h at room temperature. Washed mouse platelets were diluted to $1 \times 10^7/\text{ml}$ in MTB. Platelet were then incubated at 37°C for 4 h in the presence or absence of $1 \mu\text{M}$ CNF1. Following this, 200 μl of platelet suspension was added to coverslips and incubated at 37°C for a further hour. Coverslips were then washed with PBS and fixed with 4% PFA for 10 min, permeabilised with 0.3% Triton X100 for 5 min and stained with $1 \mu\text{g/ml}$ FITC phalloidin (green) for 30 min at room temperature. Coverslips were mounted onto glass slides with ProLong Antifade Mountant and images were obtained with a Zeiss ApoTome.2 fluorescence microscope equipped with a 60x oil immersion objective. (A) Representative images from four independent experiments. Scale bar represents 5 μm . Arrowheads indicate examples of spiky cells. Hash symbol represents a spiky cell which is then zoomed and placed at the lower left-hand corner of appropriate image. (B) Adhesion of cells in each of the conditions and (C) percentage of spread cells was calculated by manually counting cells on ImageJ software. Cells containing (D) stress fibres, (E) actin nodules and (F) spiky cells was also calculated for each condition. Data are presented as means \pm SEM of four independent experiments, (** $p < 0.01$). Con; control and FG; fibrinogen.

5.6 Effects of CNF1 on secretion and integrin activation

The next set of experiments were conducted to investigate the effects CNF1 on platelet secretion and integrin activation, processes regulated by Rho GTPase signalling (Aslan and MCCarty, 2013). In order to do so, fluorescence-activated cell sorting was performed, and results were expressed as median fluorescence intensity (MFI) since this better represent antigens which are constitutively expressed (Spurgeon, 2014). All FACS experiments were performed with the assistance of David J Riley.

5.6.1 The effects of CNF1 intoxication on platelet receptor activation

Platelet surface receptors are key components involved in influencing platelet function. In this section, flow cytometry was conducted to assess the expression of four characteristic glycoproteins: GPVI, CD41, CD42b, and CD49b (Rivera *et al.*, 2009). The expression profiles of the platelet surface receptors were investigated in unstimulated and CNF1-stimulated (1 μ M) washed platelets (6×10^8 /ml) as outlined in section 2.5.8.

Figure 5.10 shows the differences in MFI of the four platelet surface receptors upon CNF1-treatment. It is observable for CNF1 stimulation to cause a significant decrease in expression of CD41 (integrin α IIb) and CD42b (GP1b) when compared to the respective controls ($P < 0.05$). Comparable results were found between untreated and toxin-treated platelets in terms of GPVI and CD49b (integrin α 2).

The results obtained from these experiments indicate CNF1 to cause substantial modifications in platelet surface receptor expression.

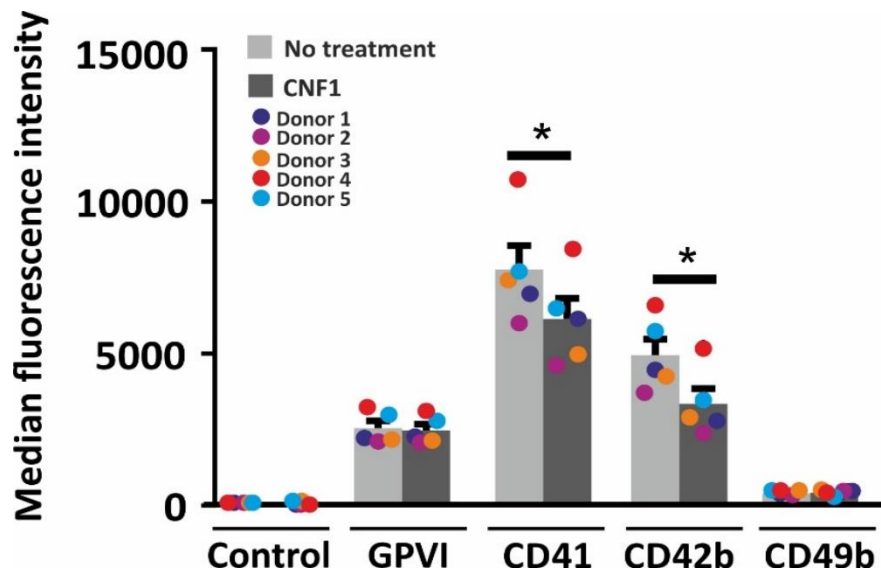


Figure 5.10 Flow cytometric analysis of the expression of platelet surface receptors in platelets treated with CNF1. Washed platelets (6×10^8 /ml) were unstimulated or stimulated with CNF1 ($1 \mu\text{M}$) and incubated at 37°C for 4 h. Following this, flow cytometry was conducted as outlined in section 2.5.8 to determine the expression levels of platelet receptors: GPVI, CD41, CD42b and CD49b. Data represent mean \pm SEM of five independent experiments. MFI was calculated with the FACSDiva software. Statistical significance was calculated between unstimulated and toxin-stimulated platelets using a paired Student's t-test ($*P < 0.05$).

5.6.2 Effects of CNF1 on integrin activation

Studies have previously demonstrated for RhoA to be required for integrin activation in platelets (Goggs *et al.*, 2015). Therefore, we hypothesised that alterations in the activation of the fibrinogen receptor (integrin $\alpha_{\text{IIb}}\beta_3$) will occur upon incubating platelets with CNF1 since the toxin has been established to target RhoA.

To investigate this, platelets were treated with CNF1 for 4h at 37°C or left untreated under the same conditions as detailed in section 5.6.1. Both groups of platelets were then stimulated with a range of agonists at various concentrations (0.1 or 0.01 U/ml thrombin, 5 or 0.5 $\mu\text{g}/\text{ml}$ collagen-related peptide (CRP), along with 10 μM ADP and 3 μM of the thromboxane analog U46619 alone or in combination). Pac-1, an antibody which specifically recognises activated $\alpha_{\text{IIb}}\beta_3$ in humans was then used to determine integrin activation in platelets via flow cytometry (section 2.5.8).

It can be seen in Figure 5.11 that CNF1 treatment of platelets resulted in a reduction in integrin activation when stimulated with any of the agonists mentioned above. In the case of thrombin and CRP, significant differences in integrin activation was found in a dose-dependent manner. We were not able to detect any significant differences in Pac-1 levels between CNF1 treated and untreated platelets when ADP or U46619 agonists were used alone to stimulate platelets, however the opposite was found upon combinational stimulation by 10 μ M of ADP and 3 μ M U46619 ($P < 0.05$).

Data gathered from these experiments suggest CNF1 has the capacity to significantly alter the level of α IIb β 3 integrin activation in platelets when stimulated with a variety of agonists, thus reinforcing CNF1 to be critically involved in modifying platelet functions via reducing the activation of the fibrinogen receptor.

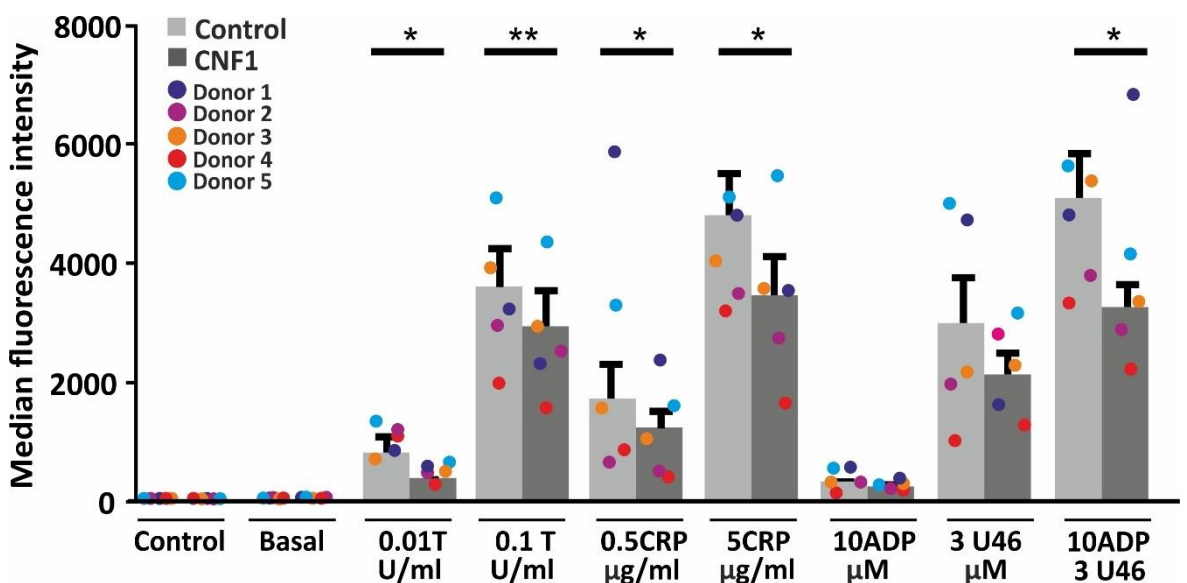


Figure 5.11 Flow cytometric analysis of integrin activation in platelets treated with CNF1.

Washed platelets (6×10^8 /ml) were either treated with CNF1 (1 μ M) or left untreated and incubated at 37°C for 4 h. Following this, flow cytometry was conducted as outlined in section 2.5.8 to determine the expression levels of α IIb β 3 activation upon stimulation with thrombin (T) (0.1 or 0.01 U/ml), CRP (5 or 0.5 μ g/ml), ADP (10 μ M), U46619 alone (3 μ M) or in combination with ADP. Data represent mean \pm SEM of five independent experiments. MFI was calculated with the FACSDiva software. Statistical significance was calculated between unstimulated and toxin-stimulated platelets using a paired Student's t-test (* $P < 0.05$ and ** $P < 0.01$).

5.6.3 The effect of CNF1 on platelet granule secretion

Next, we explored the secretory aspect of platelets. The secretion of platelet granular content is critical for a number of platelet functions, in particular to arrest bleeding. Recently, researchers have reported platelet secretion of a vast variety of cytokines and secondary mediators to be crucial to aid the immunological role of platelets (Gerdes *et al.*, 2011). It has also been previously established for Rho GTPases which generally orchestrate the rapid remodelling of the cytoskeleton, to support granule content exocytosis in platelets (Fitch-Tewfik & Flaumenhaft, 2013; Flaumenhaft, 2003; Goggs *et al.*, 2015). In this section we will explore quantitatively whether CNF1 intoxication results in defects in either alpha or dense granule secretion in platelets.

WP were prepared and incubated in the presence or absence of CNF1 as mentioned in section 5.6.2. To evaluate the effects of CNF1 treatment on α - and dense granule secretion, we examined P-selectin and CD63 expression, respectively. The same agonists detailed in section 5.6.2 were used in this experiment and flow cytometry was conducted as described in section 2.5.8.

It can be seen in Figure 5.12 and 5.13 the differences in P-selectin and CD63 expression, respectively, between untreated and CNF1 treated platelets, stimulated with various agonists.

In the case of P-selectin expression, Figure 5.12 shows a decrease in all CNF1 treated groups compared to their respective controls, except for platelets stimulated with 0.5 $\mu\text{g}/\text{ml}$ CRP and 10 μM ADP. It can also be seen that significant differences were found in P-selectin expression between control and CNF1-treated platelets upon stimulation with (0.1 U/ml) thrombin ($P < 0.01$) and 5 $\mu\text{g}/\text{ml}$ CRP ($P < 0.05$).

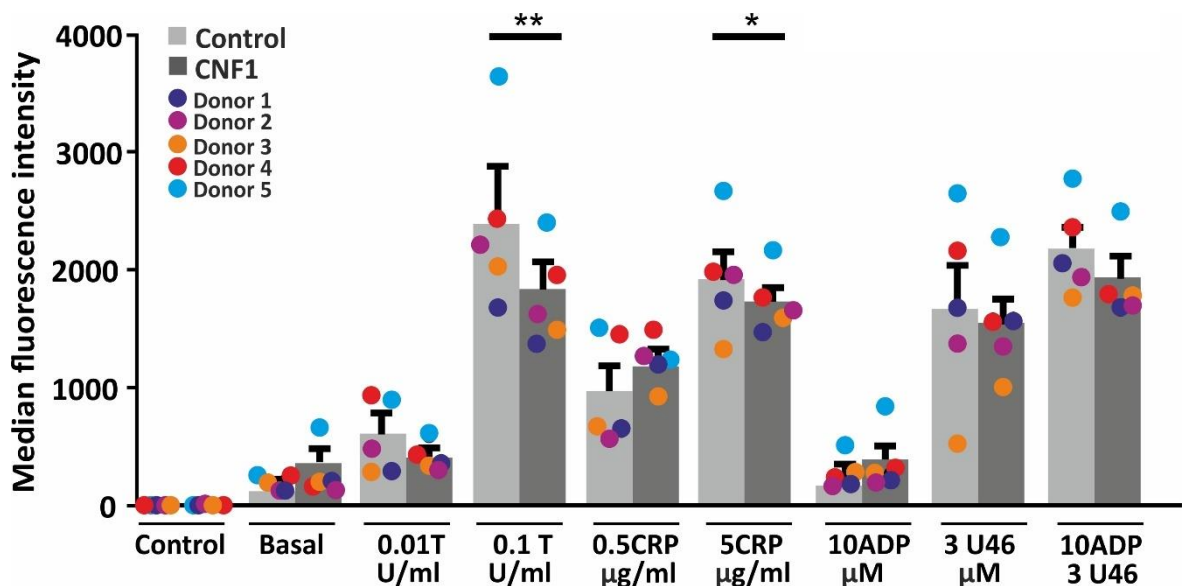


Figure 5.12 Flow cytometric analysis of alpha granule secretion in platelets treated with CNF1. Washed platelets ($6 \times 10^8/\text{ml}$) were treated with CNF1 ($1 \mu\text{M}$) or left untreated and incubated at 37°C for 4 h. Following this, flow cytometry was conducted as outlined in section 2.5.8 to determine the expression levels of P-selectin upon stimulating platelets with thrombin (T) (0.1 or 0.01 U/ml), CRP (5 or 0.5 $\mu\text{g}/\text{ml}$), ADP (10 μM), U46619 alone (3 μM) or in combination with ADP. Data represent mean \pm SEM of five independent experiments. MFI was calculated with the FACSDiva software. Statistical significance was calculated between unstimulated and toxin-stimulated platelets using a paired Student's t-test (* $P < 0.05$ and ** $P < 0.01$).

With regard to dense granule secretion, it can be observed in Figure 5.13 that ADP and/or U46619 had little effect on P-selectin expression between control and CNF1-treated platelets. In addition to this, data revealed thrombin to modify levels of CD63 expression in a dose-dependent manner, although it was found to be not statistically significant when a lower dose of thrombin was used (0.01 U/ml). The higher dose of CRP stimulation of platelets resulted in significant changes to the level of CD36 expression between control and toxin-treated platelets ($P < 0.05$).

Some of the conditions tested showed statistically significant differences between untreated and toxin-treated platelets in terms of alpha- and dense-granule secretion. Thus, suggesting CNF1 alters granule secretion of platelets quite extensively.

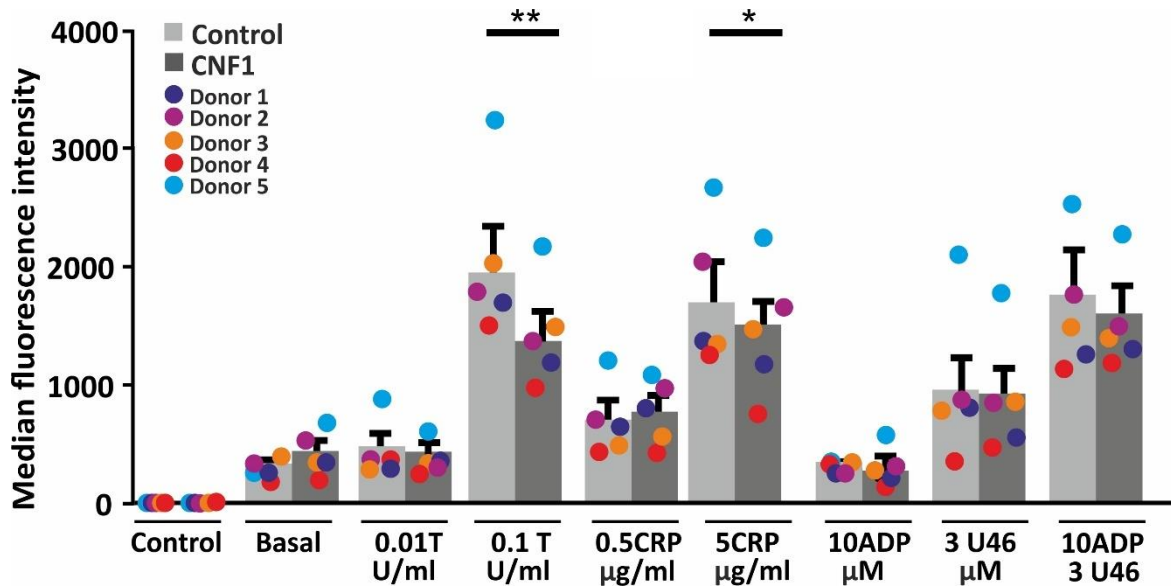


Figure 5.13 Flow cytometric analysis of dense granule secretion in platelets treated with CNF1. Washed platelets ($6 \times 10^8/\text{ml}$) were (un)treated with CNF1 ($1 \mu\text{M}$) and incubated at 37°C for 4 h. Following this, flow cytometry was conducted as outlined in section 2.5.8 to determine the expression levels of CD63 upon stimulating platelets with thrombin (T) (0.1 or 0.01 U/ml), CRP (5 or 0.5 $\mu\text{g}/\text{ml}$), ADP (10 μM), U46619 alone (3 μM) or in combination with ADP. Data represent mean \pm SEM of five independent experiments. MFI was calculated with the FACSDiva software. Statistical significance was calculated between unstimulated and toxin-stimulated platelets using a paired Student's t-test (* $P < 0.05$ and ** $P < 0.01$).

5.7 Discussion

A rising body of evidence has demonstrated for bacterial pathogens that enter the bloodstream to have evolved to target cellular and soluble elements of the host immune defence system, including platelets (Shannon, 2017). One particularly dangerous virulence that some bacteria have adapted to possess is the ability to secrete toxins or bacterial proteins which modify host cell function thus resulting in the pathogenesis of conditions such as sepsis (Hamzeh-Cognasse *et al.*, 2015).

Cytotoxic necrotising factor 1 (CNF1) is a Rho-directed toxin secreted by uropathogenic *E. coli* (UPEC) strains and have been shown to extensively modulate endothelial and epithelial cell function leading to pathological consequences. Whereas the effects of the toxin on platelets remains uncovered.

CNF1 has been found to interact with target cells via Lu/BCAM and p37/LRP (Chung *et al.*, 2003; Piteau *et al.*, 2014a). We have shown in this thesis for these receptors to be present in platelets (Appendices Figure 7.4), therefore making platelets a potential target for CNF1.

Given that the effects of CNF1 is not elucidated in platelets, and since Gram-negative associated bloodstream infections are a common cause of mortality, we decided to investigate whether these Rho-targeting pathogenic bacterial products would hinder the role of key cytoskeletal regulators (Rho GTPases) and ultimately lead to alterations in platelet functions. We therefore aim to provide insight into whether the mechanism employed by the pathogen contributes to pathological outcomes.

Since the receptors required for CNF1 binding is present in platelets, the first question to address was whether the toxin is internalised and processed in platelets. Therefore, we conducted an experiment to visualise a Rho shift which is present once GTPases have been covalently modified by the toxin (Schmidt *et al.*, 1997). Flatau *et al.*, (1997) and Brest (2003) both reported a motility shift of Rho to be present in Vero cells and lymphoid cells, respectively, post CNF1 treatment. We also found a molecular shift of Rho in CNF1-treated platelets at 4 h (Figure 5.5), thus indicating that the C-domain of the toxin leads to direct

post-translational modifications of Rho which is indicated, although indirectly, by the shift in molecular weight of Rho. However, we observed a shift in motility only when platelets were incubated with 1 μ M of toxin for 4 hours. Whereas, Schmidt *et al.*, (1997) reported a Rho shift within 2-3 hours of incubating NIH3T3 cells with the toxin. Whereas Brest (2003) found Rho shift to be present upon treating Jurkat cells with 3 nM of CNF1. The difference in results between our study and published literature in regard to time of incubation and concentration of toxin required could indicate that perhaps there is a reduced number of associated receptors in platelets or possibly that the receptors present on platelets are comparatively smaller in size. Another possible explanation is that the endocytic pathway, which is the route by which the toxin is transported into target cells (Gall-Mas *et al.*, 2018), could be less efficient in platelets. It has been demonstrated that a reduction in pH is necessary for the cleavage and translocation of the catalytic domain of CNF1 out of endosomal compartments (Knust and Schmidt, 2010). This process in platelets could require more time since platelets have fewer lysosomes (contains acid hydrolases which can alter pH when secreted) compared to nucleated cells (Fitch-Tewfik and Flaumenhaft, 2013).

In order to elucidate the uptake route of CNF1 in platelets and visualise the progression along the endocytic pathway, one could perform a pulse chase experiment followed by fractionation whereby cytosolic and membrane fractions could be analysed via SDS-PAGE. Immunocytochemistry whereby CNF1-treated platelets are stained for CNF1 in combination with endosomal markers could aid the clarification and characterisation of the CNF1 uptake route in platelets.

Even though we found the presence of a motility shift in Rho only when platelets were treated with 1 μ M CNF1 and while such concentrations are unlikely to be present in circulation upon *E. coli* bacteraemia, they could however be reached locally in a focus of infection. Another possibility would be that upon collection and clustering of bacteria by platelets in vivo such concentration would be present.

We also report in this thesis that CNF1 does not affect the stability of Rho GTPases. Although GTP hydrolysis is key in certain conditions to terminate the signalling of Rho GTPases, recently the addition of ubiquitin molecules and the subsequent proteasomal degradation has been demonstrated to regulate the small Rho GTPases (Lynch *et al.*, 2006; Chen *et al.*, 2009). Therefore, the effects of CNF1 toxin can be assumed to be counterintuitive to some extent since the permanent activation of Rho proteins leads to its rapid ubiquitinylation, hence why some researchers propose CNF1 to result in transient activation of Rho (Doye *et al.*, 2002).

Even though the results we observed differ from that of previous work by Doye *et al.*, (2002) and Munro *et al.*, (2004), as they demonstrated degradation of Rac. These divergent outcomes between the results obtained in our study could be due to a number of factors including methodological/population since they monitored degradation of Rho GTPases over a period of 24h while we stopped at 6h. However, it is also possible that degradation of Rho protein levels was not observed in our study since platelet Rho GTPases may perhaps be more stable compared to endothelial and epithelial cell lines used in their study. On the contrary, another possibility is that ubiquitinylation and/or proteasome degradation are less efficient in platelets, though this is not well-characterised.

Researchers have shown an increase in F-actin content in CNF1-treated cells (Capo *et al.*, 1998). Fiorentini and co-workers (1995) demonstrated the same in Hep-2 cells, whereas Vouret-Craviari *et al.*, (1999) found the same to be true for HUVECs treated with the toxin. Our data found an increased level of F-actin in both the control and toxin-treated groups upon thrombin stimulation, which is as expected since thrombin activates platelets which stimulates the conversion of G-actin to F-actin (Severin *et al.*, 2013). We also report for CNF1 to cause an increase in basal F-actin levels (Figure 5.7). This is compatible with switching on of the Rho GTPases, thus inducing the conversion of G-actin into F-actin.

In line with the above, it is known for platelet processes such as cell spreading requires the formation of F-actin structures. Since CNF1 targets Rho proteins which are critical partakers in the formation of such actin structures, we hypothesised abnormalities in platelet morphology to be present upon intoxication with CNF1. Indeed, in this study, we reveal for

the first time, CNF1 to induce morphological alterations in both human and mouse platelets placed on matrix proteins (Figure 5.8-9). A significant reduction in actin nodules was observed in CNF1-treated platelets. Actin nodules have been reported to be precursor to the formation of platelet structures i.e. lamellipodia and stress fibres (Calaminus *et al.*, 2008), which in turn is regulated by Rac1-WAVE-Arp2/3 axis and RhoA-ROCK/mDia1 pathways, respectively. However, recent evidence from Poulter *et al.*, (2015) suggest actin nodules to be closely associated with the Rac1 pathway rather than RhoA. Hence suggesting CNF1 to target Rac1 more than RhoA GTPases. This is coherent with the data we obtained since we noticed the proportion of cells with stress fibres (RhoA-ROCK/mDia1 pathway) was not altered, which implies that RhoA was not affected.

Data obtained lends support to numerous studies which have shown CNF1 to induce Rac1-morphological alterations in various endothelial and epithelial cells (Lerm *et al.*, 1999; Messina *et al.*, 2019). In addition to the morphological alterations observed in platelets, we found a substantial increase in the number of platelets with novel characteristic of strands radiating from the cell (spiky cells). We conclude that Rho GTPase signalling is involved in the formation of spiky structures in platelets since this characteristics was significantly reduced in untreated cells, however the key GTPase involved in inducing this alteration has not been identified although we postulate for it be Cdc42-dependent signalling since the characteristic observed were similar to that of filopodia.

Since studies have established CNF1 to result in the permanent activation of Rho proteins, we hypothesised for an increase in platelet surface expression and integrin activation upon treating platelets with CNF1. Contrary to our hypothesis, we found a modest but significant reduction in CD41 (integrin α IIb) (Figure 5.10). Furthermore, we found integrin activation was also reduced in CNF1-treated platelets stimulated with thrombin, CRP or a combination of ADP and U46619 (Figure 5.11), which essentially is in line with Figure 5.10 since less integrin expression results in less response/integrin activation. Despite the reduction in CD41 and alteration to integrin activation, adhesion of toxin-treated platelets to fibrinogen was largely unaffected (Figure 5.8-9).

We also demonstrated a reduction in platelet granule secretion once platelets were intoxicated with CNF1 (Figure 5.12 and 5.13). Along with integrin activation, platelet granule secretion is also a critical platelet process which aids the recruitment of sophisticated immune cells to site of injury/infection, thus supporting the notion that platelets partake in immune responses (Fox *et al.*, 2018). Rho GTPases have been reported to partake in aiding secretion of platelet granular content (Akbar *et al.*, 2007, 2009; Goggs *et al.*, 2015). The fact that CNF1 alters platelet secretion to some extent means platelet immunologic responses are also impaired since granules are the regions in which numerous antimicrobial peptides, cytokines and several bactericidal proteins are stored. Thus, could aid the evasion of immune response allowing *E. coli*-induced pathogenesis of sepsis in individuals. Since the toxin targets Rho GTPases which in turn regulate the platelet cytoskeleton, it could also lead to impairment in scavenging properties thus again allow the progression of infection *in vivo*.

Conclusion

In this chapter we have effectively assessed the effects of the Rho-modifying CNF1 toxin on platelet morphology and function. We show indirectly that CNF1 is taken up and processed by platelets, where it modifies Rho GTPases and induces the conversion of G-actin to F-actin. While the ability of platelets to adhere on collagen and fibrinogen was not impaired, platelet morphology was affected. By CNF1. The toxin moderately impaired integrin activation and granule secretion upon stimulation with various agonists. This study has permitted us to reinforce the importance of Rho GTPases in regulating platelet function and offers insights on how microorganisms exploit Rho signalling for their own benefit.

Chapter 6. Discussion

6.1 General discussion

Platelets are known to play an integral role in haemostasis. A rising body of evidence also propose for platelets to possess immunologic capacity (Gear and Camerini, 2003). Both functions essentially require platelet activation to occur, which in turn is facilitated through the regulation of a number of proteins via a plethora of phosphorylation-based signalling events. In addition to intracellular signalling mechanisms, some studies have shown various platelet surface receptors to mediate platelet-bacteria interactions and subsequent platelet activation, degranulation and aggregation (Ali *et al.*, 2015), thus demonstrating platelets to act as primitive immune cells. Nevertheless, research in the field of platelet-bacteria associations and their effects are in its infancy and the molecular mechanisms involved are not clearly defined.

In this thesis we add support to platelets' immune roles whereby they actively migrate and scavenge both non-infectious (FG) and infectious (bacteria) matter, through optimising and establishing a migration and scavenging assay which allows quantitative analysis of both platelet processes. In this study we focused on members of the Rho GTPase family because of their importance in regulating cytoskeletal rearrangements in platelets. We also explored the influence of tyrosine kinase signalling molecules through the use of pharmacological inhibitors, which are also commonly used in the management of malignancies. Finally, we examined the ability of Rho-targeting bacterial toxin (CNF1) to alter platelet actin dynamics and thus hinder platelet functions.

The association of bacteria or bacterial components directly or indirectly to platelet surface receptors is believed to be the initial act of host defence (Naik, 2014). It is also known for bacterial engagement to platelet receptors to be strain specific. In our study we utilised *S. aureus* Newman, which has been previously found to associate with IgGs from plasma in order to engage with platelet surface receptor FcγRIIA along with integrin αIIbβ3 to stimulate platelet activation (Arman *et al.*, 2014). We tested this by first blocking the receptor with IV.3 ab (which binds to monomeric IgGs, specifically the Fc region). Indeed, we found complete inhibition of both Newman induced aggregation as well as a significant

reduction in the ability of IV.3 antibody-treated platelets to scavenge bacteria, thus confirming *S. aureus*-platelet interactions to be influenced by FcγRIIA. In addition to this, we inhibited platelet integrin αIIbβ₃ with integrilin and found similar outcomes to that of IV.3 antibody-treated platelets (no platelet scavenging and aggregation), again confirming the involvement of GPIIb/IIIa in facilitating *S. aureus* Newman interactions with platelets.

The engagement of a ligand to FcγRIIA has been previously linked to complex and powerful platelet activation pathways via ITAM intracellular signalling cascade, as reviewed by Qiao *et al.*, (2015). Src kinases for example Lyn and Fyn, and tyrosine kinase; Syk are pathways that are downstream of FcγRIIA (Lowell, 2011). In this study, we demonstrated through the use of inhibitors dasatinib and PRT-060318, which inhibit Src and Syk respectively, that platelet scavenging properties were abolished as well as platelet aggregation, hence lending support to the fact FcγRIIA signals through the tyrosine kinase pathway to activate platelets (Yanaga *et al.*, 1995).

This is also in line with previous studies which have shown activation of FcγRIIA to cause tyrosine phosphorylation of linker for activation of T cells (LAT) which occurs downstream of Syk (independent on SLP-76) (Ragab *et al.*, 2007). This then has been found to phosphorylate and activate PLCγ2 which in turn is associated with integrin αIIbβ₃ activation and is key for facilitating bacterial-platelet interactions (Pasquet *et al.*, 1999; Arman *et al.*, 2014). Thus, by inhibiting Src and Syk which are upstream of PLCγ2 we speculate hinderance to integrin αIIbβ₃ inside-out activation and this step is critical for triggering platelet functions, hence the reason platelet aggregation and scavenging were observed to be absent. A schematic model of the proposed signalling cascade model involved in *S. aureus* Newman-induced platelet scavenging as well as platelet aggregation is depicted in Figure 6.1.

In this thesis we also report, for the first time, inhibition of platelet scavenging properties upon treatment with Ibrutinib and acalabrutinib which are BTK inhibitors commonly used in the management of haematologic malignancies i.e. chronic lymphocytic leukaemia (CLL) (Series *et al.*, 2019). Numerous researchers have shown B cell antigen receptor (BCR)-signalling to be crucial for the survival and proliferation of leukaemia cells. BTK (a member

of the Tec family) is downstream of BCR and so makes it an ideal target for CLL therapy. Upon ligand engagement with BCR, Src kinases for example Lyn is phosphorylated which then subsequently leads to the phosphorylation of Syk (Packard and Cambier, 2013). This then causes the phosphorylation of BTK as well as PLC γ 2 which then results in the activation of several molecules including PKC β and NF- κ B, which ultimately enhances cell proliferation (Singh *et al.*, 2018). In platelets, BTK have been shown to be associated with ITAM which is closely associated with Fc γ RIIA (Singh *et al.*, 2018). Thus, we propose for *S. aureus* to engage with Fc γ RIIA thus resulting in the phosphorylation of Fyn/Lyn, this then leads to the phosphorylation of BTK and PLC γ 2 downstream which then ultimately activates integrin α IIb β 3. Hence why by inhibiting BTK with ibrutinib or acalabrutinib we found platelet scavenging and aggregation to diminish (Figure 6.1).

In a number of cells, including platelets, actin cytoskeletal rearrangements in response to external stimuli are triggered via engagement of various receptors on the surface of the cell (Periayah *et al.*, 2017). Interestingly, these signals have been reported to converge internally in the cell in close association with members of the Rho GTPase family, RhoA, Rac and Cdc42 which collectively propagate signals and orchestrate the activation of platelets (Alberts *et al.*, 2002). Several studies have shown the activation of Rho GTPases to be influenced by three major elements, GEFs, GAPs and GDIs (Ota *et al.*, 2015).

Src-family of tyrosine kinases, which are downstream Fc γ RIIA have been reported to activate GEFs via phosphorylation of PI3K, which in turn acts on Rho GTPases, specifically Rac1 (Welch *et al.*, 2003; Huveneers and Danen, 2009). Studies have also found Rac1 to play a role in PI3K activation hence implying a model of platelet activation where Rho GTPases regulation is multidirectional (Aslan and McCarty, 2013). Thus, we postulate *S. aureus* Newman to interact with Fc γ RIIA along with GPIIb/IIIa, which then results in the activation and phosphorylation of SFKs downstream. This then, in addition to activating integrin inside-out signalling, can act on GEFs to activate Rho GTPases hence inducing cytoskeletal rearrangements in platelets. This justifies why morphological changes to platelets were observed when tyrosine kinase signalling molecules upstream of Rho GTPases were inhibited. The proposed pathway is depicted in Figure 6.1.

Besides activation of Rho GTPases via FcγRIIA-tyrosine kinase mediated pathway, integrin αIIbβ3 activation by fibrinogen which is associated with *S. aureus* Newman can also result in the activation of Rho GTPases via outside-in signalling (Das *et al.*, 2014). Ultimately, Rho GTPases are critical in mediating platelet shape change which in turn is essential for platelet scavenging. Therefore, it is unsurprising that upon inhibiting major Rho GTPases, the ability of platelets to scavenge was hindered. Rhosin, which inhibits RhoA activity was observed to disrupt platelet scavenging activities the most, thus implying scavenging properties of platelets to be associated more closely with RhoA than Cdc42 and Rac1.

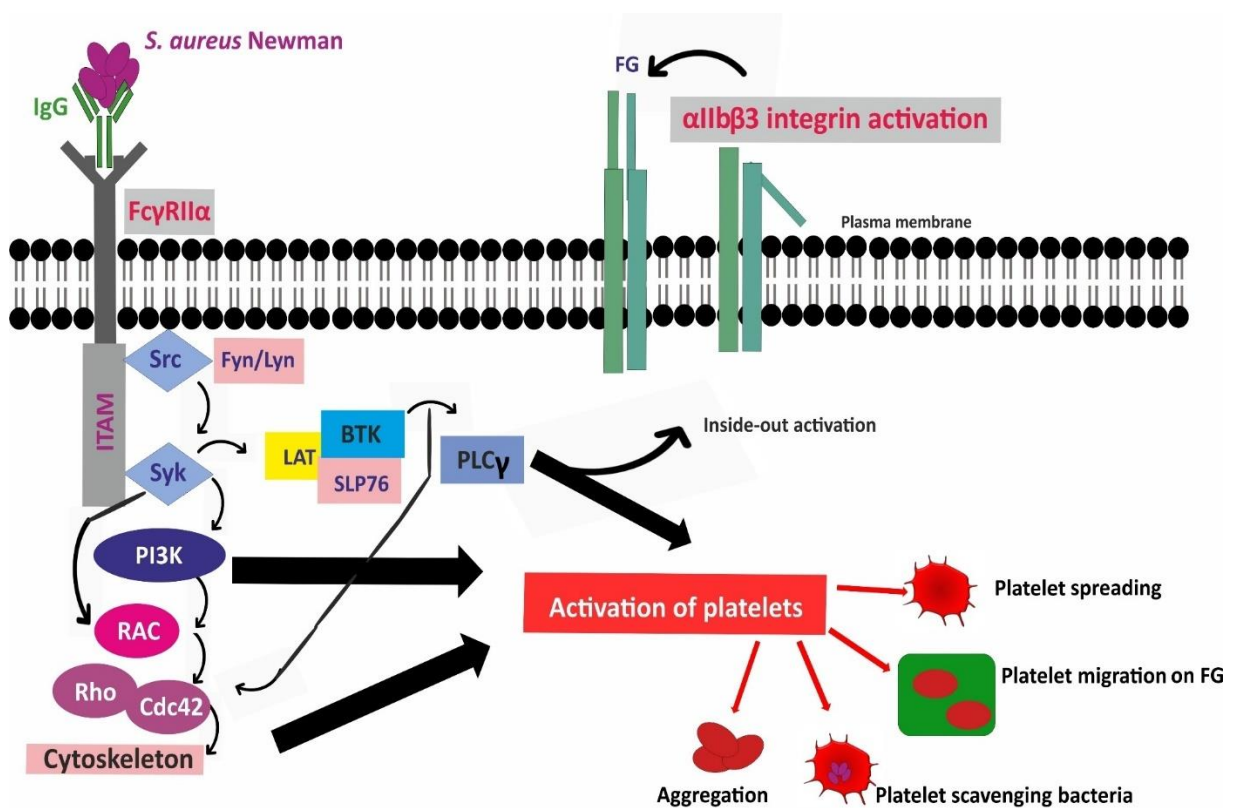


Figure 6.1 A schematic model of the platelet signalling cascade for platelet scavenging induced by *S. aureus* Newman. *S. aureus* Newman binds to FcγRIIA, which in itself is associated with an ITAM, leading to the activation and phosphorylation of Src kinases such as Lyn/Fyn. Syk is also phosphorylated resulting in activation and phosphorylation of downstream PI3K-Rac-Rho, which stimulates rearrangement of the actin cytoskeleton and promotes platelet scavenging properties. Syk phosphorylation also results in the activation of LAT-SLP76 which is associated with BTK. This subsequently activates PLCγ2, which stimulates integrin activation as well as resulting in the activation of platelets. Binding of *S. aureus* Newman also requires binding to integrin αIIbβ3, which can result in outside-in signalling, activating Rho GTPases independently to the FcγRIIA-tyrosine kinase pathway.

In addition to platelet scavenging infectious matter, we report for the first time the involvement of tyrosine kinase signalling pathway in facilitating the migration of platelets on fibrinogen. To some extent the intracellular signalling mirrors that of scavenging infectious matter. This is in line with a number of studies including those conducted by Bambach & Lämmermann, (2017); Bordon, (2018) and Deppermann & Kubes, (2018) who highlighted an association between platelet migration and scavenging capacity.

It is well established that fibrinogen binds to integrin $\alpha\text{IIb}\beta\text{3}$ (Albert and Christopher 2012). It has also been reported that integrin $\alpha\text{IIb}\beta\text{3}$ is essential for platelet migration to occur (Gaertner *et al.*, 2017). We also observed the same in our study since integrilin-treated platelets lacked the capacity to migrate thus confirming integrin $\alpha\text{IIb}\beta\text{3}$ to be critical in allowing platelets to firstly adhere to the matrix and secondly to 'peel' away from the matrix to make new associations with fibrinogen in different directions (process of cellular migration). However, we also showed inhibition of tyrosine kinase signalling molecules (which are commonly associated with ITAM receptors), to inhibit the ability of platelets to migrate on Alexa488 FG.

Src has been previously reported to be associated with integrin $\alpha\text{IIb}\beta\text{3}$. Indeed, a direct interaction between the SH3 domain of Src and the integrin- β3 cytoplasmic domain was demonstrated by Arias-Salgado *et al.*, (2005), and for this engagement to then stimulate platelet functions. Woodside *et al.*, (2001) showed the integrin- β3 -Src complex to result in subsequent recruitment and phosphorylation of Syk, which then stimulate Rac1 activation via phosphorylation of Vav1. We postulate for a similar pathway to be involved in platelet migration since blocking Src and Syk resulted in complete inhibition of platelet migratory capacity. Hence implying Rac1 activation was blocked by inhibition of proteins upstream, Src/Syk. A schematic model of the signalling involved in platelet migration is shown in Figure 6.2.

We propose platelet migration to occur via integrin- β3 -Src complex activation resulting in subsequent recruitment and activation of Syk which then phosphorylates either PI3K or PLC γ and ultimately activates cytoskeletal rearrangement via Rho-Rock-myosin II (Aburima *et al.*, 2013), Cdc42-WASp-Arp2/3 (Goggs *et al.*, 2015) or Rac1-WAVE-Arp2/3 (Aslan and

McCarty, 2013)axis. Thus, the reason inhibiting Rho GTPases or SFK resulted in an absence in platelet migration capacity.

We also found significant reduction in platelet migration ability upon treating platelets with IV.3 ab, although the alteration was not as prominent as those observed when platelets were treated with SFK/Rho GTPase inhibitors. An explanation for this observation is that platelet migration was influenced IgG, since fibrinogen we utilised were not depleted of IgGs therefore it is possible for platelets to bind IgG present on the fibrinogen matrix via FcγRIIA thus initiating tyrosine kinase mediated pathway involving Src/Syk and PI3K (shown in Figure 6.1) which ultimately acts on Rho GTPases thus modifying platelet morphology and subsequently exerting effects on platelet migration.

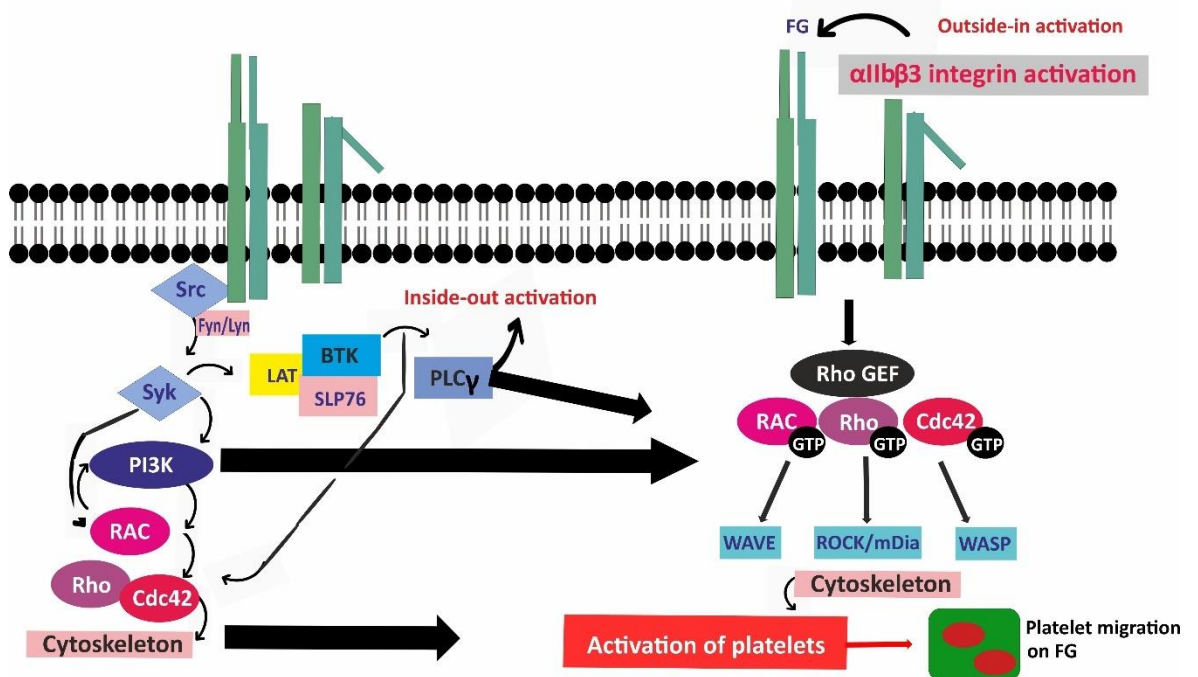


Figure 6.2 A schematic model of the platelet signalling cascade for platelet migration.

Fibrinogen (FG) binds to integrin $\alpha_{IIb}\beta_3$ resulting in activation of Rho GTPases downstream. This stimulates cytoskeletal rearrangement to occur thus aiding platelet migration processes. Alternatively, FG bind to integrin $\alpha_{IIb}\beta_3$ which in itself is associated with Src, leading to the activation and phosphorylation of Src kinases such as Lyn/Fyn. Syk is also phosphorylated resulting in activation and phosphorylation of downstream PI3K-Rac-Rho which stimulates rearrangement of the actin cytoskeleton and promotes platelet migratory properties. Syk phosphorylation also results in the activation of LAT-SLP76 which is associated with BTK. This subsequently activates PLC γ 2 which stimulates integrin activation as well as resulting in the activation of platelets.

Data from Chapter 3 and 4 confirm Rho GTPases to be critical components in regulating various platelet functions, including scavenging of bacteria and migration. We reveal in Chapter 5 the ability of CNF1 toxin produced by specific strains of *E. coli* to have the capacity to target Rho machinery in platelets resulting in alterations to platelet morphology and functions. This is in line with previously published data in epithelial and endothelial cells where CNF1 was demonstrated to induce various actin structure formations (Capo *et al.*, 1998; Gerhard *et al.*, 1998; Contamin *et al.*, 2000).

From the studies that reported morphological changes upon treating cells with CNF1, most found an increase in stress fibres (Lemichez *et al.*, 1997, Messina *et al.*, 2019). Which implies CNF1 targets RhoA specifically and if this translated in platelets we hypothesised RhoA via ROCK to mediate platelet shape change which ultimately results in stress fibre formation (Aburima *et al.*, 2013). However, in our study we found the number of cells containing stress fibres to be comparable between the control and treated group. In fact, we found CNF1 treatment to result in a significant increase in the number of platelets with actin nodules which in turn correlates with Rac1 activity (Poulter *et al.*, 2015).

In addition to this, we demonstrate the presence of a unique structure in treated group which we termed 'spiky cells'. Though the precise mechanisms involved in the formation of such structures are unknown, we postulate for Cdc42 to play a role since the morphology is to some extent similar to filopodia with the extended 'finger-like projections. Hence, it may be assumed that CNF1 targets Cdc42 activity in platelets and result to 'spiky cells' via the Cdc42-WASp-Arp2/3 axis (Aslan, 2013). A schematic model of CNF1 toxin uptake, processing and the affects it has on Rho proteins is illustrated in Figure 6.3.

The absence of increased stress fibre formation in our study was intriguing, especially since Boquet (2001) had previously mentioned for the concentration of CNF1 to determine the rate at which cytoskeletal effects would occur. He reported stress fibre formation in Hep-2 cells at 40 min when treated with Nm ranges of toxin. While we treated cells with 1 μ M for 4 hours prior to spreading platelets on matrices. This however, could be due to a number of factors although there is a strong possibility that the endocytic pathway in platelets may

be contribute to the results observed. It has been reported for CNF1 to be internalised into target cells via endocytosis (Knust and Schmidt, 2010). Endocytic pathways are present in platelets (Lowenstein, 2017). However, it is not known whether the efficiency of platelets to transport substance into its cytosol are comparable to that of nucleated cells. Hence could possibly be a reason for why we observed CNF1 effects in platelets i.e. Rho Shift only after 4 hours of incubating platelets with the toxin.

Despite all this, our data was found to be in line with findings by Lerm *et al.*, (1999) who demonstrated lamellipodia and filopodia formation to occur in HeLa cells upon CNF1 treatment. It was also found by Boquet (2001) that lymphocyte T immortalised cells to be resistant to the effects of CNF1. Therefore, it could be argued that the toxin affects each cell line differently.

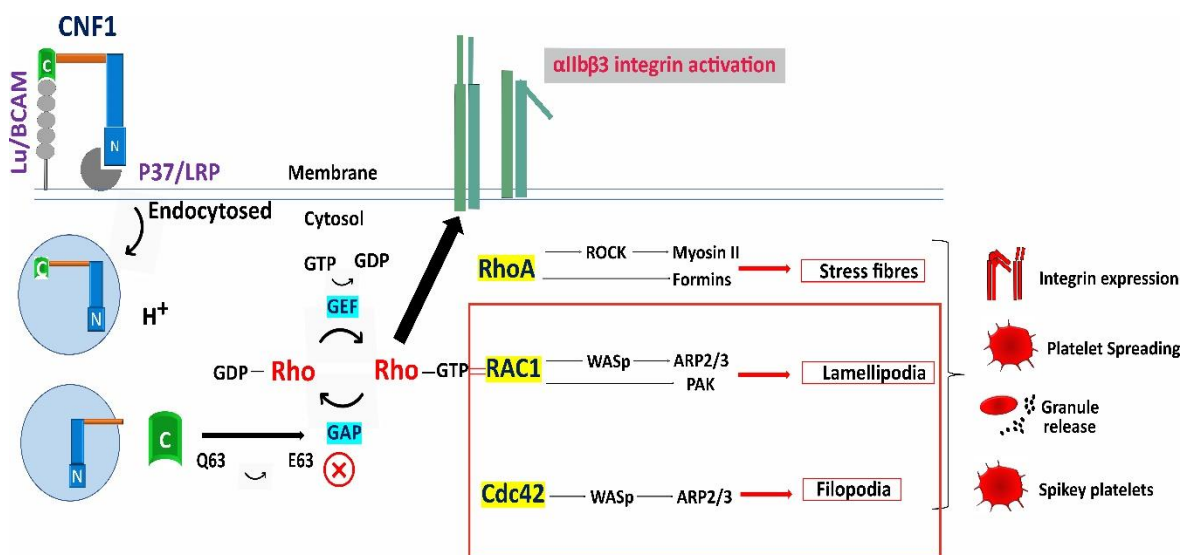


Figure 6.3 A schematic model of the effect of CNF1 on platelet signalling pathways. CNF1 binds to Lu/BCAM as well as P37/LRP which are expressed on platelets. The toxin is then postulated to be endocytosed where an increase in acidic pH cleavages and releases the catalytic domain of the toxin into the cytosol. This then results in the deamidation of key glutamine residue thus permanently locking them in the GTP-bound active state. All three major Rho GTPases (RhoA, Rac1 and Cdc42) have been proposed to be affected by the toxin in platelets. Thus, altering downstream effector proteins resulting alterations to platelet function and morphology.

In summary, the work presented in this thesis supports the notion of platelets as components of the circulating immune system. Our data confirms immunologic functions of platelets such as scavenging of bacteria and the ability to actively migrate, which occur largely through a common pathway and involve Rho GTPases and phosphorylation of tyrosine kinases. In addition to this, we have demonstrated integrin $\alpha\text{IIb}\beta\text{3}$ to be critically involved in facilitating platelet movement and collection of infectious and non-infectious matter thus for platelets to act as 'unprofessional' scavenger cells of the circulation. However, we also revealed certain bacteria to have the potential to exploit their virulence and produce toxins which are capable of attenuating platelet functions. We believe that enhancing our knowledge in the field of platelet-bacteria interactions in terms of subsequent infection-immunity balance in vivo, will reveal targets for novel therapeutic opportunities with the ultimate global aim of preventing progression of infection to sepsis.

6.2 Future work

In this thesis we have adapted an efficient method for exploring the molecular requirements for platelet migration and scavenging capacity. This in turn opens up a number of avenues for future investigations.

- To date, we have examined the role of actin, Rho GTPases, TK signalling pathways and the importance of FcγRIIIa as well as integrin αIIbβ3 in facilitating immunologic functions of platelets with regard to Newman. Numerous studies showed bacterial stimulation of platelets to be strain specific although information about the molecular mechanisms is generally ill-defined (Hamzeh-Cognasse *et al.*, 2015). Therefore, adapting the use of our migration/scavenging assay along with inhibitors targeting critical proteins, can be essentially applied to any bacterial species to study alternative signalling pathways underlying the activation of platelets. However, while deciphering the role of alternate pathways may be valuable, it may pose a problem since further optimisation maybe required i.e. to attain efficient bacterial coating on coverslips.
- The most common cause of platelet dysfunction is associated with drugs (Scharf, 2012). While the mode of action of many commonly prescribed drugs such as acetylsalicylic acid and abciximab and tirofiban are well-defined (Antoniucci, 2007), the potential effects of these drugs in impairing platelet scavenging properties and thereby increasing the risk of infections in patients is not elucidated. Likewise, a number of agents including lipid-lowering drugs (Sikora *et al.*, 2013), nonsteroidal anti-inflammatory drugs, and antibiotic (Shattil *et al.*, 1980) to name a few, has the potential to interfere with platelet reactivity and may potentially affect platelet scavenging secondarily and so the risk of infection in patients increases. This is particularly relevant in the clinical setting for patient with pre-existing conditions that compromise the host immune response such as cancer and tuberculosis. Therefore, one could test whether the drugs actually affect platelet scavenging and migration properties by utilising the adapted assay.

- It may also be of benefit to conduct time-lapse microscopy to obtain a better understanding of the process by which platelets capture and cluster *S. aureus* Newman through studying cellular dynamics. In addition to this, the analysis of platelets scavenging bacteria experiments was time-consuming and can be tedious when having to quantify a sizeable population. One could examine methods of automating parts of the steps perhaps by liaising with imaging experts or coding experts to develop a software program to allow high throughput of information.

In addition to supporting immunologic functions of platelet, we have demonstrated in this thesis for *E. coli* to exploit their virulence (produce toxins) which can then hinder platelet functions. This in turn opens up a range of research possibilities.

- Platelets encompass a diverse range of proteins and molecules which when released by activated platelets can aid the recruitment and activation of host immune cells. For example, β defensin 1 located in the extra-granular region of platelets has been reported to induce NET which then suppresses bacterial growth (Kraemer *et al.*, 2011). Therefore, one could examine the effects of CNF1 in modifying the ability of platelets 'non-professional immune cells' to recruit 'professional immune cells' such as monocytes, lymphocytes and neutrophils. This can be done by analysing factors such as NETs formation and interleukin secretion in CNF1-treated platelets.
- We found CNF1 treatment of platelets to hinder Rho GTPase activity, specifically Rac1 and Cdc42 pathways. PAK kinases are known to be effectors of Rac1 and Cdc42. It is also known for Rac1 binding to initiate autophosphorylation in PAK kinases leading to subsequent phosphorylation of downstream molecules such as LIM kinases (Aslan, Baker, *et al.*, 2013). Therefore, one could conduct experiments to determine the specificity of these pathways in CNF1 treated platelets by using inhibitors of PAK and probing for phosphorylated LIMK

Appendices

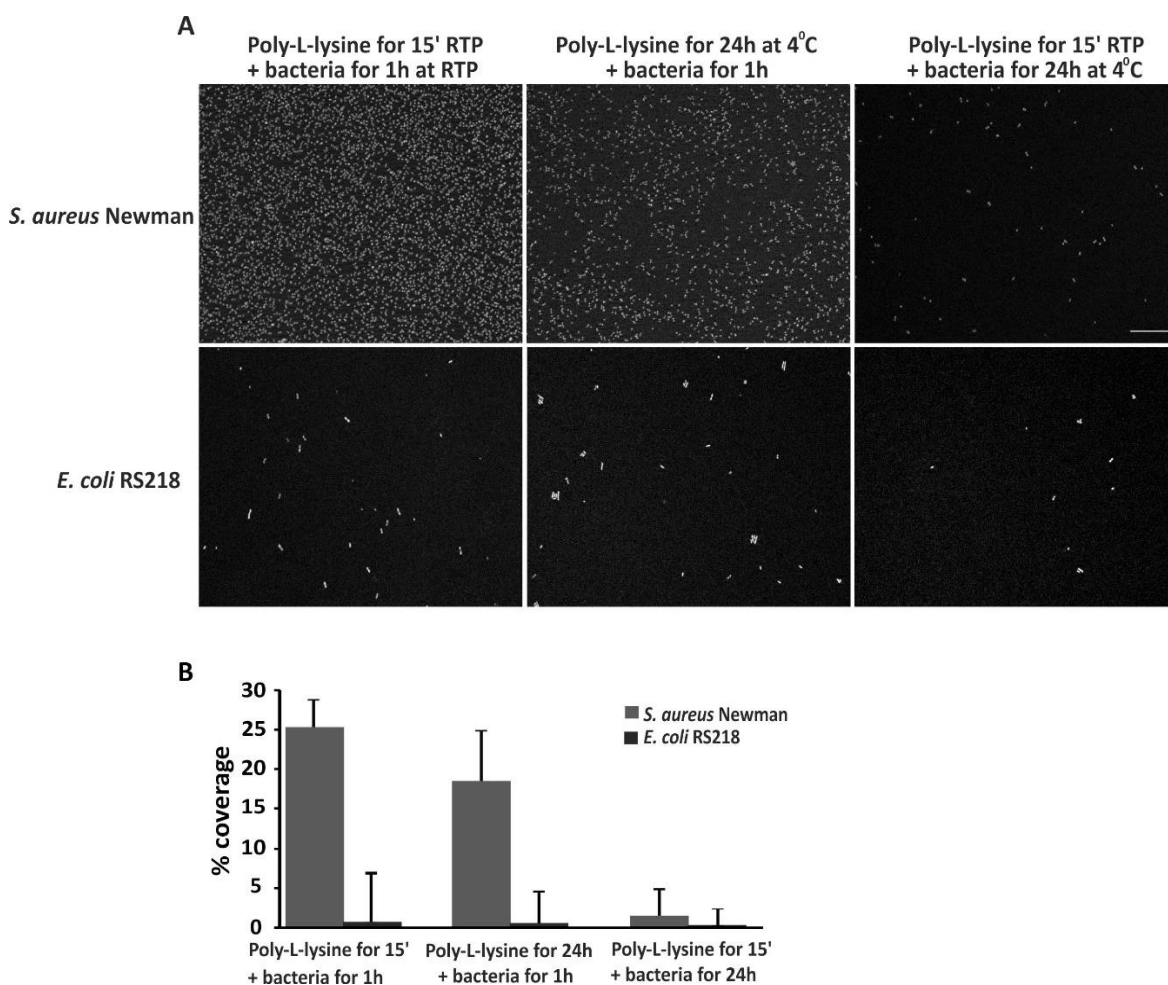


Figure 7.1 Immobilisation of *S. aureus* Newman and *E. coli* RS218 on glass coverslips. Glass coverslips were prepared by either treatment with poly-L-lysine for 15 min or overnight at 4°C. *S. aureus* Newman bacteria and *E. coli* RS218 bacteria were diluted to OD_(600nm) 1.0 in PBS from an overnight grown suspension culture. 200 µl of *S. aureus* bacterial suspension were then added to glass coverslips for either 1 h at room temperature or overnight at 4°C. The coverslips were washed with PBS and bacterial cells were fixed with 4% PFA for 10 min, permeabilised with 0.3% Triton X100 for 5 min and subsequently stained with 15 µg/ml Hoechst 33342 for 15 min at room temperature. Glass coverslips were then mounted onto glass slides with ProLong Antifade Mountant. Images were obtained with a Zeiss ApoTome.2 fluorescence microscope equipped with a 40x oil immersion objective. (A) Representative images from two independent experiments, scale bar represents 20 µm. (B) Percentage coverage of bacteria in each of the treatment conditions was calculated using ImageJ software. Data are presented as means ± SEM of two independent experiments.

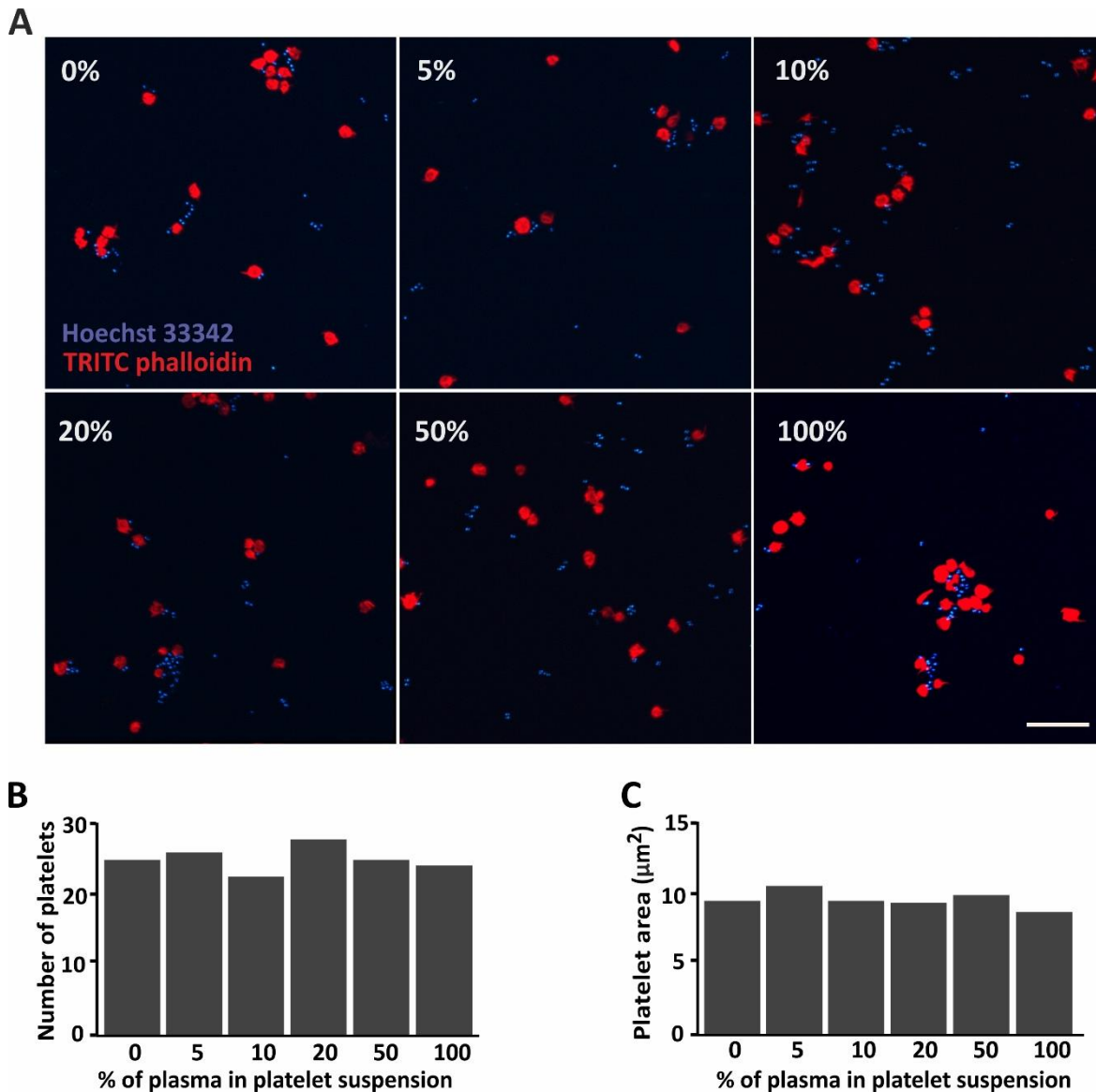


Figure 7.2 The extent to which plasma affects the attachment of bacteria and platelets to the coverslips in a scavenging assay. Human PRP was diluted to 1×10^7 /ml in varying proportions of plasma and MTB such that the final percentage of plasma was as indicated. 200 μ l of platelet suspension was then placed on coverslips containing immobilised *S. aureus* Newman and incubated at 37°C for 1 h. Unbound cells and medium from each coverslip was subsequently pipetted into separate labelled microcentrifuge tubes and spun briefly onto poly-L-lysine coated coverslips. Coverslips were then washed with PBS, fixed, permeabilised and incubated with a combination of 1 μ g/ml TRITC phalloidin (red) and 15 μ g/ml Hoechst 33342 (blue) for 30 min at room temperature. Coverslips were then mounted onto microscope slides and microscope images were obtained by using Zeiss ApoTome.2 fluorescence microscope equipped with a 40x oil immersion objective. (A) Data from one experiment. Scale bar represents 20 μ m. (B) Number of platelets per field and (C) the surface area of platelets was determined on ImageJ software.

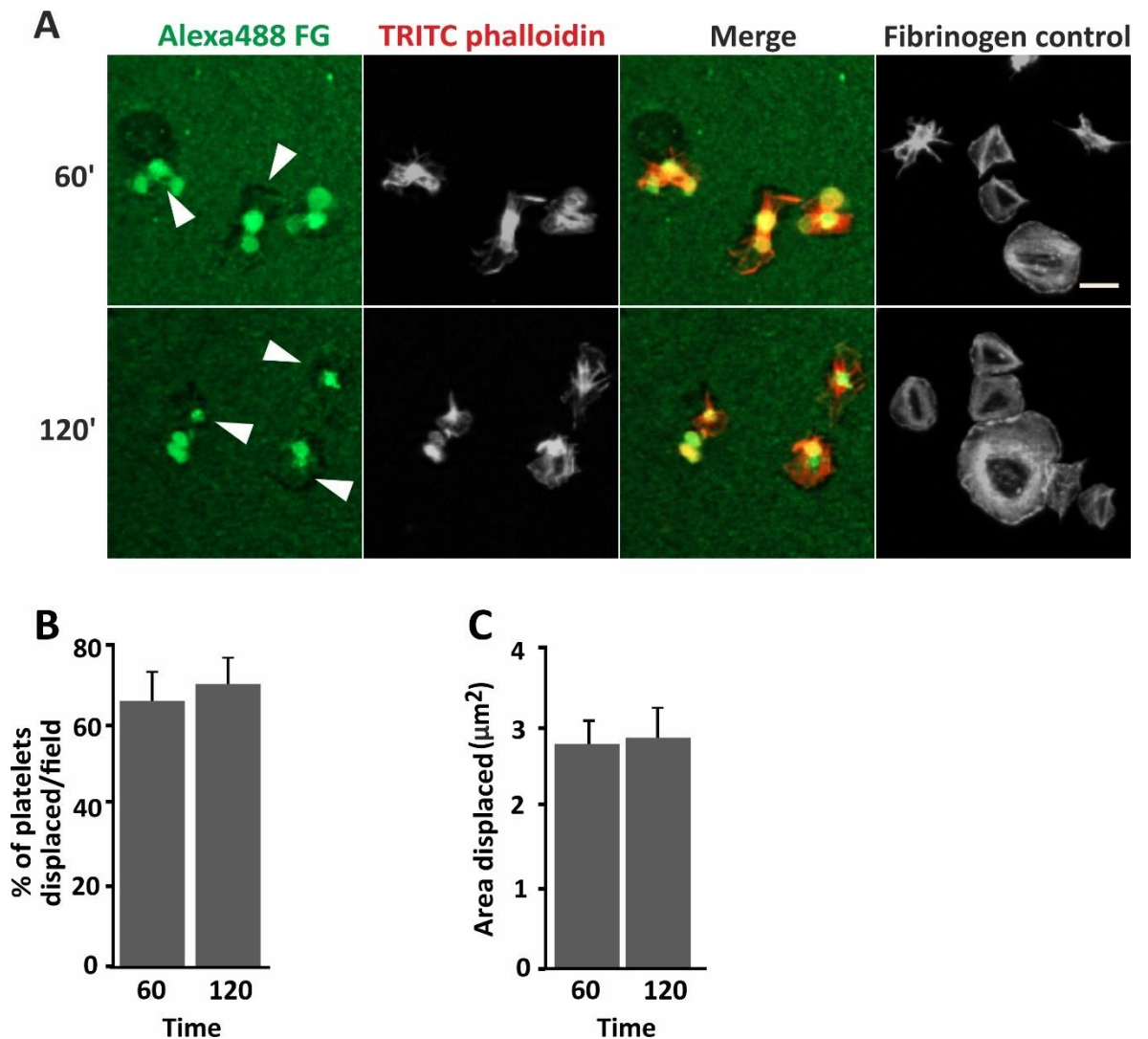


Figure 7.3 The effects of an extended platelet incubation time on the ability of platelets to migrate. Glass coverslips were acid washed with HCl for 1 h followed by dH₂O for 1 h and then silanated with HMDS for 1 min at room temperature. Coverslips were then coated with 40 $\mu\text{g}/\text{ml}$ Alexa488 fibrinogen (green) and 2 mg/ml BSA for 15 min. Platelets were diluted to $1 \times 10^7/\text{ml}$ by resuspending PRP in plasma and 200 μl was added to the coverslips and incubated at 37 °C for the indicated time. Platelets were also spread on unconjugated fibrinogen (40 $\mu\text{g}/\text{ml}$) coated coverslips in parallel. At the indicated timepoints, coverslips were washed with PBS and fixed with 4% PFA for 10 min, permeabilised with 0.3% Triton X100 for 5 min and stained with 1 $\mu\text{g}/\text{ml}$ TRITC phalloidin (grey; red on merge image) for 30 min at room temperature. Coverslips were mounted onto glass slides with ProLong Antifade Mountant and images were obtained with a Zeiss ApoTome.2 fluorescence microscope equipped with a 60x oil immersion objective. (A) Representative images. Scale bar represents 10 μm . Arrowheads indicate examples of platelet migration. (B) Percentage of migrating platelets per field was counted manually. (C) The average area of Alexa488 FG cleared by individual platelets was calculated on ImageJ software as outlined in section 2.4.7. Data are presented as means \pm SEM of three independent experiments. No statistical difference was found.

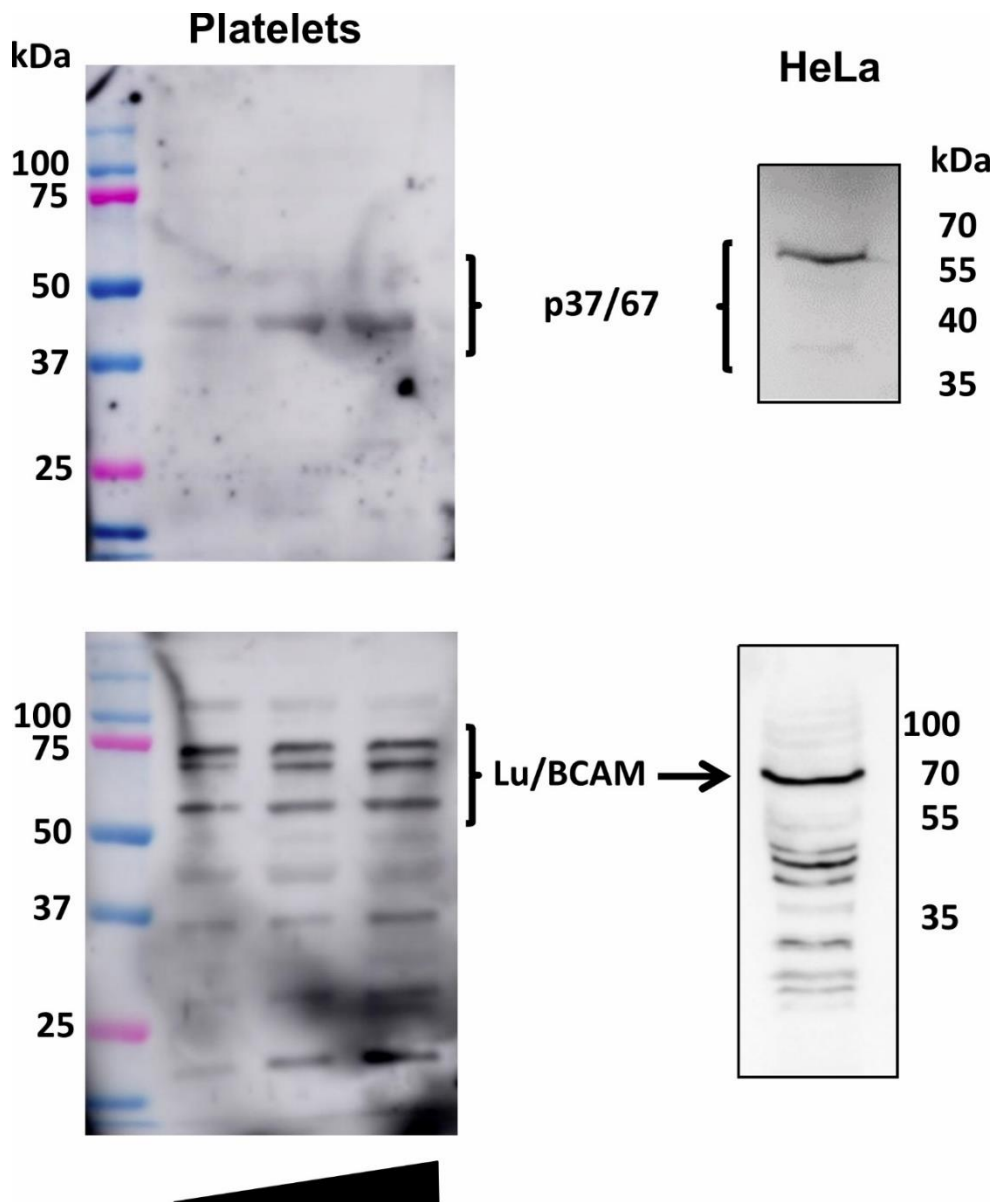


Figure 7.4 Platelets express p37/67 and Lu/BCAM laminin receptors required for CNF1 binding. Two CNF1-binding receptors, p36/64 and Lu/BCAM were identified via resolving platelet lysates (increasing amounts) by SDS-PAGE and detecting by western blotting with specific antibodies. HeLa cell lysates were used as a positive controls. Experiments were conducted by collaborators in the laboratory of Prof. G Schmidt (University of Freiburg, Germany).

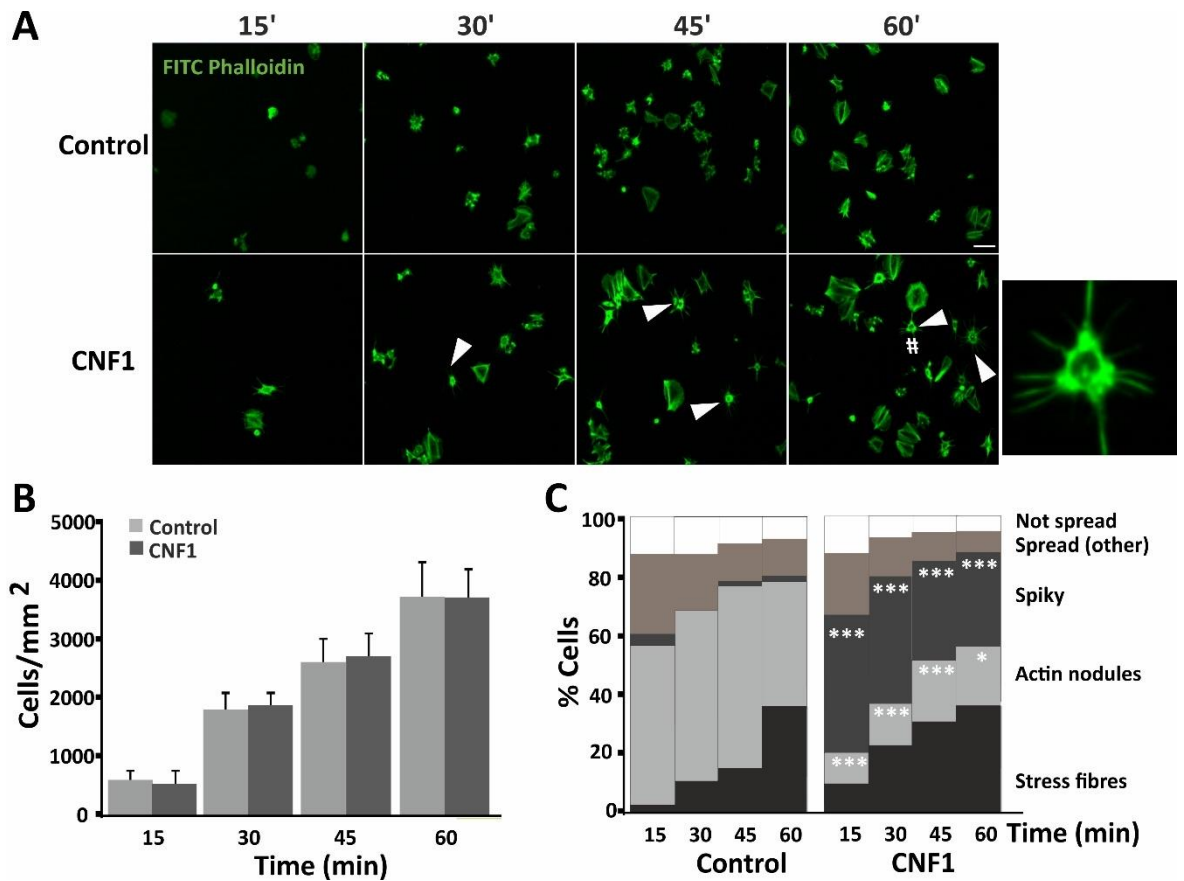


Figure 7.5 The effect of CNF1 on the ability of human washed platelets to spread on fibrinogen over time. Human washed platelets (1×10^9 /ml) were incubated at 37°C for 4 h in the presence and absence of $1 \mu\text{M}$ CNF1. Following this, the suspension was diluted to 1×10^7 /ml and $200 \mu\text{l}$ of platelet suspension was added to coverslips coated with fibrinogen or collagen ($100 \mu\text{g}/\text{ml}$). Coverslips were incubated 37°C and at indicated cells were fixed with 4% PFA for 10 min, permeabilised with 0.3% Triton X100 for 5 min and stained with $1 \mu\text{g}/\text{ml}$ FITC phalloidin (green) for 30 min at room temperature. Coverslips were mounted onto glass slides with ProLong Antifade Mountant and images were obtained with a Zeiss ApoTome.2 fluorescence microscope equipped with a 60x oil immersion objective. (A) Representative images from four independent experiments. Scale bar represents $10 \mu\text{m}$. Arrowheads indicate examples of spiky cells. Hash symbol represents an example of a spiky cell which has been zoomed and placed at the lower right-hand corner of panel A. (B) Adhesion of cells in each of the conditions and (C) percentage of spread cells were calculated by manually counting cells on ImageJ software. The proportion of cells containing (D) stress fibres, (E) actin nodules and (F) spiky cells was also calculated for each condition. Data are presented as means \pm SEM of four independent experiments. Statistical significance was calculated using a Kruskal-Wallis test ($*p < 0.05$ and $***p < 0.001$). White asterisks indicate significance relative to the corresponding control at given timepoints.

References

- Abdul Sater, H. (2017) 'Receptor Tyrosine Kinases in Human Platelets: A Review of Expression, Function and Inhibition in Relation to the Risk of Bleeding or Thrombocytopenia from Phase I through Phase III Trials', *Journal of Cancer Prevention & Current Research*. MedCrave Group, LLC, 8(6). doi: 10.15406/jcpcr.2017.08.00298.
- Ablooglu, A. J. *et al.* (2009) 'Antithrombotic effects of targeting $\alpha\text{IIb}\beta\text{3}$ signaling in platelets', *Blood*. *Blood*, 113(15), pp. 3585–3592. doi: 10.1182/blood-2008-09-180687.
- Aburima, A. *et al.* (2013) 'CAMP signaling regulates platelet myosin light chain (MLC) phosphorylation and shape change through targeting the RhoA-Rho kinase-MLC phosphatase signaling pathway', *Blood*. American Society of Hematology, 122(20), pp. 3533–3545. doi: 10.1182/blood-2013-03-487850.
- Ahrens, I., Bode, C. and Peter, K. (2005) 'Inhibition of platelet activation and aggregation', *Handbook of Experimental Pharmacology*, 170, pp. 443–462. doi: 10.1007/3-540-27661-0-16.
- Akbar, H. *et al.* (2007) 'Genetic and pharmacologic evidence that Rac1 GTPase is involved in regulation of platelet secretion and aggregation', *Journal of Thrombosis and Haemostasis*, 5(8), pp. 1747–1755. doi: 10.1111/j.1538-7836.2007.02646.x.
- Akbar, H. *et al.* (2010) 'Specific Pharmacologic Targeting of Rho GTPases Rac1, Cdc42 and RhoA Reveals Their Differential and Critical Roles In Regulation of Platelet Activation', *Blood*. American Society of Hematology, 116(21), pp. 2019–2019. doi: 10.1182/blood.v116.21.2019.2019.
- Akbar, H. *et al.* (2011) 'Gene Targeting Implicates Cdc42 GTPase in GPVI and Non-GPVI Mediated Platelet Filopodia Formation, Secretion and Aggregation', *PLoS ONE*. Edited by D. Gullberg. Public Library of Science, 6(7), p. e22117. doi: 10.1371/journal.pone.0022117.
- Akbar, H. *et al.* (2016) 'RhoA and Rac1 GTPases Differentially Regulate Agonist-Receptor Mediated Reactive Oxygen Species Generation in Platelets', *PLOS ONE*. Edited by Z. Li, 11(9), p. e0163227. doi: 10.1371/journal.pone.0163227.
- Albert, F. and Christopher N, F. (2012) 'The platelet fibrinogen receptor: from megakaryocyte to the mortuary', *JRSM Cardiovascular Disease*. SAGE Publications, 1(2), pp. 1–13. doi: 10.1258/cvd.2012.012007.
- Alberts, B. *et al.* (2002) 'How Cells Regulate Their Cytoskeletal Filaments'. Garland Science. Available at: <https://www.ncbi.nlm.nih.gov/books/NBK26809/> (Accessed: 28 September 2020).
- Ali, R. A., Wuescher, L. M. and Worth, R. G. (2015) 'Platelets: Essential components of the immune system', *Current Trends in Immunology*. Research Trends, pp. 65–78.

Allen, R. D. *et al.* (1979) 'Transformation and motility of human platelets. Details of the shape change and release reaction observed by optical and electron microscopy', *Journal of Cell Biology*. The Rockefeller University Press, 83(1), pp. 126–142. doi: 10.1083/jcb.83.1.126.

Alves, R. and Grimalt, R. (2018) 'A Review of Platelet-Rich Plasma: History, Biology, Mechanism of Action, and Classification', *Skin Appendage Disorders*, 4(1), pp. 18–24. doi: 10.1159/000477353.

Do Amaral, R. J. F. C. *et al.* (2016) 'Platelet-Rich Plasma Obtained with Different Anticoagulants and Their Effect on Platelet Numbers and Mesenchymal Stromal Cells Behavior In Vitro', *Stem Cells International*. Hindawi Limited, 2016. doi: 10.1155/2016/7414036.

An, Y. H. and Friedman, R. J. (1997) 'Laboratory methods for studies of bacterial adhesion', *Journal of Microbiological Methods*. Elsevier B.V., 30(2), pp. 141–152. doi: 10.1016/S0167-7012(97)00058-4.

An, Y. H. and Friedman, R. J. (1998) 'Concise review of mechanisms of bacterial adhesion to biomaterial surfaces', *Journal of Biomedical Materials Research*. John Wiley & Sons Inc, pp. 338–348. doi: 10.1002/(SICI)1097-4636(199823)43:3<338::AID-JBM16>3.0.CO;2-B.

Andre, P. *et al.* (2000) 'Platelets adhere to and translocate on von Willebrand factor presented by endothelium in stimulated veins', *Blood*, 96(10), pp. 3322–3328. doi: 10.1182/blood.v96.10.3322.h8003322_3322_3328.

Antczak, A. J. *et al.* (2011) 'Internalization of IgG-coated targets results in activation and secretion of soluble CD40 ligand and rantes by human platelets', *Clinical and Vaccine Immunology*. American Society for Microbiology (ASM), 18(2), pp. 210–216. doi: 10.1128/CVI.00296-10.

Antkowiak, A. *et al.* (2016) 'Cdc42-dependent F-actin dynamics drive structuration of the demarcation membrane system in megakaryocytes', *Journal of Thrombosis and Haemostasis*. Blackwell Publishing Ltd, 14(6), pp. 1268–1284. doi: 10.1111/jth.13318.

Antoniucci, D. (2007) 'Differences among GP IIb/IIIa inhibitors: Different clinical benefits in non-ST-segment elevation acute coronary syndrome percutaneous coronary intervention patients', *European Heart Journal, Supplement*. Oxford Academic, pp. A32–A36. doi: 10.1093/eurheartj/sul069.

Arciola, C. R. *et al.* (2004) 'Presence of fibrinogen-binding adhesin gene in *Staphylococcus epidermidis* isolates from central venous catheters-associated and orthopaedic implant-associated infections', *Biomaterials*, 25(19), pp. 4825–4829. doi: 10.1016/j.biomaterials.2003.11.056.

Arias-Salgado, E. G. *et al.* (2005) 'Specification of the direction of adhesive signaling by the integrin β cytoplasmic domain', *Journal of Biological Chemistry*. American Society for

Biochemistry and Molecular Biology, 280(33), pp. 29699–29707. doi: 10.1074/jbc.M503508200.

Arman, M. *et al.* (2014) 'Amplification of bacteria-induced platelet activation is triggered by FcγRIIA, integrin αIIbβ3, and platelet factor 4', *Blood*. American Society of Hematology, 123(20), pp. 3166–3174. doi: 10.1182/blood-2013-11-540526.

Arman, M. *et al.* (2015) 'Role of Platelets in Inflammation', in *The Non-Thrombotic Role of Platelets in Health and Disease*. InTech. doi: 10.5772/60536.

Arman, M. and Krauel, K. (2015) 'Human platelet IgG Fc receptor FcγRIIA in immunity and thrombosis', *Journal of Thrombosis and Haemostasis*, 13(6), pp. 893–908. doi: 10.1111/jth.12905.

Arthur, J. F. *et al.* (2008) 'Platelet receptor redox regulation', *Platelets*, pp. 1–8. doi: 10.1080/09537100701817224.

Aslan, J. E., Itakura, A., *et al.* (2013) 'p21 activated kinase signaling coordinates glycoprotein receptor VI-mediated platelet aggregation, lamellipodia formation, and aggregate stability under shear.', *Arteriosclerosis, thrombosis, and vascular biology*, 33(7), pp. 1544–51. doi: 10.1161/ATVBAHA.112.301165.

Aslan, J. E., Baker, S. M., *et al.* (2013) 'The PAK system links Rho GTPase signaling to thrombin-mediated platelet activation.', *American journal of physiology. Cell physiology*, 305(5), pp. C519–28. doi: 10.1152/ajpcell.00418.2012.

Aslan, J. E. (2019) 'Platelet Rho GTPase regulation in physiology and disease', *Platelets*. Taylor and Francis Ltd, pp. 17–22. doi: 10.1080/09537104.2018.1475632.

Aslan, J. E. and McCarty, O. J. T. (2013) 'Rac and Cdc42 team up for platelets', *Blood*. American Society of Hematology, 122(18), pp. 3096–3097. doi: 10.1182/blood-2013-08-516906.

ASLAN, J. E. and MCCARTY, O. J. T. (2013) 'Rho GTPases in platelet function', *Journal of Thrombosis and Haemostasis*. John Wiley & Sons, Ltd, 11(1), pp. 35–46. doi: 10.1111/jth.12051.

Assinger, A. *et al.* (2019) 'Platelets in sepsis: An update on experimental models and clinical data', *Frontiers in Immunology*. Frontiers Media S.A., 10(JULY), p. 1687. doi: 10.3389/fimmu.2019.01687.

Assoian, R. K. and Sporn, M. B. (1986) 'Type β transforming growth factor in human platelets: Release during platelet degranulation and action on vascular smooth muscle cells', *Journal of Cell Biology*, 102(4), pp. 1217–1223. doi: 10.1083/jcb.102.4.1217.

Van Avondt, K., van Sorge, N. M. and Meyaard, L. (2015) 'Bacterial Immune Evasion through Manipulation of Host Inhibitory Immune Signaling', *PLoS Pathogens*. Public Library of

Science, pp. 1–8. doi: 10.1371/journal.ppat.1004644.

Badimon, L. *et al.* (1988) 'Platelet thrombus formation on collagen type I. A model of deep vessel injury: Influence of blood rheology, von Willebrand factor, and blood coagulation', *Circulation*, 78(6), pp. 1431–1442. doi: 10.1161/01.CIR.78.6.1431.

Balk, S. D. *et al.* (1973) 'Roles of calcium, serum, plasma, and folic acid in the control of proliferation of normal and Rous sarcoma virus-infected chicken fibroblasts.', *Proceedings of the National Academy of Sciences of the United States of America*. National Academy of Sciences, 70(3), pp. 675–679. doi: 10.1073/pnas.70.3.675.

Bambach, S. K. and Lämmermann, T. (2017) 'Platelets, On Your Marks, Get Set, Migrate!', *Front. Plant Sci*, 27, pp. 1316–1325. doi: 10.1016/j.cell.2017.11.026.

Baranova, I. N. *et al.* (2008) 'Role of Human CD36 in Bacterial Recognition, Phagocytosis, and Pathogen-Induced JNK-Mediated Signaling', *The Journal of Immunology*. The American Association of Immunologists, 181(10), pp. 7147–7156. doi: 10.4049/jimmunol.181.10.7147.

Barkalow, K. *et al.* (1996) 'Coordinated regulation of platelet actin filament barbed ends by gelsolin and capping protein', *Journal of Cell Biology*. The Rockefeller University Press, 134(2), pp. 389–399. doi: 10.1083/jcb.134.2.389.

Bautista, M., Fernandez, A. and Pinaud, F. (2019) 'A Micropatterning Strategy to Study Nuclear Mechanotransduction in Cells.', *Micromachines*, 10(12), p. 810. doi: 10.3390/mi10120810.

Bearer, E. L. (1995) 'Cytoskeletal domains in the activated platelet', *Cell Motility and the Cytoskeleton*, 30(1), pp. 50–66. doi: 10.1002/cm.970300107.

Bearer, E. L., Prakash, J. M. and Li, Z. (2002) 'Actin dynamics in platelets', *International Review of Cytology*. Academic Press Inc., pp. 137–182. doi: 10.1016/S0074-7696(02)17014-8.

Behnke, O. (1968) 'Electron microscopical observations on the surface coating of human blood platelets', *Journal of Ultrastructure Research*. Academic Press, 24(1–2), pp. 51–69. doi: 10.1016/S0022-5320(68)80016-4.

Behnke, O. (1970) 'The morphology of blood platelet membrane systems.', *Series haematologica (1968)*, 3(4), pp. 3–16.

Behnke, O. (1992) 'Degrading and non-degrading pathways in fluid-phase (non-adsorptive) endocytosis in human blood platelets.', *Journal of submicroscopic cytology and pathology*, 24(2), pp. 169–178.

Bender, M. *et al.* (2010) 'ADF/n-cofilin-dependent actin turnover determines platelet formation and sizing', *Blood*. American Society of Hematology, 116(10), pp. 1767–1775.

doi: 10.1182/blood-2010-03-274340.

Bennett, J. S. *et al.* (1999) 'The platelet cytoskeleton regulates the affinity of the integrin α (IIb) β 3 for fibrinogen', *Journal of Biological Chemistry*. American Society for Biochemistry and Molecular Biology, 274(36), pp. 25301–25307. doi: 10.1074/jbc.274.36.25301.

Bennett, J. S., Berger, B. W. and Billings, P. C. (2009) 'The structure and function of platelet integrins', *Journal of Thrombosis and Haemostasis*, pp. 200–205. doi: 10.1111/j.1538-7836.2009.03378.x.

Bennett, J. S. and Vilaire, G. (1979) 'Exposure of platelet fibrinogen receptors by ADP and epinephrine.', *The Journal of clinical investigation*, 64(5), pp. 1393–1401. doi: 10.1172/JCI109597.

Berndt, M. C. and Andrews, R. K. (2011) 'Bernard-Soulier syndrome', *Haematologica*. Ferrata Storti Foundation, pp. 355–359. doi: 10.3324/haematol.2010.039883.

Bettex-Galland, M. and Lüscher, E. F. (1959) 'Extraction of an actomyosin-like protein from human thrombocytes', *Nature*. Nature Publishing Group, 184(4682), pp. 276–277. doi: 10.1038/184276b0.

Beynon, R. P., Bahl, V. K. and Prendergast, B. D. (2006) 'Infective endocarditis', *British Medical Journal*. British Medical Journal Publishing Group, pp. 334–339. doi: 10.1136/bmj.333.7563.334.

Billips, B. K., Schaeffer, A. J. and Klumpp, D. J. (2008) 'Molecular basis of uropathogenic Escherichia coli evasion of the innate immune response in the bladder', *Infection and Immunity*. American Society for Microbiology (ASM), 76(9), pp. 3891–3900. doi: 10.1128/IAI.00069-08.

Bishop, A. L. and Hall, A. (2000) 'Rho GTPases and their effector proteins', *Biochemical Journal*, pp. 241–255. doi: 10.1042/0264-6021:3480241.

Blair, P. and Flaumenhaft, R. (2009) 'Platelet α -granules: basic biology and clinical correlates.', *Blood reviews*. NIH Public Access, 23(4), pp. 177–89. doi: 10.1016/j.blre.2009.04.001.

Bohoněk, M. (2018) 'Cryopreservation of Platelets: Advances and Current Practice', in *Cryopreservation Biotechnology in Biomedical and Biological Sciences*. IntechOpen. doi: 10.5772/intechopen.81906.

Boquet, P. (2001) 'The cytotoxic necrotizing factor 1 (CNF1) from Escherichia coli', *Toxicon*. Elsevier Ltd, 39(11), pp. 1673–1680. doi: 10.1016/S0041-0101(01)00154-4.

Boquet, P. and Lemichez, E. (2003) 'Bacterial virulence factors targeting Rho GTPases: Parasitism or symbiosis?', *Trends in Cell Biology*. Elsevier Ltd, pp. 238–246. doi: 10.1016/S0962-8924(03)00037-0.

Bordon, Y. (2018) 'Innate immunity: Platelets on the prowl', *Nature Reviews Immunology*. Nature Publishing Group, p. 3. doi: 10.1038/nri.2017.147.

BORN, G. V. R. (1962) 'Aggregation of Blood Platelets by Adenosine Diphosphate and its Reversal', *Nature*. Nature Publishing Group, 194(4832), pp. 927–929. doi: 10.1038/194927b0.

Bradshaw, J. M. (2010) 'The Src, Syk, and Tec family kinases: Distinct types of molecular switches', *Cellular Signalling*. Cell Signal, pp. 1175–1184. doi: 10.1016/j.cellsig.2010.03.001.

Brass, L. F. *et al.* (1997) 'Signaling through G proteins in platelets: To the integrins and beyond', in *Thrombosis and Haemostasis*, pp. 581–589. doi: 10.1055/s-0038-1657593.

BRENNAN, M. P. *et al.* (2009) 'Elucidating the role of *Staphylococcus epidermidis* serine-aspartate repeat protein G in platelet activation', *Journal of Thrombosis and Haemostasis*. John Wiley & Sons, Ltd, 7(8), pp. 1364–1372. doi: 10.1111/j.1538-7836.2009.03495.x.

Brest, P. *et al.* (2003) 'Rho GTPase is activated by cytotoxic necrotizing factor 1 in peripheral blood T lymphocytes: Potential cytotoxicity for intestinal epithelial cells', *Infection and Immunity*. American Society for Microbiology (ASM), 71(3), pp. 1161–1169. doi: 10.1128/IAI.71.3.1161-1169.2003.

Brown, G. T. and McIntyre, T. M. (2011) 'Lipopolysaccharide Signaling without a Nucleus: Kinase Cascades Stimulate Platelet Shedding of Proinflammatory IL-1 β -Rich Microparticles', *The Journal of Immunology*. The American Association of Immunologists, 186(9), pp. 5489–5496. doi: 10.4049/jimmunol.1001623.

Bruce Alberts *et al.* (2002) *Molecular Biology of the Cell - NCBI Bookshelf*. Garland Science. Available at: <https://www.ncbi.nlm.nih.gov/books/NBK21054/> (Accessed: 22 February 2020).

Burkhart, J. M. *et al.* (2012) 'The first comprehensive and quantitative analysis of human platelet protein composition allows the comparative analysis of structural and functional pathways', *Blood*, 120(15), pp. e73-82. doi: 10.1182/blood-2012-04-416594.

Burridge, K. and Wennerberg, K. (2004) 'Rho and Rac Take Center Stage', *Cell*. Cell Press, pp. 167–179. doi: 10.1016/S0092-8674(04)00003-0.

Bussolino, F. *et al.* (1989) 'Platelet-activating factor enhances complement-dependent phagocytosis of diamide-treated erythrocytes by human monocytes through activation of protein kinase C and phosphorylation of complement receptor type one (CR1).', *The Journal of biological chemistry*, 264(36), pp. 21711–9.

Bustelo, X. R., Sauzeau, V. and Berenjano, I. M. (2007) 'GTP-binding proteins of the Rho/Rac family: Regulation, effectors and functions in vivo', *BioEssays*, pp. 356–370. doi: 10.1002/bies.20558.

Byrne, M. F. *et al.* (2003) 'Helicobacter pylori binds von Willebrand factor and interacts with GPIb to induce platelet aggregation', *Gastroenterology*. W.B. Saunders, 124(7), pp. 1846–1854. doi: 10.1016/S0016-5085(03)00397-4.

Calaminus, S. D. J. *et al.* (2007) 'MyosinIIa contractility is required for maintenance of platelet structure during spreading on collagen and contributes to thrombus stability', *Journal of Thrombosis and Haemostasis*, 5(10), pp. 2136–2145. doi: 10.1111/j.1538-7836.2007.02696.x.

Calaminus, S. D. J. *et al.* (2008) 'Identification of a novel, actin-rich structure, the actin nodule, in the early stages of platelet spreading', *Journal of Thrombosis and Haemostasis*, 6(11), pp. 1944–1952. doi: 10.1111/j.1538-7836.2008.03141.x.

Callan, M. B., Shofer, F. S. and Catalfamo, J. L. (2009) 'Effects of anticoagulant on pH, ionized calcium concentration, and agonist-induced platelet aggregation in canine platelet-rich plasma', *American Journal of Veterinary Research*. NIH Public Access, 70(4), pp. 472–477. doi: 10.2460/ajvr.70.4.472.

Calvete, J. J. (1999) 'Platelet integrin GPIIb/IIIa: Structure-function correlations. An update and lessons from other integrins', *Proceedings of the Society for Experimental Biology and Medicine*, pp. 29–38. doi: 10.1111/j.1525-1373.1999.09993.x.

Capo, C. *et al.* (1998) 'Effect of cytotoxic necrotizing factor-1 on actin cytoskeleton in human monocytes: role in the regulation of integrin-dependent phagocytosis.', *Journal of immunology (Baltimore, Md. : 1950)*, 161(8), pp. 4301–8.

Caprioli, A. *et al.* (1983) *Partial Purification and Characterization of an Escherichia coli Toxic Factor That Induces Morphological Cell Alterations* Downloaded from, *INFECTION AND IMMUNITY*.

Carrier, M. F., Ducruix, A. and Pantaloni, D. (1999) 'Signalling to actin: The Cdc42-N-WASP-Arp2/3 connection', *Chemistry and Biology*. Elsevier Ltd, pp. R235–R240. doi: 10.1016/S1074-5521(99)80107-0.

Caron, F. *et al.* (2017) 'Current understanding of bleeding with ibrutinib use: A systematic review and meta-analysis', *Blood Advances*. American Society of Hematology, 1(12), pp. 772–778. doi: 10.1182/bloodadvances.2016001883.

Cattaneo, M. (2009) 'Light Transmission Aggregometry and ATP Release for the Diagnostic Assessment of Platelet Function', *Seminars in Thrombosis and Hemostasis*, 35(02), pp. 158–167. doi: 10.1055/s-0029-1220324.

Cazenave, J. P. *et al.* (2004) 'Preparation of washed platelet suspensions from human and rodent blood.', *Methods in molecular biology (Clifton, N.J.)*, 272, pp. 13–28. doi: 10.1385/1-59259-782-3:013.

Cerecedo, D. (2013) 'Platelet cytoskeleton and its hemostatic role', *Blood Coagulation &*

Fibrinolysis, 24(8), pp. 798–808. doi: 10.1097/MBC.0b013e328364c379.

Chaimoff, C., Creter, D. and Djaldetti, M. (1978) 'The effect of pH on platelet and coagulation factor activities', *The American Journal of Surgery*, 136(2), pp. 257–259. doi: 10.1016/0002-9610(78)90241-6.

Chang, Y. C. *et al.* (2013) 'Rapid single cell detection of *Staphylococcus aureus* by aptamer-conjugated gold nanoparticles', *Scientific Reports*. Nature Publishing Group, 3. doi: 10.1038/srep01863.

Charest, P. G. and Firtel, R. A. (2007) 'Big roles for small GTPases in the control of directed cell movement', *Biochemical Journal*. Portland Press Ltd, pp. 377–390. doi: 10.1042/BJ20061432.

Chen, H. *et al.* (2007) 'Characterization of a novel bifunctional mutant of staphylokinase with platelet-targeted thrombolysis and antiplatelet aggregation activities', *BMC Molecular Biology*. BioMed Central, 8, p. 88. doi: 10.1186/1471-2199-8-88.

Chen, J. *et al.* (2018) 'The effect of Bruton's tyrosine kinase (BTK) inhibitors on collagen-induced platelet aggregation, BTK, and tyrosine kinase expressed in hepatocellular carcinoma (TEC)', *European Journal of Haematology*. Blackwell Publishing Ltd, 101(5), pp. 604–612. doi: 10.1111/ejh.13148.

Chen, Y. *et al.* (2009) 'Cullin Mediates Degradation of RhoA through Evolutionarily Conserved BTB Adaptors to Control Actin Cytoskeleton Structure and Cell Movement', *Molecular Cell*. Mol Cell, 35(6), pp. 841–855. doi: 10.1016/j.molcel.2009.09.004.

Cho, M. J. *et al.* (2002) 'Role of the Src family kinase Lyn in TxA₂ production, adenosine diphosphate secretion, Akt phosphorylation, and irreversible aggregation in platelets stimulated with gamma-thrombin.', *Blood*, 99(7), pp. 2442–7. doi: 10.1182/blood.v99.7.2442.

Chung, J. W. *et al.* (2003) '37-kDa laminin receptor precursor modulates cytotoxic necrotizing factor 1-mediated RhoA activation and bacterial uptake', *Journal of Biological Chemistry*. American Society for Biochemistry and Molecular Biology, 278(19), pp. 16857–16862. doi: 10.1074/jbc.M301028200.

Clark, A. (1942) 'SOME EFFECTS OF REMOVING THE NUCLEUS FROM AMOEBA', *Australian Journal of Experimental Biology and Medical Science*. Wiley-Blackwell, 20(4), pp. 241–247. doi: 10.1038/icb.1942.40.

Clawson, C. C., Rao, G. H. R. and White, J. G. (1975) 'Platelet interaction with bacteria. IV. Stimulation of the release reaction', *American Journal of Pathology*, 81(2), pp. 411–419.

Clawson, C. C. and White, J. G. (1971) 'Platelet interaction with bacteria. I. Reaction phases and effects of inhibitors.', *The American journal of pathology*, 65(2), pp. 367–80.

Clawson, C. C. and White, J. G. (1980) 'Platelet interaction with bacteria. V. Ultrastructure of congenital afibrinogenemic platelets.', *The American journal of pathology*, 98(1), pp. 197–211.

Clemetson, K. J. *et al.* (2000) 'Functional expression of CCR1, CCR3, CCR4, and CXCR4 chemokine receptors on human platelets', *Blood*. American Society of Hematology, 96(13), pp. 4046–4054. doi: 10.1182/blood.v96.13.4046.

Coburn, J., Leong, J. M. and Erban, J. K. (1993) 'Integrin $\alpha\text{IIb}\beta\text{3}$ mediates binding of the Lyme disease agent *Borrelia burgdorferi* to human platelets', *Proceedings of the National Academy of Sciences of the United States of America*. National Academy of Sciences, 90(15), pp. 7059–7063. doi: 10.1073/pnas.90.15.7059.

Cognasse, F. *et al.* (2007) 'Human platelets can activate peripheral blood B cells and increase production of immunoglobulins', *Experimental Hematology*. Elsevier Inc., 35(9), pp. 1376–1387. doi: 10.1016/j.exphem.2007.05.021.

Colville, K. *et al.* (2010) 'Effects of poly(L-lysine) substrates on attached *Escherichia coli* bacteria', *Langmuir*, 26(4), pp. 2639–2644. doi: 10.1021/la902826n.

Contamin, S. *et al.* (2000) 'The p21 Rho-activating toxin cytotoxic necrotizing factor 1 is endocytosed by a clathrin-independent mechanism and enters the cytosol by an acidic-dependent membrane translocation step', *Molecular Biology of the Cell*. American Society for Cell Biology, 11(5), pp. 1775–1787. doi: 10.1091/mbc.11.5.1775.

Cooling, L. L. W. *et al.* (1998) 'Shiga toxin binds human platelets via globotriaosylceramide (P(K) antigen) and a novel platelet glycosphingolipid', *Infection and Immunity*. American Society for Microbiology Journals, 66(9), pp. 4355–4366.

Coué, M. *et al.* (1987) 'Inhibition of actin polymerization by latrunculin A', *FEBS Letters*, 213(2), pp. 316–318. doi: 10.1016/0014-5793(87)81513-2.

Croxen, M. A. and Finlay, B. B. (2010) 'Molecular mechanisms of *Escherichia coli* pathogenicity', *Nature Reviews Microbiology*. Nature Publishing Group, pp. 26–38. doi: 10.1038/nrmicro2265.

Czapiga, M. *et al.* (2005) 'Human platelets exhibit chemotaxis using functional N-formyl peptide receptors', *Experimental Hematology*. Elsevier, 33(1), pp. 73–84. doi: 10.1016/j.exphem.2004.09.010.

D'Atri, L. P. and Schattner, M. (2017) 'Platelet toll-like receptors in thromboinflammation', *Frontiers in Bioscience - Landmark*. Frontiers in Bioscience, pp. 1867–1883. doi: 10.2741/4576.

Das, M. *et al.* (2014) 'Mechanisms of talin-dependent integrin signaling and crosstalk', *Biochimica et Biophysica Acta - Biomembranes*. Elsevier B.V., pp. 579–588. doi: 10.1016/j.bbamem.2013.07.017.

- Davidson, M. M. L. and Haslam, R. J. (1994) 'Dephosphorylation of cofilin in stimulated platelets: Roles for a GTP-binding protein and Ca²⁺', *Biochemical Journal*. Portland Press Ltd, 301(1), pp. 41–47. doi: 10.1042/bj3010041.
- Demir, M. and Kaleli, I. (2004) 'Production by Escherichia coli isolates of siderophore and other virulence factors and their pathogenic role in a cutaneous infection model', *Clinical Microbiology and Infection*. Blackwell Publishing Ltd, 10(11), pp. 1011–1014. doi: 10.1111/j.1469-0691.2004.01001.x.
- Deppermann, C. and Kubes, P. (2016) 'Platelets and infection', *Seminars in Immunology*. Academic Press, pp. 536–545. doi: 10.1016/j.smim.2016.10.005.
- Deppermann, C. and Kubes, P. (2018) 'Start a fire, kill the bug: The role of platelets in inflammation and infection', *Innate Immunity*, 24(6), pp. 335–348. doi: 10.1177/1753425918789255.
- DerMardirossian, C. and Bokoch, G. M. (2005) 'GDIs: Central regulatory molecules in Rho GTPase activation', *Trends in Cell Biology*. Elsevier, 15(7), pp. 356–363. doi: 10.1016/j.tcb.2005.05.001.
- Deuel, T. F. *et al.* (1981) 'Platelet factor 4 is chemotactic for neutrophils and monocytes', *Proceedings of the National Academy of Sciences of the United States of America*. National Academy of Sciences, 78(7 I), pp. 4584–4587. doi: 10.1073/pnas.78.7.4584.
- Djaldetti, M. *et al.* (1979) 'pH-Induced Platelet Ultrastructural Alterations: A Possible Mechanism for Impaired Platelet Aggregation', *Archives of Surgery*, 114(6), pp. 707–710. doi: 10.1001/archsurg.1979.01370300061009.
- Dmitrieff, S. and Nédélec, F. (2016) 'Amplification of actin polymerization forces', *Journal of Cell Biology*. Rockefeller University Press, pp. 763–766. doi: 10.1083/jcb.201512019.
- Dorsam, R. T., Tuluc, M. and Kunapuli, S. P. (2004) 'Role of protease-activated and ADP receptor subtypes in thrombin generation on human platelets', *Journal of Thrombosis and Haemostasis*. John Wiley & Sons, Ltd, 2(5), pp. 804–812. doi: 10.1111/j.1538-7836.2004.00692.x.
- Doye, A. *et al.* (2002) 'CNF1 exploits the ubiquitin-proteasome machinery to restrict Rho GTPase activation for bacterial host cell invasion', *Cell*. Cell Press, 111(4), pp. 553–564. doi: 10.1016/S0092-8674(02)01132-7.
- Durrant, T. N., Van Den Bosch, M. T. and Hers, I. (2017) 'Integrin α IIb β 3 outside-in signaling', *Blood*. American Society of Hematology, pp. 1607–1619. doi: 10.1182/blood-2017-03-773614.
- Dutta, D. and Willcox, M. D. P. (2013) 'A laboratory assessment of factors that affect bacterial adhesion to contact lenses', *Biology*. MDPI AG, 2(4), pp. 1268–1281. doi: 10.3390/biology2041268.

Dütting, S. *et al.* (2015) 'Critical off-target effects of the widely used Rac1 inhibitors NSC23766 and EHT1864 in mouse platelets', *Journal of Thrombosis and Haemostasis*. Blackwell Publishing Ltd, 13(5), pp. 827–838. doi: 10.1111/jth.12861.

Dütting, S. *et al.* (2017) 'A Cdc42/RhoA regulatory circuit downstream of glycoprotein Ib guides transendothelial platelet biogenesis', *Nature Communications*. Nature Publishing Group, 8(1), pp. 1–13. doi: 10.1038/ncomms15838.

Dwivedi, S. *et al.* (2010) 'Rac1-mediated signaling plays a central role in secretion-dependent platelet aggregation in human blood stimulated by atherosclerotic plaque', *Journal of Translational Medicine*. BioMed Central, 8(1), p. 128. doi: 10.1186/1479-5876-8-128.

Edward Quach, M., Chen, W. and Li, R. (2018) 'Mechanisms of platelet clearance and translation to improve platelet storage', *Blood*. American Society of Hematology, pp. 1512–1521. doi: 10.1182/blood-2017-08-743229.

Eisinger, F., Patzelt, J. and Langer, H. F. (2018) 'The platelet response to tissue injury', *Frontiers in Medicine*. Frontiers Media S.A. doi: 10.3389/fmed.2018.00317.

Eivers, M. *et al.* (2012) 'The GRAF family member oligophrenin1 is a RhoGAP with BAR domain and regulates Rho GTPases in platelets.', *Cardiovascular research*, 94(3), pp. 526–36. doi: 10.1093/cvr/cvs079.

Escolar, G., Leistikow, E. and White, J. G. (1989) 'The fate of the open canalicular system in surface and suspension-activated platelets.', *Blood*, 74(6), pp. 1983–8.

Euteneuer, U. and Schliwa, M. (1984) 'Persistent, directional motility of cells and cytoplasmic fragments in the absence of microtubules', *Nature*. Nature Publishing Group, 310(5972), pp. 58–61. doi: 10.1038/310058a0.

Eyler, C. E. and Telen, M. J. (2006) 'The Lutheran glycoprotein: A multifunctional adhesion receptor', *Transfusion*, pp. 668–677. doi: 10.1111/j.1537-2995.2006.00779.x.

Fabbri, A., Travaglione, S. and Fiorentini, C. (2010) 'Escherichia coli Cytotoxic Necrotizing Factor 1 (CNF1): Toxin Biology, in Vivo Applications and Therapeutic Potential', *Toxins*. Multidisciplinary Digital Publishing Institute (MDPI), 2(2), p. 283. doi: 10.3390/TOXINS2020283.

Falet, H. *et al.* (2002) 'Normal Arp2/3 complex activation in platelets lacking WASp', *Blood*, 100(6), pp. 2113–2122. doi: 10.1182/blood.v100.6.2113.h81802002113_2113_2122.

Falzano, L. *et al.* (1993) 'Induction of phagocytic behaviour in human epithelial cells by Escherichia coli cytotoxic necrotizing factor type 1', *Molecular Microbiology*. Mol Microbiol, 9(6), pp. 1247–1254. doi: 10.1111/j.1365-2958.1993.tb01254.x.

Falzano, L. *et al.* (2006) 'Escherichia coli cytotoxic necrotizing factor 1 blocks cell cycle G

2/M transition in uroepithelial cells', *Infection and Immunity*. American Society for Microbiology (ASM), 74(7), pp. 3765–3772. doi: 10.1128/IAI.01413-05.

Farrell, D. H. *et al.* (1992) 'Role of fibrinogen α and γ chain sites in platelet aggregation', *Proceedings of the National Academy of Sciences of the United States of America*. National Academy of Sciences, 89(22), pp. 10729–10732. doi: 10.1073/pnas.89.22.10729.

Fillon, S. *et al.* (2006) 'Platelet-Activating Factor Receptor and Innate Immunity: Uptake of Gram-Positive Bacterial Cell Wall into Host Cells and Cell-Specific Pathophysiology', *The Journal of Immunology*. The American Association of Immunologists, 177(9), pp. 6182–6191. doi: 10.4049/jimmunol.177.9.6182.

Finkenstaedt-Quinn, S. A., Ge, S. and Haynes, C. L. (2015) 'Cytoskeleton dynamics in drug-treated platelets', *Analytical and Bioanalytical Chemistry*. Springer Verlag, 407(10), pp. 2803–2809. doi: 10.1007/s00216-015-8523-7.

Fiorentini, C. *et al.* (1995) 'Escherichia coli cytotoxic necrotizing factor 1: Evidence for induction of actin assembly by constitutive activation of the p21 Rho GTPase', *Infection and Immunity*. American Society for Microbiology, 63(10), pp. 3936–3944. doi: 10.1128/iai.63.10.3936-3944.1995.

Fiorentini, C. *et al.* (1997) 'Hinderance of apoptosis and phagocytic behaviour induced by Escherichia coli Cytotoxic Necrotizing Factor 1. Two related activities in epithelial cells', *Biochemical and Biophysical Research Communications*. Academic Press Inc., 241(2), pp. 341–346. doi: 10.1006/bbrc.1997.7723.

Fitch-Tewfik, J. L. and Flaumenhaft, R. (2013a) 'Platelet granule exocytosis: A comparison with chromaffin cells', *Frontiers in Endocrinology*. Frontiers, p. 77. doi: 10.3389/fendo.2013.00077.

Fitch-Tewfik, J. L. and Flaumenhaft, R. (2013b) 'Platelet Granule Exocytosis: A Comparison with Chromaffin Cells', *Frontiers in Endocrinology*. Frontiers, 4, p. 77. doi: 10.3389/fendo.2013.00077.

FitzGerald, G. A. (1991) 'Mechanisms of platelet activation: Thromboxane A₂ as an amplifying signal for other agonists', *The American Journal of Cardiology*, 68(7). doi: 10.1016/0002-9149(91)90379-Y.

Fitzgerald, J. R. *et al.* (2006) 'Fibronectin-binding proteins of Staphylococcus aureus mediate activation of human platelets via fibrinogen and fibronectin bridges to integrin GPIIb/IIIa and IgG binding to the Fc γ RIIa receptor', *Molecular Microbiology*, 59(1), pp. 212–230. doi: 10.1111/j.1365-2958.2005.04922.x.

Flatau, G. *et al.* (1997) 'Toxin-induced activation of the G protein p21 Rho by deamidation of glutamine', *Nature*. Nature Publishing Group, 387(6634), pp. 729–733. doi: 10.1038/42743.

Flaumenhaft, R. (2003) 'ATVB In Focus Platelet Activation and the Formation of the Platelet Plug Molecular Basis of Platelet Granule Secretion', *Arterioscler Thromb Vasc Biol*, 23, pp. 1152–1160. doi: 10.1161/01.ATV.0000075965.88456.48.

Flaumenhaft, R. (2003) 'Molecular basis of platelet granule secretion', *Arteriosclerosis, Thrombosis, and Vascular Biology*, pp. 1152–1160. doi: 10.1161/01.ATV.0000075965.88456.48.

Flaumenhaft, R. *et al.* (2005) 'The actin cytoskeleton differentially regulates platelet-granule and dense-granule secretion'. doi: 10.1182/blood-2004-04.

Flaumenhaft, R. and Sharda, A. (2018) 'The life cycle of platelet granules', *F1000Research*. Faculty of 1000 Ltd. doi: 10.12688/f1000research.13283.1.

Folkman, J., Browder, T. and Palmblad, J. (2001) 'Angiogenesis research: guidelines for translation to clinical application.', *Thrombosis and haemostasis*, 86(1), pp. 23–33.

Forrester, L. J. *et al.* (1985) *Aggregation of Platelets by Fusobacterium necrophorum*, *JOURNAL OF CLINICAL MICROBIOLOGY*.

Foster, C. J. *et al.* (2001) 'Molecular identification and characterization of the platelet ADP receptor targeted by thienopyridine antithrombotic drugs', *Journal of Clinical Investigation*. The American Society for Clinical Investigation, 107(12), pp. 1591–1598. doi: 10.1172/JCI12242.

Fowler, V. G. *et al.* (2005) 'Staphylococcus aureus endocarditis: A consequence of medical progress', *Journal of the American Medical Association*. American Medical Association, 293(24), pp. 3012–3021. doi: 10.1001/jama.293.24.3012.

Fox, J. E. *et al.* (1987) 'Spectrin is associated with membrane-bound actin filaments in platelets and is hydrolyzed by the Ca²⁺-dependent protease during platelet activation.', *Blood*, 69(2), pp. 537–45.

Fox, J. E. (2001) 'Cytoskeletal proteins and platelet signaling.', *Thrombosis and haemostasis*, 86(1), pp. 198–213.

Fox, J. E. B. (1993) 'Regulation of platelet function by the cytoskeleton', in *Advances in Experimental Medicine and Biology*, pp. 175–185. doi: 10.1007/978-1-4615-2994-1_13.

Fox, J. E. B. and Phillips, D. R. (1981) 'Inhibition of actin polymerization in blood platelets by cytochalasins', *Nature*. Nature Publishing Group, 292(5824), pp. 650–652. doi: 10.1038/292650a0.

Fox, J. M. *et al.* (2018) 'CXCL4/Platelet Factor 4 is an agonist of CCR1 and drives human monocyte migration', *Scientific Reports*. Nature Publishing Group, 8(1), pp. 1–15. doi: 10.1038/s41598-018-27710-9.

Fritsma, G. (2015) 'Platelet Structure and Function', *CLINICAL LABORATORY SCIENCE*, 28(2), pp. 125–145.

Fukata, M. *et al.* (1999) 'Cell adhesion and Rho small GTPases.', *Journal of cell science*, 112 (Pt 24), pp. 4491–500.

Gadjeva, M. (2014) 'Overview', *Methods in Molecular Biology*. Humana Press Inc., pp. 1–9. doi: 10.1007/978-1-62703-724-2_1.

Gaertner, F. *et al.* (2017a) 'Migrating Platelets Are Mechano-scavengers that Collect and Bundle Bacteria', *Cell*. Cell Press, 171(6), p. 1368–1382.e23. doi: 10.1016/j.cell.2017.11.001.

Gall-Mas, L. *et al.* (2018) 'The bacterial toxin CNF1 induces activation and maturation of human monocyte-derived dendritic cells', *International Journal of Molecular Sciences*. MDPI AG, 19(5). doi: 10.3390/ijms19051408.

Gandhi, M. and Goode, B. L. (2013) 'Coronin: The Double-Edged Sword of Actin Dynamics'. Landes Bioscience.

Garcia-Souza, L. F. and Oliveira, M. F. (2014) 'Mitochondria: Biological roles in platelet physiology and pathology', *International Journal of Biochemistry and Cell Biology*. Elsevier Ltd, pp. 156–160. doi: 10.1016/j.biocel.2014.02.015.

García, S. *et al.* (2010) 'Akt activity protects rheumatoid synovial fibroblasts from Fas-induced apoptosis by inhibition of Bid cleavage', *Arthritis Research and Therapy*. BioMed Central Ltd., 12(1), p. R33. doi: 10.1186/ar2941.

Gear, A. R. L. and Camerini, D. (2003) 'Platelet chemokines and chemokine receptors: Linking hemostasis, inflammation, and host defense', *Microcirculation*, pp. 335–350. doi: 10.1038/sj.mn.7800198.

Gerdes, N. *et al.* (2011) 'Platelets regulate CD4 + T-cell differentiation via multiple chemokines in humans', *Thrombosis and Haemostasis*. Thromb Haemost, 106(2), pp. 353–362. doi: 10.1160/TH11-01-0020.

Gerhard, R. *et al.* (1998) 'Activation of Rho GTPases by Escherichia coli cytotoxic necrotizing factor 1 increases intestinal permeability in Caco-2 cells.', *Infection and immunity*, 66(11), pp. 5125–31.

Germanovich, K. *et al.* (2018) 'Effects of pH and concentration of sodium citrate anticoagulant on platelet aggregation measured by light transmission aggregometry induced by adenosine diphosphate', *Platelets*. Taylor and Francis Ltd, 29(1), pp. 21–26. doi: 10.1080/09537104.2017.1327655.

Gerrard, J. M., Rao, G. H. and White, J. G. (1977) 'The influence of reserpine and ethylenediaminetetraacetic acid (EDTA) on serotonin storage organelles of blood

platelets.', *The American journal of pathology*, 87(3), pp. 633–46.

Gerrard, J. M., White, J. G. and Peterson, D. A. (1978) 'The platelet dense tubular system: its relationship to prostaglandin synthesis and calcium flux', *Thrombosis and Haemostasis*, pp. 224–231. doi: 10.1055/s-0038-1648656.

Ghali, H. *et al.* (2016) 'Real-time detection of *Staphylococcus aureus* using Whispering Gallery Mode optical microdisks', *Biosensors*. MDPI AG, 6(2). doi: 10.3390/bios6020020.

Ghoshal, K. and Bhattacharyya, M. (2014) 'Overview of platelet physiology: its hemostatic and nonhemostatic role in disease pathogenesis.', *TheScientificWorldJournal*. Hindawi, 2014, p. 781857. doi: 10.1155/2014/781857.

Goggs, R. *et al.* (2013) 'The Small GTPase Rif Is Dispensable for Platelet Filopodia Generation in Mice', *PLoS ONE*, 8(1), p. e54663. doi: 10.1371/journal.pone.0054663.

Goggs, R., Williams, C. M., *et al.* (2015) 'Platelet Rho GTPases—a focus on novel players, roles and relationships', *Biochem. J*, 466, pp. 431–442. doi: 10.1042/BJ20141404.

Goh, W. I. *et al.* (2011) 'Rif-mDia1 interaction is involved in filopodium formation independent of Cdc42 and rac effectors', *Journal of Biological Chemistry*. American Society for Biochemistry and Molecular Biology, 286(15), pp. 13681–13694. doi: 10.1074/jbc.M110.182683.

Golebiewska, E. M. and Poole, A. W. (2015) 'Platelet secretion: From haemostasis to wound healing and beyond.', *Blood reviews*. Elsevier, 29(3), pp. 153–62. doi: 10.1016/j.blre.2014.10.003.

Goto, S. *et al.* (1995) 'Characterization of the unique mechanism mediating the shear-dependent binding of soluble von Willebrand factor to platelets', *Journal of Biological Chemistry*, 270(40), pp. 23352–23361. doi: 10.1074/jbc.270.40.23352.

Gratacap, M. P. *et al.* (2009) 'The new tyrosine-kinase inhibitor and anticancer drug dasatinib reversibly affects platelet activation in vitro and in vivo', *Blood*. American Society of Hematology, 114(9), pp. 1884–1892. doi: 10.1182/blood-2009-02-205328.

Green, F. W. *et al.* (1978) *EFFECT OF ACID AND PEPSIN ON BLOOD COAGULATION AND PLATELET AGGREGATION A possible contributor to prolonged gastroduodenal mucosal hemorrhage*, *Gastroenterology*. doi: 10.1016/0016-5085(78)90352-9.

Gross, B. S., Melford, S. K. and Watson, S. P. (1999) 'Evidence that phospholipase C- γ 2 interacts with SLP-76, Syk, Lyn, LAT and the Fc receptor γ -chain after stimulation of the collagen receptor glycoprotein VI in human platelets', *European Journal of Biochemistry*. Eur J Biochem, 263(3), pp. 612–623. doi: 10.1046/j.1432-1327.1999.00560.x.

Gu, Y. *et al.* (2003) 'Hematopoietic Cell Regulation by Rac1 and Rac2 Guanosine Triphosphatases', *Science*. American Association for the Advancement of Science,

302(5644), pp. 445–449. doi: 10.1126/science.1088485.

Gurbel, P. A., Kuliopulos, A. and Tantry, U. S. (2015) 'G-Protein-Coupled Receptors Signaling Pathways in New Antiplatelet Drug Development HHS Public Access', *Arterioscler Thromb Vasc Biol*, 35(3), pp. 500–512. doi: 10.1161/ATVBAHA.114.303412.

Hamad, O. A. *et al.* (2010) 'Complement Component C3 Binds to Activated Normal Platelets without Preceding Proteolytic Activation and Promotes Binding to Complement Receptor 1', *The Journal of Immunology*. The American Association of Immunologists, 184(5), pp. 2686–2692. doi: 10.4049/jimmunol.0902810.

Hamzeh-Cognasse, H. *et al.* (2015) 'Platelets and infections - Complex interactions with bacteria', *Frontiers in Immunology*. Frontiers Media S.A. doi: 10.3389/fimmu.2015.00082.

Han, P. and Ardlie, N. G. (1974a) 'The Influence pH, Temperature, and Calcium on Platelet Aggregation: Maintenance of Environmental pH and Platelet Function for in Vitro Studies in Plasma Stored at 37° C', *British Journal of Haematology*. John Wiley & Sons, Ltd, 26(3), pp. 373–389. doi: 10.1111/j.1365-2141.1974.tb00479.x.

Hanasaki, K., Nakano, T. and Arita, H. (1987) 'Two phasic generation of thromboxane a₂ by the action of collagen on rat platelets', *Thrombosis Research*. Elsevier, 46(3), pp. 425–436. doi: 10.1016/0049-3848(87)90130-7.

Harden, T. K., Hicks, S. N. and Sondek, J. (2009) 'Phospholipase C isozymes as effectors of Ras superfamily GTPases', *Journal of Lipid Research*. American Society for Biochemistry and Molecular Biology, p. S243. doi: 10.1194/jlr.R800045-JLR200.

Hart, M. J. *et al.* (1991) 'Identification of the human platelet GTPase activating protein for the CDC42Hs protein', *Journal of Biological Chemistry*, 266(31), pp. 20840–20848.

Hartwig, J. H. *et al.* (1995) *Thrombin Receptor Ligation and Activated Rat Uncap Actin Filament Barbed Ends through Phosphoinositide Synthesis in Permeabilized Human Platelets, Cell*.

Hartwig, J. H. (2006) 'The Platelet: Form and Function', *Seminars in Hematology*, 43(SUPPL. 1), pp. S94–S100. doi: 10.1053/j.seminhematol.2005.11.004.

Hartwig, J. H. and Desisto, M. (1988) *Mechanisms of Actin Rearrangements Mediating Platelet Activation, J. Cell Biol.*

Hartwig, J. H. and DeSisto, M. (1991) 'The cytoskeleton of the resting human blood platelet: Structure of the membrane skeleton and its attachment to actin filaments', *Journal of Cell Biology*. The Rockefeller University Press, 112(3), pp. 407–425. doi: 10.1083/jcb.112.3.407.

Hechler, B. *et al.* (2019) 'Platelet preparation for function testing in the laboratory and clinic: Historical and practical aspects', *Research and Practice in Thrombosis and Haemostasis*, 3(4), pp. 615–625. doi: 10.1002/rth2.12240.

Heemskerk, J. W. M., Bevers, E. M. and Lindhout, T. (2002) 'Platelet activation and blood coagulation', *Thrombosis and Haemostasis*, pp. 186–193. doi: 10.1055/s-0037-1613209.

Heijnen, H. F. G. and Korporaal, S. J. A. (2017) 'Platelet morphology and ultrastructure', in *Platelets in Thrombotic and Non-Thrombotic Disorders: Pathophysiology, Pharmacology and Therapeutics: an Update*. Cham: Springer International Publishing, pp. 21–38. doi: 10.1007/978-3-319-47462-5_3.

Herbert, S. *et al.* (2010) 'Repair of global regulators in *Staphylococcus aureus* 8325 and comparative analysis with other clinical isolates', *Infection and Immunity*. American Society for Microbiology Journals, 78(6), pp. 2877–2889. doi: 10.1128/IAI.00088-10.

Herr, N., Bode, C. and Duerschmied, D. (2017) 'The Effects of Serotonin in Immune Cells', *Frontiers in Cardiovascular Medicine*. Frontiers Media S.A. doi: 10.3389/fcvm.2017.00048.

Herrmann, M. *et al.* (1993) 'Adhesion of *Staphylococcus aureus* to surface-bound platelets: role of fibrinogen/fibrin and platelet integrins.', *The Journal of infectious diseases*, 167(2), pp. 312–22. doi: 10.1093/infdis/167.2.312.

Hodge, R. G. and Ridley, A. J. (2016) 'Regulating Rho GTPases and their regulators', *Nature Reviews Molecular Cell Biology*. Nature Publishing Group, pp. 496–510. doi: 10.1038/nrm.2016.67.

Hoff, J. and Hoff, J. (no date) 'Methods of Blood Collection in the Mouse'. Available at: <http://citeseerx.ist.psu.edu/viewdoc/summary?doi=10.1.1.174.5448>

Hofman, P. *et al.* (2000) 'Escherichia coli cytotoxic necrotizing factor-1 (CNF-1) increases the adherence to epithelia and the oxidative burst of human polymorphonuclear leukocytes but decreases bacteria phagocytosis.', *Journal of leukocyte biology*, 68(4), pp. 522–8. doi: 10.1189/jlb.68.4.522.

Höök, P. *et al.* (2017) 'Strong Binding of Platelet Integrin α IIb β 3 to Fibrin Clots: Potential Target to Destabilize Thrombi', *Scientific Reports*. Nature Publishing Group, 7(1), pp. 1–8. doi: 10.1038/s41598-017-12615-w.

Hornstein, I., Alcover, A. and Katzav, S. (2004) 'Vav proteins, masters of the world of cytoskeleton organization.', *Cellular signalling*, 16(1), pp. 1–11. doi: 10.1016/s0898-6568(03)00110-4.

Hou, Y. *et al.* (2015) 'Platelets in hemostasis and thrombosis: Novel mechanisms of fibrinogen-independent platelet aggregation and fibronectin-mediated protein wave of hemostasis', *The Journal of Biomedical Research*, 29(6), pp. 437–444. doi: 10.7555/JBR.29.20150121.

Hoylaerts, M. F., Vanassche, T. and Verhamme, P. (2018) 'Bacterial killing by platelets: making sense of (H) α IIb β 3', *Journal of Thrombosis and Haemostasis*. Blackwell Publishing Ltd, 16(6), pp. 1182–1186. doi: 10.1111/jth.14012.

HUFF, T. *et al.* (2002) 'Thymosin β 4 is released from human blood platelets and attached by factor XIIIa (transglutaminase) to fibrin and collagen', *The FASEB Journal*. FASEB, 16(7), pp. 691–696. doi: 10.1096/fj.01-0713com.

Huveneers, S. and Danen, E. H. J. (2009) 'Adhesion signaling - Crosstalk between integrins, Src and Rho', *Journal of Cell Science*. The Company of Biologists Ltd, pp. 1059–1069. doi: 10.1242/jcs.039446.

Hwang, J. J. and Stupp, S. I. (2000) 'Poly(amino acid) bioadhesives for tissue repair', *Journal of Biomaterials Science, Polymer Edition*, 11(10), pp. 1023–1038. doi: 10.1163/156856200743553.

Infante, E. and Ridley, A. J. (2013) 'Roles of Rho GTPases in leucocyte and leukaemia cell transendothelial migration', *Philosophical Transactions of the Royal Society B: Biological Sciences*. The Royal Society. doi: 10.1098/rstb.2013.0013.

Irie, M. and Ohgi, K. (2001) 'Ribonuclease T2', in *Methods in Enzymology*. Academic Press Inc., pp. 42–55. doi: 10.1016/S0076-6879(01)41144-X.

Israels, S. J. *et al.* (1992) 'Platelet dense granule membranes contain both granulophysin and P-selectin (GMP-140)', *Blood*, 80(1), pp. 143–152. doi: 10.1182/blood.v80.1.143.bloodjournal801143.

Jackson, S. P., Nesbitt, W. S. and Kulkarni, S. (2003) 'Signaling events underlying thrombus formation', *Journal of Thrombosis and Haemostasis*, pp. 1602–1612. doi: 10.1046/j.1538-7836.2003.00267.x.

Jennings, L. K. *et al.* (1981) *Changes in the Cytoskeletal Structure of Human Platelets Following Thrombin Activation**.

Jin, J. *et al.* (2002) 'Adenosine diphosphate (ADP)-induced thromboxane A₂ generation in human platelets requires coordinated signaling through integrin α IIb β 3 and ADP receptors', *Blood*, 99(1), pp. 193–198. doi: 10.1182/blood.V99.1.193.

Jin, J., Daniel, J. L. and Kunapuli, S. P. (1998) 'Molecular basis for ADP-induced platelet activation: II. The P2Y₁ receptor mediates ADP-induced intracellular calcium mobilization and shape change in platelets', *Journal of Biological Chemistry*. American Society for Biochemistry and Molecular Biology, 273(4), pp. 2030–2034. doi: 10.1074/jbc.273.4.2030.

Jin, J. and Kunapuli, S. P. (1998) 'Coactivation of two different G protein-coupled receptors is essential for ADP-induced platelet aggregation', *Proceedings of the National Academy of Sciences of the United States of America*. National Academy of Sciences, 95(14), pp. 8070–8074. doi: 10.1073/pnas.95.14.8070.

Jin, T. (2013) 'Gradient sensing during chemotaxis', *Current Opinion in Cell Biology*. Curr Opin Cell Biol, pp. 532–537. doi: 10.1016/j.ceb.2013.06.007.

Jiroušková, M., Jaiswal, J. K. and Collier, B. S. (2007) 'Ligand density dramatically affects integrin $\alpha\text{IIb}\beta\text{3}$ -mediated platelet signaling and spreading', *Blood*. The American Society of Hematology, 109(12), pp. 5260–5269. doi: 10.1182/blood-2006-10-054015.

Jirouskova, M., Shet, A. S. and Johnson, G. J. (2007) 'A guide to murine platelet structure, function, assays, and genetic alterations', *Journal of Thrombosis and Haemostasis*, pp. 661–669. doi: 10.1111/j.1538-7836.2007.02407.x.

Jobe, S. (2017) 'Platelet heterogeneity', in *Platelets in Thrombotic and Non-Thrombotic Disorders: Pathophysiology, Pharmacology and Therapeutics: an Update*. Springer International Publishing, pp. 55–68. doi: 10.1007/978-3-319-47462-5_5.

Jobling, L. and Eyre, L. (2013) 'Haemostasis, blood platelets and coagulation', *Anaesthesia and Intensive Care Medicine*, pp. 51–53. doi: 10.1016/j.mpaic.2012.12.001.

Johnston-Cox, H. A., Yang, D. and Ravid, K. (2011) 'Physiological implications of adenosine receptor-mediated platelet aggregation', *Journal of Cellular Physiology*, pp. 46–51. doi: 10.1002/jcp.22379.

Joo, S. J. (2012) 'Mechanisms of platelet activation and integrin $\alpha\text{IIb}\beta\text{3}$ ', *Korean Circulation Journal*. The Korean Society of Cardiology, pp. 295–301. doi: 10.4070/kcj.2012.42.5.295.

Jooss, N. J. *et al.* (2019) 'Role of platelet glycoprotein VI and Tyrosine Kinase Syk in thrombus formation on collagen-like surfaces', *International Journal of Molecular Sciences*. MDPI AG, 20(11). doi: 10.3390/ijms20112788.

Joshi, P. *et al.* (2018) 'The membrane-associated fraction of cyclase associate protein 1 translocates to the cytosol upon platelet stimulation', *Scientific Reports*. Nature Publishing Group, 8(1), p. 10804. doi: 10.1038/s41598-018-29151-w.

Kabsch, W. *et al.* (1990) 'Atomic structure of the actin: DNase I complex', *Nature*, 347(6288), pp. 37–44. doi: 10.1038/347037a0.

Kahn, M. L. *et al.* (1998) 'A dual thrombin receptor system for platelet activation', *Nature*, 394(6694), pp. 690–694. doi: 10.1038/29325.

Kahn, M. L. *et al.* (1999) 'Protease-activated receptors 1 and 4 mediate activation of human platelets by thrombin', *Journal of Clinical Investigation*. The American Society for Clinical Investigation, 103(6), pp. 879–887. doi: 10.1172/JCI6042.

Kameyoshi, Y. *et al.* (1994) 'Identification of the cytokine RANTES released from platelets as an eosinophil chemotactic factor', in *International Archives of Allergy and Immunology*. S. Karger AG, pp. 49–51. doi: 10.1159/000236751.

Kar, P. *et al.* (2012) 'A protocol for stripping and reprobing of Western blots originally developed with colorimetric substrate TMB', *Electrophoresis*, 33(19–20), pp. 3062–3065. doi: 10.1002/elps.201200333.

- Karpman, D. *et al.* (2001) 'Platelet activation by Shiga toxin and circulatory factors as a pathogenetic mechanism in the hemolytic uremic syndrome.', *Blood*, 97(10), pp. 3100–8. doi: 10.1182/blood.v97.10.3100.
- Katoh, K. *et al.* (2001) 'Rho-kinase-mediated contraction of isolated stress fibers', *Journal of Cell Biology*, 152(3), pp. 569–583. doi: 10.1083/jcb.153.3.569.
- Keane, C. *et al.* (2010) 'Invasive *Streptococcus pneumoniae* trigger platelet activation via Toll-like receptor 2', *Journal of Thrombosis and Haemostasis*, 8(12), pp. 2757–2765. doi: 10.1111/j.1538-7836.2010.04093.x.
- Keiser, H. *et al.* (1963) 'Collagen-like protein in human plasma', *Science*. *Science*, 142(3600), pp. 1678–1679. doi: 10.1126/science.142.3600.1678.
- Kerrigan, S. W. *et al.* (2002) 'A role for glycoprotein Ib in *Streptococcus sanguis*-induced platelet aggregation', *Blood*. American Society of Hematology, 100(2), pp. 509–516. doi: 10.1182/blood.V100.2.509.
- Kerrigan, S. W. *et al.* (2007) 'Molecular Basis for *Staphylococcus aureus*-Mediated Platelet Aggregate Formation Under Arterial Shear In Vitro', *Original*. doi: 10.1161/ATVBAHA.107.152058.
- Kerrigan, S. W. (2015) 'Platelet Interactions with Bacteria', in *The Non-Thrombotic Role of Platelets in Health and Disease*. InTech. doi: 10.5772/60531.
- Kerrigan, S. W. and Cox, D. (2010) 'Platelet-bacterial interactions', *Cellular and Molecular Life Sciences*, pp. 513–523. doi: 10.1007/s00018-009-0207-z.
- Keularts, I. M. L. W. *et al.* (2000) ' $\alpha(2A)$ -Adrenergic receptor stimulation potentiates calcium release in platelets by modulating cAMP levels', *Journal of Biological Chemistry*. American Society for Biochemistry and Molecular Biology, 275(3), pp. 1763–1772. doi: 10.1074/jbc.275.3.1763.
- Kiefer, F. *et al.* (1998) 'The Syk Protein Tyrosine Kinase Is Essential for Fc γ Receptor Signaling in Macrophages and Neutrophils', *Molecular and Cellular Biology*. American Society for Microbiology, 18(7), pp. 4209–4220. doi: 10.1128/mcb.18.7.4209.
- Kiefer, T. L. and Becker, R. C. (2009) 'Inhibitors of platelet adhesion.', *Circulation*, 120(24), pp. 2488–95. doi: 10.1161/CIRCULATIONAHA.109.886895.
- Kikkawa, Y. and Miner, J. H. (2005) 'Review: Lutheran/B-CAM: A Laminin receptor on red blood cells and in various tissues', *Connective Tissue Research*. Connect Tissue Res, pp. 193–199. doi: 10.1080/03008200500344074.
- Kishore Paknikar, A. (2016) *Cytoskeletal reorganization in human blood platelets during spreading*.

Klement, G. L. *et al.* (2009) 'Platelets actively sequester angiogenesis regulators', *Blood*, 113(12), pp. 2835–2842. doi: 10.1182/blood-2008-06-159541.

Klevens, R. M. *et al.* (2007) 'Invasive methicillin-resistant *Staphylococcus aureus* infections in the United States', *Journal of the American Medical Association*. American Medical Association, 298(15), pp. 1763–1771. doi: 10.1001/jama.298.15.1763.

Knust, Z. *et al.* (2009) 'Cleavage of *Escherichia coli* cytotoxic necrotizing factor 1 is required for full biologic activity', *Infection and Immunity*. American Society for Microbiology Journals, 77(5), pp. 1835–1841. doi: 10.1128/IAI.01145-08.

Knust, Z. and Schmidt, G. (2010) 'Cytotoxic necrotizing factors (CNFs)-a growing toxin family', *Toxins*. Multidisciplinary Digital Publishing Institute (MDPI), pp. 116–127. doi: 10.3390/toxins2010116.

Kostos, L. *et al.* (2015) 'Gastrointestinal bleeding in a chronic myeloid leukaemia patient precipitated by dasatinib-induced platelet dysfunction: Case report', *Platelets*. Taylor and Francis Ltd, 26(8), pp. 809–811. doi: 10.3109/09537104.2015.1049138.

Kraemer, B. F. *et al.* (2010) 'PI3 kinase-dependent stimulation of platelet migration by stromal cell-derived factor 1 (SDF-1)', *Journal of Molecular Medicine*. Springer, 88(12), pp. 1277–1288. doi: 10.1007/s00109-010-0680-8.

Kraemer, B. F. *et al.* (2011) 'Novel anti-bacterial activities of β -defensin 1 in human platelets: Suppression of pathogen growth and signaling of neutrophil extracellular trap formation', *PLoS Pathogens*. Public Library of Science, 7(11). doi: 10.1371/journal.ppat.1002355.

Kraemer, B. F. *et al.* (2012) 'Bacteria differentially induce degradation of Bcl-xL, a survival protein, by human platelets', *Blood*, 120(25), pp. 5014–5020. doi: 10.1182/blood-2012-04-420661.

Kral, J. B. *et al.* (2016) 'Platelet Interaction with Innate Immune Cells', *Transfusion Medicine and Hemotherapy*. S. Karger AG, pp. 78–88. doi: 10.1159/000444807.

Kroeze, W. K., Sheffler, D. J. and Roth, B. L. (2003) 'G-protein-coupled receptors at a glance', *Journal of Cell Science*. The Company of Biologists Ltd, 116(24), pp. 4867–4869. doi: 10.1242/jcs.00902.

Kronlage, M. *et al.* (2010) 'Autocrine purinergic receptor signaling is essential for macrophage chemotaxis', *Science Signaling*. American Association for the Advancement of Science, 3(132), p. ra55. doi: 10.1126/scisignal.2000588.

Kudinha, T. (2017) 'The Pathogenesis of *Escherichia coli* Urinary Tract Infection', in *Escherichia coli - Recent Advances on Physiology, Pathogenesis and Biotechnological Applications*. InTech. doi: 10.5772/intechopen.69030.

Kurien, B. T. and Scofield, R. H. (2006) 'Kurien, B. T., and Scofield, R. H. (2006). Western blotting.,. Methods (San Diego, Calif.), 38(4), pp. 283–93. doi:10.1016/j.ymeth.2005.11.007Western blotting.', *Methods (San Diego, Calif.)*, 38(4), pp. 283–93. doi: 10.1016/j.ymeth.2005.11.007.

Laemmli, U. K. (1970) 'Cleavage of structural proteins during the assembly of the head of bacteriophage T4', *Nature*, 227(5259), pp. 680–685. doi: 10.1038/227680a0.

Lam, F. W. *et al.* (2011) 'Platelets enhance neutrophil transendothelial migration via P-selectin glycoprotein ligand-1', *American Journal of Physiology - Heart and Circulatory Physiology*, 300(2), pp. H468-75. doi: 10.1152/ajpheart.00491.2010.

Landraud, L. *et al.* (2004) 'E. coli CNF1 toxin: A two-in-one system for host-cell invasion', in *International Journal of Medical Microbiology*. Elsevier GmbH, pp. 513–518. doi: 10.1078/1438-4221-00295.

Lapetina, E. G. and Siess, W. (1983) 'The role of phospholipase C in platelet responses', *Life Sciences*, pp. 1011–1018. doi: 10.1016/0024-3205(83)90654-9.

Laurence A. Harker *et al.* (2000) 'Effects of megakaryocyte growth and development factor on platelet production, platelet life span, and platelet function in healthy human volunteers', *Blood*, 95, pp. 2154–2522.

Leask, R. L., Jain, N. and Butany, J. (2003) 'Endothelium and valvular diseases of the heart', *Microscopy Research and Technique*. Microsc Res Tech, pp. 129–137. doi: 10.1002/jemt.10251.

Lee, G. and Arepally, G. M. (2012) 'Anticoagulation techniques in apheresis: From heparin to citrate and beyond', in *Journal of Clinical Apheresis*, pp. 117–125. doi: 10.1002/jca.21222.

Lefebvre, P. *et al.* (1993) 'Role of actin in platelet function.', *European journal of cell biology*, 62(2), pp. 194–204.

Lefrançois, E. and Looney, M. R. (2019) 'Platelet biogenesis in the lung circulation', *Physiology*. American Physiological Society, pp. 392–401. doi: 10.1152/physiol.00017.2019.

Lemichez, E. *et al.* (1997) 'Molecular localization of the *Escherichia coli* cytotoxic necrotizing factor CNF1 cell-binding and catalytic domains', *Molecular Microbiology*. Blackwell Publishing Ltd, 24(5), pp. 1061–1070. doi: 10.1046/j.1365-2958.1997.4151781.x.

Lenain, N. *et al.* (2003) 'Inhibition of localized thrombosis in P2Y₁-deficient mice and rodents treated with MRS2179, a P2Y₁ receptor antagonist', *Journal of Thrombosis and Haemostasis*. John Wiley & Sons, Ltd, 1(6), pp. 1144–1149. doi: 10.1046/j.1538-7836.2003.00144.x.

Lenehan, D. *et al.* (2016) 'Characterisation of E. coli Lipopolysaccharide Adherence to

Platelet Receptors', *Blood*. American Society of Hematology, 128(22), pp. 4906–4906. doi: 10.1182/blood.v128.22.4906.4906.

Leonard, D. *et al.* (1992) 'The identification and characterization of a GDP-dissociation inhibitor (GDI) for the CDC42Hs protein', *Journal of Biological Chemistry*, 267(32), pp. 22860–22868.

Lerm, M. *et al.* (1999) 'Deamidation of Cdc42 and Rac by Escherichia coli cytotoxic necrotizing factor 1: Activation of c-Jun N-terminal kinase in HeLa cells', *Infection and Immunity*, 67(2), pp. 496–503. doi: 10.1128/iai.67.2.496-503.1999.

Lerm, M. *et al.* (2002) 'Proteasomal degradation of cytotoxic necrotizing factor 1-activated Rac', *Infection and Immunity*. American Society for Microbiology (ASM), 70(8), pp. 4053–4058. doi: 10.1128/IAI.70.8.4053-4058.2002.

Levaditi, C. (1901) 'Et des organismes vaccines contre le vibron cholérique.', *Ann Inst Pasteur*, 15, pp. 894–924.

Levay, M. *et al.* (2013) 'NSC23766, a widely used inhibitor of Rac1 activation, additionally Acts as a competitive antagonist at muscarinic acetylcholine receptors', *Journal of Pharmacology and Experimental Therapeutics*, 347(1), pp. 69–79. doi: 10.1124/jpet.113.207266.

Levin, P. A. (2016) *Light Microscopy Techniques For Bacterial Cell Biology*.

Li, Z., Kim, E. S. and Bearer, E. L. (2002) 'Arp2/3 complex is required for actin polymerization during platelet shape change.', *Blood*, 99(12), pp. 4466–74. doi: 10.1182/blood.v99.12.4466.

Liu, D. and Mamorska-Dyga, A. (2017) 'Syk inhibitors in clinical development for hematological malignancies', *Journal of Hematology & Oncology*, 10(1), p. 145. doi: 10.1186/s13045-017-0512-1.

Livne, A. and Geiger, B. (2016) 'The inner workings of stress fibers - From contractile machinery to focal adhesions and back', *Journal of Cell Science*. Company of Biologists Ltd, 129(7), pp. 1293–1304. doi: 10.1242/jcs.180927.

Lodish, H. *et al.* (2000) 'Myosin: The Actin Motor Protein'. W. H. Freeman. Available at: <https://www.ncbi.nlm.nih.gov/books/NBK21724/> (Accessed: 29 September 2020).

Looney, M. (2018) 'Platelet Biogenesis in the Lung Circulation', *Blood*. American Society of Hematology, 132(Supplement 1), p. SCI-22-SCI-22. doi: 10.1182/blood-2018-99-109544.

Lopez, J. J. *et al.* (2007) 'Thrombin induces apoptotic events through the generation of reactive oxygen species in human platelets', *Journal of Thrombosis and Haemostasis*, 5(6), pp. 1283–1291. doi: 10.1111/j.1538-7836.2007.02505.x.

Loughman, A. *et al.* (2005) 'Roles for fibrinogen, immunoglobulin and complement in

platelet activation promoted by Staphylococcus aureus clumping factor A', *Molecular Microbiology*, 57(3), pp. 804–818. doi: 10.1111/j.1365-2958.2005.04731.x.

Louise Meyer, R. *et al.* (2010) 'Immobilisation of living bacteria for AFM imaging under physiological conditions', *Ultramicroscopy*. North-Holland, 110(11), pp. 1349–1357. doi: 10.1016/j.ultramic.2010.06.010.

Lowell, C. A. (2011) 'Src-family and Syk kinases in activating and inhibitory pathways in innate immune cells: Signaling cross talk', *Cold Spring Harbor Perspectives in Biology*. Cold Spring Harbor Laboratory Press, pp. 1–16. doi: 10.1101/cshperspect.a002352.

Lowenhaupt, R. *et al.* (1977) 'Factors which influence blood platelet migration', *J Lab Clinical Med*, 90(1), pp. 37–45.

Lowenhaupt, R. W., Miller, M. A. and Glueck, H. I. (1973) 'Platelet migration and chemotaxis demonstrated in vitro', *Thrombosis Research*. Pergamon, 3(5), pp. 477–487. doi: 10.1016/0049-3848(73)90110-2.

Lowenstein, C. J. (2017) 'VAMP-3 mediates platelet endocytosis', *Blood*. American Society of Hematology, pp. 2816–2818. doi: 10.1182/blood-2017-10-808576.

Lowry, O. H. *et al.* (no date) *PROTEIN MEASUREMENT WITH THE FOLIN PHENOL REAGENT**. Available at: <http://www.jbc.org/> (Accessed: 6 November 2019).

Lynch, E. A. *et al.* (2006) 'Proteasome-mediated degradation of Rac1-GTP during epithelial cell scattering', *Molecular Biology of the Cell*, 17(5), pp. 2236–2242. doi: 10.1091/mbc.E05-08-0779.

Mai-Prochnow, A. *et al.* (2016) 'Gram positive and Gram negative bacteria differ in their sensitivity to cold plasma', *Scientific Reports*. Nature Publishing Group, 6. doi: 10.1038/srep38610.

Mainil, J. (2013) 'Escherichia coli virulence factors', *Veterinary Immunology and Immunopathology*. Elsevier, 152(1–2), pp. 2–12. doi: 10.1016/j.vetimm.2012.09.032.

Manne, B. K., Xiang, S. C. and Rondina, M. T. (2017) 'Platelet secretion in inflammatory and infectious diseases', *Platelets*. Taylor and Francis Ltd, pp. 155–164. doi: 10.1080/09537104.2016.1240766.

Del Mar Maldonado, M. and Dharmawardhane, S. (2018) 'Targeting Rac and Cdc42 GTPases in Cancer'. doi: 10.1158/0008-5472.CAN-18-0619.

Maslow, J. N. *et al.* (1993) 'Bacterial Adhesins and Host Factors: Role in the Development and Outcome of Escherichia coli Bacteremia', *Clinical Infectious Diseases*, 17(1), pp. 89–97. doi: 10.1093/clinids/17.1.89.

Mattila, P. K. and Lappalainen, P. (2008) 'Filopodia: Molecular architecture and cellular

functions', *Nature Reviews Molecular Cell Biology*, pp. 446–454. doi: 10.1038/nrm2406.

Mayer, C. L. *et al.* (2012) 'Shiga toxins and the pathophysiology of hemolytic uremic syndrome in humans and animals', *Toxins*. Multidisciplinary Digital Publishing Institute (MDPI), pp. 1261–1287. doi: 10.3390/toxins4111261.

Maynard, D. M. *et al.* (2007) 'Proteomic analysis of platelet α -granules using mass spectrometry', *Journal of Thrombosis and Haemostasis*, 5(9), pp. 1945–1955. doi: 10.1111/j.1538-7836.2007.02690.x.

McBirney, S. E. *et al.* (2016) 'Wavelength-normalized spectroscopic analysis of *Staphylococcus aureus* and *Pseudomonas aeruginosa* growth rates', *Biomedical Optics Express*. The Optical Society, 7(10), p. 4034. doi: 10.1364/boe.7.004034.

McCarty, O. J. T. *et al.* (2005) 'Rac1 is essential for platelet lamellipodia formation and aggregate stability under flow', *Journal of Biological Chemistry*. Europe PMC Funders, 280(47), pp. 39474–39484. doi: 10.1074/jbc.M504672200.

McIntosh, R. V. *et al.* (1990) 'Freezing and Thawing Plasma', in *Cryopreservation and low temperature biology in blood transfusion*. Springer US, pp. 11–24. doi: 10.1007/978-1-4613-1515-5_2.

Meadows, T. A. and Bhatt, D. L. (2007) 'Clinical aspects of platelet inhibitors and thrombus formation.', *Circulation research*, 100(9), pp. 1261–75. doi: 10.1161/01.RES.0000264509.36234.51.

van der Meijden, P. E. J. and Heemskerk, J. W. M. (2019) 'Platelet biology and functions: new concepts and clinical perspectives', *Nature Reviews Cardiology*. Nature Publishing Group, pp. 166–179. doi: 10.1038/s41569-018-0110-0.

Menter, D. G. *et al.* (2014) 'Platelets and cancer: A casual or causal relationship: Revisited', *Cancer and Metastasis Reviews*. Kluwer Academic Publishers, pp. 231–269. doi: 10.1007/s10555-014-9498-0.

Messina, V. *et al.* (2019) 'The bacterial protein CNF1 as a new strategy against *Plasmodium falciparum* cytoadherence', *PLOS ONE*. Edited by A. G. Craig. Public Library of Science, 14(3), p. e0213529. doi: 10.1371/journal.pone.0213529.

Metcalf, P. *et al.* (1997) 'Activation during preparation of therapeutic platelets affects deterioration during storage: A comparative flow cytometric study of different production methods', *British Journal of Haematology*. Blackwell Publishing Ltd, 98(1), pp. 86–95. doi: 10.1046/j.1365-2141.1997.1572983.x.

Meysick, K. C., Mills, M. and O'Brien, A. D. (2001) 'Epitope mapping of monoclonal antibodies capable of neutralizing cytotoxic necrotizing factor type 1 of uropathogenic *Escherichia coli*', *Infection and Immunity*, 69(4), pp. 2066–2074. doi: 10.1128/IAI.69.4.2066-2074.2001.

Miajlovic, H. *et al.* (2007) 'Both complement- and fibrinogen-dependent mechanisms contribute to platelet aggregation mediated by Staphylococcus aureus clumping factor B', *Infection and Immunity*. American Society for Microbiology (ASM), 75(7), pp. 3335–3343. doi: 10.1128/IAI.01993-06.

Miajlovic, H. *et al.* (2010) 'Direct interaction of iron-regulated surface determinant IsdB of Staphylococcus aureus with the GPIIb/IIIa receptor on platelets', *Microbiology*. Microbiology Society, 156(3), pp. 920–928. doi: 10.1099/mic.0.036673-0.

MIALE, J. B. (1949) 'The role of staphylocoagulase in blood coagulation; the reaction of staphylocoagulase with coagulase-globulin to form coagulase-thrombin', *Blood*. American Society of Hematology, 4(9), pp. 1039–1048. doi: 10.1182/blood.V4.9.1039.1039.

Michelson, A. D. (1992) 'Thrombin-induced down-regulation of the platelet membrane glycoprotein Ib-IX complex', *Seminars in Thrombosis and Hemostasis*, pp. 18–27. doi: 10.1055/s-2007-1002406.

Michelson, A. D. (2013) *Platelets, Platelets*. Elsevier Inc. doi: 10.1016/C2010-0-64795-X.

Mkaddem, S. Ben *et al.* (2017) 'Lyn and Fyn function as molecular switches that control immunoreceptors to direct homeostasis or inflammation', *Nature Communications*. Nature Publishing Group, 8(1), pp. 1–13. doi: 10.1038/s41467-017-00294-0.

Moeckel, D. *et al.* (2014) 'Optimizing human apyrase to treat arterial thrombosis and limit reperfusion injury without increasing bleeding risk', *Science Translational Medicine*. American Association for the Advancement of Science, 6(248), p. 248ra105. doi: 10.1126/scitranslmed.3009246.

Moers, A. *et al.* (2003) 'G13 is an essential mediator of platelet activation in hemostasis and thrombosis', *Nature Medicine*. Presse Dienstleistungsgesellschaft mbH und Co. KG, 9(11), pp. 1418–1422. doi: 10.1038/nm943.

Moon, S. Y. and Zheng, Y. (2003) 'Rho GTPase-activating proteins in cell regulation', *Trends in Cell Biology*. Elsevier Ltd, 13(1), pp. 13–22. doi: 10.1016/S0962-8924(02)00004-1.

Mora-Rillo, M. *et al.* (2015) 'Impact of virulence genes on sepsis severity and survival in Escherichia coli bacteremia', *Virulence*. Landes Bioscience, 6(1), pp. 93–100. doi: 10.4161/21505594.2014.991234.

Moreillon, P. and Que, Y. A. (2004) 'Infective endocarditis', in *Lancet*. Elsevier Limited, pp. 139–149. doi: 10.1016/S0140-6736(03)15266-X.

Morgenstern, E. (1997) 'Human Platelet Morphology/Ultrastructure', in, pp. 27–60. doi: 10.1007/978-3-642-60639-7_2.

Moriarty, R. D. *et al.* (2016) 'Escherichia coli induces platelet aggregation in an FcγR11a-dependent manner', *Journal of Thrombosis and Haemostasis*. Blackwell Publishing Ltd,

14(4), pp. 797–806. doi: 10.1111/jth.13226.

Moroi, M. and Jung, S. M. (2004) 'Platelet glycoprotein VI: Its structure and function', *Thrombosis Research*, pp. 221–233. doi: 10.1016/j.thromres.2004.06.046.

Morrell, C. N. *et al.* (2014) 'Emerging roles for platelets as immune and inflammatory cells', *Blood*. American Society of Hematology, pp. 2759–2767. doi: 10.1182/blood-2013-11-462432.

Mullins, R. D., Heuser, J. A. and Pollard, T. D. (1998) 'The interaction of Arp2/3 complex with actin: Nucleation, high affinity pointed end capping, and formation of branching networks of filaments', *Proceedings of the National Academy of Sciences of the United States of America*, 95(11), pp. 6181–6186. doi: 10.1073/pnas.95.11.6181.

Munro, P. *et al.* (2004) 'Activation and Proteasomal Degradation of Rho GTPases by Cytotoxic Necrotizing Factor-1 Elicit a Controlled Inflammatory Response* □ S'. doi: 10.1074/jbc.M401580200.

Mustafa Ali, M. K., Sabha, M. M. and Al-Rabi, K. H. (2015) 'Spontaneous subdural hematoma in a patient with Philadelphia chromosome-positive acute lymphoblastic leukemia with normal platelet count after dasatinib treatment', *Platelets*. Informa Healthcare, 26(5), pp. 491–494. doi: 10.3109/09537104.2014.935316.

Nachmias, V. T. (1980) 'Cytoskeleton of human platelets at rest and after spreading', *Journal of Cell Biology*. The Rockefeller University Press, 86(3), pp. 795–802. doi: 10.1083/jcb.86.3.795.

Naik, U. P. (2014) 'Bacteria exploit platelets', *Blood*. American Society of Hematology, pp. 3067–3068. doi: 10.1182/blood-2014-04-565432.

Nakamura, N. *et al.* (2000) 'Phosphorylation of ERM proteins at filopodia induced by Cdc42', *Genes to Cells*. John Wiley & Sons, Ltd, 5(7), pp. 571–581. doi: 10.1046/j.1365-2443.2000.00348.x.

Neelakantan, P. *et al.* (2012) 'Platelet dysfunction associated with ponatinib, a new pan BCR-ABL inhibitor with efficacy for chronic myeloid leukemia resistant to multiple tyrosine kinase inhibitor therapy', *Haematologica*. Ferrata Storti Foundation, p. 1444. doi: 10.3324/haematol.2012.064618.

Neumüller, J., Ellinger, A. and Wagner, T. (2015) 'Transmission Electron Microscopy of Platelets FROM Apheresis and Buffy-Coat-Derived Platelet Concentrates', in *The Transmission Electron Microscope - Theory and Applications*. InTech. doi: 10.5772/60673.

Nguyen, T., Ghebrehiwet, B. and Peerschke, E. I. B. (2000) 'Staphylococcus aureus protein A recognizes platelet gC1qR/p33: A novel mechanism for staphylococcal interactions with platelets', *Infection and Immunity*, 68(4), pp. 2061–2068. doi: 10.1128/IAI.68.4.2061-2068.2000.

- Nicolson, P. L. R. *et al.* (2018) 'Inhibition of Btk by Btk-specific concentrations of ibrutinib and acalabrutinib delays but does not block platelet aggregation to GPVI', *Haematologica*, 103(12), pp. 2097–2108. doi: 10.3324/haematol.2018.193391.
- Nobes, C. D. and Hall, A. (1995) 'Rho, Rac, and Cdc42 GTPases regulate the assembly of multimolecular focal complexes associated with actin stress fibers, lamellipodia, and filopodia', *Cell*, 81(1), pp. 53–62. doi: 10.1016/0092-8674(95)90370-4.
- O'Neill, L. A. J. (2006) 'How Toll-like receptors signal: What we know and what we don't know', *Current Opinion in Immunology*, pp. 3–9. doi: 10.1016/j.coi.2005.11.012.
- O'Seaghda, M. *et al.* (2006) 'Staphylococcus aureus protein A binding to von Willebrand factor A1 domain is mediated by conserved IgG binding regions', *FEBS Journal*. John Wiley & Sons, Ltd, 273(21), pp. 4831–4841. doi: 10.1111/j.1742-4658.2006.05482.x.
- O'Shea, J. C. and Tcheng, J. E. (2002) 'Eptifibatide: A potent inhibitor of the platelet receptor integrin glycoprotein IIb/IIIa', *Expert Opinion on Pharmacotherapy*, pp. 1199–1210. doi: 10.1517/14656566.3.8.1199.
- O'Brien, L. *et al.* (2002) 'Multiple mechanisms for the activation of human platelet aggregation by Staphylococcus aureus: roles for the clumping factors ClfA and ClfB, the serine-aspartate repeat protein SdrE and protein A', *Molecular Microbiology*. John Wiley & Sons, Ltd, 44(4), pp. 1033–1044. doi: 10.1046/j.1365-2958.2002.02935.x.
- Obergfell, A. *et al.* (2002) 'Coordinate interactions of Csk, Src, and Syk kinases with α IIb β 3 initiate integrin signaling to the cytoskeleton', *Journal of Cell Biology*. The Rockefeller University Press, 157(2), pp. 265–275. doi: 10.1083/jcb.200112113.
- Offermanns, S. *et al.* (1997) 'Defective platelet activation in G α (q)-deficient mice', *Nature*. Nature Publishing Group, 389(6647), pp. 183–186. doi: 10.1038/38284.
- Offermanns, S. (2006) 'Activation of platelet function through G protein-coupled receptors', *Circulation Research*, pp. 1293–1304. doi: 10.1161/01.RES.0000251742.71301.16.
- Ogawa, M. (1993) 'Differentiation and proliferation of hematopoietic stem cells', *Blood*, 81(11).
- Ondusko, D. S. and Nolt, D. (2018) 'Staphylococcus aureus', *Pediatrics in Review*. American Academy of Pediatrics, 39(6), pp. 287–298. doi: 10.1542/pir.2017-0224.
- Ota, T. *et al.* (2015) 'Positive regulation of Rho GTPase activity by RhoGDIs as a result of their direct interaction with GAPs', *BMC Systems Biology*. BioMed Central Ltd., 9(1), p. 3. doi: 10.1186/s12918-015-0143-5.
- Packard, T. A. and Cambier, J. C. (2013) 'B lymphocyte antigen receptor signaling: Initiation, amplification, and regulation', *F1000Prime Reports*. Faculty of 1000 Ltd, 5. doi:

10.12703/P5-40.

Page, M. J. and Pretorius, E. (2020) 'A Champion of Host Defense: A Generic Large-Scale Cause for Platelet Dysfunction and Depletion in Infection', *Seminars in Thrombosis and Hemostasis*. Thieme Medical Publishers, Inc., 46(3), pp. 302–319. doi: 10.1055/s-0040-1708827.

Pal Singh, S., Dammeijer, F. and Hendriks, R. W. (2018) 'Role of Bruton's tyrosine kinase in B cells and malignancies', *Molecular Cancer*. BioMed Central Ltd., p. 57. doi: 10.1186/s12943-018-0779-z.

Palankar, R. *et al.* (2018) 'Platelets kill bacteria by bridging innate and adaptive immunity via platelet factor 4 and FcγRIIA', *Journal of Thrombosis and Haemostasis*. Blackwell Publishing Ltd, 16(6), pp. 1187–1197. doi: 10.1111/jth.13955.

Palecek, S. P. *et al.* (1997) 'Integrin-ligand binding properties govern cell migration speed through cell-substratum adhesiveness', *Nature*. Nature Publishing Group, 385(6616), pp. 537–540. doi: 10.1038/385537a0.

Pandey, D. *et al.* (2009) 'Unraveling a novel Rac1-mediated signaling pathway that regulates cofilin dephosphorylation and secretion in thrombin-stimulated platelets', *Blood*. Blood, 114(2), pp. 415–424. doi: 10.1182/blood-2008-10-183582.

Pang, L., Weiss, M. J. and Poncz, M. (2005) 'Megakaryocyte biology and related disorders.', *The Journal of clinical investigation*. American Society for Clinical Investigation, 115(12), pp. 3332–8. doi: 10.1172/JCI26720.

Pasquet, J.-M. *et al.* (1999) 'LAT Is Required for Tyrosine Phosphorylation of Phospholipase C γ 2 and Platelet Activation by the Collagen Receptor GPVI', *Molecular and Cellular Biology*. American Society for Microbiology, 19(12), pp. 8326–8334. doi: 10.1128/mcb.19.12.8326.

Patel, S. R. *et al.* (2005) 'The biogenesis of platelets from megakaryocyte proplatelets.', *The Journal of clinical investigation*. American Society for Clinical Investigation, 115(12), pp. 3348–54. doi: 10.1172/JCI26891.

Pawar, P. *et al.* (2004) ' Fluid Shear Regulates the Kinetics and Receptor Specificity of Staphylococcus aureus Binding to Activated Platelets ', *The Journal of Immunology*. The American Association of Immunologists, 173(2), pp. 1258–1265. doi: 10.4049/jimmunol.173.2.1258.

Pellegrin, S. and Mellor, H. (2007) 'Actin stress fibers', *Journal of Cell Science*. The Company of Biologists Ltd, 120(20), pp. 3491–3499. doi: 10.1242/jcs.018473.

Periayah, M. H., Halim, A. S. and Mat Saad, A. Z. (2017) 'Mechanism Action of Platelets and Crucial Blood Coagulation Pathways in Hemostasis.', *International journal of hematology-oncology and stem cell research*. Tehran University of Medical Sciences, 11(4), pp. 319–327.

Peters, C. G., Michelson, A. D. and Flaumenhaft, R. (2012) 'Granule exocytosis is required for platelet spreading: Differential sorting of α -granules expressing VAMP-7', *Blood*. American Society of Hematology, 120(1), pp. 199–206. doi: 10.1182/blood-2011-10-389247.

Petito, E., Momi, S. and Gresele, P. (2017) 'The migration of platelets and their interaction with other migrating cells', in *Platelets in Thrombotic and Non-Thrombotic Disorders: Pathophysiology, Pharmacology and Therapeutics: an Update*. Cham: Springer International Publishing, pp. 337–351. doi: 10.1007/978-3-319-47462-5_25.

Pitchford, S. C. *et al.* (2008) 'Allergen induces the migration of platelets to lung tissue in allergic asthma', *American Journal of Respiratory and Critical Care Medicine*, 177(6), pp. 604–612. doi: 10.1164/rccm.200702-214OC.

Piteau, M. *et al.* (2014) 'Lu/BCAM Adhesion Glycoprotein Is a Receptor for Escherichia coli Cytotoxic Necrotizing Factor 1 (CNF1)', *PLoS Pathogens*. Public Library of Science, 10(1). doi: 10.1371/journal.ppat.1003884.

Pleines, I. *et al.* (2009) 'Rac1 is essential for phospholipase C- γ 2 activation in platelets', *Pflügers Archiv European Journal of Physiology*. Springer Verlag, 457(5), pp. 1173–1185. doi: 10.1007/s00424-008-0573-7.

Pleines, I. *et al.* (2010) 'Multiple alterations of platelet functions dominated by increased secretion in mice lacking Cdc42 in platelets', *Blood*. Blood, 115(16), pp. 3364–3373. doi: 10.1182/blood-2009-09-242271.

Pleines, I. *et al.* (2012) 'Megakaryocyte-specific RhoA deficiency causes macrothrombocytopenia and defective platelet activation in hemostasis and thrombosis', *Blood*. American Society of Hematology, 119(4), pp. 1054–1063. doi: 10.1182/blood-2011-08-372193.

Plummer, C. *et al.* (2005) 'A serine-rich glycoprotein of Streptococcus sanguis mediates adhesion to platelets via GPIb', *British Journal of Haematology*. John Wiley & Sons, Ltd, 129(1), pp. 101–109. doi: 10.1111/j.1365-2141.2005.05421.x.

Pollard, T. D. and Cooper, J. A. (1986) 'Actin and Actin-Binding Proteins. A Critical Evaluation of Mechanisms and Functions', *Annual Review of Biochemistry*. Annual Reviews, 55(1), pp. 987–1035. doi: 10.1146/annurev.bi.55.070186.005011.

Pollard, T. D. and Cooper, J. A. (2009) 'Actin, a central player in cell shape and movement', *Science*. American Association for the Advancement of Science, pp. 1208–1212. doi: 10.1126/science.1175862.

Posner, M. G. *et al.* (2016) 'Extracellular fibrinogen-binding protein (Efb) from staphylococcus aureus inhibits the formation of platelet-leukocyte complexes', *Journal of Biological Chemistry*. American Society for Biochemistry and Molecular Biology Inc., 291(6), pp. 2764–2776. doi: 10.1074/jbc.M115.678359.

Poulter, N. S. *et al.* (2015) 'Platelet actin nodules are podosome-like structures dependent on Wiskott-Aldrich syndrome protein and ARP2/3 complex', *Nature Communications*. Nature Publishing Group, 6(1), pp. 1–15. doi: 10.1038/ncomms8254.

Qiao, J. *et al.* (2015) 'The platelet Fc receptor, FcγRIIIa', *Immunological Reviews*, 268(1), pp. 241–252. doi: 10.1111/imr.12370.

Quintás-Cardama, A. *et al.* (2009) 'Tyrosine kinase inhibitor-induced platelet dysfunction in patients with chronic myeloid leukemia', *Blood*. American Society of Hematology, 114(2), pp. 261–263. doi: 10.1182/blood-2008-09-180604.

Ragab, A. *et al.* (2007) 'Roles of the C-terminal tyrosine residues of LAT in GPVI-induced platelet activation: Insights into the mechanism of PLCγ2 activation', *Blood*. American Society of Hematology, 110(7), pp. 2466–2474. doi: 10.1182/blood-2007-02-075432.

Rana, A. *et al.* (2019) 'Shear-Dependent Platelet Aggregation: Mechanisms and Therapeutic Opportunities', *Frontiers in Cardiovascular Medicine*. Frontiers Media S.A. doi: 10.3389/fcvm.2019.00141.

Reeves, C. *et al.* (2018) 'Rotating lamellipodium waves in polarizing cells', *Communications Physics*. Nature Research, 1(1), pp. 1–11. doi: 10.1038/s42005-018-0075-7.

Reilly, M. P. *et al.* (2011) 'PRT-060318, a novel Syk inhibitor, prevents heparin-induced thrombocytopenia and thrombosis in a transgenic mouse model', *Blood*. American Society of Hematology, 117(7), pp. 2241–2246. doi: 10.1182/blood-2010-03-274969.

Reppin, F. *et al.* (2018) 'High affinity binding of escherichia coli cytotoxic necrotizing factor 1 (CNF1) to Lu/BCAM adhesion glycoprotein', *Toxins*. MDPI AG, 10(1), p. 3. doi: 10.3390/toxins10010003.

Riaz, A. H. *et al.* (2012) 'Human platelets efficiently kill IgG-opsonized E. coli', *FEMS Immunology and Medical Microbiology*. NIH Public Access, 65(1), pp. 78–83. doi: 10.1111/j.1574-695X.2012.00945.x.

Richardson, J. L. *et al.* (2005) 'Mechanisms of organelle transport and capture along proplatelets during platelet production', *Blood*. The American Society of Hematology, 106(13), pp. 4066–4075. doi: 10.1182/blood-2005-06-2206.

Ridley, A. J. *et al.* (1992) 'The small GTP-binding protein rac regulates growth factor-induced membrane ruffling', *Cell*, 70(3), pp. 401–410. doi: 10.1016/0092-8674(92)90164-8.

Riley, D. R. J. *et al.* (2019) 'Biochemical and immunocytochemical characterization of coronins in platelets', *Platelets*. Taylor and Francis Ltd, pp. 1–12. doi: 10.1080/09537104.2019.1696457.

Rivera, J. *et al.* (2009) 'Platelet receptors and signaling in the dynamics of thrombus formation', *Haematologica*, pp. 700–711. doi: 10.3324/haematol.2008.003178.

Rivero, F. (2008) 'Endocytosis and the Actin Cytoskeleton in Dictyostelium discoideum', *International Review of Cell and Molecular Biology*, pp. 343–397. doi: 10.1016/S1937-6448(08)00633-3.

Rivero, F. and Calaminus, S. (2018) 'Methods to study the roles of Rho GTPases in platelet function', in *Methods in Molecular Biology*. Humana Press Inc., pp. 199–217. doi: 10.1007/978-1-4939-8612-5_14.

Rosado, J. A., Jenner, S. and Sage, S. O. (2000) 'A role for the actin cytoskeleton in the initiation and maintenance of store-mediated calcium entry in human platelets. Evidence for conformational coupling', *Journal of Biological Chemistry*. American Society for Biochemistry and Molecular Biology, 275(11), pp. 7527–7533. doi: 10.1074/jbc.275.11.7527.

Ross, R. *et al.* (1974) 'A platelet dependent serum factor that stimulates the proliferation of arterial smooth muscle cells in vitro', *Proceedings of the National Academy of Sciences of the United States of America*. National Academy of Sciences, 71(4), pp. 1207–1210. doi: 10.1073/pnas.71.4.1207.

Rubin, E. J. *et al.* (1988) 'Functional modification of a 21-kilodalton G protein when ADP-ribosylated by exoenzyme C3 of Clostridium botulinum.', *Molecular and Cellular Biology*. American Society for Microbiology, 8(1), pp. 418–426. doi: 10.1128/mcb.8.1.418.

Saboor, M. *et al.* (2013) 'Platelet receptors: An instrumental of platelet physiology', *Pakistan Journal of Medical Sciences*. doi: 10.12669/pjms.293.3497.

Sahu, K. K. *et al.* (2016) 'Dasatinib and Dysfunction of Platelets', *Indian Journal of Hematology and Blood Transfusion*. Springer India, 32, pp. 246–247. doi: 10.1007/s12288-016-0659-x.

Salzman, E. W., Kensler, P. C. and Levine, L. (1972) 'CYCLIC 3',5'-ADENOSINE MONOPHOSPHATE IN HUMAN BLOOD PLATELETS IV. REGULATORY ROLE OF CYCLIC AMP IN PLATELET FUNCTION', *Annals of the New York Academy of Sciences*, 201(1), pp. 61–71. doi: 10.1111/j.1749-6632.1972.tb16287.x.

Sander, H. J. *et al.* (1983) 'Immunocytochemical localization of fibrinogen, platelet factor 4, and beta thromboglobulin in thin frozen sections of human blood platelets', *Journal of Clinical Investigation*. American Society for Clinical Investigation, 72(4), pp. 1277–1287. doi: 10.1172/JCI111084.

Sannes, M. R. *et al.* (2004) 'Virulence Factor Profiles and Phylogenetic Background of Escherichia coli Isolates from Veterans with Bacteremia and Uninfected Control Subjects', *The Journal of Infectious Diseases*. Oxford University Press (OUP), 190(12), pp. 2121–2128. doi: 10.1086/425984.

Saravia-Otten, P., Müller, H. P. and Arvidson, S. (1997) 'Transcription of Staphylococcus aureus fibronectin binding protein genes is negatively regulated by agr and an agr-

independent mechanism', *Journal of Bacteriology*. American Society for Microbiology, 179(17), pp. 5259–5263. doi: 10.1128/jb.179.17.5259-5263.1997.

Sarowska, J. *et al.* (2019) 'Virulence factors, prevalence and potential transmission of extraintestinal pathogenic *Escherichia coli* isolated from different sources: Recent reports', *Gut Pathogens*. BioMed Central Ltd., p. 10. doi: 10.1186/s13099-019-0290-0.

Sawyers, C. L. (1993) 'Molecular consequences of the BCR-ABL translocation in chronic myelogenous leukemia', *Leukemia and Lymphoma*. Informa Healthcare, 11(S2), pp. 101–103. doi: 10.3109/10428199309064268.

Schaks, M. *et al.* (2019) 'RhoG and Cdc42 can contribute to Rac-dependent lamellipodia formation through WAVE regulatory complex-binding', *Small GTPases*. Taylor and Francis Inc., pp. 1–11. doi: 10.1080/21541248.2019.1657755.

Scharf, R. E. (2012) 'Drugs that affect platelet function', *Seminars in Thrombosis and Hemostasis*. Semin Thromb Hemost, 38(8), pp. 865–883. doi: 10.1055/s-0032-1328881.

Schlesinger, M. (2018) 'Role of platelets and platelet receptors in cancer metastasis 06 Biological Sciences 0601 Biochemistry and Cell Biology', *Journal of Hematology and Oncology*. BioMed Central Ltd., pp. 1–15. doi: 10.1186/s13045-018-0669-2.

Schmidt, E. M. *et al.* (2011) 'Ion channels in the regulation of platelet migration', *Biochemical and Biophysical Research Communications*. Biochem Biophys Res Commun, 415(1), pp. 54–60. doi: 10.1016/j.bbrc.2011.10.009.

Schmidt, G. *et al.* (1997) 'Gin 63 of Rho is deamidated by *Escherichia coli* cytotoxic necrotizing factor-1', *Nature*, 387(6634), pp. 725–729. doi: 10.1038/42735.

Schrottmaier, W. C. *et al.* (2015) 'Aspirin and P2Y12 inhibitors in platelet-mediated activation of neutrophils and monocytes', *Thrombosis and Haemostasis*. Schattauer GmbH, 114(3), pp. 478–489. doi: 10.1160/TH14-11-0943.

Schurr, Y. *et al.* (2019) 'The cytoskeletal crosslinking protein MACF1 is dispensable for thrombus formation and hemostasis', *Scientific Reports*. Nature Publishing Group, 9(1), pp. 1–8. doi: 10.1038/s41598-019-44183-6.

Semple, J. W. and Freedman, J. (2010) 'Platelets and innate immunity', *Cellular and Molecular Life Sciences*, pp. 499–511. doi: 10.1007/s00018-009-0205-1.

Senis, Y. A., Mazharian, A. and Mori, J. (2014) 'Src family kinases: At the forefront of platelet activation', *Blood*. American Society of Hematology, pp. 2013–2024. doi: 10.1182/blood-2014-01-453134.

Series, J. *et al.* (2019) 'Differences and similarities in the effects of ibrutinib and acalabrutinib on platelet functions', *Haematologica*. Ferrata Storti Foundation, 104(11), pp. 2292–2299. doi: 10.3324/haematol.2018.207183.

SEVERIN, S. *et al.* (2013) 'A confocal-based morphometric analysis shows a functional crosstalk between the actin filament system and microtubules in thrombin-stimulated platelets', *Journal of Thrombosis and Haemostasis*. John Wiley & Sons, Ltd, 11(1), pp. 183–186. doi: 10.1111/jth.12053.

Séverin, S. *et al.* (2012) 'Distinct and overlapping functional roles of Src family kinases in mouse platelets', *Journal of Thrombosis and Haemostasis*. NIH Public Access, 10(8), pp. 1631–1645. doi: 10.1111/j.1538-7836.2012.04814.x.

Shang, X. *et al.* (2012) 'Rational design of small molecule inhibitors targeting rho subfamily rho GTPases', *Chemistry and Biology*. Cell Press, 19(6), pp. 699–710. doi: 10.1016/j.chembiol.2012.05.009.

Shannon, O. (2017) 'Determining platelet activation and aggregation in response to bacteria', in *Methods in Molecular Biology*. Humana Press Inc., pp. 267–273. doi: 10.1007/978-1-4939-6673-8_17.

Shannon, O. and Flock, J. I. (2004) 'Extracellular fibrinogen binding protein, Efb, from *Staphylococcus aureus* binds to platelets and inhibits platelet aggregation', *Thrombosis and Haemostasis*. Schattauer GmbH, 91(4), pp. 779–789. doi: 10.1160/th03-05-0287.

Sharda, A. and Flaumenhaft, R. (2018) 'The life cycle of platelet granules.', *F1000Research*. Faculty of 1000 Ltd, 7, p. 236. doi: 10.12688/f1000research.13283.1.

Shattil, S. J. *et al.* (1980) 'Carbenicillin and penicillin G inhibit platelet function in vitro by impairing the interaction of agonists with the platelet surface', *Journal of Clinical Investigation*. American Society for Clinical Investigation, 65(2), pp. 329–337. doi: 10.1172/JCI109676.

Shenker, A. *et al.* (1991) 'The G protein coupled to the thromboxane A2 receptor in human platelets is a member of the novel Gq family.', *The Journal of biological chemistry*, 266(14), pp. 9309–13.

Sheu, J. R. *et al.* (2000) 'Mechanisms involved in the antiplatelet activity of *Staphylococcus aureus* lipoteichoic acid in human platelets.', *Thrombosis and haemostasis*, 83(5), pp. 777–84.

Shin, E. K. *et al.* (2017) 'Platelet shape changes and cytoskeleton dynamics as novel therapeutic targets for anti-thrombotic drugs', *Biomolecules and Therapeutics*. Korean Society of Applied Pharmacology, pp. 223–230. doi: 10.4062/biomolther.2016.138.

Siboo, I. R., Chambers, H. F. and Sullam, P. M. (2005) 'Role of SraP, a serine-rich surface protein of *Staphylococcus aureus*, in binding to human platelets', *Infection and Immunity*. American Society for Microbiology (ASM), 73(4), pp. 2273–2280. doi: 10.1128/IAI.73.4.2273-2280.2005.

Sigismund, S. *et al.* (2012) 'Endocytosis and signaling: Cell logistics shape the eukaryotic cell

plan', *Physiological Reviews*. Europe PMC Funders, 92(1), pp. 273–366. doi: 10.1152/physrev.00005.2011.

Sikora, J. *et al.* (2013) 'Effect of statins on platelet function in patients with hyperlipidemia', *Archives of Medical Science*. Termedia Publishing, 9(4), pp. 622–628. doi: 10.5114/aoms.2013.36905.

Silhavy, T. J., Kahne, D. and Walker, S. (2010) 'The bacterial cell envelope.', *Cold Spring Harbor perspectives in biology*. doi: 10.1101/cshperspect.a000414.

Silverstein, R. L. and Nachman, R. L. (1987) 'Thrombospondin binds to monocytes-macrophages and mediates platelet-monocyte adhesion', *Journal of Clinical Investigation*. American Society for Clinical Investigation, 79(3), pp. 867–874. doi: 10.1172/JCI112896.

Smyth, S. S. *et al.* (2009) 'G-protein-coupled receptors as signaling targets for antiplatelet therapy', *Arteriosclerosis, Thrombosis, and Vascular Biology*, pp. 449–457. doi: 10.1161/ATVBAHA.108.176388.

SMYTH, S. S. *et al.* (2009) 'Platelet functions beyond hemostasis', *Journal of Thrombosis and Haemostasis*, 7(11), pp. 1759–1766. doi: 10.1111/j.1538-7836.2009.03586.x.

Sonmez, O. and Sonmez, M. (2017) 'Role of platelets in immune system and inflammation', *Porto Biomedical Journal*. No longer published by Elsevier, 2(6), pp. 311–314. doi: 10.1016/J.PBJ.2017.05.005.

SPALTON, J. C. *et al.* (2009) 'The novel Syk inhibitor R406 reveals mechanistic differences in the initiation of GPVI and CLEC-2 signaling in platelets', *Journal of Thrombosis and Haemostasis*. John Wiley & Sons, Ltd, 7(7), pp. 1192–1199. doi: 10.1111/j.1538-7836.2009.03451.x.

Spector, I. *et al.* (1999) 'New anti-actin drugs in the study of the organization and function of the actin cytoskeleton.', *Microscopy research and technique*, 47(1), pp. 18–37. doi: 10.1002/(SICI)1097-0029(19991001)47:1<18::AID-JEMT3>3.0.CO;2-E.

Speth, C. *et al.* (2013) 'Platelets as immune cells in infectious diseases', *Future Microbiology*, pp. 1431–1451. doi: 10.2217/fmb.13.104.

Spurgeon, B. E. J. (2014) *Phosphoproteomic Analysis of Platelet Signalling Cascades by Flow Cytometry*.

Ståhl, A. L. *et al.* (2006) 'Lipopolysaccharide from enterohemorrhagic *Escherichia coli* binds to platelets through TLR4 and CD62 and is detected on circulating platelets in patients with hemolytic uremic syndrome', *Blood*. The American Society of Hematology, 108(1), pp. 167–176. doi: 10.1182/blood-2005-08-3219.

Stalker, T. J. *et al.* (2012) 'Platelet Signaling', in *Handbook of experimental pharmacology*. NIH Public Access, pp. 59–85. doi: 10.1007/978-3-642-29423-5_3.

- Stefanini, L. *et al.* (2012) 'Rap1-Rac1 circuits potentiate platelet activation', *Arteriosclerosis, Thrombosis, and Vascular Biology*. NIH Public Access, 32(2), pp. 434–441. doi: 10.1161/ATVBAHA.111.239194.
- de Stoppelaar, S. F., van 't Veer, C. and van der Poll, T. (2014) 'The role of platelets in sepsis', *Thrombosis and Haemostasis*. Schattauer GmbH, 112(4), pp. 666–677. doi: 10.1160/TH14-02-0126.
- Suehiro, A. *et al.* (1993) 'Inhibitory effect of staphylokinase on platelet aggregation.', *Thromb Haemost*, 70(5), pp. 834–837.
- Sun, B. *et al.* (2001) 'Luminometric assay of platelet activation in 96-well microplate', *BioTechniques*, 31(5), pp. 1174–1181. doi: 10.2144/01315dd02.
- Suzuki, A. *et al.* (2013) 'RhoA Is Essential for Maintaining Normal Megakaryocyte Ploidy and Platelet Generation', *PLoS ONE*. Edited by K. Freson. Public Library of Science, 8(7), p. e69315. doi: 10.1371/journal.pone.0069315.
- Svensson, L. *et al.* (2014) 'Platelet activation by *Streptococcus pyogenes* leads to entrapment in platelet aggregates, from which bacteria subsequently escape', *Infection and Immunity*. American Society for Microbiology, 82(10), pp. 4307–4314. doi: 10.1128/IAI.02020-14.
- Svitkina, T. M. and Borisy, G. G. (1999) 'Arp2/3 complex and actin depolymerizing factor/cofilin in dendritic organization and treadmilling of actin filament array in lamellipodia', *Journal of Cell Biology*, 145(5), pp. 1009–1026. doi: 10.1083/jcb.145.5.1009.
- Tabak, H. F. *et al.* (2003) 'Peroxisomes start their life in the endoplasmic reticulum', *Traffic*. Blackwell Munksgaard, pp. 512–518. doi: 10.1034/j.1600-0854.2003.00110.x.
- Tanaka, K. and Itoh, K. (1998) 'Reorganization of stress fiber-like structures in spreading platelets during surface activation', *Journal of Structural Biology*. Academic Press Inc., 124(1), pp. 13–41. doi: 10.1006/jsbi.1998.4051.
- Tang, Y. Q., Yeaman, M. R. and Selsted, M. E. (2002) 'Antimicrobial peptides from human platelets', *Infection and Immunity*, 70(12), pp. 6524–6533. doi: 10.1128/IAI.70.12.6524-6533.2002.
- Tantillo, E. *et al.* (2018) 'Bacterial Toxins and Targeted Brain Therapy: New Insights from Cytotoxic Necrotizing Factor 1 (CNF1)', *International Journal of Molecular Sciences*. MDPI AG, 19(6), p. 1632. doi: 10.3390/ijms19061632.
- Thon, J. N. and Italiano, J. E. (2010) 'Platelet formation.', *Seminars in hematology*. NIH Public Access, 47(3), pp. 220–6. doi: 10.1053/j.seminhematol.2010.03.005.
- Thon, J. N. and Italiano, J. E. (2012) 'Platelets: Production, Morphology and Ultrastructure', in, pp. 3–22. doi: 10.1007/978-3-642-29423-5_1.

Thorpe, C. M. *et al.* (1999) 'Shiga Toxins Do Not Directly Stimulate Alpha-Granule Secretion or Enhance Aggregation of Human Platelets', *Acta Haematologica*. Karger Publishers, 102(1), pp. 51–55. doi: 10.1159/000040968.

Tillman, B. F. *et al.* (2018) 'Systematic review of infectious events with the Bruton tyrosine kinase inhibitor ibrutinib in the treatment of hematologic malignancies', *European Journal of Haematology*. Blackwell Publishing Ltd, pp. 325–334. doi: 10.1111/ejh.13020.

Tojkander, S., Gateva, G. and Lappalainen, P. (2012) 'Actin stress fibers - Assembly, dynamics and biological roles', *Journal of Cell Science*. The Company of Biologists Ltd, 125(8), pp. 1855–1864. doi: 10.1242/jcs.098087.

Tomaiuolo, M., Brass, L. F. and Stalker, T. J. (2017) 'Regulation of Platelet Activation and Coagulation and Its Role in Vascular Injury and Arterial Thrombosis', *Interventional Cardiology Clinics*. Elsevier Inc., pp. 1–12. doi: 10.1016/j.iccl.2016.08.001.

Torres, V. J. *et al.* (2006) 'Staphylococcus aureus IsdB is a hemoglobin receptor required for heme iron utilization', *Journal of Bacteriology*, 188(24), pp. 8421–8429. doi: 10.1128/JB.01335-06.

Towbin, H., Staehelin, T. and Gordon, J. (1979) 'Electrophoretic transfer of proteins from polyacrylamide gels to nitrocellulose sheets: Procedure and some applications', *Proceedings of the National Academy of Sciences of the United States of America*, 76(9), pp. 4350–4354. doi: 10.1073/pnas.76.9.4350.

Tran, U. *et al.* (2006) 'Staphylococcal enterotoxin B initiates protein kinase C translocation and eicosanoid metabolism while inhibiting thrombin-induced aggregation in human platelets', *Molecular and Cellular Biochemistry*. Springer, 288(1–2), pp. 171–178. doi: 10.1007/s11010-006-9134-6.

Travaglione, S., Fabbri, A. and Fiorentini, C. (2008) 'The Rho-activating CNF1 toxin from pathogenic E. coli: A risk factor for human cancer development?', *Infectious Agents and Cancer*. BioMed Central, p. 4. doi: 10.1186/1750-9378-3-4.

Trepap, X., Chen, Z. and Jacobson, K. (2012) 'Cell migration.', *Comprehensive Physiology*. NIH Public Access, pp. 2369–2392. doi: 10.1002/cphy.c110012.

Tullemans, B. M. E., Heemskerk, J. W. M. and Kuijpers, M. J. E. (2018) 'Acquired platelet antagonism: off-target antiplatelet effects of malignancy treatment with tyrosine kinase inhibitors', *Journal of Thrombosis and Haemostasis*. Blackwell Publishing Ltd, 16(9), pp. 1686–1699. doi: 10.1111/jth.14225.

Vallance, M. T. *et al.* (2017) 'Toll-Like Receptor 4 Signalling and Its Impact on Platelet Function, Thrombosis, and Haemostasis', *Mediators Inflamm*.

Vannini, E. *et al.* (2014) 'The bacterial protein toxin, cytotoxic necrotizing factor 1 (CNF1) provides long-term survival in a murine glioma model', *BMC Cancer*. BioMed Central Ltd.,

14(1). doi: 10.1186/1471-2407-14-449.

Vardon-Bounes, F. *et al.* (2019) 'Platelets are critical key players in sepsis', *International Journal of Molecular Sciences*. MDPI AG. doi: 10.3390/ijms20143494.

Varga-Szabo, D., Braun, A. and Nieswandt, B. (2009) 'Calcium signaling in platelets', *Journal of Thrombosis and Haemostasis*. Blackwell Publishing Ltd, pp. 1057–1066. doi: 10.1111/j.1538-7836.2009.03455.x.

Varga-Szabo, D., Pleines, I. and Nieswandt, B. (2008) 'Cell Adhesion Mechanisms in Platelets', *Arteriosclerosis, Thrombosis, and Vascular Biology*. Lippincott Williams and Wilkins, 28(3), pp. 403–412. doi: 10.1161/ATVBAHA.107.150474.

Veri, M. C. *et al.* (2007) 'Monoclonal antibodies capable of discriminating the human inhibitory Fcγ-receptor IIB (CD32B) from the activating Fcγ-receptor IIA (CD32A): Biochemical, biological and functional characterization', *Immunology*, 121(3), pp. 392–404. doi: 10.1111/j.1365-2567.2007.02588.x.

Verschoor, A. and Langer, H. F. (2013) 'Crosstalk between platelets and the complement system in immune protection and disease', *Thrombosis and Haemostasis*, pp. 910–919. doi: 10.1160/TH13-02-0102.

Viela, F. *et al.* (2019) 'Binding of staphylococcus aureus protein a to von willebrand factor is regulated by mechanical force', *mBio*. American Society for Microbiology, 10(2). doi: 10.1128/mBio.00555-19.

Vorchheimer, D. A. and Becker, R. (2006) 'Platelets in atherothrombosis', *Mayo Clinic Proceedings*. Elsevier Ltd, pp. 59–68. doi: 10.4065/81.1.59.

Vouret-Craviari, V. *et al.* (1999) 'Effects of cytotoxic necrotizing factor 1 and lethal toxin on actin cytoskeleton and VE-cadherin localization in human endothelial cell monolayers', *Infection and Immunity*. American Society for Microbiology, 67(6), pp. 3002–3008. doi: 10.1128/iai.67.6.3002-3008.1999.

Waller, A. K. *et al.* (2013) 'Staphylococcus aureus Lipoteichoic Acid Inhibits Platelet Activation and Thrombus Formation via the Paf Receptor'. doi: 10.1093/infdis/jit398.

Wang, L. *et al.* (2006) 'Genetic deletion of Cdc42GAP reveals a role of Cdc42 in erythropoiesis and hematopoietic stem/progenitor cell survival, adhesion, and engraftment', *Blood*. American Society of Hematology, 107(1), pp. 98–105. doi: 10.1182/blood-2005-05-2171.

Wang, Y. *et al.* (2005) 'Leukocyte engagement of platelet glycoprotein Iba via the integrin Mac-1 is critical for the biological response to vascular injury', *Circulation*, 112(19), pp. 2993–3000. doi: 10.1161/CIRCULATIONAHA.105.571315.

Wang, Y. K. *et al.* (2019) 'Comparison of Escherichia coli surface attachment methods for in

vivo single-cell microscopy', *In preparation*. doi: 10.1101/648840.

Watanabe, N. *et al.* (1999) 'Cooperation between mDia1 and ROCK in Rho-induced actin reorganization', *Nature Cell Biology*. Macmillan Magazines Ltd, 1(3), pp. 136–143. doi: 10.1038/11056.

Watson, C. N. *et al.* (2016) 'Human platelet activation by *Escherichia coli* : roles for FcγRIIA and integrin αIIbβ3', *Platelets*. Taylor and Francis Ltd, 27(6), pp. 535–540. doi: 10.3109/09537104.2016.1148129.

Weber, A. *et al.* (1994) 'Tropomodulin caps the pointed ends of actin filaments', *Journal of Cell Biology*, 127(6 I), pp. 1627–1635. doi: 10.1083/jcb.127.6.1627.

Weber, A. (1999) 'Actin binding proteins that change extent and rate of actin monomer-polymer distribution by different mechanisms', *Molecular and Cellular Biochemistry*. Springer, 190(1/2), pp. 67–74. doi: 10.1023/A:1006984010267.

Welch, H. C. E. *et al.* (2002) 'P-Rex1, a PtdIns(3,4,5)P3- and gβγ-regulated guanine-nucleotide exchange factor for Rac', *Cell*. Cell Press, 108(6), pp. 809–821. doi: 10.1016/S0092-8674(02)00663-3.

Welch, H. C. E. *et al.* (2003) 'Phosphoinositide 3-kinase-dependent activation of Rac', *FEBS Letters*. Elsevier, pp. 93–97. doi: 10.1016/S0014-5793(03)00454-X.

Wencel-Drake, J. D. *et al.* (1986) 'Ultrastructural localization of coagulation factor V in human platelets.', *Blood*, 68(1), pp. 244–9.

White, J. G. (1972) 'Interaction of membrane systems in blood platelets.', *American Journal of Pathology*. American Society for Investigative Pathology, 66(2), pp. 295–312.

White, J. G. (1979) 'Current concepts of platelet structure', *American Journal of Clinical Pathology*, pp. 363–378. doi: 10.1093/ajcp/71.4.363.

White, J. G. and Burris, S. M. (1984) 'Morphometry of platelet internal contraction', *American Journal of Pathology*. American Society for Investigative Pathology, 115(3), pp. 412–417.

Williams, C. M. *et al.* (2015) 'Leukemia-associated Rho guanine-nucleotide exchange factor is not critical for RhoA regulation, yet is important for platelet activation and thrombosis in mice', *Journal of Thrombosis and Haemostasis*. Blackwell Publishing Ltd, 13(11), pp. 2102–2107. doi: 10.1111/jth.13129.

Woodside, D. G. *et al.* (2001) 'Activation of Syk protein tyrosine kinase through interaction with integrin β cytoplasmic domains', *Current Biology*. Cell Press, 11(22), pp. 1799–1804. doi: 10.1016/S0960-9822(01)00565-6.

Woronowicz, K. *et al.* (2010) 'The platelet actin cytoskeleton associates with SNAREs and

participates in α -granule secretion', *Biochemistry*. NIH Public Access, 49(21), pp. 4533–4542. doi: 10.1021/bi100541t.

Worth, R. G. *et al.* (2006) 'Platelet Fc γ RIIA binds and internalizes IgG-containing complexes', *Experimental Hematology*, 34(11), pp. 1490–1495. doi: 10.1016/j.exphem.2006.06.015.

Woulfe, D. *et al.* (2004) 'Signaling receptors on platelets and megakaryocytes.', *Methods in molecular biology (Clifton, N.J.)*, pp. 3–32. doi: 10.1385/1-59259-783-1:003.

Woulfe, D. S. (2005) 'Platelet G protein-coupled receptors in hemostasis and thrombosis', *Journal of Thrombosis and Haemostasis*. John Wiley & Sons, Ltd, pp. 2193–2200. doi: 10.1111/j.1538-7836.2005.01338.x.4

Wurpel, D. J. *et al.* (2014) 'F9 fimbriae of uropathogenic Escherichia coli are expressed at low temperature and recognise Galb1-3GlcNAc-containing glycans', *PLoS ONE*. Public Library of Science, 9(3). doi: 10.1371/journal.pone.0093177.

Xavier, C.-P. *et al.* (2013) 'Evolutionary and Functional Diversity of Coronin Proteins'. Landes Bioscience. Available at: <https://www.ncbi.nlm.nih.gov/books/NBK6170/> (Accessed: 17 September 2020).

Yada, Y. *et al.* (1989) 'Inhibition by cyclic AMP of guanine nucleotide-induced activation of phosphoinositide-specific phospholipase C in human platelets', *FEBS Letters*. John Wiley & Sons, Ltd, 242(2), pp. 368–372. doi: 10.1016/0014-5793(89)80503-4.

Yan, J. and Jin, T. (2012) 'Signaling network from GPCR to the actin cytoskeleton during chemotaxis', *BioArchitecture*. Informa UK Limited, 2(1), pp. 15–18. doi: 10.4161/bioa.19740.

Yanaga, F. *et al.* (1995) 'Syk interacts with tyrosine-phosphorylated proteins in human platelets activated by collagen and cross-linking of the Fc γ -IIA receptor', *Biochemical Journal*. Portland Press Ltd, 311(2), pp. 471–478. doi: 10.1042/bj3110471.

Yeaman, M. R. *et al.* (1998) 'Platelet microbicidal proteins and neutrophil defensin disrupt the Staphylococcus aureus cytoplasmic membrane by distinct mechanisms of action', *Journal of Clinical Investigation*. American Society for Clinical Investigation, 101(1), pp. 178–187. doi: 10.1172/JCI562.

Yeaman, M. R. (2010) 'Platelets in defense against bacterial pathogens', *Cellular and Molecular Life Sciences*. Springer, pp. 525–544. doi: 10.1007/s00018-009-0210-4.

Yeaman, M. R. and Bayer, A. S. (2000) 'Staphylococcus aureus, platelets, and the heart', *Current Infectious Disease Reports*. Springer Science and Business Media LLC, 2(4), pp. 281–298. doi: 10.1007/s11908-000-0005-0.

Yoshimura, K. *et al.* (1998) 'No direct effects of Shiga toxin 1 and 2 on the aggregation of human platelets in vitro [10]', *Thrombosis and Haemostasis*. Schattauer GmbH, pp. 529–

530. doi: 10.1055/s-0037-1615248.

Youssefian, T. *et al.* (2002) 'Host defense role of platelets: Engulfment of HIV and *Staphylococcus aureus* occurs in a specific subcellular compartment and is enhanced by platelet activation', *Blood*, 99(11), pp. 4021–4029. doi: 10.1182/blood-2001-12-0191.

Yurttas, N. O. and Eskazan, A. E. (2019) 'Tyrosine Kinase Inhibitor–Associated Platelet Dysfunction: Does This Need to Have a Significant Clinical Impact?', *Clinical and Applied Thrombosis/Hemostasis*. SAGE Publications Inc., p. 107602961986692. doi: 10.1177/1076029619866925.

Yusuf, M. Z. *et al.* (2017) 'Prostacyclin reverses platelet stress fibre formation causing platelet aggregate instability', *Scientific Reports*. Nature Publishing Group, 7(1). doi: 10.1038/s41598-017-05817-9.

Zapotoczna, M. *et al.* (2013) 'Iron-regulated surface determinant B (IsdB) promotes *Staphylococcus aureus* adherence to and internalization by non-phagocytic human cells', *Cellular Microbiology*. John Wiley & Sons, Ltd, 15(6), pp. 1026–1041. doi: 10.1111/cmi.12097.

Zhang, G. *et al.* (2009) 'Lipopolysaccharide Stimulates Platelet Secretion and Potentiates Platelet Aggregation via TLR4/MyD88 and the cGMP-Dependent Protein Kinase Pathway', *The Journal of Immunology*. The American Association of Immunologists, 182(12), pp. 7997–8004. doi: 10.4049/jimmunol.0802884.

Zhang, Z. *et al.* (2018) 'Reversible senescence of human colon cancer cells after blockage of mitosis/cytokinesis caused by the CNF1 cyclomodulin from *Escherichia coli*', *Scientific Reports*. Nature Publishing Group, 8(1), p. 17780. doi: 10.1038/s41598-018-36036-5.

Zharikov, S. and Shiva, S. (2013) 'Platelet mitochondrial function: From regulation of thrombosis to biomarker of disease', in *Biochemical Society Transactions*, pp. 118–123. doi: 10.1042/BST20120327.

Zhou, L. and Schmaier, A. H. (2005) 'Platelet Aggregation Testing in Platelet-Rich Plasma Description of Procedures With the Aim to Develop Standards in the Field', *American Journal of Clinical Pathology*. Oxford University Press (OUP), 123(2), pp. 172–183. doi: 10.1309/y9ec-63rw-3xg1-v313.

Zucker-Franklin, D. (1997) 'Platelet Structure and Function', in *Thrombopoiesis and Thrombopoietins*. Totowa, NJ: Humana Press, pp. 41–62. doi: 10.1007/978-1-4612-3958-1_2.

Zuidscherwoude, M., Green, H. L. H. and Thomas, S. G. (2019) 'Formin proteins in megakaryocytes and platelets: regulation of actin and microtubule dynamics', *Platelets*. Taylor and Francis Ltd, pp. 23–30. doi: 10.1080/09537104.2018.1481937.